Functional Oligothiophenes: Molecular Design for Multidimensional Nanoarchitectures and Their Applications[†]

Amaresh Mishra, Chang-Qi Ma, and Peter Bäuerle*

Institute of Organic Chemistry II and Advanced Materials, Ulm University, Albert-Einstein-Allee 11, 89081 Ulm, Germany

Contents

[†] Dedicated to Prof. M. S. Wrighton (Washington Univ. in St. Louis), pioneer in organic and molecular electronics, on the occasion of his 60th birthday.
* Corresponding author: Telephone: +49-731-50-22850. Fax: +49-731-50-22840. E-mail: peter.baeuerle@uni-ulm.de.

1. Introduction

Functional oligothiophenes have attracted comprehensive interest among researchers all over the world and have

Amaresh Mishra (right) received his Ph.D. degree in 2000 from the Sambalpur University, India, under the coguidance of Prof. G. B. Behera and Prof. R. K. Behera, working on dye–surfactant interactions in microheterogeneous media. He started his postdoctoral research career in 1999 at the University of South Florida, Tampa, and subsequently at the University of Akron, Ohio, working with Prof. G. R. Newkome, where he gained knowledge in the area of supramolecular and dendrimer chemistry. Later, he joined the Tata Institute of Fundamental Research, Mumbai, in 2002 as a Visiting Fellow working with Prof. N. Periasamy, where he was involved in the synthesis and photophysical studies of organic light emitting materials. In 2005, he joined in the group of Prof. Peter Bäuerle, University of Ulm, Germany, as an Alexander von Humboldt Fellow. His present research interests are centered on chemistry of functional oligothiophenes, donor–acceptor-based conjugated dyes, and metal complexes toward applications in solar energy conversion and molecular electronic and photonic devices.

Chang-Qi Ma (left) received his bachelor's degree in chemistry from Beijing Normal University in 1998. In 2003 he obtained his Ph.D. degree at the Technical Institute of Physics and Chemistry, Chinese Academy of Sciences in Beijing with Professor B.-W. Zhang. After that he was a postdoctoral research assistant at Heriot-Watt University in Edinburgh, U.K., with Dr. G. Cooke, until he joined the research group of Prof. P. Bäuerle at the University of Ulm in 2004 as an Alexander von Humboldt fellow, where he is currently a research associate. His main research interests focus on the design and synthesis of novel π-conjugated organic materials for the application in organic electronics, e.g. organic solar cells.

Peter Bäuerle (center) received his Ph.D. in organic chemistry from University of Stuttgart (Germany, 1985) working with Prof. F. Effenberger. After a postdoctoral year at MIT, Boston, Massachusetts, in the group of Prof. M. S. Wrighton, he carried out independent research at the University of Stuttgart and received his habilitation (1994). After being Professor of Organic Chemistry at the University of Würzburg (Germany, 1994–95), he became Director of the Institute for Organic Chemistry II and Advanced Materials at the University of Ulm (Germany, since 1996). Current research interests of the group include development of novel organic semiconducting and conducting materials, in particular, conjugated poly- and oligothiophenes. Synthetic strategies and new reactions for their functionalization, structure–property relationships, self-assembling properties, and applications in electronic devices, in particular organic solar cells, are investigated. Results have been published in about 200 peer-reviewed scientific papers, 3 book chapters, and 7 patents. For his work in the field of plastic electronics he was awarded with the René Descartes Prize of the European Union (2000). Guest Professorships at the University of Osaka (Japan, 2002), Université Rennes 1 (France, 2004), and Melbourne (Australia, 2008) followed. He is cofounder of Heliatek GmbH, Dresden/Ulm, a spin-off company devoted to the production of organic solar cells (2006). Since October 2008 he has served as Dean of the Faculty for Natural Sciences at the University of Ulm.

actually been advanced to be among the most frequently used π-conjugated materials, in particular as active components in organic electronic devices and molecular electronics.[1,2] More recently, the traditional linear systems have been vastly extended to higher dimensionalities and novel topologies. A multitude of various not only esthetic but also func-

Chart 1.1
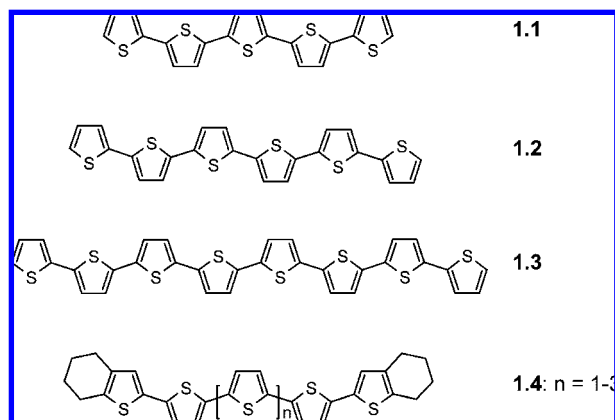
tional molecular architectures have been established and characterized.

Two key reasons count for this development: Thiophene chemistry is well established and has been developed for a long time. There are uncountable methods to modify the core molecule,[3,4] but more importantly, thiophenes are ideal building blocks in transition metal-catalyzed cross-coupling reactions which have been enormously developed in the past decades and nowadays provide the basis for the synthesis of most conjugated π-systems.[5] Besides the enormous and attractive potential of structural variation which allows tuning of the electronic properties in a wide range, the second reason why these materials are successful is their outstanding chemical and physical properties. They are typically stable in various oxidation states and can be readily characterized by many methods. Their unique electronic, optical, and redox properties are intriguing, as well as their unique self-assembling properties on solid surfaces or in the bulk. Finally, the high polarizability of sulfur atoms in thiophene rings leads to a stabilization of the conjugated chain and to excellent charge transport properties, which are one of the most crucial assets for applications in organic and molecular electronics.

In parallel to the remarkable development of π-conjugated polymers as conductors and semiconductors, a renaissance of oligothiophenes was launched in 1989 when Garnier and Fichou realized that also shorter conjugated oligomers such as α-sexithiophene (**1.2**) can be used as an active semiconductor materials in organic field-effect transistors (OFETs).[6,7] Later on, the implementation of structurally defined end-capped oligothiophenes (**1.4**: $n = 1-3$) in organic light emitting diodes (OLEDs)[8] was demonstrated in 1993, and that of α-quinquethiophene (**1.1**) and α-octithiophene (**1.3**) in organic solar cells (OSC)[9] was demonstrated in 1995 (Chart 1.1).

Furthermore, it turned out that the structurally defined and monodisperse oligomers are excellent model compounds for the corresponding polydisperse polymers, which include chain length distributions, defects, and interruptions of the conjugated chains.[10] The monitoring of the various properties in dependence of the chain length allowed establishing valuable structure–property relationships and extrapolations to the polymer.[11] Nearly for all basic π-conjugated polymers, manifold series of corresponding oligomers have been produced,[2] and finally this development led to a division of organic electronics into two worlds or philosophies: On one hand, conjugated polymers are used which can be rather simply and cheaply produced by polymerization of corresponding monomers and processed from solution, but they

Chart 2.1
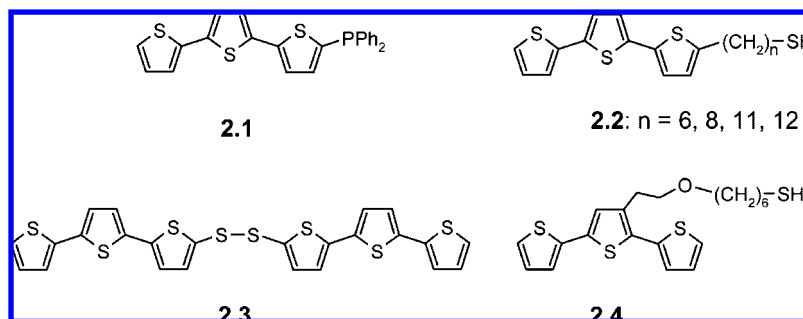
include the disadvantage of less defined molecular structures and consequently result in less perfect thin films. On the other hand, there is the field of structurally defined π-conjugated oligomers which in fact are synthetically demanding and built up in multiple step protocols but typically are processed by vacuum evaporation techniques guaranteeing more defect-free layers and films.

In the last 5−10 years, the number of publications about functionalized oligothiophenes, which can be considered as a third generation of advanced conjugated materials, dramatically increased. It was recognized that with functional groups additional and novel properties to those of the π-conjugated systems can be created which are important for many applications. Furthermore, novel molecular architectures having more complicated conjugated structures and sophisticated topologies other than linear systems have emerged as a consequence of increased versatility of thiophene chemistry and currently represent a most interesting and quickly spreading field of research. Since in most applications an ordering of the conjugated systems leads to improved properties, the control and understanding of the correlation between structure and self-organizational behavior which can be governed by functional groups and their intermolecular forces also became very important. In general, the increase of dimensionality in π-conjugated systems can lead to different superstructures in the solid state and to multidirectional charge transport.

Therefore, we felt that a review on oligothiophenes under the aspects of functionalization and molecular architecture is overdue. We tried to comprehensively take into account the results obtained in the field of functionalized oligothiophenes, in which the conjugated backbone either contains exclusively thiophene moieties or mixed systems but is built up of at least a bithiophene unit using a great variety of coupling reactions. We have tried to draw a complete image of current activities from the viewpoint of synthetic chemists in this area and their role in the field of organic/molecular electronics. The order in the article comes from the dimensionality and the type of functional groups in the oligothiophenes. Their consequences on properties and device performances were taken into account where data was available. The immense and quite recent citations included herein come from extensive literature searches using SciFinder and Scopus search engines and are very actual, covered until December 2007. It is also noteworthy that out of ~770 citations presented in this review, in excess of 540 cover the period of 2000−2007, which itself tells the story of this dynamic development. Nevertheless, our apologies are extended to those who have made contributions in this area but whose work we missed. We deliberately excluded related functionalized polythiophenes, because it would go

beyond the scope of this article. This field also has seen an enormous development and deserves a review on its own. We also did not take into account several of the structures which were already reviewed under various aspects in order to avoid repetition, and the interested reader is referred to corresponding review articles.[12−36]

2. Functionalized Linear Oligothiophenes

Oligothiophenes[1,12,37,38] and their functional derivatives have been extensively studied because of their numerous applications in OLEDs,[17,19,27] OFETs,[39−42] chemosensors,[43,44] biosensors,[45,46] and electrochromic devices[47,48] among others. In this regard, the functionalization of oligothiophenes has allowed us to develop materials with specific electronic properties, which arise from both the backbone and the functional groups.[49] In this section, we will focus exclusively on the synthesis and application of functional oligothiophenes related to their self-assembly, redox activity, metal chelating, molecular recognition, and biological activity. On the other hand, few functional polythiophenes are discussed wherever necessary and significant.

Functional oligothiophenes are generally synthesized by either oxidative homocoupling (lithiation followed by addition of $CuCl_2$ or $Fe(acac)_3$) or metal-catalyzed C−C-coupling, such as Kumada-,[50] Suzuki-,[51,52] Sonogashira-,[53] Stille-,[54] and Negishi-[55] type reactions.[56] Various characterization methods such as absorption and emission spectroscopy as well as cyclic voltammetry are normally used to analyze the electronic properties of these materials.

2.1. Oligothiophenes Containing Surface Active Groups

Organic molecular devices which comprise conjugated molecules suitably connected by self-assembly to a metal surface are of growing interest in the field of molecular scale electronics.[57,58] Among them, oligothiophenes are viewed as ideal systems, since they are electron rich and provide the outstanding ability to acquire positive charges and to transport them through self-assembled monolayers (SAMs) or thin films. Experimental and theoretical studies have been carried out to understand the assembling and electrical behavior of surface-bound, thiol-terminated conjugated oligomers based on thiophene or 2-thienylethynylene.[59−61] Thiols, disulfides, or phosphines are known as good surface anchoring groups not only for flat surfaces but also for nanoparticles.[62] In this respect, Wolf et al. recently reported the attachment of phosphine-tethered terthiophenes **2.1** (Chart 2.1) to Au nanoparticles which on elelctrochemical treatment

Chart 2.2

2.5: n = 1, 2

2.6: n = 1, 2

2.7: n = 1, 2
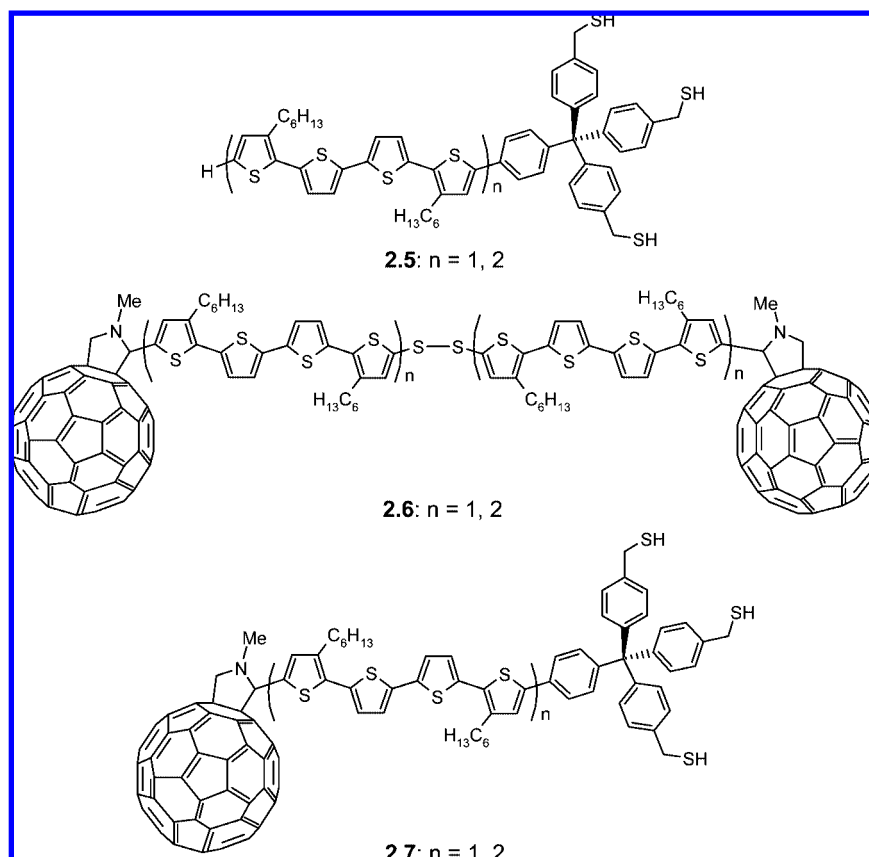
formed a cross-linked network of π-conjugated bridges and metal nanoparticles.[63,64]

The self-assembling properties of oligothiophenes were originally reported by Liedberg et al. using thiol- and disulfide-functionalized terthiophenes (Chart 2.1).[65] Undecylthiol-terminated terthiophene **2.2** (n = 11; 85%) was prepared from bithiophene in seven steps, and the final transformation to the thiol was carried out using thiourea. Bis(2,2′:5′,2″-terthien-5-yl)disulfide (**2.3**) was prepared by lithiation of α-terthiophene with n-butyl lithium (n-BuLi) and successive reaction of the monolithiated species with elemental sulfur in 58% yield. The formation of SAMs from these compounds on Au surfaces was obtained by solution processing *via* a sulfur−gold bond. Terthiophene **2.2** (n = 11) showed a rapid self-assembly in minutes and anchoring *via* thiol-groups leading to highly organized structures in which the tilt angle of the 3T units was 14° with respect to the surface. On the other hand, monolayers of **2.3** formed very slowly (required 24 h of equilibration) and showed corresponding tilt angles of 33°. A strong electronic coupling of the oligomers and the Au substrate has been proposed. Michalitsch et al. synthesized a series of similar alkylthiol-functionalized oligothiophenes **2.2** (n = 6, 8, 12) by employing Kumada cross-coupling reactions to build up the π-conjugated part. Conversion of the terminal bromines to thiols was achieved *via* formation of the corresponding isothiouronium salts by reaction with thiourea, which was subsequently cleaved by tetraethylenepentaamine.[66−68]

Terthiophene **2.4** having an 7-oxa-nonylthiol side chain attached to the β-position of the oligothiophene was obtained starting from 3-(hydroxyethyl)thiophene in 26% overall yield.[68] Terthiophene **2.4** was adsorbed on Pt- or Au-surfaces to form densely packed SAMs and subsequently was electropolymerized. The resulting thin films showed high electrochemical stability.[69]

Otsubo et al. prepared oligothiophene dyads **2.5** which at one terminus bore a thiol-functionalized tripod consisting of a central tetraphenylmethane unit and three methylthiol groups as "pads" (Chart 2.2).[70] The SAM-forming compounds were prepared by Stille coupling of the stannylated oligothiophene and 4-bromophenyl-tris(4-S-acetylthiomethylphenyl)methane in the presence of Pd(PPh₃)₄, which subsequently was deprotected to the desired thiol by alkaline hydrolysis. The thiol groups acted as rigid anchors to Au surfaces, and consequently, the oligothiophene unit pointed outward and promoted charge transfer. The system was tested in OLEDs (Au-SAM **2.5**/TPD/Alq₃/Mg−Ag) and an improvement of the electroluminescence (EL) was observed. The operating voltage at a luminance of 100 cd m^{-2} decreased from 9.5 V for the bare Au device to 8.5 V for the SAM **2.5** (n = 2) device and to 6.3 V for the SAM **2.5** (n = 1) device.[71] This finding revealed that the SAM of **2.5** (n = 2) compared to **2.5** (n = 1) is less compact on a Au-surface due to the longer conjugated chains.

The same research group reported the synthesis of fullerene-functionalized oligothiophenes **2.6** (n = 1, 2) in which two units are coupled through a disulfide bridge (Chart 2.2).[72] Later on, the synthesis of [60]fullerene-linked quater- and octithiophene **2.7** (n = 1, 2) was reported which bore the above-described thiol-functionalized tripod **2.5** (n = 1, 2), allowing the formation of well-organized SAMs.[73] Photoelectrochemical measurements were performed using the cell structure Au/SAM **2.6** or **2.7**/methyl viologen/Pt. In a photoelectrochemical cell, the modified Au-electrode acted as working electrode and methyl viologen (MV^{2+}) as an electron carrier. In comparison to a photoelectrochemical cell

Scheme 2.1

Reagents and conditions: (i) 1. Mg/THF, 2. S₈, 3. CH₃COCl; (ii) NH₄OH; (iii) 1. *t*-BuLi, 2. S₈, 3. CH₃COCl

Scheme 2.2

Reagents and conditions: (i) 1. BuLi, 2. S₈, 3. ethyl 3-bromopropionate; (ii) NBS; (iii) Pd(PPh₃)₄; (iv) 1. DBU, 2. CH₃COCl.
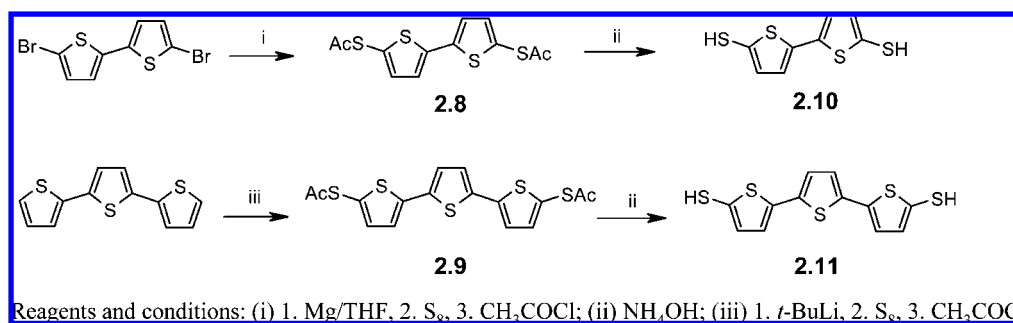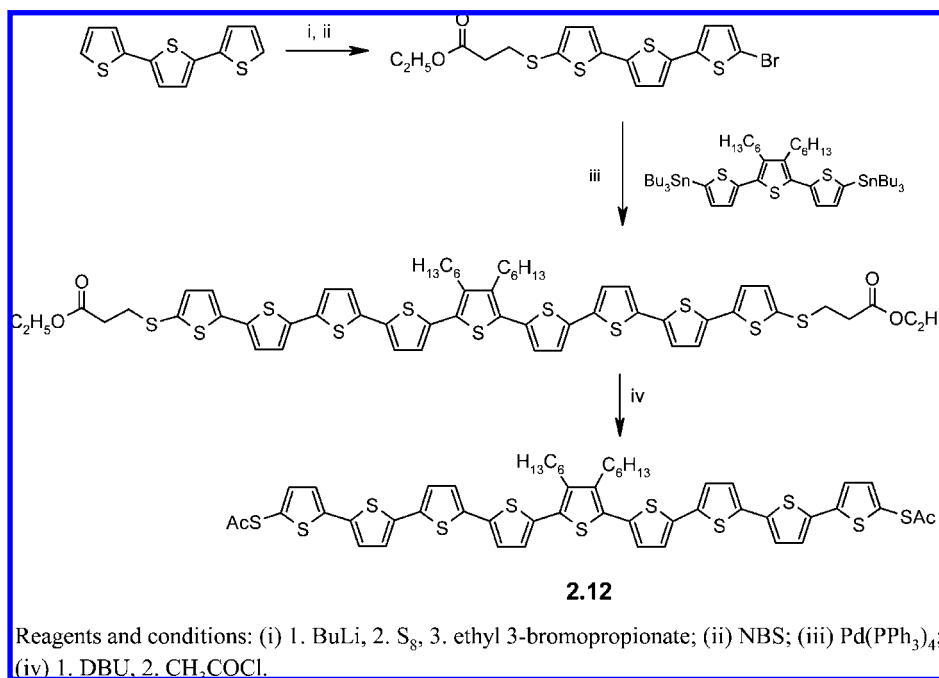
containing disulfide-bridged **2.6** (*n* = 1), an increase in the photoelectrochemical response and in photocurrent density by a factor of 190 has been observed for **2.7** (*n* = 1).

Dithiol-based bi- and terthiophenes for their utilization as SAMs in molecular scale electronics have been synthesized.[74] Functional bithiophene **2.8** was prepared by sulfurization of the Grignard reagent of 5,5′-dibromo-2,2′-bithiophene followed by acetylation Scheme 2.1. In contrast, terthiophene **2.9** was obtained by lithiation of α-terthiophene using *t*-BuLi and subsequent treatment by sulfurization and acetylation with acetyl chloride. Thiol derivatives **2.10** and **2.11** were then prepared by deprotection with ammonium hydroxide. The self-assembling properties and molecular orientation in SAMs were investigated by cyclic voltammetry, grazing incidence Fourier transform infrared spectroscopy (GI-FTIR), ellipsometry, and contact angle measurements. A positive shift of the oxidation potential of the terthiophene unit in the SAM of **2.11** compared to that of **2.9** in solution (Δ*E* = 0.11 V) was observed.

Sugawara et al. recently prepared the same terthiophene **2.9** and a nonathiophene **2.12**, which at both termini were functionalized with thioacetate groups for the attachment to gold nanoparticles.[75] Nonithiophene **2.12** was prepared in six steps starting from monolithiated α-terthiophene, which was reacted with elemental sulfur, quenched with ethyl 3-bromopropionate, and subsequently brominated with NBS

at the other α-position. Stille-type coupling of the resulting terthiophene and a distannylated terthiophene gave the nonamer, which was transformed by acetylchloride to thioacetylated nonithiophene **2.12** in an overall yield of 24% (Scheme 2.2). Oligomers **2.9** and **2.12** were attached to gold nanoparticles by *in situ* removal of acetyl groups using aqueous ammonia. The self-assembling properties of the oligomers on gold nanoparticles and the resulting formation of a network structure due to the bifunctional character of the oligothiophenes were investigated by field emission-scanning electron microscopy (FE-SEM). The number of oligothiophenes attached to a nanoparticle was estimated to be ~110 for the terthiophene and ~70 for the nonamer derivative, resulting in an average diameter of 4 nm for a nanoparticle. Conductivity measurements revealed an electron transport mechanism between the nanoparticles and π-bridging oligothiophenes which is a prerequisite for developing molecular nanocircuits.

Huang et al. prepared a series of oligothiophenes functionalized with thiocyanate groups at the termini (Chart 2.3).[76] Terthiophene **2.13** was prepared in 89% yield by reaction of α-terthiophene with bromine and KSCN. On the other hand, 5-bromoterthiophene was dimerized in a Ni-catalyzed homocoupling reaction followed by thiocyanation, giving sexithiophene **2.14** in 86% yield. Nonithiophene **2.15** was built up in 72% yield by Kumada-type cross-coupling of the

Chart 2.3
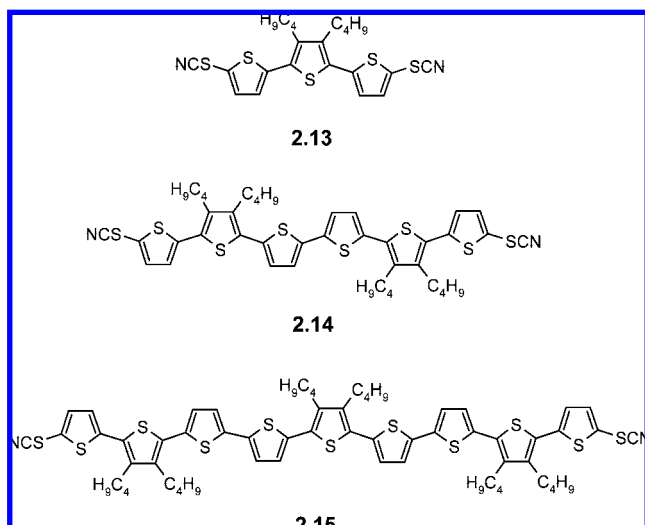
Grignard reagent of 5-bromoterthiophene and 5,5″-dibromo-3′,4′-dibutyl[2,2′:5′,2″]terthiophene to give the parent nonamer, which successively was brominated and transformed to the thiocyanate. Corresponding dithiol derivatives were prepared by reduction of respective thiocyanates with LiAlH$_4$, which then were given to 2-dodecanethiol-protected gold nanoparticles (3.3 ± 1 nm) assembled between gold electrodes. By *in situ* thiol-to-thiol ligand exchange, oligothiophene dithiol-bridged gold nanoparticles were produced, finally bridging the two electrodes by means of Au−S bonds. The morphologies and current−voltage (I−V) characteristics of the self-assembled films were studied by scanning electron microscopy (SEM), and atomic force microscopy (AFM) and their photoresponsive properties were discussed.

Zotti et al. prepared star-shaped terthiophene **2.17** in which a tris(terthienyl)methane unit is attached to the terminus of a hexylthiol.[77] The intermediate tris(terthienyl)hexylbromide **2.16** was synthesized from tris(thienyl)methane by lithiation with *n*-BuLi and alkylation with dibromohexane. The terthienyl units were built up by successive cycles of bromination and cross-coupling reaction with thienylmagnesium bromide. Conversion to the thiol was performed *via* formation of an isothiouronium salt that was subsequently cleaved by tetraethylene pentamine (Scheme 2.3). Formation of SAMs of **2.17** on ITO-coated gold nanoparticles has been studied, and a red shift of the gold-nanoparticle surface plasmon absorption band (Δλ = 25 nm) with enhanced intensity was observed. Multilayering of **2.17** and gold nanoparticles was performed by repetitive dipping of a SAM of **2.17** into the colloidal gold solution and a solution of **2.17**. The formation of multilayers further red-shifted the surface plasmon band (Δλ = 60 nm). Multilayer formation, polymerization of terthiophene on a gold surface, and the increase in conductivity was also discussed.

Recently, Aso et al. reported the synthesis of long oligothiophenes (24-mers) with the length of ca. 10 nm bearing anchor units at both termini (protected thiophenyl or alkyne group). Starting from a bromotetrahexyl-sexithiophene, dibromododecithiophene **2.18** was obtained in 59% yield by oxidative homocoupling with ferric perchlorate. Pd^0-catalyzed Stille-type coupling of **2.18** with corresponding stannylated sexithiophene gave functional oligothiophenes **2.19a** and **b** in 48 and 39% yields, respectively (Scheme 2.4). The use of these oligomers as molecular wire in single molecule electronics was proposed.[78]

Soluble isocyanide-terminated oligothiophenes **2.21** up to a long heptadecamer were prepared, which in an extended form results in a length of 7 nm. Stille-type coupling of 2-bromo-5-(4-formamidophenyl)thiophene with stannylated quaterthiophene followed by bromination yielded **2.20** (n = 4) as an intermediate building block. Corresponding higher oligomers **2.20** (n = 8, 12, 16) were prepared by cycles of Stille-type coupling and bromination. Isocyanides **2.21** (n = 4, 8, 12, 16) were finally obtained by dehydration of the corresponding formamides **2.20** using triflic anhydride under basic condition (Scheme 2.5).[79] Oligothiophenes **2.21** (n = 4, 8, 12, 16) were characterized by UV−vis, fluorescence, and cyclic voltammetric (CV) measurements. With the increase in conjugation length, the absorption maximum shifts from 409 to 430 nm and the emission maximum from 542 to 555 nm. The isocyanide group in the "molecular wires" allowed specific binding to Pt-surfaces and the formation of SAMs. CVs of **2.21** in solution and as SAMs revealed that with increasing conjugation length the first oxidation potential decreases for solution measurement but increases in the SAM, indicating decelerated electron transfer in SAMs.

Analogous thienylene−ethynylene oligomers **2.23** terminated at both ends with isocyanide groups were synthesized by the same research group *via* Sonogashira-type coupling of ethynylated and iodinated thiophene derivatives (Scheme 2.6), spanning 11 nm when extended.[80] In this case, the final isocyanides **2.23** were prepared by hydrolysis of the formamides **2.22** with triphosgene. CVs of SAMs of diisocyanides **2.23** on Pt-electrodes showed that the first oxidation potential is reduced from 1.04 V for the shortest **2.23** (n = 0) to 0.52 V for the longest oligomer **2.23** (n = 8). This result suggested that conjugation was extended over the entire length of the oligomer in the SAM.

In a recent paper, Nuckolls et al. reported the conduction of current through oligothienylene−ethynylene units which act as molecular bridges between single walled carbon nanotubes (SWNTs).[81] The carboxylic acid-terminated SWNTs were prepared by precise oxidative cutting of SWNT with oxygen plasma using an electron-beam lithography technique. The size of the gap between SWNTs was approximately 10 nm as measured by AFM. Coupling of carboxylic acid-modified SWNTs with diamine derivatives **2.24** which were formed by alkaline hydrolysis of **2.22** filled the gap between the SWNTs *via* amide bondings. In addition, the potential use of these amide-linked SWNTs in sensors and switches and the understanding of electron transfer at the molecular level in these devices were described.

2.2. Self-Assembling Hybrid Oligothiophenes

Another approach for the supramolecular organization of π-conjugated molecules works by noncovalent bonds and is defined as "chemistry beyond the molecule".[82] Self-assembly offers an attractive tool to construct well-organized π-conjugated materials. In a recent review, Meijer et al. proposed that it is possible not only to study material properties at the supramolecular level but also to tune the macroscopic properties of π-conjugated systems.[26] These authors extensively revisited the supramolecular organization, molecular interactions, and self-assembling behavior of different π-conjugated systems at the nanoscale level and described different approaches such as (1) thermotropic and lyotropic liquid-crystalline phases of π-conjugated systems to create shape-persistent objects; (2) the removal of solubilizing groups in

Scheme 2.3

Reagents and conditions: (i) n-BuLi, Br(CH$_2$)$_6$Br; (ii) NBS; (iii) 2-thienylmagnesium bromide
PdCl$_2$(PPh$_3$)$_2$; (iv) 1. NH$_2$CSNH$_2$, 2. Tetraethylene pentamene.

Scheme 2.4

Reagents and conditions: (i) 1. Fe(ClO$_4$)$_3$, CHCl$_3$, rt, 2. NH$_2$NH$_2$/H$_2$O; (ii) Pd(PPh$_3$)$_4$, toluene, reflux.

Scheme 2.5

Reagents and conditions: (i) Pd(PPh$_3$)$_4$, toluene, reflux; (ii) NBS, CHCl$_3$; (iii) triflic anhydride, diisopropylethylamine, CH$_2$Cl$_2$.
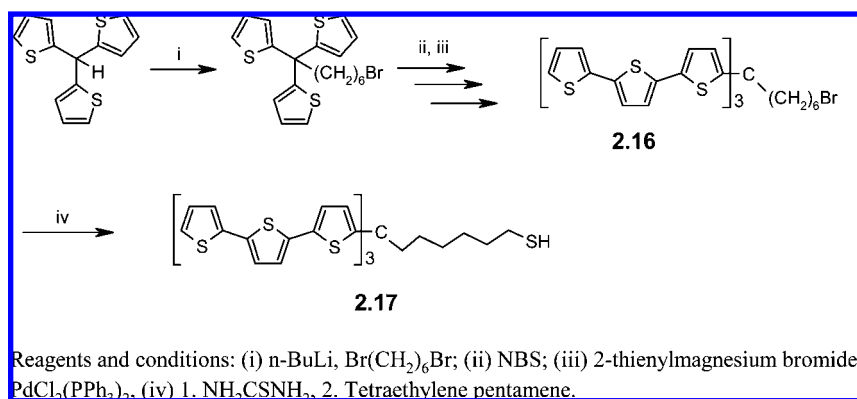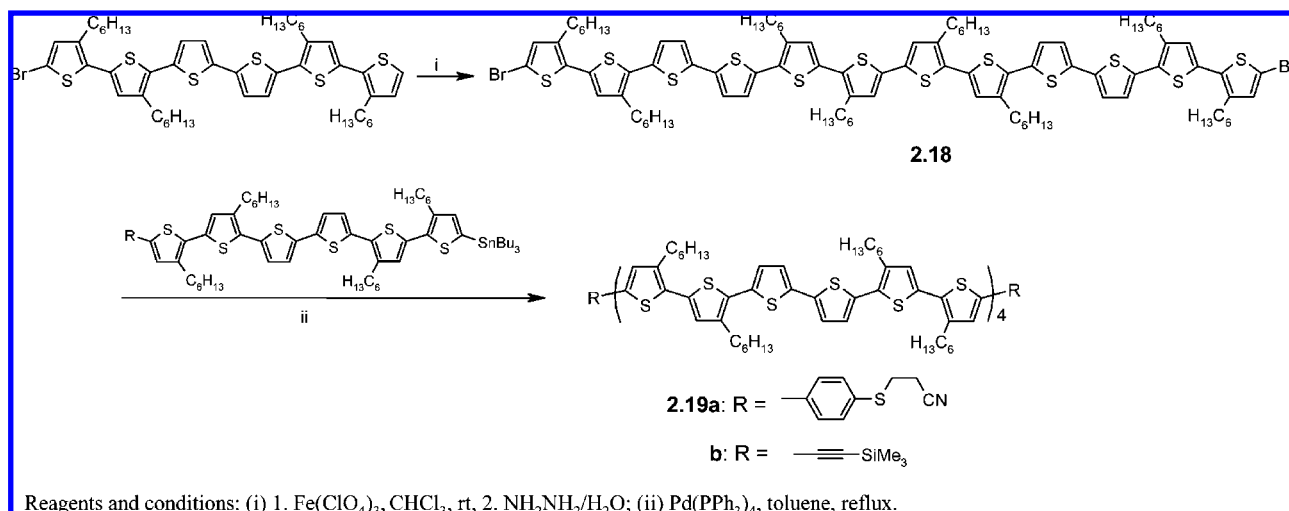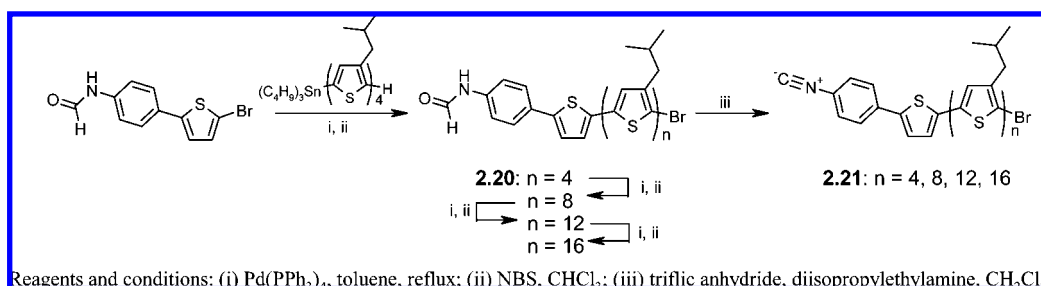
an additional processing step after self-assembly; and (3) manipulation of alignment layers required to obtain long-range ordering in plastic electronics devices in order to fix self-organized π-conjugated systems. Furthermore, they stated that the vertical or homeotropic alignment of self-assembled objects is extremely difficult and still a great challenge.

Polyesters **2.25** and **2.26** based on alternate semiconducting oligothiophenes and flexible insulating aliphatic esters were reported in 1995 by Hong and Miller (Chart 2.4).[83,84] Although the conjugation in the polymer is interrupted by the alkyl ester chain, these polymers exhibited high conductivity due to the π-stacking between the oxidized oligothiophene units in the polymer chain, which make them useful candidates for photodiode applications.

Kilbinger and Feast prepared dibromo derivative **2.27**, consisting of two α-brominated bithiophene units linked by

a polyethylene glycol chain (PEG). Stille-type coupling of **2.27** with 2,5-bis(trimethylstannyl)thiophene or 5,5′-bis(tri-methylstannyl)-2,2′-bithiophene yielded block copolymers **2.28** and **2.29** comprising semiconducting oligothiophene and insulating PEG blocks (Scheme 2.7). These polymers tended to aggregate in dioxane/water mixtures, which was manifested by a blue shift of the absorption maxima ($\Delta\lambda = 26$ nm for **2.28** and $\Delta\lambda = 38$ nm for **2.29**) and by strong quenching of the fluorescence.[85]

Preparation of a similar copolymer **2.32** containing sexithiophene units which are alternately linked by a hydrophobic alkyl and a hydrophilic PEG chain was achieved by Suzuki-type cross-coupling of dibromo derivative **2.27** with bisboronic ester **2.31** (Scheme 2.8).[86] The latter compound was synthesized by Stille-type cross-coupling of bisstannylated derivative **2.30** and a bromobithiophene endowed with boronic ester functionality at the other terminal

Scheme 2.6

2.23: n = 0, 2, 4, 6, 8

i

2.22: n = 0, 2, 4, 6, 8

ii

2.24: n = 0, 2, 4

Reagents and conditions: (i) triphosgene, CH₂Cl₂, (ii) NaOH, MeOH, reflux

Chart 2.4

2.25

2.26

α-position. However, the synthesized copolymer **2.32** was found to be insoluble in common organic solvents.

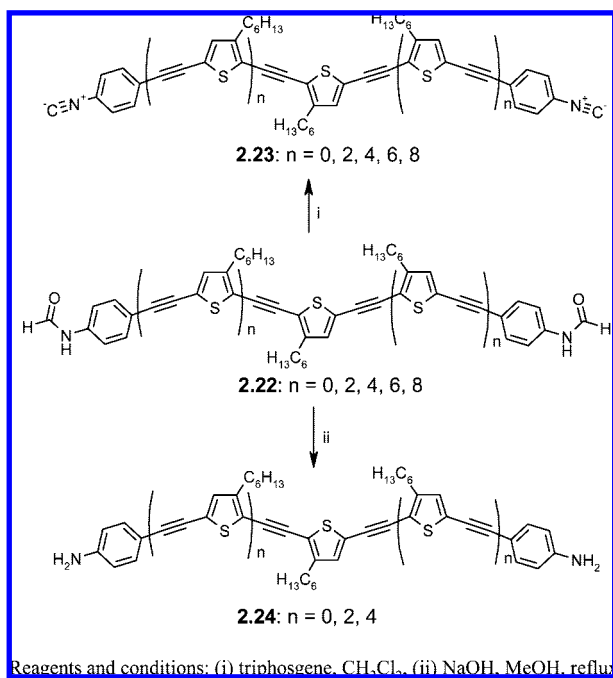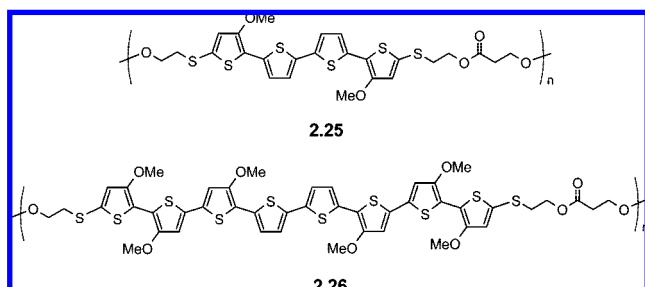Meijer et al. studied the chiroptical and self-assembling properties of various quinque-, sexi-, and septithiophenes substituted at both ends by chiral oligo(ethyleneglycol) chains which carried an α, β, δ, or ε methyl group (Scheme 2.9).[87−89] Compounds (**2.34**: $m = 3$, β; **2.34**: $m = 4$, α, β, δ, ε; and **2.34**: $m = 5$, β) were prepared by Pd[0]-catalyzed Stille-type coupling of the corresponding chiral bromo derivatives **2.33** with distannylated oligothiophenes. Self-assembly of these oligomers in butanol solution was studied by UV−vis, fluorescence, and circular dichroism (CD) measurements. By decreasing the temperature, a blue shift in the absorption spectrum and a red shift in the emission spectrum was observed, indicating H-type aggregation. The large blue shift in the UV−vis spectrum found for these aggregates indicated that the structures are tightly packed, resulting in a strong exciton coupling. CD measurements for **2.34** ($m = 4$, β) showed that the magnitude of the observed Cotton effect in the aggregate decreases gradually as the chiral methyl groups move away from the thiophene unit. They further demonstrated that the aggregation behavior on solid surfaces can be controlled by modulating the nature of the substrate.[90,91] AFM images for **2.34** ($m = 4$, β) on graphite generated one-dimensional nanowires while, on mica, platelets are formed. AFM images on silicon substrates showed left-handed helical aggregate formation. Thus, the formation of chiral assemblies

in the solid state was induced by the presence of a stereocenter in the side chain and the type of substrate.

Furthermore, Schenning et al. demonstrated the use of strong magnetic forces as a tool to control the magnetic deformation of spherical nanocapsules, assembled from bolaamphiphilic sexithiophene **2.34** ($m = 4$; β), into oblate spheroids.[92]

Supramolecular organization of chiral oligothiophenes **2.34** ($m = 3$, 5; β) was studied by means of absorption, photoluminescence, and time-resolved spectroscopy, which revealed the formation of H-aggregates due to strong intramolecular interactions.[93] These studies showed that the stability of the assemblies depends on the π-conjugation length and the position of the stereocenter with respect to the π-conjugated core.

Advincula et al. synthesized a water-soluble sexithiophene bolaamphiphile **2.35** bearing cationic end groups by Stille-type reaction of bisstannylated bithiophene and 5-bromo-hexyl-5′-bromobithiophene followed by quaternization using trimethylamine (Chart 2.5). The bolaamphiphile showed aggregation behavior in aqueous solution and in a thin film cast from THF/water mixtures which was studied by absorption, fluorescence, and AFM techniques.[94,95]

Meijer et al. reported an amphiphilic sexithiophene **2.36** bearing an amide-functionality and a bolaamphiphilic sexithiophene **2.37** terminated with ammonium groups (Chart 2.5).[96] The amide-functionalized oligothiophene **2.36** showed a higher tendency for aggregation compared to the corresponding ester derivative **2.34**, which was assigned to the strong hydrogen-bonding ability together with $\pi−\pi$ interactions. Compound **2.37**, bearing ammonium groups, formed complexes with chiral polypeptides such as poly(glutamate) and DNA in aqueous medium. The polypeptide acts as a chiral template and directs the formation of metastable assemblies *via* helical stacks.

Block copolymer **2.40** with a low polydispersity of 1.1 was prepared by ring closure of 1,4-dicarbonyl precursor **2.39** using an excess of Lawesson's reagent (Scheme 2.10).[97] The latter compound was synthesized by coupling of 2 equiv of formylated α-terthiophene **2.38** endowed with a polystyrene chain at the other α-terminus with the bis-Mannich base 5,5″-bis[3-(dimethylamino)propionyl]-2,2′:5′,2″-terthiophene. TEM and SFM measurements showed that **2.40** self-assembled into spherical, micellar structures with average diameters of 12 nm, which corresponds to about 60 block copolymer molecules per aggregate.

A diblock copolymer **2.41** based on polystyrene and a regioregularly alkylated nonathiophene showed a high glass transition temperature (~102 °C) and was prepared by the coupling of the nonathiophene aldehyde and a living anionic polystyrene (Chart 2.6). No microphase separation was observed by transmission electron microscopy (TEM) measurements, probably due to the low molecular weight and small volume fraction of the oligothiophene moiety compared to that of polystyrene in the copolymer system.[98]

Recently, Hayakawa and Yokoyama synthesized polystyrene oligothiophene block copolymers **2.42−2.44** (Chart 2.6) by Stille-type coupling reaction of mono- or bis-trimethyl-stannyl-2,2′-bithiophene and bromobithiophene(s) endowed with a polystyrene chain.[99] Scanning electron microscopy (SEM) images showed that block copolymers **2.42** and **2.43** containing quaterthiophene termini formed hexagonally packed microporous structures on silicon wafers (1.7 and 2.1 μm size) *via* self-assembly templating processes with

Scheme 2.7

Reagents and conditions: (i) 2,5-bis(trimethylstannyl)thiophene, Pd(PPh₃)₄, 120 °C; (ii) 2,2'-bis(trimethylstannyl)bithiophene, Pd(PPh₃)₄, 120 °C

Scheme 2.8

Reagents and conditions: (i) Pd(PPh₃)₄ dry toluene, reflux; (ii) **2.27**, 1M Na₂CO₃, Pd(PPh₃)₄ toluene, reflux.
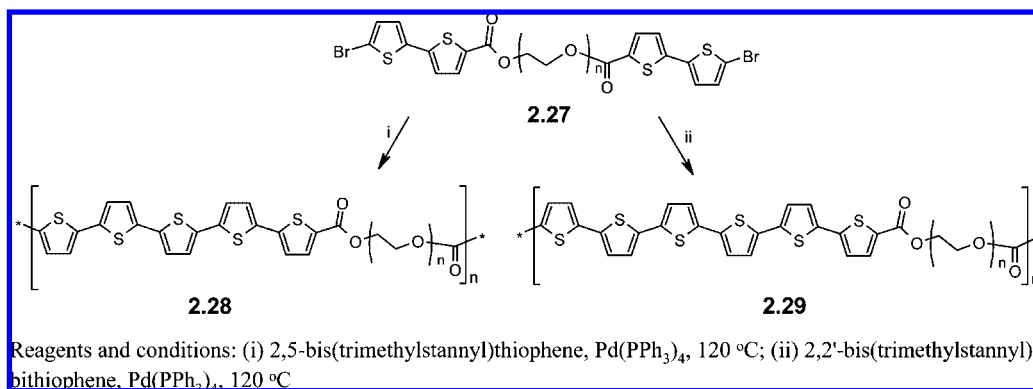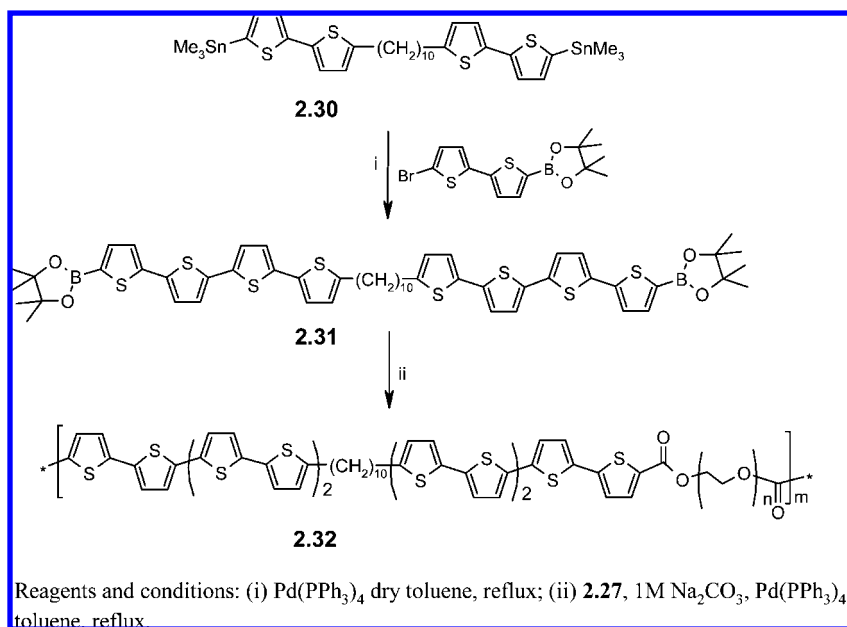
Scheme 2.9
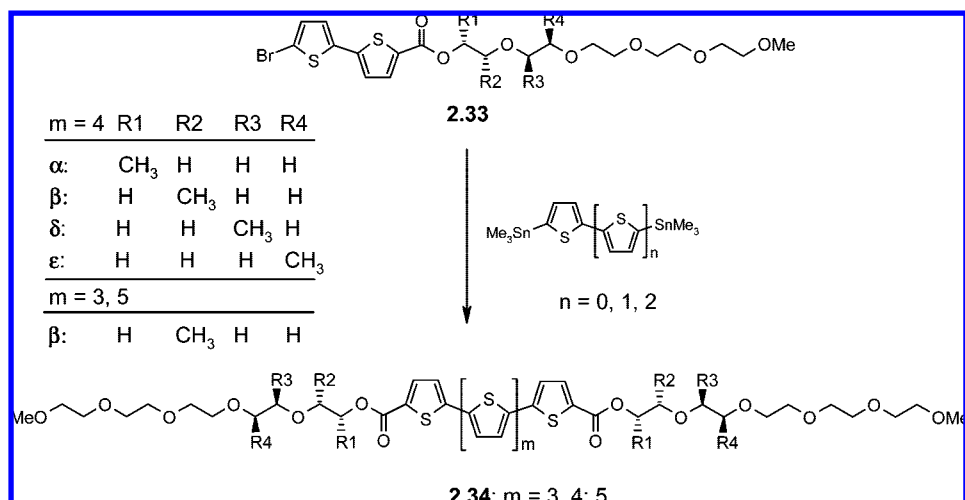
water droplets. Both polymers behaved as emulsifiers during the process of film formation, and the quarterthiophene units remained at the interior of the micropores. In contrast, SEM images of block copolymer **2.44** containing a central sexithiophene unit did not show a periodic microporous structure in the film. The authors concluded that a block copolymer containing the rod segment at the terminal

position is necessary for the formation of an ordered film, because it works as an emulsifier and effectively stabilizes the water droplets.

Shinkai et al. reported a series of organogelators **2.45** (*n* = 2−4) bearing two cholesterol groups at the α-termini of quater-, quinque-, and sexithiophenes (Chart 2.7).[100] Gelators **2.45** (*n* = 2, 3) were prepared by reaction of an amino-

Chart 2.5

2.35

2.36

2.37

Scheme 2.10

2.38

2.39

2.40

Reagents and conditions: (i) NaCN, DMF; (ii) Lawesson's reagent.
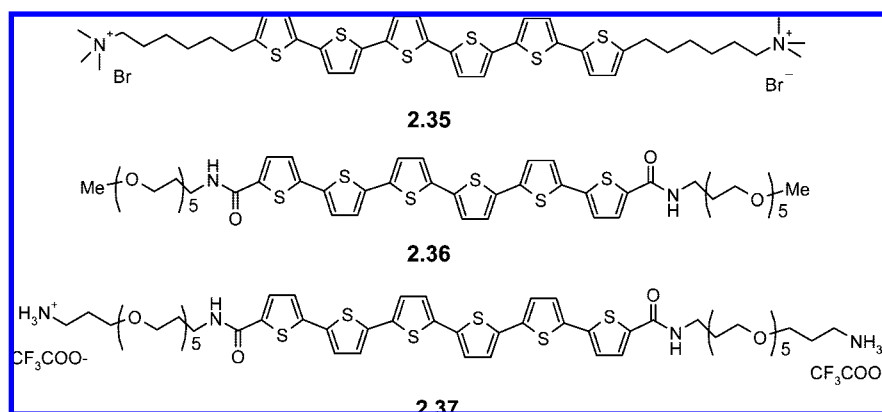
terminated cholesterol derivative and 5-bromo-2-thiophen-ecarboxylic acid chloride followed by Stille-type coupling with distannylated bi- and terthiophenes to build up the oligothiophene backbone. Compound **2.45** ($n = 4$) was prepared by reaction of the same chloresterol derivative with 5-bromo-2,2′-bithiophene-5′-carboxylic acid chloride followed by Stille coupling with distannylated bithiophene. These oligothiophenes acted as organogelators for various organic solvents and showed unique thermochromic behavior through the sol−gel phase transition. UV−vis measurement in tetrachloroethane showed a gelation-induced blue shift, which suggests formation of H-type aggregates *via* self-assembly. TEM and SEM measurements of these gelators further confirmed their self-assembly to form fibrous network structures (Figure 2.1.). Moreover, AFM measurements revealed the formation of unimolecular left-handed helical aggregates in which the oligothiophenes are stacked in an H-aggregation mode.

A series of oligothiophenes attached to chiral cyclohexyl diamine/diimine were recently reported by Melucci and co-workers.[101−103] The imine derivatives **2.46** ($n = 1−4$) were prepared by condensation of diaminocyclohexane with corresponding formylated oligothiophenes under conventional or microwave heating in moderate to good yields. Further reduction of the imine groups using a hydride source gave corresponding amino derivatives **2.47** in good yields (Scheme

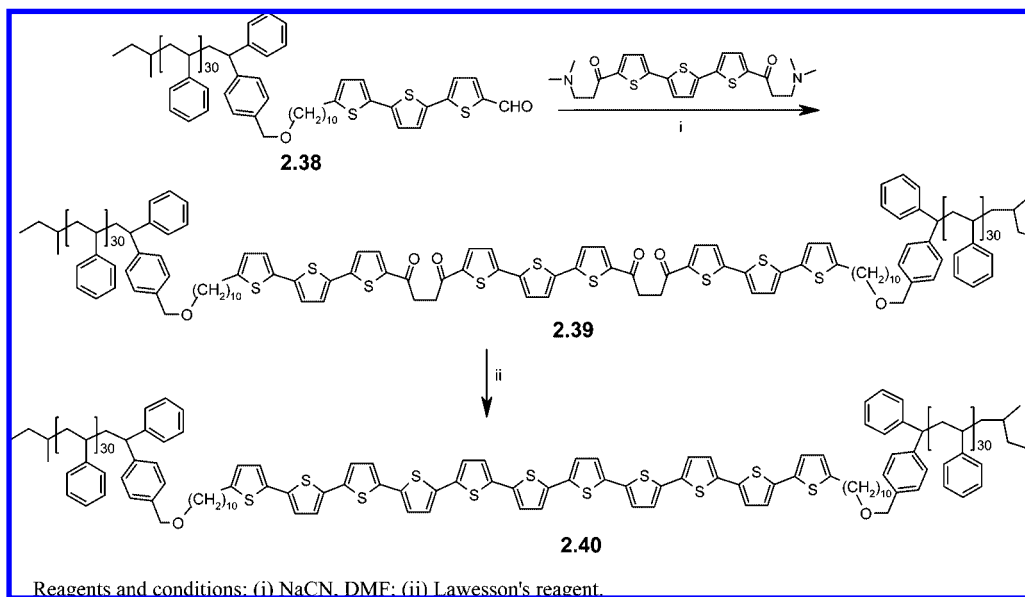2.11). CD measurements carried out for **2.46** ($n = 1−4$) in solution showed a strong bisignated Cotton effect which was ascribed to a helical arrangement of the oligothiophenes. In contrast, only a weak bisignated Cotton effect with a positive sign could be detected for **2.47** ($n = 2−4$) and no CD-signal was observed for **2.47** ($n = 1$).[102] The intensity of the Cotton effect for diimines was significantly greater compared to that of corresponding diamines, which was attributed to the conformational rigidity in the former class of compounds due to C=N groups. Based on these measurements, the authors claimed that the size of the attached oligothiophene moiety and the chiral cyclohexyl diimine/diamine group determined the conformational flexibility of the molecules and consequently their molecular and supramolecular helicity in solution and in the solid state.

2.3. Oligothiophenes as Pendant Groups Grafted to Polymer Backbones

Another approach to create block copolymers is to introduce pendant conjugated oligomer blocks to nonconjugated polymer backbones. The formed polymer films are expected to exhibit characteristic properties of the pendant oligomers. Shirota et al. prepared a series of polyvinyl polymers **2.48a**−**d** containing conjugated oligothiophenes as pendant groups (Chart 2.8).[104,105] The vinyl monomers were

Chart 2.6

2.41

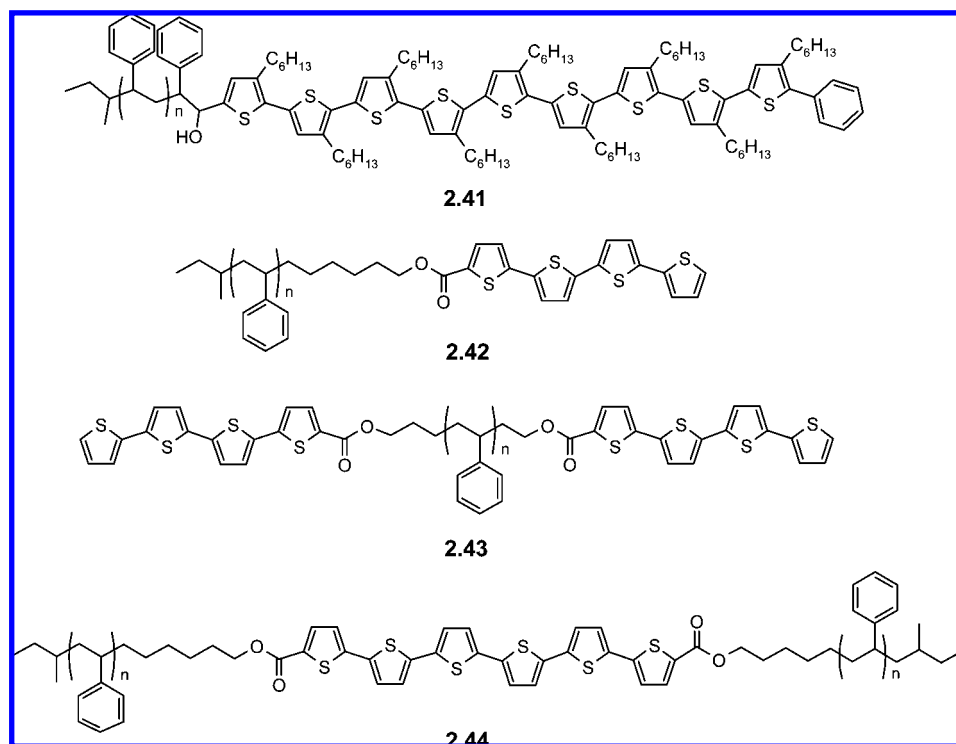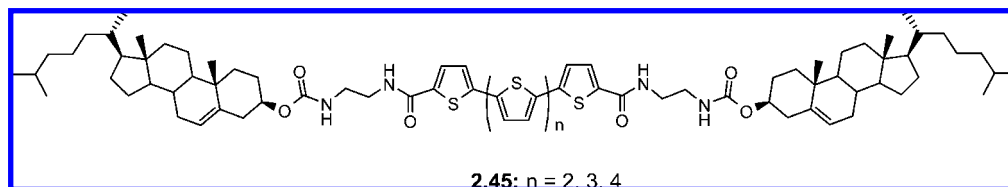**2.42**

2.43

2.44

Chart 2.7

2.45: n = 2, 3, 4

synthesized by treatment of formylated oligothiophenes with *n*-BuLi/methyltriphenylphosphonium bromide *via* Wittig reaction. The polymers were prepared by anodic polymerization of the corresponding vinyl monomers in the presence of tetra-*n*-butylammonium perchlorate. These polymers showed a reversible color change by electrochemical doping and dedoping, which made them suitable for applications in the field of electrochromic displays. Another series of methacrylate polymers **2.49a−d** containing pendant ter-, quater-, quinque-, and sexithiophene units was prepared by radical polymerization of the corresponding methacrylates.[106] The monomers were synthesized by reduction of analogous formylated oligothiophenes with $NaBH_4$ to yield the corresponding alcohols followed by reaction with methacryloyl chloride. Thin films of these poly(methacrylates) with pendant oligothiophenes also showed electrochromic behavior due to their reversible color change upon electrochemical oxidation and reduction in acetonitrile containing $LiClO_4$ as supporting electrolyte.

Similar polyvinyl polymers **2.50** containing pendant oligothiophenes were prepared *via* radical polymerization. In this series, the oligothiophene moieties were endowed with an alkyl substituent at the other terminal position (Chart 2.8).[107] Self-assembly induced white photoluminescence (400−700 nm range) was reported, possibly due to intra- and interchain interaction of the oligothiophenes, which formed a type of supramolecular arrangement suitable for charge transport in the device.

Hayakawa and Horiuchi incorporated an end-capped terthiophene unit to a poly(styrene-*β*-substituted isoprene) block copolymer backbone. Thus, an oligothiophene bearing an acid chloride functionality was reacted with the polymer pendant alcohol groups to afford polymer **2.51** (Chart 2.9) with a very low polydispersity of 1.08 ($M_n = 55000$).[108] SEM and polarized optical microscope (POM) images of cast films of the polymer confirmed the formation of hexagonally packed micropores with a narrow size distribution (~1.5 μm in diameter). TEM images of the film revealed a phase-separated cylindrical nanostructure consisting of π-conjugated oligothiophene molecules, which were self-aligned perpendicular to the substrate.

Block copolymers **2.52** and **2.53** were prepared by emulsion copolymerization of styrene and methylmethacrylated terthiophenes in the presence of a fluorinated anionic surfactant using $K_2S_2O_8$ as a free-radical initiator (Chart 2.9).[109] Polymer solutions were deposited on a hydrophilic surface by a microfluid lithography technique to induce formation of hexagonally self-assembled fluorescent nanobeads. SEM measurement revealed that the nanobeads can be organized in ordered two-dimensional patterns (Figure 2.2.). The average nanobead size (100−400 nm) as determined by SEM measurement was controlled by varying the concentration of surfactant used, which decreased with an increase in the surfactant concentration. The self-aggregation into nanobeads was embodied by the styrene chains, while the specific optical functions came from the attached olig-
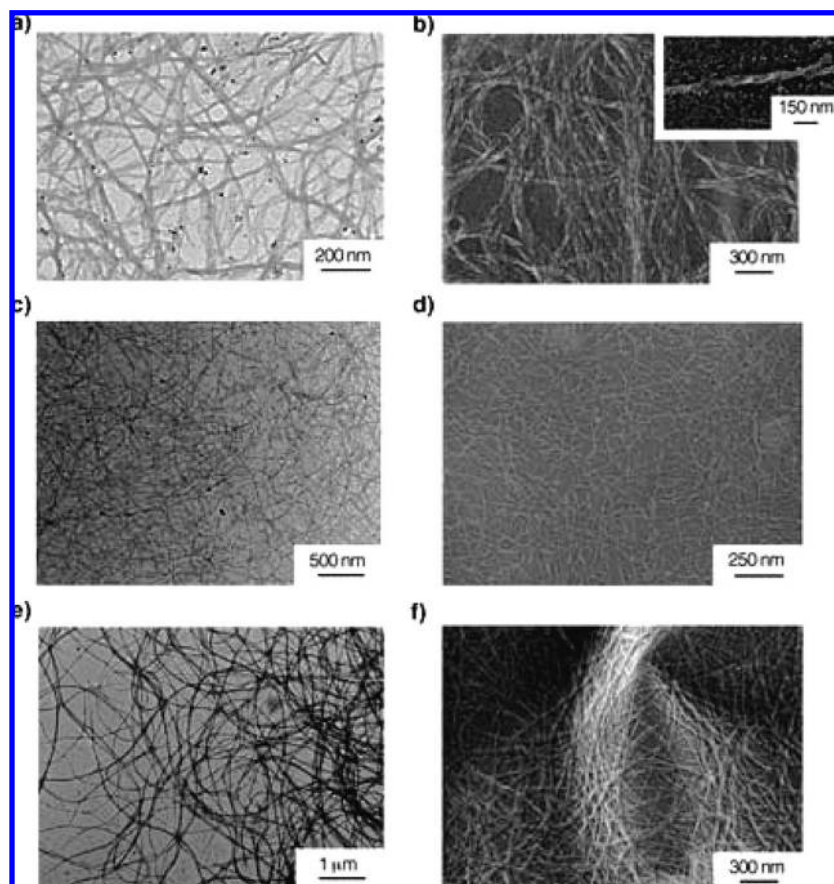
Figure 2.1. TEM (left) and SEM (right) images of xerogels prepared from **2.45**: $n = 2$ (top), $n = 3$ (middle), and $n = 4$ (bottom) gels. Conditions: (a) [**2.45**, $n = 2$] = 1.5 mM in tetrachloroethane (TCE); (b) [**2.45**, $n = 2$] = 1.0 mM in toluene; (c and d) [**2.45**, $n = 3$] = 2.9 mM in TCE; (e and f) [**2.45**, $n = 4$] = 3.8 mM in TCE. (Reproduced with permission from ref 100. Copyright 2005 Wiley-VCH.)

Scheme 2.11

n = 1-3, R = H   **2.46**   **2.47**
n = 4, R = C$_6$H$_{13}$

Reagents and condition: (i) MgSO$_4$, DCM, reflux or Microwave irradiation; (ii) NaBH$_4$ or NaBH$_3$CN
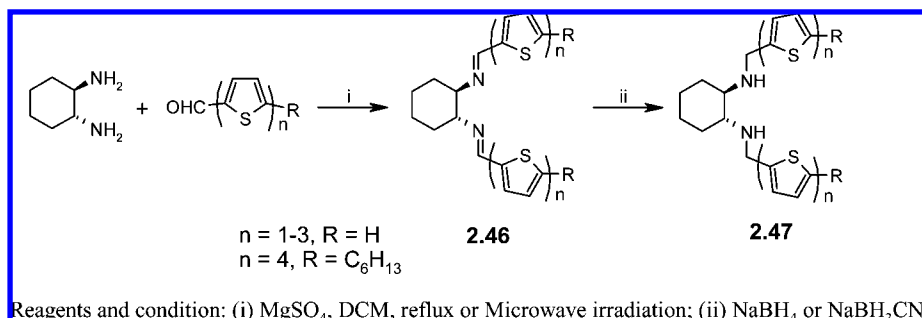
othiophenes. Furthermore, photoluminescence and pump−probe measurements showed that the formation of self-assembled nanobeads does not influence the optical signature of the terthiophene units.

Zhao et al. synthesized homopolymer **2.55** ($M_n = 65217$; PDI = 1.08) containing phenyl end-capped quaterthiophenes by ring-opening metathesis polymerization of norbornene derivative **2.54** by using a Grubbs' catalyst (Scheme 2.12).[110] TGA analysis of the polymer revealed good thermal stability up to 411 °C. UV−vis spectra of the polymer in chloroform solution showed bands at 422 nm, whereas 435 nm was measured in thin films due to the extended conjugated systems. A photovoltaic device fabricated by using the layer sequence Al/polymer **2.55**/ITO showed an open circuit voltage of $V_{oc} = 0.7$ V and a moderate short circuit current of $I_{sc} = 0.7$ μA cm^2. The device stability was good under ambient conditions.

2.4. Oligothiophenes as Liquid Crystalline Materials

The molecular orientation of π-conjugated structures is an important factor for high charge-carrier mobilities in OFETs. Long α,α'-dialkylated oligothiophenes up to a hexamer and an octamer have been widely studied in OFETs, because of their ease of synthesis and high molecular ordering.[20,111−114] Due to moderate solubility, these oligomers often have to be purified by vacuum sublimation techniques in order to obtain high purity, which is a prerequisite to obtain good self-assembling properties together with enhanced mobilities. From this point of view, liquid crystalline (LC) oligothiophenes have been recognized as a new type of self-organized organic semiconductor because they can form homogeneous thin films with high charge carrier mobilities. The LC formation can be tuned by appropriate choice of

Chart 2.8

2.50: R = CH$_3$, m = 0
R = C$_6$H$_{13}$, m = 0,

2.48: m = 0, R = H
2.49: m = 1, R = CH$_3$

Chart 2.9

2.51

2.52

2.53
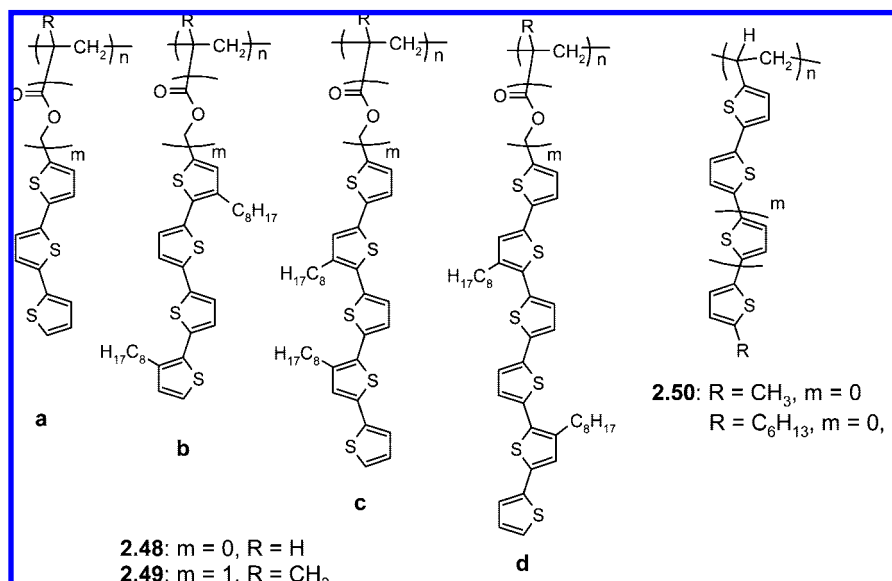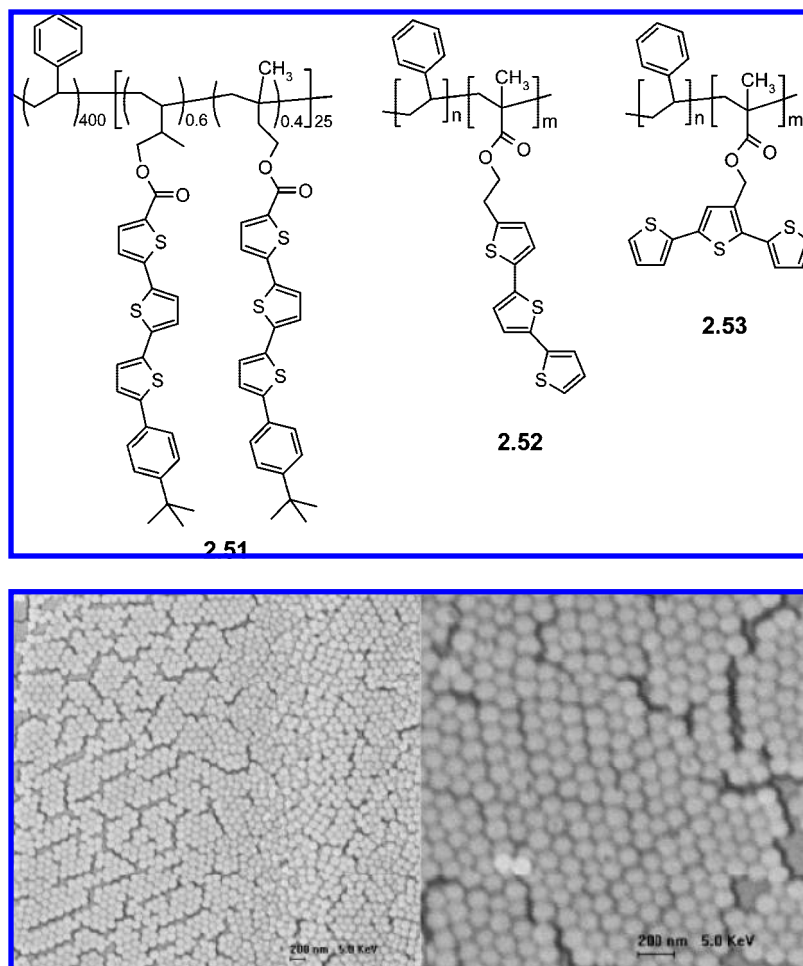
Figure 2.2. SEM micrograph images of microfluidic-induced self-assembly of nanobeads formed from copolymer **2.52**. (Reproduced with permission from ref 109. Copyright 2005 American Chemical Society.)

side chains. In this context, various α,α′-disubstituted oligothiophenes **2.56** have been synthesized and studied for their liquid crystalline properties (Chart 2.10).[115−118] It has already been revealed that terthiophenes substituted with different alkyl chains at the terminal α-positions exhibit

smectic LC-phases whereas corresponding quaterthiophenes showed smectic and nematic LC-phases.[115,116] In addition, the length of the attached alkyl groups played a crucial role in the LC behavior of these materials. For example, 5,5‴-dipropylquaterthiophene **2.56a** (R^1 = R^2 = C$_3$H$_7$) showed a

Scheme 2.12

Reagents and conditions: (i) CH_2Cl_2, $CH_2=CHOC_2H_5$.
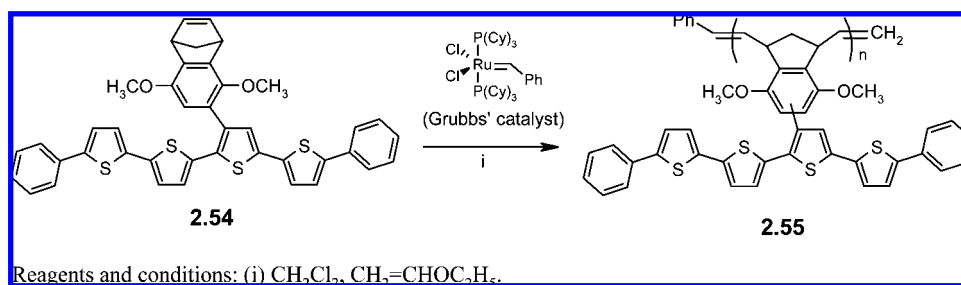
Chart 2.10
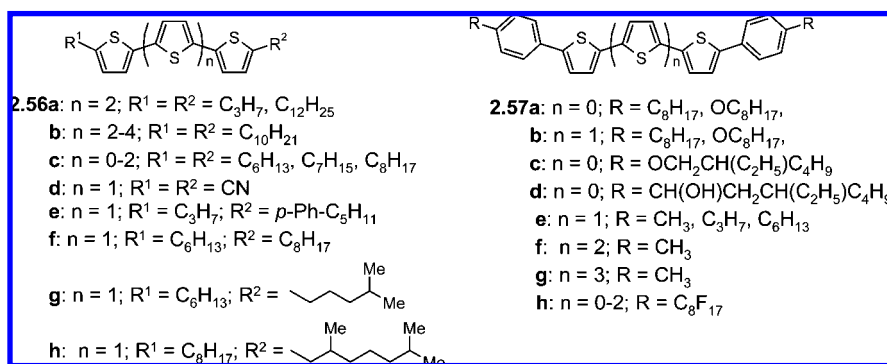
nematic LC-phase whereas didodecyl derivative **2.56a** (R^1 = R^2 = $C_{12}H_{25}$) formed more ordered phases at higher temperatures.[116]

Ponomarenko and Kirchmeyer synthesized didecyloligothiophenes **2.56b** by employing Kumada cross-coupling and/or Cu-catalyzed oxidative homocoupling reactions.[117] Due to the formation of high order in its LC-phase, α,α'-didecyl quaterthiophene **2.56b** (n = 2) is reported to be the most promising material for solution processable OFETs, as compared to quinque- or sexithiophene derivatives **2.56b** (n = 3, 4).

Byron et al. reported a four-step synthesis of symmetrical α,α'-dialkyloligothiophenes **2.56c** by repetitive Friedel−Crafts acylation followed by Wolff−Kishner reduction of α-terthiophene.[115] Although this approach provided fair to excellent yields, it required a relatively large number of synthetic steps. Thus, there is still a demand for a practical and simple route to synthesize these derivatives. More recently, Geerts et al. described an improved high yield synthesis of alkylated oligothiophenes **2.56c** using n-BuLi/t-BuOK as lithiating agent, whereby the addition of t-BuOK considerably enhanced the reactivity of lithiated oligothiophenes toward alkyl halides.[118] The charge carrier transport properties of **2.56c** (n = 1; R^1 = R^2 = C_8H_{17}) were measured by Funahashi and Hanna by time-of-flight (TOF) measurements, showing a mobility of 5×10^{-4} cm^2 V^{-1} s^{-1} in a nonordered SmC phase (87.8−91.3 °C) which increased up to 10^{-2} cm^2 V^{-1} s^{-1} by the formation of a hexagonal molecular order in a SmG phase between 63.9 and 72 °C.[119] Azumi et al. reported a nematic liquid crystalline phase at 205 °C for nonalkylated 5,5″-dicyanoterthiophene (**2.56d**) upon cooling, indicating the importance of the substituents for the formation of LC-mesophases.[120]

Compound **2.56e**, bearing an additional phenyl group, exhibited ambipolar charge carrier transport in a highly ordered smectic phase. By TOF-measurement, high hole and electron mobilities of 0.07 and 0.2 cm^2 V^{-1} s^{-1}, respectively, were observed.[121] It has also been reported that the OFET-performance of **2.56e** was largely influenced by the pretreatment of the substrate surface with silane agents. Octyltrichlorosilane enhanced the performance and led to a good hole mobility of 0.04 cm^2 V^{-1} s^{-1} in ambient atmosphere compared to 0.02 cm^2 V^{-1} s^{-1} observed on hexamethyldisilazane treated SiO_2 surfaces.[122]

Terthiophenes **2.56f−h**, which were synthesized by employing Suzuki cross-coupling and carbanion alkylation steps, showed that the branching of the side chain and desymmetrization of the molecule are two important factors for tailoring the thermotropic LC-properties of the oligothiophene mesogens.[123] Terthiophene **2.56f** with two different linear alkyl chains has nearly the same LC-transition temperature as that of α,α'-dihexylterthiophene. In contrast, introduction of branched side chains as in case of **2.56g** and **2.56h** decreased the transition temperature relative to that of the linear analogue. Compound **2.56h** with a bulkier substituent showed LC-behavior at room temperature (23−49 °C), which could be an essential factor for the fabrication of flexible organic semiconducting devices.

Locklin et al. synthesized some soluble bi- and terthiophenes **2.57a,b** (Chart 2.10) substituted with alkyl- and alkoxyphenyl groups by Stille and Suzuki coupling reactions. Compound **2.57a** showed a high field-effect mobility of 0.18 cm^2 V^{-1} s^{-1} and an on/off ratio of 10^7 when the molecules were deposited at a substrate temperature of 50 °C.[124] Although replacement of the linear alkyl groups by branched substituents in **2.57c,d** increased the solubility of the molecules, the mobilities of these semiconductors in OFETs decreased dramatically over several orders of magnitude.[125]

Frisbie et al. prepared a series of alkylphenyl-substituted oligothiophenes **2.57e−g** by Stille-type reaction of 2-bromo-5-(4-alkylphenyl)thiophene and corresponding distannylated moieties.[126,127] All compounds showed p-type transport character and hole mobilities in the range of 0.03 cm^2 V^{-1} s^{-1} and improved I_{on}/I_{off} ratios approaching a record 10^9 for **2.57f** (n = 2) at room temperature. These findings revealed that increasing alkyl chains do not improve the molecular

Chart 2.11

2.58a: R = C$_4$H$_9$
b: R = C$_6$H$_{13}$
c: R = C$_{10}$H$_{21}$

2.59

2.60

2.61 (n = 4−8)

2.62

2.63a: n = 0; R = C$_6$H$_{13}$
b: n = 1; R = C$_3$H$_7$

2.64a: R^1 = CH$_3$; R^2 = H; R^3 = C$_3$H$_7$
b: R^1 = H; R^2 = CH$_3$; R^3 = C$_3$H$_7$
c: R^1 = H; R^2 = CH$_3$; R^3 = C$_{12}$H$_{25}$
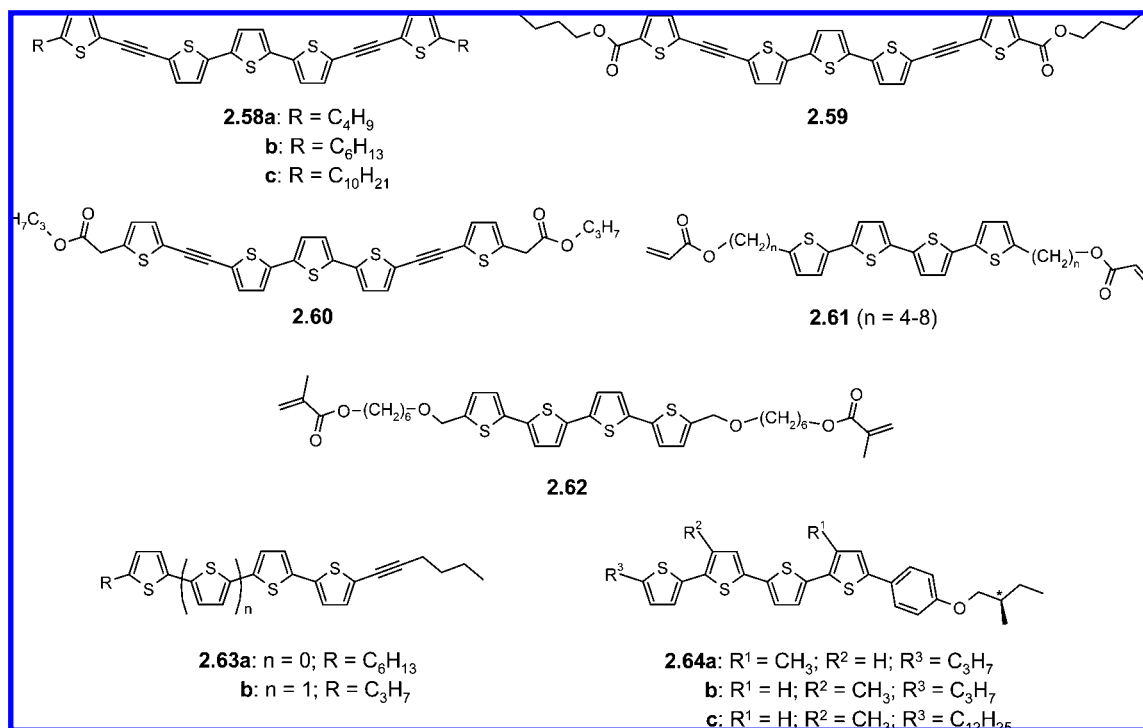
ordering; however, the addition of phenyl groups greatly improves the on/off ratio in OFETs.

Replacement of alkyl groups by perfluorooctyl chains in **2.57h** (n = 0−2) increased the thermal stability and sublimation yield, respectively. These oligomers can be sublimed well below their melting point. Thin films of **2.57h** showed n-type semiconducting behavior and charge carrier mobilities ranging from ∼10^{-6} to ∼0.1 cm^2 V^{-1} s^{-1}, which strongly depended on the substrate temperature.[128]

Ikeda et al. prepared an alkyl-capped quinquethiophene with acetylene spacers **2.58a** (Chart 2.11), which upon heating showed a transition from crystalline to a nematic LC-phase at 101 °C and a transition from the mesophase to an isotropic phase at 194 °C.[129] On cooling, along with a transition from the isotropic phase to the nematic phase at 191 °C, a monotropic smectic B phase between 90 and 54 °C was observed. In a photoreorientation measurement, **2.58a** was doped as guest dye for both polar and nonpolar LC hosts, and a decrease of threshold light intensities about 135−180 times was observed compared to nondoped LCs. Simultaneously, a strong enhancement of the optical field-induced reorientation due to a change in molecular polarizability between the ground and the excited-state of the dye was observed. The same group further synthesized two ester-functionalized oligomers **2.59** and **2.60** (Chart 2.11), in which for **2.59** a smectic phase between 201 and 130 °C as well as a nematic phase between 141 and 114 °C for **2.60** were observed.[130] These changes in the phase behavior were ascribed to the change in the position of the carbonyl group in the oligomers. These oligomers were also used as guest dyes in dye-doped LCs, and the effect on the photoinduced reorientational behavior was examined. The photoinduced formation of a defraction ring for **2.59** was observed at a lower threshold light intensity of 11 W cm^{-2} when compared to the cases of **2.58a** (30 W cm^{-2}) and **2.60** (27 W cm^{-2}). This behavior was ascribed to the extended π-electron delocalization of **2.59** in the excited state.

Recently, van Breemen et al. synthesized other oligothiophenes **2.58b** and **2.58c** with longer alkyl substituents. These compounds form semiconducting films over large areas with highly ordered morphologies due to their LC nature. By thermal annealing, these compounds formed self-assembled monodomain films in a single-crystalline monoclinic morphology with lamellae parallel to the substrate. In OFETs, an increase of the hole mobility to 1 × 10^{-2} cm^2 V^{-1} s^{-1} was measured by the time-of-flight technique.[131]

Huisman et al. studied the LC behavior of semiconducting oligothiophenes **2.61** (n = 4−8) (Chart 2.11), which were substituted by polymerizable acrylate groups.[132] By using these materials for the fabrication of OFETs, it was observed that the use of polymer films resulted in a decrease in mobility by a factor of 10 compared to the cases of transistors made from the bisacrylate monomer. For example, the charge carrier mobility of **2.61** (n = 6) after polymerrization was 6 × 10^{-4} cm^2 V^{-1} s^{-1} compared to 4 × 10^{-3} cm^2 V^{-1} s^{-1} before polymerization.

McCulloch et al. synthesized methacrylate-functionalized LC oligothiophene **2.62**, which formed a smectic crystalline phase and showed a moderate field-effect mobility of 5 × 10^{-3} cm^2 V^{-1} s^{-1} due to its poor alignment in the film.[133] Photopolymerization of these oligomers reduced the field-effect mobility by a factor of 10, which was ascribed to the reduced degree of ordering due to cross-coupling.

By using Kumada and Sonogashira-type cross-coupling reactions, Funahashi and Hanna synthesized LC materials **2.63a,b** (Chart 2.11) comprising asymmetrically substituted oligothiophene cores bearing alkyl and acetylene groups at each α-terminus.[134] Due to the extended intermolecular interaction of the π-conjugated systems, smectic LC phases with highly ordered films over a wide temperature range (including ambient temperatures) were observed. A high hole mobility of 0.1 cm^2 V^{-1} s^{-1} was observed for **2.63b**, which is comparable to that measured for polycrystalline materials.

Chart 2.12
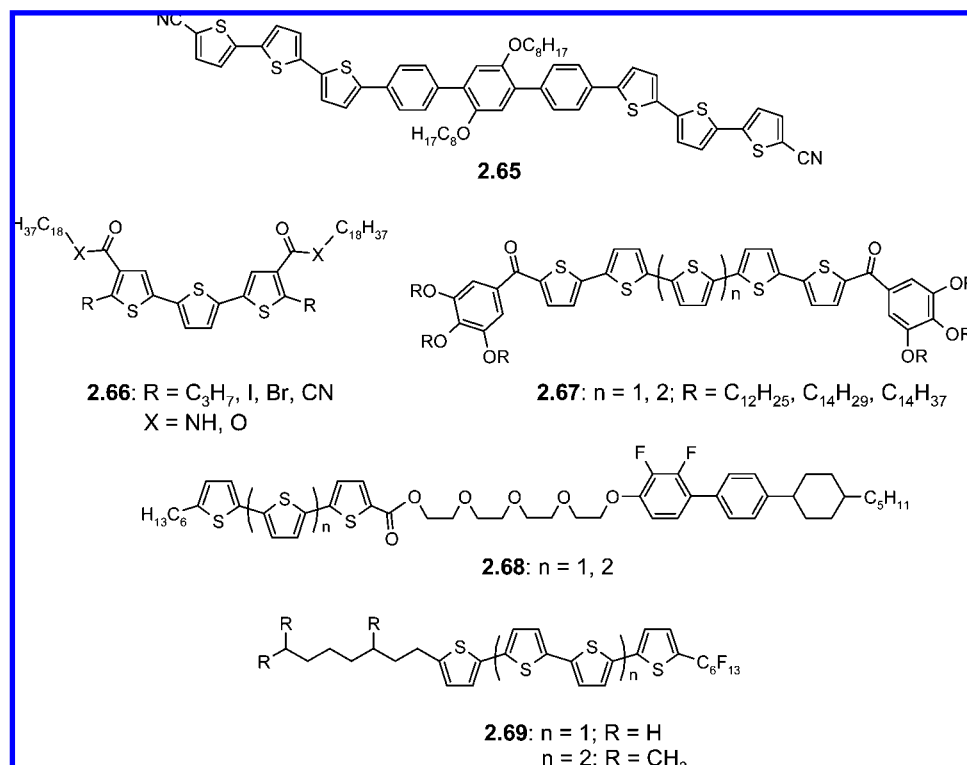
This may possibly be ascribed to the small intermolecular distances of 3.9 Å between the smectic layers.

Chiral oligomers **2.64a−c** (Chart 2.11) were prepared by sequential Kumada cross-coupling reactions, halogenation, and final Suzuki-type coupling of iodinated quaterthiophenes with 4-[(S)-2-methylbutoxy]phenylborate.[135−137] These compounds have the same aromatic core structure, which is responsible for the carrier transport process, whereas the presence of different alkyl chain and methyl group substitutions influenced the molecular self-organization. Compound **2.64a** formed only a chiral nematic phase, while, for the oligomers **2.64b** and **2.64c**, an additional chiral smetic C phase was observed at temperatures below the chiral nematic phase. The electron mobility in the chiral nematic phase of all the three compounds increased monotonically with the temperature. On the contrary, the temperature dependence of the hole mobility was rather different among the three compounds. In the chiral nematic phase of **2.64a**, the hole mobility increases with an increase in temperature; conversely, a temperature-independent mobility was observed in the chiral nematic phase of **2.64b**. In the chiral nematic phase of **2.64c**, the hole mobility decreased with an increase in temperature.[137] A reduced hole mobility on the order of $\sim 2 \times 10^{-4}$ cm^2 V^{-1} s^{-1} at 120−150 °C and an electron mobility of $<10^{-4}$ cm^2 V^{-1} s^{-1} was measured for all three compounds by the TOF technique.

Cyano-substituted oligothiophene **2.65** (Chart 2.12) was prepared by a Suzuki-type coupling reaction of 5-bromo-5″-cyanoterthiophene and the bis-boronic acid of the inner terphenyl building block.[138] The presence of terminal cyano groups in the extended molecular backbone facilitated the formation of a nematic LC-phase by melting at 204 °C and clearing at 343 °C.

To develop oligothiophene-based LC materials capable of hydrogen bonding, Liu et al. synthesized a series of terthiophene derivatives **2.66** (X = NH) (Chart 2.12) in which

the functional groups (C$_3$H$_7$-, I-, Br-, CN-) were attached to the α-position and the stearylamide groups to the β-position of terminal thiophenes.[139,140] Although **2.66** (R = I, Br, CN) displayed the formation of a smectic A phase, **2.66** (R = C$_3$H$_7$) did not show any liquid crystallinity. IR measurements revealed both a stretching vibration band at ~ 3300 cm^{-1} due to hydrogen bonding and a sharp free N−H stretching absorption at 3419 cm^{-1}. Furthermore, the same authors prepared ester-functionalized terthiophene derivatives **2.66** (X = O) which were not LC active, thus suggesting that intermolecular hydrogen bonding between the amide groups in **2.66** (X = NH) played an important role in the LC-phase formation.[139]

Kato et al. prepared some π-conjugated oligomers **2.67** (n = 1, 2) (Chart 2.12) where the alkoxy-substituted benzene groups were attached to the termini of the oligothiophenes *via* carbonyl groups.[141] Friedel−Crafts reaction of 2-bromothiophene with 3,4,5-trimethoxybenzoyl chloride gave 5-(3,4,5-trimethoxybenzoyl)-2-bromothiophene. Pd^0-catalyzed coupling of the product with 2-tributylstannylthiophene and bromination using NBS gave 5-bromo-5′-(3,4,5-trimethoxybenzoyl)-2,2′-bithiophene. Subsequent deprotection of the methoxy groups by BBr$_3$ afforded the corresponding alcohols, which were then reacted with alkyl halides under basic conditions to give the building blocks with longer alkoxy side chains. These were finally coupled with bis-borylated thiophene or bithiophene to give the corresponding oligomers **2.67** (n = 1, 2) in excellent yields. Compared to other liquid crystalline oligothiophenes which show nematic and/or smectic mesophases, these alkoxy-substituted materials exhibited thermotropic columnar mesophases. Intermolecular π−π interactions between oligothiophene moieties and nanosegregation of the aromatic cores from the surrounding alkoxy groups facilitated self-organization into one-dimensional columnar structures.

Oligothiophene-based LC materials **2.68** ($n = 1, 2$) (Chart 2.12) containing a 2,3-difluoro-4′-(4-*trans*-pentylcyclohexyl)biphenyl unit linked to the oligothiophenes by a tetra(ethylene oxide) (TEO) spacer were prepared by condensation of oligothiophene carboxylic acids with corresponding hydroxy-terminated TEO derivatives.[142] Compound **2.68** ($n = 1, 2$) formed enantiotropic smectic A phases in wide temperature ranges (33−138 °C for $n = 1$; 113−170 °C for $n = 2$). The attachment of a fluoro-substituted cyclohexylbiphenyl mesogenic unit to one terminus of the oligothiophenes thermally stabilized the smectic A phases. Meijer et al. earlier reported that chiral oligothiophene **2.34** ($m = 4, \beta$, Scheme 2.7) containing terminal oligo(ethylene oxide) units exhibited smectic phases between 180 and 200 °C.[88]

Geerts et al. recently synthesized liquid crystalline oligothiophenes **2.69** ($n = 1, 2$) (Chart 2.12) comprising two incompatible peripheral substituents, such as alkyl and perfluoro alkyl groups which were attached to the core by Suzuki-type cross-coupling reactions.[143] Compound **2.69** ($n = 1$) formed a smectic A mesophase when cooling from 220 °C (isotropic liquid) to 200 °C, whereas **2.69** ($n = 2$) formed an insoluble material and no phase transitions were observed before decomposition at 250 °C.

Tschierske et al. recently synthesized a series of liquid crystalline quaterthiophenes **2.70** bearing two terminal polar hydrogen bonding groups to provide a bolaamphiphilic structure.[144] These materials were synthesized by Pd⁰-catalyzed cross-coupling reactions of α,α′-dibromo-quaterthiophene and glycerol-functionalized phenyl boronic acid (Scheme 2.13). Compound **2.70a** with two dodecyl chains at the oligothiophene core showed an enantiotropic liquid-crystalline phase, whereas compound **2.70b** bearing additional methyl groups at the phenyl ring showed only a monotropic (metastable) mesophase on cooling from the isotropic melt. In contrast, compound **2.70c**, in which the methyl groups were replaced by longer hexyl chains, was not liquid-crystalline. This finding indicated that longer peripheral chains inhibit LC phase formation, probably by disrupting hydrogen bonding between the polar groups. A honeycomb-like network of square cylindrical structures involving π-conjugated oligothiophenes was proposed for compound **2.70a**, which forms a complex liquid-crystalline phase. This arrangement opens new possibilities for the directed organization of π-conjugated organic materials into complex superstructures and patterns for the design of functional devices by means of liquid-crystal self-assembly.

Three liquid-crystalline semiconducting oligothiophenes containing rigid dithienothiophene (**2.71**), benzothiadiazole (**2.72**), and carbazole (**2.73**) cores were synthesized by Pd⁰-catalyzed Suzuki coupling reactions of the dibromo derivatives of the core molecules and corresponding oligothienyl boronic esters (Chart 2.13).[145] Polarized optical microscopy (POM) and differential scanning calorimetry (DSC) analyses revealed highly ordered smectic mesophases for co-oligomers **2.71** ($n = 0$) and **2.72** ($n = 0$). Derivatives **2.71** ($n = 1$) and **2.73** showed some degree of phase transition, whereas no LC behavior was observed for **2.72** ($n = 1$). X-ray diffraction (XRD) studies performed at various temperatures showed that the smectic order is retained in the crystalline state upon cooling across the transition temperature, affording cast films with a more favorable morphology for OFET applications.

Scheme 2.13

2.70a: R = H; **b**: R = CH₃; **c**: R = C₆H₁₃

Reagents and conditions: (i) a. Pd(PPh₃)₄, DME, aq. NaHCO₃; (ii) MeOH, HCl.

Chart 2.13

2.71: n = 0, 1

2.72: n = 0, 1

2.73
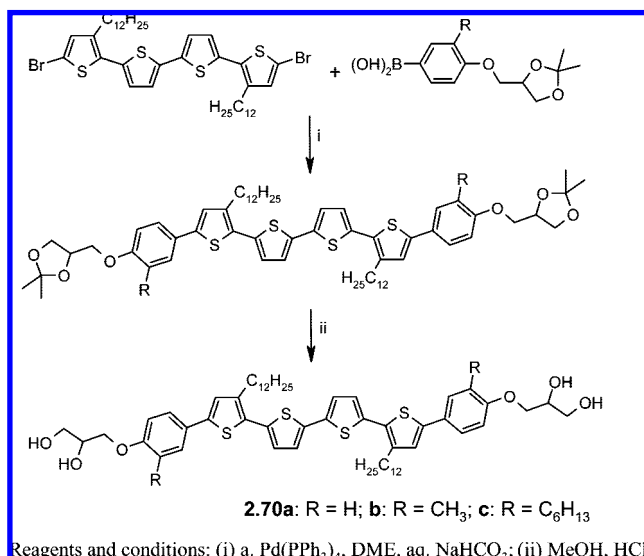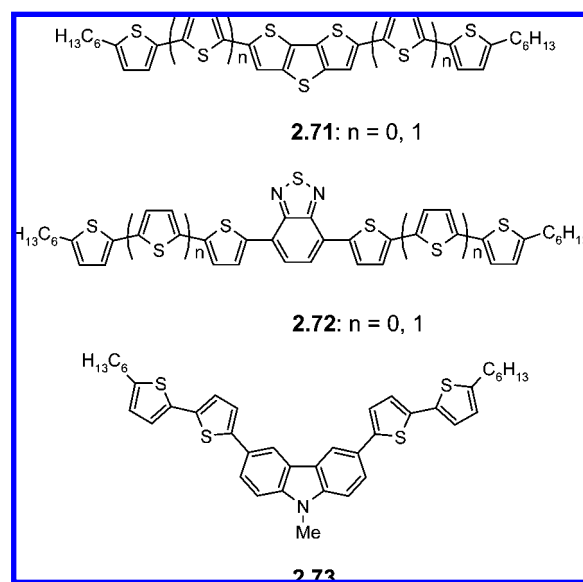
2.5. π-Dimeric Model System

Previous studies concerning redox states of linear conjugated oligothiophenes as models for polarons and bipolarons in conjugated polymers did not fully address the influence of intermolecular interactions on the electronic structure of π-conjugated systems in the solid state. Various studies proposed the formation of π-dimers as charge carriers. However, the formation of these π-dimers has been explored only by analyzing low-temperature electronic spectra of oligothiophenes in various oxidation states. Detailed structural information of the aggregates was not well established.[146−149] Furthermore, it was also difficult to distinguish the intrinsic spectrum of the associated π-dimeric species from that of the monomer.

In contrast to the case for linear systems, Otsubo et al. prepared a first example of cyclophane-type π-dimeric model compound **2.76**, containing two quinquethiophene units separated by ethyl spacers.[150] The synthesis included Kumada-type coupling of 1,2-bis(5-bromo-2-thienyl)ethane and 3-octylthiophene magnesium bromide to obtain bithiophene derivative **2.74** (Scheme 2.14). Successive bromination by

Scheme 2.14

Reagents and conditions: (i) Ni(dppp)Cl$_2$, ether, reflux; (ii) NBS, CHCl$_3$-acetic acid, RT; (iii) TMS-acetylene Pd(PPh$_3$)$_4$, CuI, Et$_3$N, 80 °C; (iv) KOH, benzene-MeOH, RT; (v) Cu(OAc)$_2$, pyridine, 45 °C; (vi) Na$_2$S·9H$_2$O, KOH, dioxane, reflux.
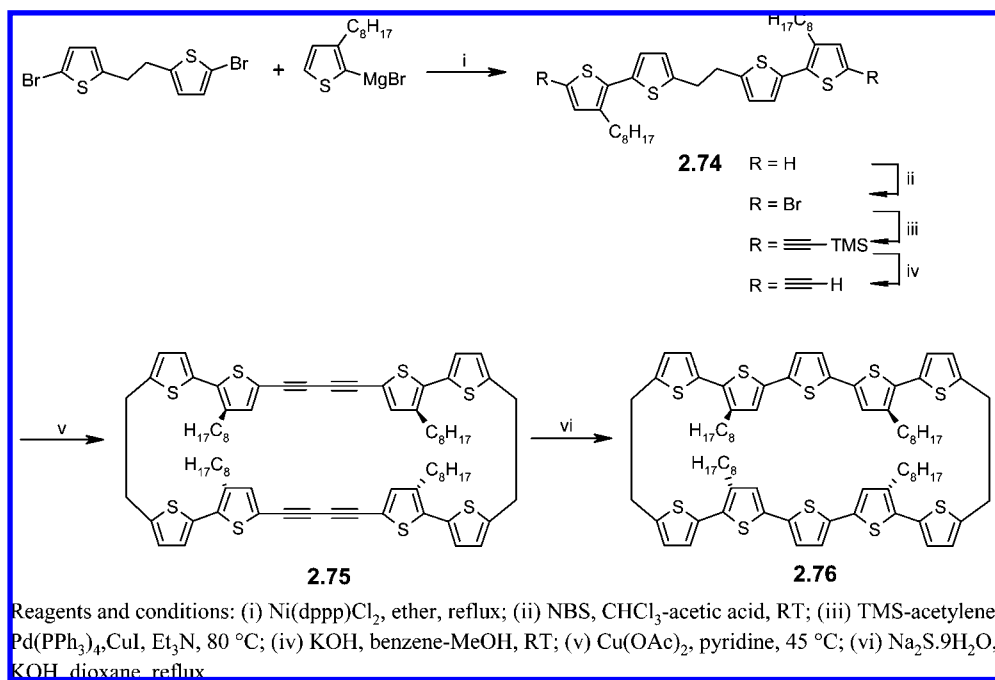
Chart 2.14
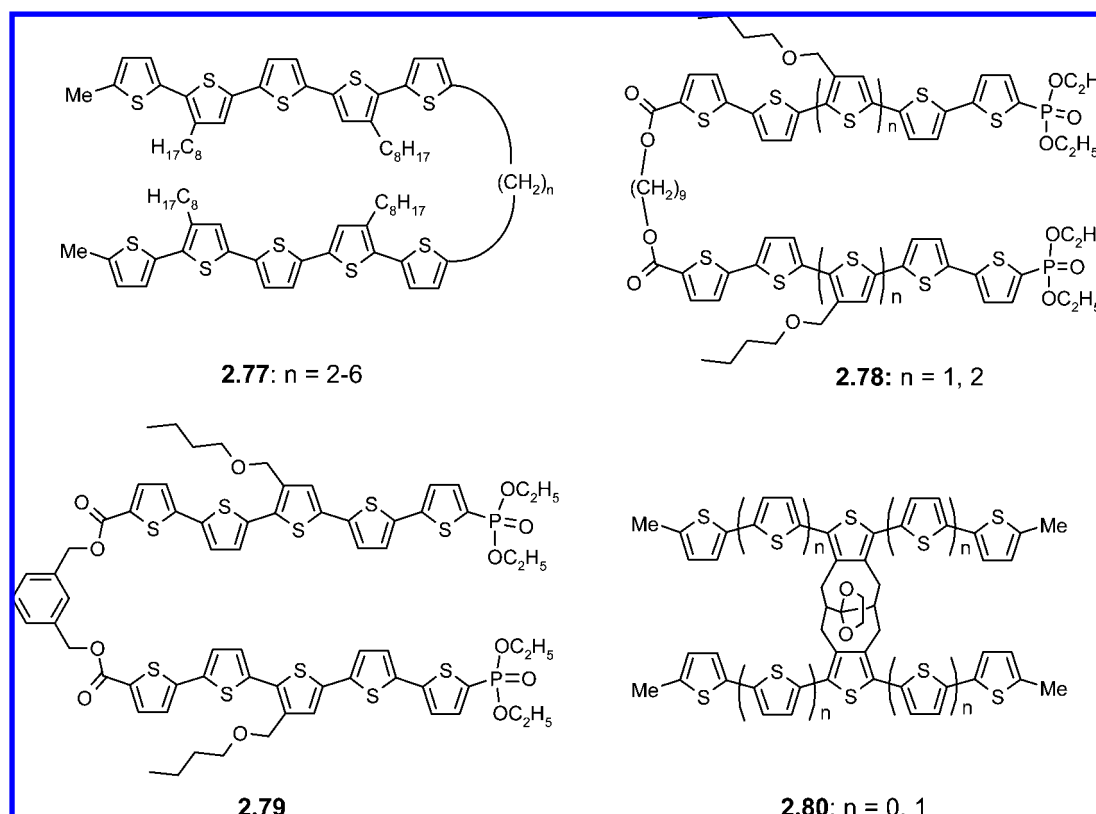
NBS and reaction with trimethylsilylacetylene, followed by deprotection of the trimethylsilyl group, generated the bisethynyl intermediate. Eglinton-type coupling of the later compound under dilution conditions yielded cyclic dimer **2.75** in 22%. Final treatment of **2.75** with Na$_2$S afforded the desired cyclophane **2.76** in moderate yield. The formation of a π-dimer was observed upon two-electron oxidation of cyclophane **2.76** at room temperature.

The same research group reported the preparation of pincer-type oligomers **2.77** ($n = 2-6$) as an open-chained

counterpart in which two methyl end-capped quinquethiophenes were separated by an alkyl spacer (Chart 2.14).[151] π-Dimerization including strong electronic interaction was observed upon two-electron oxidation of **2.76** and **2.77** by FeCl$_3$, resulting in the formation of polaronic bands in the near-infrared (NIR) region of the absorption spectra.[152] Detailed electrochemical properties were also discussed.

Edder and Fréchet prepared oligothiophene-based systems **2.78** and **2.79** (Chart 2.14), in which one end of the oligothiophene units was linked to alkyl/phenyl ester bridges

Chart 2.15
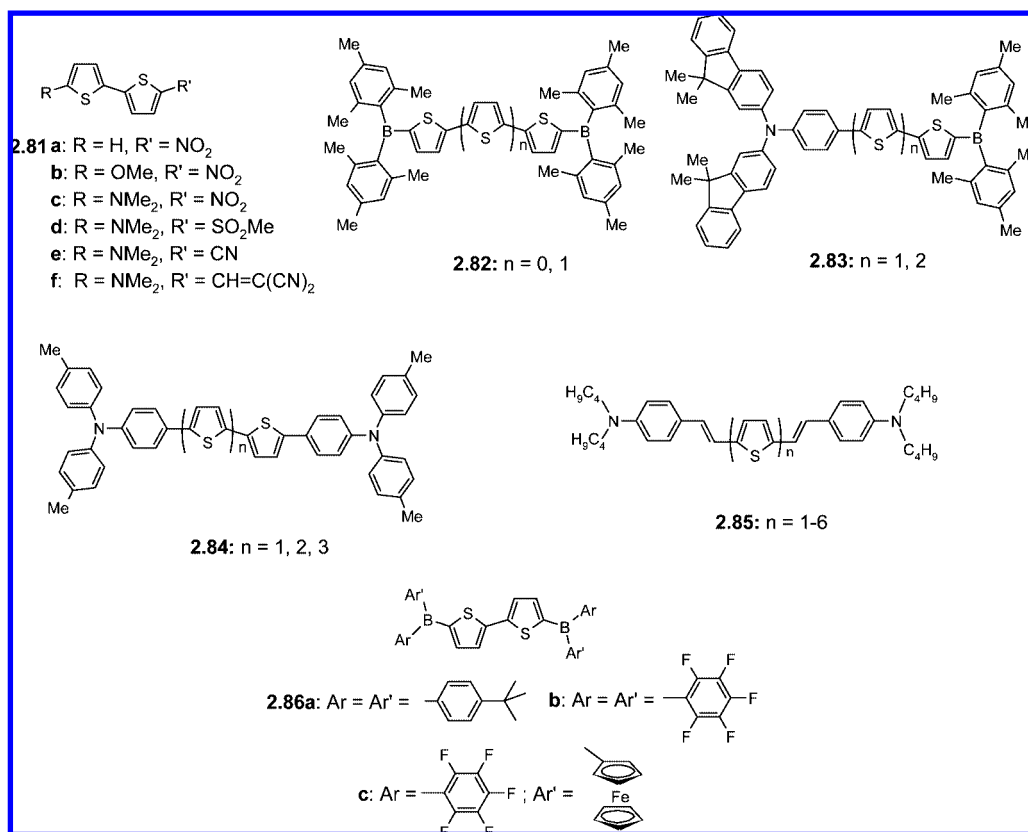
and the other end to diethylphosphate groups. By esterification of 5-carboxy-2,2′-bithiophene with 1,9-dihydroxynonane or 1,3-dihydroxymethylbenzene, corresponding bridged bithiophenes were obtained as building blocks. Further bromination using NBS followed by Stille-type coupling reaction with the corresponding stannyl derivatives afforded **2.78** ($n = 1$) in 34%, **2.78** ($n = 2$) in 10%, and **2.79** in 11% yield.[153] The authors suggested that the presence of diethylphosphate binding groups at the α-termini may possibly allow us to use these compounds as electroactive surfactants for semiconducting nanoparticles and organic electronics.

In a recent report, Collard et al. synthesized cofacially stacked π-dimeric model oligothiophenes **2.80** (Chart 2.14), in which two oligothiophene units are fused to a bicyclo-[4.4.1]undecane core.[154] One- and two-electron oxidation of these stacked oligomers afforded radical cations and dications that served as models for polarons and bipolarons in *p*-doped conjugated polymers and demonstrated the effect of π-stacking on the electronic structure of these species. Splitting of the oxidation wave in cyclic voltammetry measurements and lowering of the oxidation potential was observed for **2.80** compared to the case for the corresponding linear oligothiophene, which indicated strong interchain interactions and stabilization of the radical cations. In the case of **2.76**, those effects were not observed.

2.6. Donor, Acceptor, and Donor−Acceptor (D−A) Mixed Systems

Thiophene-containing D−A-substituted π-systems have been extensively studied in relation to their application in organic electronics. Nonlinear optical (NLO) measurements of such push−pull systems showed enhanced second-order

polarizabilities (β) compared to the phenyl counterparts. These increased nonlinearities were attributed to the partial decrease of the aromatic character and increased π-overlap between the thiophene units. Various electron donors (alkyl, -NR₂, -OMe, -SMe, etc.) and acceptors (-NO₂, -CHO, -SO₂Me, -CN, etc.) have been introduced to oligothiophene backbones, not only to study electron and energy transfer processes but also because of their prospects as active molecules in electronic devices. The changes in physical properties (e.g., absorption, fluorescence, electrochemistry, etc.) of these derivatives strongly depended on the nature of both the π-conjugation and the type of D−A substitution.[155−160]

Effenberger et al. synthesized a series of D−A-based bithiophenes **2.81a−f** (Chart 2.15) by employing Negishi- and Stille-type coupling reactions, where the *tert*-amine or methoxy groups acted as donor and nitro, cyano, methylsulfone, and dicyanovinylene groups as acceptor. A strong solvatochromic behavior was observed in their absorption spectra due to the D−A substitution.[161]

Shirota et al. synthesized amorphous electron-transporting oligothiophenes **2.82** ($n = 0, 1$), in which dimesitylboryl acceptor groups were introduced at both α-termini of the oligothiophene moiety (Chart 2.15). The presence of dimesitylboryl groups prevented the crystallization of the oligothiophenes due to the resulting nonplanar structure and gave rise to stable amorphous glasses when molten samples were cooled upon standing in air. They exhibited very high thermal and chemical stabilities. Because of their high photoluminescence quantum yields, they have been investigated as active layers in OLEDs. Increased luminance was reported for OLED devices using oligothiophene **2.82** ($n = 1$) as electron transporting material and tris(8-quinolinato)aluminum (Alq₃) as the emitting layer.[162,163]

Scheme 2.15

Reagents and conditions: (i) 1, BBr$_3$, RT, 2, MeSCu, CH$_2$Cl$_2$, 100 °C for 24 h.
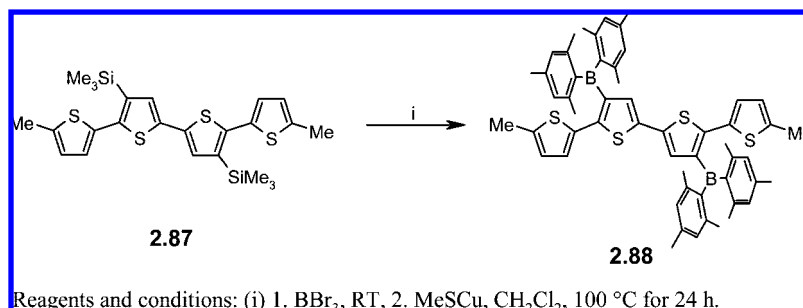
The same research group furthermore prepared D–A-capped oligothiophenes **2.83** (Chart 2.15) in which one of the dimesitylboryl units of **2.82** was replaced by a triphenylamine-type donor.[164] Compounds **2.83** ($n = 1, 2$) were synthesized via Suzuki coupling of N,N-bis(fluorenyl)-4-bromoaniline and the boronic ester of the basic oligothiophene followed by lithiation and further coupling with dimesitylboron fluoride. Cyclic voltammetry measurements showed reversible oxidation and reduction processes to generate stable radical cations and anions, respectively. Due to their high glass transition temperatures around 120 °C and strong fluorescence, these materials acted as good emitters in OLEDs emitting multicolored light. Furthermore, depending on the π-conjugation length, they also acted as good color-tuning host materials for emissive dopants.

A series of oligothiophenes **2.84** ($n = 1–3$) (Chart 2.15) bearing triarylamine units at either terminus have been prepared using the Grignard coupling reaction of 4-bromophenyl-bis(4-methylphenyl)amine with the corresponding dibromooligothiophene.[165] These compounds exhibited high glass transition temperatures ($T_g = 90–98$ °C) and displayed high performance in bilayer electroluminescent devices when used as an emitting layer with hole-transport ability.[166] FT-IR and Raman spectroscopic studies of these materials also pointed to their amorphous nature. This together with their high thermal stability promotes these compounds to good candidates as active components in optoelectronic devices.[167]

A similar type of donor-capped hole-transporting oligothiophene **2.85** ($n = 1–6$) (Chart 2.15) was synthesized by a combination of Wittig–Horner–Emmons olefination and Pd-catalyzed Stille coupling. The aminoalkyl groups control the ionization potential of these materials, whereas the energy gap and electron affinity depend on the conjugated chain length of the oligothiophene.[168] X-ray structure analyses clearly showed that the crystal packing is influenced by an odd or even number of thiophene units in the bridge.

Jäkle et al.[169] prepared organoboranes, which contained a common bithiophene linker and different aryl-substituted borons. Borylated bithiophene **2.86a** (Chart 2.15) was synthesized in 74% yield by reaction of a distannylated precursor with bis-p-tert-butylphenylated boron bromide. Derivatives **2.86b** and **2.86c** were prepared from dibromoboryl-functionalized bithiophene, which was obtained by reaction of 2,2′-bis(trimethylsilyl)-5,5′-bithiophene and boron tribromide via B–Si exchange. Treatment of the precursor building block with 4 equiv of pentafluorophenyl copper yielded **2.86b** in 71% yield. In contrast, **2.86c** was obtained in 77% yield by selective reaction of the precursor building block with stannylated ferrocene and successive reaction with pentafluorophenyl copper. The influence of the substituents, electronic communication between the Lewis acidic boron centers, and cooperativity effects in the binding of pyridine

were studied using various spectroscopic techniques and cyclic voltammetry.

The same group further elaborated the transmetalation B–Si exchange to borylate at the β-position of oligo- or polythiophene backbones.[170] For example, reaction of trimethylsilyl-substituted quaterthiophene **2.87** with BBr$_3$ and then with mesitylcopper at elevated temperature afforded β-boryl-substituted tetramer **2.88** in 61% yield (Scheme 2.15). The influence of the electron deficient boryl groups on the electronic properties was discussed.

Yamaguchi et al. recently prepared a series of 3-boryl-2,2′-bithiophene-based triads **2.90** in which a dimesitylboryl unit at a β-position of the central bithiophene acted as an acceptor.[171] The parent compound 3-dimesitylboryl-2,2′-bithiophene **2.89** was synthesized by lithiation of 3-bromo-2,2′-bithiophene followed by reaction with dimesitylboron fluoride (Scheme 2.16). Dibromination of **2.89** with 2 equiv of NBS followed by Pd-catalyzed cross-coupling reactions with appropriate aryl boronic acids or aryl stannanes gave the π-extended co-oligomers **2.90a–e** in moderate to good yields. Tuning the electron-donating ability of the π-conjugative framework by attachment of different (donor) end groups resulted in intense solution and solid-state emission, covering a wide range from blue (477 nm) to deep red (660 nm). This feature was attributed to steric congestion of the 3-boryl group, which prevents intermolecular interactions and self-quenching of the fluorescence, and a large Stokes shift (100–200 nm) arising from an intramolecular charge-transfer (ICT) transition was also detected.

Bäuerle et al. synthesized and characterized a series of oligothiophenes **2.91** consisting of two to four thiophene units and comprising pyrrolidino donor groups at the outer β-position of the terminal thiophene rings (Chart 2.16).[172] With increasing chain length of the oligothiophene, the absorption maximum was red-shifted by ~35–50 nm compared to unsubstituted oligothiophenes, while cyclic voltammetry showed a negative shift of the oxidation potentials. Interestingly, the presence of pyrrolidino groups enhanced the electropolymerization ability of these oligothiophenes, whereas, e.g. the unsubstituted quaterthiophene did not electropolymerize.

Various diarylamino-capped bithiophenes were prepared by Pd-catalyzed coupling of dihalogenated bithiophenes with diarylamines.[173,174] Higher homologues of diphenylamino- and phenothiazino-substituted oligothiophenes **2.92** and **2.93** (Chart 2.16) were synthesized by Hartmann et al. in 13–45% yield by Pd-catalyzed reaction of stannylated diarylamino-capped smaller oligothiophenes and dibrominated thiophene-based central units.[175] The same group recently reported successful synthesis of diphenylamino-capped oligothiophenes **2.92** ($n = 5, 6, 7$) up to a nonamer by the same route.[176,177] Alternatively, bi- and quaterthiophenes **2.92**
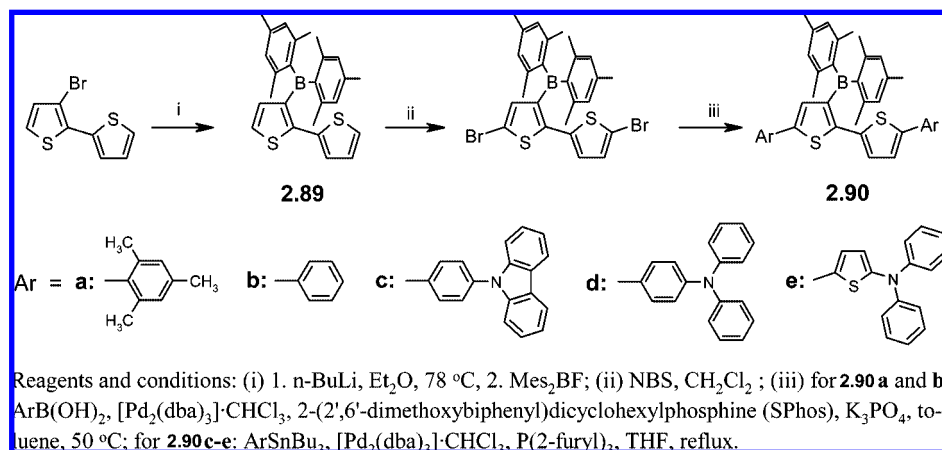
Scheme 2.16

Reagents and conditions: (i) 1. n-BuLi, Et$_2$O, 78 °C, 2. Mes$_2$BF; (ii) NBS, CH$_2$Cl$_2$; (iii) for **2.90 a** and **b** ArB(OH)$_2$, [Pd$_2$(dba)$_3$]·CHCl$_3$, 2-(2',6'-dimethoxybiphenyl)dicyclohexylphosphine (SPhos), K$_3$PO$_4$, toluene, 50 °C; for **2.90 c-e**: ArSnBu$_3$, [Pd$_2$(dba)$_3$]·CHCl$_3$, P(2-furyl)$_3$, THF, reflux.
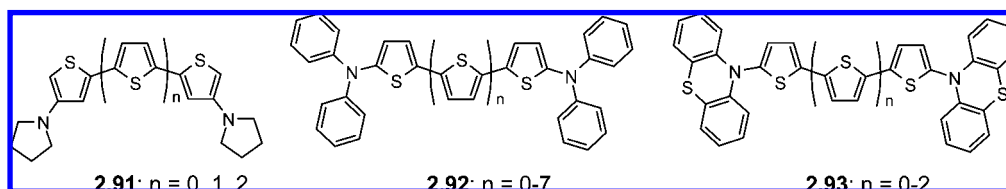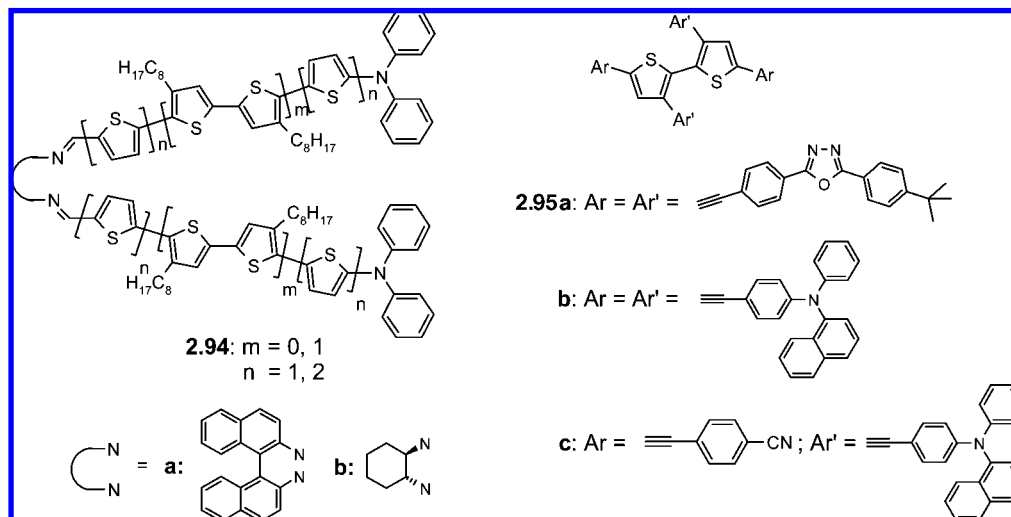
Chart 2.16

Chart 2.17

($n = 0$, 2) were prepared by oxidative dimerization of 2-diphenylamino-substituted thiophene and bithiophene with TiCl$_4$. These oligomers were easily electrochemically oxidized, giving stable radical cations, which were studied by electron spin resonance (ESR) and spectroelectrochemical measurements.

A series of interesting tweezer-like oligothiophenes **2.94a,b**, which are held together by chiral binaphthyl- or cyclohexyl-diamine units and are end-capped with diphenylamino donor groups, were prepared by condensation of oligothiophene aldehydes and the diamines in the presence of molecular sieves to give corresponding Schiff bases **2.94a,b** in 12−46% yield (Chart 2.17).[178] The formylated diphenylamino-oligothiophene precursors were prepared by a combination of Suzuki and Stille-type reactions. Enhanced first order hyperpolarizabilities (β_{HRS}) were reported for these oligomers due to the presence of the chiral centers and the tweezer-type structure, which disfavored the formation of centrosymmetrical dimeric assemblies.

Recently, it has been demonstrated that large two-photon absorption cross-sections (σ) can be obtained by the proper choice of donor and/or acceptor substituents in bithiophenes **2.95a−c** (Chart 2.17). Upon excitation at 800 nm, quadrupolar-type chromophore **2.95c** exhibited the largest σ value (1120 GM) in CH$_2$Cl$_2$.[179]

Oligothiophene-fluorene co-oligomers **2.96** (Chart 2.18) endowed with two hexyl groups at both termini of the fluorine units were synthesized using Suzuki or Stille coupling reactions, and their transport behavior was investigated in OFETs. Highly ordered polycrystalline films were obtained by vacuum evaporation. Charge carrier mobilities as high as 0.12 cm^2 V^{-1} s^{-1} and on/off ratios of 10^5 were achieved for fluorene-substituted bithiophene **2.96** ($n = 1$).[180,181]

Promarak et al. prepared a series of 9,9-dialkylated fluorene-capped oligothiophenes **2.97**[182] and **2.98**[183] (Chart 2.18). The strategy adopted for the synthesis of oligomers **2.97** was sequential Suzuki cross-coupling and bromination

Chart 2.18

2.96: n = 1-3

2.97: n = 1-4

2.98a: n = 0, 2, 4; R = C_6H_{13}
b: n = 1; R = C_8H_{17}

2.99: n = 0; m = 0
n = 0; m = 1
n = 1; m = 1
n = 2; m = 1

2.100: n = 0-2
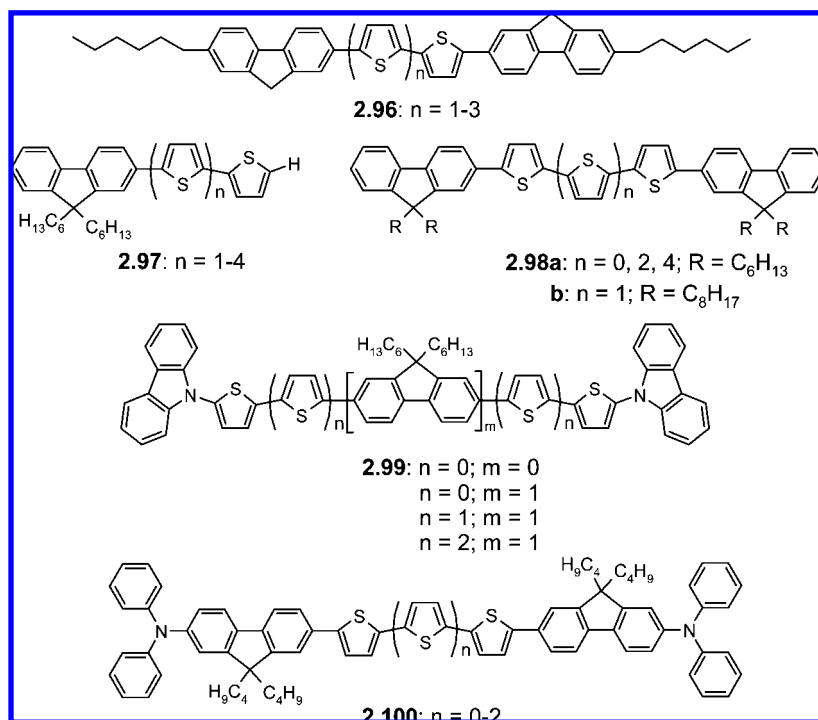
reactions, whereas oligomers **2.98a** were synthesized *via* Ni-catalyzed reductive dimerization. Co-oligomers of carbazole-oligothiophene-fluorene **2.99** were also synthesized. Reaction of dibromofluorene with 2-thiophene boronic acid under Suzuki coupling conditions afforded a fluorene-thiophene oligomer. Repeated bromination and Suzuki-type coupling afforded dibrominated oligothiophene-fluorenes. Final coupling of the resulting dibromo compounds with carbazole under Ullmann coupling conditions furnished **2.99** in good yields.[184−186] The optical, electrochemical, and thermal properties of these materials are tuned by varying the conjugation length of the oligothiophene segment. Noticeable red shifts in absorption and emission spectra and decreased oxidation potentials of the co-oligomers were observed with increasing number of thiophene units. The incorporation of terminal carbazole and central fluorene units in **2.99** had significant effects on improved solubility and morphology and had promise as potential hole-transporting and light-emitting layers in OLED devices.

Leclère et al.[187] prepared analogous terthiophene **2.98b** end-capped with 9,9-dioctyl-substituted fluorene units which formed well-defined monolayers in the solid state with a herringbone-type organization of the molecules and assembled into micrometer-long stripe-like structures. This oligothiophene-fluorene showed structureless absorption and structured emission both in solution and in the solid state. In comparison to solution spectra, the absorption was red-shifted by only 17 nm in the solid state, while emission was red-shifted by ~75 nm. The difference in shape between the absorption and emission was attributed to increased local polarizability and/or planarity of the molecule in the excited state. Polarized confocal microscopy indicated that the structural order leads to a polarized emission along the long axis of the stripes with red-shifted emission originating from well-defined aggregates, which could be promising for optoelectronic applications.

In order to enhance the OLED-performance, ambipolar diphenylamino end-capped fluorenyloligothiophenes **2.100**

($n = 0−2$) were synthesized by cross-coupling reaction of diiodo- or dibromooligothiophenes and corresponding diphe-nylaminofluorenyl boronic esters (Chart 2.18).[188,189] In addition to typical hole transport properties, these co-oligomers also facilitated efficient electron transport, in which the central oligothiophene core can act as an electron-accepting unit.

Skabara et al.[190,191] prepared sexithiophenes **2.101** and **2.102** bearing pendent 1,3-dithiol-2-ylidene-fluorene and fused tetrathiafulvalene (TTF) units, respectively (Chart 2.19). The optical band gap of **2.101** determined from UV−vis absorption spectra ($E_g^{opt} = 1.9$ eV) and the electrochemically determined band gap were equal ($E_g^{CV} = 1.9$ eV), indicating the donor−acceptor character of the compound. Whereas the longest wavelength absorption arose due to an intramolecular charge transfer (ICT) from the dithiole donor to the electron deficient fluorene moiety, the lowest oxidation potential came from the sexithiophene unit. Photovoltaic cells fabricated from blends of **2.101** with PCBM revealed modest power conversion efficiencies of 0.1%. While the power conversion efficiency is low, the photocurrent spectrum indicated that the ICT process was also involved in the conversion of absorbed light to current. This represents an interesting example in which pendant donor−acceptor moieties are attached to the conjugated backbone in order to improve the light harvesting efficiency. Electrochemical measurements of α,α′-dodecyl-capped derivative **2.102** revealed simultaneous oxidation through sexithiophene and TTF units.

Oligothiophenes end-capped with cyano (**2.103**)[192−194] or cyano-containing groups, such as dicyanovinylene (DCV) (**2.104**),[195] tricyanovinylene (TCV) (**2.105**, **2.106**),[196,197] and dicyanomethylene (**2.107**),[194,198−202] were prepared and investigated by various groups (Chart 2.20). The incorporation of these quite strong electron-accepting groups into oligo-thiophene backbones induced strong bathochromic shifts in their optical spectra and lowered the HOMO−LUMO gap. For example, UV−vis spectra of **2.105b** and **2.105a** (*n* =

Chart 2.19
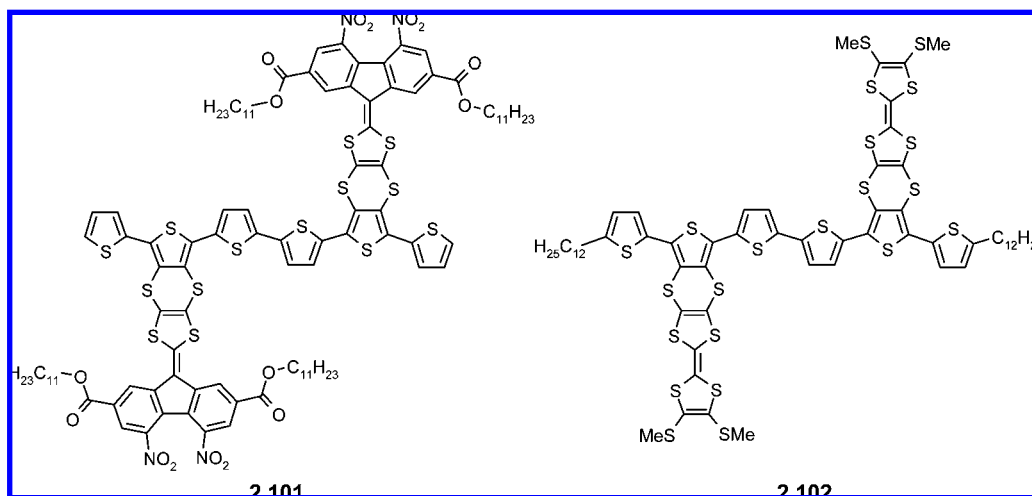
Chart 2.20
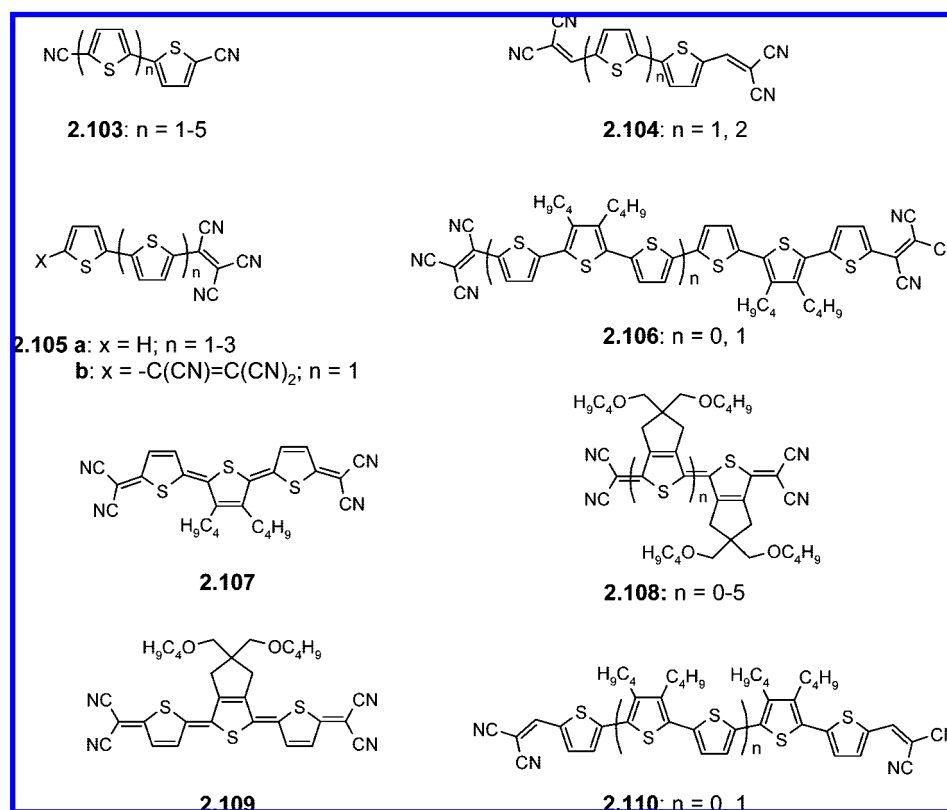
1) showed the longest wavelength absorptions at 504 and 485 nm, respectively, which are at considerably lower energies compared to that for bithiophene (304 nm). TCV-terminated oligomers **2.106** ($n = 0, 1$) were prepared in moderate yields by dilithiation of the basic oligothiophene building blocks using n-BuLi followed by treatment with tetracyanoethylene. The introduction of TCV groups dramatically lowered the band gap as compared to that of the parent oligothiophenes. X-ray structure analyses revealed that π-stacking is frequently observed for thiophenes capped with one or more electron-withdrawing groups on the terminal α-positions. These results suggested that these compounds may be used as n-type semiconductors and more likely exhibit ambipolar charge transport characteristics; that is, they can be used as p- and n-type semiconductors depending on the sign of the gate bias in an OFET.

Quinoidal terthiophene **2.107** (Chart 2.20) bearing butyl substituents at the central thiophene ring and dicyanomethylene terminal groups was prepared by a Pd-catalyzed cross-coupling reaction of dibromoterthiophene and malononitrile in the presence of sodium hydride, followed by oxidation of the dianion with Br_2.[199] Compound **2.107** exhibited a planar geometry which is stabilized by the dicyanomethylene caps. X-ray structure analysis of **2.107** revealed that the molecules form face-to-face π-stacked dimers and the intermolecular face-to-face distance is alternately 3.47 and 3.63 Å. Vapor- and solution-deposited films of **2.107** behave as n-type semiconductors in OFETs exhibiting electron mobilities of 5×10^{-3} and 2×10^{-3} cm^2 V^{-1} s^{-1}, respectively,[199] which were further improved to 0.2 cm^2 V^{-1} s^{-1} by changing the film morphology in the device.[203]

Scheme 2.17

Reagents and conditions: (i) *n*-BuLi, 1 eq. I$_2$, -78 °C, THF; (ii) NaH, CH$_2$(CN)$_2$, Pd(PPh$_3$)$_4$, THF; (iii) 1,3-dithiole-2-thione, dimethyl sulfate, Et$_3$N, CH$_3$COOH; (iv) benzo[d]-1,3-dithiole-2-thione, dimethyl sulfate, Et$_3$N, CH$_3$COOH; (v) POCl$_3$, DMF; (vi) NBS, DMF-CHCl$_3$; (vii) benzene-1,2-dithiol, *p*-TsOH, benzene; (viii) NaH, CH$_2$(CN)$_2$, Pd(PPh$_3$)$_4$, THF.
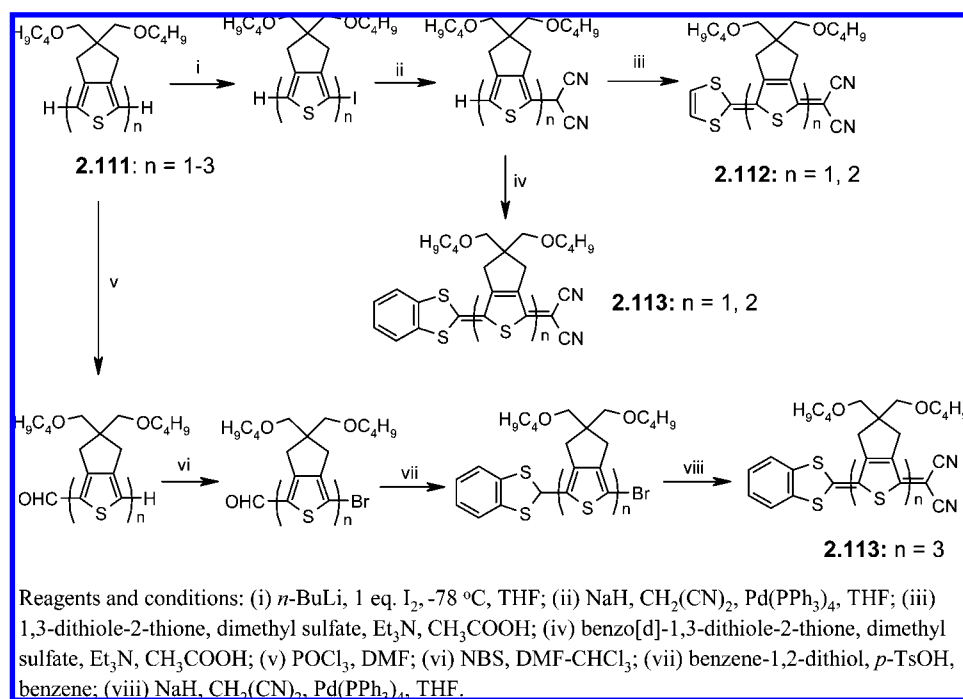
Otsubo et al. synthesized a series of highly soluble dicyanomethylene derivatives **2.108** (*n* = 0−5) following a procedure similar to that reported for **2.107** (Chart 2.20).[201] The absorption spectra of these compounds were shifted to the NIR region. For example, derivative **2.108** (*n* = 5) showed a longest wavelength absorption at 1012 nm and a less intense absorption at 1371 nm due to the extended quinoidal structure. The higher homologues **2.108** (*n* = 4, 5) existed as equilibrium mixtures of closed-shell and biradical species, as demonstrated by ESR measurements. The biradicaloid nature of these longer quinoidal oligothiophenes was further confirmed by Raman spectroscopy in combination with quantum chemical calculations.[204]

However, oligomers **2.108** (*n* = 0−5) were found not to be a suitable organic semiconductor in organic electronic applications because of the steric crowding of the solubilizing side chains, which reduces intermolecular interactions in the solid state. To retain such high solubility and simultaneously good intermolecular interactions in the solid state, analogous dicyanomethylene-substituted quinoidal terthiophene **2.109** was prepared and a highly soluble material with n-type charge transport behavior was obtained.[205] Utilization of spin-coated thin films of **2.109** as active semiconducting material in OFETs showed high electron mobilities of up to 0.16 cm^2 V^{-1} s^{-1}.

López Navarrete et al. reported that direct substitution of oligothiophenes by cyano groups as presented in **2.103** as well enhances the electron affinity of the oligomers by stabilizing the radical anions or dianions, which promotes them to prospective *n*-channel materials.[206] The application of some of these dicyano derivatives in OFETs has been reviewed recently.[207]
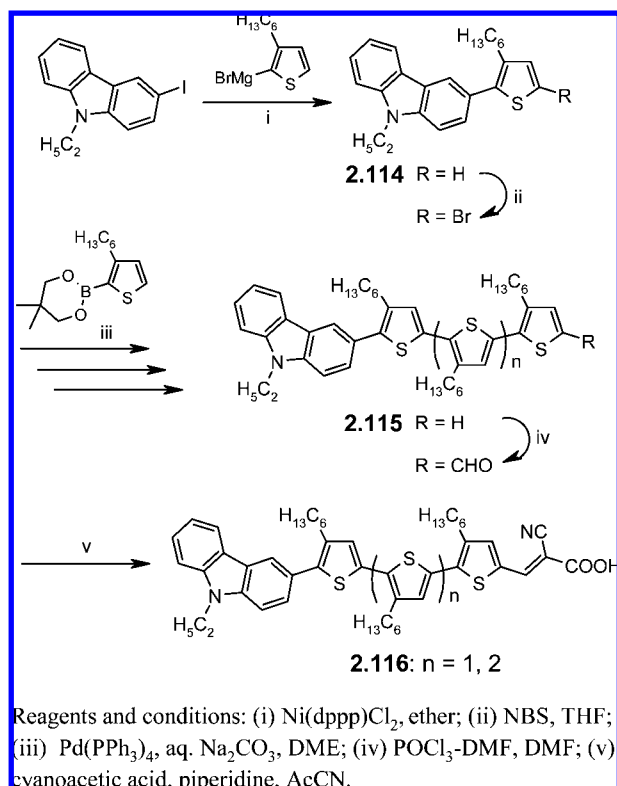
Leo and Bäuerle et al. recently reported the synthesis of low-band gap acceptor-capped oligothiophenes designed for the use in bilayer heterojunction solar cells. Dicyanovinyl (DCV) was the acceptor of choice and butyl side chains served for solubility. Quinquithiophene **2.110** (*n* = 1) (Chart 2.20) was prepared as a deep-purple solid from corresponding

butyl-substituted quinquethiophene, that successively was converted to the dialdehyde by Vilsmeier−Haack formylation and further transformed to the DCV derivative by Knoevenagel condensation with malononitrile in basic medium. The UV−vis spectrum in solution showed the longest wavelength absorption at 513 nm, whereas a significant bathchromic shift to 573 nm and a broadened absorption band was observed in thin films, causing a decrease of the optical band gap to 1.77 eV. Solar cells fabricated using **2.110** (*n* = 1) as donor and fullerene-C$_{60}$ as acceptor showed a maximum power conversion efficiency of 3.4% under illumination with simulated sun light.[208,209]

In a continuation of this work devoted to the application of DCV-substituted oligothiophenes in OSCs, the same authors further reported solar cells comprising a blended layer of terthiophene **2.110** (*n* = 0) and C$_{60}$.[210,211] Photoinduced and transient absorption spectroscopy were used to study triplet exciton dynamics in thin films of the pure oligomer and its blends with fullerene-C$_{60}$. Enhanced generation of triplet excitons on the oligomer was achieved *via* a back and forth exciton transfer which was termed as ping-pong effect.

Otsubo et al. further prepared a series of novel D−A-based quinoidal thiophenes **2.112** and **2.113** in which 1,3-dithiol-2-ylidene units acted as donor and dicyanomethylene units as acceptor.[212] For the preparation of dyads **2.112** (*n* = 1, 2) and **2.113** (*n* = 1, 2), oligomers **2.111** were monoiodinated using *n*-BuLi and elemental iodine, which were then subjected to a Pd^0-catalyzed substitution reaction with sodium dicyanomethanide according to the Takahashi method[213,214] (Scheme 2.17). Finally, coupling of the intermediate with 2-methylthio-1,3-dithiolium methyl sulfate or 2-methylthiobenzo[d]-1,3-dithiolium methyl sulfate gave the target compounds in moderate to good yields. On the other hand, trimer **2.113** (*n* = 3) was prepared by another route starting from **2.111** (*n* = 3). The synthesis included monoformylation of **2.111** (*n* = 3) and subsequent bromination with NBS at the other terminal α-position to afford the functional ter-

Scheme 2.18

Reagents and conditions: (i) Ni(dppp)Cl$_2$, ether; (ii) NBS, THF; (iii) Pd(PPh$_3$)$_4$, aq. Na$_2$CO$_3$, DME; (iv) POCl$_3$-DMF, DMF; (v) cyanoacetic acid, piperidine, AcCN.

thiophene intermediate. After conversion of the formyl group of the intermediate into the thioacetal group by reaction with benzene-1,2-dithiol, the bromo group was transformed into the dicyanomethylene group under basic conditions to give **2.113** (n = 3) in a very low yield. Owing to the extensive π-conjugation of the quinoidal skeleton, these oligomers showed strong red-shifted absorptions in the NIR regime.

2.6.1. Donor–Acceptor Substituted Oligothiophenes for Dye-Sensitized Solar Cells

Dye-sensitized solar cells (DSSC) have attracted considerable attention as organic/inorganic hybrids in the search for alternatives for silicon-based solar cells. Since the groundbreaking work by Grätzel and co-workers showing highest power conversion efficiencies up to 11% by using Ru complexes adsorbed on nanocrystalline TiO$_2$,[215] in the past few years, the possibility to develop DSSCs based on pure D–A-substituted organic chromophores has been realized by several groups.

Koumura et al. prepared ter- and quaterthiophenes **2.116** (n = 1, 2) in which N-ethylcarbazole and cyanoacrylic acid were attached at either terminus of the oligothiophene core for their utilization as active components in DSSCs (Scheme 2.18).[216] The synthesis started by coupling of the Grignard reagent of 2-bromo-3-hexylthiophene and 3-iodo-9-N-ethylcarbazole to yield carbazole-substituted thiophene **2.114**. Successive cycles of bromination at the terminal thiophene unit and consecutive Suzuki-type coupling reactions with 3-hexylthiophene-2-boronic ester gave intermediate ter- and quaterthiophenes **2.115**. Their formylation and final condensation with cyanoacetic acid in basic medium afforded corresponding D–A-oligothiophenes **2.116** in 70−90% yields. UV−vis absorption spectra of **2.116** showed red-shifted maxima at 463 (n = 1) and 473 nm (n = 2), respectively. Fabrication of DSSCs based on **2.116** resulted

in high incidence monochromatic photon-to-current conversion efficiencies (IPCE) of ∼70% in the range of 400−650 nm and good maximum power conversion efficiencies (η) of 7.7 and 5.6% under AM 1.5 illumination.

Recently, a series of oligothiophene-based D−A triads containing tetrahydroquinoline as donor part and cyanoacrylic acid as acceptor unit were prepared as sensitizers for application in DSSCs.[217] Suzuki-type reaction between tetrahydroquinoline boronic acid and corresponding α-bromo-ω-formyl-oligothiophenes yielded formylated dyad **2.117** (n = 1, 2) (Scheme 2.19). Oligomer **2.119** (n = 1, 2) was prepared by the mono-Wittig olefination of bis-formylated oligothiophenes with the phosphonium salt of tetrahydroquinoline. Knoevenagel condensation reaction of the respective aldehydes with cyanoacetic acid afforded triads **2.118** and **2.120** in moderate to good yields. All triads showed redshifted π−π* absorption bands in the range of 455 to 475 nm due to the D−A substitution. Fabrication of DSSCs based on dyes **2.120** (n = 1, 2) gave moderate efficiencies of η = 2.35 and 1.91% under AM 1.5 illumination. On the contrary, better performances were observed for dyes **2.118** (n = 1, 2), which gave maximum η values of 4.53 and 3.44%. These results suggested that the presence of a double bond as spacer in **2.120** (n = 1, 2) is not a suitable construction rule for higher efficiencies in DSSCs. In contrast, the removal of the double bond in **2.118** (n = 1, 2) gave more rigid molecular structures and therefore is promising for higher solar-to-electricity conversion efficiencies in DSSCs.

Ko et al. reported some D−A-substituted oligothiophene-based dyes **2.121**−**2.124** (Chart 2.21).[218−222] The bulkier electron-donating fluorenylamino moieties were used to prevent aggregation and to increase the thermal stability of the dyes. Cells based on **2.121a** exhibited an IPCE of 91% at ∼520−540 nm, whereas this value decreases to 58% for cells prepared from **2.121b** containing an additional double bond.[218] The maximum η value decreased from 8.01% for dye **2.121a** to 4.78% for **2.121b**. Additionally, a decrease in short-circuit current density (J_{sc}) from 14 to 10.5 mA cm^{-2} was noticed. Furthermore, cells consisting of dyes **2.122** and **2.123** showed maximum η values of 7.43 and 5.15%, respectively.[220,221] The maximum efficiencies were reduced to 2.47 and 2.95%, respectively, by replacing the fluorenylamino groups by julolidine as donor moiety in **2.124a,b**. This could be assigned to the low molar extinction coefficient of these dyes compared to the case of fluorenyl amino-substituted dyes.[222]

Sensitizers **2.125** (Chart 2.21) consisting of thienothiophene-bridging units which absorb at 488 nm showed a high overall conversion efficiency (η) of 6.23% in DSSC.[223] All above studies further suggested that it might be essential to incorporate a bulky conjugated electron-donating group to prevent stacking and a rigid π-conjugative spacer to harvest the solar spectrum effectively.

2.6.2. Fluoroalkyl- and Fluoroarene-Substituted Oligothiophenes

A majority of oligothiophene derivatives exhibit hole-transporting (p-type) semiconducting behavior. On the other hand, electron-transporting (n-type) oligothiophenes are still limited but of great interest in recent years, because of their tunable chemical and physical properties. Recently, it has been demonstrated that π-conjugated systems substituted with electron-withdrawing perfluoroalkyl groups generally lower the LUMO level and therefore facilitate electron injection,
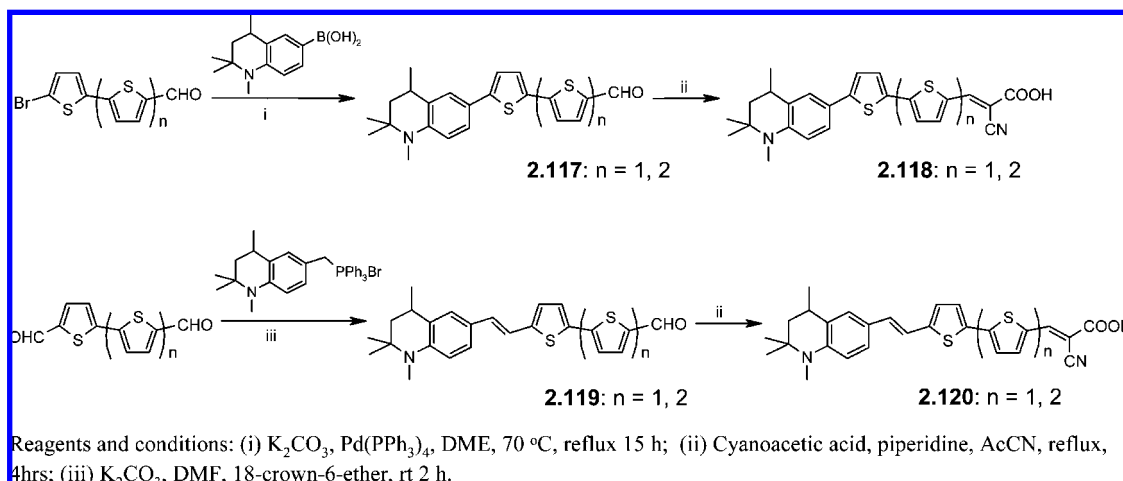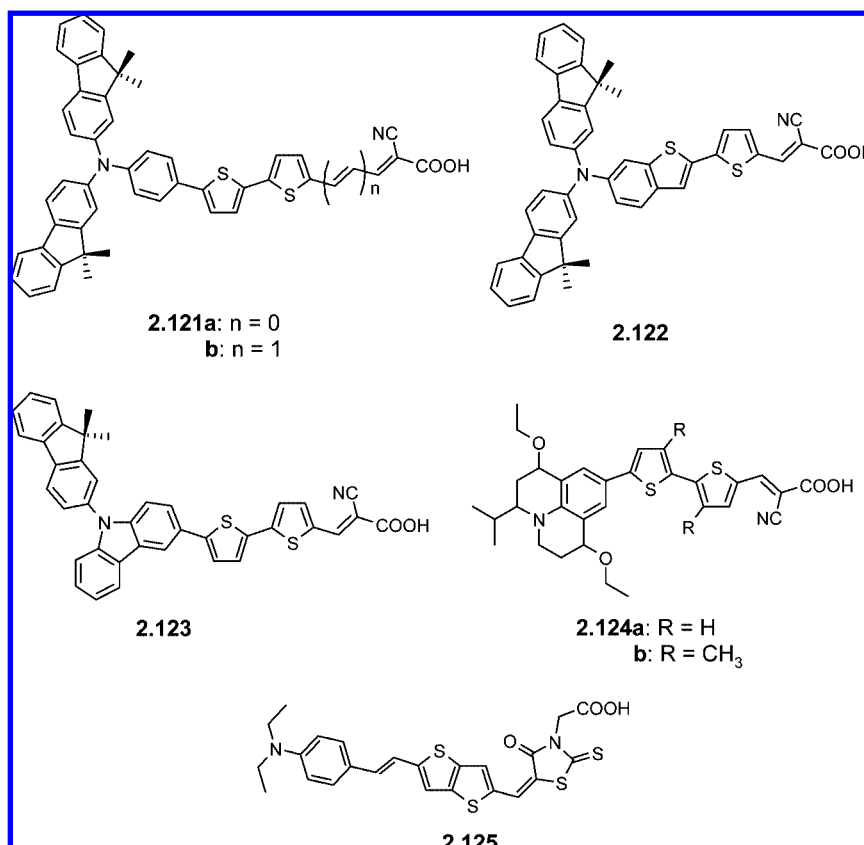
Scheme 2.19

Reagents and conditions: (i) K$_2$CO$_3$, Pd(PPh$_3$)$_4$, DME, 70 °C, reflux 15 h; (ii) Cyanoacetic acid, piperidine, AcCN, reflux, 4hrs; (iii) K$_2$CO$_3$, DMF, 18-crown-6-ether, rt 2 h.
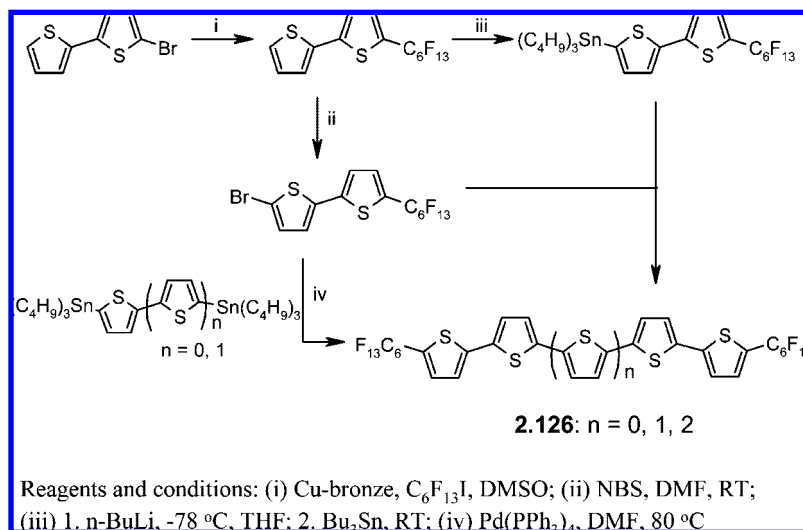
Chart 2.21

leading to an increased n-type character.[207,224] Among π-conjugated systems, perfluoroalkyl-terminated oligothiophenes are leading n-channel semiconductors because of their high solubility, excellent thermal stability, and volatility. A recent review by Tian and Yang described the effect of fluorine-substitutions on the photochromic materials based on 1,2-dithienylethene.[225]

Marks et al. reported the synthesis and properties of the first fluoroalkyl-functionalized thiopene-based materials **2.126** (n = 0−2) as the efficient n-type counterparts of the widely studied p-type dihexyl-oligothiophenes.[226,227] The oligomers were prepared by Stille-type cross-coupling reaction as depicted in Scheme 2.20. Introduction of terminal-perfluorinated hexyl chains to the oligothiophene core substantially enhanced the thermal stability, volatility, and

electron affinity vs the parent α,α′-dihexyl-substituted oligothiophenes. Thermal and XRD studies indicated that fluoro substituted derivatives exhibit close intermolecular π−π stacking. The presence of fluorohexyl groups in **2.126** imparts sufficient electron-withdrawing ability and lowered the HOMO/LUMO energy levels, allowing electron injection to exceed hole injection.

The introduction of carbonyl groups between the quater-thiophene and perfluohexyl units in **2.127** (Scheme 2.21) further lowered the LUMO level and showed improved stability and unique charge transport characteristics.[228,229] DSC and polarized optical micrograph measurements revealed that incorporation of carbonyl groups improved the intermolecular packing and imposed long-range ordering, as reflected by the presence of a smectic LC phase. OFETs

Scheme 2.20

Reagents and conditions: (i) Cu-bronze, $C_6F_{13}I$, DMSO; (ii) NBS, DMF, RT; (iii) 1. n-BuLi, -78 °C, THF; 2. Bu$_3$Sn, RT; (iv) Pd(PPh$_3$)$_4$, DMF, 80 °C

Scheme 2.21

Reagents and conditions: (i) MeLi, $C_6F_{13}I$, Et$_2$O; (ii) Br$_2$, CH$_2$Cl$_2$; (iii) MnO$_2$, CH$_2$Cl$_2$ (iv) Pd(PPh$_3$)$_4$, DMF, 100 °C
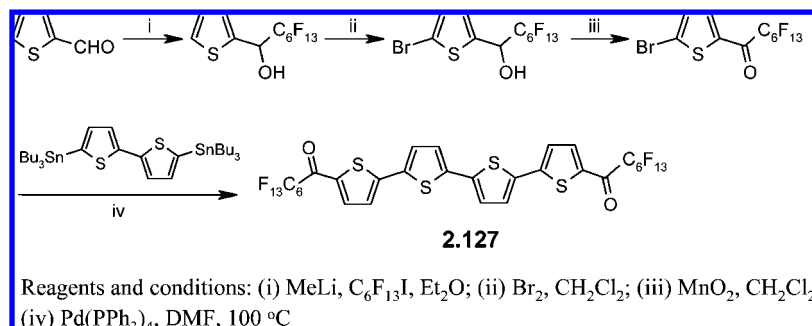
fabricated from **2.127** were found to be air sensitive and showed n-type character with improved charge carrier mobilities of 0.32 cm^2 V^{-1} s^{-1} compared to 6×10^{-2} cm^2 V^{-1} s^{-1} for analogous quaterthiophene **2.126** ($n = 0$) without carbonyl groups.[230] Recently, it has been demonstrated that, after proper dielectric surface modification (nonpolar polystyrene coatings on SiO$_2$) in interfacial studies of air sensitive semiconductors (generally high LUMO energy), n-type mobilities were significantly improved: values approaching ~2 cm^2 V^{-1} s^{-1} for **2.127** were measured.[231] In contrast, the device performance of air-stable n-type and p-type semiconductors is not significantly affected by the same dielectric surface modifications.

A family of perflouoroarene-oligothiophenes (**2.128**–**2.130**) were synthesized to assess the influence of perfluoroarene introduction and regiochemistry on the molecular and thin-film transistor properties.[232] These materials were synthesized by Stille-type reaction between bromo and the corresponding stannylated or distannylated oligothiophene(s) (for synthesis of **2.128**, see Scheme 2.22). Crystal structure analyses of perfluoroarene-substituted oligomers revealed that all compounds exhibited close cofacial packing of electron-rich and electron-deficient subunits. OFET measurements demonstrated that the oligomer **2.128** behaves as n-type semiconductor, while **2.129** and **2.130** (Chart 2.22) exhibited p-type behavior. By optimizing the growth conditions, a large n-channel mobility approaching ~0.5 cm^2 V^{-1} s^{-1} and I_{on}/I_{off} ratios > 10^8 were achieved for **2.128**.[233] This n-type character of **2.128** was explained in terms of optimum molecular packing in the solid state and charge localization in the molecule. The lowest mobility of 4×10^{-5} cm^2 V^{-1}

Scheme 2.22

Reagents and conditions: (i) Pd(PPh$_3$)$_4$.
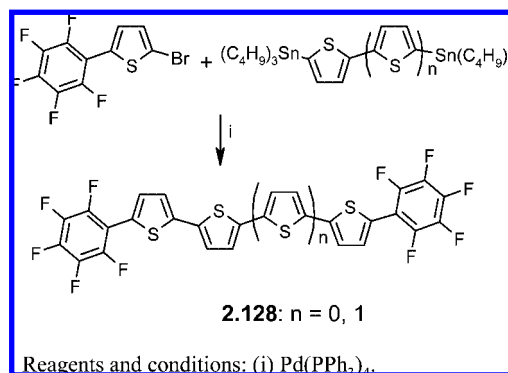
s^{-1} obtained for **2.130** was clarified in terms of steric repulsions between the central perfluoroarene groups, resulting in pronounced distortion from the planarity.

Phenacyl-quaterthiophene **2.131** (Chart 2.22) was synthesized by Friedel–Craft acylation of pentafluorobenzoylchloride and 2-bromothiophene followed by coupling with 5,5′-bis(tributylstannyl)-2,2′-bithiophene. Thin film OFETs of **2.131** fabricated from vapor- and solution-cast films exhibited high electron mobilities up to ~0.51 and ~0.25 cm^2 V^{-1} s^{-1}, respectively, which were slightly higher compared to those of compound **2.128**.[234]

Frisbie et al. synthesized an α,α′-(perfluoro-3,6-dioxadecanoate)quaterthiophene **2.133** in 70% yield by Stille-type reaction of **2.132** and distannylated bithiophene. The precursor **2.132** was prepared by lithiation of 2,5-dibromothiophene followed by reaction with a fluoroalkoxy methyl ester

Chart 2.22

2.129

2.130

2.131

Scheme 2.23

2.132

2.133

Reagents and conditions: (i) n-BuLi, C₄F₉OC₂F₄OCF₂COOMe, BF₃.Et₂O; (ii) Pd(PPh₃)₄, DMF, 85 °C
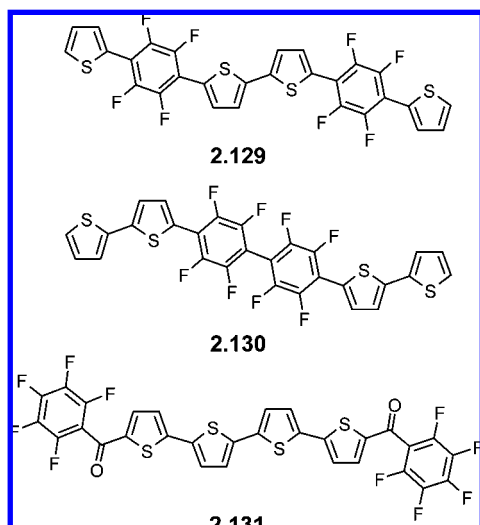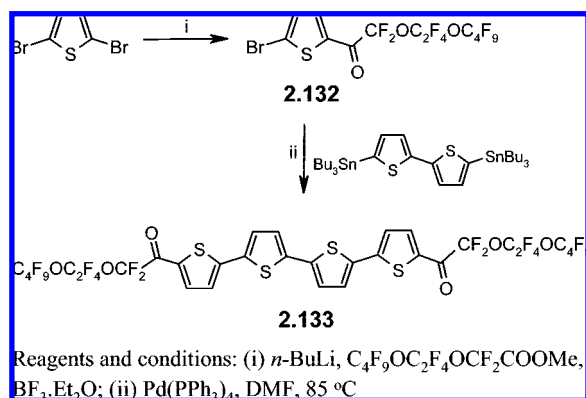
(Scheme 2.23). Ambipolar transport with reasonable electron and hole mobilities was reported for thin films of **2.133** grown over a wide range of temperatures.

The synthesis of hexafluorocyclopenta[c]thiophene-based oligothiophenes as n-type semiconductors was recently realized by Aso et al.[236] The building block **2.135** was prepared in ~70% overall yield from 2,5-dibromo-cyclopenta[c]thiophene-4,6-dione **2.134** by the treatment with N-fluoro-6-(trifluoromethyl)pyridinium-2-sulfonate (MEC-04B) followed by formation of the bis-1,3-dithiolane derivative and further desulfurative fluorination with HF·pyridine (Scheme 2.24). The building block **2.135** was used to build up the trimer **2.136** (n = 0) by coupling with stannylated thiophene or perfluorothiophene. Hexamer **2.136** (n = 1) was accomplished via sequential Stille-type reaction, iodination, and subsequent Pd⁰-catalyzed reductive homocoupling in 20−30% yields. Introduction of the central hexafluorocyclopantene unit in **2.136** (n = 0, R = H) showed a red-shifted absorption band (Δλ = 20 nm) compared to nonsubstituted terthiophene. Cyclic voltammetry measurement revealed a lowering of the HOMO−LUMO energy levels which indicated that the fluorinated unit acts as net electron acceptor. Attachment of the terminal perfluorohexyl units prompted a further positive shift of the oxidation and reduction potentials. On the other hand, the introduction of terminal perfluorinated units in the hexamer does not influence the HOMO−LUMO energy levels and absorption was nearly at the same wavelength.

A series of difluoromethylene-bridged oligomers **2.137** and **2.138** were built up via Stille-type reactions (Chart 2.23).[237] The central difluoromethylene-bridged bithiophene building block was prepared from the corresponding ketone following a similar procedure as mentioned above for fluorination of **2.135**. X-ray structure analysis revealed that the attached difluoromethylene-bridge was responsible for the coplanarity of the molecules. This was further confirmed by a red shift of the $\pi-\pi^*$ absorption band and a positive shift of the reduction potential leading to a lowering of the LUMO level compared to that of α,α'-perfluorinated oligothiophenes. In OFETs, these oligomers showed n-type semiconducting behavior with electron mobilities approaching 10^{-2} cm² V⁻¹ s⁻¹.

2.7. Oligothiophene S,S-Dioxides

The group of Barbarella has developed a method to obtain a new class of thiophene-based materials that are rather electron-deficient and easier to reduce than oxidize. Taking advantage of the hypervalent nature of the sulfur atom in thiophenes, they selectively introduced two oxygen atoms to the sulfur nuclei of one or more thiophene units in the conjugated backbone, generating so-called S,S-dioxides. These derivatives were prepared by peroxide-mediated oxidation of the thiophene sulfur using m-chloroperbenzoic acid (m-CPBA) in dichloromethane. By performing theoretical calculations, Tanaka et al. in 1989 first proposed the lowering of the HOMO−LUMO gap and high stability of S,S-dioxide derivatives compared to oligothiophenes.[238] The dearomatization of the thienyl rings of the oligothiophenes by selective introduction of S,S-dioxides significantly increases the electron affinity of the molecules and modifies the energies of both HOMO and LUMO. Thus, oligomers containing thiophene S,S-dioxides have smaller energy gaps than the precursor oligothiophenes. Additionally, the photo- and electroluminescence efficiencies in the solid state were enhanced.

A first series of S,S-dioxide-functionalized oligothiophenes was synthesized by one step oxidation of oligothiophenes using m-CPBA.[239] In the oxidation of quaterthiophene, regioisomers of both mono- and bis-S,S-dioxide were formed which had to be separated by chromatography. Terminal thiophene units were found to be more reactive toward oxidation compared to internal thiophenes. For example, oxidation of 5,5′-bis(dimethyl-tert-butylsilyl)terthiophene gave only mono-oxidized (**2.139**) and dioxidized (**2.140**) products in 17−45% yield, respectively. On the other hand, oxidation of silyl-capped quaterthiophene gave two isomeric monosulfones (**2.141** and **2.142**) and the disulfone **2.143** in 8−25% yield (Chart 2.24).

Barbarella et al.[240] further reported the regioselective synthesis of single isomeric oligothiophene S,S-dioxides up to pentamer **2.144** by successive implementation of thiophene-S,S-dioxides in the reaction sequence. Using Stille-type coupling reactions between mono- and dibrominated thiophene S,S-dioxides and the appropriate thienyl stannanes[241] gave low to moderate yields of the final oligomer (Scheme 2.25). A red shift of the absorption maxima (Δλ ~ 90−120 nm) was also observed by the introduction of S,S-dioxide groups. A dramatic decrease of the LUMO energy level which comes from the increase in electron affinity has also been found. Electrochemical studies revealed that the successive introduction of oxygen atoms to the thienyl rings leads to a positive shift of both the reduction and oxidation potentials
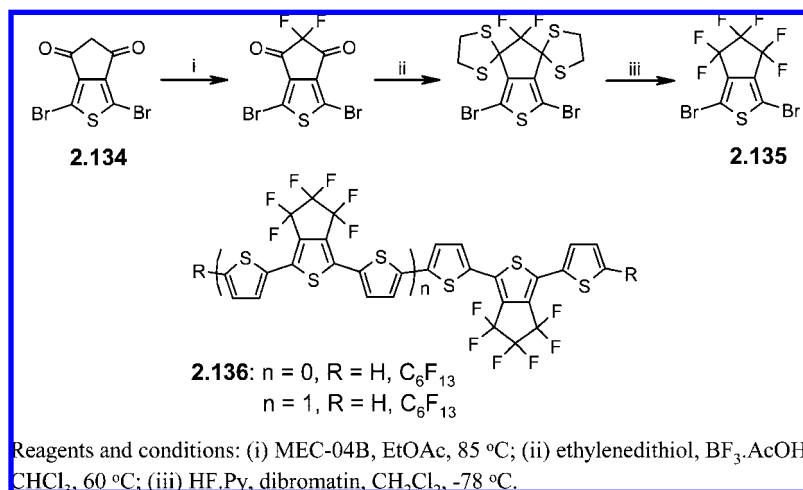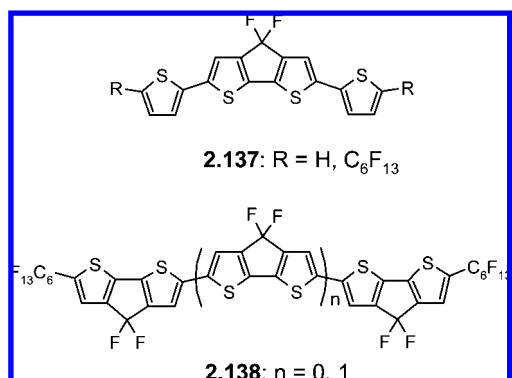
Scheme 2.24

Reagents and conditions: (i) MEC-04B, EtOAc, 85 °C; (ii) ethylenedithiol, BF₃·AcOH, CHCl₃, 60 °C; (iii) HF·Py, dibromatin, CH₃Cl₃, -78 °C.

Chart 2.23

which leads to a decreased LUMO and HOMO energy level. For example, pentamer **2.144** showed redox potentials of E°_{ox} = 1.46 V and E°_{red} = −0.82 V vs Ag/Ag⁺ in comparison to E°_{ox} = 0.92 V and E°_{red} = −2.13 V vs Ag/Ag⁺ observed for the corresponding unsubstituted quinquethiophene, finally resulting in a smaller band gap (ΔE_g = 0.77 eV). Due to the anodic shift of their reduction potentials, S,S-dioxide derivatives exhibited n-type semiconducting behavior.[242]

Jiang and Tilley reported a versatile and high yielding synthetic method for the preparation of thiophene-1-oxides using zirconocene coupling of diynes.[243] For example, the reaction of a diyne **2.145** with zirconocene afforded intermediate metallacycles **2.146**, which on subsequent treatment with gaseous SO₂ gave thiophene-1-oxides **2.147** in 75−80% yield (Scheme 2.26). Further oxidation of the latter oxides with m-chloroperbenzoic acid (m-CPBA) resulted in thiophene-1,1-dioxides **2.148** in high yield. Compared to both, 1,1-dioxides and thiophenes, thiophene-1-oxides **2.147** showed a red shift in absorption.

Barbarella et al. further introduced linear and bulky alkyl groups at the β-positions of quinquethiophene S,S-dioxides (**2.149−2.151**) in order to tune the absorption and photoluminescence properties.[244,245] S,S-dioxides **2.149** and **2.150** (Chart 2.25) showed quite high solid state photoluminescence efficiencies (Φ = 11% and 37%) compared to those of their unsubstituted counterparts 3″,4″-dihexylquinquethiophene (Φ = 2%).[246] Introduction of alkyl substituents at the β-position as in **2.150** and **2.151** increased the EL efficiencies due to distortion of the conjugated backbone. This effect prevents quenching of the fluorescence due to hindered exciton migration to quenching sites.[247] The fabrication of bilayer

OLED-devices using these derivatives showed low turn-on voltages with high EL efficiencies.[248] Furthermore, the use of these oligothiophene-S,S-dioxide derivatives as electron acceptor materials in organic photovoltaic devices was proposed.[249]
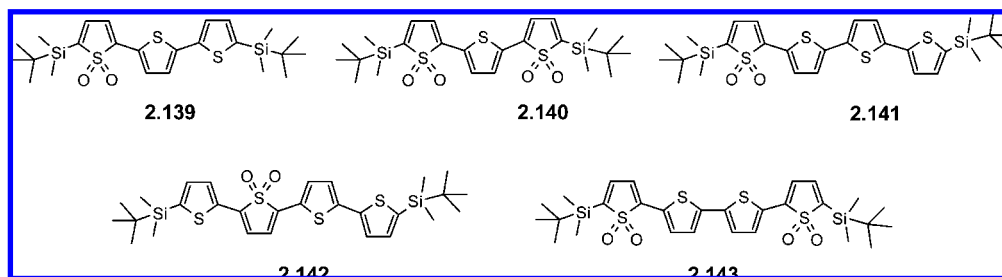
Amir and Rozen recently developed a new elegant method for the preparation of all-S,S-dioxide oligothiophenes **2.153** by treatment of alkyl-capped oligothiophenes **2.152** with oxygen transfer agent HOF·CH₃CN, which possesses a truly electrophilic oxygen center.[250] The synthetic route provided high yielding and rapid S,S-dioxide transformations (1−40 min at 0 to −10 °C, Scheme 2.27) without formation of regioisomers as previously reported by the Barbarella group. Compared to starting materials and partially oxygenated S,S-dioxides, which showed a single broad absorption band, the corresponding all-S,S-dioxides displayed structured bands due to the rigidification of the π-conjugated backbone. Furthermore, these all-S,S-dioxides showed a large bathochromic shift in the absorption spectra that indicates a considerable narrowing of the HOMO−LUMO gap.

Recently, Mann et al. synthesized quinoid-type terthiophene S,S-dioxide **2.155** in 83% yield by oxidation of quinoidal terthiophene **2.154** with m-CPBA (Scheme 2.28).[251] The interesting finding here is the high selectivity at the β-substituted thiophene ring. This selectivity for the central ring is reverse of that observed in the unsubstituted systems reported by Barbarella et al. (vide supra), and it can be rationalized that the center ring is more electron-rich than the outer rings, which bear electron-accepting dicyanomethane groups. To further confirm the selectivity of this oxidation process, the authors synthesized ter- and sexithiophene-S,S-dioxides **2.156** (n = 1, 2) without electron-withdrawing groups at the termini in 57 and 37% yield, respectively.[252] Further structural evidence came from an X-ray crystallographic analysis and NMR spectroscopy. In general, the oxidation of terthiophenes to thiophene-1,1-dioxides causes a red shift in the absorption ($\Delta\lambda$ = 71 nm) whereas oxidation of quinoid derivative **2.154** to the quinoidal thiophene-1,1-dioxide **2.155** caused a blue shift ($\Delta\lambda$ = 85 nm).

2.8. Dye-Functionalized Oligothiophenes

Roncali et al. recently prepared macrocyclic azobenzene-functionalized quaterthiophenes **2.157−2.159** (Chart 2.26) containing a bithiophene, a 3,3′-dimethoxybithiophene, or a bis-3,4-ethylenedioxythiophene unit, respectively.[253,254] The

Chart 2.24

2.139   **2.140**   **2.141**

2.142   **2.143**

Scheme 2.25

2.140 (40%)   (16%)

2.144 (40%)

Reagents and conditions: (i) *m*-chloroperbenzoic acid, CH₂Cl₂; (ii) Pd(AsPh₃)₄, Toluene.

Scheme 2.26

2.145: n = 0, 1   **2.146**: n = 0, 1

2.147: n = 0, 1   **2.148**: n = 0, 1

Reagents and conditions: (i) Cp₂Zr; (ii) SO₂ gas; (iii) *m*-CPBA, CH₂Cl₂, rt.

Chart 2.25

2.149   **2.150**   **2.151**

Scheme 2.27

2.152   **2.153**: n = 0, 1, 2
R = *t*-Bu, Br

Scheme 2.28

2.154   **2.155**

2.156: n = 1, 2

Reagents and conditions: (i) *m*-CPBA, CH₂Cl₂, rt.
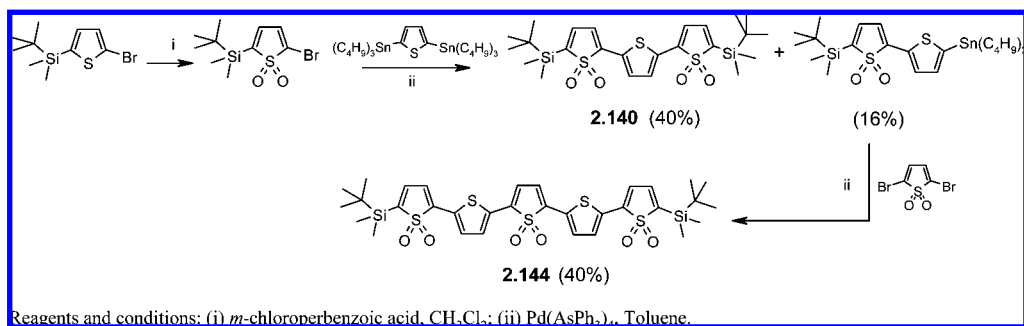
bridging azobenzene groups were implemented at the internal β-position of the two terminal thiophene rings of the quaterthiophene unit in a one pot reaction by deprotection of the corresponding thiolate groups of bis-cyanoethylsulfanyl quaterthiophenes with cesium hydroxide. Subsequently,

Chart 2.26

2.157   **2.158**   **2.159**

Scheme 2.29

2.160   **2.161 a: n = 1**
                   b: n = 2
                   c: n = 3

ring closure was achieved by coupling the intermediates with bis-*p*-bromomethylazobenzene under high dilution conditions. The X-ray crystallographic structure showed that the two systems lie in parallel planes with a short interplane distance. An X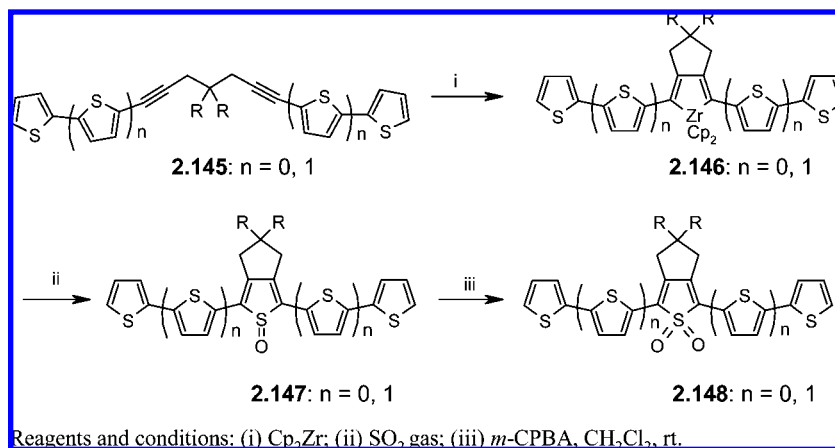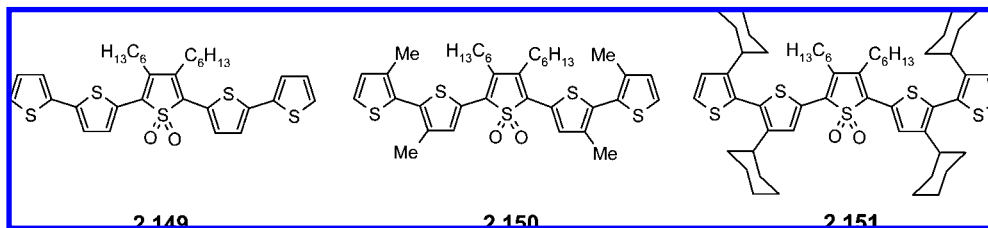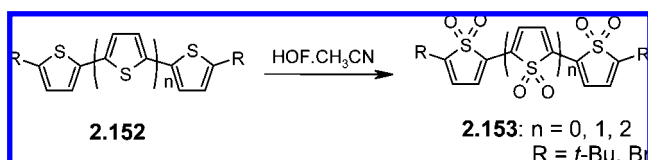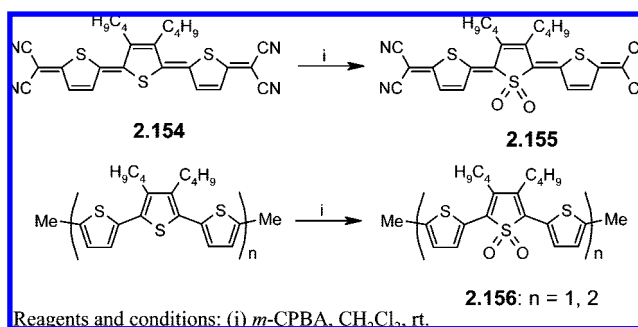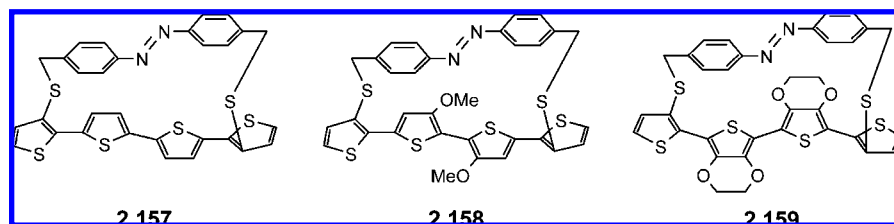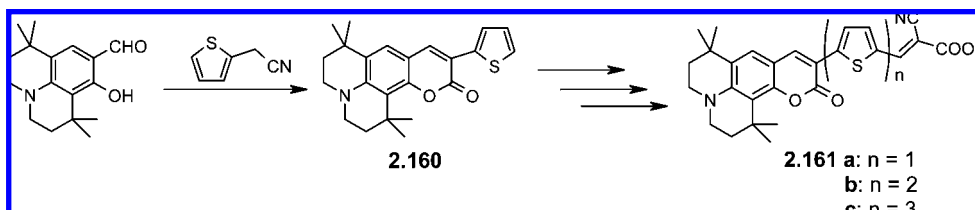-ray analysis for **2.157** and **2.158** showed that the quaterthiophene and azobenzene units are oriented in two quasiparallel planes whereby the quaterthiophene chain showed a *syn−anti-syn* conformation. On the other hand, hybrid molecule **2.159** adopted an *all-anti*-conformation in the conjugated π-system of the thiophene rings which is stabilized by noncovalent intramolecular sulfur−oxygen interactions. ^{1}H NMR, UV−vis, and cyclic voltammetry studies unequivocally showed that a *trans* to *cis* photoisomerization of the azobenzene group induces dimensional and conformational changes and thus reversible modifications of the electronic properties of the basic π-conjugated system. Upon UV-irradiation of oligomer **2.157**, an increase in the HOMO level and a narrowing of the HOMO−LUMO gap was observed. Only limited conformational changes were observed for **2.158** due to steric hindrance between the methoxy groups. In contrast, for **2.159**, a decrease in the HOMO energy level and consequently an increase of the band gap was found as a consequence of the specific structural rearrangement.

To improve the efficiency of DSSCs, Hara et al. synthesized a series of oligothiophene derivatives **2.160** and **2.161** functionalized with a coumarin dye.[255,256] Thiophene-coumarin dyad **2.160** was prepared by reaction of 9-formyl-8-hydroxyjulolidine and 2-thienyl-acetonitrile in the presence of acetic acid and piperidine. Vilsmeyer−Haack formylation of the resulting coumarin **2.160** by DMF/POCl₃ followed by condensation with cyanoacetic acid gave **2.161a** as dark green crystals. Hybrid molecules **2.161b,c** (Scheme 2.29) were prepared from **2.160** by stepwise bromination, Pd-catalyzed coupling with thiophene-2-boronic acid, formylation, and final condensation with cyanoacetic acid in good yields. The UV−vis spectrum of the dyes showed absorption maxima at 501−511 nm, which were blue-shifted by ∼30 nm when adsorbed onto nanocrystalline TiO₂ surfaces. Solar energy conversion efficiencies of 5.8% for **2.161a**, 8.1% for **2.161b**, and 6.4% for **2.161c** with rapid electron injection from the dye to the conduction band of TiO₂ (<100 fs) were reported. The kinetics of the electron transport in terms of electron diffusion coefficient and electron lifetime (τ) has been studied for these coumarin-dye-sensitized nanocrystalline TiO₂ electrodes by intensity-modulated photocurrent and
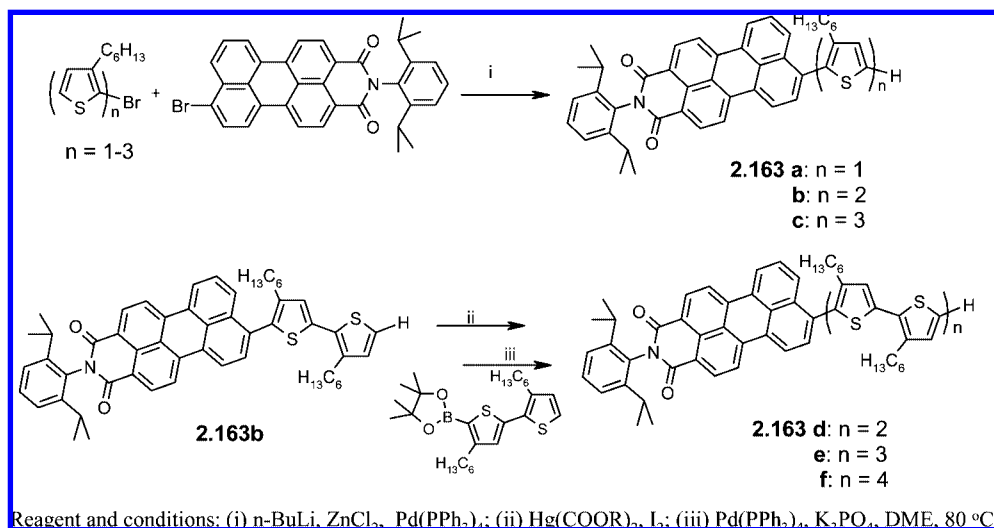
Chart 2.27

2.162
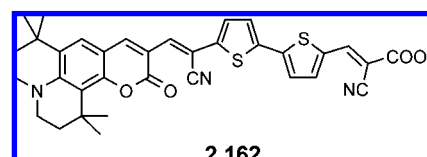
photovoltage spectroscopy. The smaller lifetime (τ) for the coumarin-based DSSCs suggested that the back-electron transfer process which corresponds to recombination of electrons from the TiO₂ conduction band and I₃⁻ ions from the electrolyte occurred more easily.[257]

Employing a similar synthetic approach, the same group recently reported a new coumarin dye **2.162** (Chart 2.27) which more intensively absorbs at longer wavelength (λ = 552 nm, ε = 97400 L mol⁻¹ cm⁻¹) compared to **2.161b** (λ = 511 nm, ε = 64300 L mol⁻¹ cm⁻¹).[258] The key to this accomplishment was the introduction of one more cyano group to the molecular core which reduced the band gap. This dyad molecule exhibited near-unity light harvesting efficiency and incident photon-to-electron conversion efficiency over a wide spectral region in 6 μm thick transparent TiO₂ films. DSSCs based on dye **2.162** showed good long-term stability and power-conversion efficiencies of around 6% under continuous light-soaking stress for up to 1000 h.

Bäuerle and Müllen et al. reported a series of novel D−A systems **2.163a−f** (Scheme 2.30) consisting of head-to-tail coupled oligo(3-hexylthiophenes) covalently linked to perylenemonoimide, where the length of the oligothiophene units differed from a thiophene up to an octithiophene.[259] Dyads **2.163a−c** were synthesized *via* effective Pd⁰-catalyzed Negishi-type cross-coupling between zincates of α-bromothiophenes with brominated perylenemonoimide. Derivatives **2.163d−f** were synthesized starting from **2.163b** by successive iodination and Suzuki-type coupling reactions with the boronic ester of bithiophene in excellent yields. UV−vis measurements showed broad π−π* absorption between 300 and 550 nm with high extinction coefficients. The optical band gaps were calculated to be 2.12−2.22 eV. Increased quenching of the fluorescence was observed with increasing number of thiophene units due to the occurrence of intramolecular photoinduced electron transfer processes. The fabrication of OSCs based on a blend of **2.163d** or **2.163f** with PCBM revealed moderate power conversion efficiencies up to 0.5% under a simulated terrestrial sun spectrum.

Scheme 2.30

Reagent and conditions: (i) n-BuLi, ZnCl₂, Pd(PPh₃)₄; (ii) Hg(COOR)₂, I₂; (iii) Pd(PPh₃)₄, K₃PO₄, DME, 80 °C

Scheme 2.31

Reagent and conditions: (i) Pd(OAc)₂/P(tBu)₂, hydroquinone, CsCO₃, DMA
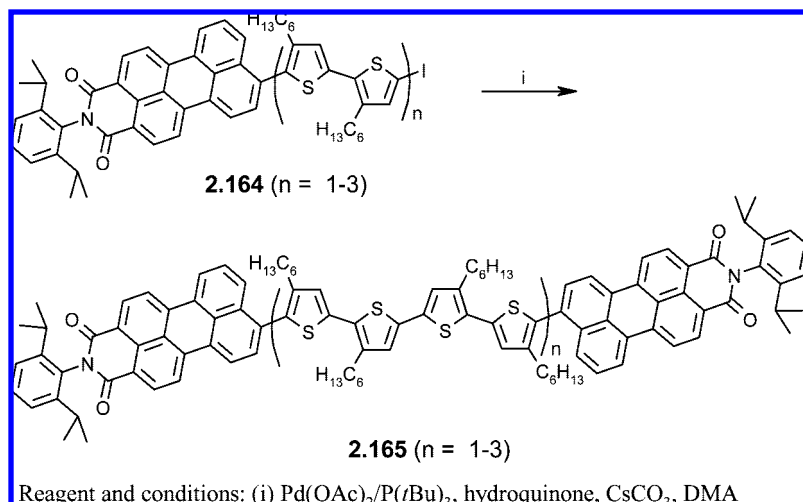
In the same way, Bäuerle et al. prepared a series of novel acceptor−donor−acceptor triads **2.165** ($n = 1−3$) (Scheme 2.31), consisting of head-to-tail-coupled oligo(3-hexylthiophene)s integrated between two terminal perylenemonoimides.[260] These hybrid materials, which differ by the length of the oligothiophene units from a quaterthiophene up to a dodecithiophene, were synthesized by an effective Pd⁰-catalyzed Ullmann-type homocoupling reaction of iodo derivatives **2.164** (Scheme 2.18). UV−vis measurements performed for **2.165** ($n = 1−3$) showed absorption maxima between 492 and 523 nm, which are characteristic values for perylene dyes. By increasing the length of the oligothiophene unit in **2.165**, a spectral broadening with tailing to the low energy side of the band was observed. Thus, a decrease of the optical band gap to 2.11 eV was reported. Transient absorption and time-resolved fluorescence measurements revealed that charge transfer (CT) bands appeared only in benzonitrile solution, whereas no evidence of CT states was found in toluene.[261]

Another series of donor−acceptor−donor triads **2.166** (Scheme 2.32) based on oligothiophenes and perylenebisimide were prepared by Zhu et al., where the perylene unit was used as a core.[262] The thiophene moieties were introduced to the perylene core by Suzuki or Stille-type coupling reactions. UV−vis spectra of **2.166a−c** showed bathochro-

Scheme 2.32

a: R = [structure] **b**: R = [structure] **c**: R = [structure]

Reagent and conditions: (i) Pd(PPh₃)₄, K₂CO₃, reflux, 24 h; (ii) Pd(PPh₃)₂Cl₂, dry DMF, 70 °C, 24 h
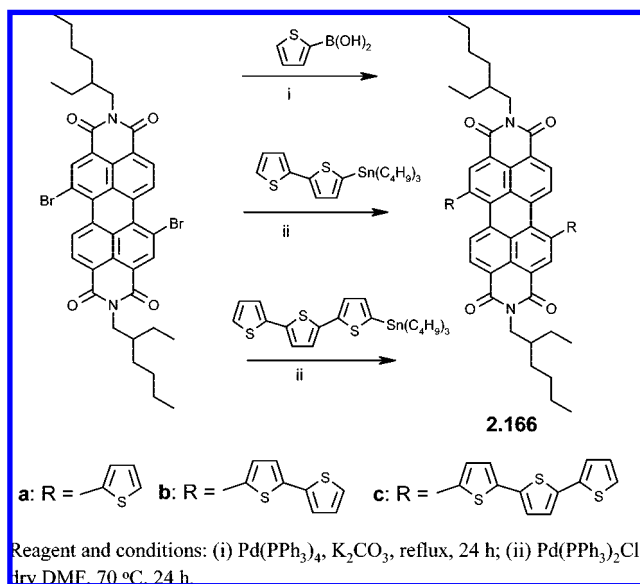
mic shifts of the absorption in comparison to the perylene dye. Furthermore, broad and structureless absorption bands were observed. Cyclic voltammetry measurements showed

Scheme 2.33

2.167: n = 0, 2
Closed form

Open form

2.168: n = 1, 2
Closed form

Open form

Scheme 2.34

2.169: n = 0, 1; R = *o*-F, *p*-OMe

Reagents and conditions: (i) acyl chloride (1.04 equiv), SnCl$_4$ (1.04 equiv), CH$_2$Cl$_2$, -4 to 23 °C; (ii) sodium acetylide (1.4–2.0 equiv), DMSO, acetylene, 2–3 h; (iii) 2-naphthol, PPTS (5 mmol%), 23 °C to reflux, CH$_2$Cl$_2$; (iv) n-BuLi, CuCl$_2$ (1.6–2.0 equiv).
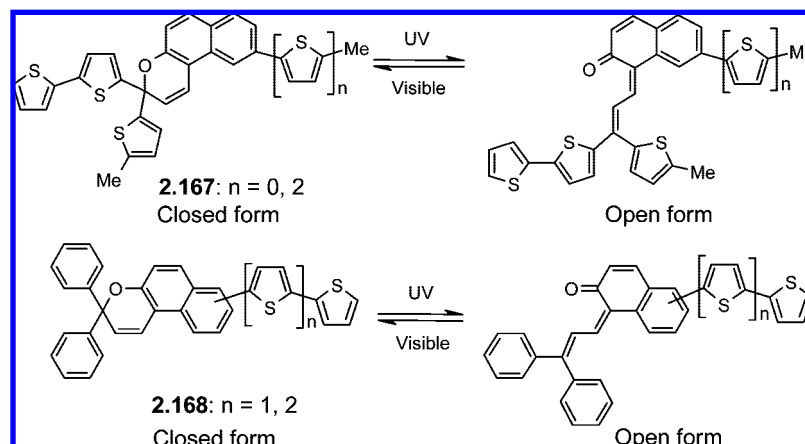
a decrease of the band gap by increasing the length of the oligothiophene unit. Due to the presence of electron-withdrawing perylenebisimide moieties in the backbone of π-conjugated polymers which were formed by electrochemical polymerization of **2.166b** and **2.166c**, reversible *n*-doping characteristics and good electron-transporting properties were realized.

Various napthopyran-substituted oligothiophenes **2.167** and **2.168** in which the thiophene units were linked to a naphthalenic ring at different positions have been synthesized as photochromic materials.[263−266] The oligomers were prepared by a combination of condensation reaction of substituted 2-napthol with 1,1-diarylprop-2-yn-1-ol, at room temperature, using pyridinium *p*-toluenesulfonate as catalyst, and metal-catalyzed Suzuki-type cross-coupling reactions. Most of the compounds showed photochromic behavior under UV irradiation in solution as well as in a polymeric matrix (Scheme 2.33).[267] When optically excited, these compounds undergo a structural change passing from a neutral closed form to a strongly polarized open form, causing a large bathochro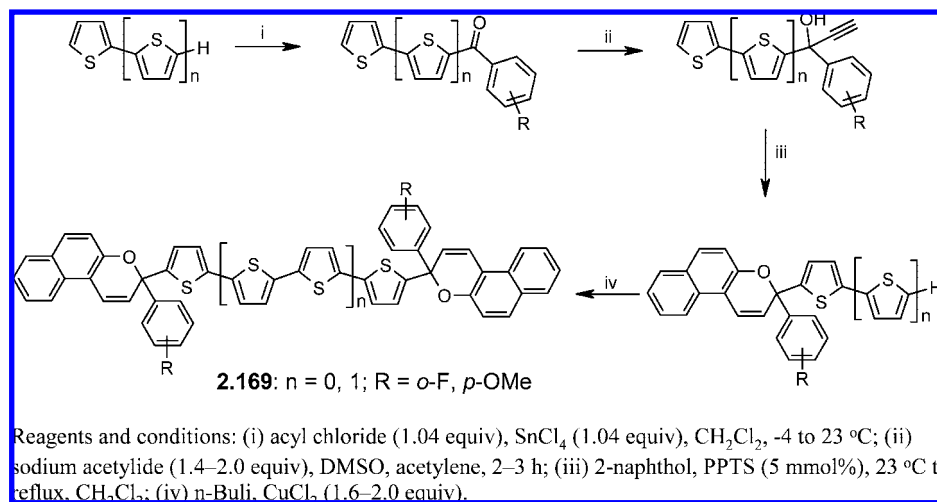mic shift of the main absorption band. The photochromic process was also accompanied by a large increase in electrical conductivity.[268] It has been demonstrated that the photochromic properties strongly depend on the number and position of the thienyl units.

Bi- and quaterthiophene-linked bisnapthopyrans **2.169** (*n* = 0, 1) were synthesized by Carreire et al. under the same aspect as photochromic materials.[269] The oligomers were

synthesized as depicted in Scheme 2.34 by using Friedel−Craft acylation of thiophene and bithiophene under Lewis acidic conditions, reaction with sodium acetylide, successively with 2-napthol, and finally oxidative homocoupling using the system *n*-BuLi/CuCl$_2$. Sequential and temperature-dependent photochromism was observed in these oligomers, and cross-talk between the two chromophores was found to be dependent on the length of the oligothiophene linker.

2.9. Oligothiophenes Containing Redox Active Groups

2.9.1. Fullerene-Functionalized Oligothiophenes

Fullerene-C$_{60}$ has been extensively studied as an ultrafast and efficient electron-acceptor material for conjugated oligomers and polymers in photovoltaic devices.[270] Later on, a soluble C$_{60}$ derivative (PCBM) was discovered for its use in OSCs by solution processing. In OSCs, blending of PCBM with regioregular P3HT gave power conversion efficiencies of up to 3.5% after annealing of the devices.[271] Higher efficiencies of more than 5% using P3HT and PCBM in bulk-heterojunction tandem solar cells have been recently reported.[272,273] Other alkyl and ethyleneoxide-substituted polythiophenes have been prepared to generate good conversion efficiencies in OSCs.[274−276]

Due to the successful use of PCBM as acceptor material in solar cells, various attempts have been made to covalently

Chart 2.28
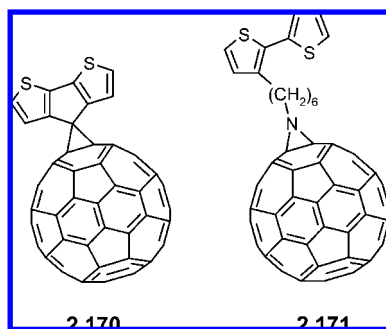
link C_{60} to an oligothiophene backbone in order to prepare D−A-based materials for photovoltaic devices by tuning their electronic properties.[29,30,277,278] The attachment of fullerene units prevented large scale phase separation in thin films, and despite the inclusion of bulky fullerene units, the soluble polymers retained their high order in thin films. However, the efficiency of such devices has been limited by competition between photoinduced electron transfer and energy transfer which occurs from the donor component to the fullerene.

The first dyad molecule in which a fullerene was covalently linked to an oligothiophene **2.170** (Chart 2.28) was realized by Zotti et al. as a precursor for a corresponding polythiophene. An azo-transfer reaction of lithiated cyclopentadithiophene and tosylazide followed by reaction with C_{60} in toluene at room temperature gave a D−A compound in which the fullerene unit was appended at the bridging carbon of the cyclopentadithiophene ring.[279] The conjugated polymer obtained by electrochemical polymerization of **2.170** on an ITO electrode showed a broad absorption band with a maximum at 440 nm and tailing to 700 nm. Due to the electron withdrawing effect of the attached fullerene unit, the oxidation potential of **P2.170** was shifted to higher potentials compared to that of the parent poly(cyclopentadithiophene). The proximity of the fullerene and thiophene units in the polymer could lead to a better phase separation in OSCs. Later on, Ferraris et al. synthesized fullerene-bithiophene dyad **2.171** (Chart 2.28) by introducing a hexyl spacer, which not only increased the solubility but also prevented fullerene−bithiophene interactions.[280] **2.171** was prepared by coupling of fullerene with an azidoalkyl-functionalized bithiophene in chlorobenzene. The polymer showed an absorption maximum at 480 nm, which is similar to that of conventional polythiophene, demonstrating no ground-state interaction between polythiophene and fullerene units.

Neugebauer et al. attached a polymerizable bithiophene building block to fullerene via a phenylethylene glycol spacer (**2.172**) (Scheme 2.35).[281,282] The synthesis was performed via double Williamson etherification and subsequent coupling with C_{60} by azomethineylide cycloaddition reaction. Although the donor (polythiophene) backbone and the pendant acceptor units (fullerene) in the resulting polymer did not interact in the ground state, a photoinduced electron transfer from the polythiophene to the fullerene units occurred in the excited state. A charge separated state was generated, as demonstrated by ESR measurements.

Terthiophene−fullerene dyad **2.173** (Chart 2.29), in which the fullerene unit was attached to the β-position of the central thiophene unit through a rigid ethynyl spacer, has been prepared by Komatsu et al.[283] The synthesis was ac-

complished by lithiation of 3′-ethynylterthiophene[284] to generate the lithium acetylide, which subsequently was reacted with C_{60} to form the ethynylated fullerenyl anion. By treatment of the latter with methyl iodide, dyad **2.173** was obtained in 35% yield. Another terthiophene−fullerene dyad **2.174** (Chart 2.29) was prepared in 64% yield by following a similar approach. In this system, the two terminal thiophene units in **2.173** consisted of EDOT groups.[285] The precursor oligomer was synthesized by Stille-type coupling of stannylated EDOT[286] and 2,3,5-tribromothiophene to give a 3′-bromoterthiophene which then was coupled with trimethylsilylacetylene followed by deprotection of the silyl group. Compared to the case of **2.173** cyclic voltammetry of dyad **2.174** showed a lowering of the oxidation potential by 350 mV, indicating the enhanced donor ability of the EDOT units and the higher planarity of the system.[283] Corresponding polymers were electroactive in the p- and n-doped state and displayed electrochromism. Efficient photoelectrochemical responses of these polymers have been discussed in comparison to those of the parent nonsubstituted polymers.

Fullerene-C_{60} containing terthiophene **2.175** (Chart 2.29), in which a fullerene unit was attached to the central thiophene through a pyrazine ring, was prepared in 92% yield by coupling of diketobisfulleroid and 3′,4′-diaminoterthiophene in a mixture of o-dichlorobenzene and acetic acid.[287] The band gap (E_g) of **2.175** was determined to be as low as 0.18−0.30 eV depending on the type of measurement. The polymer obtained by electrochemical polymerization of **2.175** could be useful for photovoltaic conversion, if electron transfer from the polythiophene backbone to the fullerene moiety takes place in the ground state through the covalently bound thieno[3,4-b]pyrazine units.

Recently, Fréchet et al. prepared diblock copolymer **2.176** (Chart 2.29) by reaction of norbornene-functionalized C_{60} and a shorter poly(3-hexylthiophene) by ring-opening metathesis polymerization using Grubbs' catalyst.[288] No phase segregation was observed in blends of P3HT and PCBM by addition of copolymer **2.176** (17 wt %) due to the lowering of interfacial energy between polymer and PCBM. The photovoltaic device showed a conversion efficiency of 2.7% and high stability. No degradation was observed by increasing the annealing time from 0.1 to 10 h at 140 °C. The authors argued that the diblock copolymer can improve the device performance by reducing thermal phase segregation.

D−A-substituted α-quinquethiophene **2.178** capped by an anthracene and a C_{60} unit has been synthesized via [4 + 2] cycloaddition reaction of C_{60} with anthrylquinquethieno-o-quinodimethane as intermediate, which was generated in situ by cheletropic extrusion of SO_2 from the precursor cyclic sulfone **2.177** (Scheme 2.36).[289] Energy transfer from the anthracene donor to the fullerene acceptor has been observed for the triad. Photoinduced-electron transfer processes in the triad were observed in low temperature ESR measurements.[290]

Roncali et al. synthesized D−A system **2.179** (Chart 2.30) by 1,3-dipolar cycloaddition of the azomethine ylide of dimethylaniline-substituted dithienylethylene to C_{60}.[291] The blue shift of the $\pi-\pi^*$ absorption band of **2.179** (λ_{max} = 436 nm) compared to that of the precursor formyl derivative (λ_{max} = 467 nm) was possibly due to disruption of the conjugation. This result was also supported by the negative

Scheme 2.35

Reagents and conditions: (i) K_2CO_3, acetone, reflux, 8 h; (ii) N-methylglycine, C_{60}, chlorobenzene, reflux

2.172

Chart 2.29

2.173   **2.174**   **2.175**

2.176: m = 25, n = 2-10

Scheme 2.36

2.177   **2.178**

Reagents and conditions: (i) C_{60}, chlorobenzene, reflux.
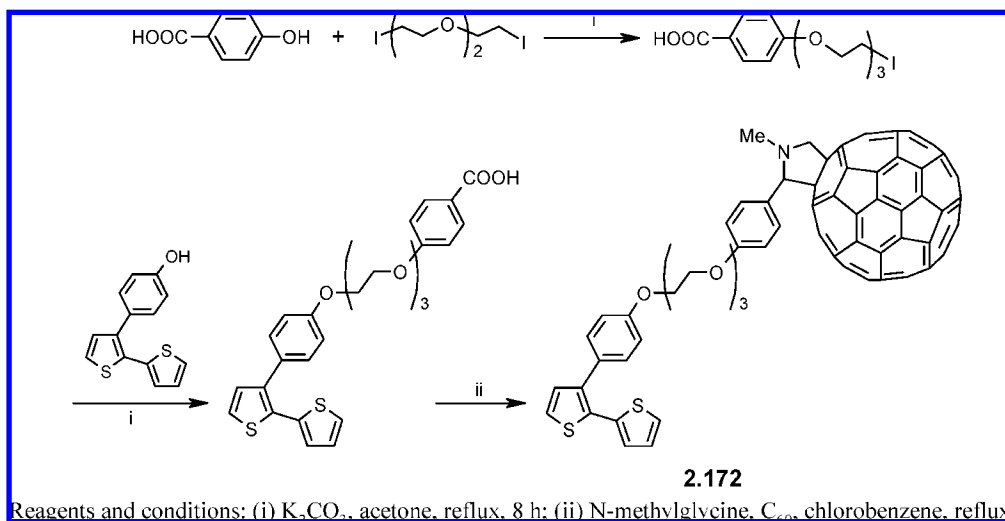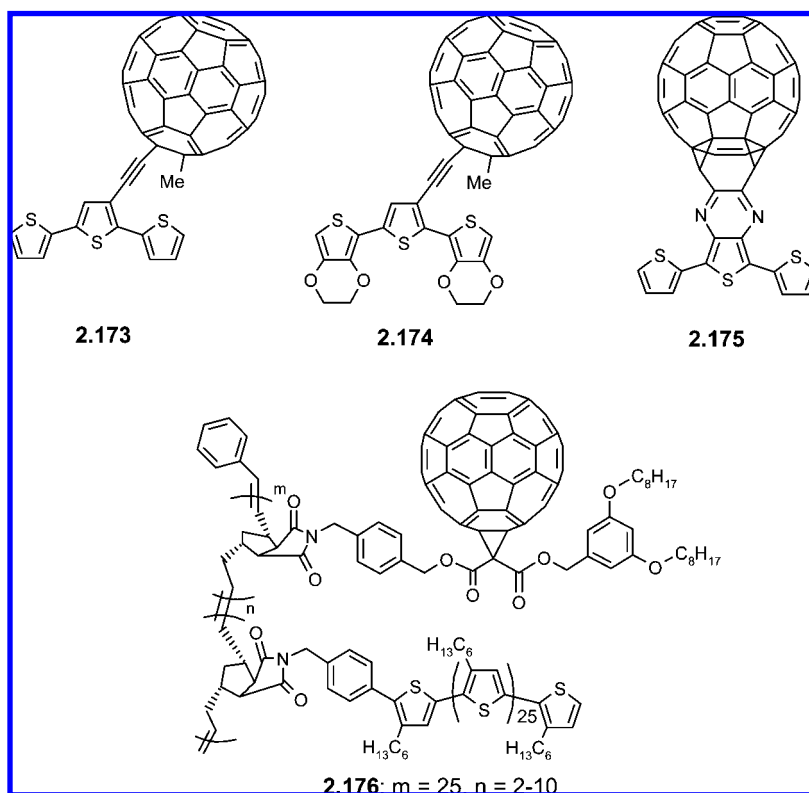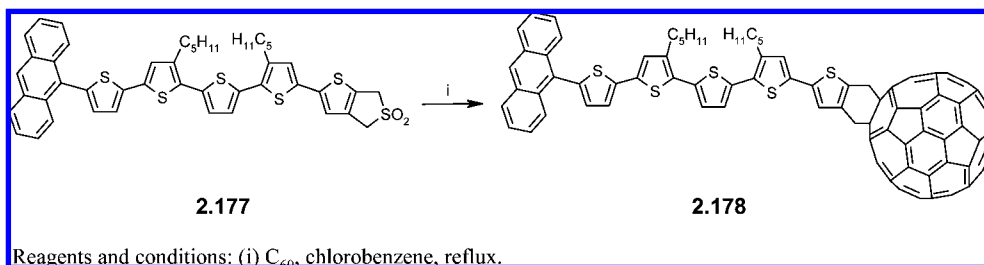
shift of the oxidation and reduction potentials in cyclic voltammetry measurements compared to that of the formyl derivative.

Otsubo et al. synthesized C_{60}-linked quater-, octi-, dodeci-, and hexadecathiophene dyads **2.180** (Chart 2.30).[292] The

quaterthiophene precursor was prepared by Ni-catalyzed Kumada-type coupling of 2,2′-dibromobithiophene with the Grignard reagent of 3-hexyl-2-bromothiophene. Octi-, dodeci-, and hexadecathiophene oligomers were isolated in 10−37% yields from one-pot oxidative coupling of the

Chart 2.30

2.179

2.180: n = 1-4

2.181: n = 0-2

Chart 2.31

2.182: n = 1-4

2.183: n = 1-4

2.184: n = 4-6
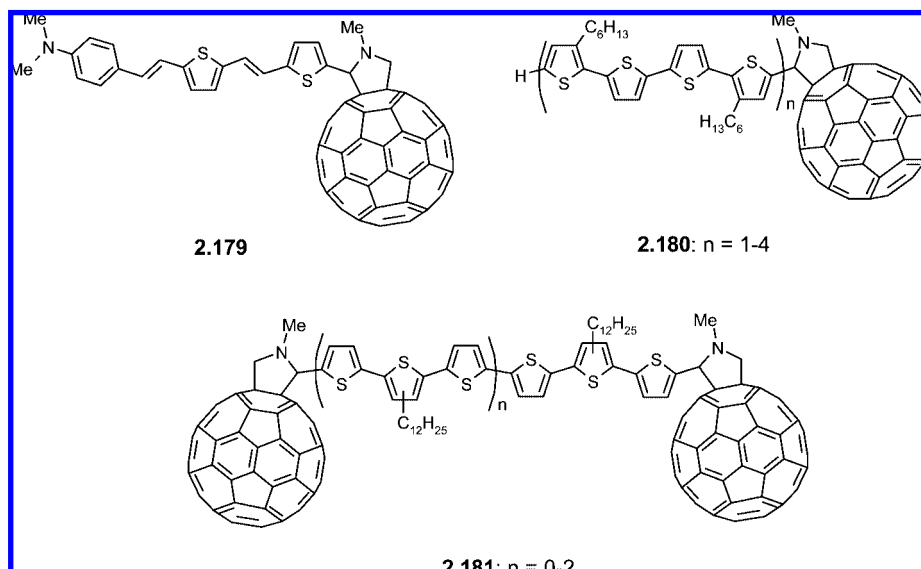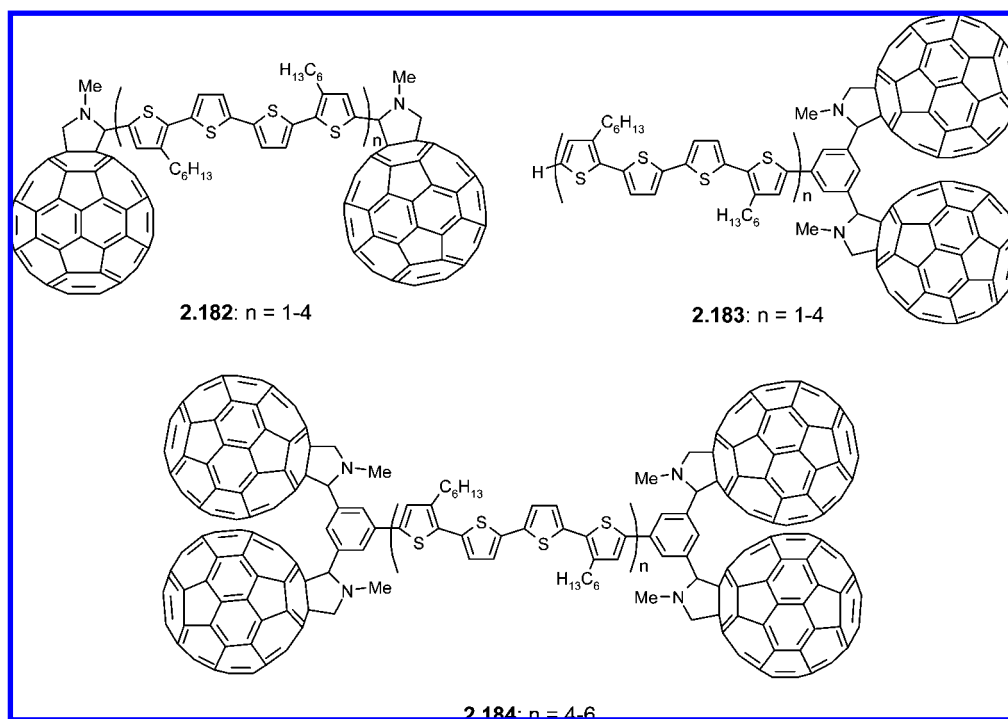
quaterthiophene precursor using the system LDA/CuCl$_2$. Formylation of these oligothiophenes followed by coupling with C$_{60}$ and *N*-methylglycine according to Prato's method[293] afforded corresponding dyads in 40, 31, and 29% yields, respectively. Photophysical studies of these dyads in nonpolar solvents such as toluene revealed efficient energy transfer from the photoexcited oligothiophene unit to the fullerene moiety and an efficient photoinduced electron transfer in polar solvents such as benzonitrile and in the solid state.[294,295] Due to the photocurrent generation (7% for *n* = 3 and 9.7% for *n* = 4) observed for these dyads, they were discussed as useful materials for photovoltaics. Thus, a cell structure consisting of Al/**2.180** (*n* = 4)/Au gave a rather low power conversion efficiency of 0.32% upon illumination from the Al side with monochromatic light.[296]

Janssen et al. prepared a series of C$_{60}$-oligothiophene-based triads **2.181** (*n* = 0−2) (Chart 2.30) where C$_{60}$ is tethered at

both ends of an oligothiophene.[297] Vilsmeier−Haack formylation of the basic oligothiophenes afforded corresponding dialdehydes, which were converted to the desired triads **2.181** by Prato reaction with C$_{60}$. The effect of conjugation length on the energy- and electron-transfer processes in solution and in the solid state was investigated using photoinduced absorption (PIA) and time-resolved fluorescence spectroscopy. A very fast singlet-energy transfer from the oligothiophene donor to the fullerene acceptor has been reported in toluene. In solid films, energy transfer was predominant for the terthiophene (*n* = 0) whereas electron transfer processes took place for the higher oligomers (*n* = 1, 2).

A similar series of triads **2.182** (*n* = 1−4) (Chart 2.31), containing fullerene units on each α-terminus of oligothiophenes, has been reported by Otsubo et al.[298] Triads **2.182** were synthesized by following a synthetic procedure similar to that discussed earlier for the series **2.180**. Due to the poor

Scheme 2.37

Reagents and conditions: (i) NBS, CS$_2$–DMF; (ii) Pd(PPh$_3$)$_4$, THF; (iii) C$_{60}$, N-methylglycine
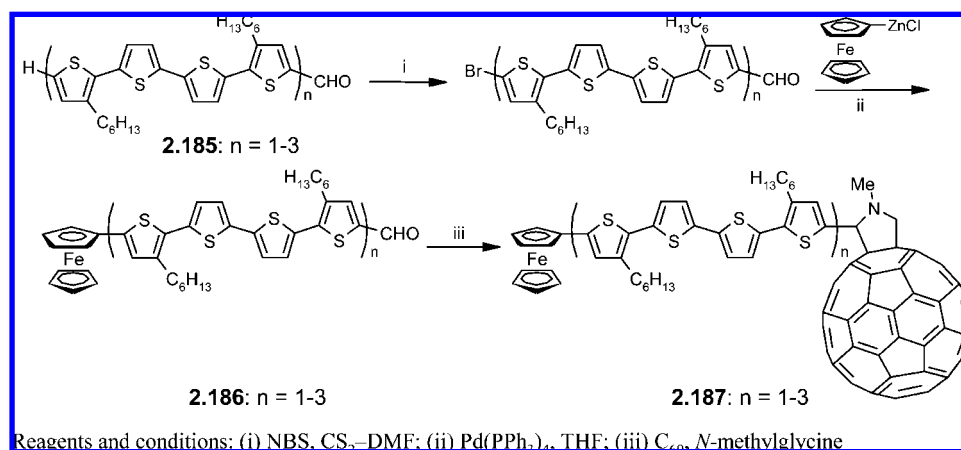
solubility and film forming ability of these triads, the same authors subsequently prepared another series of triads **2.183** ($n = 1-4$), where two fullerene units are connected through a phenyl linker at one terminus of the oligothiophene core.[298] The precursor for **2.183** ($n = 1$), quaterthienyl-substituted isophthalaldehyde, was prepared by Stille-type coupling of the stannylated quaterthiophene and 5-bromoisophthalaldehyde. The higher precursors ($n = 2-4$) were prepared from the above quaterthienyl-isophthalaldehyde by cycles of bromination and Stille-type coupling reaction with stannylated quaterthiophene. Prato reaction of the dialdehydes with C$_{60}$ gave corersponding triads **2.183** ($n = 1-4$) in 38−50% yield.

A strong quenching of the oligothiophene fluorescence was observed by increasing the number of C$_{60}$ units. Due to the good film forming properties of **2.180** ($n = 4$) and **2.183** ($n = 4$), solution-processed ambipolar OFETs were fabricated. Moderate hole mobilities of 4.8×10^{-5} cm^2 V^{-1} s^{-1} and 1.1×10^{-5} cm^2 V^{-1} s^{-1} were reported for **2.180** ($n = 4$) and **2.183** ($n = 4$), respectively.[299] Increasing the number of pendant fullerene units in **2.183** constituted an improved network for electron transport and rendered them to good photovoltaic materials compared to dyads **2.180**. High photocurrent generation (14 and 25%, respectively) for **2.183** ($n = 3, 4$) was observed, which is almost double that of **2.180**. In a photovoltaic device using a cell structure Al/**2.183** ($n = 3, 4$)/Au, moderate maximum power conversion efficiencies of 0.50% ($n = 3$) and 0.65% ($n = 4$) have been reported.[298]
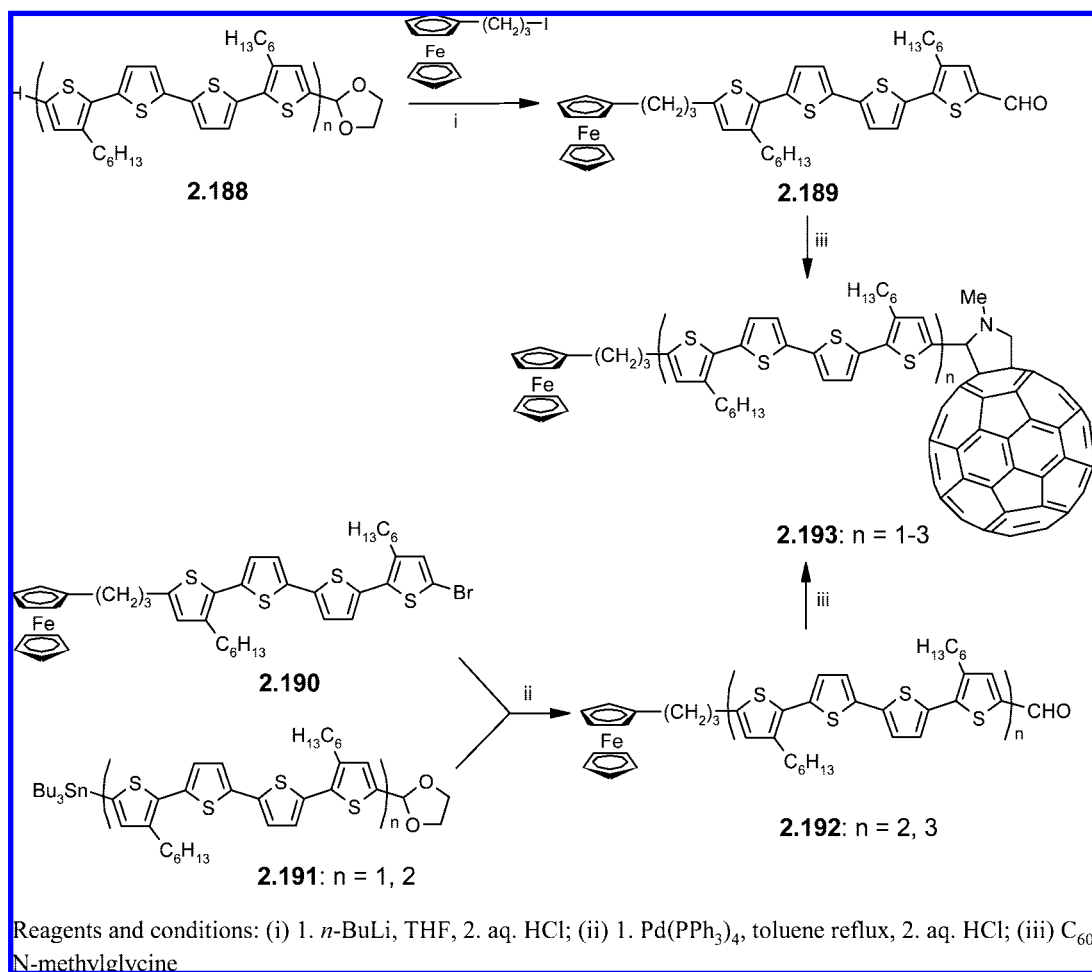
An oligothiophene−fullerene pentad **2.184** (Chart 2.31) was recently synthesized, in which four pendant fullerenes are coupled to the two termini of longer oligothiophene chains.[300] An efficient intramolecular electron transfer process was observed in the excited-state for these pentads. In a sandwich device Al/**2.184** ($n = 6$)/Au, a photocurrent generation of 14% was reported, which is similar to the value for triad **2.183** ($n = 3$).

To promote photoinduced electron transfer processes, different ferrocene−oligothiophene−fullerene triads have been synthesized, in which ferrocene units are coupled to the oligothiophene chains either directly, as in **2.187**, or via an alkyl spacer, as in **2.193**.[301] The precursor dyads **2.186** ($n = 1-3$) were obtained from corresponding oligothiophene carbaldehydes **2.185** ($n = 1-3$) via bromination and subsequent Pd^0-catalyzed cross-coupling reaction with ferrocenylzinc chloride (Scheme 2.37). In the other case, compounds **2.193** ($n = 1-3$) were prepared via two different
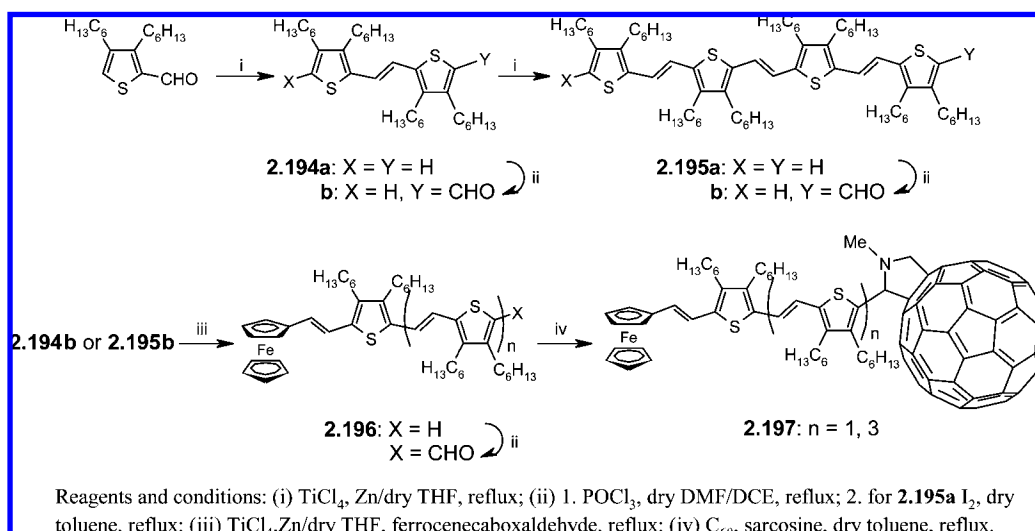
routes (Scheme 2.38). Lithiation of acetal-protected quaterthiophene **2.188** with n-BuLi followed by treatment with 3-iodopropylferrocene gave precursor **2.189** in 24% yield. The ferrocenylpropyl−oligothiophene−carbaldehydes **2.192** ($n = 2, 3$) were synthesized in ∼60% yield by Pd^0-catalyzed coupling of bromo-ferrocenylpropyl-quaterthiophene **2.190** and stannyl-derivatives of acetal-protected octi- and dodecithiophene **2.191** ($n = 1, 2$). Finally, C$_{60}$ was introduced to the other terminus of the oligothiophene using Prato's protocol to obtain the corresponding triads **2.187** and **2.193** in 40−50% yields, respectively. All triads showed absorption maxima in the range of 402−463 nm corresponding to the oligothiophene moieties and at ∼330 nm and ∼700 nm due to the presence of the fullerene units. The direct attachment of electron-donating ferrocene units in triads **2.187** evidently contributed to the stabilization of the charge-separated states, thus promoting a more efficient intramolecular electron transfer than that observed for nonconjugated derivatives **2.193**. However, the charge-separated state is more effectively maintained in **2.193** compared to **2.187**. This result showed that the lifetime of charge-separated states is longer by preventing the π-conjugation between the ferrocene and the oligothiophene moieties.[302]

Ferrocene−oligothienylenevinylene−fullerene (Fc-OTV-C$_{60}$) triads were prepared as candidates to study photoinduced charge separation processes.[303] Successive cycles of McMurry reaction and Vilsmeier formylation starting from 2-formyl-3,4-dihexylthiophene yielded dimer **2.194a** and tetramer **2.195a** in good yields (Scheme 2.39). McMurry coupling of monoformylated dimer **2.194b** and tetramer **2.195b** with ferrocene (Fc) carboxaldehyde afforded dyads **2.196**, which on further formylation and reaction with C$_{60}$ gave triads **2.197** ($n = 1, 3$) in ∼25% yield. Photoinduced intramolecular processes were studied by nanosecond transient absorption spectra and time-resolved fluorescence lifetime measurements. Strong quenching of the fluorescence was observed for **2.197** ($n = 1, 3$) in both polar and apolar solvents, indicating the efficient photoinduced charge-separation processes from Fc-OTV dyads to the excited singlet state of C$_{60}$ moieties. Fluorescence quenching followed by charge separation was found to be more efficient for **2.197** ($n = 3$) compared to **2.197** ($n = 1$). These results suggested that the introduction of the Fc-donor moiety at the longer OTV chain in C$_{60}$-OTV dyad systems effectively increases the ability and efficiency of the charge-separation processes and the lifetimes of the charge separated state.

Scheme 2.38

Reagents and conditions: (i) 1. *n*-BuLi, THF, 2. aq. HCl; (ii) 1. Pd(PPh$_3$)$_4$, toluene reflux, 2. aq. HCl; (iii) C$_{60}$, N-methylglycine

Scheme 2.39

Reagents and conditions: (i) TiCl$_4$, Zn/dry THF, reflux; (ii) 1. POCl$_3$, dry DMF/DCE, reflux; 2. for **2.195a** I$_2$, dry toluene, reflux; (iii) TiCl$_4$, Zn/dry THF, ferrocenecaboxaldehyde, reflux; (iv) C$_{60}$, sarcosine, dry toluene, reflux.

Roncali's group reported the synthesis of dyads **2.198** and triad **2.199** (Chart 2.32) based on C$_{60}$ moieties attached to OTVs[15,304] for studying intramolecular photoinduced processes.[305,306] The covalently bound dyads and a triad were prepared by reaction of corresponding formylated OTVs with C$_{60}$ and *N*-methylglycine. Upon photoexcitation of the OTV moieties, ultrafast singlet energy transfer to C$_{60}$ occurred with subsequent quenching of the OTV fluorescence. Afterward, the C$_{60}$ fluorescence was quenched by a rapid intramolecular electron transfer process to yield an intramolecularly charge-separated ion pair (C$_{60}$$^{\bullet-}$−OTV$^{\bullet+}$). The detailed intramolecular photoinduced energy- and electron-transfer processes in polar and apolar solvents have been discussed, showing that an ultrafast energy transfer precedes the electron transfer process.[306] Owing to the small HOMO−LUMO gap, the utilization of these compounds in organic photovoltaics can be envisaged.[305]

Chart 2.32

2.198: n = 1, 2, 3, 5   **2.199**

Scheme 2.40

2.200: n = 2, 4, 6   **2.201**: n = 2, 4, 6

2.202: n = 2, 4

2.203: n = 2, 4

Reagents and conditions: (i) 1. LDA, ether, -78 to 0 °C, 2. DMF, -78 °C to RT; (ii) C$_{60}$, N-methylglycine, toluene, reflux.
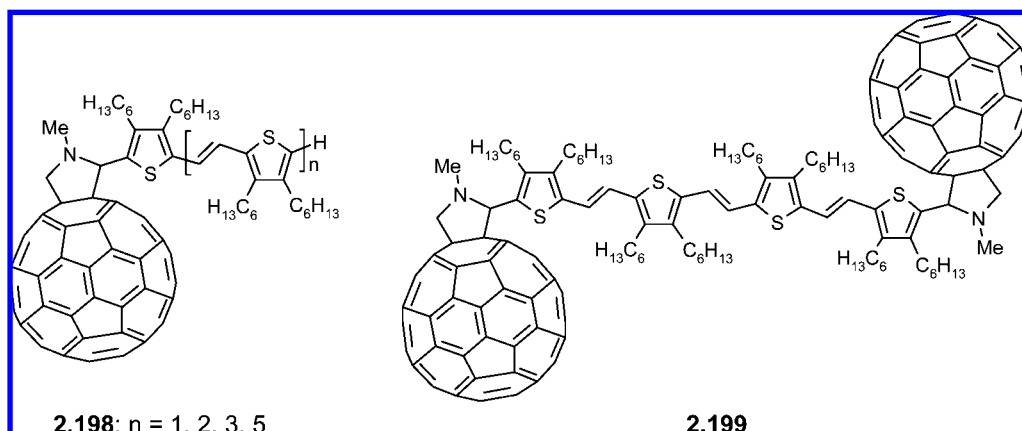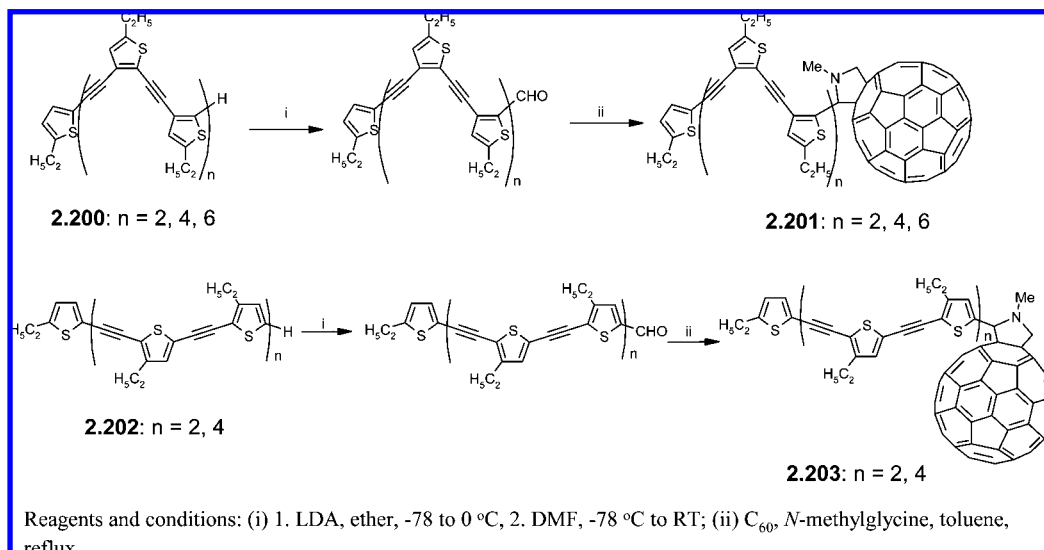
Otsubo et al. synthesized C$_{60}$-linked coil-shaped oligo(2,3-thienylethynylenes) **2.201** and rod-shaped oligo(2,5-thienyl-ethynylenes) **2.203**.[307] The key building blocks **2.200** and **2.202** were obtained by repeated application of Pd^0-catalyzed cross-coupling reactions of terminal alkynes and thienyl iodides followed by coupling with 2-ethyl-5-iodothiophene (Scheme 2.40).[308] The free α-position of the building blocks was then formylated, and the resulting aldehydes were reacted with C$_{60}$ to yield corresponding dyads **2.201** and **2.203** in 40−50% yields. Fluorescence measurements in toluene solutions revealed photoinduced intramolecular interactions between the oligomers and C$_{60}$, which occurred in a through-space fashion for **2.201** due to its coil-conformation and in a through-bond fashion for **2.203**.

Roncali et al. developed an approach to synthesize functional oligothiophenes **2.207** and **2.208** that have been coupled singly or doubly to C$_{60}$ units through the β-positions of the terminal thiophene(s).[309] The thiol-protected quater-thiophene precursor **2.204** was synthesized by Stille-type coupling of 2-bromo-3-(2-cyanoethylsulfanyl)thiophene with di(tributylstannyl)bithiophene (Scheme 2.41). Stepwise depro-tection of the thiolate groups by CsOH and successive reactions with iodopentane and 2-bromoethanol gave **2.205**. Esterification of **2.205** with 3-chloro-3-oxoethylpropanoate gave corresponding monoester **2.206**, which by single Bingel-type reaction with C$_{60}$ afforded dyad **2.207** in 35% yield. Single-step deprotection of **2.204** with 2 equiv of CsOH and

subsequent reactions as above led to doubly coupled qua-terthiophene **2.208** (Chart 2.33) in 40% yield. The electronic properties, redox behavior, and photoinduced absorptions were investigated in solution. Compared to **2.207**, fast intramolecular energy and electron transfer were reported for **2.208**, most likely due to the imposed face-to-face orientation of the oligothiophene part and C$_{60}$ in **2.208**.

Applying the similar reaction procedure as in Scheme 2.40, two polymerizable bithiophene-functionalized dyads **2.209** and **2.210** (Chart 2.33) were prepared as mixtures which were separated by chromatography in 13−24% yield, respec-tively.[310] Electropolymerization of the two compounds showed enhanced conjugation and improved stability in the resulting polymers under redox cycling. Significant enhance-ment of the photocurrent which was measured for these polymers revealed their potential utility for OSCs.

In order to continue the study of photoinduced charge separation processes in oligothiophene-based materials, Ot-subo et al. recently synthesized two dual oligothiophene-fullerene[C$_{60}$] triads **2.211** and **2.212** (Chart 2.34) in which a quaterthiophene and an octithiophene unit were separated by a propyl chain.[311] The synthesis was performed by conventional Stille-type coupling reaction, Vilsmeier formy-lation, and finally Prato reaction with C$_{60}$. As studied by UV−vis and cyclic voltammetry measurements, no electronic interactions were observed in the ground state. On the other hand, the emission spectra were markedly perturbed by
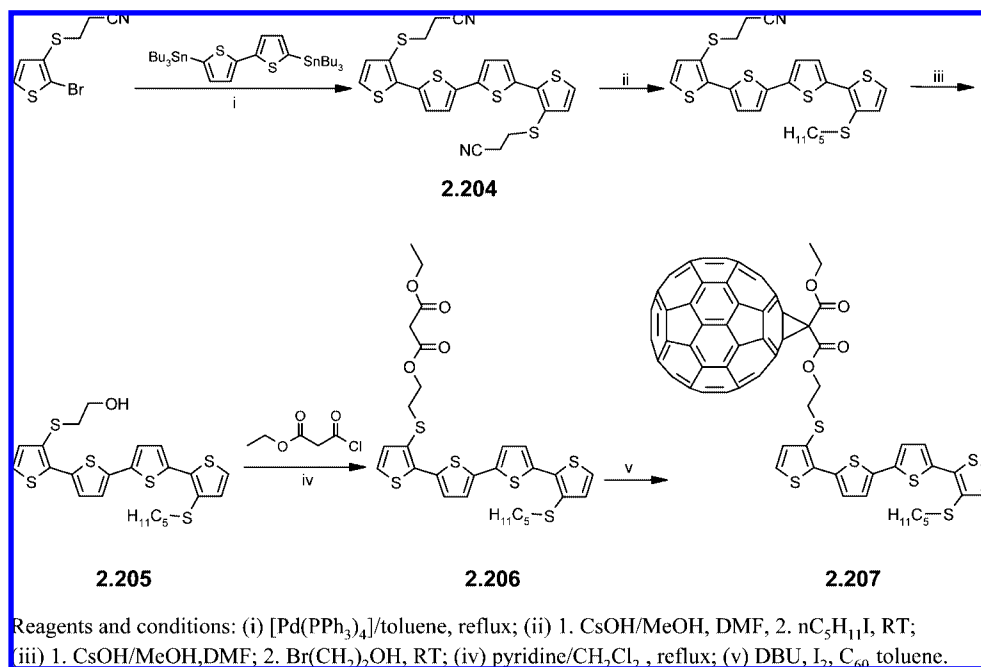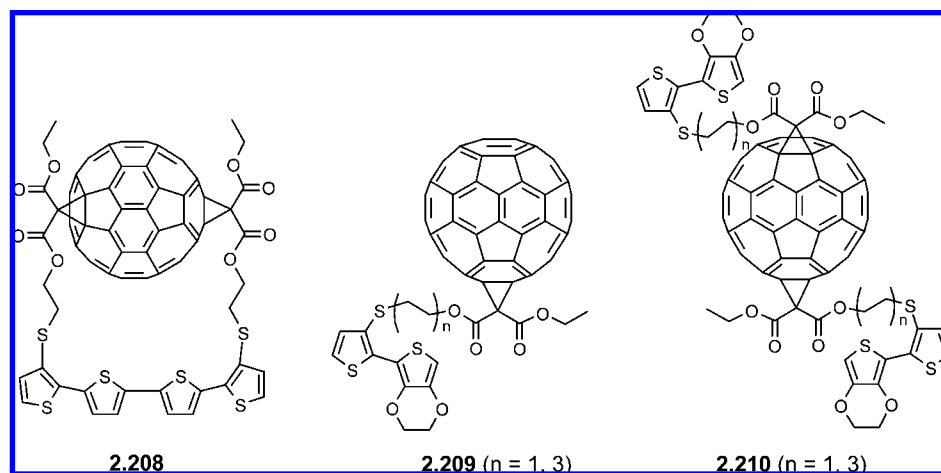
Scheme 2.41

2.204

2.205   **2.206**   **2.207**

Reagents and conditions: (i) [Pd(PPh$_3$)$_4$]/toluene, reflux; (ii) 1. CsOH/MeOH, DMF, 2. nC$_5$H$_{11}$I, RT;
(iii) 1. CsOH/MeOH,DMF; 2. Br(CH$_2$)$_2$OH, RT; (iv) pyridine/CH$_2$Cl$_2$, reflux; (v) DBU, I$_2$, C$_{60}$ toluene.

Chart 2.33

2.208   **2.209** (n = 1, 3)   **2.210** (n = 1, 3)

electron and/or energy transfer from the oligothiophene to the fullerene unit. In particular, it has been revealed that triad **2.211** undergoes photoinduced electron transfer leading to a long-distance charge separated state. OSCs based on **2.211** showed improved photovoltaic performance in comparison to devices made from **2.212**.

D−A triads **2.213** (Chart 2.34) based on tetrathiafulvalene and oligothiophenes as combined donor and fullerene as acceptor were synthesized by Stille-type coupling reaction of bromooligothiophenes and stannylated tetrathiafulvalene. The attachment of the fullerene was achieved by successive reaction with the system fullerene/*N*-methylglycine.[312] An increased photocurrent generation was observed for triads **2.213** in comparison to oligothiophene−fullerene dyads **2.180**.

Bassani et al. explored the 1:1 hydrogen-bonded supramolecular complex formation between a barbituric acid-substituted fullerene and the complementary Hamilton-type receptor including thienylenevinylenes (TVs). The fullerene unit was reorganized and placed between two TV side arms of the receptor unit (**2.214**, Chart 2.35).[313] Due to the close proximity of the redox-active fullerene and TV moieties

within the assembly, strong ground-state D−A interactions were observed. Ultrafast time-resolved transient absorption measurements revealed a fast photoinduced electron transfer from the TV donor to the fullerene acceptor unit, suggesting a strong binding between the redox centers.

The same research group utilized a hydrogen bonding motif to synthesize a linear dyad **2.215** based on a melamine-terminated oligothiophene donor and a complimentary barbituric acid-functionalized fullerene as acceptor (Chart 2.35).[314] The melamine moieties were introduced at the two termini of the oligothiophene unit by a Schiff base reaction of the dialdehyde end groups and tetraaminopyrimidine. Hydrogen bonding formation with complimentary barbituric acid-substituted fullerenes allowed uniform film growth with greater charge separation ability. A 2.5-fold enhancement of photocurrent generation was observed when compared to analogous systems comprising non-hydrogen-bonded C$_{60}$, which was ascribed to high molecular-level ordering. The modification of gold electrode surfaces with SAMs bearing hydrogen-bonding molecular recognition end groups was seen to further enhance the photovoltaic response of the corresponding functional supramolecular device, thus indi-
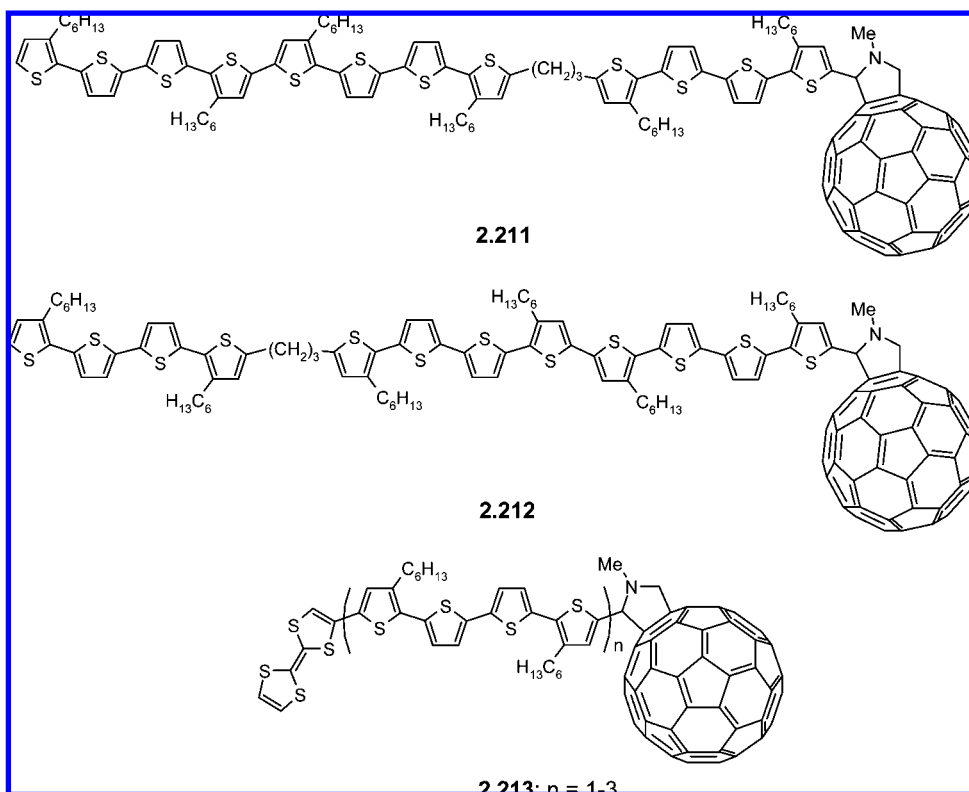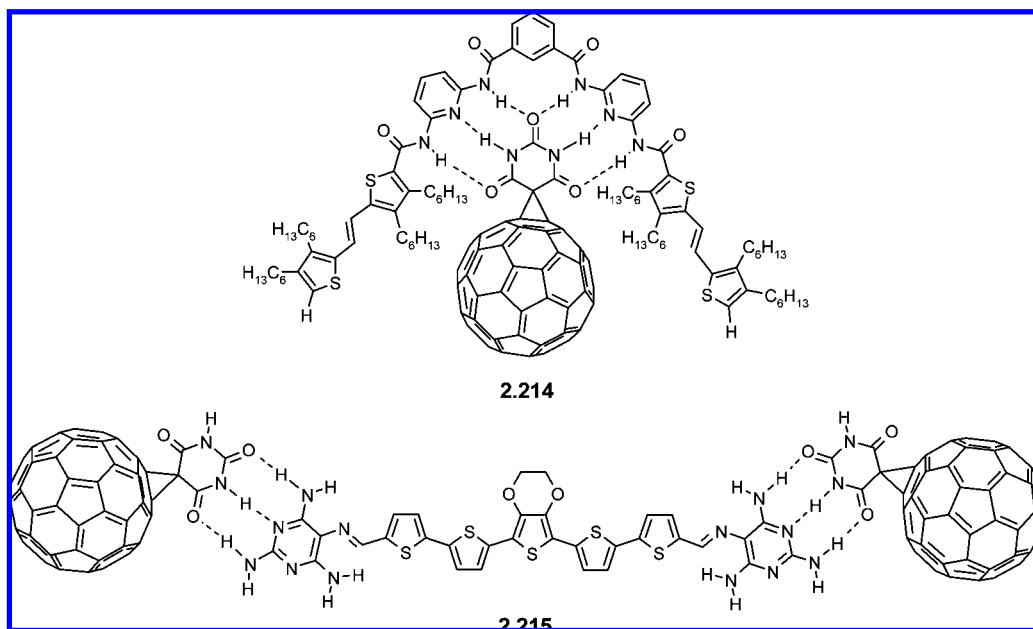
Chart 2.34

2.211

2.212

2.213: n = 1–3

Chart 2.35

2.214

2.215

cating the advantage of the supramolecular hydrogen bonding motif in electronic devices.[315]

A liquid crystalline septithiophene−fullerene dyad was synthesized, in which the fullerene unit is attached to the central thiophene *via* an oxyethylene spacer.[316] Septithiophene **2.218** was prepared in two steps by Pd[0]-catalyzed reaction of brominated terthiophene **2.216** and ethyleneglycol-substituted 2,5-bis-stannylthiophene **2.217** followed by cleavage of the tetrahydropyranyl ether using pyridinium *p*-toluenesulfonate (Scheme 2.42). Esterification of **2.218** with the acid chloride of the fullerene (a derivative of PCBM which is frequently used in OSCs) afforded dyad **2.219** in

40% yield. By thermal annealing, supramolecular fibrous nanostructure formation was observed in solid films, which was assigned to the self-assembly *via* π−π interaction of the oligothiophene groups. Implementation of the dyads in OSCs showed a rather low power conversion efficiency of 0.15%, which was attributed to the inefficient charge transfer due to unsuitable molecular packing in the film.

2.9.2. Porphyrin-Functionalized Oligothiophenes

In D−A based dyads and triads, porphyrins have been used either as acceptors in energy transfer systems or as donors
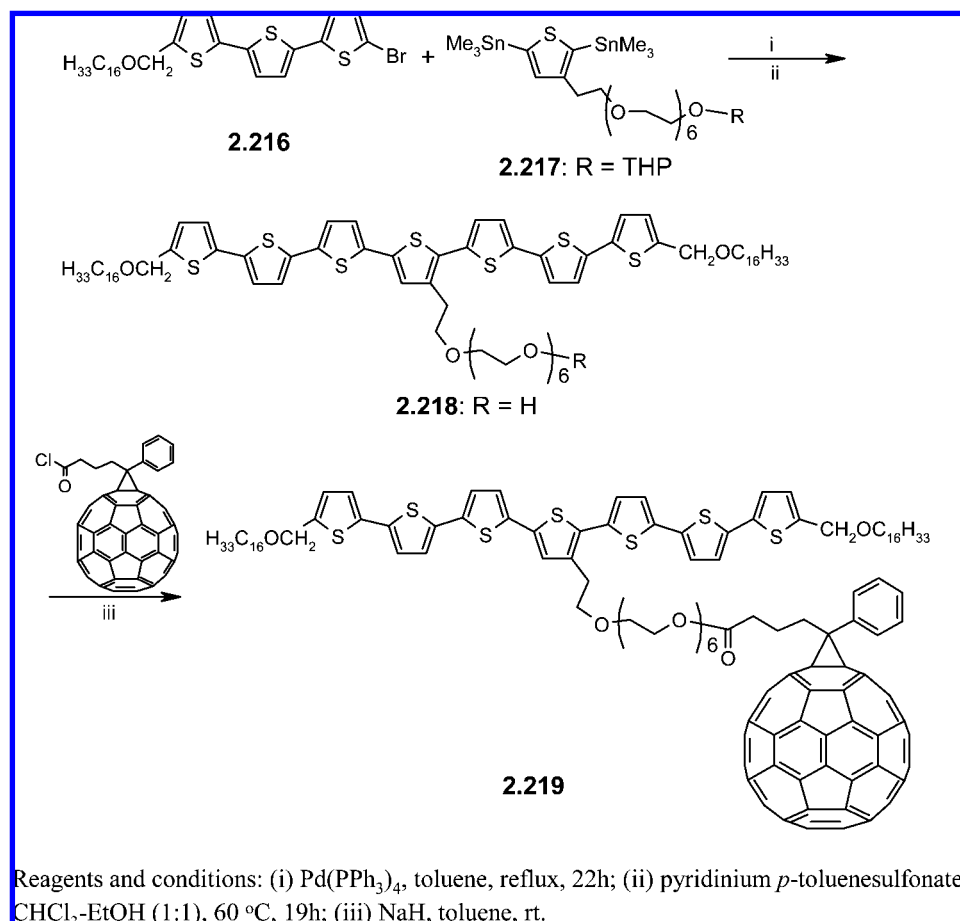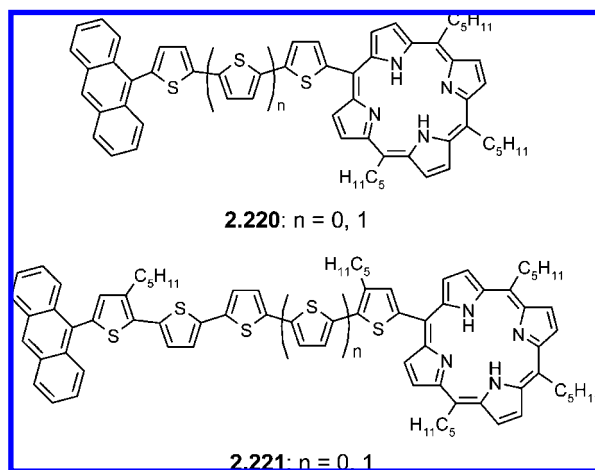
Scheme 2.42

Reagents and conditions: (i) Pd(PPh₃)₄, toluene, reflux, 22h; (ii) pyridinium *p*-toluenesulfonate, CHCl₃-EtOH (1:1), 60 °C, 19h; (iii) NaH, toluene, rt.

Chart 2.36

2.220: n = 0, 1

2.221: n = 0, 1

in electron transfer systems. Although symmetrical thienyl-based porphyrin derivatives were synthesized decades ago, the synthesis of unsymmetrically substituted meso-(oligo)thienyl porphyrins was first realized in 1995 by the group of Effenberger.[317] Few examples[317,318] of this type of structures such as **2.220** and **2.221** (Chart 2.36) became available. They were synthesized by reaction of anthrone with a lithiated oligothiophene, followed by conversion to the corresponding aldehyde by Vilsmeier−Haack formylation, which was reacted in an acid-catalyzed condensation with pyrrol and hexanal to the final porphyrin following a protocol developed by Lindsey et al.[319] The general drawback of this method when applied to the synthesis of unymmetrical porphyrins

often includes a low statistical yield of the desired products (2−10%) as well as potentially tedious purification steps.

In an effort to study efficient energy transfer in conjugated D−A systems, Effenberger and co-workers further synthesized the symmetrical anthraquinone−oligothiophene−porphyrin triad **2.225** (Scheme 2.43), in which quinquethiophene bridges are terminally linked to the *meso*-position of a porphyrin ring and on the other side to the 9-position of an anthracene moiety.[318] Cross-coupling reactions of 5,5′-dibromoterthiophene with the Grignard reagent of 2-bromo-3-pentylthiophene yielded quinquethiophene **2.222**. Lithiation of the resulting quinquethiophene followed by reaction with anthrone gave 9-anthryl-substituted dipentylquinquethiophene **2.223**. By applying Vilsmeier−Haack formylation, corresponding aldehyde **2.224** was prepared, which upon a 4-fold reaction with pyrrole in the presence of borontrifluoride etherate and subsequent oxidation with *p*-chloranil yielded the porphyrin−oligothiophene−anthracene triad **2.225** in about 3−4% yield. The linear D−A triad **2.226** was also prepared by condensation of aldehyde **2.224** with pyrrole and hexanal in a yield of 3% which had to be separated from other possible isomers (Chart 2.37).[318] Steady-state fluorescence and picosecond time-resolved fluorescence measurements revealed that selective excitation of the anthracene donor (254 nm) leads to an efficient unidirectional intramolecular energy transfer to the emitting porphyrin (650−800 nm) *via* the oligothiophene bridges.

Krebs et al. synthesized zinc porphyrin **2.227**, which was linked to regioregular octi(3-hexylthiophene) by a Stille-type coupling reaction of a stannyl derivative of the octithiophene and 5,15-dibromo-10,20-bis(3,5-di-*tert*-butylphenyl)zinc(II)-

Scheme 2.43

Reagents and conditions: (i) Mg, Et$_2$O; (ii) 5,5''-dibromoterthiophene, NidpppCl$_2$, Et$_2$O; (iii) 1. *n*-BuLi, Et$_2$O, anthraquinone, 2. HCl, MeOH/Toluene; (iv) POCl$_3$, DMF; (v) 1. pyrrole, BF$_3$·Et$_2$O/EtOH, 2. p-chloranil, reflux
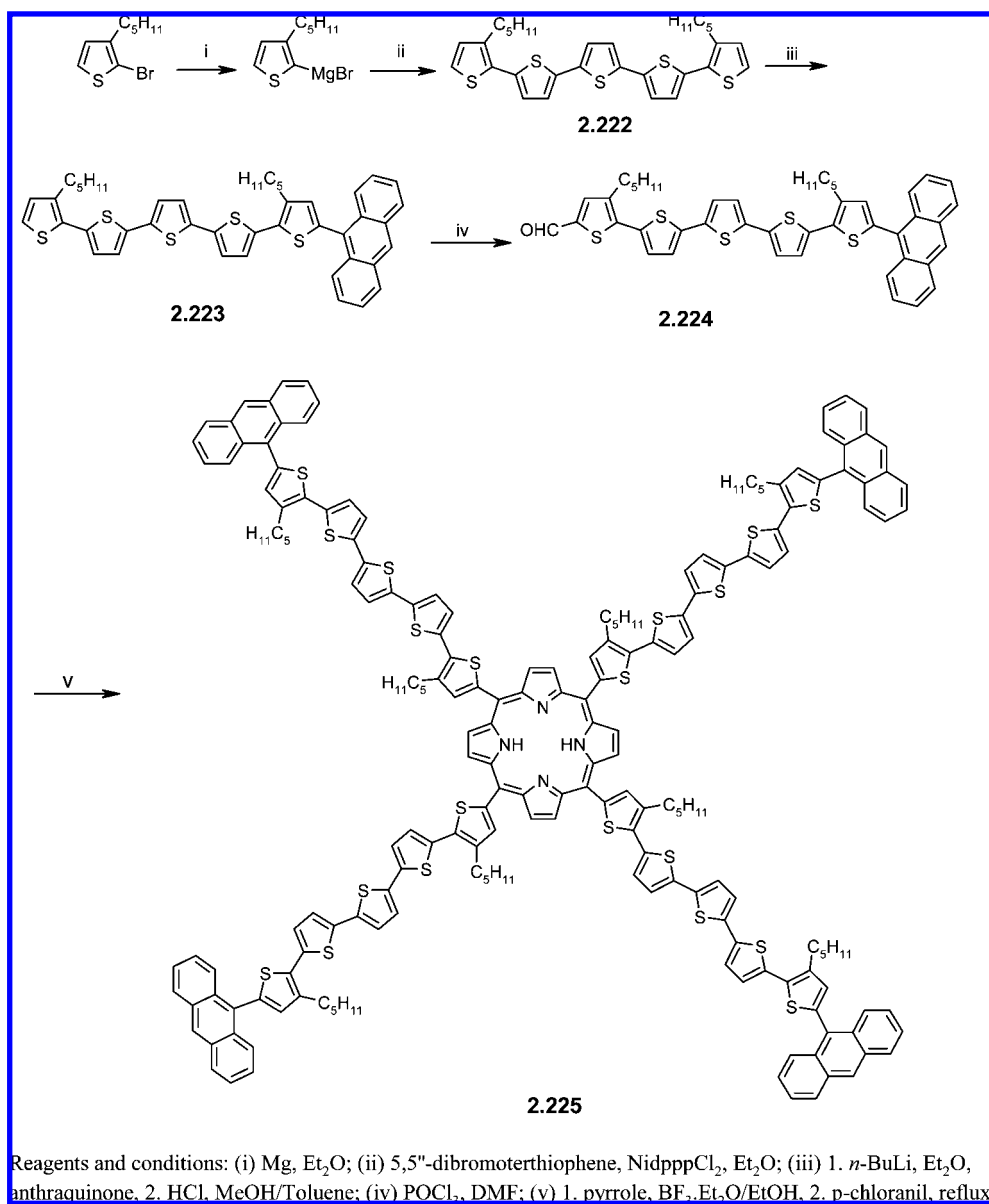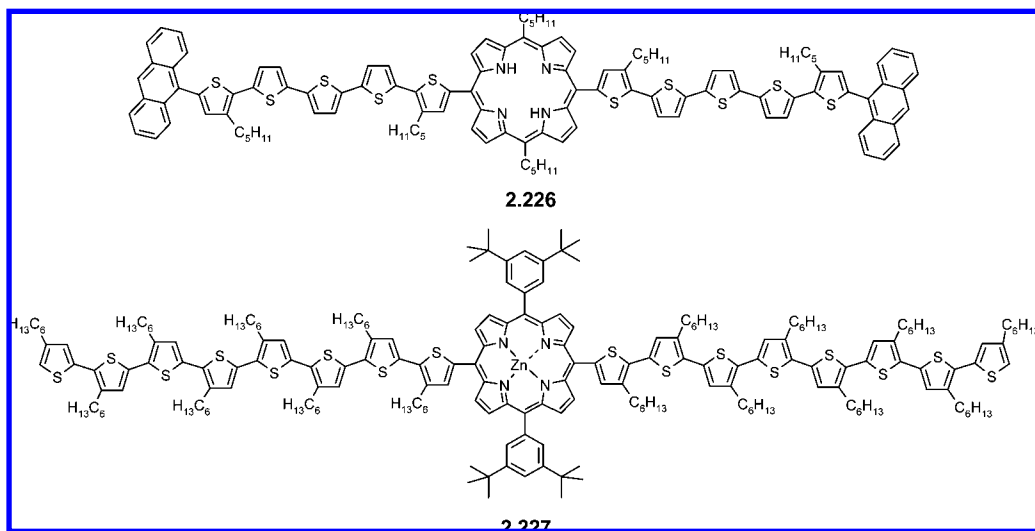
Chart 2.37

porphyrin in 15% yield (Chart 2.37).[320] A photovoltaic device based on **2.227** showed a rather poor photovoltaic response, which was ascribed to the internal conversion of the energy absorbed by the Zn-porphyrin constituent.
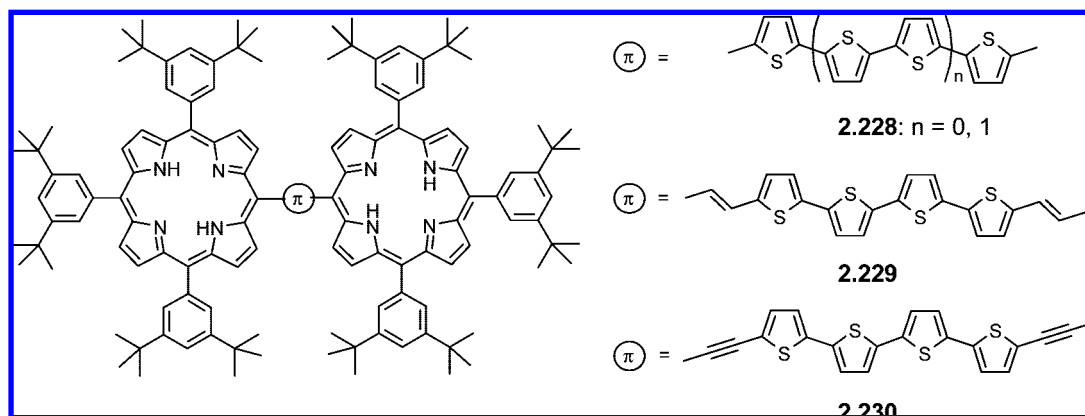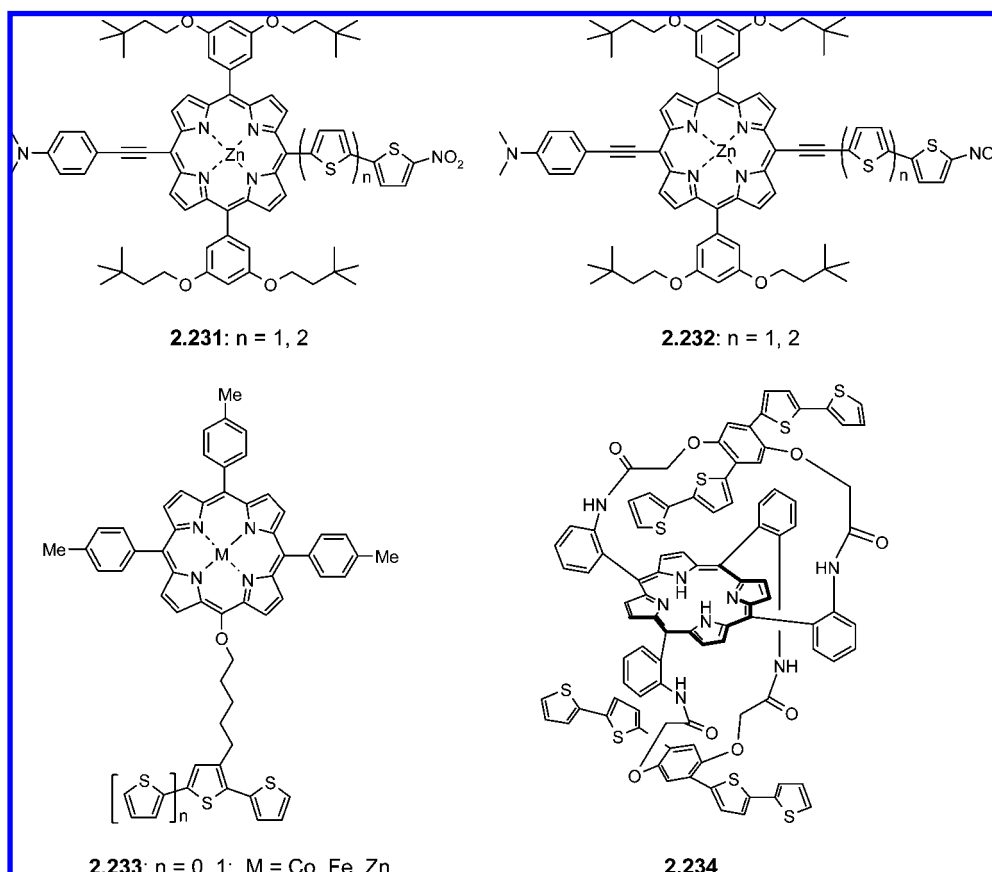
Chart 2.38

Chart 2.39

2.231: n = 1, 2

2.232: n = 1, 2

2.233: n = 0, 1; M = Co, Fe, Zn

2.234

Odobel et al. prepared a series of porphyrin—oligothiophene-based triads **2.228**—**2.230** in which two porphyrin units are connected to an oligothiophene bridge *via* single (**2.228**), double (**2.229**), and triple (**2.230**) bonds, respectively (Chart 2.38).[321] These compounds demonstrated the influence of the oligothiophene bridge on interporphyrin electronic interactions. The synthesis of the new triads was carried out by Pd[0]-catalyzed cross-coupling reactions of 5-iodo-10,15,20-{3,5-bis(*tert*-butylphenyl)}porphyrin and the appropriately substituted oligothiophenes. Spectroscopic and computational studies allowed establishing structure—property relationships, which clearly showed the effect of the different bridging linkers on the electronic communication between the porphyrin and oligothiophene units. A high photoinduced electron transfer rate constant was reported for oligomer **2.230** including an ethynyl linker. Thus, it was proven that oligothiophenes attached *via* ethynyl groups are viable

bridging modules to promote high electronic coupling between porphyrin units and can be suitable for the construction of artificial photosynthetic systems and related devices.

A series of conjugated (porphyrinato)zinc(II)-based chromophores **2.231** and **2.232** (Chart 2.39) containing nitroo-ligothienyl electron-accepting moieties have been synthesized using metal-catalyzed cross-coupling reactions involving the boronic ester of (porphyrinato)zinc(II) and 5-bromo(porphyrinato)zinc(II) and corresponding halogenated and ethynylated oligothienyl precursors.[322] In **2.231** (*n* = 1, 2) these acceptor moieties are appended directly to the *meso*-position of the porphyrin, while in **2.232** (*n* = 1, 2) a *meso*-ethynyl linker between the porphyrin and thiophene units was used. UV—vis absorption measurement performed for **2.231** showed a Soret band at ~457 nm and Q-bands at 580 and 640 nm, whereas the addition of an ethynylene spacer in **2.232** provoked a red shift of the Soret band to ~467 nm. Only

one Q-band at 683 nm was observed irrespective of the number of thiophene units. On the other hand, the emission spectra of derivatives **2.231** showed a blue shift of about 7 nm for the terthiophene derivative in comparison to the bithiophene analogue. Similarly, a 14 nm blue shift was observed for **2.232** derivatives by increasing the length of the oligothiophene moiety. In agreement with well-established structure−property relationships, these chromophores showed a decrease in the $S_0 \rightarrow S_1$ transition energy and an increase in the first hyperpolarizability with increasing conjugation length. For these neutral dipolar materials, large dynamic hyperpolarizabilities were determined by hyper-Rayleigh light scattering measurements and proved their applicability in electrooptic and telecommunication technology.

Schäferling and Bäuerle reported a series of bi- and terthiophenes attached to *meso*-tetraphenylporphyrins *via* an alkoxy spacer **2.233** (Chart 2.39).[323,324] After metalation of the porphyrin moieties, electrooxidative polymerization led to the corresponding metal-complexed porphyrin-appended polythiophenes. A lack of polymerizing ability was observed for the metal-free porphyrin−oligothiophene dyad due to the presence of free nitrogens in the porphyrin unit, which are known to inhibit the polymerization process due to interactions with the thiophene radical cations. The electrochemical and spectroscopic properties of the polymer films revealed the superimposition of the electronic properties of the individual π-systems. Spectroelectrochemical experiments and conductivity measurements pointed to a mixed charge transport mechanism. The functionalized polythiophenes showed higher stability in comparison to analogues without the porphyrin moiety due to a partial charge transfer from the conducting backbone to the porphyrin moieties. Furthermore, the redox wave obtained for the porphyrin subunits in the polymer represented a sensitive probe for external chemical stimuli promoting these hybrid polymers to potential candidates as amperometric sensors for the detection of polychlorinated phenols.

Swager et al. synthesized doubly strapped porphyrin **2.234** suitable for fluoride ion recognition, owing to the presence of two small hydrogen-bonding cavities (Chart 2.39).[325] Due to the presence of bithiophene units, electropolymerization of **2.234** gave a cross-linked conducting polymer possessing good conductivity. The conductivity of the polymer decreased upon addition of fluoride ions, and a shift of the porphyrin redox waves was observed. Thus, these systems are useful as highly selective alosteric fluoride recognition systems.

In another approach, Officer et al. prepared a series of dyads, where oligothiophenes were attached to the porphyrin unit through α- (**2.235**) and β-linkages (**2.236**) (Chart 2.40).[326] Dyads **2.235** were synthesized by condensation of 2-formyloligothiophenes with pyrrole by trifluoroacetic acid-catalyzed reaction followed by oxidation. Condensation of 3′-formyl-2,2′:5′,2″-terthiophene with pyrrole using a Lewis acid as catalyst gave **2.236** in ~30% yield.

Nonmetalated terthiophene derivative **2.237** (17%) was prepared by the condensation of bispyrrylmethane with 3′-formylterthiophene in trifluoroacetic acid, whereas the quinquethiophene derivative **2.238** was prepared by condensation of bispyrrylmethane and 3″-formylquinquethiophene with a Lewis acid as catalyst (Chart 2.40). ^{1}H NMR analysis of the free-base porphyrins **2.237** and **2.238** indicated an inseparable statistical mixture of ββ- and αβ-conformations. Terthiophene-Zn(II)porphyrin **2.239** was prepared as the *trans*

Chart 2.40

2.235: n = 0, 1, 2   **2.236**

2.237: R = H; M = 2H or Zn   **2.239**: M = Zn
2.238: R = 2-thienyl; M = 2H or Ni

Chart 2.41

2.240: M = 2H, n = 1-3
2.241: M = Zn, n = 1-2

2.242: n = 1, 3
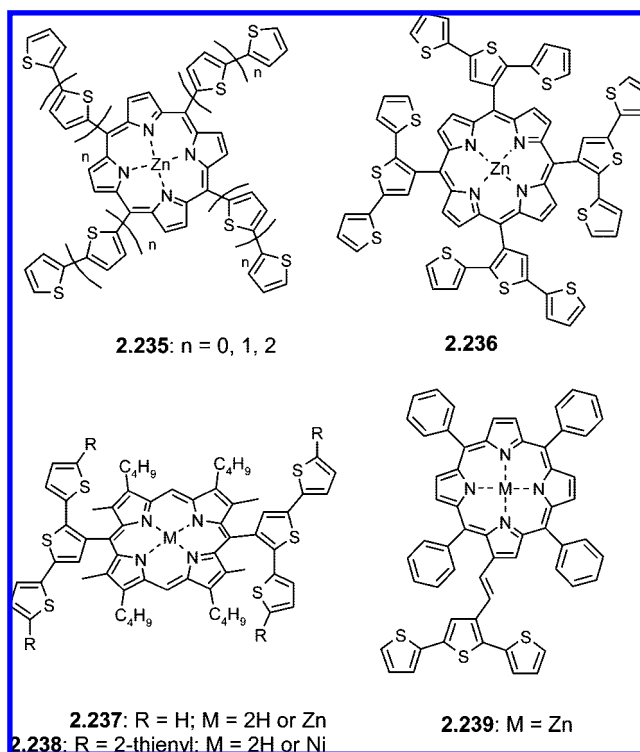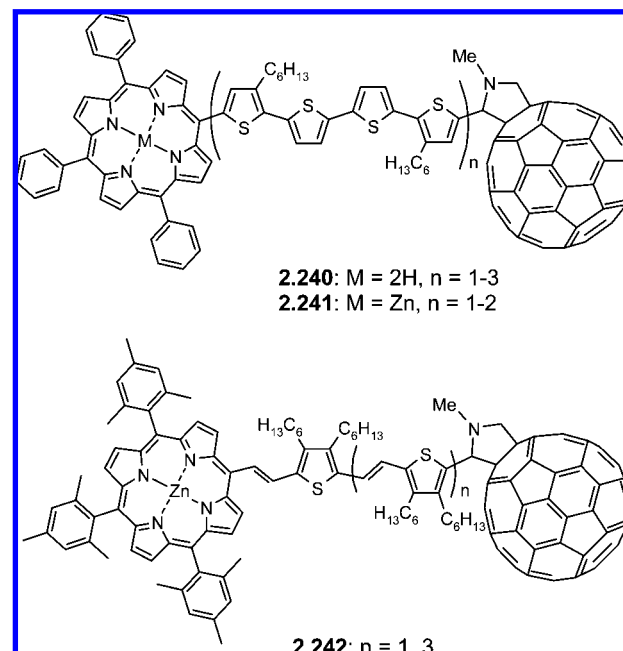
isomer by Wittig-reaction of 3′-formyl-2,2′:5′,2″-terthiophene and a phosphonium salt of tetraphenylporphyrin by irradiation with a tungsten lamp at elevated temperature (Chart 2.40). All porphyrin derivatives were easily metalated in high yields using Zn, Cu, or Ni salts. The electropolymerization of these derivatives led to polymeric architectures containing metalloporphyrins useful for sensory applications.

Ito et al. reported the synthesis of triads **2.240** (n = 1−3) (Chart 2.41) that incorporate a porphyrin as donor and fullerene as acceptor unit which are bridged by quater-, octi-, and dodecithiophenes.[327] The authors employed a one-pot procedure by reaction of formylated oligothiophenes with 3

Scheme 2.44

Reagents and conditions: (i) Pd(PPh₃)₄; (ii) BuLi, Bu₃SnCl; (iii) DMF, POCl₃; (iv) C₆₀, N-methylglycine
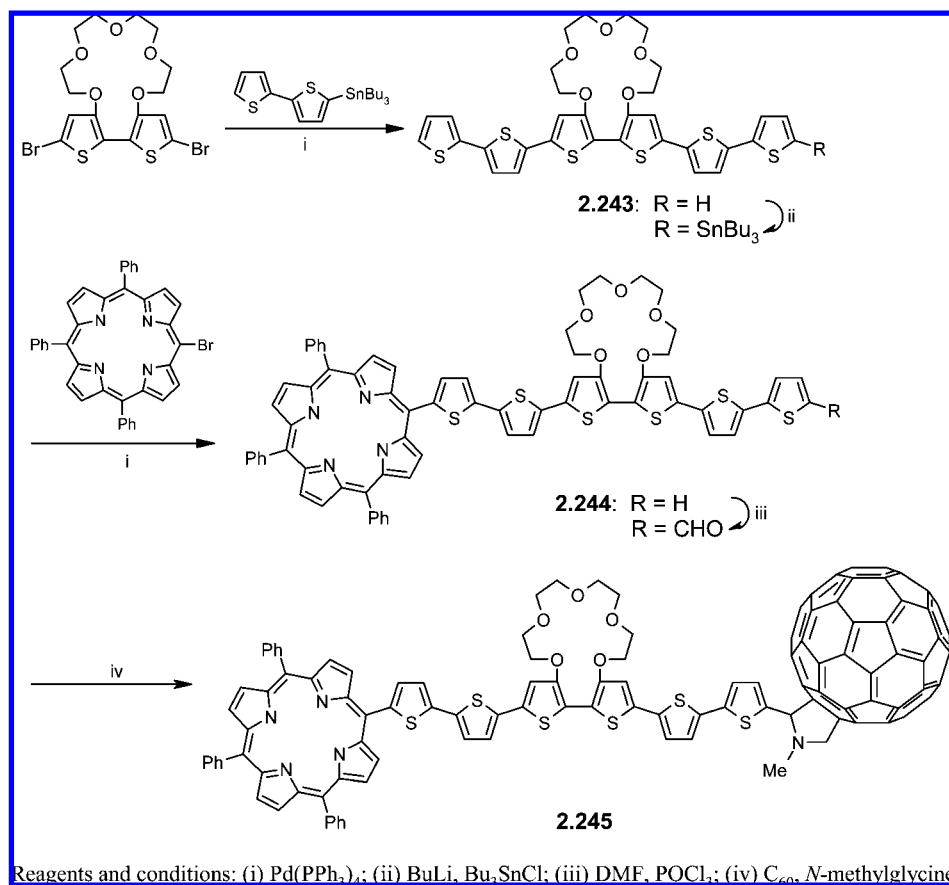
equiv of benzaldehyde and 4 equiv of pyrrole in the presence of trifluoroacetic acid. Subsequent oxidation with p-chloranil gave intermediate porphyrin−oligothiophene dyads in 2−9% yield. Formylation of the dyads at the other end and coupling with fullerene and N-methylglycine afforded triads **2.240** in 40−50% yields. Efficient quenching of the porphyrin fluorescence has been observed due to electron transfer to the fullerene unit *via* the oligothiophene spacer. The extent of quenching decreased with increase of the oligothiophene chain length. The same authors further prepared Zn complexes **2.241** (n = 1, 2) and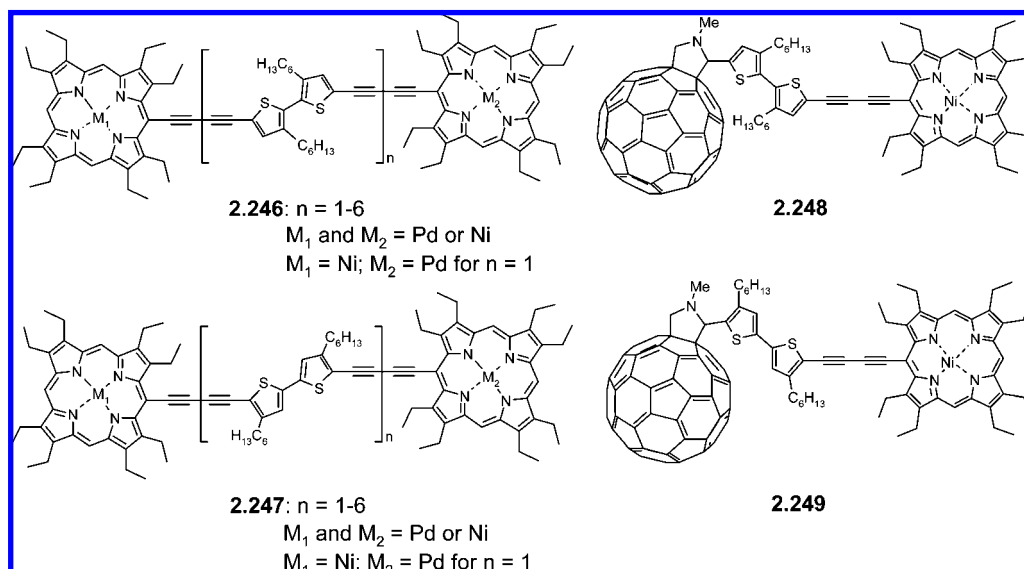 studied the effect of solvent polarity on the lifetimes of the charge-separated states.[328] Compared to the case of the free-base triads **2.240**, the lifetime of the Zn-complexed triads **2.241** was found to be ∼30 times longer in o-dichlorobenzene. Zn porphyrin−fullerene-containing triads **2.242** (n = 1, 3) linked by oligothienyle-nevinylenes (OTVs) were synthesized by Wadsworth−Emmons olefination between a phosphonate−Zn-porphyrin and alkyl substituted bisformyl-OTVs under stoichiometric control followed by 1,3-dipolar cycloaddition with N-methylglycine and C₆₀ in chlorobenzene.[329] Photoinduced energy and electron transfer processes from the excited singlet state of Zn-porphyrin to C₆₀ *via* the oligothiophene or OTV bridge were discussed in all systems depending on the length of the conjugated bridge and solvent polarity.

The synthesis of the similar porphyrin−oligothiophene−fullerene triad **2.245** was published by Otsubo et al. in which two central thiophene units were bridged by a crown ether ring (Scheme 2.44).[330] Sexithiophene **2.243** was prepared by cross-coupling of crown ether-appended dibromobithiophene and stannylated bithiophene. Further stannylation of **2.243** and reaction with bromoporphyrin gave dyad **2.244**, which

was formylated and finally coupled with C₆₀ and N-methylglycine to yield triad **2.245** in 25%. Efficient intramolecular electron transfer was observed in **2.245** from the photoexcited porphyrin moiety to the fullerene through the sexithiophene. However, complexation with sodium cations by the crown ether caused complete suppression of electron transfer as a result of a drastic conformational change of the sexithiophene backbone. Furthermore, decomplexation of the crown ether units in the hybrid system by addition of the same amount of 15-crown-5 resumes the photoinduced electron transfer. This on/off switching phenomenon indicated that the polyether-bridged sexithiophene can function as a complexation-gated molecular wire.

Acetylene-functionalized porphyrin−bithiophene−porphyrin triads **2.246** and **2.247** were synthesized in ∼8−9% yield by Higuchi et al. using oxidative cross-coupling reactions of corresponding ethynyl derivatives of octaethylporphyrin-Ni and 5,5′-bisethynyldihexylbithiophene in the presence of anhydrous copper(II) acetate in a mixture of pyridine and methanol (Chart 2.42).[331,332] Higher homologues containing 2−5 units of the dihexylbithiophene-diethynyl systems were simultaneously obtained from the same reaction in only 1−3% overall yield. The analysis of the UV−vis spectra in solution indicated that the position of the hexyl groups at the thiophene dramatically affects the electronic communication between the two terminal porphyrin rings. **2.246** showed an intense Soret band at 454 nm and broad Q-bands at 562 and 593 nm, whereas **2.247** showed a clear splitting of the Soret band with maxima at 440 and 484 nm and a Q-band at 601 nm. Thus, the tail-to-tail orientation of the 3-hexylthiophene rings in **2.247** raised the HOMO and lowered the LUMO levels of the extended porphyrin systems effectively,

Chart 2.42

2.246: n = 1-6
M₁ and M₂ = Pd or Ni
M₁ = Ni; M₂ = Pd for n = 1

2.248

2.247: n = 1-6
M₁ and M₂ = Pd or Ni
M₁ = Ni; M₂ = Pd for n = 1

2.249

while the head-to-head orientation in **2.246** did not show any significant effect.

Using a similar approach as that described for the Ni complexes of **2.246** and **2.247** (Chart 2.42), Higuchi and co-workers further synthesized a series of symmetrical Pd complexes. The syntheses of unsymmetrical Pd−Ni mixed-metal complexes of **2.246** (n = 1) and **2.247** (n = 1) were carried out by coupling octaethylporphyrin-Ni acetylene and a 5-bromo-5′-ethynylbithiophene precursor followed by a second Sonogashira coupling with trimethylsilyl acetylene. Deprotection with K₂CO₃ and final coupling with octaethylporphyrin-Pd acetylene were followed by an Eglinton-type coupling.[333,334] The ¹H NMR spectral data revealed that all the triads possessed fairly simple skeletal features. IR spectral measurements demonstrated that the diethynylene linkage for the tail-to-tail series contributed more efficiently to an extension of the resonance structure with the porphyrin and dihexylbithiophene units, regardless of the number of bithiophene units. Electrochemical and optical measurements of the unsymmetrical complexes revealed a strong electronic communication between the two terminal porphyrin rings, which was more effective in the case of the tail-to-tail isomers. The absorption spectra of both head-to-head and tail-to-tail series of the Pd complexes displayed slight hypsochromic shifts compared to those of the corresponding Ni complexes. The change in electronic properties due to both the orientation and the number of bithiophene units was also discussed.

In another approach, Higuchi and co-workers prepared the orientational isomers of octaethylporphyrin−dihexylbithiophene−fullerene triads **2.248** and **2.249** in which the porphyrin and fullerene units are attached at both ends of the bithiophene moiety (Chart 2.42).[335] The oligomers were build up by oxidative coupling of 5-formyl-5′-ethynyldihexylbithiophenes with (ethynylporphyrinato)Ni(II) to give corresponding monoaldehydes. Further condensation of the corresponding aldehydes with C₆₀ and N-methylglycine afforded compounds **2.248** and **2.249** in 20 and 25% yield, respectively. The electronic and electrochemical properties of the triads were studied, showing that the orientation of the dihexyl-bithiophene group not only affects the electronic structure of the triads but also their molecular motional behavior.

2.9.3. Ferrocene-Functionalized Oligothiophenes

Lin et al. synthesized a series of rigid molecular rods **2.250** and **2.251** (n = 1, 2) in which thiophene units were end-capped with ferrocenyl groups through vinyl or ethynyl linkages (Chart 2.43).[336] Compound **2.250** was prepared from 5-(2-ferrocenylvinyl)thiophene-2-carboxaldehyde by a Mc-Murray reaction using TiCl₄/Zn in 92% yield. Ferrocene-capped oligothiophenes **2.251** (n = 1, 2) were synthesized by Sonogashira-type cross-coupling reaction of ethynylferrocene with corresponding dibromo(oligo)thiophenes. These compounds displayed two absorption bands, one a low energy d−d transition due to a charge transfer from the ferrocenyl group to the oligothiophene core and another high energy π−π* transition band coming from the oligothiophene unit. Cyclic voltammetry performed for **2.250** and **2.251** revealed single two electron transfer processes at lower potentials which indicated a weak ferrocene−ferrocene interaction. A single oxidation wave was observed at higher potential due to the oligothienyl group.

Wong et al. synthesized a series of ethynyl-terminated oligothiophene−ferrocene dyads, which were used to prepare stable platinum(II) complexes **2.252** (Chart 2.43).[337] The ethynyl-terminated dyads were synthesized by a Pd(II)-catalyzed Sonogashira-type coupling reaction of ethynylferrocene with an excess of corresponding dibromooligothiophenes. This was followed by a second Sonogashira coupling reaction with trimethylsilylacetylene and deprotection of the silyl group by K₂CO₃. These ethynyl ligands were used to prepare corresponding Pt complexes **2.252** as red crystalline solids by reaction with trans-[Pt(PBu₃)₂Cl₂]/CuI in basic medium. Single crystal X-ray structure analyses showed that the oligothiophene units are in a coplanar arrangement and attached to the Pt center in a trans-orientation. A decrease in the energy of the π−π* transition of the oligothienyl bridges was observed due to the incorporation of Pt(II), which indicates an enhancement in the degree of π-delocalization through the Pt center. Cyclic voltammetry measurements showed two oxidation peaks, which correspond to the ferrocenyl and the thienyl groups, respectively. It was found that the thienyl moieties were stabilized against oxidation by incorporation of the Pt centers. Similarly to that observed for **2.250** and **2.251**, a weak
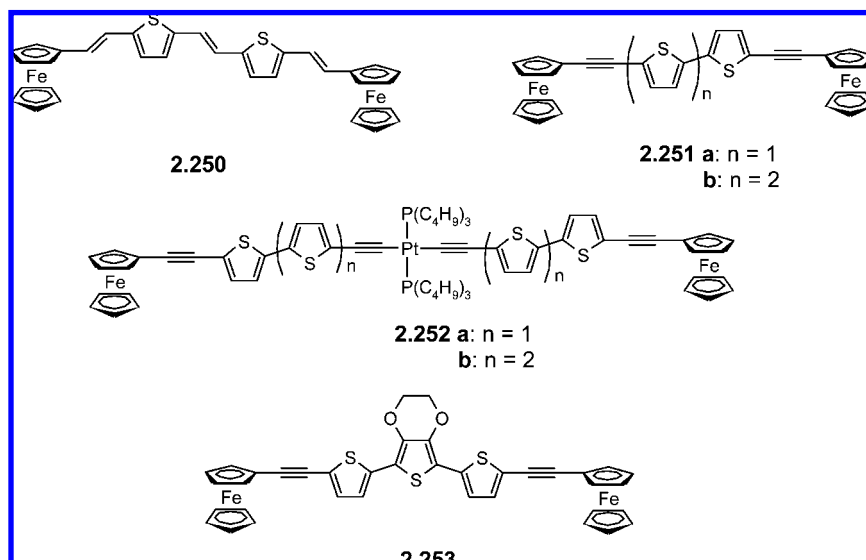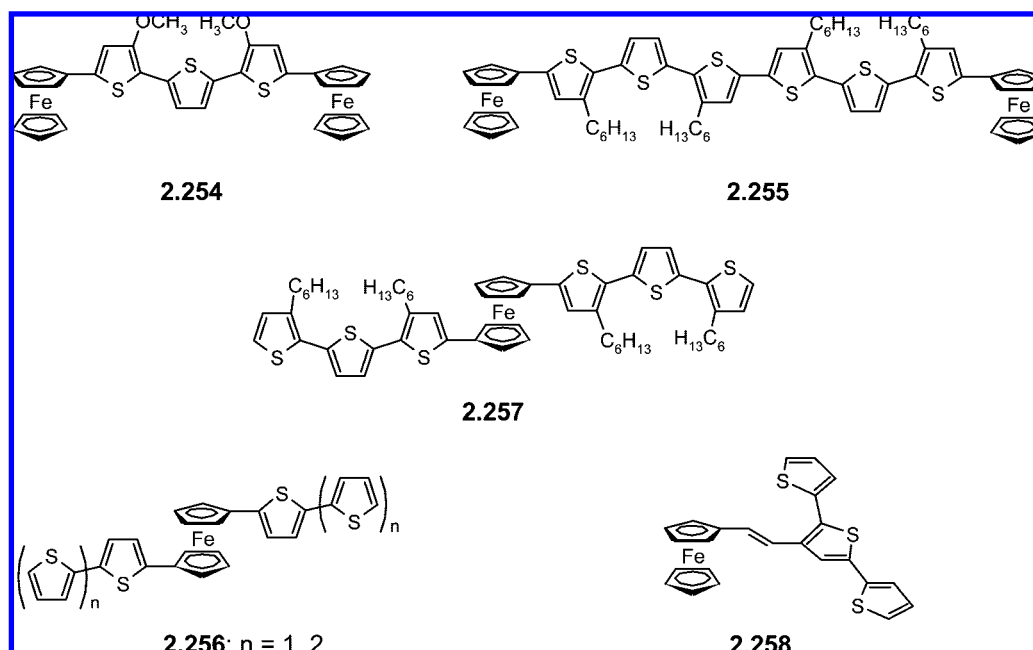
Chart 2.43

2.250

2.251 a: n = 1
b: n = 2

2.252 a: n = 1
b: n = 2

2.253

Chart 2.44

2.254

2.255
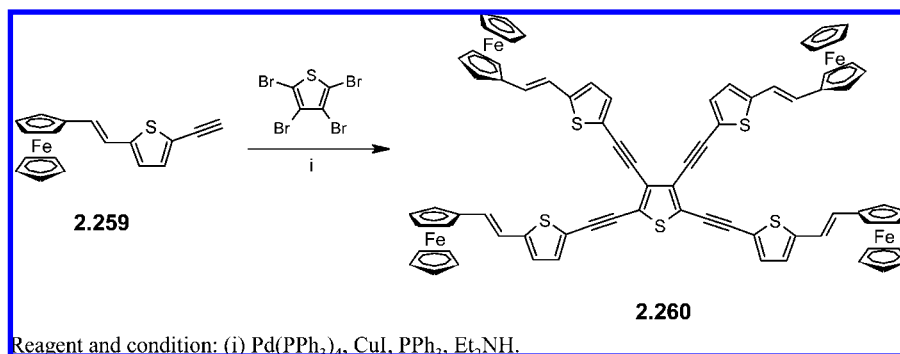
2.257

2.256: n = 1, 2

2.258

ferrocene−ferrocene interaction through the alkynyl−platinum−oligothiophene bridge was observed for **2.252**. In addition, a slight negative shift of the Fc/Fc⁺ redox potential in **2.252** compared to **2.251** indicated some degree of electron delocalization into the platinum unit in the former molecule, which is in agreement with the results obtained from theoretical studies.

Wolf et al. synthesized ethynylferrocenyl-capped ter-thiophene derivative **2.253**, in which the central thiophene unit was an EDOT moiety (Chart 2.43).[338] The π−π* absorption band of **2.253** was red-shifted in comparison with that of **2.251b** (Δλ = 17 nm) due to the presence of the central EDOT unit. In cyclic voltammetry, **2.253** exhibited one reversible wave which was assigned to the Fe^{II/III} oxidation and an irreversible wave at higher potential due to oligothiophene oxidation. Oxidation of the ferrocene centers generated corresponding monocations and dications, which were responsible for the oligothiophene-to-ferrocene charge transfer transitions observed in the near-IR region.

These results demonstrated an intramolecular charge delo-calization and charge transfer transitions along the rigid oligothiophene backbone.

Sato et al. synthesized ferrocenyl-terminated terthiophene **2.254** and sexithiophene **2.255** using Negishi-type cross-coupling reactions of ferrocenylzincate and corresponding dihalogenated oligothiophenes (Chart 2.44).[339] Cyclic vol-tammetry measurements of **2.254** showed three oxidation waves, where the first two were assigned to the redox processes of the ferrocene and the third wave to the terthiophene moiety. This result suggested a strong electronic interaction between the two terminal ferrocene units, indicat-ing charge transfer between the two units through the terthiophene. In contrast, compound **2.255** showed only two oxidation waves, from which the first one was ascribed to the ferrocene and the second to the sexithiophene unit, suggesting that no communication occurs between the ferrocenyl termini.[340]

Scheme 2.45

Reagent and condition: (i) Pd(PPh₃)₄, CuI, PPh₃, Et₂NH.

Higgins et al.[341] synthesized oligothiophene-substituted ferrocenes **2.256** ($n = 1$) and **2.257** by Stille-type coupling reaction of 1,1′-bis(tributylstannyl)ferrocene and 5-iodooligothiophenes in 19 and 28% yield, respectively (Chart 2.44). Cyclic voltammetry of the dyads revealed reversible redox waves coming from the ferrocene moiety. Electropolymerization of the oligomers gave electrochromic ferrocene−oligothiophene copolymers. Interestingly, during repetitive scanning the ferrocene wave diminished and eventually disappeared with the formation of the polymer. New redox waves appeared which were assigned to the reversible oxidation of quater- and sexithiophene units, respectively. Wolf et al.[342] prepared similar compounds **2.256** ($n = 1, 2$) in 34 and 53% yield, respectively. In this case, electropolymerization in dry CH_2Cl_2 gave polymers which showed the presence of ferrocene redox waves in the polymer film.[343] This result revealed that it was essential to carry out electropolymerization under absolutely dry conditions and the presence of a trace amount of water caused the formation of brittle black precipitates on the electrode, as well as the disappearance of the ferrocenyl redox wave after a couple of scans.

Chen et al.[344] prepared terthiophene-functionalized ferrocene **2.258**, in which the ferrocene unit is attached at the β-position of the central thiophene ring *via* a vinylene spacer (Chart 2.44). Wittig reaction of ferrocenylmethyltriphenylphosphonium bromide and 3-formyl-2,2′:5′,2″-terthiophene[345] under basic medium gave **2.258** in 69% yield. The product was isolated as a *cis/trans* mixture, which afterward was converted to the *all-trans* isomer by iodine. A homopolymer of **2.258** showed the characteristic redox behavior of both the ferrocene and the terthiophene moiety. Due to the existence of a π−π* transition and a polaronic band upon oxidation, a broad absorption ranging from 300 to 1100 nm was observed in the polymer film. A linear increase in the ferrocene oxidation peak was found in the presence of cytochrome-*C*, rendering this system to have potential as biosensors.

Thomas and Lin synthesized star-shaped ferrocene−oligothiophene **2.260** using a Pd^0-catalyzed coupling of acetylene derivative **2.259** and tetrabromothiophene (Scheme 2.45).[346] A strong absorption was reported for **2.260** at 390 nm due to the π−π* transition of the oligothiophene unit and at 500 nm due to the d−d transition of the metal centers. Cyclic voltammetry measurements performed on **2.260** showed a cathodic shift of the ferrocene oxidation compared to that of the free acetylene **2.259** ($\Delta E_p = 0.12$ V). This behavior was attributed to the extended conjugation in the molecule. Although a weak electronic interaction of the ferrocene and the central oligothiophene core has been noticed in **2.260**, no electronic communication was observed between the ferrocenyl units.

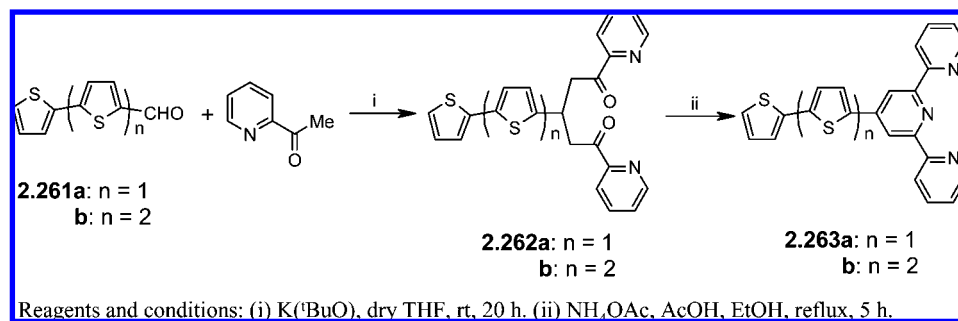## 2.10. Oligothiophenes Containing Transition Metal Chelating Ligands

Incorporation of polypyridyl ligands into π-conjugated systems receives growing interest. Their complexation with transition metal ions directly influences the electronic properties of the conjugated oligomers and polymers, thus allowing us to tune them specfically. The behavior of these polypyridyl complexes generally depends on the way the molecules are designed. If the complexes are directly coordinated to the backbones, a strong electronic coupling results, or if they are separated by spacers, a weaker electronic coupling can be expected.[347,348]

The design of oligothiophene-based polypyridyl chelating ligands and the tuning of their properties by complexation with transition metal ions are crucial for their applications in organic solar cells, sensors, catalysis, and electrochromics.[43,349−351]
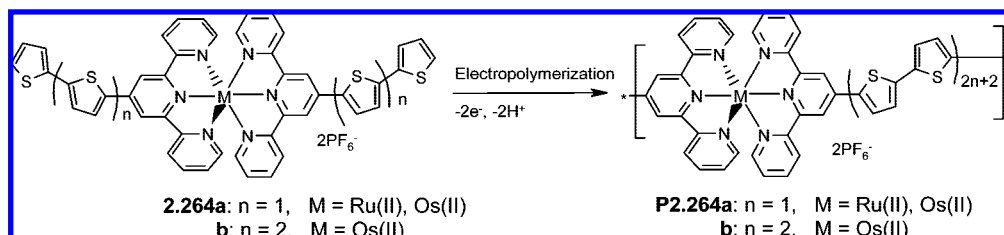
2.10.1. Terpyridine-Functionalized Oligothiophenes

Tridentate 2,2′:6′,2″-terpyridine (tpy) is a strong transition-metal binding ligand used to facilitate and control the assembly of molecular architectures.[352,353] The synthesis of the first terpyridine-functionalized oligothiophenes 2.263 ($n = 1, 2$) was reported by the group of Constable (Scheme 2.46).[354−356] Diketones 2.262 ($n = 1, 2$) were prepared by a reaction of 2,2′-bithiophene-5-carbaldehyde **2.261a** or 2,2′,5′,2″-terthiophene-5-carbaldehyde **2.261b** with 2-acetylpyridine in the presence of potassium *tert*-butoxide as base. Ring closure of the resulting diketone **2.262** using ammonium acetate in acetic acid medium finally gave the hybrid molecules **2.263**. Metal complexation of the terpyridines with $RuCl_3 \cdot 3H_2O$ and $K_2[OsCl_6]$ was performed by microwave irradiation under reducing conditions to give Ru- and Os-terpy complexes **2.264a,b** in a yield of 25−30%. The Ru-based complexes displayed characteristic singlet metal-to-ligand charge transfer (¹MLCT) absorption bands at ∼500−515 nm, whereas, for the Os-based complexes, both ¹MLCT and ³MLCT transitions were observed in solution. Electropolymerization of complexes **2.264** generated rodlike conjugated metallopolymers **P2.264** containing [Ru(terpy)₂]²⁺ or [Os(terpy)₂]²⁺ units in the main chain connected by either quater- or sexithienyl moieties (Scheme 2.47).[355,357] From cyclic voltammetry studies, the mutual interaction between the metal and oligothiophene bridges was discussed. *In-situ* conductivity measurements of the polymer films indicated
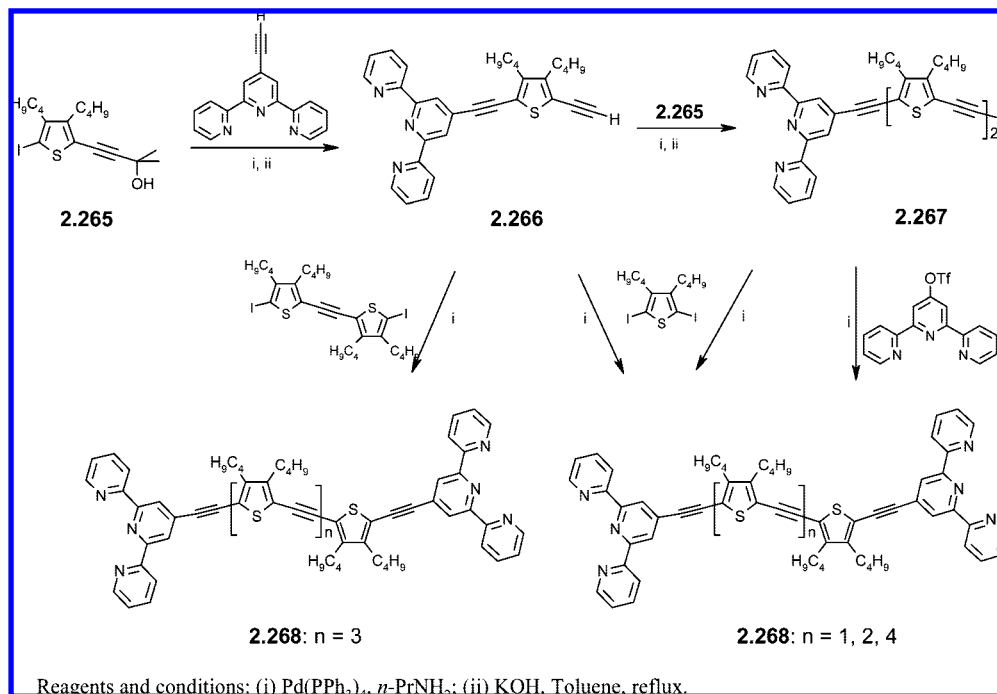
Scheme 2.46

Reagents and conditions: (i) K(ᵗBuO), dry THF, rt, 20 h. (ii) NH₄OAc, AcOH, EtOH, reflux, 5 h.

Scheme 2.47

Scheme 2.48

Reagents and conditions: (i) Pd(PPh₃)₄, n-PrNH₂; (ii) KOH, Toluene, reflux.

that charge transport rates can be significantly enhanced by a better matching of the redox potentials of the metal center and the conjugated bridge.[356] Thus, by specifically controlling the electrochemical behavior, spectroscopic properties, and direction of energy transfer, these materials could provide new possibilities to enhance charge transport rates in electronic devices.

Ziessel et al. prepared a novel series of molecular wires **2.268**, in which oligo(2,5-diethynyl-3,4-dibutylthiophene) units were end-capped with rigid terpyridine ligands.[358,359] The precursor oligomer **2.266** was synthesized in 80% yield by Pd⁰-catalyzed coupling of propargyl alcohol protected 5-iodo-3,4-dibutylthiophene **2.265** and ethynylterpyridine and subsequent deprotection of the propargyl group under basic conditions (Scheme 2.48). Repetition of the reaction sequence yielded the end-protected higher oligomer **2.267** in 86%

yield. Coupling of the intermediate oligomers **2.266** and **2.267** and diiodo-functionalized dibutylthiophenes using Sonogashira-type coupling reactions produced the desired bis-terpyridine derivatives **2.268** (n = 1−4) in moderate to good yields.

Complexation of the ligands **2.268** (n = 1−4) by using cis-[Ru(terpy)(DMSO)Cl₂] afforded mono- and binuclear Ru(II) complexes **2.269** and **2.270** as red solids (Chart 2.45).[360] The structures of these Ru complexes were well supported by ¹H NMR and FAB mass spectroscopy. Absorption spectra of the metal complexes exhibited both ligand-centered (LC) and MLCT transitions, whereas the emission behavior was dominated by long-lived ³MLCT-based luminescence.[361] The electrochemical results obtained for the complexes indicated that oxidation of the Ru center(s) [Ruᴵᴵ/Ruᴵᴵᴵ] occurred in the same potential range. Multiple reduction

Chart 2.45

2.269: n = 1-4

2.270: n = 1-4
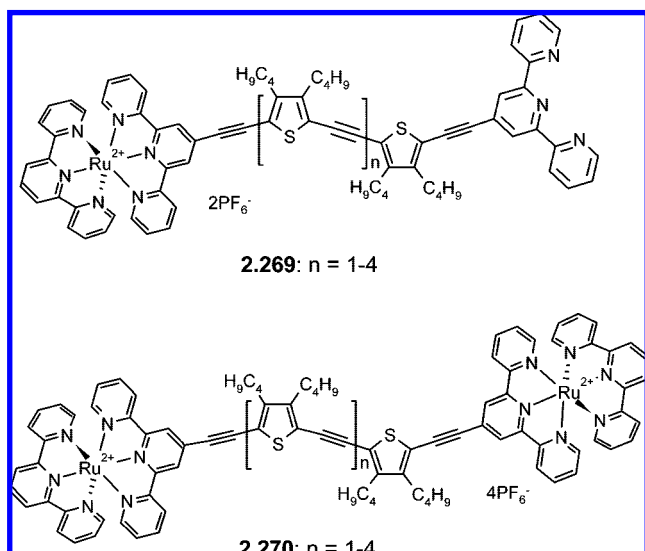
waves were observed, which corresponded to the various terpyridine segments. For mononuclear complexes **2.269** (*n* = 2−4) additional irreversible thiophene-based oxidations and terpyridine reduction waves were reported.

Odobel et al. synthesized heteroleptic Ru(terpy)$_2$ complexes **2.272** and **2.273**, which were substituted with a phosphonic acid moiety at one end and a bi- or terthiophene at the other end (Scheme 2.49).[362] The oligothiophene-substituted terpyridine ligands were prepared by a Stille-type coupling reaction of stannylated terpyridine and corresponding bromo-oligothiophenes. Ru(II) complexes **2.272** and **2.273** were prepared by complexation of paramagnetic Ru(III) adduct 2,2′:6′,2″-terpyridine-4′-diethylphosponate **2.271** and corresponding oligothienyl terpyridine under reductive conditions and final hydrolysis of the ethyl group by mild trimethylbromosilane. In DSSCs, poor photovoltaic efficiencies of ∼0.08% were observed by using these Ru complexes as sensitizers and poly(octylthiophene) as hole conductor, which was attributed to the low electron injection efficiency into the TiO$_2$ photoanode. This finding was also supported by spectroscopic and electrochemical investigations performed on **2.272** and **2.273**, which showed that the LUMOs of these complexes are localized on the terpyridine−oligothiophene and not on the terpyridine−phosphonic acid which binds to the TiO$_2$ surface.

Recently, Jørgensen et al. synthesized a mixed multidomain oligomer **2.274** (Chart 2.46) designed for solar cell applications containing different functionalities, such as a zinc porphyrin, a bis-terpy-Ru(II) complex, a (dimethylamino)phenyl-terminated nonithiophene, and a cyanovinyl oligophenylenevinylene terminated by a benzoic ester.[363] Although compound **2.274** contained all the photophysical and electronic functionalities needed for solar cells, a bulk heterojunction device made using **2.274** as active layer showed very low power conversion efficiencies of ∼10^{-4}%. This result was attributed to the presence of the zinc porphyrin−Ru(II)terpy dyad, which efficiently transformed the excited-state to a long-lived MLCT-mediated charge separated state, but it is inefficient at generating and separating charge carriers.

2.10.2. Bipyridine-Functionalized Oligothiophenes

Guillerez et al. prepared π-conjugated polymer **2.277** containing alternate regioregular quater(3-octylthiophene) units[364] and 2,2′-bipyridine-Ru(II) complexes (Scheme 2.50).[365] The polymer was obtained in two different ways: In the first case, the polymer backbone **2.275** was constructed *via* Stille-type cross-coupling reactions of 5,5′-dibromo-2,2′-bipyridine and bisstannylated-quaterthiophene prior to the metal complexation with Ru(bipy)$_2$Cl$_2$. This approach had the drawback of the uncertainty of the incorporation of the metal ion into the polymer. In the second case, reaction of the bisstannyl derivative with the preconstructed metallic core **2.276** gave metal-containing polymer. A general drawback found for both strategies was that the polymers were not regioregular due to the unsymmetrical heterocoupling of the two bifunctional units. The structure of the polymer was confirmed by ^{1}H NMR spectroscopy, from which the chain length of the polymer was estimated and compared to the results of gel permeation chromatography (GPC) and light-scattering experiments. UV−vis measurements showed that the delocalization of π-electrons in the conjugated polymer chain involves both oligothiophene and ruthenium chelating bipyridine units. Electrochemical measurements revealed strong electronic interaction between the π-conjugated backbone and the Ru(II)-polypyridyl complexes.

Other soluble metal−organic polymers **2.278** and **2.279** (Chart 2.47) containing Os(II) and Ru(II) polypyridyl complexes fused with π-conjugated oligo(3-octylthiophenes) have been reported.[366] The photophysical and electrochemical studies performed for these complexes showed strong electronic interactions between the metal center and the π-conjugated segments. Week MLCT luminescence and long-lived transient absorptions were reported for these complexes due to the presence of an energetically low-lying $^3\pi-\pi^*$ state of the thiophene−bipyridine system. The authors claimed that, to produce metal−organic materials that display efficient MLCT emission, it is necessary to keep the energy of the $^3\pi-\pi^*$ state of the π-conjugated system above the energy level of the MLCT state. From ESR measurements, strong spin−orbit coupling was observed in the reduced (n-doped) state of these complexes, indicating that the injection of charge occurs preferentially on the metalated bipyridine units of the polymer backbone, which acts as an electronic gate.[367]

Pappenfus and Mann prepared bipyridine-capped oligothiophene ligands **2.281** as well as their respective binuclear Ru(II) complexes **2.282** (Scheme 2.51).[368]Precursor sexithiophene **2.280** was synthesized by oxidative coupling of terthiophene with BuLi/Fe(acac)$_2$. Bisstannyl derivatives of ter- and sexithiophene were prepared by lithiation followed by quenching with trimethylstannyl chloride. These compounds were then *in situ* coupled to 4-bromo-2,2′-bipyridine using Stille-type cross-coupling reactions to give ligands **2.281** (*n* = 1, 2) in 60−70% yields. Complexation of these ligands with *cis*-Ru(bipy)$_2$Cl$_2$·2H$_2$O in 2-methoxyethanol afforded the corresponding Ru(II) complexes **2.282** in 80−90% yield. The complexes were characterized by ^{1}H NMR and MALDI-TOF mass spectrometry. UV−vis spectra of ligands **2.281** (*n* = 1, 2) in dichloromethane solution displayed low energy bands at 398 nm (*n* = 1) and 431 nm (*n* = 2), respectively, which were attributed to the π−π* transition of the conjugated π-system and a high-energy band at 282 nm corresponding to the π−π* transition of the bipyridine units. Ru(II) complexes

Scheme 2.49

Reagents and conditions: (i) AgBF₄, EtOH, DMF; (ii) Me₃SiBr, DMF.

Chart 2.46

2.274

Scheme 2.50

Reagents and conditions: (i) Pd(PPh₃)₂Cl₂, DMF, 120 °C; (ii) Ru(bipy)₂Cl₂, ethanol, reflux.
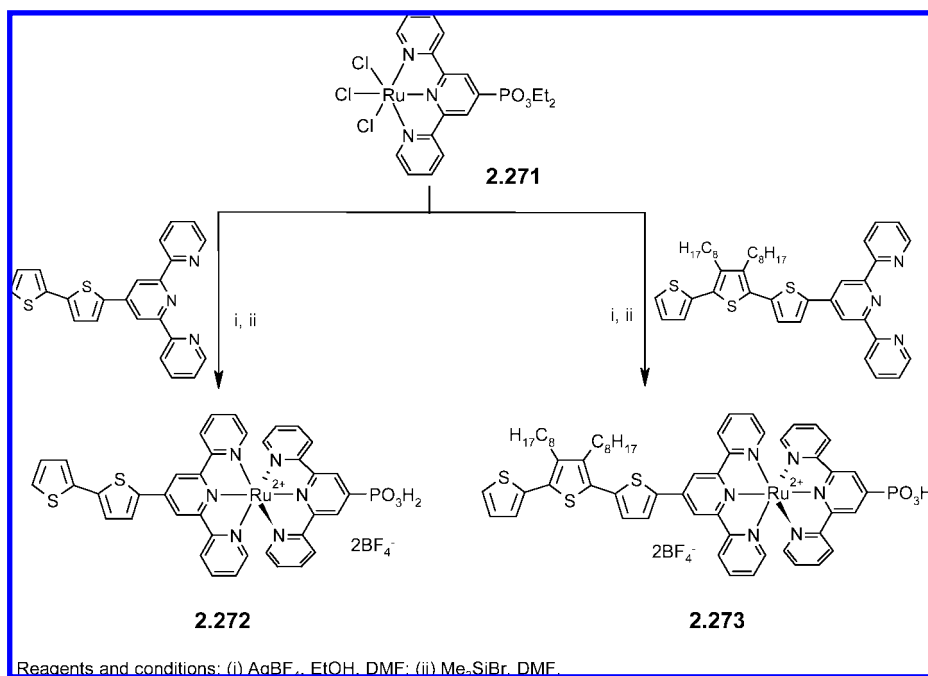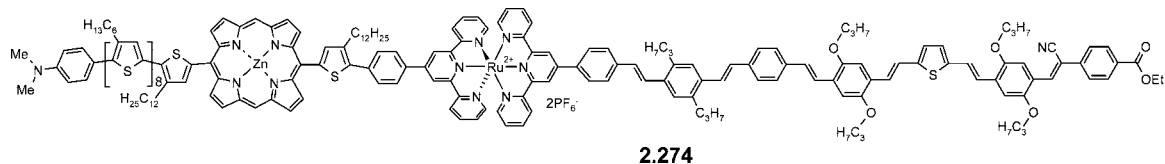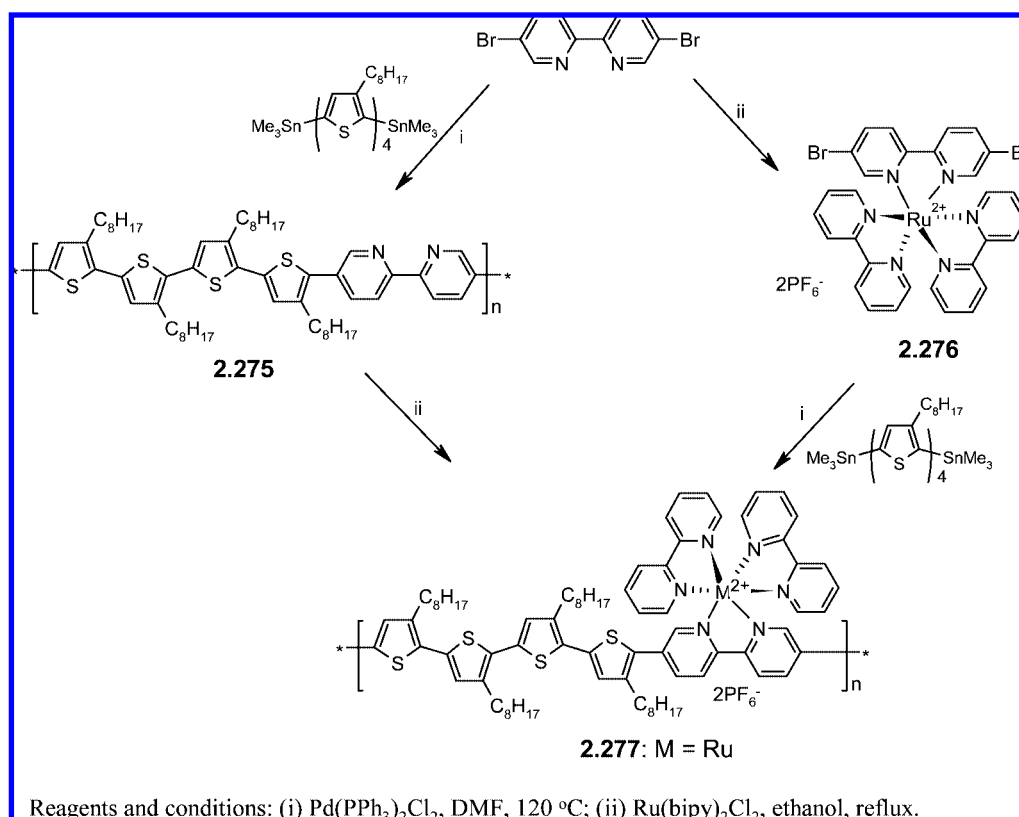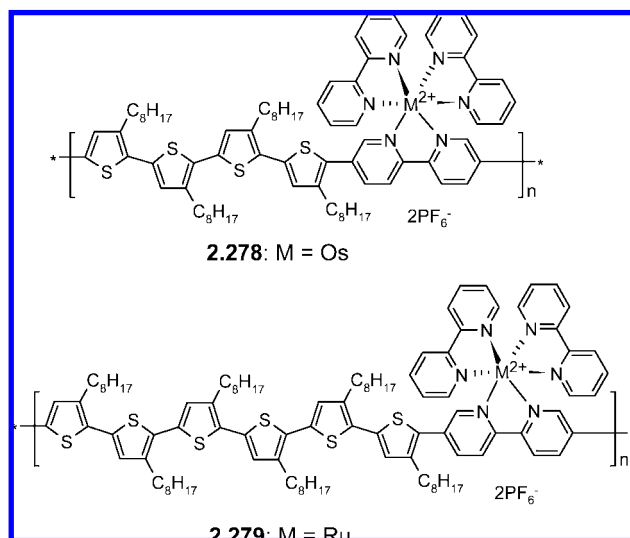
2.282 (*n* = 1, 2) showed a strong intense band at 290 nm due to the bipyridine units together with a broad red-shifted

MLCT transition at about 475 nm due to the overlapping of the low energy π−π* transition of the oligothiophene unit

Chart 2.47

2.278: M = Os

2.279: M = Ru

with the MLCT band. Cyclic voltammetry experiments conducted on the Ru complexes revealed an electrochemically reversible redox behavior. The first oxidation peak potentials at 1.15 V for **2.282** ($n = 1$) and at 0.87 and 0.99 V (vs SCE) for **2.282** ($n = 2$) were assigned to the oxidation of the ter- and sexithiophene bridge, whereas the redox wave at ~1.33 V corresponded to the simultaneous oxidation of the metal centers. Multiple two-electron reduction processes were observed, in which the first reduction wave was attributed to the reduction of the bipyridine units of the bridging ligand, followed by the subsequent reduction of additional bipyridine units.

Barbieri, Ziessel, and co-workers[369] synthesized another series of binuclear Ru(II) complexes **2.287** and **2.288**, in which the complexing units are attached at both termini of a ter- or quinquethiophene *via* ethynyl spacers (Scheme 2.52). Terthiophene derivative **2.285** was prepared by Pd⁰-catalyzed coupling of diiodoterthiophene **2.283** and 5-ethynyl-2,2′-bipyridine, whereas ligand **2.286** was synthesized by reaction of the bisethynyl derivative of quinquethiophene **2.284** and 5-bromo-2,2′-bipyridine. Complexation with [Ru(bipy)₂Cl₂] afforded the desired complexes **2.287** and **2.288** in 76 and 63% yield. The complexes displayed a low energy ¹MLCT absorption maximum at 442 nm and a high energy band at 287 nm due to the ¹π–π* transition of the bipyridine units. Weak emission was reported for complex **2.287** ($\lambda_{em} = 647$ nm, $\Phi_f = 4 \times 10^{-4}$), which is consistent with a ³MLCT nature,[361,370] whereas **2.288** was reported to be nonfluorescent. Cyclic voltammetry measurements of these binuclear Ru(II) complexes showed that the first reduction step takes place at the bipyridine ligands bearing an ethynylene group, whereas the first oxidation takes place at the oligothiophene bridge. Further oxidations corresponded to the weakly interacting Ru^II → Ru^III metal centers.

Bair and Harrison synthesized a series of unsymmetrical bi- and quaterthiophenes **2.293** ($n = 0$, 1) containing Ru(II)bipyridine and phosphonic acid groups at the termini (Scheme 2.53).[371] Phosphonation of bithiophene and subsequent stannylation gave **2.289** as precursor building block. Cross-coupling of stannylated bithiophene **2.289** to an appropriate bromobipyridine unit afforded the precursor ligands **2.290**. On the other hand, quaterthiophene-based ligands **2.292** were prepared by the cross-coupling of **2.289** and 5-bromo-5′-bipyridyl-2,2′-bithiophenes **2.291**. Finally,
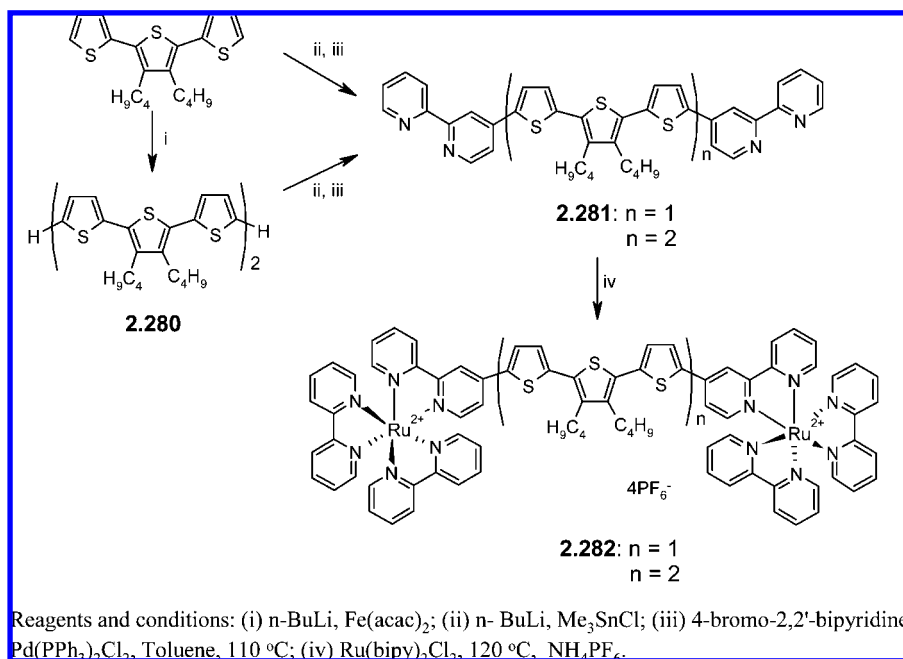
hydrolysis of the phosphonic esters to the corresponding acids was facilitated using trimethylsilyl bromide. Complexation of the ligands with [Ru(bipy)₂Cl₂] afforded the respective complexes in 70–80% yield. All complexes showed both π–π* and MLCT-based transitions, which are red-shifted to those of Ru(bipy)₃²⁺ by 12–30 nm. No significant difference in absorption was observed between the 4- and 5-bipyridine-substituted derivatives **2.292** and **2.293**, respectively.

Wolf et al. prepared metal complexes **2.294** ($n = 0$, 1), in which ruthenium(II) bis(bipyridyl) groups were coordinated to 3″-phosphino-oligothiophenes[372,373] *via* a diphenylphosphine linker and a thienyl sulfur (*P,S* bonding) (Scheme 2.54).[373,374] Upon treatment with a base, switching of the thiophene coordination from Ru–S (*P,S* bonding) in **2.294** to Ru–C (*P,C* bonding) in **2.295** was observed, resulting in substantial changes of the electronic properties of the oligothiophene ligands. This process was reversible upon addition of acid to **2.295**, resulting in the regeneration of the *S*-coordinated complexes **2.294**. X-ray structure analysis confirmed the *P,S* and *P,C* coordination mode of the complexes and suggested that the *P,C*-bonding mode is more flat than the *P,S*-bonding. Red shifts of the π–π* and MLCT transitions were observed by switching from the *P,S*- to the *P,C*-coordinated complexes, which further confirmed the increased planarity of the oligothiophene chain in the latter complex. Both bonding modes resulted in remarkable quenching of the ligand-based luminescence due to thermal population of a low-lying Ru-centered nonemissive energy level.[373] Cyclic voltammetric measurements of the *P,S*-coordinated complexes **2.294** ($n = 0$, 1) revealed large positive shifts of the oxidation potentials ($\Delta E = 0.7–1.0$ V) whereas for *P,C*-coordinated complexes **2.295** ($n = 0$, 1) the oxidation potentials were even lower than those of the free ligands ($\Delta E = 0.5$ V).
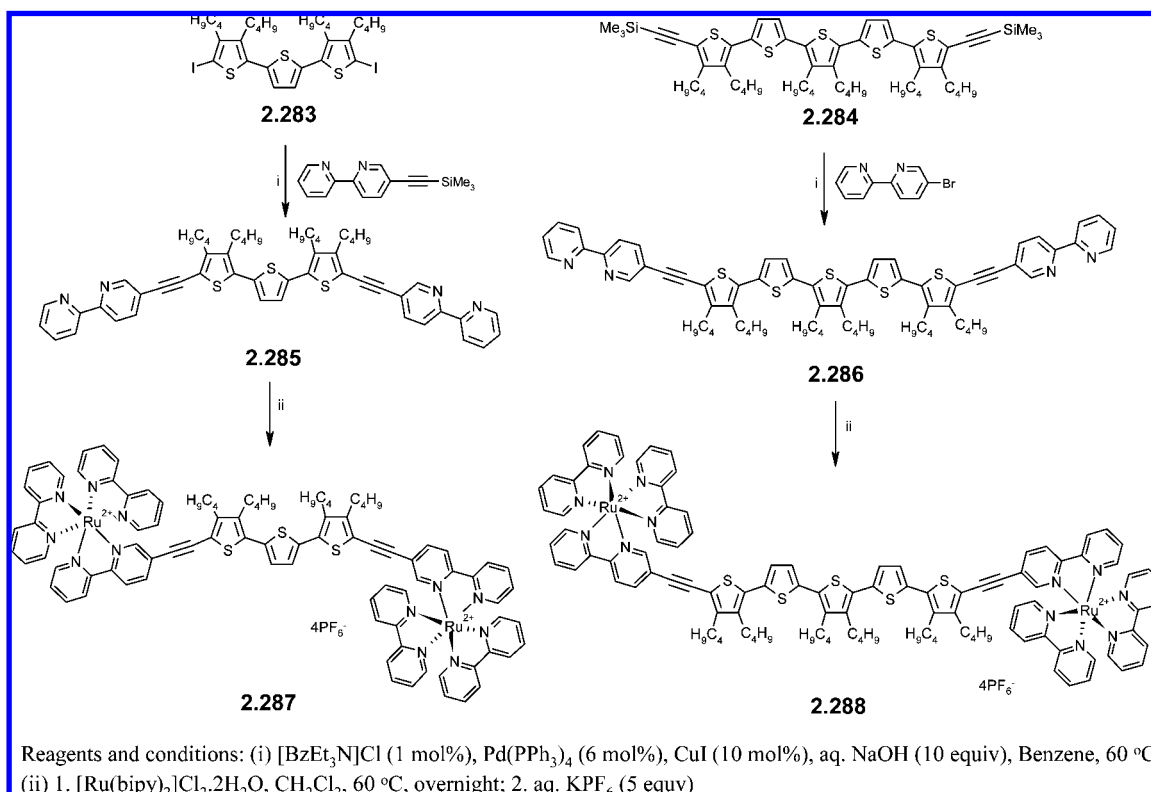
Transient absorption measurements performed for the *P,C*-coordinated complex **2.295** ($n = 1$) showed the formation of long-lived transient species with a lifetime of 2.2 μs, which suggested that the HOMO level is located at the quinquethiophene chain, whereas the terthiophene derivative **2.295** ($n = 0$) showed a metal-based HOMO with a very short-lived transient (<1 μs).[375]

To develop novel 3-dimensional architectures around the metal center, Swager et al. synthesized bithiophene-functionalized bipyridines and their corresponding Ru(II) complexes **2.296** and **2.297** (Chart 2.48).[376] The ligands were prepared by Stille cross-coupling of stannylated bithiophene and corresponding 4,4′- or 5,5′-dibromobipyridines. The ruthenium complexes were prepared by reaction of the ligands with RuCl₃·xH₂O in DMF under refluxing conditions. The complexes showed low energy MLCT absorption bands at 454 nm for **2.296** and at 507 nm for **2.297** along with high energy ligand-centered absorption bands at 310 and 404 nm, respectively. In comparison, unsubstituted [Ru(bipy)₃]²⁺ absorbs at 290 and 452 nm. The MLCT absorption band of **2.296** nearly coincided with that of [Ru(bipy)₃]²⁺, suggesting that the *meta*-relationship between oligothiophene units and the ruthenium center exerted little influence on the MLCT absorption bands. Upon electrochemical polymerization, these complexes formed three-dimensional networks which displayed both metal bipyridyl-based and oligothienyl-based redox processes. Moderate conductivity was observed in the polymers due to strong interactions between the electroactive ruthenium centers through the conjugated oligothiophene units. The conductivity observed for poly-**2.297** indicated

Scheme 2.51

Reagents and conditions: (i) n-BuLi, Fe(acac)$_2$; (ii) n- BuLi, Me$_3$SnCl; (iii) 4-bromo-2,2'-bipyridine, Pd(PPh$_3$)$_2$Cl$_2$, Toluene, 110 °C; (iv) Ru(bipy)$_2$Cl$_2$, 120 °C, NH$_4$PF$_6$.

Scheme 2.52

Reagents and conditions: (i) [BzEt$_3$N]Cl (1 mol%), Pd(PPh$_3$)$_4$ (6 mol%), CuI (10 mol%), aq. NaOH (10 equiv), Benzene, 60 °C; (ii) 1. [Ru(bipy)$_2$]Cl$_2$.2H$_2$O, CH$_2$Cl$_2$, 60 °C, overnight; 2. aq. KPF$_6$ (5 equv)
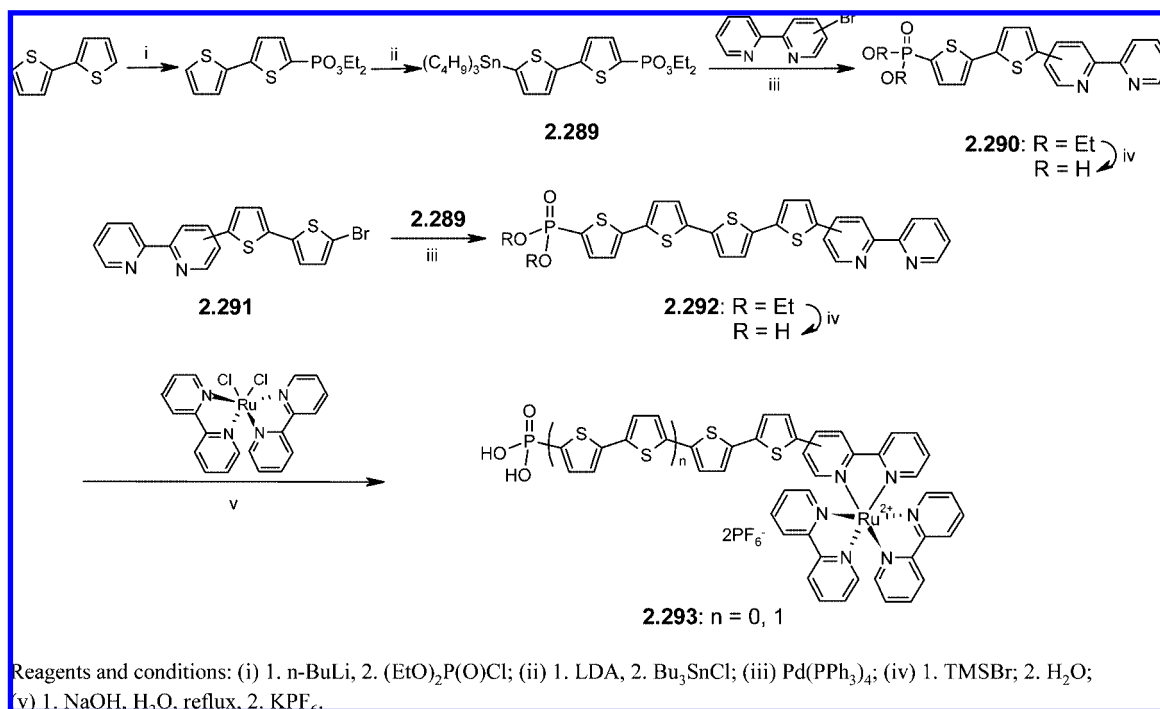
that there is an effective conjugation of the oligothienyl backbone and the ruthenium centers.

Roncali et al. synthesized functionalized bithiophene–bipyridine-based metal complexes **2.298** and **2.299** to prepare corresponding conjugated polymers by electrochemical polymerization (Chart 2.48).[377] The precursor ligand contained a polymerizable bithiophene, consisting of a thiophene and an EDOT unit, which was attached to the bipyridine ligand through an alkylsulfanyl linker. The electrochemical polymerization of the complexes formed three-dimensional networks which exhibited the typical signature of both the

π-conjugated polythiophene backbone and the immobilized metal complex.

Very recently, Wu et al. prepared novel Ru(II) complex **2.300** (Chart 2.49), which was used as sensitizer in DSSCs.[378] The new complex was synthesized from 4,4′-dicarboxylic acid-2,2′-bipyridine and 4,4′-bis(5-octyl-2,2′-bithiophenyl)-2,2′-bipyridine in the presence of [RuCl$_2$(p-cymene)]$_2$ and subsequent treatment with an excess of NH$_4$NCS. An UV–vis spectrum of the complex in DMF showed a MLCT-based transition at 553 nm along with two additional bands at 400 and 312 nm, which corresponded to the π−π*

Scheme 2.53

Reagents and conditions: (i) 1. n-BuLi, 2. (EtO)$_2$P(O)Cl; (ii) 1. LDA, 2. Bu$_3$SnCl; (iii) Pd(PPh$_3$)$_4$; (iv) 1. TMSBr; 2. H$_2$O; (v) 1. NaOH, H$_2$O, reflux, 2. KPF$_6$.

Scheme 2.54

2.294: n = 0, 1   **2.295**: n = 0, 1
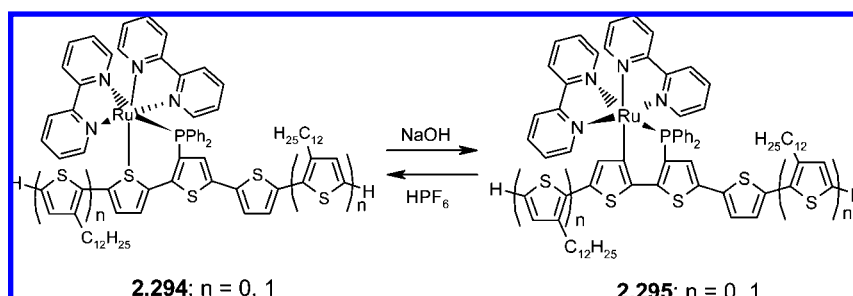
transition of the ligands. Semiempirical calculations performed for **2.300** confirmed that the HOMO level of the complex is localized on the Ru center and NCS ligands, while the LUMO level is located on the dicarboxylated bipyridine which binds to the TiO$_2$, thus allowing better electron injection from the excited Ru center to the TiO$_2$ surface. The absorption coefficient of **2.300** was higher compared to that of the widely used photosensitizer *cis*-di(thiocyanato)-bis(2,2′-bipyridyl-4,4′-dicarboxylate) ruthenium(II) (**2.301**, commonly known as N3-dye) due to the presence of bithiophene units in one of the ligands. Solar cells based on **2.300** displayed high current densities (I_{sc}) and gave high power conversion efficiencies of 8.54% under AM 1.5 illumination. This value is 10% higher than that of the standard complex **2.301** measured under the same experimental conditions.

2.10.3. Phenanthroline-Functionalized Oligothiophenes

Ru(II) complex **2.302** (Chart 2.49) based on dicarboxylated bipyridine and bithienyl-substituted phenanthroline was prepared and tested as photosensitizer in DSSCs.[379] The power conversion efficiency of the cell obtained under AM 1.5 sunlight illumination was 3.42%, which is lower than that of the previously reported cells with **2.300** and **2.301** under the same experimental conditions. This lowering of efficiency was ascribed to the partial localization of the

HOMO level on the ancillary ligand of the complex instead of being only located on the metal center and NCS group.

Araki et al. synthesized terthiophene-substituted phenanthroline **2.303** by Ni-catalyzed coupling of the Grignard reagent of terthiophene and 3,8-dibromophenanthroline (Scheme 2.55).[380] Ligand **2.304** was obtained by treatment of **2.303** with bromine and KSCN. Ru(II) complexes **2.305** and **2.306**, which were obtained by reaction of the ligands with [Ru(bipy)$_2$(OH$_2$)$_2$](NO$_3$)$_2$, showed a broad UV−vis absorption peaking at 442 nm corresponding to the combination of terthiophene $\pi-\pi^*$ and Ru-centered ^{1}MLCT transitions. The authors observed that electropolymerization of **2.306** generates polymer **P2.306** having alternate sexithiophene and Ru(II)-polypyridine complexes, resulting in compact electrochromic films on ITO electrodes at low surface concentrations. At higher surface concentrations, the formation of a fibrous polymer loosely bound to the electrode was favored. The utilization of this polymer as a functionalized molecular wire between nanogap electrodes to generate stable molecular devices was also explored.

The groups of Ziessel and Bäuerle prepared heterobinuclear Ru(II)- and Os(II)-polypyridine complexes **2.307** (Chart 2.50) linked through a quinquethiophene bridge with an intermetal separation of about 1.9 nm.[381] The ligand was prepared in 27% yield by Pd^0-catalyzed coupling of 2-iodo-1,10-phenanthroline and biszincated hexabutylquin-
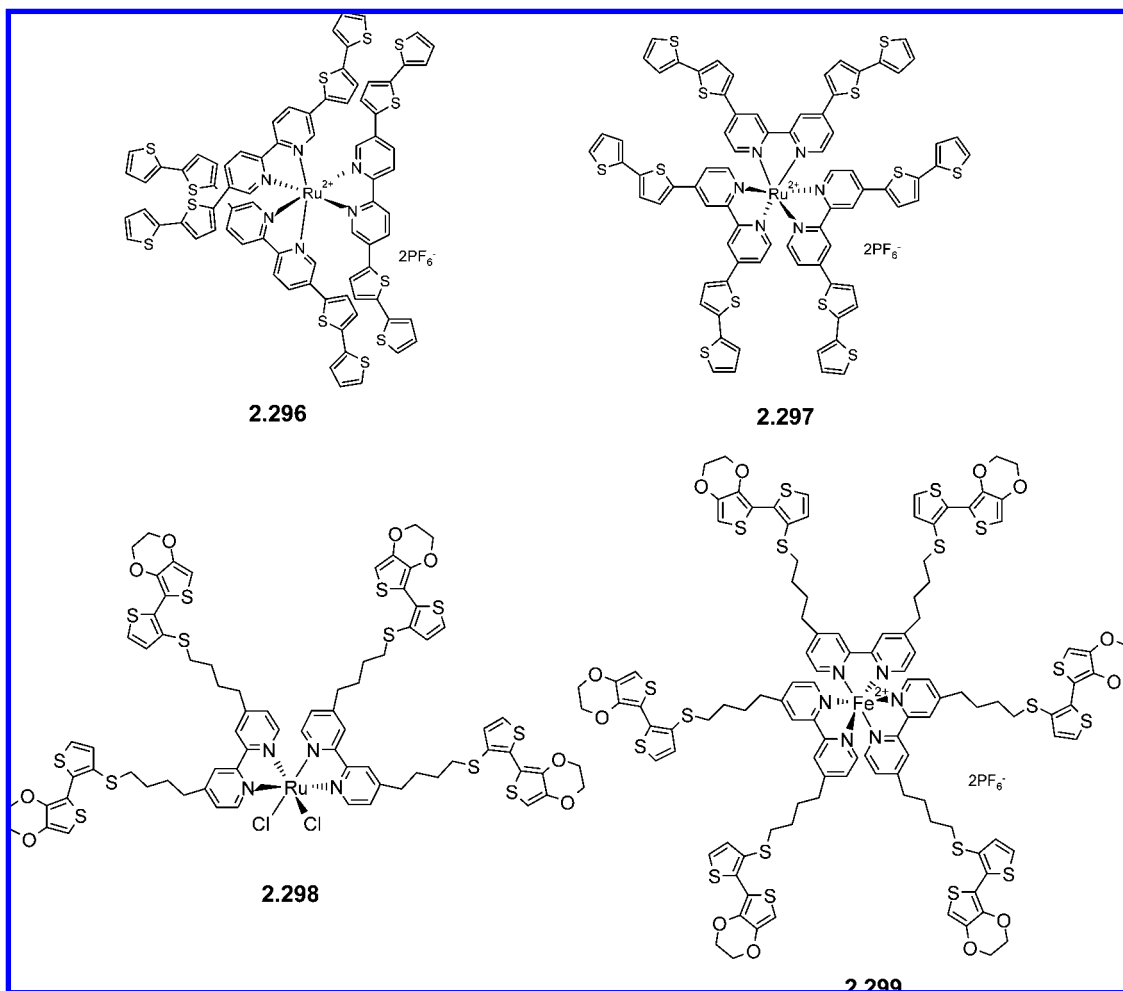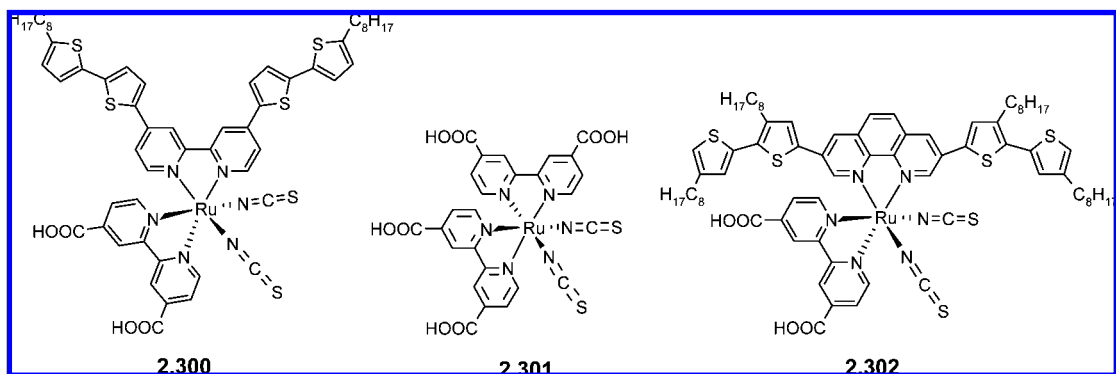
Chart 2.48

2.296

2.297

2.298

2.299

Chart 2.49

2.300

2.301

2.302

quethiophene, which on stepwise complexation with Ru(bipy)₂Cl₂ and Os(bipy)₂Cl₂ gave the desired metal complex **2.307** in 45% overall yield. The UV−vis spectrum of **2.307** showed the lowest energy band at 418 nm, corresponding to the overlap of the $\pi-\pi^*$ transitions of the oligothiophene and the ^{1}MLCT transition of the metal-based termini. An additional weak band at 615 nm was observed, corresponding to direct singlet−triplet absorption, leading to the population of the Os-centered ^{3}MLCT states. Irrespective of the excitation wavelength, a pure Os-based emission at 718 nm was observed due to the flow of excitation energy from the Ru complex to the luminescent Os-terminus through the oligothiophene chain.

In a recent report, Gordon et al. synthesized novel multicomponent Re(I) complex **2.308** (Chart 2.50), containing a hole-transporting β-substituted terthiophene unit at one end and an electron-transporting 1,3,4-oxadiazole at the other end of a central emissive Re(I) polypyridyl complex.[382] UV−vis spectra of the complex showed a MLCT absorption maximum at 409 nm and a weak and broad emission band at 474 nm. Electrochemical analysis revealed a band gap energy of 1.9 eV. Considering the low HOMO level of −5.38 eV, the complex represents a good hole transport material for OLEDs. On the other hand, the small band gap of **2.308** may also cause inefficient conversion of excitons into radiation, as is reflected in the low quantum yield.
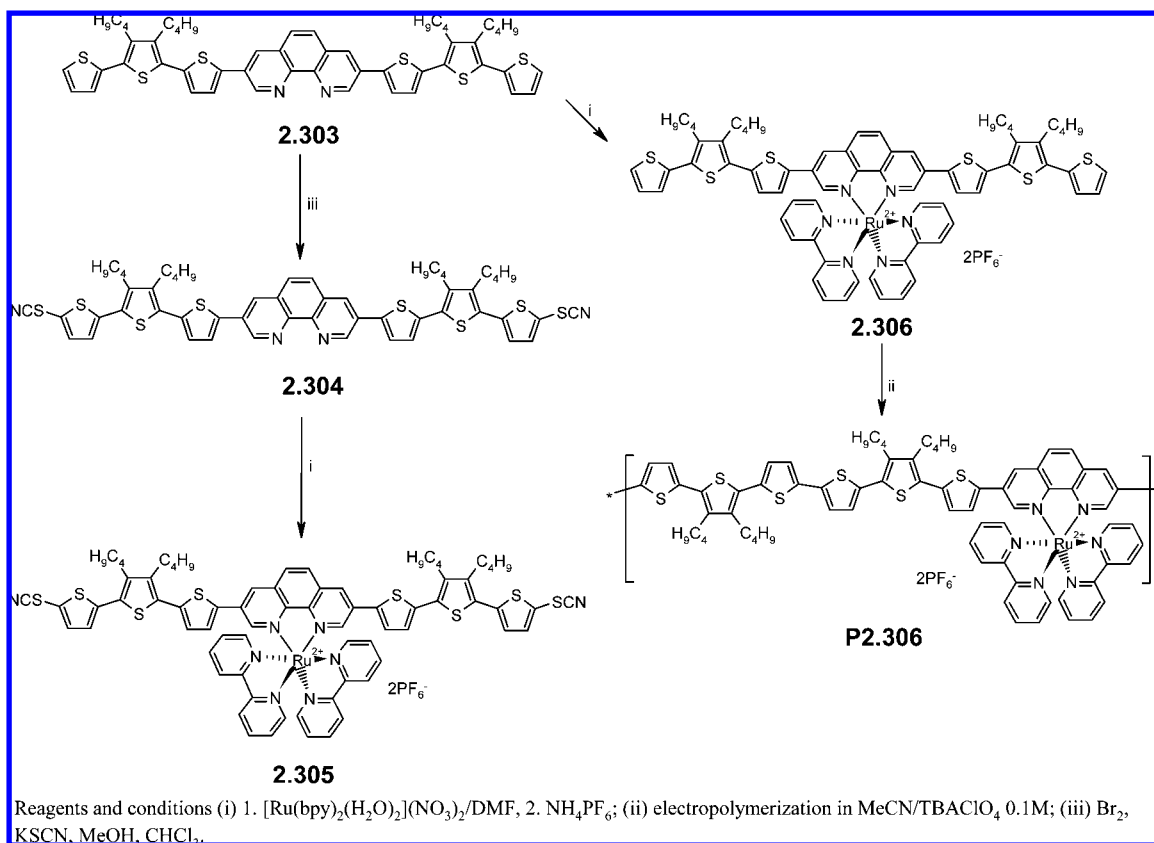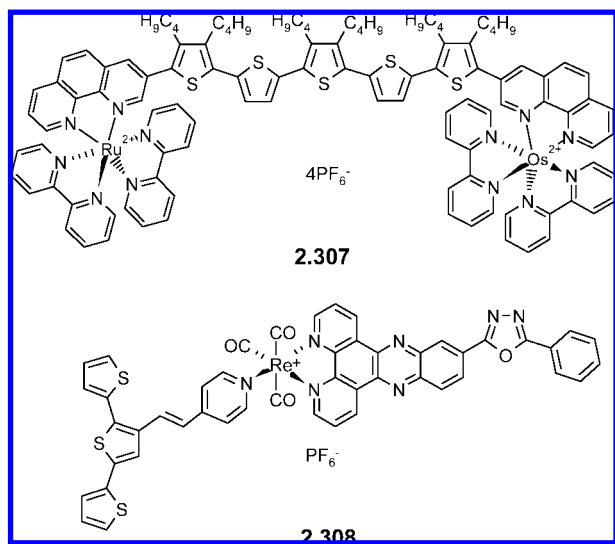
Scheme 2.55

Reagents and conditions (i) 1. [Ru(bpy)$_2$(H$_2$O)$_2$](NO$_3$)$_2$/DMF, 2. NH$_4$PF$_6$; (ii) electropolymerization in MeCN/TBAClO$_4$ 0.1M; (iii) Br$_2$, KSCN, MeOH, CHCl$_3$.

Chart 2.50

fluorescence spectroscopy showed a red shift of the low energy π−π* transition with respect to the parent oligothiophenes, which confirmed the extended π-conjugation between the oligothiophene and phenanthroline subunits. Characterization of the redox properties displayed additional evidence for the role of [1,10]phenanthroline as a π-bridging unit.

Furthermore, ethynyl-substituted and crescent-shaped ligands **2.312** (n = 0, 1) were obtained from **2.310** (n = 1) and **2.311** by iodination and successive Sonogashira-type coupling with trimethylsilyl acetylene (Scheme 2.56).[385] Cu(I) complexation of **2.312** (n = 0, 1), afforded homoleptic bis-phenanthroline complexes **2.313** (n = 0, 1) in 95 and 89% yield, respectively.[384] Here, the oligothiophene units in the ligands are arranged in two different directions around the pseudotetrahedral Cu(I) center. The formation of interlocked π-conjugated macrocycles and catenanes of these Cu(I) complexes **2.313** (n = 0, 1) is discussed in detail in section 4.2.2.

2.10.4. Other Ligand-Functionalized Oligothiophenes

Several metal chelating units have been incorporated to thiophenes, including Schiff-base complexes **2.314** and **2.315**,[386−388] and metal clusters **2.316** and **2.317** (Chart 2.52).[284,389] Polymers obtained from Schiff bases **2.314** and **2.315** showed the electrochromic behavior of the polythiophene backbone, which was influenced by the coordinating metal center. An alkali metal sensory effect has been reported for complex **2.315**, bearing a crown ether group. Metal cluster **2.316** (R = H) was prepared by reaction of 3′-ethynylterthiophene and [Mo$_2$(η-C$_5$H$_5$)$_2$(CO)$_4$] in toluene at room temperature in 75% yield, whereas **2.316** (R = Ph) was prepared with 3′-phenylethynylterthiophene at 80 °C in 25% yield. X-ray structure analysis of cluster **2.316** (R =

Bäuerle et al. recently developed an efficient synthetic route toward a series of phenanthroline-based oligothiophenes. Among the series of 2,2′-(oligothienyl)bis[1,10]-phenanthrolines (**2.309**),[383] 2,9-bis(oligothienyl)[1,10]-phenanthrolines (**2.310**)[383] and 2,9-bis(quaterthienyl)[1,10]-phenanthroline (**2.311**)[384]were synthesized by employing Negishi-type cross-coupling reactions (Chart 2.51). Derivatives **2.309** and **2.310** were obtained in moderate to high yield from the reaction of 2-iodo[1,10]phenanthroline or 2,9-diiodo[1,10]phenanthroline with *in situ* generated α-zincated ter- and quinquethiophenes. Ligand **2.311** was prepared by Pd^0-catalyzed coupling of the zincated terthiophene and iodinated 2,9-bis(thien-2-yl)phenanthroline. UV−vis and
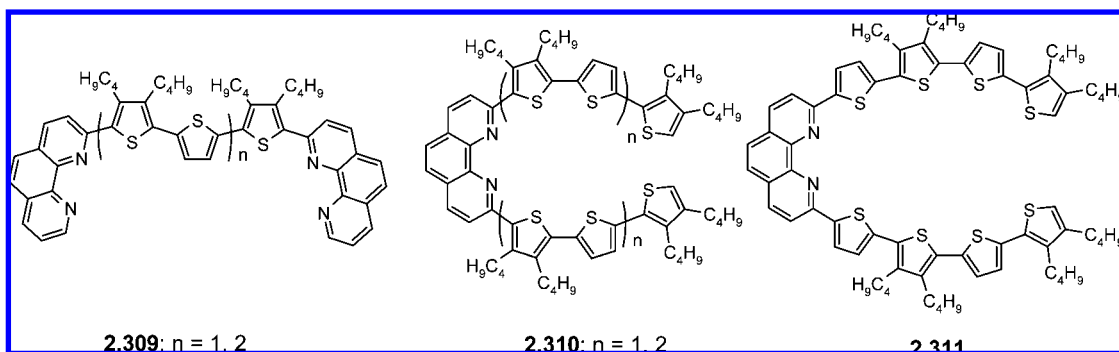
Chart 2.51

2.309: n = 1, 2   **2.310**: n = 1, 2   **2.311**

Scheme 2.56

2.312: n = 0, 1   **2.313**: n = 0, 1

Reagents and conditions: (i) Cu[CH₃CN]₄BF₄, CH₃CN, CH₂Cl₂

Chart 2.52

2.314: M = Cu, Ni   **2.315**: M = Cu, Ni   **2.316**: R = H, Ph   **2.317**
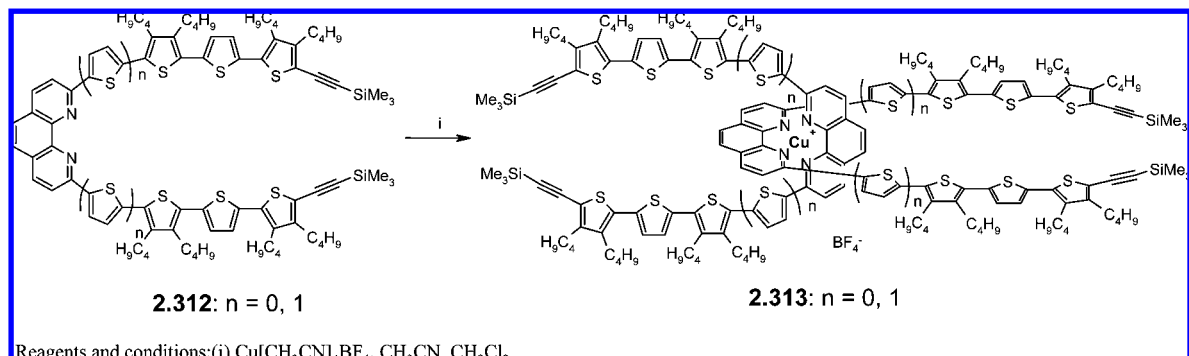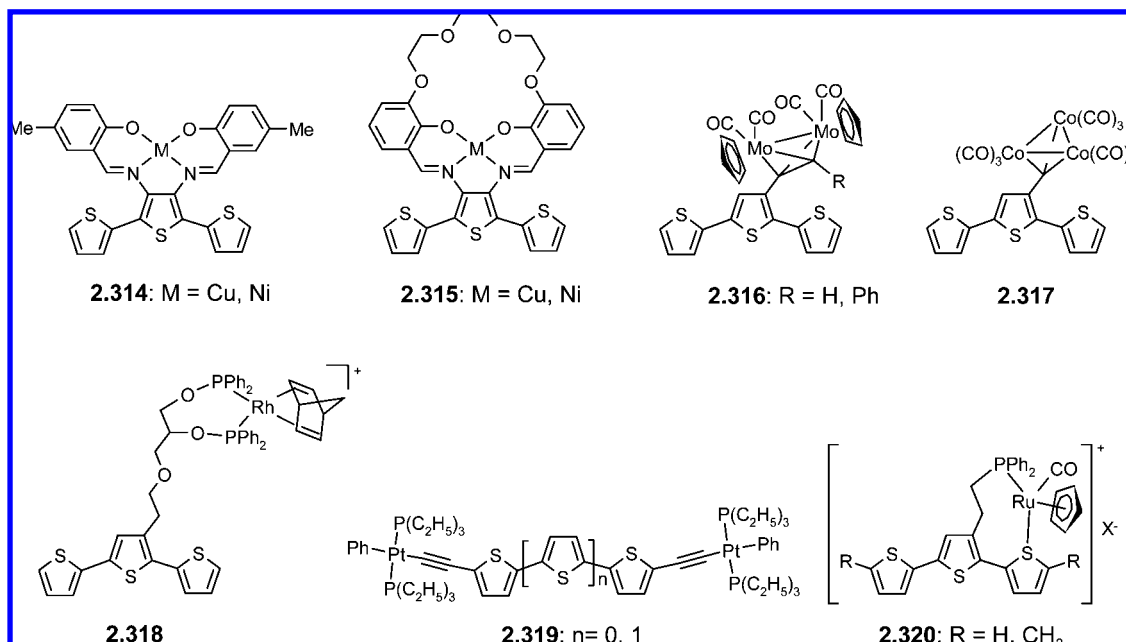
2.318   **2.319**: n= 0, 1   **2.320**: R = H, CH₃

H) showed that the two Mo centers departed from coplanarity of the middle thiophene ring. This out-of-plane behavior of the Mo centers with respect to the conjugated backbone was also seen in the electrochemical polymerization, which allowed the formation of electroactive films on the electrode surface. The terthiophene−cobalt carbonyl cluster complex **2.317** was prepared by reaction of 3′-chloromercurio-2,2′: 5′,2″-terthiophene and HCCo₃(CO)₉. The formation of electroactive films on electrode surfaces by electropolymerization was also reported.

Higgins and Mirkin successfully prepared electroactive polymers from metal cluster-functionalized terthiophene

2.318 (Chart 2.52). Oxidation of the terthiophene was possible due to its lower oxidation potential (0.6 V) in comparison to that of the Rh metal (∼0.9 V).[390]

Lewis et al. reported a series of dinuclear platinum complexes of acetylene-functionalized oligothiophenes **2.319** (n = 0, 1) (Chart 2.52).[391] The structures were established by X-ray crystallographic analyses. The complexes showed red-shifted absorption maxima compared to those of the parent ethynylated oligothiophenes ($\Delta\lambda = 38$ nm for **2.319**, n = 1), which indicates that the platinum center acts as net electron acceptor.

Chart 2.53

2.321: n = 1, 2   **2.322**   **2.323**

2.324: n = 1, 2   **2.325**: n = 1, 2 M = Pd, Pt   **2.326**: R = H, Ph, Thienyl, butyl

2.327   **2.328**   **2.329**: n = 1, 2 M = Pd, Cu, Zn
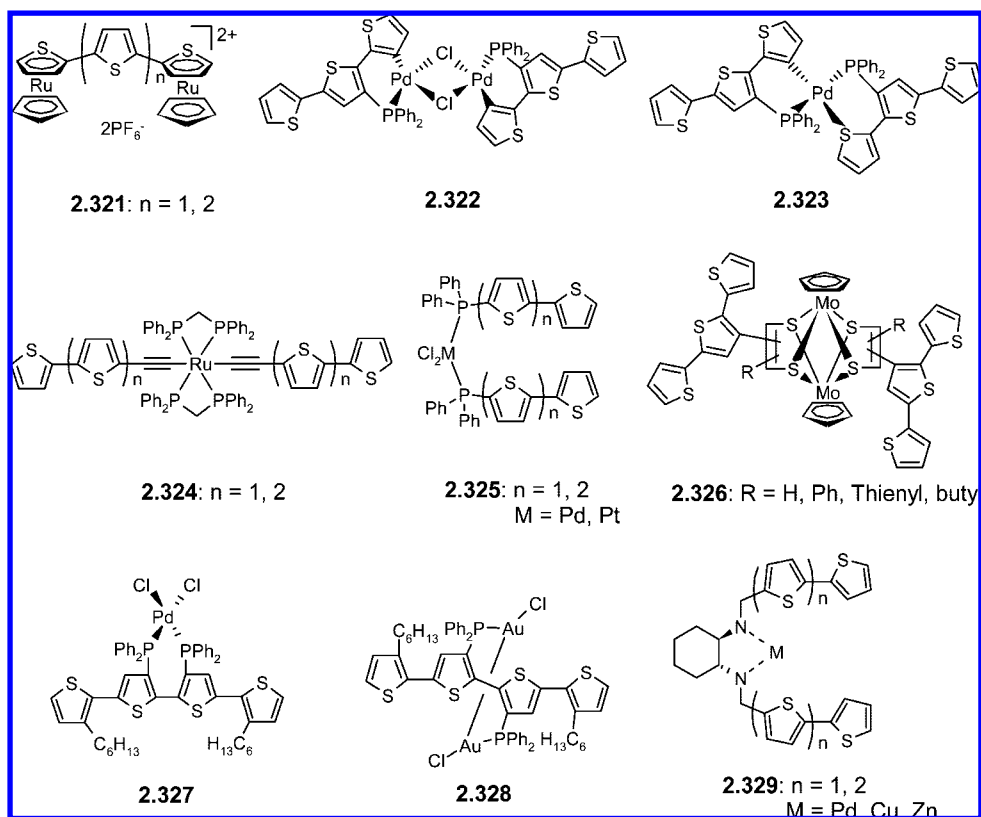
Ruthenium complexes of phosphin-containing terthiophene ligands **2.320** were synthesized with the aim to prepare oligomers or polymers with redox-switchable hemilabile ligands (Chart 2.52).[392] Interestingly, the ligand that is η^1-bound to the terminal thiophene was easily displaced when 4 equiv of acetonitrile were added. Spectroelectrochemical investigations of the corresponding electrochemically generated polymer revealed that the ruthenium centers showed a reversible and switchable intramolecular interaction with the polymer backbone.

Graf and Mann reported the synthesis of metal complexes **2.321** (*n* = 1, 2), in which terminal thiophenes of ter- and quaterthiophene moieties were directly complexed with cyclopentadienyl-Ru(I) (CpRu) (Chart 2.53).[393,394] Delocalization of positive charges on the uncomplexed oligothiophene(s) was favored upon oxidation, while electrons added upon reduction were localized only on the complexed terminal thiophene ring and CpRu. Although the complexes were thoroughly studied by several NMR methods and CV, UV−vis and fluorescence measurements were not reported.

Phosphinoterthiophenes having σ-bonded Pd-complexes (**2.322**, **2.323**) were prepared by the group of Wolf using 3′-diphenylphosphino-2,2′:5′,2″-terthiophene[372] and PdCl₂ in acidic medium (Chart 2.53).[395,396] The presence of *cis*- and *trans*-isomers has been comfirmed from ³¹P NMR specroscopy. Electropolymerization of these complexes showed large electronic interactions between Pd moieties and the polythiophene backbone, which produced an increase in conductivity of the polymer film. The increase in conductivity observed for **2.322** was attributed to the charge delocalization along the extended polythiophene chain and π-stacking, whereas for **2.323** a contribution from cross-metal delocalization was considered. The electropolymerization of a ruthenium complex of oligothienylacetylide (**2.324**) has been

reported to generate molecular wires based on alternate oligothiophene−ruthenium units.[397]
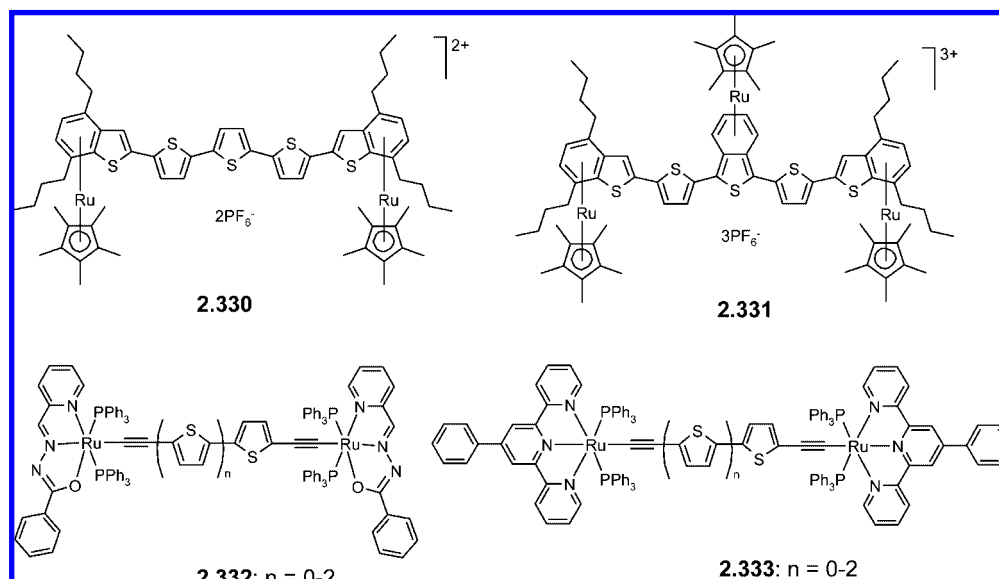
Some Pd and Pt complexes **2.325** (Chart 2.53) containing diphenylphosphino-substituted oligothiophenes were prepared and characterized by X-ray structure analysis, which showed π−π interaction between the oligothiophene rings in the solid state.[398] Third order nonlinear optical behavior was observed for complex **2.325** (*n* = 2), which was significantly stronger for the Pd complex compared to the corresponding Pt complex, suggesting that the metal center has a significant influence on nonlinear absorption.[399]

Kim et al. synthesized a series of terthiophene−organomolybdenum cluster complexes **2.326** (Chart 2.53) which were isolated as a mixture of *syn-* and *anti*-isomers.[400] After electropolymerization, the polymeric clusters exhibited an electrochromic response due to the electronic synergistic interaction of the metal sulfide clusters and the polythiophene backbone.

Wolf et al. prepared Pd and Au complexes **2.327** and **2.328** in which phosphine substituents are located on adjacent rings (Chart 2.53).[401] The structures were confirmed from X-ray crystallographic analysis, and changes in the interannular torsion angles due to backbone substitution and the metal groups were observed. In the metal complexes, both red shifts in the π−π* absorption transitions and a decrease in the oxidation potentials of the oligothiophene π-system due to the large interannular torsion angles were described, relative to unsubstituted oligomers. Electropolymerization of these complexes has not been reported.

Umani-Ronchi et al. recently explored the use of chiral C_2-symmetrical diamino-oligothiophenes **2.329** (Chart 2.53) as chiral ligands in palladium-,[101,402,403] copper-,[404] and zinc-catalyzed[403] enantioselective transformations. The key role played by these chiral ligands in a high level of enantiose-

Chart 2.54

2.11. Oligothiophenes Containing Recognition Groups

The following paragraph compiles a series of oligothiophenes endowed with recognition groups such as calixarenes, cyclodextrins, and crown ethers. The main reason for the functionalization of oligothiophenes with these recognition groups was to modulate the electrooptical properties of corresponding conducting polymers generated by electropolymerization of these oligomers and their selective host−guest interactions.
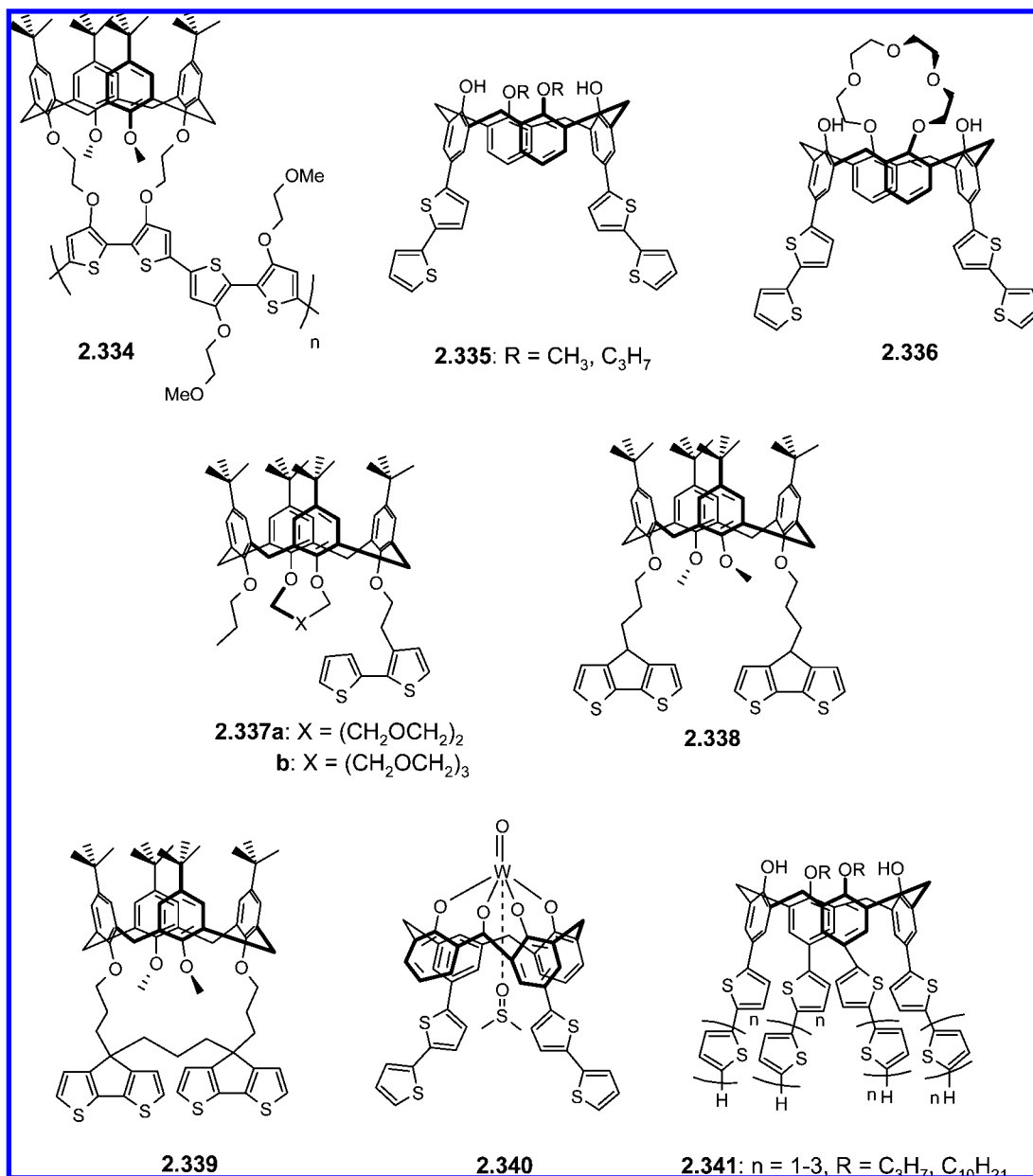
2.11.1. Calixarene-Functionalized Oligothiophenes

In 1995, Swager et al. synthesized the first calixarene-coupled diiodinated bithiophene, which afforded copolymer **2.334** (Chart 2.55), by Stille-type cross-coupling with distannylated 3,3′-bis(methoxyethoxy)bithiophene.[409] Selective recognition of Na^+ ions was studied by UV−vis spectroscopy and cyclic voltammetry. After addition of 0.5 mM of Na^+, cyclic voltammetric measurements showed a positive shift of the oxidation potential of about +100 mV with a simultaneous dramatic decrease in conductivity. This finding was attributed to an electrostatic effect of the Na^+ ions and reduced electron-donating ability of the sodium bound oxygen atoms of the calixarene.

Recently, the same group reported the synthesis of calixarene-functionalized bithiophenes **2.335** (Chart 2.55). Stille-type cross-coupling of the dihalo derivatives of calixarene and 5-stannyl-2,2′-bithiophene gave the hybrid compounds in 88 and 64% yield, respectively.[410] Electrochemical polymerization in CH_2Cl_2 solution resulted in polymers with zigzag conformation having alternate calixarene and quaterthiophene units. A decrease in conductivity of the polymer was observed when CH_3CN was used instead of CH_2Cl_2. The conductivity was recovered by the addition of trifluoroacetic acid, suggesting a proton-doped behavior of the conducting polymer.

Crown ether-functionalized calixarene **2.336** (Chart 2.55), in which two bithiophene units were attached at the termini of a calixarene moiety, was prepared by a similar procedure described above for **2.335**.[411] Polymer films formed by electropolymerization of **2.336** in CH_2Cl_2 or acidic CH_3CN

lectivity was further evidenced by crystallographic analysis. Especially, unprecedented noncovalent van der Waalls interactions between the inner thiophene and the metal center proved to be essential to create the stereochemical environment necessary in order to ensure high levels of chemical and optical yields.

The catalytic activity was further explored by electropolymerization of the Pd complex of ligand **2.329** ($n = 2$) on graphite elelctrodes.[405] The prepared thin polymer films were efficient in catalyzing several cross-coupling reactions including the Suzuki-, Heck-, and Sonogashira-type in good yields. This heterogeneous organometallic polymer film was reported to be easily recovered and reused without loss of activity.

Ru metal π-complexes of benzoanellated oligothiophenes **2.330** and **2.331** (Chart 2.54) were prepared by reaction of a benzoterthiophene-capped oligothiophene and [CpRu-(CH_3CN)_3]PF_6, to result in a η^6-coordination of the metal fragment. Spectroscopic and electrochemical results clearly showed the influence of the Ru centers on the conjugated oligothiophene unit.[406,407] Compared to the case of **2.330**, an additional η^6-complexation of the central benzo[c]thiophene unit in tris-metallated complex **2.331** showed a very low first reduction potential and a decrease in the first oxidation potential and consequently of the band gap. Significant red shifts in absorption and emission spectra were observed for complex **2.331** relative to **2.330**. The influence of the additional η^6-benzo[c]thiophene complexation was attributed to the enhanced quinoidal character of the oligothiophene ligand.[407]

In a recent report, Chen et al. synthesized a series of oligothiophenes **2.332** ($n = 0−2$) and **2.333** ($n = 0−2$) capped with ruthenium complexes (Chart 2.54).[408] Electrochemical and UV−vis−NIR studies confirmed that metal−metal charge transfer was observed. Furthermore, it was clearly demonstrated that, with increasing number of thiophene groups in the bis(ethynyl)oligothiophene bridge, intramolecular electron transfer is progressively reduced with a smooth transition from almost electronic delocalization ($n = 0$) to localization ($n = 2$). It was interesting that the presence of electron-rich ligands in complexes **2.332** was more favorable for electronic communication than the corresponding electron-deficient ligands in **2.333**.

Chart 2.55

solutions exhibited a conductivity of 0.6 S/cm. An increase in conductivity up to 5.2 S/cm was observed by addition of Ca^{2+} ions, whereas the addition of K$^+$ ions reduced the conductivity to <1% of its original value. The enhancement of conductivity upon addition of Ca^{2+} ions was discussed in terms of the dominant charge balance between the polymer backbone and the bound metal ions.

Mori et al. reported the synthesis of 1,3-bridged propoxy-calix[4]crown ethers **2.337** with a pendant 2,2′-bithienyl-3-hexyl unit (Chart 2.55).[412] Electropolymerization of **2.337** in CH$_2$Cl$_2$/CH$_3$CN mixtures formed chemically modified electrodes which were coated with poly(vinylchloride) membranes containing a lipophilic cation exchanger to avoid the sensitivity of the polymer toward dissolved oxygen. An ion-selective response of the coated polymer electrodes shows potential in both potentiometric and amperometric recognition sensors.

Sannicolò et al. synthesized cyclopentadibithiophenes (CPDT) **2.338** and **2.339** functionalized with calixarene moieties (Chart 2.55).[413] **2.338** was prepared by alkylation

of CPDT with 1,3-dibromopropane in the presence of *n*-BuLi at −70 °C, followed by reaction with the calix[4]arene in basic medium. **2.339** was synthesized in three steps, starting from a stoichiometry-controlled alkylation of CPDT with 1,3-dibromopropane, followed by reaction with the calix[4]arene under basic conditions and final methylation using NaH/MeI. Electropolymerization of the monomers formed insoluble cross-linked polymers. Quartz crystal microbalance (QCM) analyses showed that the adsorption constants of the calix-arene-functionalized polymers were extremely high for toulene. In fact, these materials displayed an adsorption capacity even more efficient than that shown for the highly sorbent Ni(SCN)$_2$(4-picoline)$_4$ complex. It is interesting to note that the adsorption properties of calixarene-functional-ized polymers for toluene are by a magnitude of three orders higher than those exhibited for an analogous polymer without calixarene units.

Vigalok and Swager synthesized a unique bithiophene-functionalized tungsten-capped calixarene **2.340** (Chart 2.55), in which the calixarene cavity showed Lewis acidic behav-

Chart 2.56

2.342: n = 0, 0.25, 0.5, 1
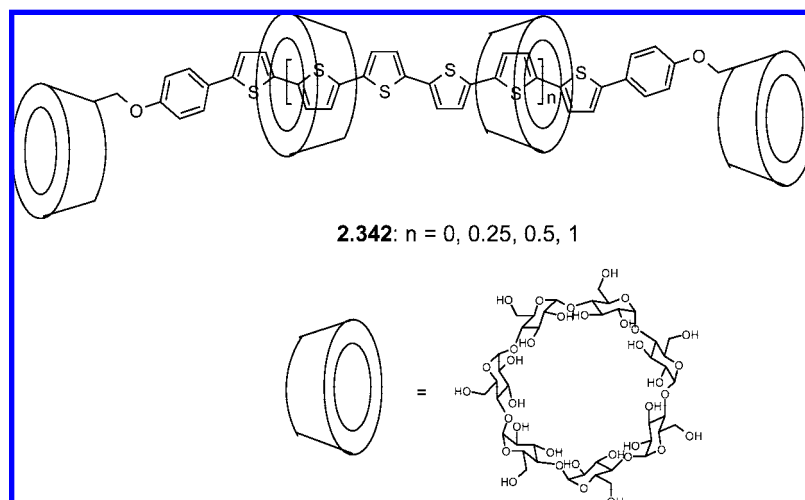
ior.[414] Compound **2.340** was prepared by complexation of a dibromocalixarene with $WOCl_4$ to form a calixarene tungsten-oxo derivative, in which the W=O bond was further masked with ethylene glycol. Bithiophene moieties were attached to the calixarene by Stille-type cross-coupling reactions, and finally deprotection of the glycol unit in $DMSO/H_2O$ afforded **2.340** as its DMSO-adduct, in which DMSO was complexed to the tungsten atom through the calixarene cavity. Reaction of **2.340** with various formamides afforded corresponding host−guest adducts. The replacement of DMSO by forma-mide guest molecules was confirmed by the appearance of a formyl signal in the 3−4 ppm range in ^{1}H NMR spectra. Conducting polymers were prepared by electropolymerization of **2.340** in the presence of different guest molecules, and the formation of 1:1 complexes was observed. The polymer containing monosubstituted formamides showed slightly lower conductivity (∼20−30 S/cm) relative to the H_2O adduct (∼40 S/cm). The conductivity was significantly lowered for the disubstituted formamide complexes (∼4−5 S/cm).

Sun et al. recently synthesized a series of calix[4]arene derivatives **2.341** endowed with four oligothiophene moieties (Chart 2.55).[415] Bromination of the different tetraalkoxycalix-[4]arenes with NBS followed by cross-coupling reaction with thienylmagnesium bromide in the presence of $PdCl_2$(dppf) as catalyst afforded the corresponding tetra(thienyl)calix[4]-arenes. Higher homologues up to quaterthiophenes were obtained in yields of 70−80% by repeating the sequence of bromination and cross-coupling with thienylmagnesium bromide. Absorption and emission spectra of the compounds were measured in chloroform solution and compared with corresponding 2-(4-alkoxy-3,5-dimethylphenyl)oligothiophenes. A strong intrachromophoric interaction between the oligo-thiophene arms was reported for **2.341**, resulting in slightly blue-shifted absorption and red-shifted emission bands compared to the case of the parent 2-(4-alkoxy-3,5-dimeth-ylphenyl)quaterthiophene.

Harada et al.[416] synthesized a series of β-cyclodextrin end-capped oligothiophene-rotaxanes **2.342** (Chart 2.56) by employing Suzuki-coupling reactions of bisborylated bi- and terthiophene-rotaxanes with iodophenyl-cyclodextrin. Quater- and sexithiophene derivatives were isolated from the same reactions and were separated by reverse phase HPLC. The inclusion of rotaxanes and their influences were studied by ^{1}H NMR. Although no change in the absorption behavior was observed, the fluorescence efficiency effectively in-

creases in the presence of the rotaxane due to suppression of intermolecular interactions. The recognition of guest molecules by terminal cyclodextrins was also investigated.

2.11.2. Crown Ether-Functionalized Oligothiophenes

Macrocyclic crown ethers are among the most investigated receptors and are able to complex various metal cations. The first series of oligothiophenes functionalized with 12-crown-4 (**2.343**: n = 0, 1) and 18-crown-6 (**2.344**) via flexible alkoxy spacers were reported by Bäuerle et al. (Chart 2.57).[417,418] The oligomers were synthesized with 66, 48, and 72% yield, respectively, by reaction of ω-brominated alkyl(oligo)th-iophenes and 12-crown-4-methanol or 18-crown-6-methanol using tetrabutylammonium hydrogen sulfate as phase transfer catalyst. Compounds **2.343** (n = 0, 1) were easily electropo-lymerized to the corresponding crown-ether-functionalized poly(alkylbithiophene) **P2.343** (n = 0) and poly(alkylter-thiophene) **P2.343** (n = 1). The polymer films formed by electropolymerization of the oligomers were characterized in monomer-free electrolytes showing two redox waves. Very low potentials (0.45 and 0.86 V vs Ag/Ag$^+$) were measured for **P2.343** (n = 0). In contrast, the higher potential (0.60 and 0.96 V vs Ag/Ag$^+$) for **P2.343** (n = 1) was attributed to its shorter conjugation length with an average of 15−18 thiophene units. During electrochemical polymerization of bithiophene **2.344**, moderate film forming ability was observed due to the steric hindrance of 18-crown-6 unit. UV−vis spectra of **P2.344** were blue-shifted in comparison to those of **P2.343** (n = 0) (Δλ = 61 nm), ascribed to the close proximity of the crown ether units in the former, which induces conformational change and led to the distortion of the thiophene rings due to steric repulsion. The influence of alkali metal ions on the redox behavior of the polymers could be rationalized in terms of host−guest interactions of the crown ethers and metal ions. Polymers **P2.343** were more suitable for Li$^+$, which at concentrations as low as 5×10^{-5} M affected the CV response visually, whereas the 18-crown-6 cavity in **P2.344** was more selective toward K$^+$ compared to Li$^+$ or Na$^+$.

Zotti et al. reported cyclopentadithiophene precursors comprising a 16-crown-5-ether ring **2.345** which is coplanar relative to the bithiophene unit and a 15-crown-5-ether **2.346** perpendicular to the bithiophene unit (Chart 2.57).[419] Elec-tropolymerization of the monomers resulted in extensively

Chart 2.57

2.343: n = 0, 1 2.344

2.345 2.346 2.347 2.348; n = 1, 2

2.349: n = 1, 2; m = 0, 1 2.350
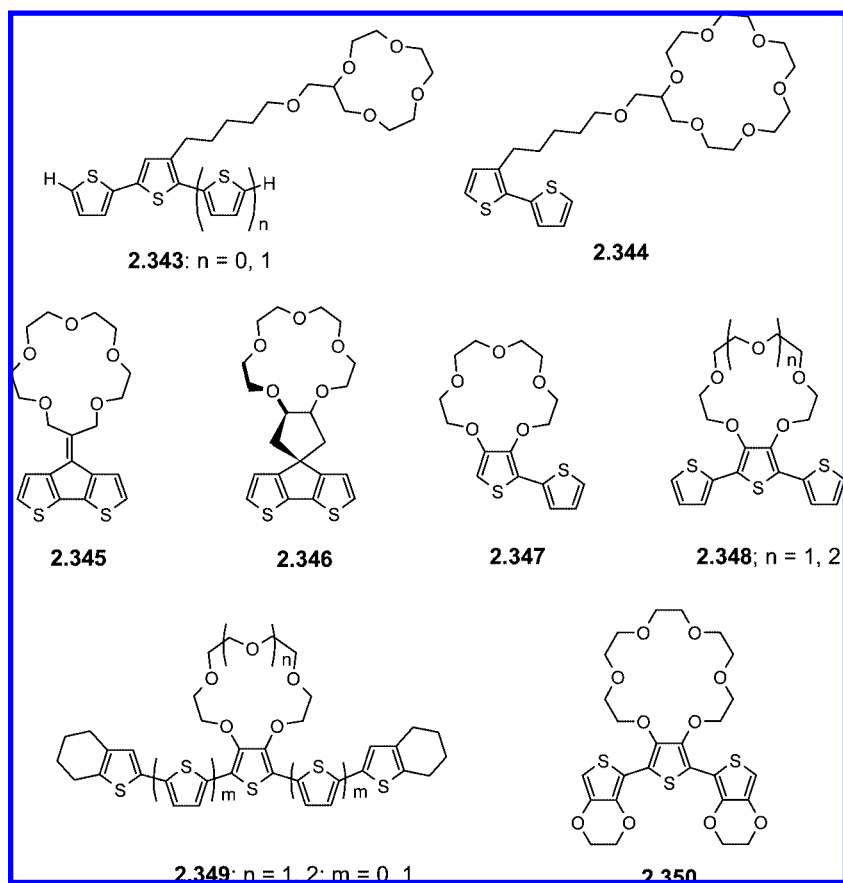
conjugated polymers due to the decrease in steric interaction between the crown ether and the π-conjugated backbone. Polythiophene **P2.345** showed redox processes at lower potentials than that for **P2.346**, which was attributed to the strong π-dimerization of the radical cations in the case of the former polymer and the closer packing of the polymer chains. Increased conjugation was further supported by absorption spectra of these polymers in their neutral state. A 350 mV positive shift of the oxidation potential was observed for **P2.345** in the presence of Na$^+$ ions compared to that observed in the presence of the Et$_4$N$^+$ ions, which was explained by a sandwich-coordination of the Na$^+$ ions to the crown ether moieties. On the other hand, **P2.346** was insensitive to changes of cationic species in solution.

Bi- and terthiophenes **2.347** and **2.348** ($n = 1$), in which 15-crown-5 units were directly attached to one of the thiophenes, were synthesized by Stille-type cross-coupling reactions (Chart 2.57).[420] The redox behavior was largely influenced by the recognition process of the metal cations. Thus, the oxidation potential of **2.347** was more affected by the presence of Na$^+$ ions ($\Delta E_p = 48$ mV) than by Li$^+$ (23 mV) or K$^+$ (22 mV) ions, whereas **2.348** ($n = 1$) showed a negligible effect upon addition of metal cations.
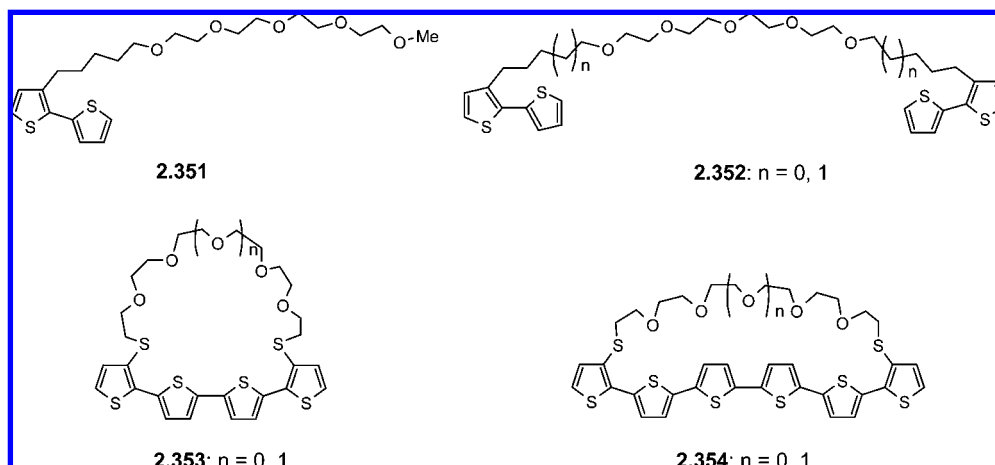
Furthermore, Bäuerle et al. reported a series of end-capped oligothiophene derivatives **2.349** (Chart 2.57), in which the crown ether moieties were attached directly to the 3,4-position of the central thiophene unit.[421] The compounds were synthesized by Pd^0-catalyzed cross-coupling reactions of 2,5-dibromothieno-crown ethers and the corresponding stannyl derivatives of end-capped oligothiophenes. Electrochemical investigations performed for **2.349** in the presence of metal cations showed that the redox behavior was strongly

influenced by the molecular recognition process and by the polarity of the solvent. An anodic shift of the oxidation potentials was observed in the presence of Li$^+$, Na$^+$, K$^+$, NH$_4$$^+$, and Ba^{2+} ions. The 1:1 complexes were formed due to electrostatic interactions between complexed cations and the redox center. All oligomers showed the highest recognition toward divalent Ba^{2+} ions, which was 2−3 times larger than that toward monovalent cations. Therefore, the largest shifts of about 0.3 V were observed for those oligomers containing a 18-crown-6 unit (**2.349**, $n = 2$). Furthermore, the magnitude of the cation-induced shifts depended on the host/guest complementarity, which can be defined by considering the inner diameter of the macrocycle and the size of the complexed cation.
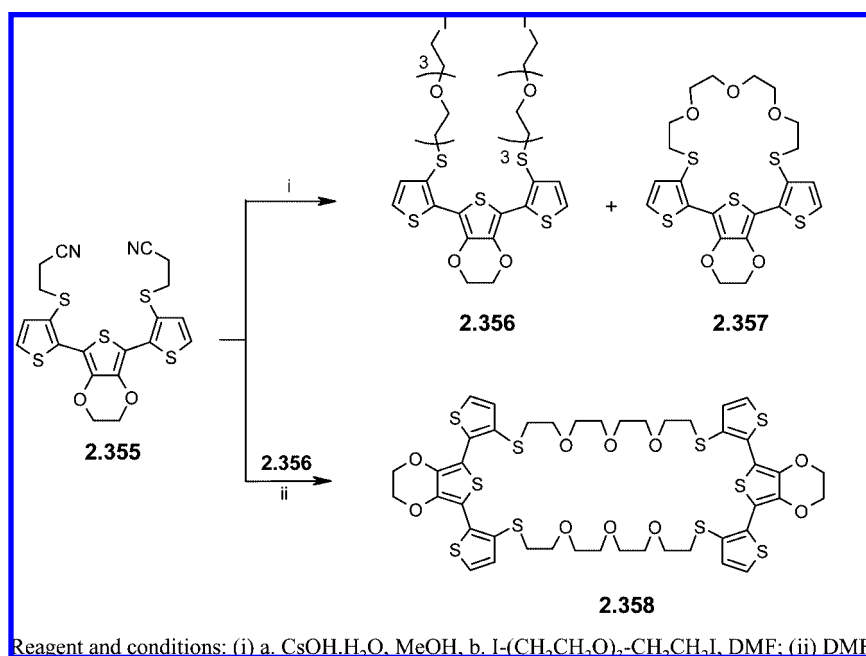
Terthiophene **2.348** ($n = 2$) and EDOT-containing derivative **2.350**, in which 18-crown-6 moieties were directly attached to the 3,4-position of the central thiophene ring, were prepared by the group of Zotti (Chart 2.57).[422] These oligomers showed maximum absorption at 365 and 366 nm, respectively, which were significantly blue-shifted ($\Delta\lambda = 20−30$ nm) after the addition of 0.1 M Na$^+$ or K$^+$ ions. The polymer films prepared by electropolymerization of the oligomers showed little influence by the addition of alkali metal ions. Furthermore, electrochemical quartz crystal microbalance analysis of the alkali metal coordination ability of the polymer films in acetonitrile solution revealed a lower degree of coordination, which was attributed to the loss of degrees of freedom in the crown-ether moiety.

Compounds **2.351** and **2.352** ($n = 1$) were synthesized in 50 and 40% yield by the reaction of 3-(5-bromopentyl)-2,2′-bithiophene with tetraethylene glycol monomethyl ether and tetraethylene glycol, respectively, in the presence of a phase

Chart 2.58

2.351

2.352: n = 0, 1

2.353: n = 0, 1

2.354: n = 0, 1

Scheme 2.57

2.355

2.356

2.357

2.358

Reagent and conditions: (i) a. CsOH.H₂O, MeOH, b. I-(CH₂CH₂O)₃-CH₂CH₂I, DMF; (ii) DMF

transfer catalyst (Chart 2.58).[418] The electrochemical polymerization of **2.351** in the presence of alkali metal ions generated a polymer which showed a positive shift of the oxidation potential ($\Delta E_p = 50-160$ mV) compared to the case of a polymer formed in the absence of the metal ions. In contrast to this behavior, polymerization of **2.352** in the presence of alkali metal ions gave a polymer with increased conjugation length and showed a negative shift of the oxidation potential ($\Delta E_p = 20-40$ mV). UV−vis absorption maxima of **P2.351** and **P2.352** in the absence of metal ions were observed at 508 and 482 nm, respectively. Upon addition of metal ions, a 17−30 nm blue shift was observed for **P2.351** and a 22−29 nm red shift for **P2.352**. These results were explained in terms of preorganization of the bithiophene units in the presence of alkali metals.

Blanchard et al. reported a decrease of 0.3 V in the oxidation potential of **P2.352** ($n = 0$) when it is polymerized in the presence of Ba²⁺ ions. This effect was attributed to a template effect associated with the interaction between the oligooxyethylene segments and Ba²⁺ ions during the electropolymerization process.[423]

Roncali et al.[424] recently synthesized some macrocyclic oxyethylene-bridged oligothiophenes **2.353** and **2.354** in which oxyethylene groups were attached to the internal β-position of both terminal thiophenes *via* a sulfide linkage (Chart 2.58). ¹H NMR and UV−vis spectroscopic analysis of the macrocycles in the presence of metal ions (Ba²⁺, Sr²⁺, Pb²⁺) revealed the formation of 1:1 complexes and resulted in conformational transitions in the π-conjugated system. Absorption spectra of **2.353** showed small red shifts in the presence of metal cations, whereas no change was observed for **2.354**. Furthermore, the cation binding abilities of these macrocycles and their influence on the electrochemical responses were also discussed.

Recently, macrocycle **2.357** derived from a terthiophene bearing a median EDOT unit was synthesized in 41% yield by a ring closure reaction under high dilution conditions of diiodooligooxyethylene and a dithiolate which was prepared by thiolate deprotection of bis(2-cyanoethylsulfanyl)terthiophene **2.355** (Scheme 2.57).[425] During the synthesis of **2.357**, diiodo compound **2.356** was also formed in low yield, which on further ring-closure under high dilution condition using the deprotected dithiolate gave macrocycle **2.358** in

Chart 2.59

2.359; n = 0, 1   **2.360**
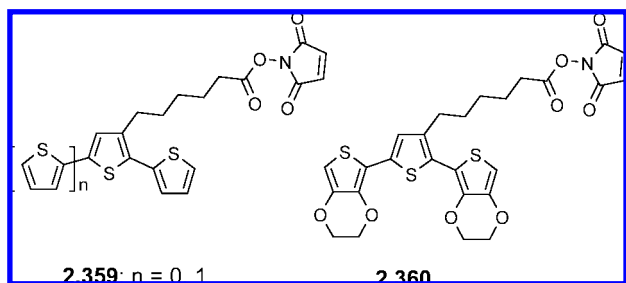
36% yield. The metal cation complexing properties of the compounds were studied by ^{1}H NMR, UV−vis spectroscopy, and cyclic voltammetry. Compound **2.358** showed no complexing ability toward metal ions. In contrast, compound **2.357** exhibited interesting complexing properties toward Pb^{2+}. However, because of the self-rigidification of the conjugated structure by the median EDOT unit, cation complexation did not produce any noticeable conformational change in the conjugated system, in contrast to compounds **2.353** without EDOT units.

2.12. Biologically Active Oligothiophenes

Over the past decade, conjugated polymers (CPs) have been widely implemented in amperometric biosensors.[426−428] The integration of biomolecules to the backbone of CPs is a difficult process and a key challenge toward the design and preparation of biosensory materials. The functionalization of CPs can be achieved in various ways: (1) the attachment of biomolecules to the oligomer backbone prior to their polymerization; (2) the attachment of biomolecules to the polymer backbone during the polymerization process; and (3) the attachment of biomolecules by covalent linkages to reactive CP films. In the last two cases, however, it is difficult to estimate the ratio of biofunctionality to the CP backbones.

The characterization of different biofunctionalities attached to the backbone of oligomers and polymers is usually carried out by cyclic voltammetric and UV−vis spectroscopic measurements. Additionally, it is also well-known that fluorescence techniques provide useful information concerning structure, distance, orientation, complexation, and location of biomolecules. Furthermore, time-resolved spectroscopy reveals the dynamics and kinetics of the attached biomolecules. As a result, many strategies for fluorescence labeling of biomolecules, especially with oligothiophenes, have been developed in recent years due to their wide absorption and emission windows depending on the conjugation length.

Bäuerle and co-workers reported the attachment of *N*-hydroxysuccinimide (NHS) esters to bi- and terthiophenes **2.359** (Chart 2.59).[426,429] Their syntheses were performed by conversion of 3-bromopentyl-substituted oligothiophenes to nitriles and successively to carboxylic acids in overall yields of 70−87%. Treatment of the carboxylic acids with oxalyl chloride formed corresponding acid chlorides, which then reacted with NHS to give the corresponding active ester-functionlized oligothiophenes **2.359** in about 70% yield. After electrochemical polymerization, postfunctionalization of the active ester groups at the polymer surface was carried out with amino groups of enzymes, such as glucose oxidase, by immersion of modified electrodes in phosphate buffer solutions of the protein. The advantage of these functionalized polythiophene-modified electrodes as amperometric sensors was the high redox stability of the polythiophene films, in

which deterioration by enzymatically generated H$_2$O$_2$ is less probable. A novel effective method for the postfunctionalization of polythiophene surfaces with reactive amines and their utilization in sensor applications was presented.[426,429]
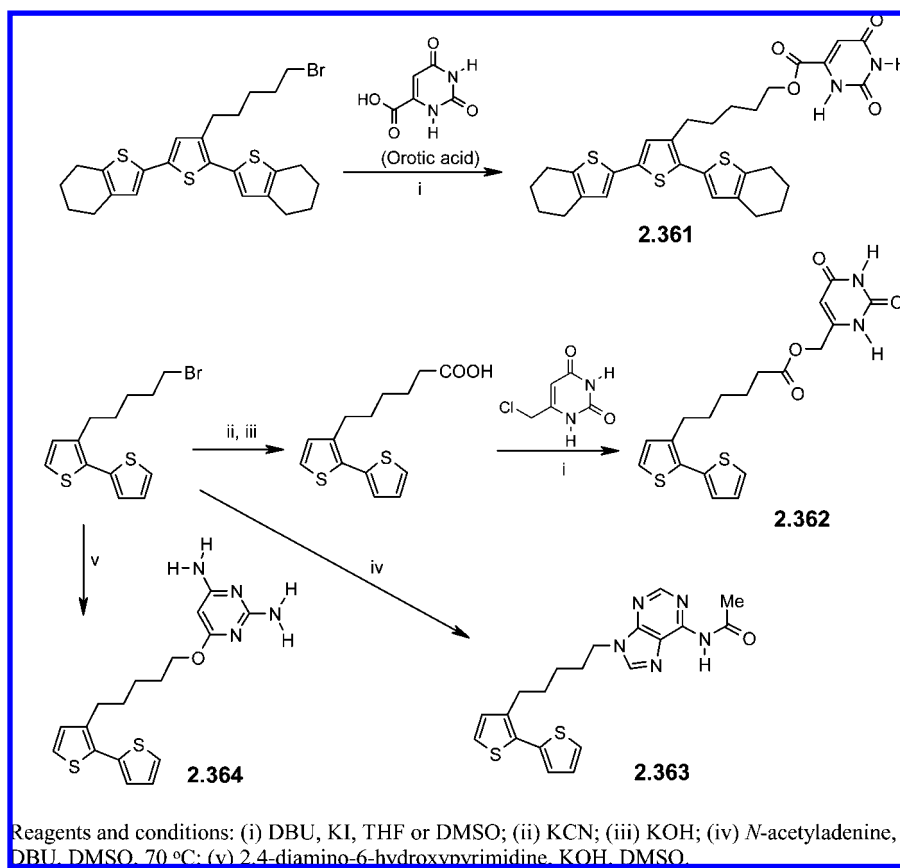
As realized later, the polymers formed from **2.359** were electrochemically inactive in aqueous environments due to the hydrophobic polythiophene chains. Thus, analogous oligothiophene **2.360** (Chart 2.59) bearing EDOT groups was synthesized in order to improve the performance of the corresponding polymer in aqueous electrolytes for biosensor applications.[430]

Furthermore, Bäuerle et al. prepared uracil-substituted "end-capped" terthiophene **2.361** and bithiophene **2.362** (Scheme 2.58).[431,432] **2.361** was prepared by reaction of 5-bromopentyl-substituted terthiophene with orotic acid in 38% yield. Bithiophene derivative **2.362** was synthesized by conversion of 3-(5-bromopentyl)-2,2′-bithiophene to the nitrile and carboxylic acid followed by reaction with 6-(chloromethyl)uracil in 36% yield. The molecular recognition properties of **2.361** and **2.362** with complementary acetyl-9-octyladenine and 2,4-diacetamido-6-pentoxypyrimidine were studied by cyclic voltammetry in CH$_2$Cl$_2$ solutions. A positive shift of the oxidation potential ($\Delta E = 20-130$ mV) was observed upon addition of complimentary nucleobases to the electrolyte.
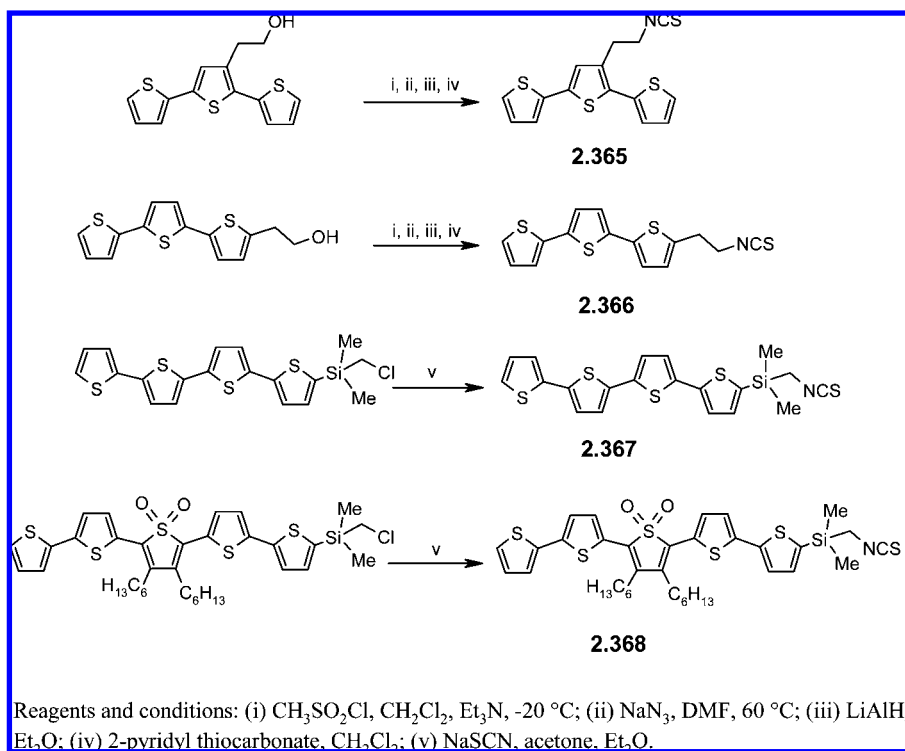
Adenine-functionalized bithiophene **2.363** was synthesized in 82% yield by coupling 3-(5-bromopentyl)-2,2′-bithiophene with *N*-acetyladenine in DMSO in the presence of DBU as base (Scheme 2.58),[432] whereas diaminopyrimidine-substituted bithiophene derivative **2.364** (87%) was prepared by reaction with 2,4-diamino-6-hydroxypyrimidine and KOH as base.[433] The bithiophenes were electropolymerized to their corresponding polymers. The interaction of **P2.363** and **P2.364** with complementary nucleobases revealed large changes in their electrochemical properties.[432] The multiple hydrogen bonds formed could be identified in ^{1}H NMR spectra due to the downfield shift of N*H*-protons. Cyclic voltammetry and spectroelectrochemical measurements demonstrated that successive addition of complementary bases to the nucleobase-substituted polymers led to a specific tuning of the electrochemical and optical properties of the backbone. These results further demonstrated that although the molecular recognition groups are not in direct conjugation with the polymer backbone, the chemical information based on the formation of specific hydrogen bonds was transformed into changes of the electrooptical response of the conjugated polymer.

Due to their variable absorption and emission wavelengths, oligothiophenes can also be used as unique photostable fluorescent markers for biomolecules. Thus, Barbarella et al. reported the introduction of isothiocyanate functionalities into oligothiophene backbones. These can react with amino groups of lysine residues to form urea bonds without affecting the optical properties of the oligothiophene. Consequently, they can be used as fluorescent markers.[434,435] Terthiophenes **2.365** and **2.366** were prepared in four steps by transformation of corresponding alcohols to isothiocyanates as depicted in Scheme 2.59. In a different approach, oligomers **2.367** and **2.368** were prepared by conversion of chloromethylsilanes to corresponding isothiocyanates by reaction with sodium thiocyante. Absorption and emission spectra of the oligomers in dichloromethane solutions showed a red shift upon increasing the conjugation length. Reaction of isothiocyanates **2.365**−**2.368** with amino groups of lysine residues as a part of bovine serum albumin (BSA) forms

Scheme 2.58

Reagents and conditions: (i) DBU, KI, THF or DMSO; (ii) KCN; (iii) KOH; (iv) *N*-acetyladenine, DBU, DMSO, 70 °C; (v) 2,4-diamino-6-hydroxypyrimidine, KOH, DMSO.

Scheme 2.59

Reagents and conditions: (i) CH₃SO₂Cl, CH₂Cl₂, Et₃N, -20 °C; (ii) NaN₃, DMF, 60 °C; (iii) LiAlH₄ Et₂O; (iv) 2-pyridyl thiocarbonate, CH₂Cl₂; (v) NaSCN, acetone, Et₂O.
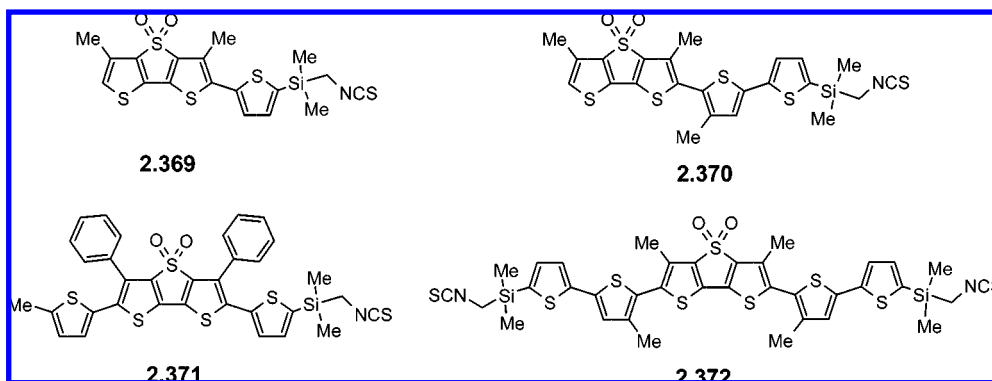
oligothiophene—BSA conjugates, which showed high photoluminescence and chemical stabilities. Conjugation of *S,S*-dioxide derivative **2.368** with monoclonal anti-CD8 antibody was also studied, and an increase in the fluorescence intensity was reported upon increasing the fluorophore—protein molar ratio.

Barbarella et al. further synthesized some fused *S,S*-dioxide oligothiophenes comprising terminal isothiocyanate functionalities **2.369**−**2.372** (Chart 2.60).[436] The compounds were prepared by Stille-type cross-coupling of mono- and dibrominated rigid cores and appropriate (chloromethyl)dimethylsilyl thienyl stannanes followed by conversion of the

Chart 2.60

2.369 **2.370**

2.371 **2.372**

Scheme 2.60

2.373 **2.374**

2.375

Reagents and conditions: (i) benzylbromide, DBU, toluene, rt, 15h; (ii) Hg(C$_5$H$_{11}$O$_2$)$_2$/I$_2$, CH$_2$Cl$_2$:AcOH (95:5), 0 °C-rt, 18h; (iii) 4,3'-dihexyl-2,2'-bithiophene-5-boronic acid, Pd(PPh$_3$)$_4$, CsF, THF, reflux; (iv) Bu$_4$NOH, THF, reflux; (v) 1. ByBOP, DIPEA, CH$_2$Cl$_2$ DMF (9:1), 2. 90% TFA.
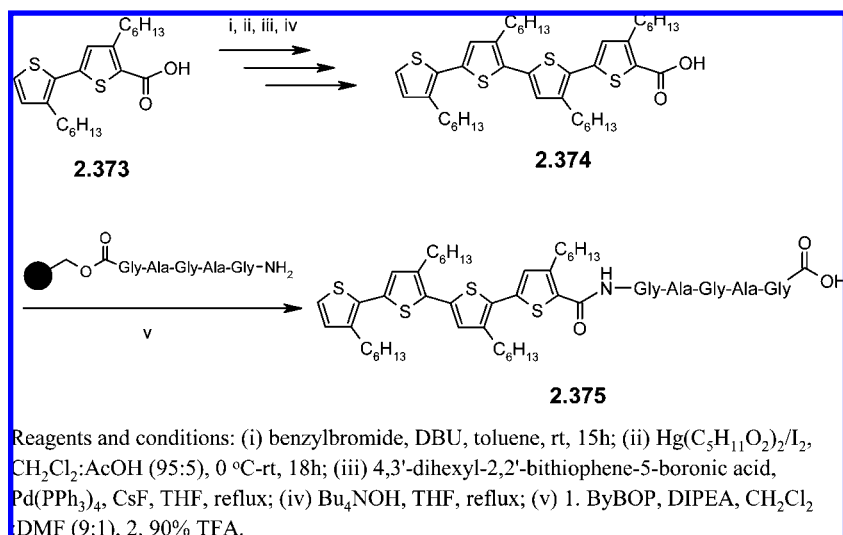
chloride to the isothiocyanate functionality by treatment with NaSCN in acetone. The photoluminescence spectrum of **2.369** showed green emission at 514 nm, whereas oligomers **2.370**–**2.372** exhibited yellow and orange emissions with maxima at 540, 550, and 566 nm, respectively. Compared to known fluorescent labeling agents such as fluorescein isothiocyanate, these oligothiophene isothiocyanates had high photostability and chemical stability. The reaction of isothiocyanates with the monoclonal antibodies anti-CD3 and anti-CD8 in basic phosphate buffer formed stable thiourea-bonded bioconjugates with variable emission properties and showed their potential use as fluorescent markers.

Utilization of solid phase synthetic techniques for the preparation of oligothiophene–peptide conjugates was realized by Bäuerle et al.[437] Regioregular 5-carboxyquater(3-hexylthiophene) **2.374** was synthesized starting from 4,3'-dihexyl-2,2'-bithiophene-5-carboxylic acid **2.373** (Scheme 2.60).[438,439] First, the carboxylic acid group was protected as a benzyl ester, and then, it was iodinated at the other α-terminus and cross-coupled with 4,3'-dihexyl-2,2'-bithiophene-5-boronic ester. After deprotection of the benzyloxy carbonyl group, the product was reacted with the resin-bound silk-inspired glycine- and alanine-containing pentapeptide sequence (Gly-Ala-Gly-Ala-Gly), affording **2.375** in 24% yield.

STM measurements on highly ordered pyrolytic graphite (HOPG) surfaces displayed the formation of superstructures of conjugate **2.375** due to its hydrogen bonding-mediated self-assembly. From FTIR measurements, the formation of

Chart 2.61

2.376 **2.377**

2.378
(DMTr = 4,4'-Dimethoxytriphenylmethane)
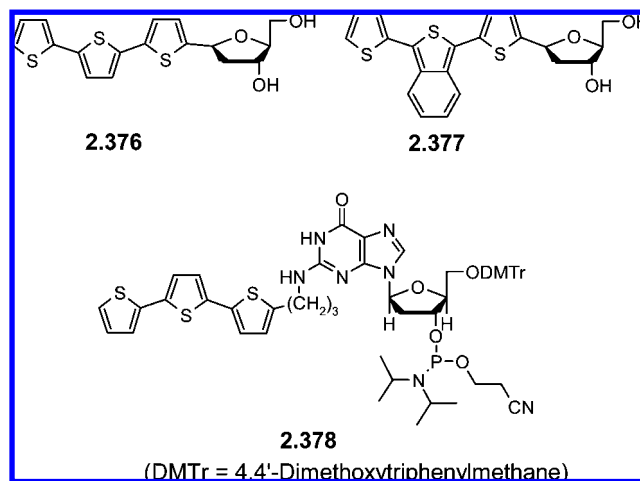
an antiparallel β-sheet structure was proposed. Cyclic voltammetry on **2.375** in dichlomethane solution showed a positive shift of the first oxidation potential compared to the case of the basic quarterthiophene which was attributed to the electron withdrawing effect of the peptide residue.

Kool et al. reported the synthesis of deoxyriboses **2.376** and **2.377** (Chart 2.61), in which the terthiophene-based fluorophore is attached to the C1-position of the deoxyribose unit, in fact replacing the DNA base in a corresponding nucleoside.[440] The conjugates were synthesized by cadmium-mediated reaction of the Grignard reagent of brominated

Scheme 2.61

Reagents and conditions: (i) 2-cyanoethyl-N,N-diisopropyl-chlorophosphite, DIPEA, CH$_2$Cl$_2$; (ii) 1. Oligonucleotide tetramer, solid-phase synthesis; 2. concentrated NH$_3$, 50 °C.

Chart 2.62

2.381: n = 0, 1, 2   **2.382a**: R = SMe, R$_1$ = H   **2.383**: n = 0, 1, 2
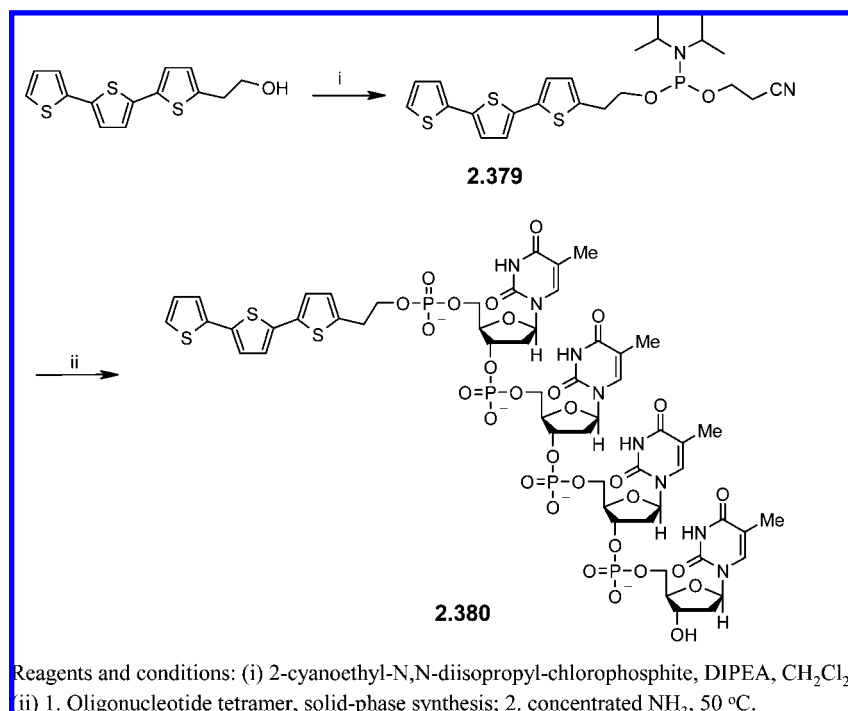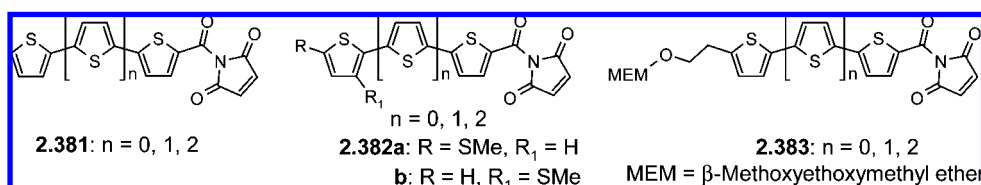 **b**: R = H, R$_1$ = SMe   MEM = β-Methoxyethoxymethyl ether

terthiophene precursors with Hoffer's chlorosugar (2-deoxy-3,5-di-O-(p-toluoyl)-D-ribofuranosyl chloride). The toluoyl protecting groups on the sugar moieties were then removed using sodium methoxide to generate the free dioxyribose. Due to the color tuning abilities of these fluorophores, they are potentially useful as probes to study the structure and dynamics of nucleic acids and their complexes with proteins.

Terthiophene-functionalized guanine nucleotide **2.378** was synthesized for its incorporation into the minor grove of DNA without alteration of duplex stability (Chart 2.61).[441] Pulse radiolysis measurements of **2.378**-modified oligodeoxynucleotides showed the formation of a stable terthiophene radical cation in DNA. The authors further proposed that the incorporation of several terthiophene moieties along the DNA sequence may be useful for carrying holes along the modified DNA. Capobianco et al. synthesized an oligonucleotide label comprising fluorescent terthiophene **2.380** *via* the phosphoramidite approach (Scheme 2.61).[442] A precursor phosphoramidite **2.379** was prepared from 5-(2-hydroxyethyl)terthiophene by reaction with 2-cyanoethyl-N,N-diisopropyl-chlorophosphite in anhydrous conditions. Coupling of **2.379** with the corresponding oligonucleotide (tetramer of a thymidine-sugar) was performed by solid phase synthesis, and the product was characterized by ^{1}H and ^{31}P NMR spectroscopy. UV−vis measurements revealed a typical absorption band at 260 nm due to the thymidine derivative and at 356 nm due to the terthiophene unit. A blue emission at ∼450 nm was found. Fluorophore **2.380** was reported to be highly photostable under prolonged UV illumination.

Recently, Barbarella et al. synthesized a series of oligothiophenes **2.381**−**2.383** bearing *N*-succinimidyl ester groups as markers for monoclonal antibodies and oligonucleotides (Chart 2.62).[443−445] For the synthesis of these oligomers, 5-bromo-2-thiophenecarboxaldehyde was converted to the corresponding carboxylic acid derivative and then reacted with NHS to afford active ester-functionalized monothiophene. Repetitive bromination and Stille-type coupling reactions afforded the oligomers in good overall yields. These compounds were covalently attached to the amino groups of biopolymers under mild conditions, to obtain chemically and optically stable bioconjugates. The labeling of antibodies and bovin serum albumin (BSA) with these fluorophores has been investigated by fluorescence measurements showing high photoluminescence and optical stability.

Konradsson and Inganäs et al. have recently prepared terthiophene **2.384** from 3-hydroxyethyl-thiophene by bromination with NBS, tosylation, substitution with Boc-protected L-serine, and final coupling with a bisborylated thiophene (Scheme 2.62).[446] Successive deprotection of the Boc-groups and oxidative polymerization gave a corresponding zwitterionic semiconducting polythiophene **P2.384** with rather short chains of three to five repeating units, as determined by MALDI-TOF measurements. The shift of the absorption maxima from 434 to 484 nm in aqueous solution by modifying pH indicated protonation and deprotonation of the terminal amino and carboxylic groups, which induced a coil-to-rod transformation of the polyelectrolytic backbone. The polymer was used as optical probe in the detection of
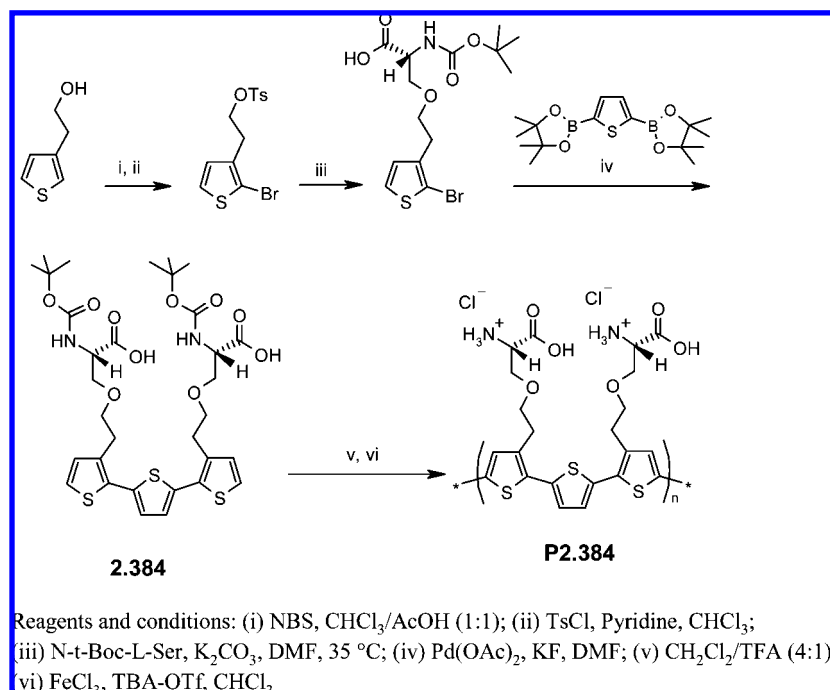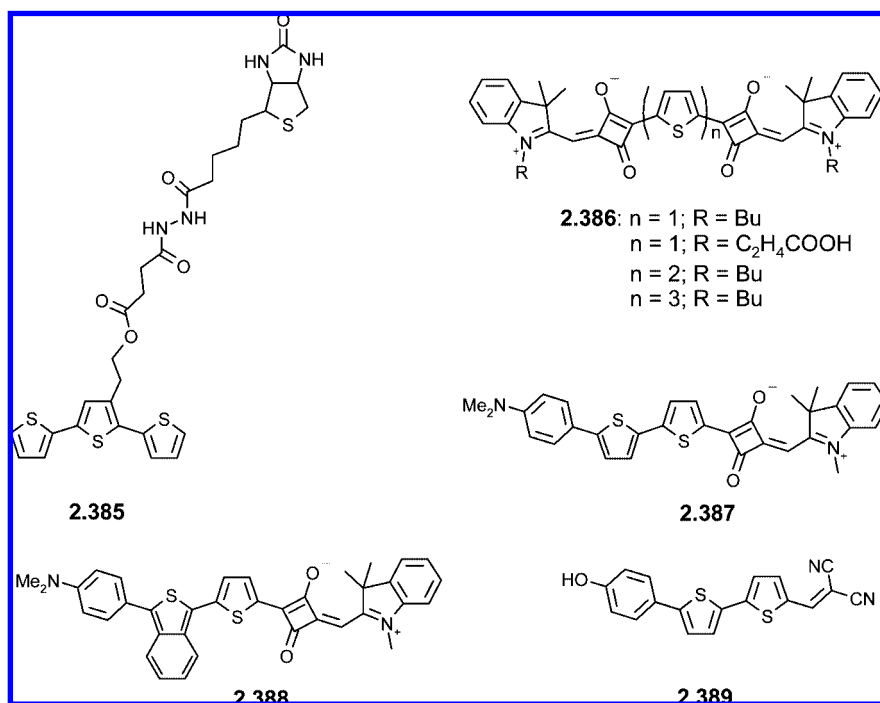
Scheme 2.62

2.384

P2.384

Reagents and conditions: (i) NBS, CHCl$_3$/AcOH (1:1); (ii) TsCl, Pyridine, CHCl$_3$;
(iii) N-t-Boc-L-Ser, K$_2$CO$_3$, DMF, 35 °C; (iv) Pd(OAc)$_2$, KF, DMF; (v) CH$_2$Cl$_2$/TFA (4:1);
(vi) FeCl$_3$, TBA-OTf, CHCl$_3$

Chart 2.63

2.385

2.386: n = 1; R = Bu
n = 1; R = C$_2$H$_4$COOH
n = 2; R = Bu
n = 3; R = Bu

2.387

2.388

2.389

amyloid fibril formation of bovin insulin (BI) and chicken lysozyme in acidic medium. Upon interaction with BI, a drastic increase of the emission intensity was observed along with a blue shift of the emission maximum from 600 to 560 nm. This may be due to the interaction of the polyelectrolyte and BI originating from a more twisted conformation due to noncovalent interactions. TEM, SEM, and optical images revealed the formation of bundles of electroactive luminescent wires of up to ∼100 μm length and width ∼10 μm, in which the wires were built from **P2.384** integrated into the amyloid fibrils of BI *via* a self-assembly process.[447]

Higgins et al. synthesized a biotin-functionalized terthiophene **2.385** by reaction of biotin hydrazide and a

terthiophene which was functionalized by a succinimidyl active ester (Chart 2.63).[448] The copolymerization of **2.385** with terthiophene on a Pt-electrode formed poly(terthiophene) films containing intact biotin moieties. The binding of 5 × 10^{-14} mol of glycoprotein avidin to the pendant biotin units of the polymer film resulted in a positive shift of the oxidation potential due to specific interactions and blocking of the ion transport to and from the polymer by the bound protein.

Some bis-squaraine derivatives **2.386** have been prepared as NIR emissive fluorophores, where two squaraine units were linked by oligothiophene spacers (Chart 2.63).[449] These dyes showed absorption bands at ∼780 and

~700 nm with high molar extinctions. Additionally, by increasing the number of thiophene units, blue shifts in the absorption bands were observed. This blue shift suggested that the planar π-conjugation in the chromophore might be inhibited by a torsion between the thiophene units. This nonplanarity of the thiophene rings was also supported by NMR spectroscopy, in which an upfield shift of the thiophene protons with increasing thiophene units was observed. The noncovalent interactions with human serum albumin (HSA) and BSA have been studied in trizma buffer and showed the formation of 1:1 complexes concomitant with a fluorescence enhancement.

Swager and Bacskai et al. reported donor−acceptor-based squarylium dyes **2.387** and **2.388** (Chart 2.63) in which the dimethylaminophenyl donor and squaraine acceptor were inetrconnectetd by a bithiophene unit.[450] These dyes showed stong absorption at 650 and 690 nm and NIR emission at 670 and 820 nm, respectively. They can preferentially bind to the myelin protein present in the brain tissue sections. Their unique emission behavior in the NIR wavelength allowed using them in combination with visible light fluorophores in multichannel detection of the fluorescent signals.

The same authors further synthesized push−pull type dicyanovinyl-functionalized 4-hydroxyphenylbithiophene **2.389**, which was used as a contrast agent in the imaging of Alzheimer's diseases (Chart 2.63).[451] The precursor molecule was prepared by Pd⁰-catalyzed coupling of 5-tributylstannyl-2,2′-bithiophene and *tert*-butyldimethylsilyl-protected 4-iodophenol. The product was converted to the aldehyde by n-BuLi/DMF, condensed with malononitrile, and finally deprotected to give bithiophene **2.389**. A strong fluorescence quenching was observed in aqueous media due to a nonemissive intramolecular charge transfer process. An *in vitro* binding study with aggregated amyloid β-protein showed a 70 nm red shift of the absorption maxima and a simultaneous 400-fold enhancement of the emission due to the strong dye−protein binding.
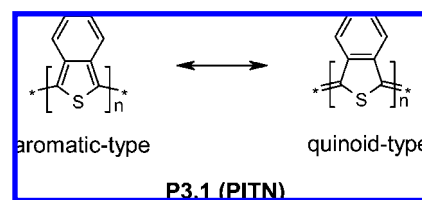
3. Fused Thiophenes

Soon after the discovery of (semi)conducting polymers, much effort was devoted to the development of low band gap polymers in view of their interesting properties and potential to serve as intrinsically conductive polymers. Various chemical approaches to lower and to tune the band gap of conjugated polymers have been reported.[13,452] Among others, the use of ring-fused thiophene units in conjugated polymer backbones is a convenient one. In comparison to "normal" thiophene units, ring-fused or annulated thiophenes exhibit an extended π-conjugation and more rigid structures. Both features would contribute to a lowering of the polymer band gap and to an increase of the intermolecular interactions in solid films. The following discussion will elaborate on recent progress in developing fused thiophene-based materials.

3.1. Aromatic and Heteroaromatic Ring-Fused Thiophenes

3.1.1. Benzo[c]thiophene Analogues

The first example of a fused thiophene-based material was reported by Wudl et al. in 1984.[453] In this pioneering work, poly(isothianaphthene) (PITN, **P3.1**) was synthesized by electrochemical polymerization of isothianaphthene, also

Scheme 3.1

P3.1 (PITN)

named benzo[c]thiophene. Both theoretical and experimental investigations[452,454,455] have demonstrated that the fused benzene ring in benzo[c]thiophene increases the quinoid character of the electronic ground state in PITN, causing a band gap of ~1.0 eV, which is about half that of polythiophene (2.0 eV, Scheme 3.1).[456,457] Alkyl- or alkoxy-substituted soluble PITNs **P3.2** were also developed (Chart 3.1). However, such chemical modifications did not lead to significant changes in the band gap of the polymers. Like parent polymer **P3.1**, these polymers showed band gaps of around 1.0 eV.[458−460]

Dithienylbenzo[c]thiophene **3.3** (Chart 3.1) was synthesized independently by different research groups.[461−464] Electrochemical polymerization of **3.3** led to a corresponding polythiophene with a band gap of 1.6 eV, which is in between those of **P3.1** and polythiophene.[461] From a similar standpoint, further extended polymers from naphtha[2,3-c]thiophene **P3.4** and dithienyl derivative **P3.5** were prepared *via* electropolymerization.[465,466] Compared to polythiophene, both polymers showed a smaller band gap of ~1.5 eV for **P3.4** and one of only 0.65 eV in the case of **P3.5**.

Bäuerle et al. have developed a series of end-capped benzo[c]thiophene-based oligomers **3.6**.[407,467] In comparison to corresponding α-oligothiophenes, these benzo[c]thiophene-based oligomers exhibited a significant red shift in the absorption spectra.[407] For example, the maximum absorption of **3.6** (n = 1, R = H) was red-shifted by 80 nm compared to that of α-quinquethiophene.[468] Metal complexes of compounds **3.6** were also synthesized and are discussed in detail in section 2.10.4 (*vide supra*). Alkyl-substituted terthiophenes incorporating a central benzo[c]thiophene were successfully dimerized to form hexathiophenes **3.7** in reasonable yields by using FeCl₃ or phenyliodine(III)-bis(trifluoroacetate) as oxidant.[469] All sexithiophenes showed red-shifted absorption bands with maxima at 504−510 nm, suggesting an extended π-conjugation system. Oxidative coupling of noncapped terthiophenes yielded higher oligomers. As an example, trimer **3.8**, which can be viewed as a modified nonithiophene, was isolated.[470]

Vilsmeier−Haack formylation of 1,3-dithienylbenzo[c]thiophene gave monoaldehyde **3.9a** (Chart 3.2), while dialdehyde **3.9b** was synthesized by dilithiation of 1,3-dithienylbenzo[c]thiophene followed by reaction with DMF. Both compounds were reacted to various corresponding vinylenes by Knoevenagel condensation or Wittig reaction.[470] By a Pd⁰-catalyzed C−N coupling reaction, diarylamino-capped 1,3-dithienylbenzo[c]thiophene oligomers **3.10** were synthesized by Thelakkat et al.[471] The compound exhibited extensive absorptions in the range of 300−620 nm. The electron-donating diarylamino groups increased the HOMO energy, making them promising candidates for light-harvesting and hole-transport materials in organic solar cells.

Substitution at the benzene ring of the benzo[c]unit was performed with this type of compound to fine-tune the properties of the resulting materials. In this respect, Vander-
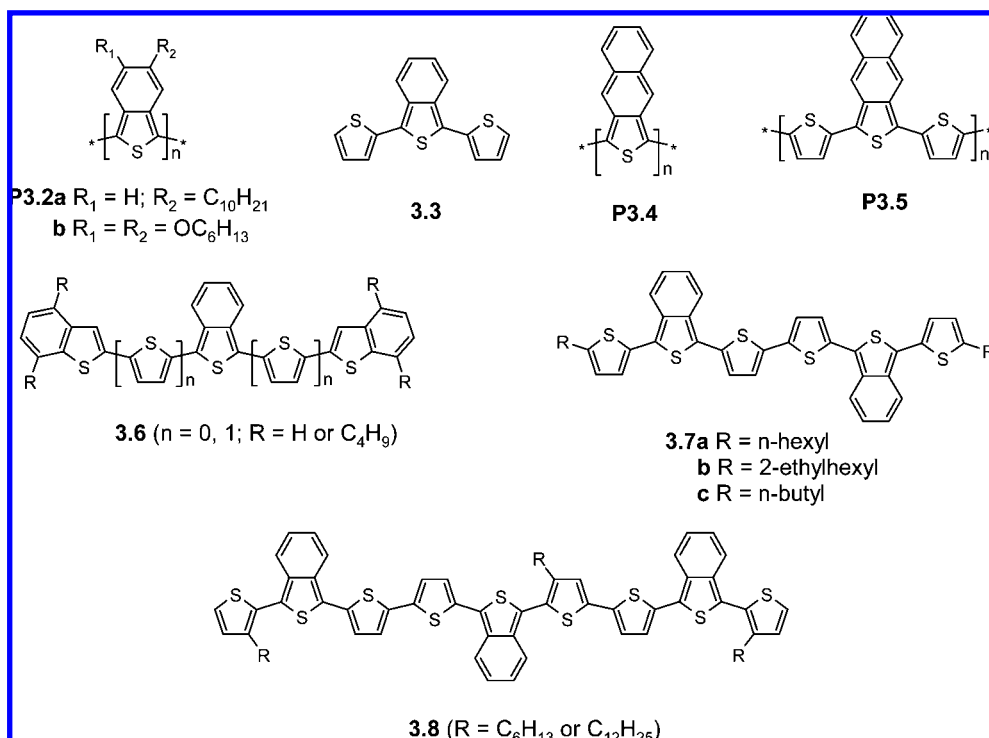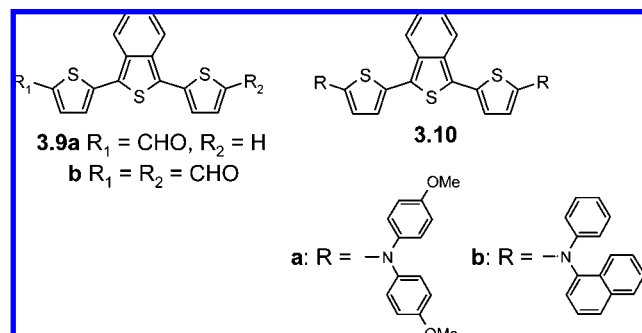
Chart 3.1

Chart 3.2

zande et al. reported the facile synthesis of 5,6-dichloro-1,3-dithienylbenzo[c]thiophenes **3.11a−c**.[459,472] These dichloroterthiophenes served as precursors for synthesizing 5,6-disubstituted 1,3-dithienylbenzo[c]thiophenes. As an example, Pd⁰-catalyzed coupling reaction of **3.11a** with an alkyl Grignard reagent gave 5,6-dioctyl-1,3-dithienylbenzo[c]thiophene **3.11d**.[459] Chemical polymerization of the 5,6-modified monomers with $FeCl_3$ yielded polymers with band gaps of 1.4−1.8 eV, which were similar to that of poly-(dithienylbenzo[c]thiophene) **P3.3**.[459] Application of these polymers as donor and fullerene PCBM as acceptor in bulk heterojunction solar cells (BHJSC) was also investigated and reported. A moderate overall power conversion efficiency of 0.3% and an internal power conversion efficiency (IPCE) of 24% were obtained for PMMA/poly-**P3.11c**/PCBM (1:2:6) blended devices.[472]

In 2001, Wudl et al. reported the synthesis of poly(benzo[c]thiophene-N-2″-ethylhexyl-4,5-dicarbodiimide) **P3.12** (Chart 3.3), which had a broad absorption band with a maximum at 832 nm and an onset absorption at 1000 nm corresponding to a band gap of E_g = 1.24 eV. Cyclic voltammograms of **P3.12** exhibited an oxidation potential of 0.88 V and a reduction potential of −1.10 V vs SCE, showing p- and n-dopable properties of **P3.12**. Compared

to the parent polymer PITN, both oxidation and reduction are shifted to positive potentials due to the electron-withdrawing effect of the imide group.[473]

The same research group developed a copolymer consisting of 3,4-ethylenedioxythiophene (EDOT) and benzo[c]thiophene-N-2″-ethylhexyl-4,5-dicarbodiimide. Copolymer **P3.13** was synthesized via Pd⁰-catalyzed coupling reaction of distannylated EDOT and a dibromo benzo[c]thiophene derivative. Analogous copolymer **P3.14** was prepared by electrochemical oxidative polymerization of terthiophene precursor **3.14**, which was synthesized via coupling reaction of stannylated EDOT and 2,9-dibromobenzo[c]thiophene-N-2′-ethylhexyl-4,5-dicarboxyimide in the presence of a Pd⁰-catalyst. Both polymers were p- and n-dopable and highly stable, and band gaps of ∼1.10 eV, slightly lower than that of **P3.12**, were determined.[474,475]

3.1.2. Benzo[b]thiophene Analogues

Benzo-annulation at the 2,3-position of thiophene rings results in another class of useful building blocks for constructing organic electronic materials. Chart 3.4 depicts examples of these building blocks, benzo[b]thiophene (**3.15**), benzo[1,2-b:4,5-b′]dithiophene (**3.16**), benzo[2,1-b:3,4-b′]dithiophene (**3.17**), and benzo[1,2-b:3,4-b′:5,6-b″]-trithiophene (**3.18**), which represent planar and rigid structures with extended π-conjugated systems. These structural elements allow greater intermolecular overlap of the molecules in the solid state and consequently provide high charge carrier mobilities.

Quaterthiophene analogues **3.19**, which comprise terminal benzo[2,3-b]thiophene (n = 0) or naphtho[2,3-b]thiophene (n = 1) groups, exemplified the fusing effect. The field-effect mobilities of **3.19** were around 10^{-2} cm² V⁻¹ s⁻¹, which is around five times higher than that of quaterthiophene under the same conditions.[476,477]
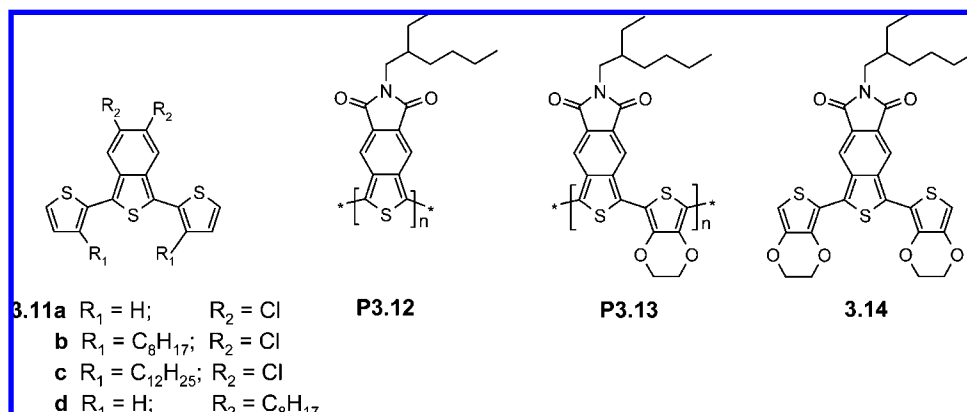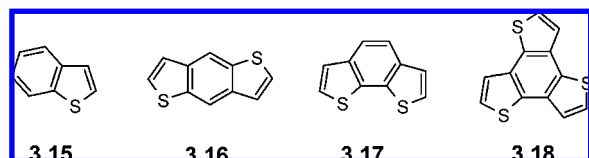
Chart 3.3

3.11a R₁ = H;   R₂ = Cl   **P3.12**   **P3.13**   **3.14**
   b R₁ = C₈H₁₇; R₂ = Cl
   c R₁ = C₁₂H₂₅; R₂ = Cl
   d R₁ = H;   R₂ = C₆H₁₇

Chart 3.4

3.15   **3.16**   **3.17**   **3.18**

In the area of charge transporting materials, pentacene is one of the most prominent systems, and high mobilities up to 1–2 cm² V⁻¹ s⁻¹ have been achieved. Anthradithiophenes **3.20**–**3.21** (Chart 3.5) represent thieno-fused pentacene analogues; however, all these compounds were obtained as inseparable mixtures of *syn*- and *anti*-isomers. In comparison to the case for pentancene, the terminal thiophene rings increase the benzenoid character of the conjugation system, thus lowering the HOMO levels and increasing the band gap. As a consequence, such a chemical modification enhances the stability of the materials. Katz et al. first reported the application of anthradithiophene **3.20** in solution processed OFETs, and mobilities of 0.01–0.02 cm² V⁻¹ s⁻¹ were measured for 2,8-dihexyl[2,3-*b*:6,7-*b′*]anthradithiophenes **3.20b**.[478] Interestingly, dihexyl and didodecyl derivatives **3.20b** and **3.20c** showed in vacuum-deposited OFET devices higher hole carrier mobilities (>0.1 cm² V⁻¹ s⁻¹) than that of nonsubstituted anthradithiophene **3.20a** (0.02–0.09 cm² V⁻¹ s⁻¹), although quite a large volume is occupied by insulating alkyl chains. Evidently, alkyl chains support forming favorable molecular organization and packing for good charge transport in solid films. Anthony et al. developed (trialkylsilyl)ethynyl-functionalized anthradithiophenes **3.21**, which are well soluble and chemically stable.[479] The molecular packing of these compounds in the solid state greatly depended on the type of alkyl chain in the silylenthynyl group. (Triethylsilyl)ethynyl derivative **3.21b** showed a strong 2-D π-stacking arrangement with a small π–π facing distance of 3.25 Å. High hole mobilities of 1.0 cm² V⁻¹ s⁻¹ were measured in **3.21b**-based OFET devices.[480]

The same research group reported the application of anthradithiophenes in organic solar cells (OSC). Ethyl-modified **3.21d** was quite stable and did not undergo Diels–Alder cycloaddition reactions with fullerene derivative PCBM[60], offering the opportunity to fabricate bulk heterojunction OSCs using **3.21d** as donor and PCBM[60] as acceptor. Annealing of **3.21d**/PCBM[60] blended films resulted in a crystallization of **3.21d** within the blends and the formation of unusual spherulite motifs. AFM analysis on the spherulites showed a network of anthradithiophene crystallites dispersed in an amorphous matrix composed
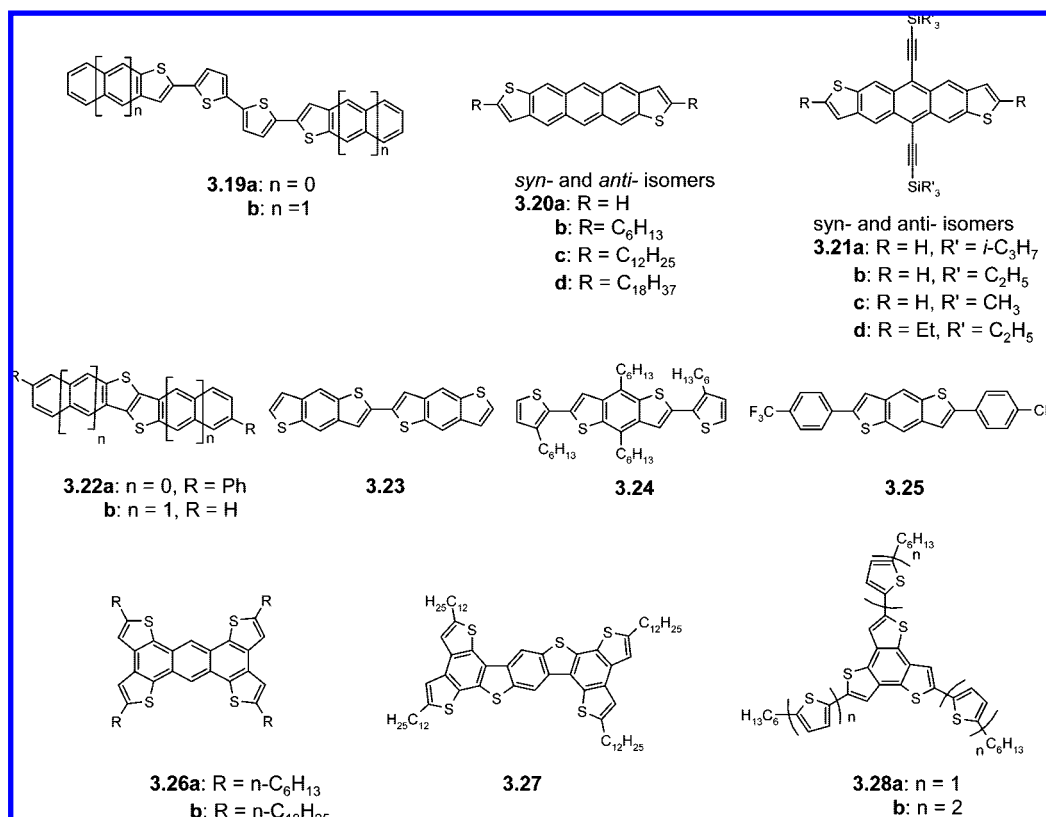
primarily of fullerene. The best devices with 82% coverage of spherulites showed a power conversion efficiency of 1%, which is among the best performances for solution-processed small molecule based photovoltaic cells.[481]

Takimiya et al. developed another type of thiophene-modified acenes **3.22** (Chart 3.5). These molecules had also the structural motif of an acene but included a central thienothiophene unit. This construction blocked the typical photodimerization, which commonly occurs in higher acenes, and consequently increased the stability of the materials in OFET device applications. 2,7-Diphenyl[1]benzothieno[3,2-*b*]benzothiophene **3.22a** and dinaphtho[2,3-*b*:2′,3′-*f*]thieno[3,2-*b*]thiophene **3.22b** showed the highest hole mobilities of 2.0 and 2.9 cm² V⁻¹ s⁻¹, respectively.[482,483]

Katz et al. first reported on benzodithiophenes for use as organic semiconductors (Chart 3.5). In their first publication, hole transfer mobilities of 0.04 cm² V⁻¹ s⁻¹ were measured for a dimer of *anti*-benzo[1,2-*b*:4,5-*b′*]dithiophene (**3.23**).[484] Alkyl chain modified benzodithiophene **3.24** showed good solubility and was chemically polymerized. Corresponding polymer **P3.24** gave well-organized lamellar layered structures in the solid state, which was confirmed by two-dimensional grazing-incidence X-ray diffraction (GIXRD). OFET devices based on polymer **P3.24** had saturation mobilities of 0.15–0.25 cm² V⁻¹ s⁻¹ with a current on/off ratio of 10⁵–10⁶ when measured under ambient conditions, which suggested an excellent stability of the polymer in device applications.[485] Interestingly, introduction of strong electron-withdrawing groups to the benzodithiophene unit converted the semiconducting characteristics of the materials from p-type to n-type. As an example, 4-trifluoromethylphenyl end-capped compound **3.25** showed a high electron transport mobility of 0.044 cm² V⁻¹ s⁻¹.[486]

Higher fused oligomers, such as **3.26** and **3.27** were also developed. A hole mobility of 0.012 cm² V⁻¹ s⁻¹ was measured for vacuum deposited films of **3.26a**. A high stability of **3.26a** based OFET devices was reported, which can be attributed to the low-lying HOMO energy level (E = −5.57 eV) as well as the high energy band gap (E_g = 2.93 eV) of the compound.[487] Compound **3.27** with an extended planar structure favors highly ordered self-assembly by π–π stacking to form nano- and microstructures. The shape and size of nano- and microstructures of **3.27** can be easily controlled and tuned by using different solvents and casting on various substrates. The self-assembled microstructures in solution were confirmed by ¹H NMR and absorption spectroscopy. SEM micrograph images confirmed the formation of microwires *via* self-assembly. Microwires prepared by

Chart 3.5

3.19a: n = 0
b: n = 1

syn- and *anti-* isomers
3.20a: R = H
b: R = C₆H₁₃
c: R = C₁₂H₂₅
d: R = C₁₈H₃₇

syn- and anti- isomers
3.21a: R = H, R' = *i*-C₃H₇
b: R = H, R' = C₂H₅
c: R = H, R' = CH₃
d: R = Et, R' = C₂H₅

3.22a: n = 0, R = Ph
b: n = 1, R = H

3.23

3.24

3.25

3.26a: R = n-C₆H₁₃
b: R = n-C₁₂H₂₅

3.27

3.28a: n = 1
b: n = 2

solution-processing of **3.27** showed a high mobility of 0.01 cm² V⁻¹ s⁻¹ in an OFET.[488]

Roncali et al. have synthesized star-shaped and π-conjugated oligothiophenes **3.28** (Chart 3.5) by attaching thiophene and bithiophene arms to the benzotrithiophene core (**3.18**) *via* Stille coupling reactions.[489] Compared to the case of a linear system, UV−vis data showed a red shift of the absorption maxima (**3.28a**, 357 nm; **3.28b**, 404 nm) for the star-shaped material due to extended π-conjugation through the core, which was corroborated by the successive decrease of the oxidation potential with increasing number of thiophene units. Heterojunction OSCs based on a blend of **3.28b** as hole transporter and *N*,*N*′-bis(tridecylperylenedicarboxyimide) as electron transport layer were fabricated and exhibited moderate power conversion efficiencies of 0.8%.[490]

3.1.3. Heteroaromatic Ring-Fused Oligothiophenes

In poly(benzo[*c*]thiophene) systems such as PITN, steric hindrance between benzo-H and thiophene-S atoms of adjacent thiophene rings creates a twist, resulting in a reduced π-conjugation in the polymeric backbone (Scheme 3.2). Replacement of the 4-CH group in the benzo[*c*]thiophene unit by nitrogen would diminish steric hindrance, which has been proven by X-ray structure analysis of **3.29** (Chart 3.6). The torsion angle between the central thienopyridine moiety and the thiophene unit on the nitrogen side is only 3.5°, whereas it is 39° on the CH side.[491] Based on these findings, heteroaromatic ring-fused thiophenes, such as thieno[3,4-*b*]pyrazine **3.30**, thienothiadiazole **3.31**, and thiadiazolothienopyrazine **3.32**, were proposed as another type of important fused thiophene building blocks for the construction of donor−acceptor type low-band gap polymers (Chart 3.6).

Substituted thieno[3,4-*b*]pyrazines are generally synthesized by condensation of 3,4-diaminothiophene with substi-
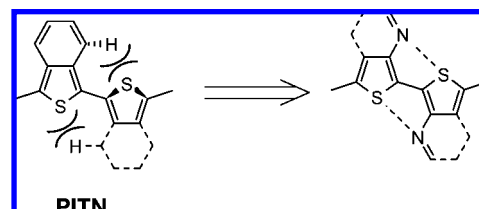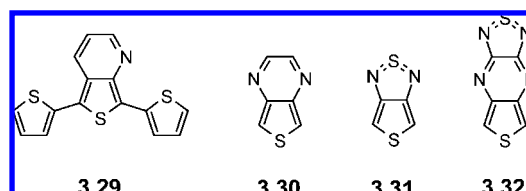
Scheme 3.2

PITN

Chart 3.6

3.29   **3.30**   **3.31**   **3.32**

tuted 1,2-diones (Scheme 3.3).[492,493] By this synthetic approach, various alkyl-substituted thieno[3,4-*b*]pyrazines **3.33** were synthesized and chemically polymerized with FeCl₃. The resulting polymers were highly soluble in organic solvents due to the alkyl side chains and had low band gaps of 0.8−1.1 eV.[458,492,493] There has been no report on successful electrochemical polymerization of thieno[3,4-*b*]pyrazine derivatives, and a popular hypothesis holds that the failure is due to the quenching of the created radical cations by the pyrazine ring.[494] However, Rasmussen et al. indicated that the reason may lie in the monomers' trait of easy overoxidation.[495,496] Under an oxidation potential as low as possible (∼1.4 V), electrochemical polymerization of dialkylated derivatives **3.33** was achieved. These electrochemically generated polymers have very low band gaps of ca. 0.69 eV, complying with the value of theoretical calculations (0.70 eV). However, this value is lower than
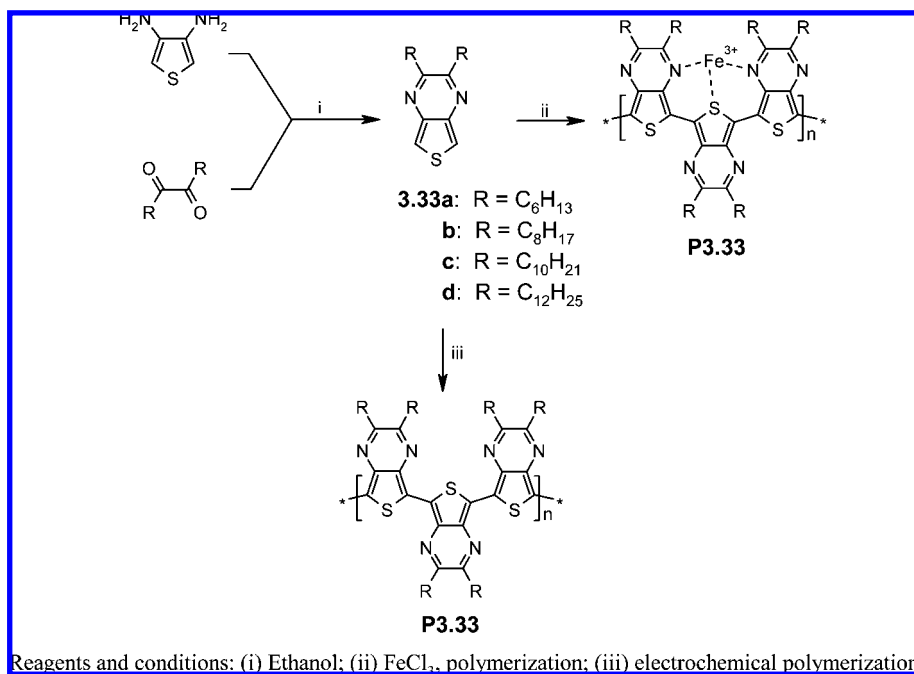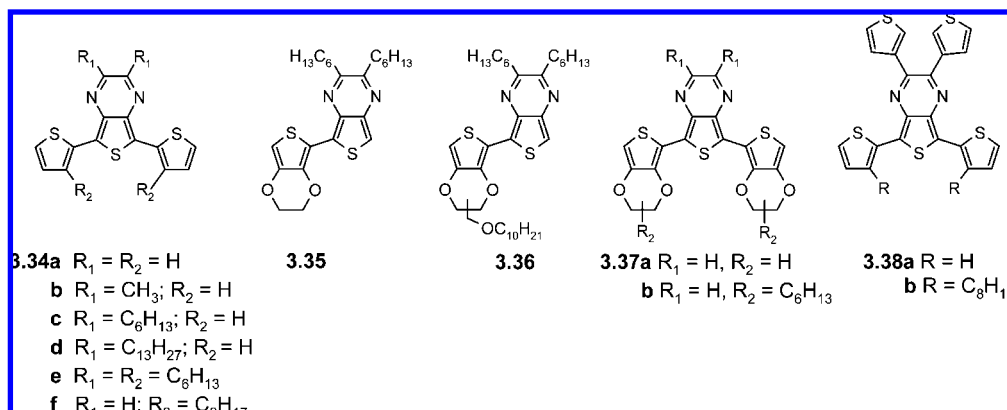
Scheme 3.3

3.33a: R = C_6H_{13}
b: R = C_8H_{17}
c: R = $C_{10}H_{21}$
d: R = $C_{12}H_{25}$

P3.33

P3.33

Reagents and conditions: (i) Ethanol; (ii) FeCl₃, polymerization; (iii) electrochemical polymerization

Chart 3.7

3.34a R₁ = R₂ = H
 b R₁ = CH₃; R₂ = H
 c R₁ = C₆H₁₃; R₂ = H
 d R₁ = C₁₃H₂₇; R₂ = H
 e R₁ = R₂ = C₆H₁₃
 f R₁ = H; R₂ = C₈H₁₇

3.35

3.36

3.37a R₁ = H, R₂ = H
 b R₁ = H, R₂ = C₆H₁₃

3.38a R = H
 b R = C₈H₁₇

that of the polymers synthesized by chemical oxidation with FeCl₃ (~1.0 eV). The authors proposed that Fe³⁺ chelation within the conjugated backbone results in a significant backbone twisting and a consequently increased band gap.[496]

In 1994, Yamashita et al. reported a series of 5,7-di(thienyl)thieno[3,4-b]pyrazines **3.34a–e** (Chart 3.7). Except for trimer **3.34e**, all other co-oligomers were electrochemically polymerized to corresponding polymers, which are ambipolar and can be oxidized at 0.80 to 1.00 V and reduced at −1.10 to −1.50 V vs SCE. Their band gaps varied from 1.0 to 1.5 eV depending on the substitution pattern.[497]

Recently, Wudl et al. synthesized thienopyrazine-based trimer **3.34f** (Chart 3.7) by attaching octyl groups at the 3 position of the thiophene ring.[498] Oligomer **3.34f** was chemically polymerized with FeCl₃ to generate thienopyrazine-based polymer **P3.34f**. The polymer covered a very broad absorption range from 300 to 980 nm, featuring a good sunlight harvesting ability. Polymer **P3.34f**/PCBM (1:1) blended bulk-heterojunction OSCs exhibited a maximum IPCE value of 6% at λ = 660 nm. Under white light illumination (100 mW cm⁻²), the devices showed a low overall power conversion efficiency of 0.085%, possibly due to the low V_{oc} (0.22 V) resulting from the relatively high

HOMO level of **P3.34f**, which diminishes the energy difference between the HOMO of **P3.34f** and the LUMO of PCBM.

Roncali et al. synthesized bithiophenic precursors **3.35** and **3.36** consisting of electron donating EDOT and electron deficient dihexylthienopyrazine units (Chart 3.7). The electrogenerated polymers of these precursors **3.35** and **3.36** showed excellent stability under reductive redox cycling conditions. **P3.35** retained 80% of its original electroactivity after 250 potentials scans. A very small band gap of 0.36 eV was estimated from the absorption onset of solid films.[499] However, the solubility of **P3.35** is poor, which might be attributed to the tight molecular packing of the polymeric chains originating from the intra- and intermolecular N···S and O···S interactions. To improve solubility, a long alkoxymethyl chain was introduced at the dioxoethylene bridge. The electrochemically generated polymer **P3.36** thus had a higher solubility than **P3.35**. The oxidation potential of **P3.36** was by 0.36 V more negative than that of **P3.35**, indicating a higher polymerization degree. However, the band gap of **P3.36** was about 0.83 eV, which is quite a bit higher than that of **P3.35**. The authors rationalized this rather unexpected effect by the increased distance between the
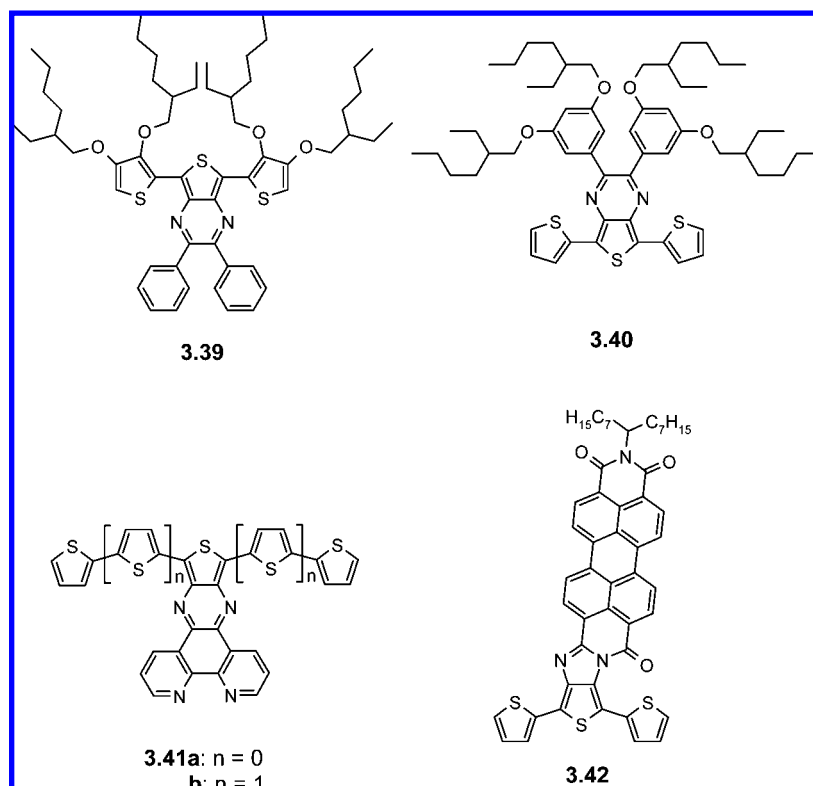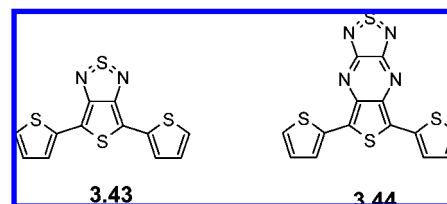
Chart 3.8

3.39

3.40

3.41a: n = 0
b: n = 1

3.42

polymer chains and hence decreased interchain interactions due to steric interactions of the alkoxymethyl side chains.[500]

Cooligomers **3.37** consisting of EDOT and thienopyrazine were synthesized by Berlin et al. (Chart 3.7).[501,502] Similar to other thienopyrazine-based polymers, electrochemically generated polymers of **3.37** exhibited ambipolar electroactivity. **P3.37a** had an *in situ* conductivity of 0.5 S cm^{-1} in the oxidized state and 0.01 S cm^{-1} in the reduced state while corresponding values for alkylated derivative **P3.37b** were 15 and 0.03 S cm^{-1}. Both polymers had broad absorption bands peaking at 950 nm, suggesting small band gaps.[501]

Recently, polymers based on 2,3-di(3-thienyl)thieno[3,4-*b*]pyrazine **3.38** have attracted much attention due to their green color and application prospect in electrochromic devices (Chart 3.7).[503] Electrochemical polymerization of **3.38a** performed under low potential yielded polymer **P3.38a**, giving a very saturated green color in the neutral state. In the oxidized form, these absorptions were depleted and resulted in a transmissive pale brown polymer. Terthiophene **3.38b** had a better solubility and could be polymerized by chemical oxidants such as FeCl$_3$ or CuCl$_2$. The mild oxidant CuCl$_2$ gave better polymers **P3.38b**, whereas strong oxidant FeCl$_3$ overoxidized the monomer and gave a purple, insoluble polymer.[504−507]

More recently, 5,7-dithienylthienopyrazine derivatives **3.39** and **3.40** were used to synthesize corresponding polymers (Chart 3.8).[508] Both polymers were soluble in organic solvents and had an intensive absorption ranging from 600 to 950 nm. Polymer **P3.40** had a band gap of 1.2 eV which is slightly smaller than that of **P3.39** (1.28 eV). Application of the polymers as blends with PCBM in bulk-heterojunction OSCs resulted in rather low open circuit voltages of 0.39 and 0.56 V, respectively, which can be attributed to the low oxidation potential and the therefore high-lying HOMOs of the polymers. External quantum efficiencies (EQEs) exceeding 15%

Chart 3.9

3.43

3.44

in the 700−900 nm region and power conversion efficiencies of 1.1% were determined for **P3.40**/PCBM devices.

Oligothiophenes **3.41** which are linked with larger π-conjugated pyrazinophenanthrolines were synthesized and investigated. The condensation of phenanthroline rings to the oligothiophene core generated n-type semiconductor characteristics. Phenanthroline-oligothiophene **3.41a** showed an electron mobility of 2 × 10^{-4} cm^2 V^{-1} s^{-1}, while 6 × 10^{-5} cm^2 V^{-1} s^{-1} was found for **3.41b**. Interestingly, compound **3.41b** showed ambipolar behavior in OFETs, and hole mobilities of 6 × 10^{-5} cm^2 V^{-1} s^{-1} were measured.[509] Another example with an even larger extended π-conjugation is represented by perylenemonoimide-fused terthiophene **3.42** (Chart 3.8). The terthiophene was synthesized by condensation of 3′,4′-diamino-2,2′:5′,2″-terthiophene and *N*-(10-pentadecyl)-3,4,9,10-perylenetetracarboxylic acid-3,4-anhydride-9,10-imide in the presence of zinc acetate. Terthiophene **3.42** showed a low band gap of 1.4 eV. Electrochemical polymerization of **3.42** yielded corresponding polymer **P3.42** with an even more diminished band gap of 0.9 eV.[510]

Yamashita et al. have synthesized thieno-thiadiazole and thiadiazolo-thienopyrazine-based terthiophenes **3.43** and **3.44** (Chart 3.9).[511−513] X-ray structure analysis of **3.43** showed a nearly coplanar structure of the three rings.[511] Both monomers have strong absorptions in the red-NIR regime peaking at 618 and 990 nm, respectively.[511,514] Electropolymerization

Chart 3.10

3.45　　　　**3.46**　　　　**3.47**

3.48　　　　**3.49**
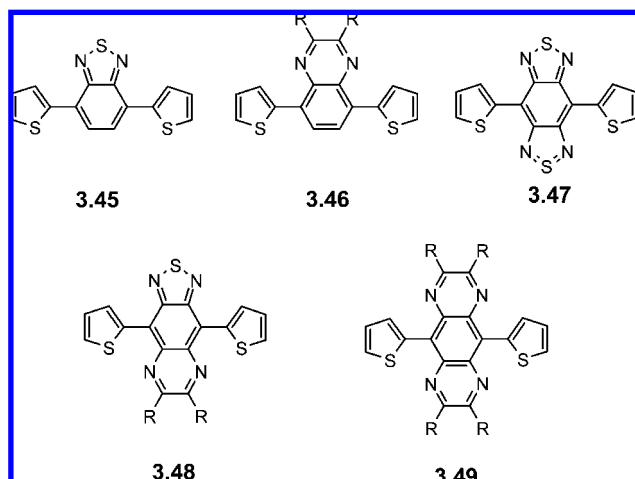
of **3.43** and **3.44** yielded corresponding polymers with very low band gaps of 0.9 and 0.3 eV, respectively, which are among the smallest band gap values ever reported.[512,513]

3.1.4. Other o-Quinoidal Acceptor-Based Low Band Gap Materials

Benzanellated heterocycles, such as benzothiadiazoles or quinoxalines, are rather electron-deficient systems with increased quinoid character in the ground state. Combination of these o-quinoid acceptors with electron-donating thiophene units yields a class of building blocks for the construction of low band gap materials with alternating D−A units in the main chain. Yamashita et al. have reported a family of thiophene-based trimeric systems, such as 4,7-di-2-thienyl-2,1,3-benzothiadiazole **3.45**, 5,8-di-2-thienyl-quinoxaline **3.46**, 4,8-di-2-thienylbenzo[1,2-*c*:4,5-*c*′]bis[1,2,5]thiadiazole **3.47**, 4,9-di-2-thienyl[1,2,5]thiadiazolo[3,4-*g*]quinoxaline **3.48**, and 4,9-di-2-thienylpyrazine[2,3-*g*]quinoxaline **3.49** (Chart 3.10). Electrochemical polymerization of these monomers resulted in regular copolymers with very small band gaps of 0.5−1.4 eV depending on the strength of the acceptor unit in the main chain.[515]
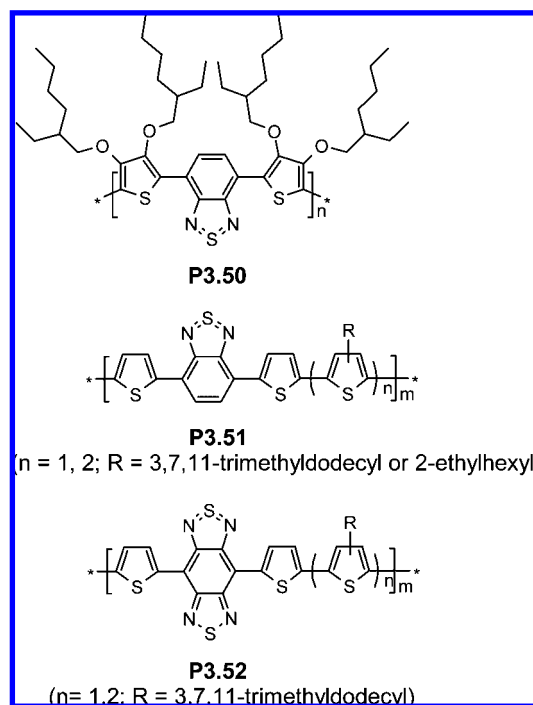
Janssen et al. reported the polymerization of 4,7-bis(5-bromo-3,4-bis[2-ethylhexyloxyl]-2-thienyl)-2,1,3-benzothiadiazole *via* a Ni(COD)₂-catalyzed coupling reaction and obtained soluble high molecular weight polymer **P3.50** (Chart 3.11).[516] The band gap of **P3.50** was determined to be 1.55 eV from the onset of the absorption spectrum in the solid film. OSCs with **P3.50**/PCBM blends showed an extended spectral response up to 800 nm, and a power conversion efficiency of 0.9% was obtained for this device.

Bundgaard and Krebs recently reported similar conjugated copolymers **P3.51** and **P3.52** based on benzothiadiazole **3.45** and benzobis(thiadiazole) **3.47** as acceptors showing band gaps of ~1.7 eV and ~0.7 eV, respectively. Due to their small band gaps, these polymers were discussed as promising candidates as light harvesting materials in OSCs.[517]

3.2. Thienothiophenes

Thienothiophenes (TTs) in general contain two annulated thiophene rings, of which four isomers exist, namely thieno[3,4-*c*]thiophene **3.53**, thieno[3,4-*b*]thiophene **3.54**, thieno[3,2-*b*]thiophene **3.55**, and thieno[2,3-*b*]thiophene **3.56** (Chart 3.12). All four compounds are sulfur-rich, planar, and rigid molecules, among which derivative **3.53** has a limited

Chart 3.11

P3.50

P3.51
(n = 1, 2; R = 3,7,11-trimethyldodecyl or 2-ethylhexyl)

P3.52
(n= 1,2; R = 3,7,11-trimethyldodecyl)

stability due to its nonclassical electronic character.[13,518] The other derivatives have been widely used to construct conjugated and low band gap polymers due to their electron-richness and planar fused chemical structure.

3.2.1. Thieno[3,4-b]thiophene Analogues

Thieno[3,4-*b*]thiophene **3.54** was already synthesized in 1967,[519] while the polymer based on **3.54** was only reported 30 years later. Pomerantz et al. described the synthesis of 2-decylthieno[3,4-*b*]thiophene **3.57a**, aiming at corresponding soluble polymers.[520,521] By chemical polymerization of **3.57a** with FeCl₃, chloroform soluble **P3.57a** was obtained with an average molecular weight (M_n) of 52000. 2-Phenyl-substituted thieno[3,4-*b*]thiophene **3.57b** was synthesized by Neef et al. through a two-step reaction starting with 3,4-dibromothiophene (Chart 3.13).[522] **P3.57b** was obtained by electrochemical polymerization and, similar to PITN, **P3.57a** and **P3.57b** exhibited a quite small band gap of around 0.8−0.9 eV.

Polymers based on unsubstituted thieno[3,4-*b*]thiophene **3.54** and thieno[3,4-*b*]furane **3.58** were synthesized and investigated by Sotzing et al. (Chart 3.13).[523−525] The band gaps for **P3.54** and **P3.58** were determined to be 0.85 and 1.03 eV, respectively. Both polymers showed high optical transparency in the neutral and oxidized states, which is important for applications as optical transparent electrodes. Polymer **P3.54** is insoluble in organic solvents; however, the authors demonstrated that chemically polymerized **P3.54** can be sulfonated with fuming sulfuric acid to afford a water processable polymer.[526] In two other publications, the same group reported polymerization of thienothiophene **3.54** in aqueous dispersions utilizing poly(styrene sulfonate) (PSS) as polyelectrolyte. The resulting conducting polymer showed a band gap of about 1.0 eV and high stability as a water dispersion. A cross-linked structure of **P3.54**-PSS as shown in Scheme 3.4 was proposed by the authors.[527,528]

Symmetrical thieno[3,4-*b*]thiophene dimers, 2,2′-bis-(thieno[3,4-*b*]thiophene) **3.59**, 4,4′-bis(thieno[3,4-*b*]thiophene)
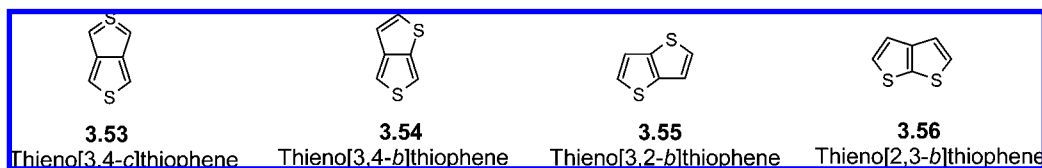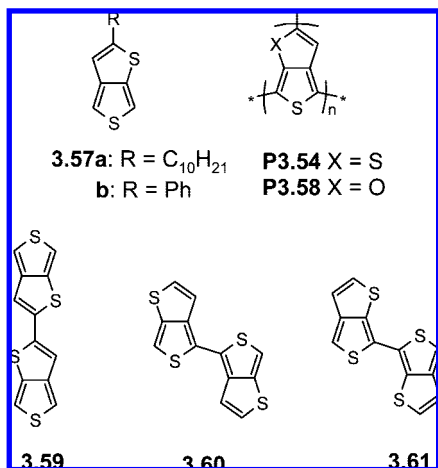
Chart 3.12

3.53
Thieno[3,4-*c*]thiophene

3.54
Thieno[3,4-*b*]thiophene

3.55
Thieno[3,2-*b*]thiophene

3.56
Thieno[2,3-*b*]thiophene

Chart 3.13

3.57a: R = C$_{10}$H$_{21}$
b: R = Ph

P3.54 X = S
P3.58 X = O

3.59   **3.60**   **3.61**

3.60, and 6,6′-bis(thieno[3,4-*b*]thiophene) **3.61** were synthesized and electrochemically polymerized by Sotzing et al. (Chart 3.13).[529] Due to the extended π-conjugation, these dimers had lowered oxidation potentials in comparison to the monomer **3.54** ($\Delta E = 0.17-0.41$ eV). Corresponding polymers exhibited small band gaps of ca. 0.9 eV, which were very close to that of **P3.54**.[530]

3.2.2. Thieno[3,2-b]thiophene Analogues

Electrochemical and chemical polymerization of thieno[3,2-*b*]thiophene **3.55** were already investigated in the 1980s, resulting in polymers which were insoluble in organic solvents.[531,532] In 1997, Fuller et al. developed a convenient four step route to thieno[3,2-*b*]thiophene **3.55** and its brominated derivatives.[533] TT **3.55** was obtained from 3-bromothiophene in an overall yield of 51% (Scheme 3.5). Bromination of thieno[3,2-*b*]thiophene-2-carboxylic acid **3.62** gave 2,3,5-tribromothieno[3,2-*b*]thiophene **3.63** in a high yield of 93%. Further bromination of **3.63** by lithiation with LDA followed by treatment with bromine yielded tetrabromothieno[3,2-*b*]thiophene **3.64** in 78%. Finally, derivative **3.64** was converted to 3,6-dibromothieno[3,2-*b*]thiophene **3.65** with zinc and acetic acid in 76% yield.

Lim et al. developed TT-based semiconductors for OFETs by synthesizing co-oligomers **3.66** and **3.67**, which consisted of **3.55** and fluorene or biphenyl units. Corresponding copolymer **P3.69** was synthesized as well. In compounds **3.68** and **P3.70** the fused thiophenes have been replaced by flexible bithiophene units (Chart 3.14).[534−536] X-ray crystal structure analysis of oligomer **3.67** indicated a nearly coplanar structure of the biphenylene groups with the thienothiophene core, while the fluorene units in **3.66** were slightly distorted. In thin film OFET devices, the more rigid and planar structure of **3.67** afforded good charge transport mobilities of 0.08−0.09 cm^2 V$^{−1}$ s$^{−1}$, which were slightly higher than those of **3.66** and **3.68** (0.05−0.06 cm^2 V$^{−1}$ s$^{1−}$).[537−539] Comparison of the performance of copolymers **P3.69** and **P3.70** showed that the charge carrier mobility is

three times higher for polymer **P3.69** (1.1 × 10$^{−3}$ cm^2 V$^{−1}$ s$^{−1}$), which contains the more rigid TT unit.[534] In addition, the rigid TT unit in **P3.69** caused a narrow fluorescence band, which in OLED devices (ITO/PEDOT/**P3.69**/LiF/Al) resulted in a pure green emission.[535]

Kwon et al. utilized hexyl-substituted thieno[3,2-*b*]-thiophene to end-cap naphthalene and anthracene, which resulted in mixed systems **3.71** and **3.72** (Chart 3.15). Both compounds formed highly ordered polycrystalline solid films *via* vacuum deposition. A high hole transport mobility of 0.14 cm^2 V$^{−1}$ s$^{−1}$ was measured for **3.72**, while that of **3.71** was lower (0.084 cm^2 V$^{−1}$ s$^{−1}$).[540] Choi et al. built up star-shaped materials for OFET applications which included phenylene cores. Due to the starburst structure, **3.73** had excellent solubility and could be utilized for solution-processed devices. A moderate charge carrier mobility of 2.5 × 10$^{−4}$ cm^2 V$^{−1}$ s$^{−1}$ was measured for **3.73** and ascribed to the random orientation of the molecules in the solid film.[541]
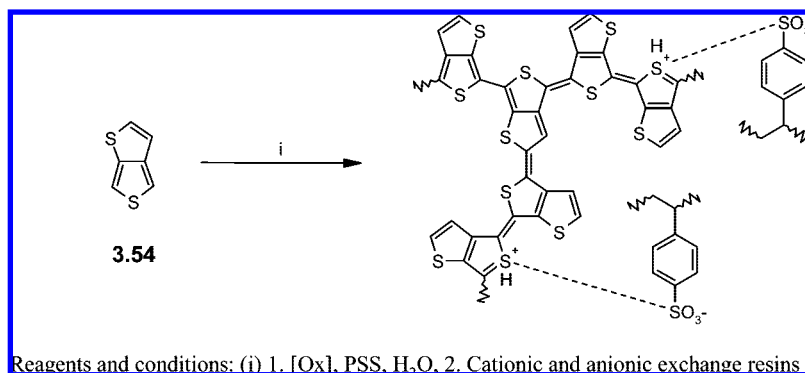
Substitution of the β-positions of TTs increases steric hindrance in mixed systems, causing a blue shift in the absorption spectra. The recently published work of Miguel and Matzger clearly showed this trend. For comparison, β,β′-bisnonyl-substituted TT **3.75** (Chart 3.16) had a maximum absorption at 353 nm, which is 20 nm blue-shifted in comparison to the case of nonsubstituted derivative **3.74**. If the steric hindrance is further increased, as represented in dimer **3.78** ($\lambda^{max} = 296$ nm), an additional blue shift of 40 and 57 nm in comparison to the cases of parent compounds **3.77** and **3.76**, respectively, was noticed. The steric hindrance is on the other hand reduced by the insertion of an ethynyl spacer between the TT units. Thus, compound **3.79** showed a maximum absorption at 383 nm,[542] which is 87 nm red-shifted relative to the case of **3.78**. The same trends were also seen for the corresponding polymers.[542,543]

McCulloch et al. reported less sterically hindered but soluble copolymers **P3.80** made of TTs and thiophenes (Chart 3.16).[544] Interestingly, these polymers exhibited liquid crystalline properties and formed large crystalline domains in thin solid films, thus offering the potential for fabrication of "quasi-single-crystal" transistors. For both polymers, high charge carrier mobilities of 0.2−0.6 cm^2 V$^{−1}$ s$^{−1}$ were measured in OFETs under nitrogen atmosphere.

Dimethoxylated TT **3.81** along with its dimer **3.82** were recently synthesized by Roncali et al. (Scheme 3.6).[545] X-ray crystallographic structure analysis of **3.81** showed a self-rigidification of the conjugated backbone through noncovalent sulfur−oxygen interactions between two adjacent TT units. Electrochemical polymerization of monomer **3.81** led to polymer **P3.81** with a relatively low oxidation peak potential of 0.2 V (vs Ag/AgCl) and a moderate band gap of 1.7 eV.

TTs which were linked *via* β-positions, as represented in structures **3.83** and **3.84** (Chart 3.17), were recently reported by Matzger et al.[546] In thienothiophene units, the C−H···π interactions is reduced in the crystalline state and favors the formation of π-stacks. Single crystal structure analysis of

Scheme 3.4

Reagents and conditions: (i) 1. [Ox], PSS, H₂O. 2. Cationic and anionic exchange resins

Scheme 3.5

Reagents and conditions: i) 1. LDA; 2. N-formylpiperidine; ii) HSCH₂CO₂Et/K₂CO₃; iii) LiOH;
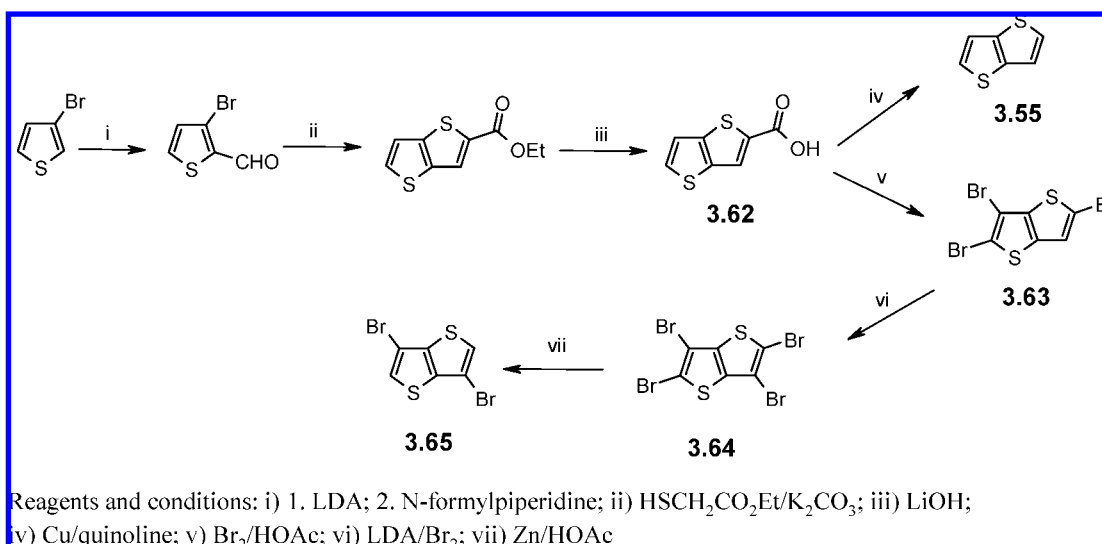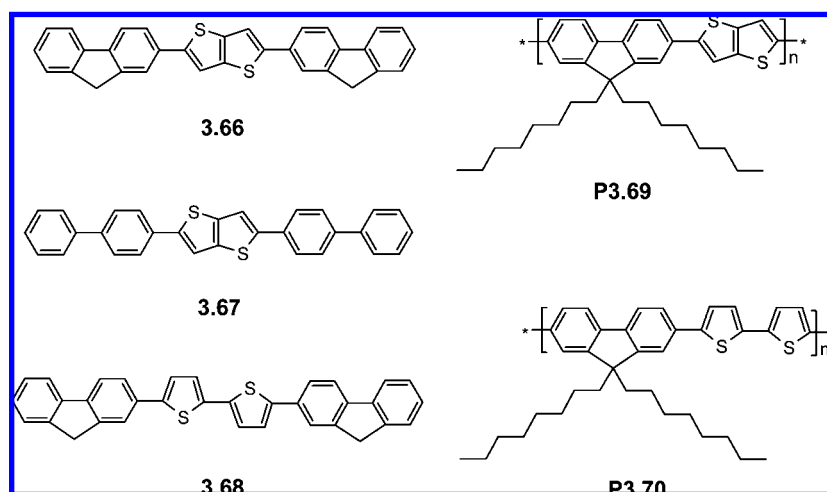iv) Cu/quinoline; v) Br₂/HOAc; vi) LDA/Br₂; vii) Zn/HOAc

Chart 3.14

3.83 and **3.84** released nearly coplanar structures for the TT units and edge-to-face π-stacking of the molecules in the solid state. The molecular packing of these β-linked TTs is quite different from that of the α-linked isomers, which rather adopt herringbone arrangments.[547]

3.2.3. Thieno[2,3-b]thiophene Analogues

Unlike the other isomers, thieno[2,3-b]thiophene **3.56** is a cross-conjugated system unable to form a fully conjugated pathway in conjugated oligomers or polymers. As shown in Scheme 3.7, the incorporation of thieno[2,3-b]thiophene **3.56** into a conjugated polymer would restrict the effective conjugation length of the polymer as well as lower its ionization potential (i.e., HOMO level).

Despite this cross-conjugation, McCulloch et al. demonstrated that polymers **P3.85** in OFETs exhibit high charge carrier mobilities of 0.15 cm² V⁻¹ s⁻¹ and on/off ratios of 10⁵ in addition to excellent stability (Chart 3.18).[548] In a later
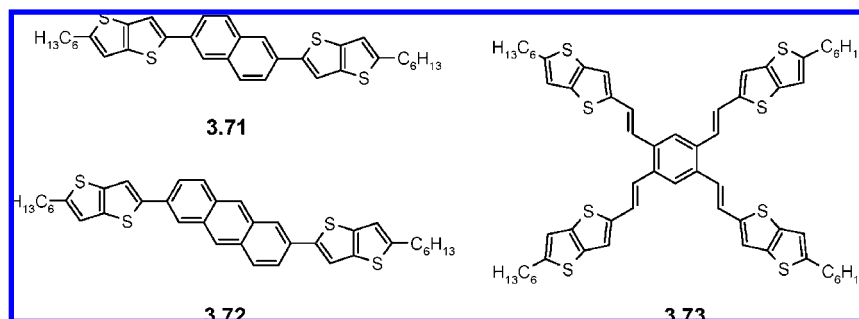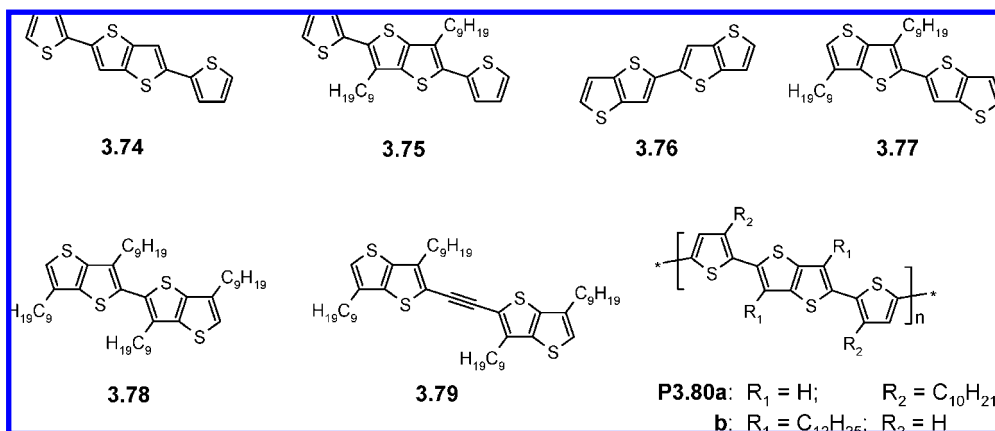
Chart 3.15

3.71

3.72

3.73

Chart 3.16

3.74

3.75

3.76

3.77

3.78

3.79

P3.80a: $R_1 = H$; $R_2 = C_{10}H_{21}$
b: $R_1 = C_{12}H_{25}$; $R_2 = H$

Scheme 3.6

3.55   **3.64**   **3.65**   **3.81**

3.82   **P3.81**

Reagents and conditions: (i) $Br_2/CHCl_3$; (ii) Zn/AcOH; (iii) MeONa, CuO, KI; (iv) 1. BuLi, 2. Bu_3SnCl 3. $CuCl_2/Pd(OAc)_2$

Chart 3.17

3.83   **3.84**
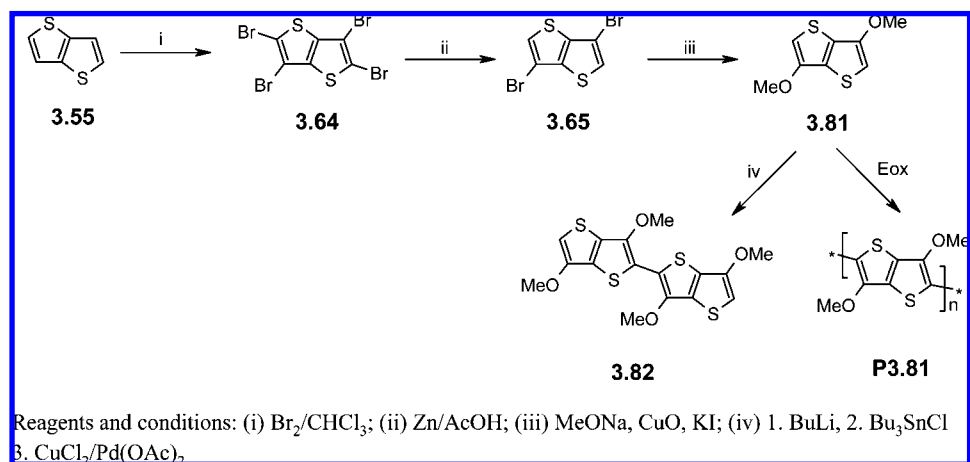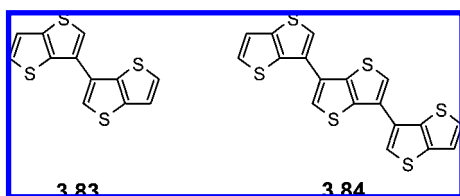
publication, the authors reported ambipolar OFETs based on blended layers of **P3.85a** and PCBM showing good electron mobilities of 9×10^{-3} cm^2 V^{-1} s^{-1} and hole mobilities of 4×10^{-3} cm^2 V^{-1} s^{-1}.[549,550]

Hergué and Frère synthesized 3,4-ethylenedioxythieno[2,3-*b*]thiophene and EDOT-based co-oligomer **3.86**. Due to the multiplication of S···O intramolecular interactions, **3.86**

should bear a self-rigidified structure. Cyclic voltammograms of **3.86** exhibited a first irreversible oxidation peak at 0.81 V (vs Ag/AgCl), which is 150 mV anodic compared to trimeric EDOT, suggesting a lower HOMO energy level. Electropolymerization of **3.86** gave the corresponding polymer, which due to the disruption of the conjugation through the thieno[2,3-*b*]thiophene units was more difficult to oxidize than PEDOT. On the other hand, a good stability in the neutral state under ambient conditions was found.[551]

3.3. β,β'-Bridged Bithiophenes

Annulation of bithiophenes by bridging the β- and β'-position leads to useful building blocks for the construction of functional materials. These include dithienothiophene (DTT) **3.87**, dithienosilole (DTS) **3.88**, cyclopentadithiophene (CPDT) **3.89**, dithieno[3,2-*b*:2'3'-*d*]pyrrole (DTP) **3.90**, and
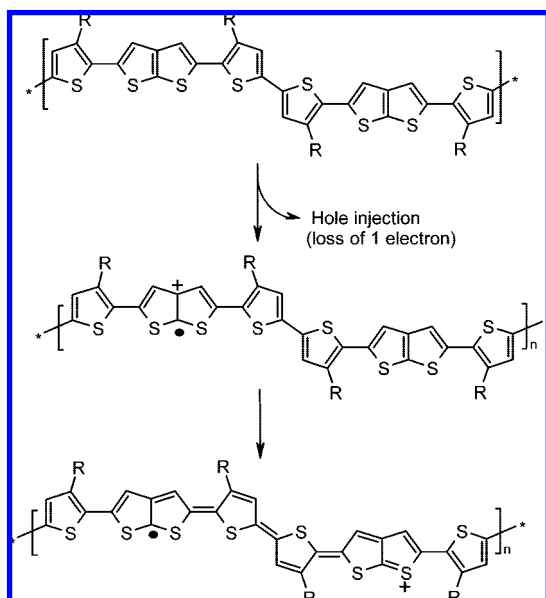
Scheme 3.7

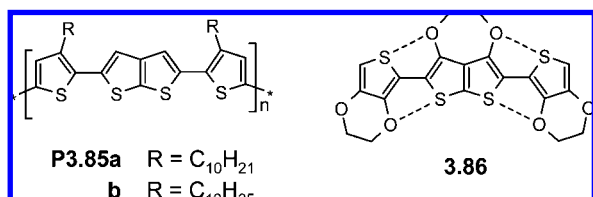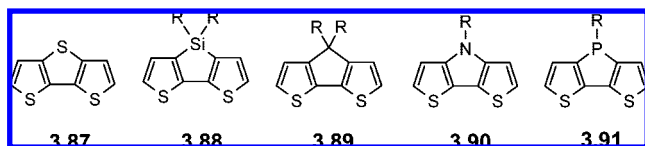Hole injection
(loss of 1 electron)

Chart 3.18

P3.85a R = C$_{10}$H$_{21}$
    b R = C$_{12}$H$_{25}$

3.86

Chart 3.19

3.87 **3.88** **3.89** **3.90** **3.91**

dithieno[3,2-*b*:2′3′-*d*]phosphole (DTPh) **3.91** and their derivatives (Chart 3.19).

3.3.1. Dithienothiophene (DTT) Analogues

Like its thienothiophene (TT) analogues, DTT **3.87** represents a sulfur-rich, planar, and rigid π-conjugated system, which has been widely used as a building block in functional materials. A recent review discussed the progress in the synthesis of dithienothiophenes and its derivatives.[24] In this section, we will therefore only emphasize the latest developments concerning synthesis and applications of DTT-based compounds.

Due to the planar and rigid structure of DTT, analogues have been developed as p-type semiconductors for OFETs. Friend et al. reported the synthesis and application of α-linked DTT dimer **3.92** (Chart 3.20).[552] X-ray structure analysis of **3.92** revealed a completely planar molecule and strong intermolecular S···S interactions in the solid state. In addition, DTT **3.92** showed a well ordered face-to-face π−π stacking and efficient molecular orbital overlap of the units. Good charge carrier mobilities of 0.02−0.05 cm^2 V^{-1} s^{-1} were measured for **3.92** in OFET devices.

Matzger et al. developed a β,β′-linked dimer of dithienothiophene **3.93**. Similar to the α-linked isomer **3.92**, isomer **3.93** showed a coplanar structure for the two

dithienothiophene units and formed columns of face-to-face stacked molecules with an intermolecular distance of 3.57 Å.[546] Application of **3.93** in OFETs was not reported yet.

Zhu et al. reported the synthesis and application of a benzannulated DTT, dibenzo[*d,d*′]thieno[3,2-*b*:4,5-*b*′]-dithiophene **3.94** (Chart 3.20).[553] Synthesis of **3.94** was successfully achieved starting form benzo[*b*]thiophene in three steps. **3.94** had a very low-lying HOMO level of −5.60 eV and a large band gap of 3.46 eV, which provide a high stability of the materials in device applications. High mobilities of 0.51 cm^2 V^{-1} s^{-1} and an on/off ratio larger than 10^6 were measured for vacuum-deposited devices.

The same research group further developed α-substituted DTT derivatives **3.95a−c** for applications in OFETs (Chart 3.20).[554] Compounds **3.95** were synthesized *via* a Pd^0-catalyzed coupling reaction of 2,6-dibromodithieno[3,2-*b*:2′,3′-*d*]thiophene with corresponding boronic acids. Highly crystalline films were observed for all these compounds. A high charge carrier mobility of 0.42 cm^2 V^{-1} s^{-1} and an on/off ratio of 5 × 10^6 were measured for diphenyl derivative **3.95b**. It is worth noting that these DTT derivatives have lower HOMO levels than comparable nonfused oligothiophenes, thus resulting in higher stabilities and on/off ratios.

Destri et al. reported the synthesis of fluorene-DTT cooligomers **3.95d**.[555] Electrochemical investigations showed reversible oxidation waves and suitable HOMO energy levels relative to high work-function electrodes. Pentafluorophenyl-modified DTT **3.95e** was synthesized by Otsubo et al. *via* a Pd^0-catalyzed coupling reaction of 2,6-dibromodithieno[3,2-*b*:2′,3′-*d*]thiophene with pentafluorophenyl boronic acid.[556] However, the application of these fluorinated compounds in organic electronic devices was not reported.

Barbarella et al. described organic light-emitting transistors (OLETs) based on thiophene oligomer **3.96** (Chart 3.20).[557] **3.96** was synthesized *via* a microwave-assisted Suzuki coupling reaction of 3,5-dimethyl-2,6-diiododithieno[3,2-*b*:2′,3′-*d*]thiophene and 5-hexyl-5′-(4,4,5,5-tetramethyl-1,3,2-dioxaborolan-2-yl)-2,2′-bithiophene. Organic light emitting transistors (OLETs) were successfully fabricated by both vacuum sublimation and drop casting of **3.96**.

In the solid state, dimesitylborane-substituted DTT **3.97** showed a broad blue-green and a weak red emission (Chart 3.20). The red fluorescence originated from the cross-like dimer of **3.97**, which was confirmed by photophysical and theoretical investigation. OLEDs made of ITO/PEDOT:PSS/**3.97**/LiF/Al showed not only blue-green emission originating from the isolated molecules, but also an intensive red emission with a peak at 680 nm coming from the dimer. The superposition of both emissions gave white light with an external quantum efficiency of 0.35%.[558]

The use of DTT units as conjugated spacers for nonlinear optical materials was also described.[559,560] Lee et al. reviewed recent intensive research on application of 1,6-distyryl-DTT derivatives **3.98** for two-photon absorption materials (Chart 3.21).[561]

Choi et al. utilized fused dithienothiophene units as building blocks to create phenylene-cored star-shaped compound **3.99**, which has a solubility of more than 15 mg/mL in chlorobenzene and offers processability of the materials from solution for device applications (Chart 3.22). Drop-cast films of **3.99** exhibited good polycrystallinity, which was verified by X-ray diffraction analysis. A good charge carrier mobility of 2.5 × 10^{-2} cm^2 V^{-1} s^{-1} was measured

Chart 3.20

3.92 **3.93** **3.94** **3.95a**: Ar =

b: Ar =

c: Ar =

d: Ar =

3.96 **3.97** **e**: Ar =

Chart 3.21

3.98

a: Ar = Ar' =

b: Ar = Ar' =

c: Ar = 　　　Ar' =
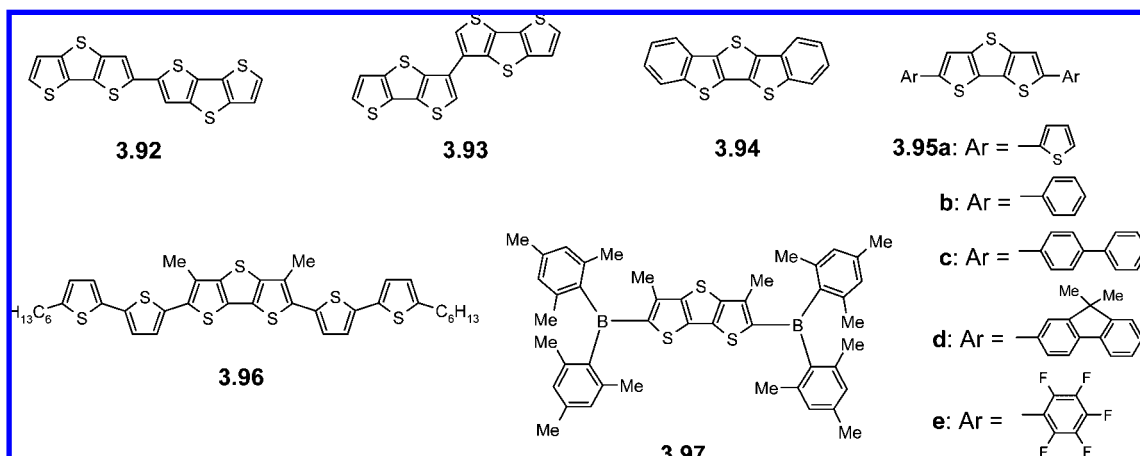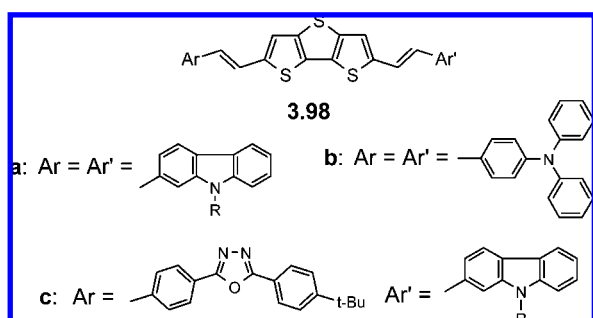
for **3.99**, much higher than that of the corresponding bithiophene derivative **3.100** (6.0×10^{-3} cm^2 V^{-1} s^{-1}).[541]

3.3.2. Dithieno[3,2-b:2′3′-d]thiophene-4,4-dioxides

Thiophenes can be converted into the corresponding S,S-dioxides by oxidation with hydrogen peroxide. Such a chemical modification of thiophene rings usually leads to an increased electron affinity and higher fluorescence quantum yield. The systems then behave rather as a diene than as an aromatic thiophene.[242,245] Barbarella's group has intensively studied the influence of thiophene-S,S-dioxide building blocks in oligothiophenes (described in detail in sections 2.7 and 2.12). The implementation of the sulfon group into fused DTT was represented in 3,5-dimethyl-2,6-bis(3-methylthienyl)dithieno[3,2-b:2′3′-d]thiophene-4,4-dioxide (DTTO) **3.102** (Chart 3.23).[248,562] X-ray powder diffraction measurements in combination with theoretical calculations demonstrated that DTTO **3.102** does not form dimers in the solid state, resulting in an increased fluorescence quantum yield.[563] The DTTO system is easy to modify, and thus, it is possible to tune the fluorescence over the entire visible range. Therefore, applications of DTTO derivatives in OLEDs and as fluorescence markers in biological systems[436] have been investigated by Barbarella et al. (see also Chapter 2.7 and 2.12).[564]

3.3.3. Dithienosilole (DTS) Analogues

Due to the $\sigma^* - \pi^*$ interaction between silicon and the butadiene moiety, silole rings possess a low lying LUMO energy level, which endues with better electron injection and transport ability in thin films. For example, siloles bearing electron-withdrawing groups such as pyridine showed excellent electron transport properties in OLED devices.[565]

Dithienosilole (DTS) **3.88** is formed by fusing the β,β'-position in bithiophene with a silyl group. Ohshita et al. have reported the synthesis and application of a series of 2,6-diaryl-DTSs **3.103**. Compared to their parent bithiophene analogues, the DTS derivatives showed red-shifted absorption and fluorescence, indicating an extended π-conjugation. OLEDs using **3.103a** as electron transport and Alq$_3$ as emitting layer showed excellent electron transport properties and high brightness.[566] Lee et al. synthesized triarylamine-containing DTS derivatives **3.103d,e** (Chart 3.24). The incorporation of triarylamines resulted in an improved hole-transport ability. OLEDs consisting of DTS **3.103d** as emitting layer showed bright green emission with an efficiency of 1.2%.[567]

Kunai et al. synthesized copolymers **P3.104** including DTS and silane blocks via Ni^0-catalyzed Kumada-type coupling reactions (Chart 3.25). OLEDs based on these materials were fabricated and investigated. The results indicated that introduction of the dithienosilole moiety into the silane improved the electron-transport ability of the materials.[568]

Following a similar approach, Jen et al. developed copolymer **P3.105**, a copolymer of 9,9-dihexylfluorene and 4,4-diphenyl-DTS. The relatively small ratio of DTS units in the polyfluorene chain acted as electron and energy traps. In a double-layer device using **P3.105** as the emitting layer, a bright green emission of the DTS moieties was found originating from efficient energy transfer from the oligofluorene sites. A maximum external quantum efficiency of 1.64% indicated improved charge injection and recombination in the DTS-modified layer.[569]

3.3.4. Cyclopentadithiophene (CPDT) Analogues

Bridging the β,β'-position, bithiophenes with sp^2 or sp^3 carbons lead to cyclopentadithiophenes (CPDTs), which are frequently used as monomers or building blocks for conjugated polymers. These include 4H-cyclopenta[2,1-b:3,4-b′]dithiophene **3.106**, 4-mono- or 4,4-disubstituted 4H-cyclopenta[2,1-b:3,4-b′]dithiophene **3.107** and **3.89**, 4H-cyclopenta[2,1-b:3,4-b′]dithiophene-4-one **3.108** and its acetal **3.110**, 4-dicyanomethylene-4H-cyclopenta[2,1-b:3,4-b′]dithiophene **3.109**, and other 4-substituted derivatives such as TTF-derivative **3.111** or dimer **3.112**. The principal chemical transformations of CPDT-derivatives are depicted in Scheme 3.8 and typically start from cyclopentadithiophenone **3.108**. Progress of CPDT-based systems was recently reviewed by Coppo and Turner.[570]
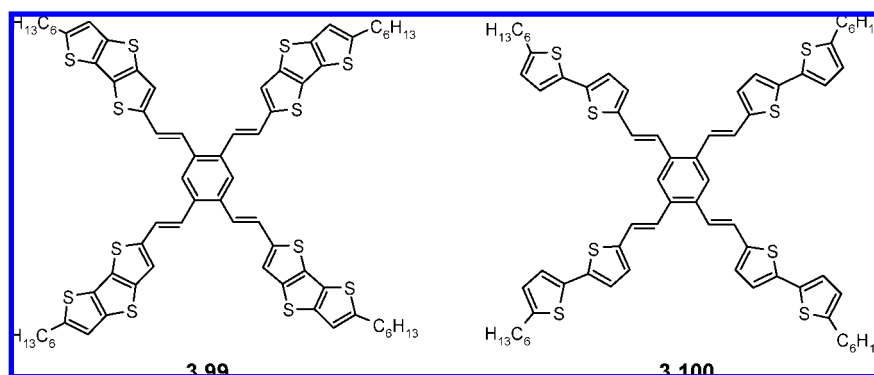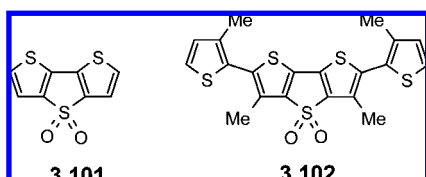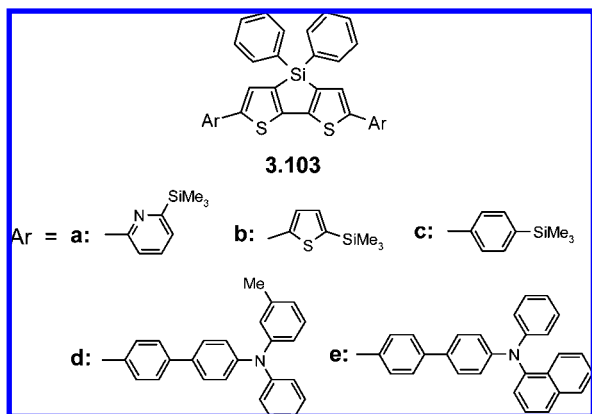
Chart 3.22

Chart 3.23

Chart 3.24

The family of CPDTs **3.106**, **3.107**, and **3.89** can be regarded as thiophene analogues of fluorene. Big efforts have been devoted to developing CPDT-based conjugated polymers. Results showed that polymers from dialkylated CPDT **3.89** have higher solubility but lower conductivity (2−40 S cm^{-1}) in comparison to polymers from monoalkylated **3.107** (80−300 S cm^{-1}). The lower conductivity of **P3.89** could be due to weaker interchain interactions caused by the introduction of the second alkyl chain.[571]

Bäuerle et al. synthesized end-capped oligothiophenes **3.113**, which had a diphenylated CPDT building block in the center and showed good solubilities due to the nonplanar structure of the bridging 4,4-diphenylmethane group (Chart 3.26).[467]

CPDT derivatives **3.108** and **3.109** contain electron withdrawing groups and were used as building blocks for low band gap polymers. Homopolymers of **3.108** and **3.109** exhibited low band gaps of 1.2[572] and 0.8 eV,[572,573] respectively. The corresponding copolymers **P3.114** and **P3.115**, containing EDOT, units were developed by Berlin et al. (Chart 3.26).[501] Because the acid-catalyzed hydrolysis of dioxolane-protected CPDT **3.110** can be readily performed, it has been used as precursor for the functionalization of ketone **3.108**. This strategy has been applied for the synthesis of dithienylcyclopentadithiophenone **3.118**, which has been

obtained in an overall yield of 46% and formally represents a quaterthiophene. Distannylated acetale **3.116** was coupled to 2-bromo-5-perfluoroheptanoylthiophene in a Stille-type reaction to give acetal **3.117**, which then was transformed to ketone **3.118** (Scheme 3.9). Due to the poor solubility of **3.118**, thin solid films of **3.118** were made from soluble **3.117**, followed by a treatment with H$_2$O−HCl vapor and annealing. The resulting films showed good charge carrier mobilities of 0.01 cm^2 V^{-1} s^{-1} in OFET devices.[228]

In contrast to CPDTs **3.108** and **3.109**, 4-(1,3-dithiol-2-ylidene)-4H-cyclopenta[2,1-*b*;3,4-*b*′]dithiophene **3.111** contains an electron-donating 1,3-dithiole moiety, resulting in a low oxidation potential of 0.8 V.[574] X-ray structure analysis of unsubstituted **3.111** showed strong intermolecular S···S interactions in the solid state. High conductivities were measured for corresponding homopolymers.[574,575]

In 2003, Pickup et al. reported the electrochemical polymerization of Δ$^{4,4'}$-dicyclopenta[2,1-*b*:3,4-*b*′]dithiophene **3.112**, yielding the corresponding probably cross-linked polymer with a band gap lower than 0.5 eV.[576] The same research group later reported the electrochemical copolymerization of **3.112** with EDOT.[577] The resulting polymer had an even smaller band gap of 0.1−0.3 eV. However, the conductivities of the doped polymers were as low as 10^{-5} S cm^{-1}.

### 3.3.5. Nitrogen and Phosphor Atom Bridged Bithiophenes

Dithienopyrrols and -phospholes as nitrogen- and phosphor-bridged bithiophenes were developed and investigated in the same line. Rasmussen et al. described an efficient synthetic route to N-functionalized dithieno[3,2-*b*:2′,3′-*d*]pyrroles (DTP, **3.90**) by palladium-catalyzed C−N coupling reactions (Scheme 3.10).[578] Compared to the synthesis of Zanirato et al.,[579] this new method not only simplifies the synthetic procedure but also significantly increases the total yield. An X-ray structure analysis of **3.90b** showed a completely planar structure of the DTP-fused ring system. A more recent work by the same research group described the synthesis of DTP-based oligothiophenes **3.119** and **3.120** (Chart 3.27). The fused and rigid DTP oligomers had higher fluorescence efficiencies in comparison to parent oligothiophenes.[580] A polymeric DTP **P3.121** functionalized with chiral side chains was developed by Samyn et al.;[581] however, the resulting polymer showed a relatively poor solubility. Cyclic voltammograms of **P3.121** gave two oxidation peaks at 0.5 and 0.8 V (vs Ag/AgCl), a band gap of 2.1 eV, and a conductivity of 6 S cm^{-2} after iodine doping.

Baumgartner et al. reported the synthesis of novel dithieno[3,2-*b*:2′,3′-*d*]phosphole derivatives (DTPh) **3.122** and **3.123**

Chart 3.25

P3.104

m = 1, 2   R = Ph, p-Tol

Ar =

P3.105a: m = 0.9, n = 0.1
b: m = 0.95, n = 0.05
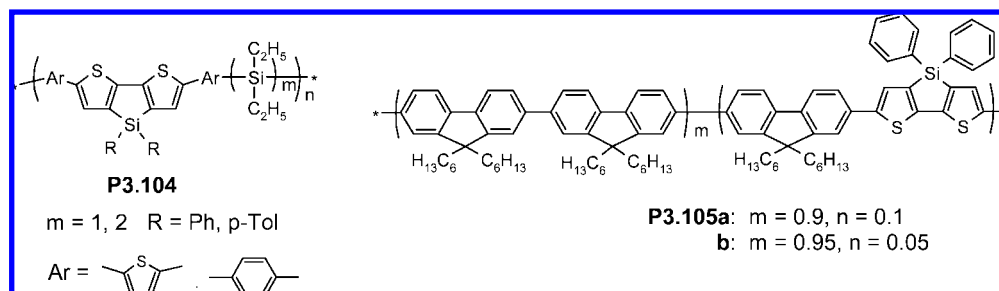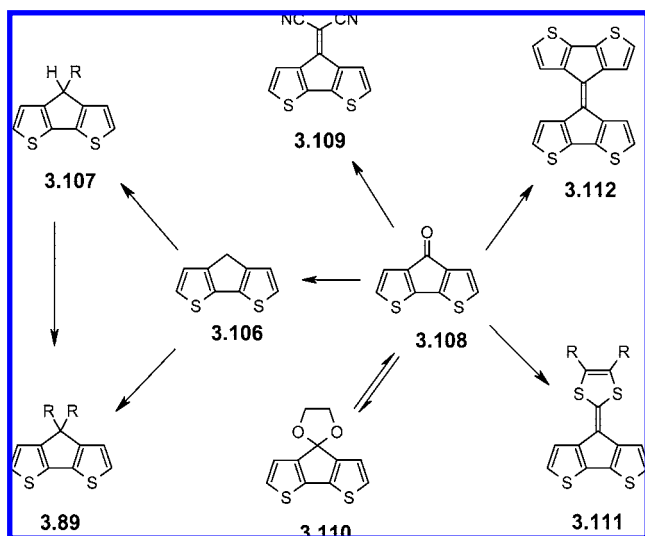
Scheme 3.8

(Scheme 3.11). All DTPh species displayed strong blue emission. Chemical modification of the central phosphorus atom, by means of oxidation or complexation with Lewis acids or transition metals, can be readily performed, owing to its nucleophilic nature. Therefore, it is possible to tune the chemical and physical properties of the compounds.[582−584]

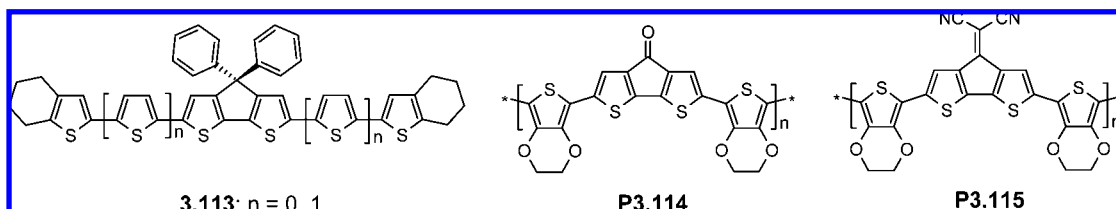## 3.4. Thienoacenes

3.4.1. S-Anellated α-Oligothiophenes

Annulation of α-oligothiophenes with a sulfur bridge through the β-positions of adjacent thiophenes leads to linear thienoacenes **3.125**, which are planar and rigid π-conjugated molecules with a very low C/H ratio (Chart 3.28). Compared to linear acenes **3.124**, the lower C/H ratio of thienoacenes would weaken the role of C−H···π interactions in the solid state.[585] Such an effect along with strong intermolecular S···S interactions of thienoacenes and efficient molecular orbital overlap, which were confirmed, e.g., by X-ray structure analysis of **3.92**, endues thienoacenes with promising application prospects in optoelectronic devices. To date, linear thienoacenes with thiophene units up to eight have been synthesized and characterized. Small thienoacenes such as thienothiophene and dithienothiophene units have already been discussed above. Here, we will discuss thienoacenes with more than three thiophene units. Annulation of α-oligothiophenes to higher thioacenes can be achieved either by bridging the 3,3′-position with sulfur and then coupling to the α-carbon atoms, (strategy A, Scheme 3.12) or by first forming the C−C bond followed by ring closure of the 3,3′-position with a sulfur bridge (strategy B).

The first synthetic route to tetrathienoacene **3.128** and pentathienoacene **3.130** was developed by Kobayashi et al. (Scheme 3.13) utilizing synthetic approach A shown in Scheme 3.12.[586,587] After metal−halogen exchange with n-BuLi, 3-bromothieno[3,2-b]thiophene **3.126** was quenched with sulfide to yield precursors **3.127** and **3.129**. Following oxidative homocoupling with the system n-BuLi/CuCl₂, the two precursor molecules were transformed to target compounds **3.128** and **3.130** in 60% and 20% yield, respectively. The moderate yield for the synthesis of pentathienoacene **3.130** is caused from the low solubility of the precursor **3.129**. Zhu et al. investigated pentathienoacene **3.130** in OFET devices and found a higher stability in air in comparison to pentacene due to the larger HOMO−LUMO energy gap.[588] A good hole transport mobility of 4.5×10^{-2} cm² V⁻¹ s⁻¹ was determined.
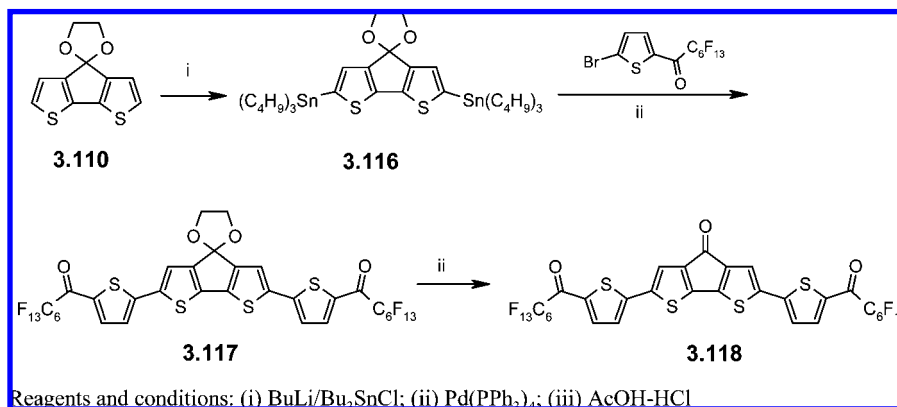
Matzger et al. utilized the same synthetic strategy to construct higher thienoacenes, such as pentathienoacene **3.130** and heptathienoacene **3.137** (Scheme 3.14). In this case, triisopropylsilyl (TIPS) groups were introduced to block the terminal reactive α-positions as well as to improve the solubility of the products. By an interesting "halogen dance" reaction, β-bromo substituted TT **3.131** and DTT **3.134** were obtained from corresponding α-bromosubstituted precursors. Pd-catalyzed coupling of β-bromo-substituted TT **3.131** and DTT **3.134** with hexabutyldistannan gave corresponding sulfides **3.132** and **3.135** in excellent yields (95% and 75%, respectively). TIPS-protected thienoacenes **3.133** and **3.136** were obtained by oxidative coupling of the sulfides with BuLi/CuCl₂. Fluoride-activated deprotection gave the desired products **3.130** and **3.137** in overall yields of 31% and 27%, respectively.[585] This more efficient method allows for large scale synthesis of higher oligo(thienoacenes).

Alkyl-substituted thienoacenes were synthesized by He and Zhang recently.[589] In this report, β-decyl-substituted tetrathienoacene **3.140** was synthesized from 2,3,4,5-tetrabromothieno[3,2-b]thiophene **3.64**. By a key ring closure reaction of thienothiophene-based diketone **3.138**, a diester of pentathienoacene **3.140** was synthesized in an overall yield of 22% in 5 steps (Scheme 3.15A). 3,6-Didecylpentathienoacene **3.143** was obtained by synthetic strategy B shown in Scheme 3.12. 3-Bromo-6-decylthieno[3,2-b]thiophene **3.141** was coupled to corresponding dimer **3.142** using LDA/CuCl₂. Lithium−halogen exchange of **3.142** with n-BuLi followed by reaction with bis(phenylsulfonyl)sulfide gave the desired product **3.143** in a yield of 45%. Attempts to synthesize 3,7-didecylheptathienoacene **3.146** by the same synthetic route were not successful due to the low solubility of dimeric precursor **3.145**. However, by using Matzger's coupling method,[585] alkylated heptathienoacenes **3.149** were synthesized in good yields (Scheme 3.15D).[589]
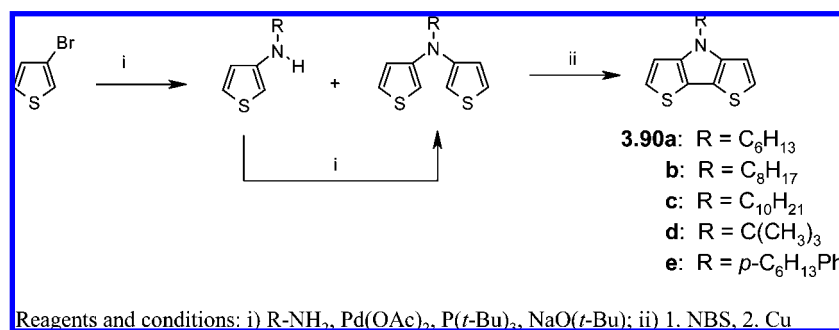
Chart 3.26

3.113: n = 0, 1   **P3.114**   **P3.115**

Scheme 3.9

Reagents and conditions: (i) BuLi/Bu₃SnCl; (ii) Pd(PPh₃)₄; (iii) AcOH-HCl

Scheme 3.10

3.90a: R = C_6H_{13}
   b: R = C_8H_{17}
   c: R = $C_{10}H_{21}$
   d: R = $C(CH_3)_3$
   e: R = p-C_6H_{13}Ph

Reagents and conditions: i) R-NH₂, Pd(OAc)₂, P(t-Bu)₃, NaO(t-Bu); ii) 1. NBS, 2. Cu

Chart 3.27

3.119   **3.120**   **P3.121**

Scheme 3.11

3.122   **3.123**
R = Ph or t-Bu   R = Ph or t-Bu
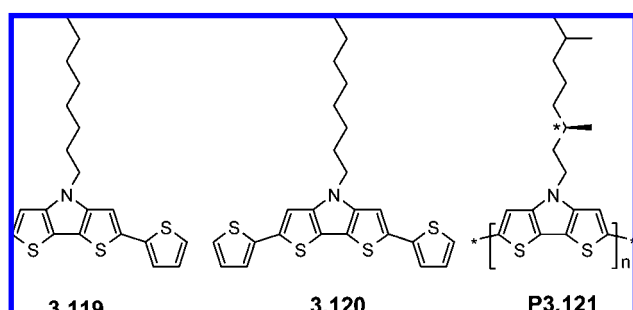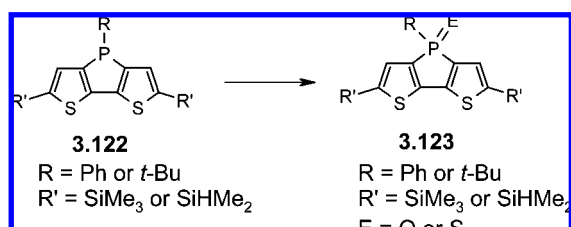R' = SiMe₃ or SiHMe₂   R' = SiMe₃ or SiHMe₂
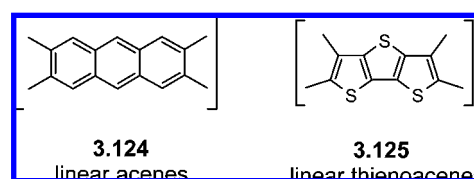   E = O or S

Although tetrathienoacene **3.128** was successfully synthe-sized by the synthetic methods discussed above (Scheme 3.13), synthesis of higher thienoacenes with even fused thiophene rings by either approach will be much more
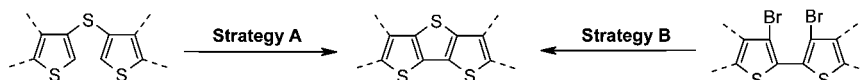
Chart 3.28

3.124   **3.125**
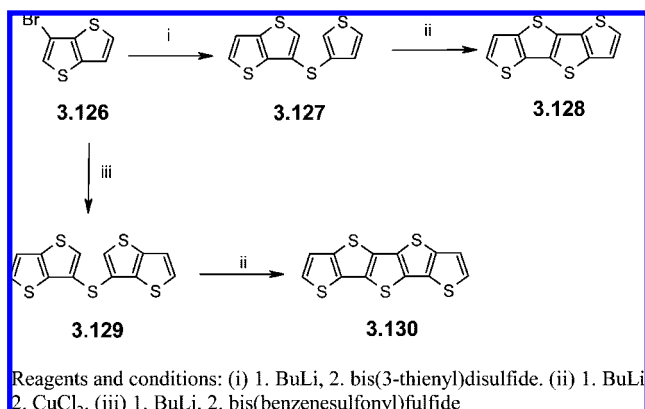linear acenes   linear thienoacenes

difficult, owing to the required asymmetric dimeric precursor. Yamaguchi et al. recently reported a general synthesis method to oligothienoacenes consisting of even fused thiophene rings starting from dithienylacetylene precursors (Scheme 3.16).[590] In this synthetic approach, intramolecular double cyclization of thienylacetylene to thiophene-fused thieno[3,2-*c*](1,2-dithiin) is the key reaction step. For example, TMS-protected dithienylacetylene **3.150** was lithi-ated by lithium−halogen exchange and then quenched with elemental sulfur to form dithiolated intermediate **3.151**, which underwent a 5-*endodig* mode cyclization to give thieno[3,2-*b*]thienylthiophenedithiolate **3.152**. Oxidative workup with K₃[Fe(CN)₆] in NaOH aqueous solution yielded dithiin **3.153**. Reductive dechalcogenation of **3.153** gave TMS-protected tetrathienoacene **3.154** in a yield of 56%.

By the same synthetic approach, TIPS-protected hexa-thienoacene **3.157** was synthesized starting from bis(3-bromothieno[3,2-*b*]thienyl)acetylene **3.155** in an overall

Scheme 3.12

Scheme 3.13

Reagents and conditions: (i) 1. BuLi, 2. bis(3-thienyl)disulfide. (ii) 1. BuLi, 2. CuCl₂. (iii) 1. BuLi, 2. bis(benzenesulfonyl)fulfide

yield of 25%.[590] Utilizing bis(thienothienyl)acetylene **3.158** as starting material, 2-fold intramolecular double cyclization gave the fused 1,2-dithiin **3.159** in 42% yield. Although **3.159** was obtained as a mixture of isomers, subsequent dechalcogenation of the mixture gave octathienoacene **3.160** in a yield of 51%. (Scheme 3.17) Single crystal X-ray structure analyses of the neutral octathienoacene and its dication were determined showing that in the neutral state **3.160** has a benzenoid structure with a large bond alternation of about 0.04 Å, whereas its dication has a quinoid structure in which two cationic charges are mainly localized on the terminal rings. This might be the reason for the absorption of thienoacenes which is blue-shifted when compared to the case of the corresponding linear α-oligothiophenes.

Bis(o-haloaryl)diacetylenes undergo intramolecular triple cyclization through a similar reaction procedure, producing thienoacenes with odd-numbered fused thiophene rings. As an example, dithienyl-diacetylene **3.161** was dilithiated with n-BuLi and then quenched by elemental sulfur to yield fused 1,2-dithian **3.162**. Subsequent dechalcogenation with copper metal afforded TMS-protected penta(thienoacene) **3.163**, which was obtained in 22% yield. Starting from 2,2′-(1,3-butadiyne-1,4-diyl)bis[3-bromobenzo[b]thiophene] **3.164**, intramolecular triple cyclization *via* dilithiation followed by reaction with elemental sulfur produced benzo[b]-fused penta(thienoacene) **3.166** in an overall yield of 55% (Scheme 3.18).[591,592] Recently, Yamaguchi et al. reported high mobilities of 0.25−0.5 cm² V⁻¹ s⁻¹ for transistors based on benzoannulated penta(thienoacene) crystals **3.166**.[593] In comparison to the well developed pentacene, thienoacenes showed much higher stability in OFETs applications. Although there is no published work yet, higher thienoacenes can be expected to be even better candidates for OFET devices due to their rigid planar molecular structures and high stabilities.

Tsuchida et al. developed a novel approach to 2,6-dimethyloligo(thienoacenes) **3.170** and linear poly(thienoacene) **3.174** (Scheme 3.19 and 3.20).[594] In this method, the corresponding thienoacenes were prepared by oxidation of 3-(alkylsulfanyl) precursors **3.167** and **3.171**, respectively, followed by an intramolecular ring closure condensation with triflic acid. Dealkylation of the resulting λ⁴-alkylsulfanyliumdiyl-fused oligo(thienoacenes) **3.169** and **3.173** in reflux-

ing pyridine gave 2,6-dimethyldithienophene **3.170a**, 2,6-dimethylpenta(thienoacene) **3.170b**, and poly(thienoacene) **3.174** in overall yields of 84−88% in a three-step reaction. Polymer **3.174** was an insoluble and infusible dark red powder. A solid film of **3.174** on a glassy carbon disk electrode was prepared *in situ* by dealkylation of the λ⁴-alkylsulfanyliumdiyl groups of **3.173** in a film, which was obtained by spin-coating of a solution of **3.173**. The redox properties of the poly(thienoacene) along with its precursors were investigated by cyclic voltammetry. All compounds revealed a first oxidation peak in the range of $E_p^a \approx 1.0-1.4$ V (vs Ag/AgCl) and broad reductive waves. The band gap of poly(thienoacene) **3.174** was determined from the difference between the onset potential of oxidation and reduction and resulted in the extremely low value of 0.4 eV. The conductivity of an iodine-doped film of poly(thienoacene) **3.174** was measured to be 300 S cm⁻¹. It is worthy to point out that the spectroscopic data of the oligo(thienoacenes) presented in this paper were quite different from those in previous papers.[591,595] The band gap obtained here was greatly different from the value (2.21 eV) estimated by extrapolation of the energy of the longest wavelength absorption versus the number of double bonds.

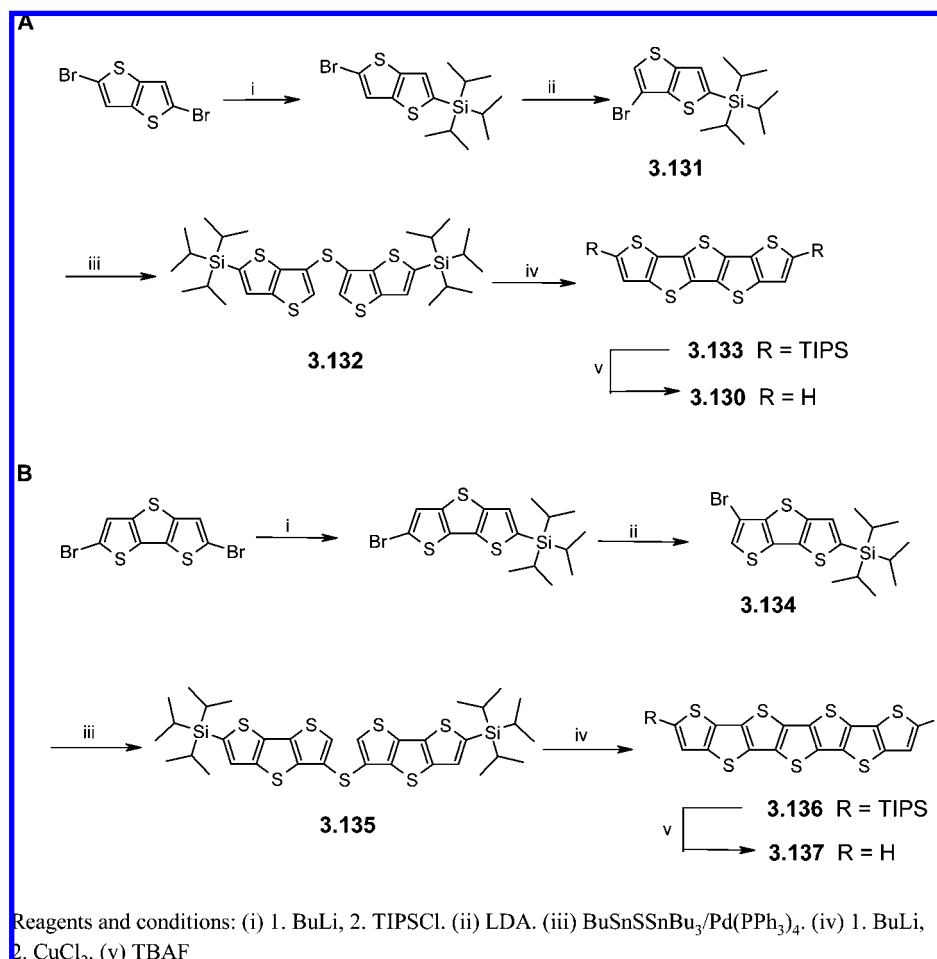### 3.4.2. S-Anellated β-Oligothiophenes

Annelation of 3,3′-bithiophene with a sulfur bridge produces the isomer of DTT. Scheme 3.21 illustrates the approach to synthesize the smallest homologue of the series of S-annelated β-oligo(thienoacenes), dithieno[2,3-b:3′,2′-d]thiophene **3.175**.[587,596] Similar approaches were used to get higher S-annelated β-oligo(thienoacenes).[55,597]

Nenajdenko et al. developed a unique synthesis toward fused β-oligothiophenes,[598] in which thieno[2,3-b]thieno[3′,2′:4,5]thieno[3,2-d]thiophene **3.178** was obtained in three steps from 3-bromothiophene with an overall yield of 23%. Isomer **3.179** was also synthesized by a similar strategy and isolated in 25% overall yield (scheme 3.22).

Very recently, the same research group reported the successful synthesis of octathio[8]circlene (**3.182**).[599] **3.182** has the molecular formula $C_{16}S_8$ (or simply $(C_2S)_8$) and can be classified as a new form of carbon sulfide. **3.182** was synthesized in an overall yield of 80% starting from tetrathiophene **3.180**, which was easily obtained in 70% yield from 3,4-dibromothiophene (Scheme 3.23).[600] The circlene was completely insoluble in common organic solvents. However, solid-state magic-angle spinning ¹³C NMR confirmed the highly symmetric structure of **3.182** (two signals at δ = 125 and 138 ppm). X-ray powder diffraction data analysis revealed a completely flat structure of the molecule.

Rajca et al. first reported synthesis and separation of optically active fused heptamer **3.185**. The helical thienoacene was obtained by condensation of 4,4′-dibromo-5,5′-bis(trimethylsilyl)dithieno[2,3-b:3′,2′-d]thiophene **3.183**. In the key annelation step, the authors used (−)-sparteine as the chiral inducing reagent to form the chiral lithiated precursor **3.184**. (−)-[7]Helicene (**3.185**) was obtained in yields of 20−37% with enantiomeric excesses (ee) of 19−47% (Scheme 3.24). An alternative approach to highly optically pure [7]helicene was developed by the same research group by a resolution-

Scheme 3.14

Reagents and conditions: (i) 1. BuLi, 2. TIPSCl. (ii) LDA. (iii) BuSnSSnBu$_3$/Pd(PPh$_3$)$_4$. (iv) 1. BuLi, 2. CuCl$_2$. (v) TBAF

based approach (Scheme 3.25). Lithiation of racemic helicene **3.187** by LDA afforded the dilithiated species, which was quenched with chiral menthyl-substituted chlorosiloxane [(−)-MenthSiCl] to obtain the protected diastereomeric mixture (±)-**3.188**. This was further separable by column chromatography. After desilylation with trifluoroacetic acid (TFA), highly optically pure [7]helicene **3.189** was obtained.[601,602]

More recently, the higher carbon−sulfur [11]helicene **3.192** was synthesized by the same research group by annulation of **3.191** mediated with (−)-sparteine (Scheme 3.26).[603] An X-ray structure analysis of **3.190** showed an almost planar geometry of the molecule.[598] However, increasing the number of annulated thiophenes led to a twist of the skeleton, yielding helical molecules.

In another publication, the synthesis of phenyl-condensed carbon−sulfur [7]helicene (**3.195**) was presented. Here, (−)-*B*-chlorodiisopinocamphenylborane was used to selectively reduce racemic diketone **3.193** to alcohol (+)-**3.194**, which then can be separated from unreacted (−)-**3.193**. The separated alcohol (+)-**3.194** was then reoxidized by pyridinium chlorochromate (PCC) to enantiomerically pure diketone (+)-**3.193**. Intramolecular McMurry reaction of both diketones, (+)-**3.193** and (−)-**3.193**, respectively, with TiCl$_3$/Zn/DME gave target molecules (+)-**3.195** and (−)-**3.195** with ee values of 50−90% (Scheme 3.27).[604]
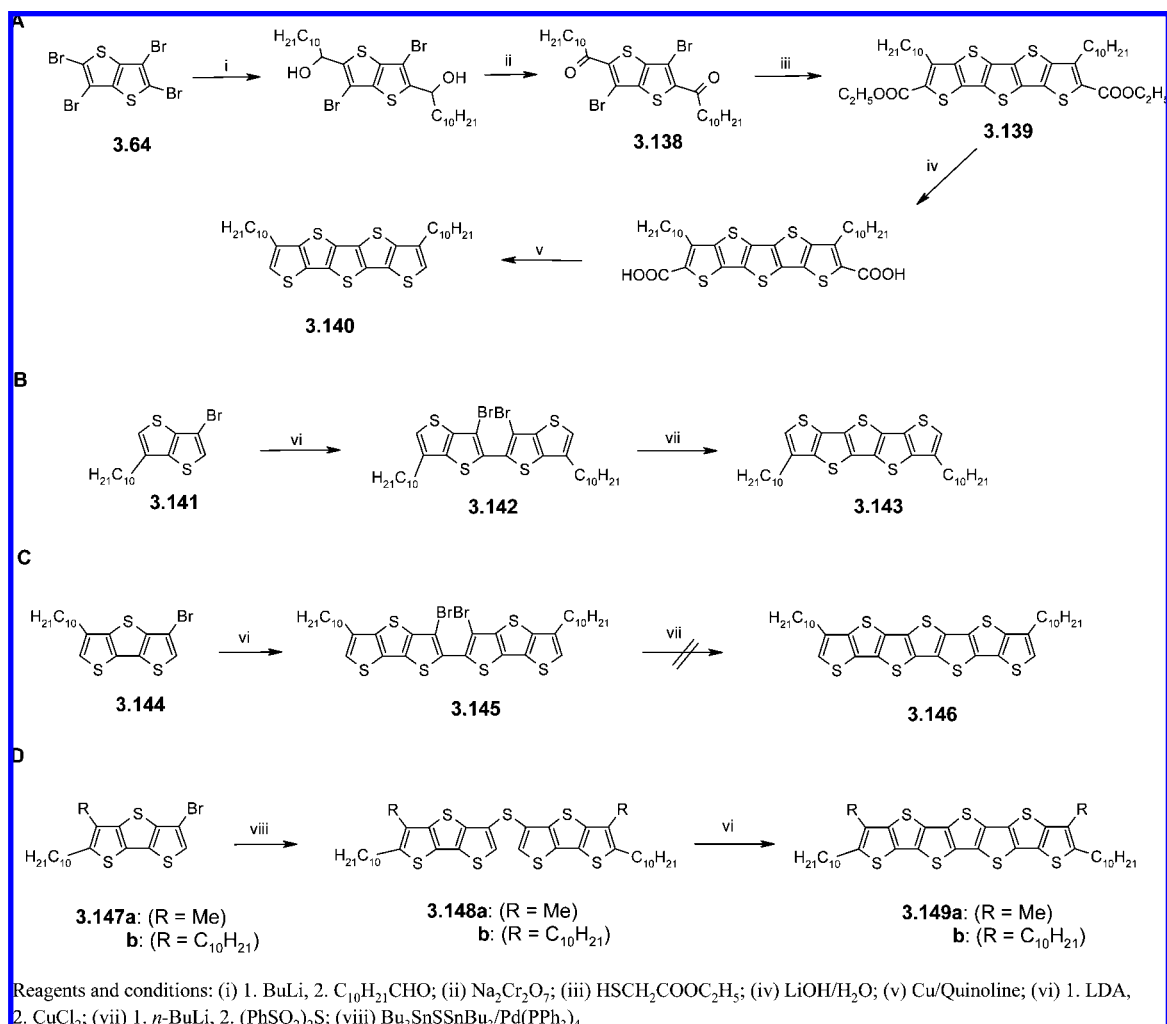
4. Macrocyclic Thiophenes

In the previous sections, linear and bandlike thiophene-based conjugated oligomers and polymers have been pre-
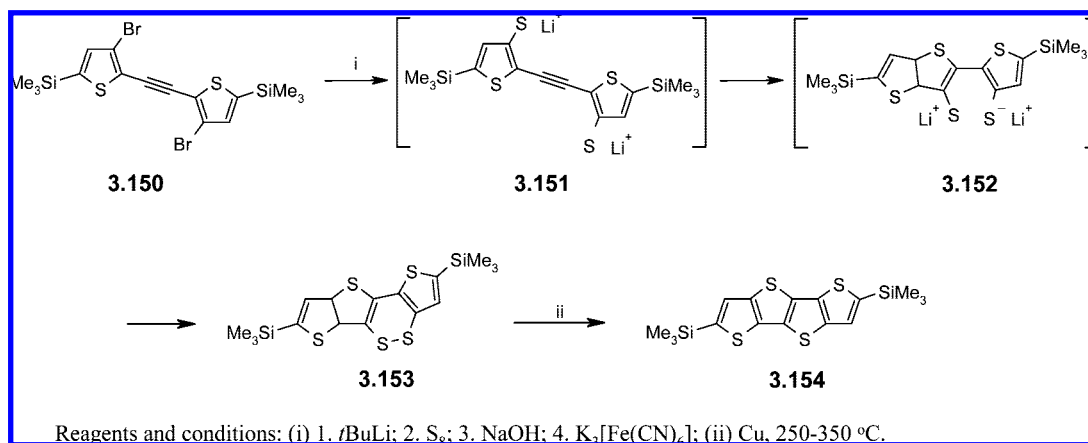
sented. In numerous investigated series of monodisperse linear oligothiophenes, the physical properties are well correlated to the structural parameters, such as chain and conjugation length of the oligomers, and thus, valuable information concerning structure−property relationships of these π-conjugated systems become accessible. However, sometimes the physical properties of such well-defined oligomers, in particular for the shorter ones, are influenced by undesired perturbing end effects on the conjugated chain.[37] In this respect, corresponding fully π-conjugated and shape-persistent macrocycles represent model systems, which in comparison to usual linear oligomers and polymers have the distinct advantage to ideally combine an "infinite" defect-free π-conjugated chain of an idealized polymer with the advantages of a structurally well-defined oligomer, but excluding perturbing end effects. This renders them as interesting candidates for various future perspectives and applications in organic and molecular electronics also with respect to host−guest interaction, aggregation, and self-assembly on surfaces (Figure 4.1).

In this section, thiophene-based "conjugated" macrocycles, made of sp^2- or sp-carbons in the perimeter, are described. Conjugation is put into quotation marks, because in several described systems thiophene units are linked *via* β-positions, which results in cross-conjugation and interruption of the conjugation. The section is divided up into three parts: the first one describes macrocycles containing purely thiophenes (section 4.1), the second one describes those containing thiophenes mixed with other unsaturated moieties such as

Scheme 3.15

Reagents and conditions: (i) 1. BuLi, 2. $C_{10}H_{21}CHO$; (ii) $Na_2Cr_2O_7$; (iii) $HSCH_2COOC_2H_5$; (iv) $LiOH/H_2O$; (v) Cu/Quinoline; (vi) 1. LDA, 2. $CuCl_2$; (vii) 1. n-BuLi, 2. $(PhSO_2)_2S$; (viii) $Bu_3SnSSnBu_3/Pd(PPh_3)_4$.

Scheme 3.16

Reagents and conditions: (i) 1. tBuLi; 2. S_8; 3. NaOH; 4. $K_3[Fe(CN)_6]$; (ii) Cu, 250-350 °C.

phenylenes, heterocycles, ethenylenes, and ethynylenes (section 4.2), and the third part collects representative thiophene-containing porphyrinoid macrocycles or thiaporphyrin derivatives (section 4.3).

All systems, in principle, can be regarded as annulene derivatives, and many of them have been prepared with this viewpoint. With the venue of conducting polymers and organic electronics, more recently, emphasis has been put, rather, on the design of thiophene-based macrocycles
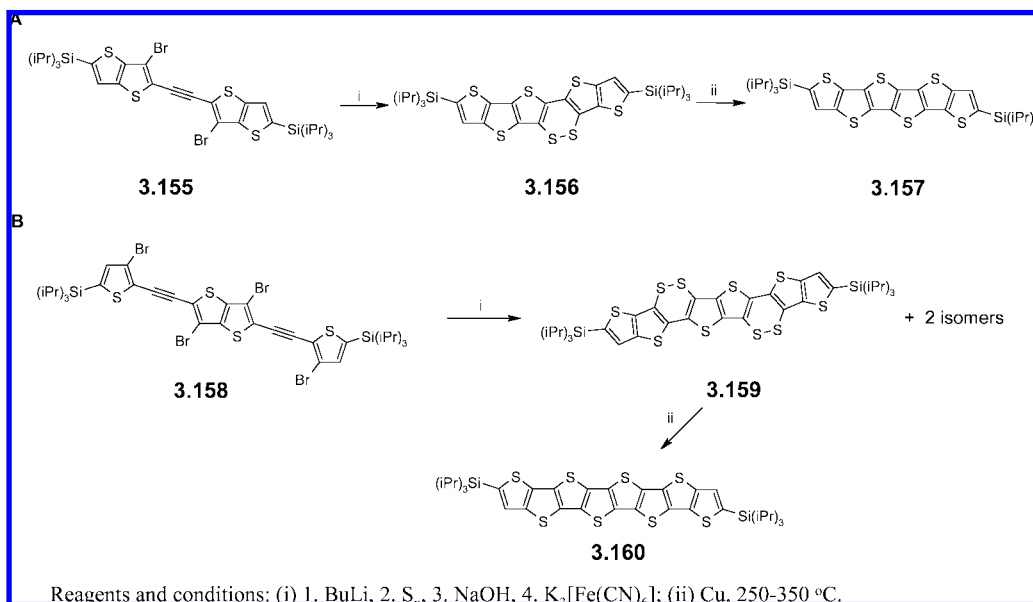
which are model systems and show interesting electronic properties.

4.1. Macrocycles Based Only on Thiophenes

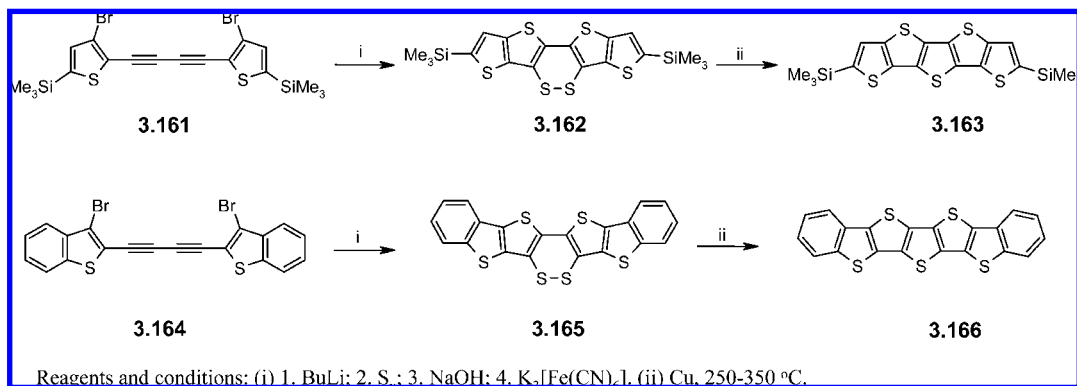### 4.1.1. Linkages Including β-Positions of Thiophene Units Leading to Cross-conjugated Cyclo[n]thiophenes

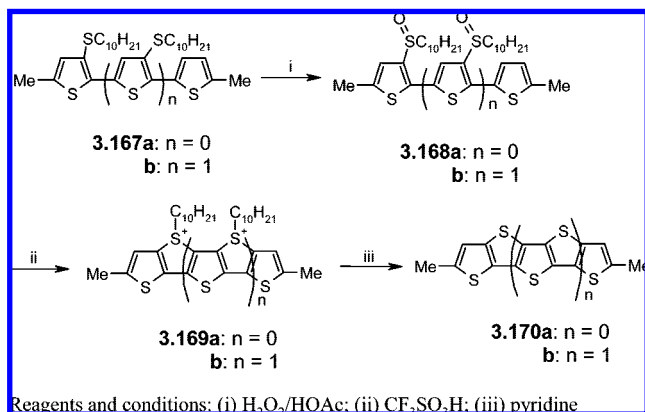Cyclobutadithiophene **4.1** can formally be regarded as the smallest member of the cyclothiophenes. Also known as

Scheme 3.17

Reagents and conditions: (i) 1, BuLi, 2, S$_n$, 3, NaOH, 4, K$_3$[Fe(CN)$_6$]; (ii) Cu, 250–350 °C.

Scheme 3.18

Reagents and conditions: (i) 1. BuLi; 2. S$_n$; 3. NaOH; 4. K$_3$[Fe(CN)$_6$], (ii) Cu, 250–350 °C.

Scheme 3.19

Reagents and conditions: (i) H$_2$O$_2$/HOAc; (ii) CF$_3$SO$_3$H; (iii) pyridine

Scheme 3.20

Reagents and conditions: (i) H$_2$O$_2$/HOAc; (ii) CF$_3$SO$_3$H; (iii) pyridine

Scheme 3.21

Reagents and conditions: (i)1.LDA, 2. (PhSO$_2$)$_2$S; (ii) 1. LDA, 2. CuCl$_2$

cyclo[2]thiophene or cyclodi(3,4-thienylene), it has been prepared by Shepherd as the most stable of the four possible isomeric dithia-analogues of biphenylene.[605] In the ^{1}H NMR spectrum of **4.1**, a paramagnetic shift for the α-thiophene protons has been found, indicating a cyclobutadienoid or [4]-annulenoid structure. In the UV spectrum, absorptions are red-shifted (334, 318 nm) compared to that of thiophene (230 nm), providing evidence of electronic interaction and conjugation between the two thiophene units.

The next higher homologue, cyclo[3]thiophene or cyclo-tri(3,4-thienylene) **4.2**, represents an "exocyclic benzene"
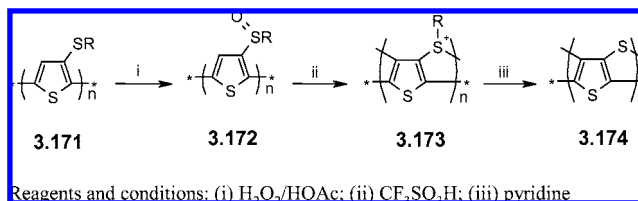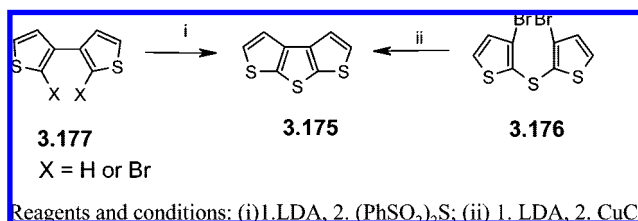
containing [c]-fused thiophene rings and has been synthesized in about 40% yield from hexakis(bromomethyl)benzene and sodium sulfide and subsequent oxidation of the resulting trisulfide with chloranil.[606] Very recently, Bendikov et al. prepared the same compound in one step by Ni-catalyzed cyclotrimerization of 3,4-dibromothiophene in 40% yield. It had to be separated from the simultaneously formed cyclotetramer **4.8** (40% yield). An X-ray structure analysis

Scheme 3.22

Reagents and conditions: (i) 1. LDA, 2. S, 3. CH$_2$Br$_2$; (ii) 1. BuLi, 2. Me$_2$NCO$_2$Et; (iii) BuLi/HMPA, -80 °C-RT; (vi) HMPA, 150-200 °C; v) NBS
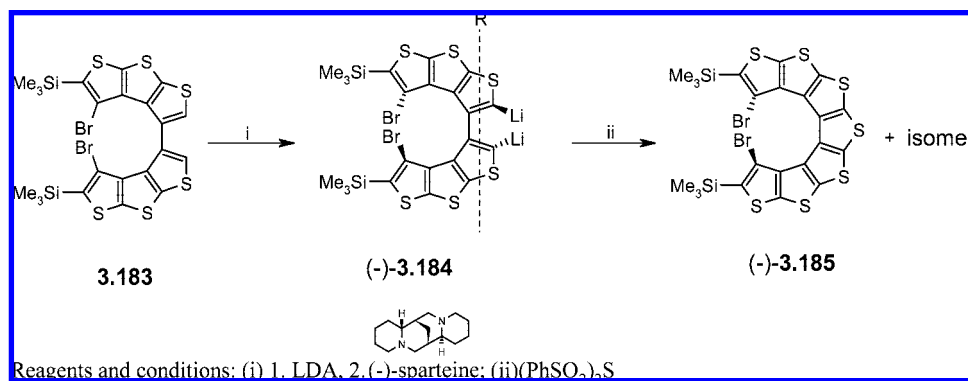
Scheme 3.23

Reagents and conditions: (i) LDA (16 equiv), Sulfur (16 equiv); (ii) aq. HCl; (iii) vacuumm pyrolysis

Scheme 3.24

Reagents and conditions: (i) 1. LDA, 2. (-)-sparteine; (ii)(PhSO$_2$)$_2$S

Scheme 3.25

| 3.186 R = TMS | (-)-3.188 (38 - 50 %) | (-)-3.189 (96% ee 97 +%) |
| 3.187 R = H | (+)-3.188 (40 -45 %) | (+)-3.189 (93 % ee -93 %) |

Reagents and conditions: (i) TFA, CHCl$_3$, RT; (ii) 1. LDA, 2. (-)-MenthSiCl
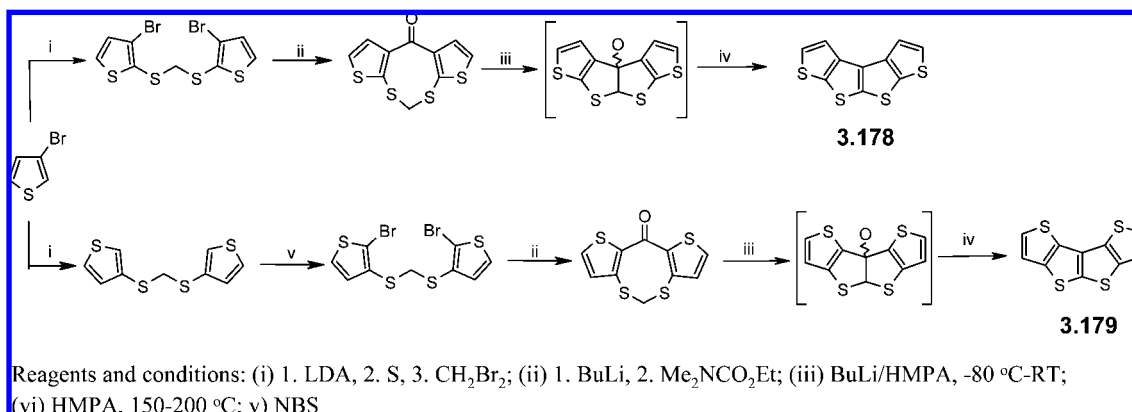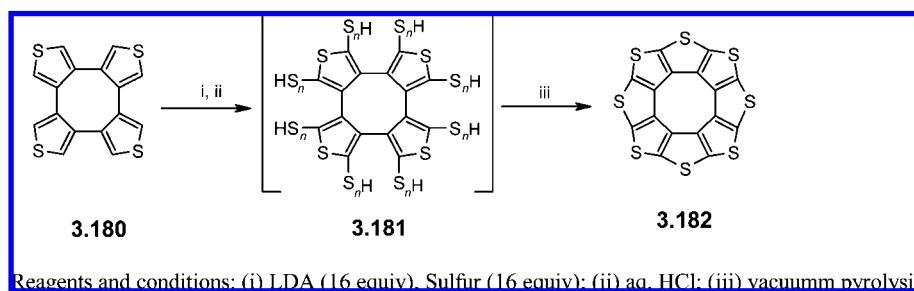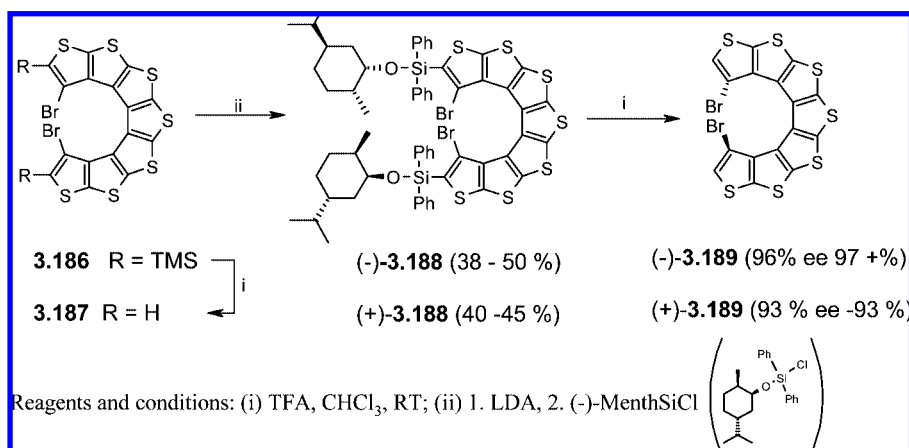
of **4.2** showed practically planar molecules with D_{3h} symmetry. It was found that the aromatic C–C bonds of the central six-membered ring with 1.451 Å were unusually long whereas the exocyclic double bonds were relatively short (1.36–1.37 Å) and can be considered rather as a [6]radialene than a [6]annulene. UV spectra of **4.2** showed besides the strong absorption for the thiophene rings at 254 nm redshifted absorption peaks which are ascribed to interactions

Scheme 3.26

Reagents and conditions: (i) Pd(P(t-Bu)₃)₂, K₃PO₄, toluene; (ii) LDA, (−)-sparteine; (iii) (PhSO₂)₂S

Scheme 3.27

Reagents and conditions: (i) (−)-B-chlorodiisopinocamphenylborane, column chromatography; (ii) PCC; (iii) TiCl₃, Zn, DMF.
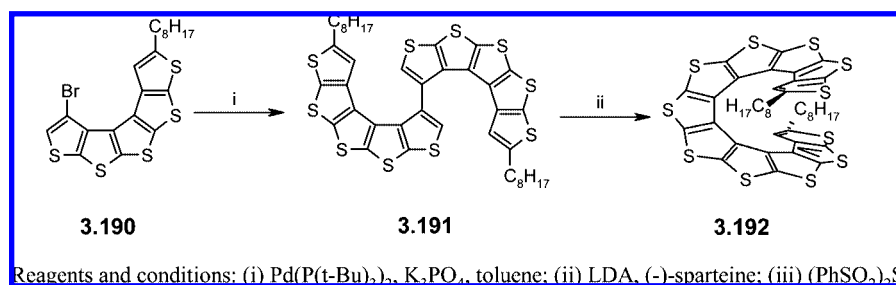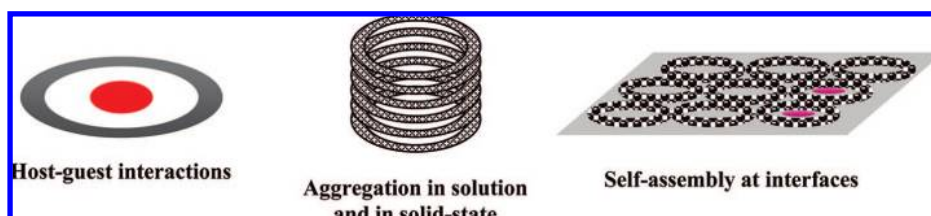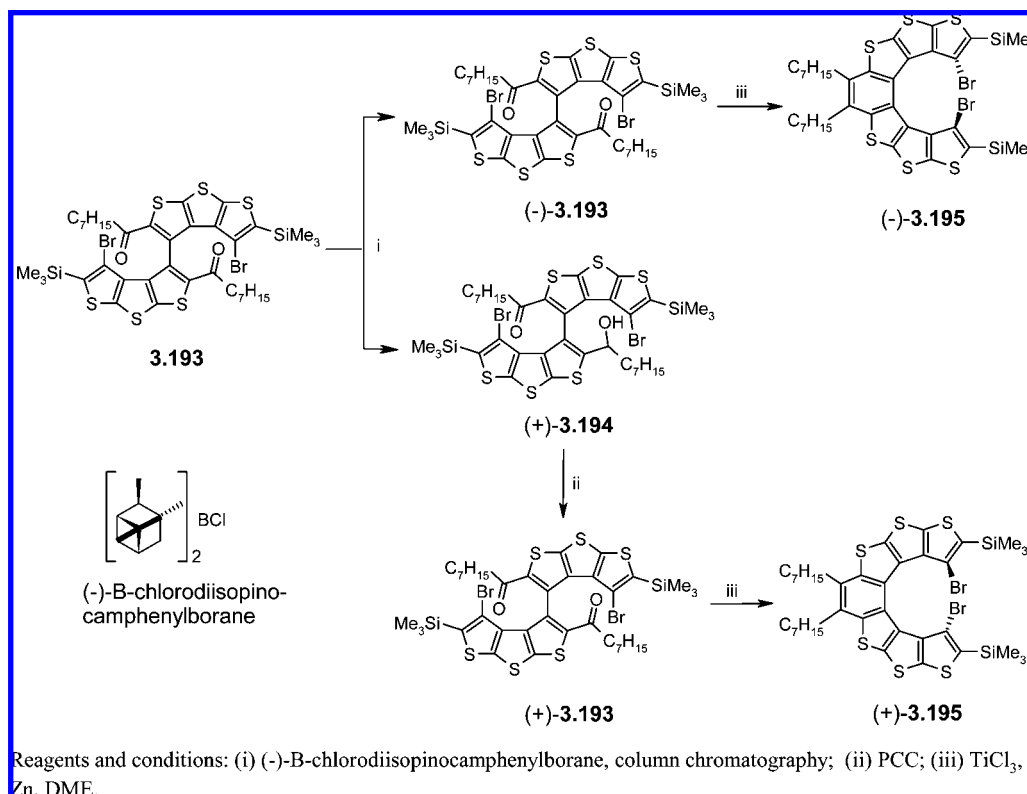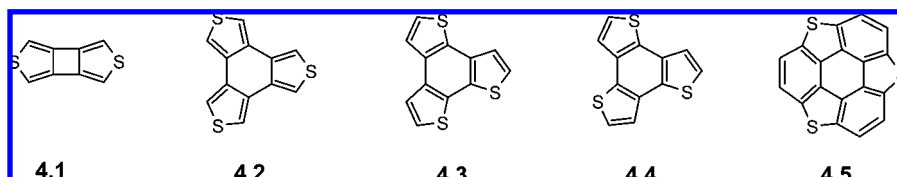

Figure 4.1. Properties of shape-persistent macrocycles.

between the heterocyclic rings through the central ring.[607] Other benzotrithiophene isomers **4.3** and **4.4** containing [*b*]-fused thiophene rings were made by photocyclization of terthiophenes in 69% and 34% yield.[608] Cyclotri[2,3-thienylene] **4.4** was later more efficiently prepared as a single regioisomer by oxidative photocyclization of 2,3′:3,2″-terthiophene in 60% yield and has been used as a core for the construction of star-shaped oligothiophenes.[489,609] The UV spectrum of trisbenzo[*c*] isomer **4.2** showed its longest wavelength absorption at 320 nm whereas trisbenzo[*b*] isomer **4.4** absorbs at appreciably lower wavelength (286 nm), a trend which also has been found for benzo[*c*]thiophene (343 nm) in comparison to benzo[*b*]thiophene (298 nm).[606] Recently, cyclo[3]thiophene **4.2** has been used as starting

material for the synthesis of a bowl-shaped thia analogue **4.5** of corannulene (Chart 4.1).[610]

The synthesis of cyclo[4]thiophenes was already reported in 1975 by Kauffmann et al.[611] Partly cross-conjugated cyclotetra(2.3-thienylene)s **4.6**−**4.8** were prepared by oxidative coupling reactions of various lithiated bithiophene precursors (Scheme 4.1). Starting from 2,2′-dibromo-3,3′-bithiophene or 3,3′-dibromo-2,2′-bithiophene, **4.6** was obtained in 18-25% yield, whereas 4,4′-dibromo-3,3′-bithiophene gave isomeric cyclotetramer **4.8** (23% yield). Both systems can be regarded as thiophene-fused [8]annulene or cyclooctatetraene (COT) derivatives. Analogous reaction of 3,3′-dibromo-2,2′-bithiophene gave instead cyclosexi(2.3-thienylene) **4.9**, a thiophene-fused [12]annulene, although in very

Chart 4.1

Scheme 4.1

Reagents and conditions: (i) n-BuLi, CuCl₂.

Scheme 4.2

Reagents and conditions: (i) n-BuLi, CuCl₂.
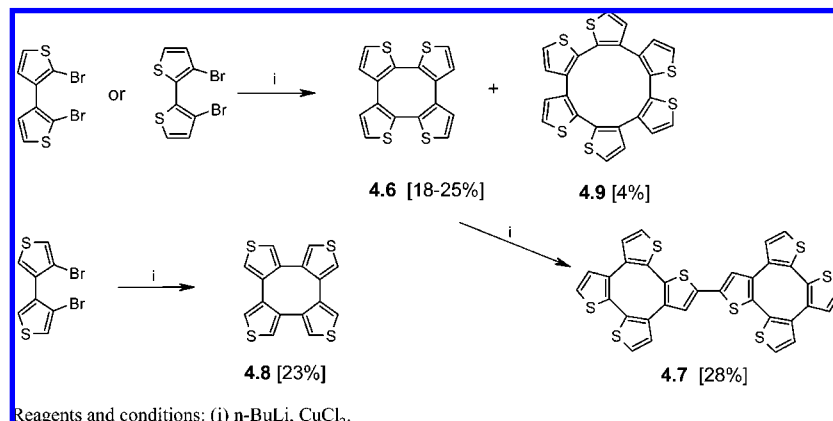
Chart 4.2

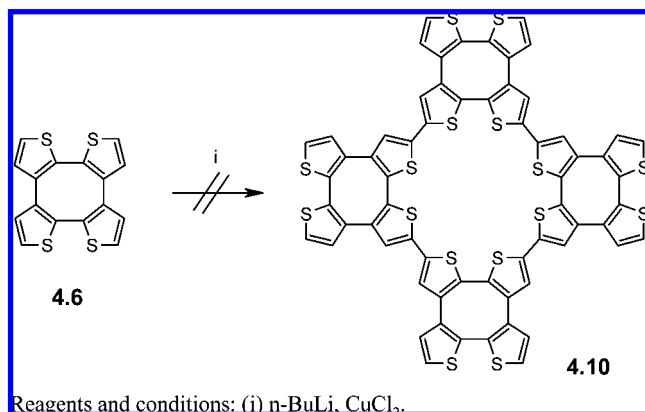low yield. Lithiation of the macrocycles typically led only to monolithiated species, and oxidative coupling of 2-lithio-cyclotetrathiophene **4.6** gave the interesting structure of "dimeric" cyclotetrathiophene **4.7** (28% yield) (Scheme 4.1). Due to the interruption of the electronic pathway, which is caused by α,β- or β,β-linkages of the thiophene units, and due to a highly distorted structure with the thiophene rings being twisted to each other by 54°, as confirmed by X-ray structure analysis of **4.7**,[612] these macrocycles were expected to be only very weakly conjugated. By bonding character, they rather resembled an octamethylene-cyclooctane than a COT. For example, [8]annulene **4.6** had an absorption maximum of $\lambda_{max}= 278$ nm, which lies lower than that of the corresponding cyclotrimer **4.2** and in between those of a 2,2′-bithiophene ($\lambda_{max}= 302$ nm) and 3,3′-bithiophene ($\lambda_{max}= 263$ nm).[37] Cyclotetrathiophene **4.8** later on has been synthesized in one step from 3,4-dibromothiophene by modern Ni-catalyzed cross-coupling reactions in 70% yield.[613]

The ambitious aim of Kauffmann et al. to synthesize a "supercyclopolythiophene" as represented in **4.10** (Scheme 4.2) could not be achieved due to the failure of a second lithiation of **4.6**.[614] The inner perimeter of hypothetical **4.10** corresponds to an α-conjugated cyclo[8]thiophene which was
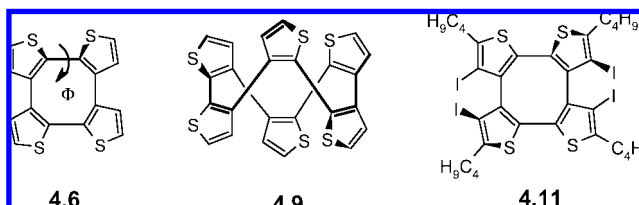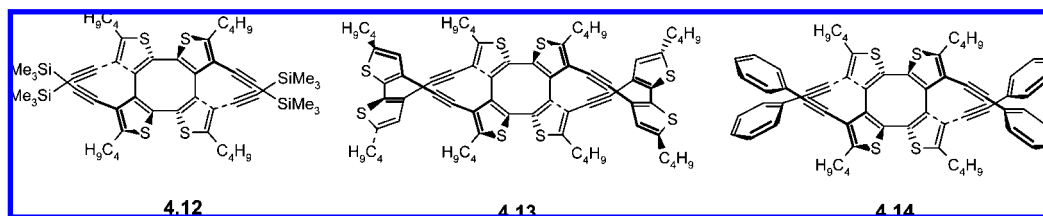
synthesized nearly 20 years later by Bäuerle et al. in a completely different way (*vide infra*).
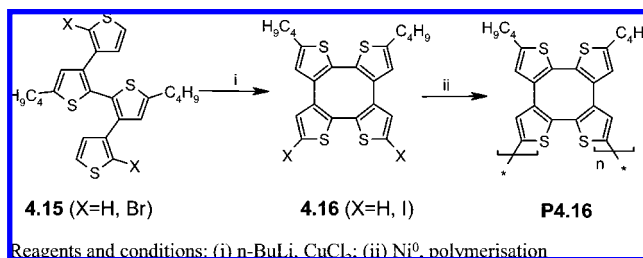
Despite the emergence of polythiophenes in 1981 and their continuing success story as (semi)conducting polymers which triggered an enormous amount of thiophene chemistry,[1] Kauffmann's thiophene-based annulenes were taken up only very recently by Marsella et al. as building blocks for π-functional materials with applications as "molecular actuators". The synthesis now was performed using modern transition metal-catalyzed coupling and cyclization reactions. Detailed structural characterization showed that the twisted nature of these annulenes gives rise to helical and tubular scaffolds (Chart 4.2).[615,616]

Reversible redox-induced conformational changes in these COT-derivatives (boat-shaped in the antiaromatic neutral state and planar in the aromatic 2⁻-state) predetermined them for molecular models for actuation. Functionalization of cyclotetra[2,3-thienylene] as a modular building block for the synthesis of double-helical structures was achieved by halogenation to **4.11** (X = I) and successive Pd/Cu-catalyzed Sonogashira-type cross-coupling of TMS-protected ethynylene groups to the four β-positions of the thiophene units to form extended double helical system **4.12**. In an analogous tandem cross-coupling reaction between a 3,3′-ethynylene-substituted 2,2′-bithiophene and the tetraiodo derivative of **4.11** under high dilution conditions, ladder-type octathienyl oligomer **4.13** was isolated in a remarkable 28% yield. The phenyl-capped derivative **4.14** was synthesized in 35% yield from the same tetraiodo cyclotetrathiophene **4.11** and phenylacetylene. Interestingly, crystals of **4.14** showed homo-
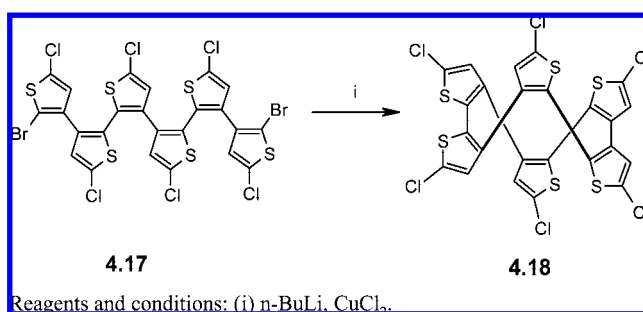
Chart 4.3

Scheme 4.3

4.15 (X=H, Br)   **4.16** (X=H, I)   **P4.16**

Reagents and conditions: (i) n-BuLi, CuCl₂; (ii) Ni⁰ polymerisation

Scheme 4.4

4.17   **4.18**

Reagents and conditions: (i) n-BuLi, CuCl₂.

Scheme 4.5

4.19: R=TMS, H

4.20: n =3-9

Reagents and conditions: (i) CuCl₂, CuCl, pyridine, RT, pseudo high-dilution

chiral double-helical polymeric strands due to intermolecular edge-to-face interactions of phenyl rings (Chart 4.3).[617]

Synthesis of a poly[tetra(2,3-thienylene)] **P4.16** was realized by typical Ni⁰-catalyzed cross-coupling polymerization of halogenated tetramer **4.16**, which in turn was prepared effectively from quaterthiophene **4.15** by oxidative coupling in 48% yield (Scheme 4.3).[615,616] The polymer, a poly([8]-annulene), which was soluble in organic solvents due to the butyl side chains, showed electronic properties typical for polythiophenes; a measurement of actuation, however, could not be obtained.

In addition, Iyoda et al. recently reported the synthesis of variants of tetra[2,3-thienylene] which are planar, in contrast to Marsella's derivatives.[600] With respect to thiophene-based [12]annulene **4.9**, which was first synthesized by Kauffmann et al. in low yields, Marsella and his group extended this scaffold by preparing hexachloro-substituted hexa(2,3-thienylene) **4.18** starting from 3,3′-bithiophene. The oxidative macrocyclization of the terminally lithiated hexachloro-sexithiophene **4.17** with copper chloride gave the tubular structure in 20% yield (Scheme 4.4). The poor π-orbital overlap within the [12]annulene framework is represented by the onset of absorption at very high energies (320 nm) compared to the case for α-conjugated sexithiophene and distorsions of the thiophene units by 103° on average, which were determined by X-ray crystallography.[618]

4.1.2. Linkages Including α-Positions of Thiophene Units Leading to Conjugated Cyclothiophenes

The feasibility and importance of fully α-conjugated cyclothiophenes was supported by theoretical calculations
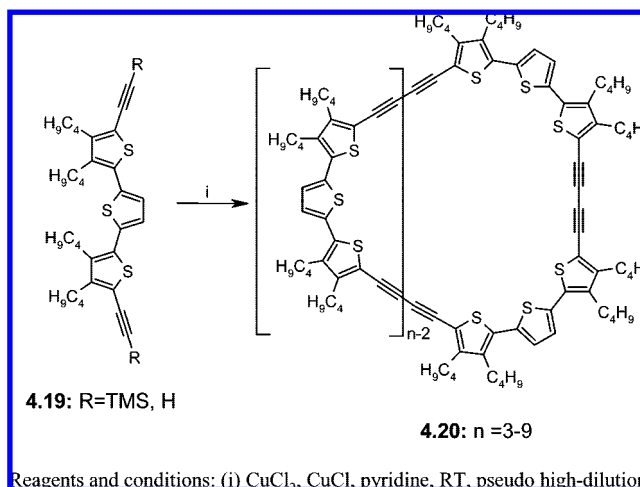
which were carried out in 1995 by Tol on cyclo[12]thiophene and on its corresponding charged species. These calculations revealed a nearly nonstrained and coplanar structure with an all-syn conformation of the thiophene rings. Most interestingly, charging of this cyclic structure led to a radical cation which is delocalized only over a semicircle and subsequently to a doubly oxidized species which exists as two cation radicals, each located on one semicircle and not in a dicationic quinoidal form as for linear oligothiophenes.[619]

The synthesis of the first fully α-conjugated cyclothiophenes was realized in the year 2000 by Bäuerle et al. based on a statistical macrocyclization of terminally bis-ethynylated oligothiophenes **4.19** and **4.21**, respectively. In this common method to prepare macrocycles, oligomerization and macrocyclization are involved at the same time.[620−624] Oxidative coupling of terthiophene **4.19** by a modified Eglington−Glaser variant under pseudo-high-dilution conditions gave a mixture of macrocyclic terthiophene-butadiynes **4.20** (n = 3−9), as expected in a moderate overall yield of 8.7% (Scheme 4.5).

The pure macrocycles from the cyclotrimer to the cyclononamer were isolated by separation with preparative HPLC, whereby the formation of the cyclotetramer (4%) and cyclotrimer (2.6%) was favored. The structures were proven by NMR and MALDI-TOF-MS.[625−627] Accordingly, quinquethiophene **4.21** was cyclized to give a mixture of cyclo(quinquethiophene-butadiynes) **4.22** (n = 2−6) in 13.5% overall yield (Scheme 4.5). In this case, the cyclotrimer (8%) is formed in excess (Scheme 4.6).

Another strategy other than the less efficient statistical approach is represented by an intramolecular macrocyclization of doubly functionalized longer oligomers. Here, the final cyclization step usually yields only one product; however, the unavoidable pitfall is the more time-consuming stepwise synthesis of the corresponding precursor of defined length.[620−624] The availability of well established synthetic methods for constructing longer oligothiophenes[628,629] gave

Scheme 4.6

4.21: R=TMS, H

4.22: n=2-6

Scheme 4.7

4.23: R=TMS, H

4.24

4.25
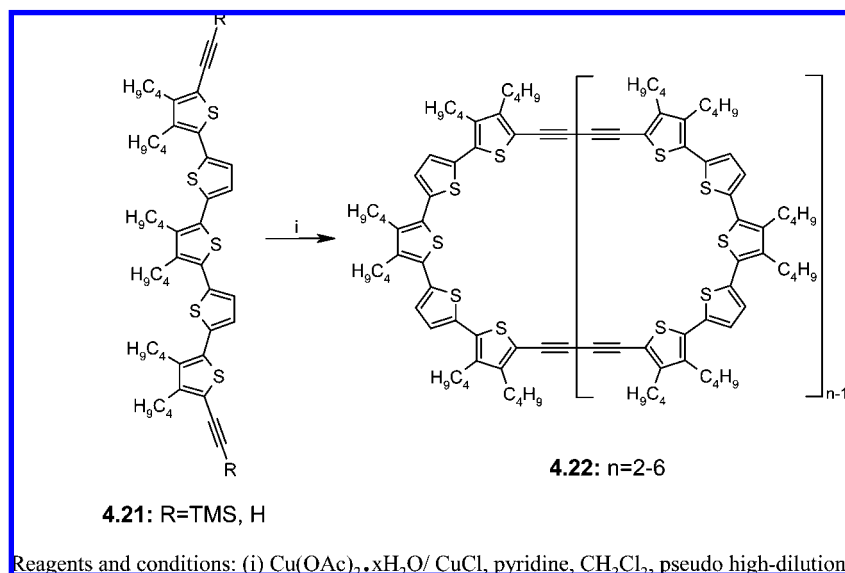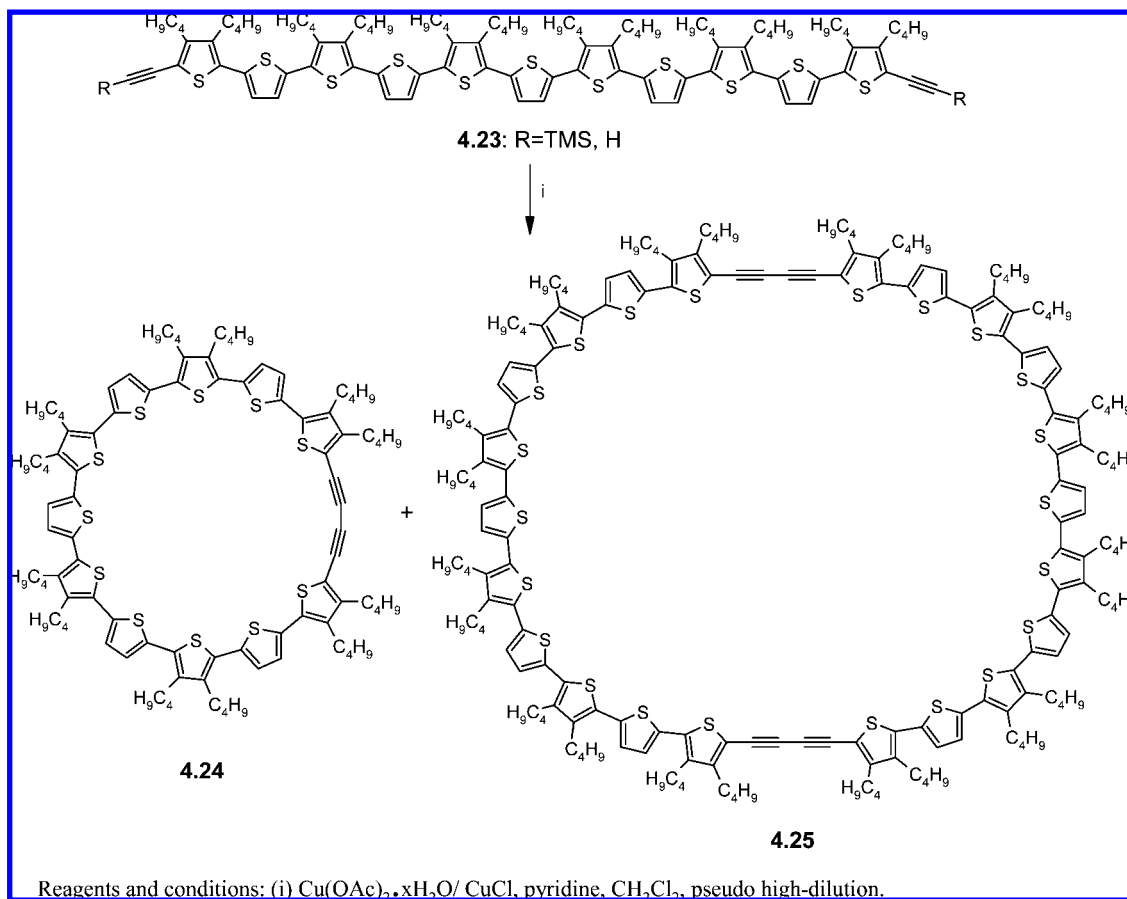
the option to investigate a one-step intramolecular cyclization of diethynylated 11-mer **4.23** which was carried out under modified Eglinton reaction conditions. The red microcrystalline product consisted of two macrocycles which were separated to yield cyclo(undecithiophene-butadiyne) **4.24** (31%, m/z = 1622.4), formed by an intramolecular reaction, and the corresponding giant 96-membered dimer **4.25** (18%, m/z = 3245.3), formed by an intermolecular reaction (Scheme 4.7).[626] A comparison of the overall yield for both approaches results in 4.6% for the intramolecular macrocy-

clization (7 steps starting from quinquethiophene) and only 2.4% for the statistical intermolecular method (three steps starting from quinquethiophene).

Di(oligo)thienyl-butadiynes reacted with sulfide to give the corresponding α-conjugated oligothiophenes in excellent yields.[611,614,630,631] Analogous reaction of macrocycles **4.20** (n = 3), **4.20** (n = 4), and **4.22** (n = 3), respectively, with sodium sulfide gave fully α-conjugated cyclo[12]thiophene **4.26**, cyclo[16]thiophene **4.27**, and cyclo[18]thiophene **4.28** in 23%, 7%, and 27% yield, which correspond to 52−64%

Scheme 4.8

4.20 (n=1, m=1), **4.20** (n=1, m=2)
4.20 (n=2, m=1)

4.26

4.27

4.28
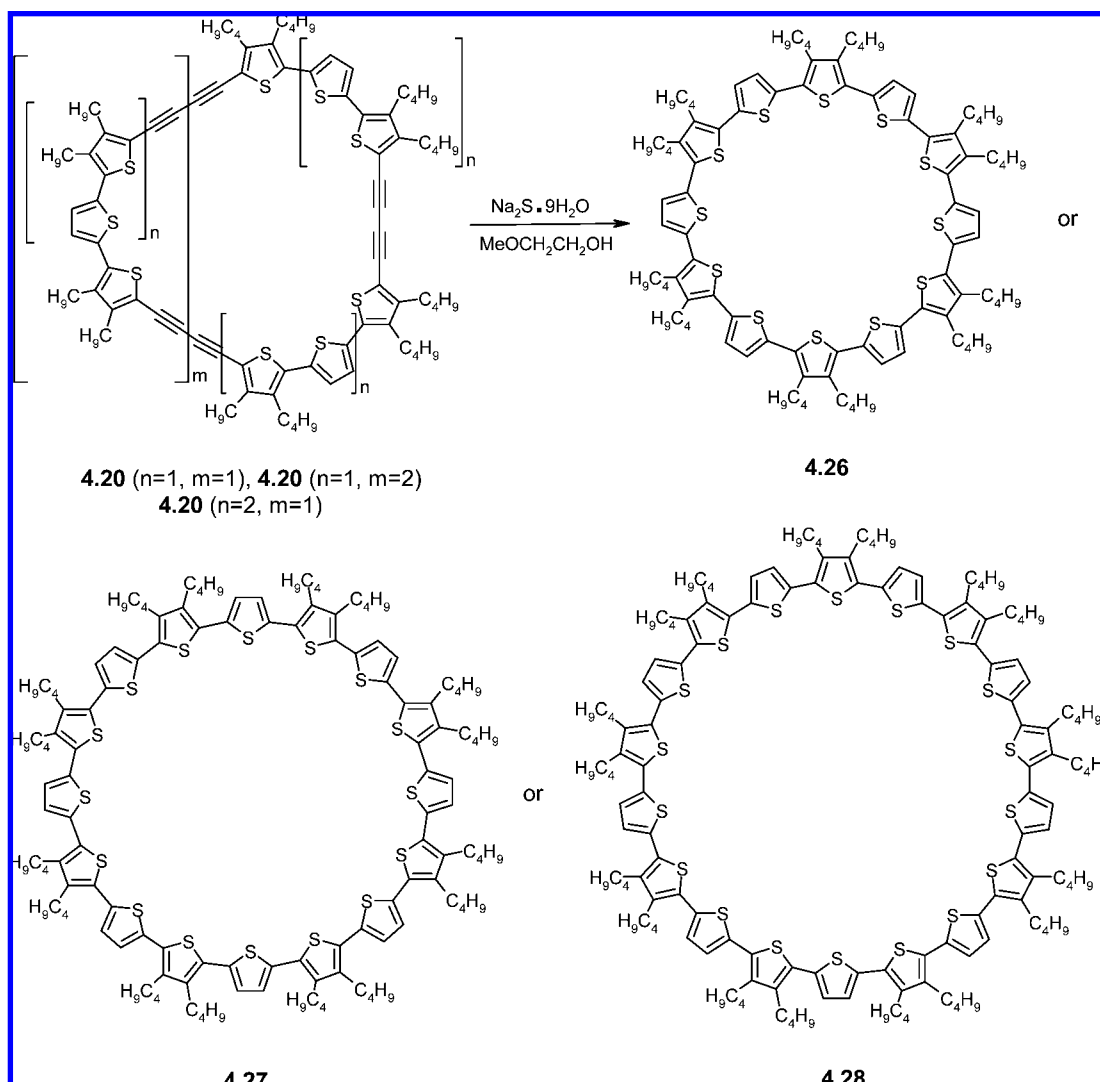
per reaction step (Scheme 4.8). The three cyclothiophenes are stable orange to red microcrystalline solids which are well soluble in most common organic solvents. Despite the fact that these macrocycles could be considered as $(4n)\pi$ antiaromatic [48]-, [64]-, and [72]-annulenes (36, 48, and 54 ring members), no obvious ring current shifts are observed, indicating benzenoid rather than annulenoid character. According to semiempirical calculations, they form cavities in the nanometer regime with 1.28, 1.81, and 2.00 nm inner diameter. The calculated strain energies of the macrocycles were rather low (0.0−1.8 kcal/mol).

In general, kinetically controlled macrocyclization reactions are low-yielding processes which lead to a mixture of cyclic products. An alternative and more promising approach includes the use of templates, as well as cyclizations under thermodynamic control. Template-directed synthesis can be a powerful tool to prepare macrocycles in high yields, but mostly a lot of effort must be put toward developing suitable templates with the required structural and functional properties.[620−624,632] Moreover, the method is limited to certain cases where adequate functionalities in the core allow noncovalent or covalent interactions with the template. The advantages of performing macrocyclization reactions under thermodynamic control have been clearly pointed out in the field of supramolecular chemistry.[633−638] In the directional-bonding approach elaborated independently by Fujita and

Stang,[639−641] cis complexes of transition metals are used to self-assemble with organic ligands to form well-ordered supramolecular cyclic structures under thermodynamic equilibrium.

In this respect, Bäuerle et al. have now developed a novel and effective protocol for the synthesis of conjugated macrocycles in which conveniently accessible bis-ethynylated building blocks and transition metal precursor complexes self-assemble to form stable, coordinatively bound metallamacrocycles. Most importantly, the transition metal units were subsequently expelled under simultaneous formation of C−C bonds, leading to the conjugated macrocycles. Thus, by reaction of cis-Pt(dppp)Cl₂ and bis-ethynylated terthiophene **4.19** in the presence of CuI and NEt₃, bisplatinamacrocycle **4.29** was isolated in 91% yield (Scheme 4.9). Reductive 1,1-eliminations for C−C coupling products from Pd σ-acetylide complexes are well-known to effectively proceed in the catalytic cycle of the Sonogashira−Hagihara reaction[53] or the Pd-catalyzed version of the Glaser coupling.[642,643] In a newly developed reaction, 1,1-reductive elimination of the Pt(dppp) "corners" from bismetallacycle **4.29** was achieved with iodine under simultaneous C−C bond formation and preservation of the cyclic structure in cyclodimeric terthiophene-butadiyne **4.30** (54% yield). It represented the smallest (26-membered, 32-annulene) macrocycle in the homologous series, which, however, never
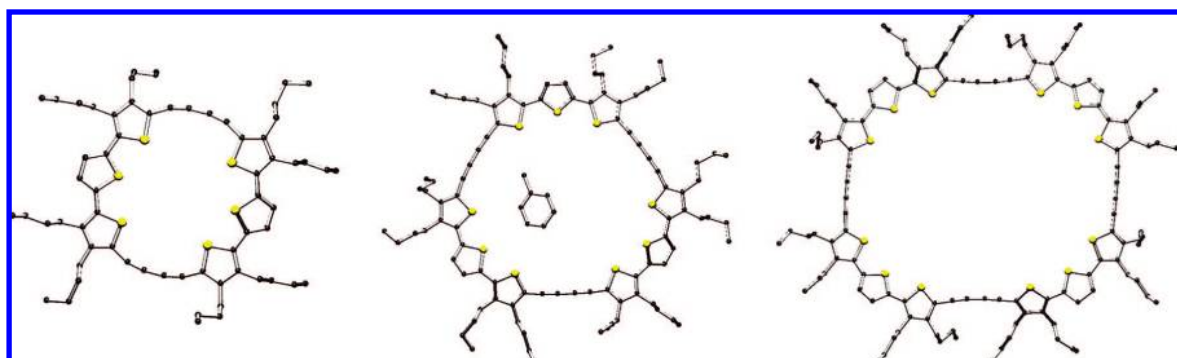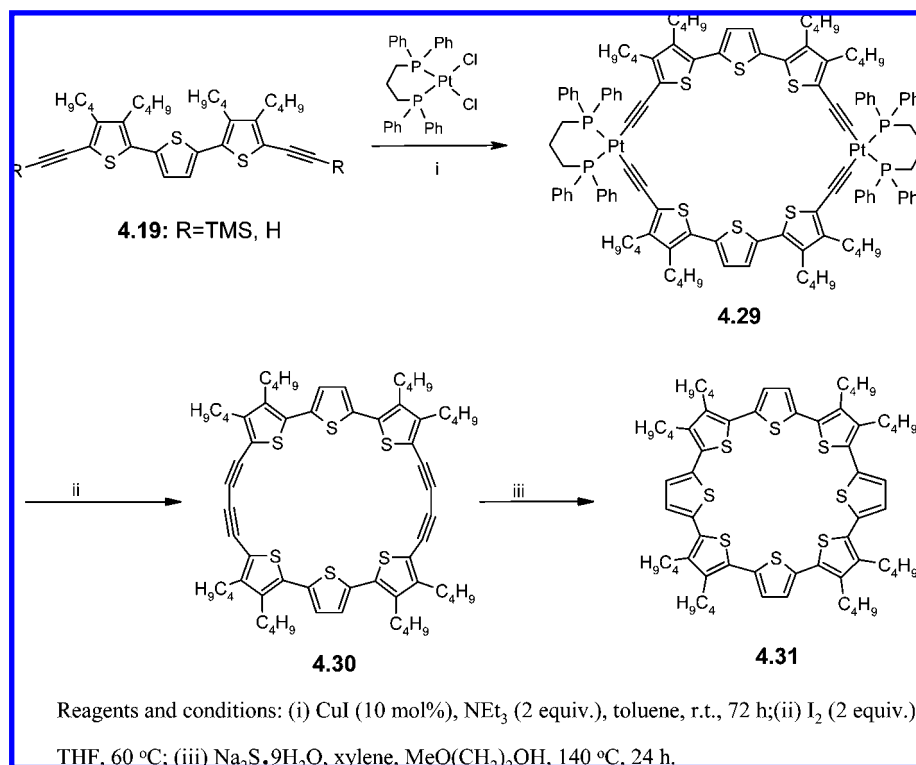
Scheme 4.9

Reagents and conditions: (i) CuI (10 mol%), NEt₃ (2 equiv.), toluene, r.t., 72 h;(ii) I₂ (2 equiv.), THF, 60 °C; (iii) Na₂S·9H₂O, xylene, MeO(CH₂)₂OH, 140 °C, 24 h.

Figure 4.2. X-ray structure analyses of macrocyclic terthiophene-butadienes **4.30** (left), **4.20** ($n = 1$, $m = 1$) (middle), and **4.20** ($n = 1$, $m = 2$) (right). (Left figure reproduced with permission from ref 644. Copyright 2003 Royal Society. Middle figure reproduced from ref 627. Copyright 2006 University of Ulm. Right figure reproduced with permission from ref 625. Copyright 2000 Wiley-VCH.)

could be detected in the previous random cyclooligomerization reactions.

Terthiophene-butadiyne **4.30** was finally reacted with sodium sulfide in DMSO to give octabutylcyclo[8]thiophene **4.31** in 36% yield. The rather moderate yield in this reaction seems to be due to the ring strain in the starting macrocycle, as confirmed by X-ray structure analysis (vide infra)[644] and the resulting cyclo[8]thiophene.

X-ray structure analyses of macrocyclic terthiophene-butadienes **4.20** ($n = 1$, $m = 2$),[625–627] **4.20** ($n = 1$, $m = 1$),[627,645,646] and **4.30**[644] showed that with decreasing ring size the increasing strain energy is taken up by the butadiyne units, which in the case of the smallest macrocycle **4.30** were severely bowed with angles of 160°–167° (Figure 4.2). Despite the distortion of the thiophene rings and the butadiyne units in **4.28**, the 32π-electron perimeter shows remarkable conjugation. In the ¹H NMR spectrum, a substantial upfield shift of the thiophene β-protons in comparison to those of the next larger members in the series ($\Delta\delta \geq 0.2$ ppm) shows antiaromatic behavior. Interestingly,

in the crystal lattice, the macrocycles are packed in a way that they form channels or tubes of ≥1 nm in diameter.

The control of structural order on the molecular level in semiconducting materials has important consequences on their electronic properties.[647,648] Therefore, the programmed assembly of π-conjugated materials in nanoscale architectures[649] as well as surface patterning with nanometer-sized objects[650,651] has recently received much attention and is a crucial step for applications in organic or molecular electronics. The adsorption and self-assembling properties of various cyclothiophenes and cyclo(oligothienyl-butadiynes) were investigated by in situ scanning tunnelling microscopy (STM) at the solution/graphite (HOPG) interface (Figure 4.3).[625–627,645,646] Typically, the macrocycles physisorbe spontaneously and order in a "honeycomb" pattern with hexagonal symmetry. The STM images show an excellent long-range ordering of the submolecularly resolved individual macrocycles. Corroborative semiempirical calculations revealed that a "spider-like" conformation in which the butyl side chains are uniformly bent downward is preferred. The bent alkyl side
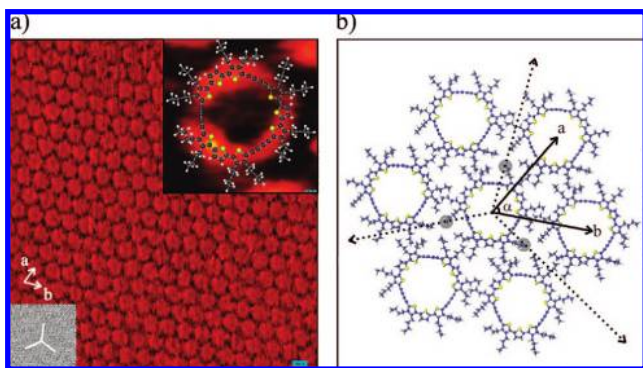
Figure 4.3. (a) STM images of macrocycle **4.20** ($n = 1$, $m = 1$) at the solution−HOPG interface, showing long-range ordering (60 × 60 nm^2). The inset (bottom left) shows the underlying graphite, including the three main crystallographic axes. The inset (top right) shows the STM image of an individual macrocycle (2.7 × 2.7 nm^2) overlaid with a theoretically calculated molecule. (b) Calculated model of a hexagonal crystal of **4.20** ($n = 1$, $m = 1$) showing the lattice vectors (solid line) and the crystallographic axes of the HOPG (dashed line). (Reproduced with permission from ref 646. Copyright 2002 Wiley-VCH.)

chains are responsible for the interaction of the circular structures with the surface and with alkyl side chains of adjacent molecules via van der Waals forces.

The controlled hierarchical construction of hybrid multilayers[57,652] comprising (electronic) functions on the molecular scale is a major challenge. Highly organized monolayers of hexagonally packed ring-shaped cyclo[12]-thiophene **4.26** can be used as a veritable template to epitaxially grow 3D-nanoarchitectures with C$_{60}$-fullerenes which uniquely adsorb and self-assemble in a second layer.[58] Submolecularly resolved STM images allow the investigation of 1:1 complexes consisting of a ring-shaped p-type and a spherical n-type semiconductor for which the dynamics of the coadsorption and the complexation site on the macrocycle were analyzed (Figure 4.4). The electronic properties of the complexes were elucidated by means of scanning tunnelling spectroscopy exhibiting I/V curves with rectifying behavior.[58]

Due to the circular structure of thiophene-based macrocycles, they represent model systems, which in comparison to usual linear conjugated oligomers and polymers have the distinct advantage of ideally combining an "infinite" defect-free π-conjugated chain of an idealized polymer with the advantages of a structurally well-defined oligomer, but excluding perturbing end effects. In this sense, the optical properties of cyclothiophenes **4.26**−**4.28** have been compared to those of a series of the parent linear compounds. Surprisingly, the maximum absorption wavelength of a cyclothiophene corresponded to that of an oligothiophene chain of about half the length. This means that the cyclothiophene spectra were blue-shifted with respect to the spectra of linear derivatives with the same number of repeat units but showed the same intensity.[653] This phenomenon was explained by theoretical calculations in the frame of Frenkel exciton theory which clearly showed that the differences in the absorption spectra are caused by different selection rules as a consequence of their different geometries. Cyclothiophenes have transition dipoles mainly arranged in the ring plane with a very small perpendicular component. As a consequence, the S$_0$−S$_1$ transition at lowest energy is forbidden, and therefore, the main absorption band corresponds to the S$_0$−S$_2$ transition. However, for the smallest macrocycles **4.30** and **4.31**, which are strained and distorted

from planarity, a weak new band at lower energies appears which can be ascribed to the S$_0$−S$_1$ transition. Interestingly, depending on the excitation energy for those macrocycles, dual fluorescence from both the S$_1$ and the S$_2$ states can be detected, which is a very rare case (Figure 4.5).[627,654]

In a very recent theoretical paper on cyclothiophenes with ring sizes from 6−30 repeating units, Bendikov et al. studied *syn-* and *anti*-conformations using density functional theory (DFT).[655] The properties of the *anti*-conformers in neutral and charged states change systematically with increasing ring size whereas *syn*-conformers lose planarity and cannot be correlated. Cyclothiophenes are revealed as a good model for polythiophenes, and it was identified that *syn*-cyclo[14]thiophene should have an even lower HOMO−LUMO gap than that of polythiophene (Figure 4.6). The authors proposed that this fully conjugated cyclothiophene and circular structure would be an excellent target for novel materials with low band gap. In the same sense and in view of potential electronic materials, Fabian and Hartmann very extensively calculated cyclo[n]thiophenes ($n = 2-18$) on the DFT level as well as their mono- and dications. Furthermore, their absorption behavior was evaluated in dependence of their symmetry.[656]

4.2. Mixed Macrocycles Based on Thiophenes and Other Unsaturated Units

4.2.1. Mixed Macrocycles Based on β-Substitution in Thiophene Units

In an effort to overcome steric interactions due to β-substitutents in cyclotetra(2,3-thienylenes) **4.6** (*vide supra*), Marsella et al. have synthesized expanded thiophene-fused didehydro[12]annulene **4.32**, which incorporated two additional ethynylene groups between the β-positions of the cyclic structure (Scheme 4.10).[657] Regiospecific halogenation of a 2,2′-bithiophene and Sonogashira-type cross-coupling with the ethynylated counterpart were key elements of the synthetic strategy, which was also used to prepare a further extended macrocycle **4.33** (Chart 4.4), making use of quadrupolar interactions of the central phenylene units.[658]

Trithienocyclotriyne (TTC) **4.34**, which can be regarded as expanded benzo[1,2-*b*:3,4-*b*′:5,6-*b*″]trithiophene **4.4**, was prepared by Youngs et al. by cyclization of the Cu(I) salt of 2-iodo-3-ethynylthiophene in 21% yield (Scheme 4.11). X-ray structure analysis of TTC showed a planar molecule including more strain and a larger cavity than this of tribenzocyclotriyne (TBC). The low conjugation in the macrocycle due to α−β linkages in the thiophene units can be estimated from the maximum absorption at 308 nm. TTC was used as a ligand in the reaction with Co$_2$(CO)$_8$ to give a tetracobalt complex **4.35**, in which two of the alkynes of TTC bind to hexacarbonyl dicobalt moieties.[659]

An isomer of TTC **4.34**, in which the macrocycle is built up from 3,4-substituted thiophene units, was synthesized by the same group with the aim to develop liquid crystalline materials, in particular discotic mesogens. 2,5-Alkynylated 3-ethynyl-4-iodothiophenes were cyclized with the catalytic system Pd^0/Cu(I) to give colorless cyclotriynes **4.36** in yields up to 25% (Scheme 4.12). An X-ray structure analysis of one derivative showed that in the crystal the cyclotriyne cores do not interact.[660] Similar reaction of a dimethylated thiophene yielded cyclotetramer **4.37**, which is formed preferentially over the trimer in the cyclization of 3-ethynyl-4-iodo-2,5-dimethylthiophene (Scheme 4.13).[661]
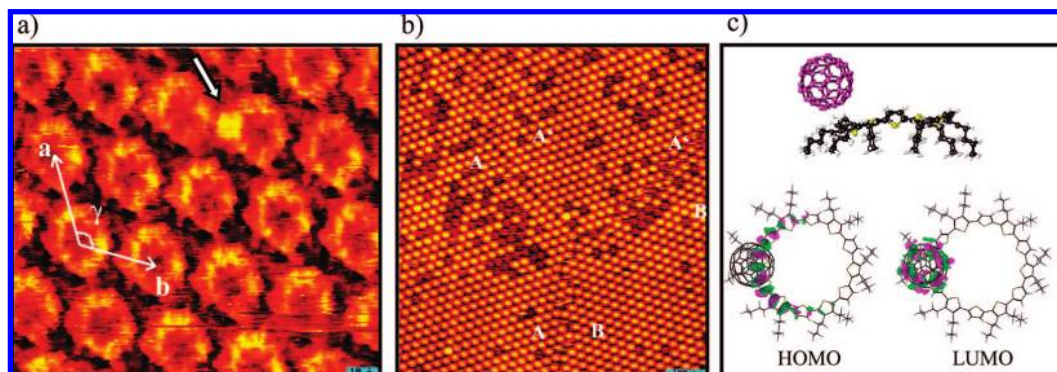
Figure 4.4. (a) STM images of submolecularly resolved cyclo[12]thiophene **4.26** (11.6 × 8.7 nm^2) on HOPG including a C[12]T-C60 complex (white arrow). (b) Short-range STM image of C[12]T-C60 complexes, including some noncomplexed macrocycles (deep red) and different domains (A, A′, and B) (79 × 79 nm^2). (c) Structural model of the 1:1 D−A complex (top) and charge distribution in the HOMO and LUMO (bottom). (Reproduced with permission from ref 58. Copyright 2006 Wiley-VCH.)
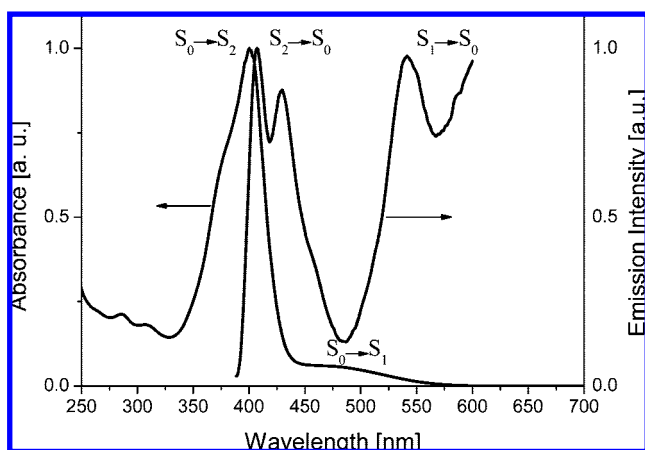

Figure 4.5. Absorption and emission spectrum of cyclo(terthienyl-butadiene) **4.30**. (Reproduced from ref 627. Copyright 2006 University of Ulm.)

Haley et al. synthesized thiophene analogues **4.38**−**4.40** of didehydro-tribenzo[18]annulene by Eglington cyclooligomerization in order to study their optical properties in comparison to the basic [18]annulene system (Chart 4.4). The C_3-symmetric **4.38** involving 2,3-thienylenes connected by butadiyne units can be regarded as the next higher expanded macrocycle in the series benzo[1,2-*b*:3,4-*b*′:5,6-*b*′′]trithiophene **4.4** and trithienocyclotriyne (TTC) **4.34**.[662]

Tilley et al. developed the very effective synthesis of zirconacyclopentadiene-coupled macrocycles. One of the examples has been reacted with disulfurdichloride to give mixed macrocycle **4.41**, in which three 3,4-thienylene units are connected by *p*-phenylene units and are responsible for cross-conjugation (Chart 4.4).[663]

Functional macrocycles **4.42** and **4.43** with photochromic reactivity were prepared and investigated by Ko et al. (Chart 4.5). Macrocycle **4.42** was built up by Sonogashira-type coupling of two semicircles containing two photoswitchable dithienylene ethene units each (9% yield). The reaction of the bis-ethynylated precursor with *trans*-Pt(PEt$_3$)Cl$_2$ more effectively led to metallamacrocycle **4.43** (27%). Due to the β-substitition in the dithienylene ethene units, the macrocycles were not fully conjugated, indicated by the maximum absorptions at 313 and 325 nm, respectively. By irradiation, the solutions turned blue, and one or two of the four photochromic groups could be closed, consequently increasing the conjugation length ($\lambda_{max} = 602$ and 625 nm). Further

ring closure to a fully conjugated macrocycle was not observed.[664]

4.2.2. Mixed Macrocycles Including α-Substitution in Thiophene Units

In 1965, the first thiophene-derived annulene **4.44**, a heterocyclic derivative of [18]annulene with three sulfur bridges, was reported and obtained in a low-yielding multistep procedure.[665] This compound later on has been prepared more efficiently by McMurry coupling of 2,5-thiophenedicarboxaldehyde in 38% yield by Cava et al.[666] Additionally, the corresponding tetrasulfide **4.45** was isolated in nearly 5% yield (Scheme 4.14). An X-ray structure analysis confirmed suggestions from spectroscopic and theoretical investigations that the macrocycle is not planar and the three thiophene units are totally out of plane. Furthermore, no significant ring current and additional aromaticity than that provided by the thiophene units has been found in NMR spectra. Thus, [18]annulene trisulfide **4.44** may be viewed as a combination of independent thiophene and vinylene units rather than as a conjugated annulene.

When a reductive coupling of 5,5′-bithiophene-dicarboxaldehyde was carried out under high dilution conditions, two products were obtained after chromatographic workup. The yellow tetrathiaporphycene **4.46** was obtained first in 10.5% yield (Scheme 4.15).[666] This 4nπ-thiophene analogue of porphycene, an isomer of porphyrin constructed from two bithiophene and two vinylene units, is quite stable and without an obvious ring current. From the absorption maximum at 336 nm, it can be seen that the molecule must be nonplanar with only moderate conjugation. Oxidation of **4.46** to an 18π aromatic dication was not successful. As a second fraction, the corresponding cyclotrimer, hexathia-[30]annulene **4.47** was isolated in 13.5% yield. Despite the fact that the macrocycle is a $(4n + 2)\pi$-system, also no obvious extra-aromatic ring current was detected and the absorption maximum at 384 nm allows us to assume as well a nonplanar molecule. The nonplanarity of both macrocycles was confirmed independently by Merz et al. by X-ray structure analysis.[667]

Analogous McMurry coupling of the next higher homologue, 5,5′′-terthiophene-dicarboxaldehyde with TiCl$_4$ and zinc gave hexathiahomoporphycene **4.48**, a 28π macrocycle, in a yield of 64% (Scheme 4.16).[668] In its UV−vis spectrum,
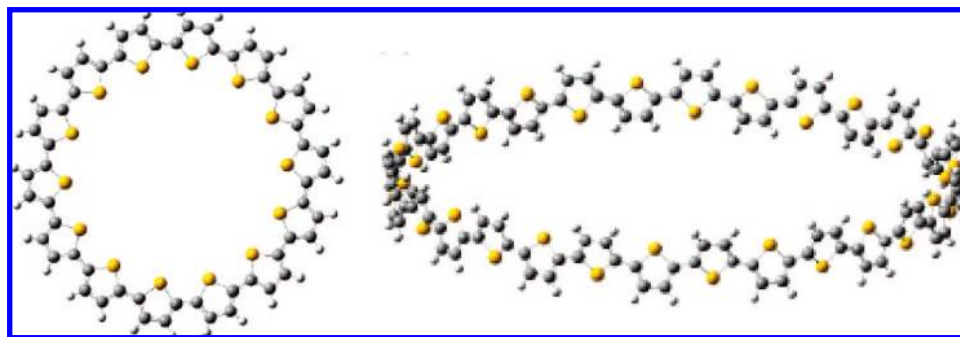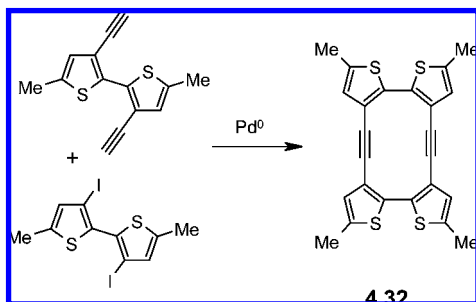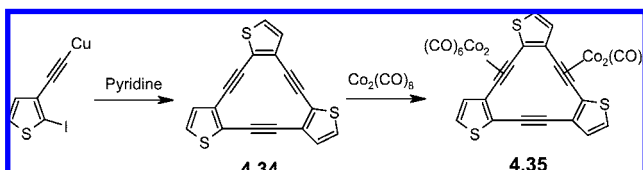
Figure 4.6. DFT-calculated structures of *syn*-cyclo[14]thiophene and *anti*-cyclo[30]thiophene. (Reproduced with permission from ref 655. Copyright 2006 American Chemical Society.)
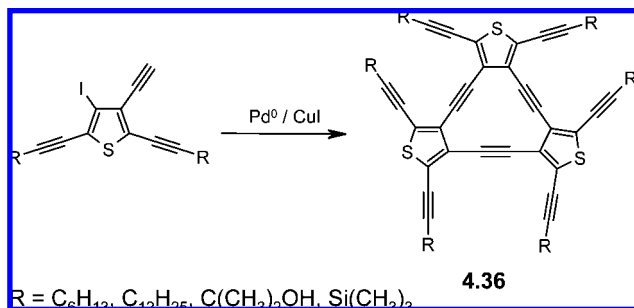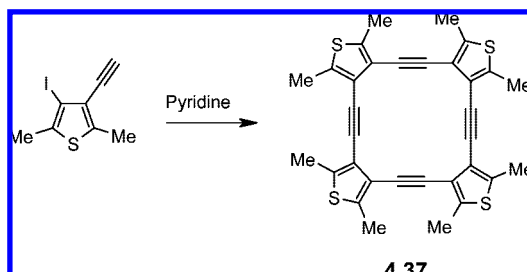
Scheme 4.10

Scheme 4.11

Scheme 4.12

R = C$_6$H$_{13}$, C$_{12}$H$_{25}$, C(CH$_3$)$_2$OH, Si(CH$_3$)$_3$

Scheme 4.13

a strong maximum at 431 nm was found, indicating partial conjugation. When concentrated sulfuric acid was added to macrocycle **4.48**, a purple 26π dication **4.49** with an absorption maximum at 885 nm was obtained which is typical for porphyrins. Greatly deshielded protons in the NMR spectrum indicate a strong ring current effect.

Mixed macrocycles built from thiophenes, ethenylene, and ethynylene units have been synthesized by Oda et al. McMurry coupling of diformyldithienylacetylene gave only traces of cyclodimer **4.50**, and cyclotrimer **4.51** was isolated as the main product (15% yield) (Scheme 4.17). Cyclodimer **4.50** was then synthesized by another route starting from diformyl-1,1-dichloro-2,2-di(2-thienyl)ethene, which was coupled to cyclodimer **4.52**, comprising exocyclic double bonds. By treatment with *n*-BuLi, these double bonds rearranged to endocyclic triple bonds, giving **4.50** in 30% yield (Scheme 4.18). An X-ray structure analysis showed that macrocycle **4.50** is nearly planar, which is in contrast to the twisted structure of analogue **4.45**. As a consequence, the molecule seems to be strained, because the triple bonds are bent to 165°. However, as for the comparable annulene derivatives, NMR data of **4.50** do not show extra ring currents in the 24π periphery.[669]

The same authors extended the structural variety of thiophene-based macrocycles by synthesizing [24]annulene **4.53**, in which two 2,2′-bithiophene units are connected *via* butatriene groups (Chart 4.6). The macrocycle showed clear paratropicity (antiaromaticity) whereas the dianion, a 26π electron system which is obtained by alkali reduction, was strongly diatropic (aromatic).[670]

Macrocyclization *via* McMurry coupling was very recently used by Iyoda et al. to synthesize large thienylene-ethynylene-vinylene macrocycles **4.54** in a statistical approach.[671] Reaction of a longer oligo(thienylene-ethynylene) dialdehyde, which was made from thiophene in 12 steps, with TiCl$_4$ and zinc resulted in a statistical distribution of macrocycles with various sizes (Scheme 4.19). The main product, a cyclodimer, corresponds to a [60]annulene and was isolated in 30% yield after chromatographic workup and consisted of the three possible isomers *E/E*, *E/Z*, and *Z/Z* in the ratio 18:1:3. As higher homologues and very large macrocycles, the cyclotrimer was isolated in 9%, the cyclotetramer in 6%, the cyclopentamer in 4%, and the cyclohexamer in 2% yield. The optical and redox properties of the series of macrocycles **4.54** showed full conjugation which correlates with ring size. Very recently, the X-ray structure analyses, AFM images, and electrooptical properties of this series of macrocycles were reported.[672]

A mixed cyclothiophene including phenylene units was synthesized by Tobe et al. Macrocycle **4.55** (Chart 4.6) was made including four alternating 2,5-thienylene and 1,3-phenylene units and is similar in shape to cyclo[8]thiophene **4.31**. Definitely, the *meta*-branched phenylene units helped to form the macrocycle and reduced strain energy, but interrupted the overall conjugation.[673] The synthesis of a corresponding pyridine-containing macrocycle **4.56** was

Chart 4.4

Chart 4.5

Scheme 4.14

4.44 (38%)   **4.45** (5%)

Reagents and conditions: (i) TiCl₄/Zn, Pyridine, THF, reflux

Scheme 4.15

4.46 (10.5%)   **4.47** (13.5%)

Reagents and conditions: (i) TiCl₄/Zn, Pyridine, THF, reflux
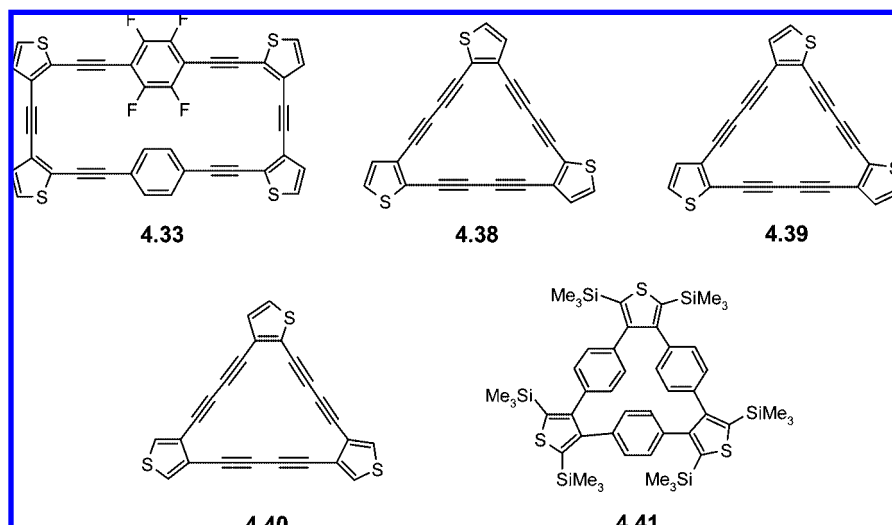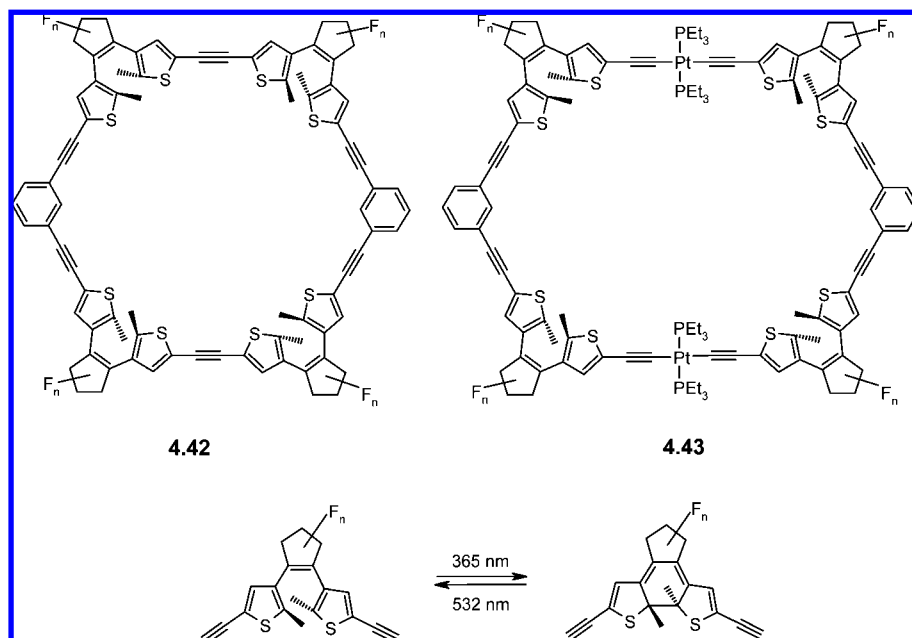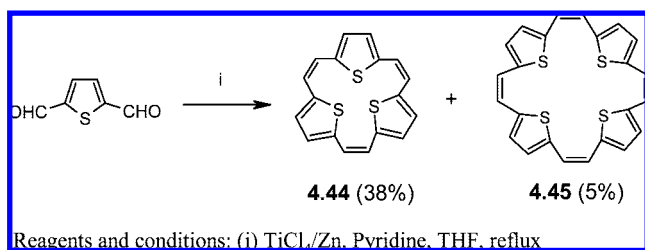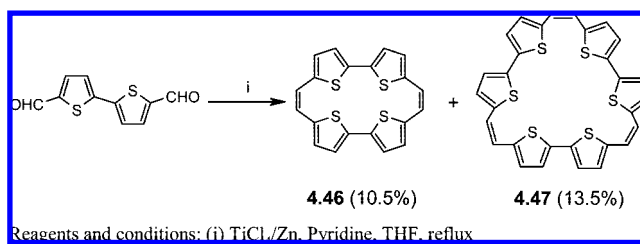
attempted, but the ring-closure reactions of penta- and heptacyclic precursors failed.[674]

A literally giant macrocycle **4.57** with an inner diameter of about 12 nm and a periphery made from exclusively conjugated ethynylene- or butadiyne-linked 2,5-thienylene and *p*-phenylene units has been synthesized by Mayor et al.[675] The giant ring with a mass of 11690 emu corresponds to a [320]annulene(!) and was obtained by a convergent buildup of a linear hexadecamer, which was cyclized by modified Eglington conditions under high dilution (38% yield) (Scheme

4.20). The absorption maximum of **4.57** at 461 nm was slightly bathochromically shifted with respect to the linear precursor and lies close to the extrapolated limit for an infinite chain length (462 nm), indicating full conjugation.

A synthetic approach to interlocked thiophene-based macrocycles which represent novel π-conjugated topologies was very recently developed by Bäuerle et al. These novel molecules would combine their outstanding electronic material benefits with the specific properties of the topological structure, e.g. circumrotation in catenanes or ring shuttling

Scheme 4.16

4.48 (64%)

4.49

Reagents and conditions: (i) TiCl₄/Zn, Pyridine, THF, reflux; (ii) H₂SO₄ (98%)

Scheme 4.17

4.50 (traces)   **4.51** (15%)

Reagents and conditions: (i) TiCl₄/Zn, Pyridine, THF, reflux

Scheme 4.18

4.52   **4.50** (30%)

Reagents and conditions: (i) TiCl₄/Zn, Pyridine, THF, reflux; (ii) BuLi
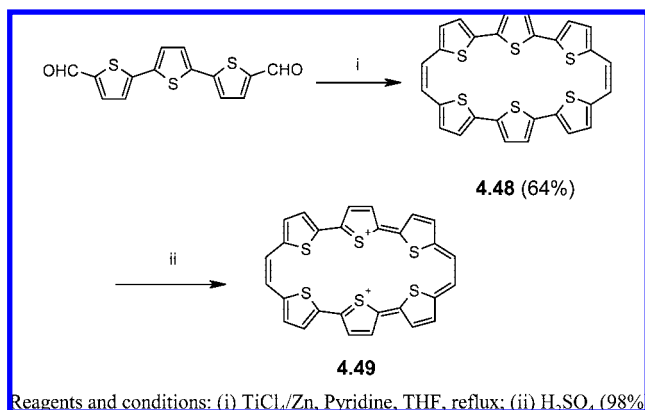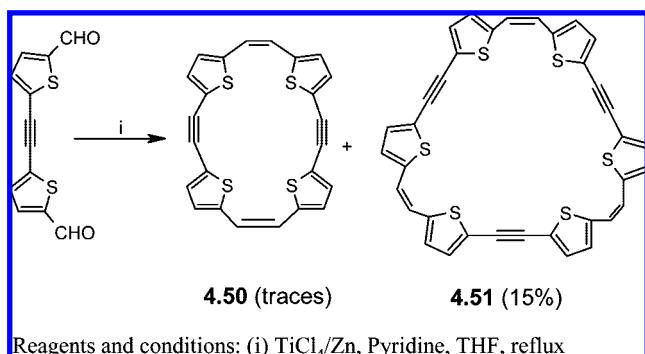
in rotaxanes. In contrast to many already existing, quite flexible intertwined molecules, fully conjugated building blocks involve more rigid structural elements, making their preparation a major synthetic challenge. The first attempt toward conjugated catenanes based on interlocked, conjugated terthienyl-phenanthroline-butadiyne macrocycles ended with a Cu(I)-catenate **4.58** (Chart 4.7).[383] Mutual steric constraints from the relatively small macrocycles (28-membered rings) prevented demetalation and formation of the Cu-free [2]catenane.

The synthesis and characterization of an expanded Cu(I)-catenate **4.61** and the first demetalated conjugated [2]catenane **4.62** by using quaterthiophene instead of terthiophene units was accomplished by the same group. Cyclization of **2.313** under pseudohigh dilution Eglington conditions surprisingly led to monomacrocycle **4.59** (50% yield) instead of the expected [2]catenate (Scheme 4.21). Apparently, closure of the first macrocycle generates steric constraints disentangling the second crescent-shaped precursor.

By application of the recently developed Pt-templated macrocyclization protocol (*vide supra*) to the bis-phenanthroline Cu(I) complex, an interlocked tris-metalated Pt(II)−Cu(I)−Pt(II)-catenate **4.60** was obtained from precursor **2.313**. Elimination of the Pt corners with iodine under

simultaneous C−C bond formation afforded Cu(I)-catenate **4.61**, which represented the higher homologue of Cu(I)-catenate **4.58**. In this case, due to the larger ring sizes (34-membered), decomplexation of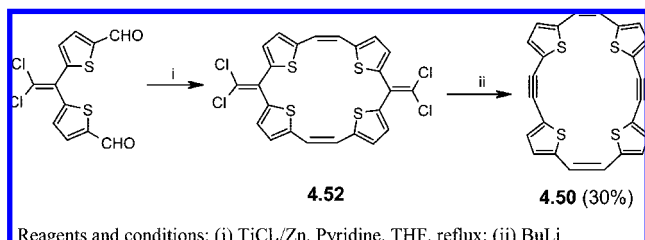 the Cu(I) center was achieved by reaction with KCN, and "conjugated catenane" **4.62** was isolated in pure form after chromatography (Scheme 4.22). Evidence for the interlocked structure of **4.62** came from ¹H NMR spectroscopy as well as tandem mass spectrometry.[384]
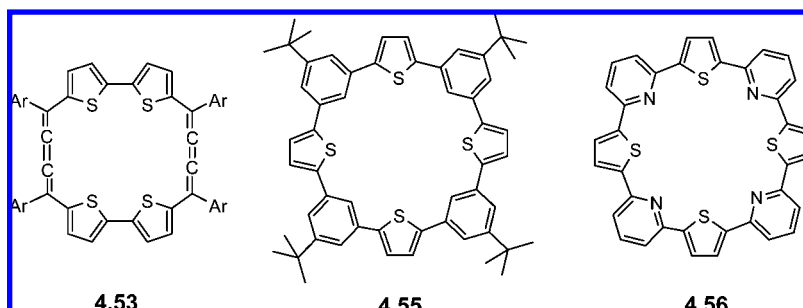
[2]Catenane **4.62** is a unique molecular system in which both conjugated macrocycles are mechanically kept in close proximity and may influence each other electronically "through space". Investigating the optical and redox properties of **4.62** in comparison to macrocycle **4.59** gave clear evidence for a mutual interference of its two rings. Interestingly, very recently, a theoretical paper by Fomine et al. appeared in which [2]catenanes and trefoil knots made exclusively of thiophene units were calculated with DFT methods. Catenanes with more than 18 thiophene units and knots with more than 22 thiophene units were predicted to be viable synthetic targets with interesting electronic properties.[676] Calculations on mono- and dications of oligothiophene catenanes and knots were reported recently.[677]

Several mixed macrocycles combining thiophene and other five-membered heterocyclic rings were synthesized as analogues of corresponding thiophene-based macrocycles. One series containing thiophene, furane, and pyrrole moieties **4.63**−**4.65** was made by stepwise cyclocondensation reactions as heterocyclic derivatives of [18]annulene and analogues of **4.44** (*vide supra*) (Chart 4.8).[678,679] All four compounds were found to be nonplanar, nonaromatic compounds without complete cyclic delocalization of the 18π-electrons on the carbon periphery. They can be regarded rather as consisting of three heterocycles linked by three olefinic vinylene groups.

Intermediate structures between thiophene-based annulenes and extended porphyrin systems are given by mixed macrocycles **4.66** and **4.67** (R = C₃H₇), which were prepared by Ti⁰-mediated coupling of corresponding dialdehydes and are analogous to structures **4.48** and **4.50**, respectively.[680,681] These macrocycles represent (4n + 2)π aromatic [18]- and [26]annulenes due to the possibility to incorporate oxidized pyrrole units, as they are present in porphyrins. Cava et al. synthesized comparable *N,N*-dialkylated annulenes **4.68** (R = Me, C₁₂H₂₅) comprising four thiophene and two pyrrole units by McMurry coupling of tricyclic aldehydes.[668] The alkylation of the pyrrole nitrogens prevented oxidized aromatic forms, and like **4.50** compounds **4.68** existed as (4n)π antiaromatic [28]annulenes. Interestingly, in an ongoing work, Cava et al. used a template strategy to synthesize corresponding bicyclic *N,N*-bridged macrocycles **4.69** by an intramolecular McMurry coupling (Chart 4.9).[682] Depending on the length of the bridge (R = (CH₂)₄, (CH₂)₆, (CH₂)₃O(CH₂)₂O-(CH₂)₃) the yields varied from 24% to 58%. Absorption spectra and cyclic voltammetry of the three macrocycles showed that with the extension of the bridge less rigidity and distortion is obtained, leading to a better overall conjugation.

Extended thiophene pyrrol macrocycles **4.70** and **4.71** were prepared by similar intermolecular coupling of pentacyclic dialdehydes in 17−37% yield. Two tricyclic derivatives **4.71** were made in which two pyrrole units were linked by longer alkyl and ether chains already present in the precursor aldehydes (Chart 4.10).

Chart 4.6

4.53   **4.55**   **4.56**

Scheme 4.19

4.54

Reagents and conditions: (i) TiCl$_4$/Zn, Pyridine, THF, reflux.

Scheme 4.20

(n = 16)

4.57: n = 16

Reagents and conditions: (i) Cu(OAc)$_2$, Pyridine.

Chart 4.7

4.58
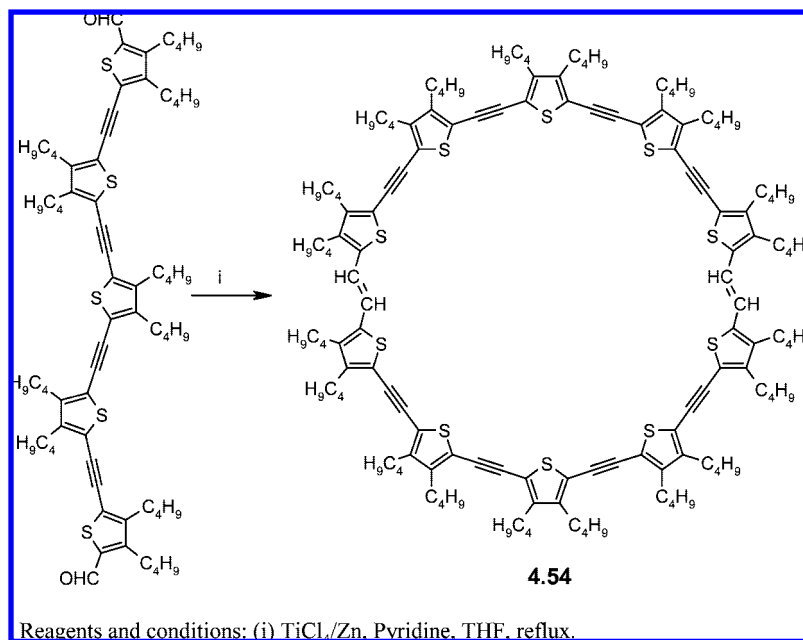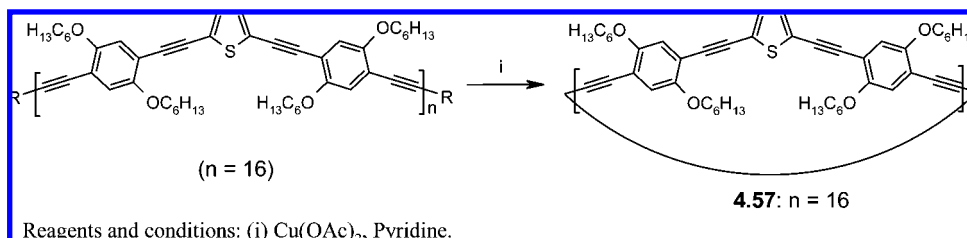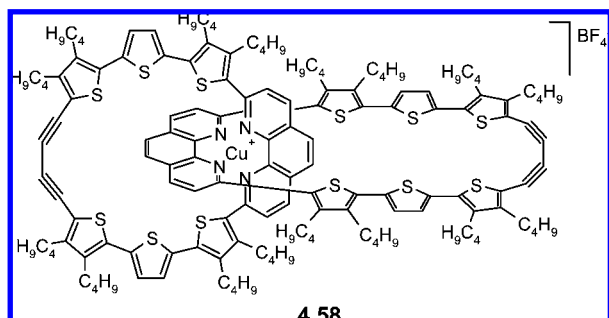
4.3. Thiophene-Based Porphyrinoid Macrocycles

In the last paragraph, it became evident that there is a smooth transition from the discussed mixed thiophene-based macrocycles toward porphyrins which are bridged heterocyclic structural variants of fully aromatic [18]annulene. Compared to the numerous studies on porphyrins, sulfur-bridged analogues have been much less investigated. Vogel's tetrathiaporphyrin dication **4.72** is one of the first and prominent representatives and was provided together with oxygen- and selenium-analogues **4.73** and **4.74** in a three-step synthesis starting from furfuryl alcohol (Scheme 4.23).[683,684] Compound **4.72** was a violet solid and showed absorptions up to 700 nm in the UV−vis spectrum comparable to dialkylated porphyrin dications. An X-ray structure analysis exhibited nonplanarity with a distortion of the thiophene rings up to 23°. In coincidence with NMR data, this deviation from planarity did not weaken the aromaticity and electron delocalization. In contrast to the benzoid/annulenoid macrocycles described in paragraph 4.2.2, this system can be regarded as [18]annulene. The neutral form of tetrathiaporphyrin **4.72** would correspond

Scheme 4.21

2.313   **4.59**

Reagents and conditions: (i) Cu(OAc)₂, CuCl₂.

Scheme 4.22

2.313

4.60

4.61   **4.62**

Reagents and conditions: (i) CsF, Pt(dppp)Cl₂; (ii) I₂/THF; (iii) KCN.

Chart 4.8

4.63   **4.64**   **4.65**
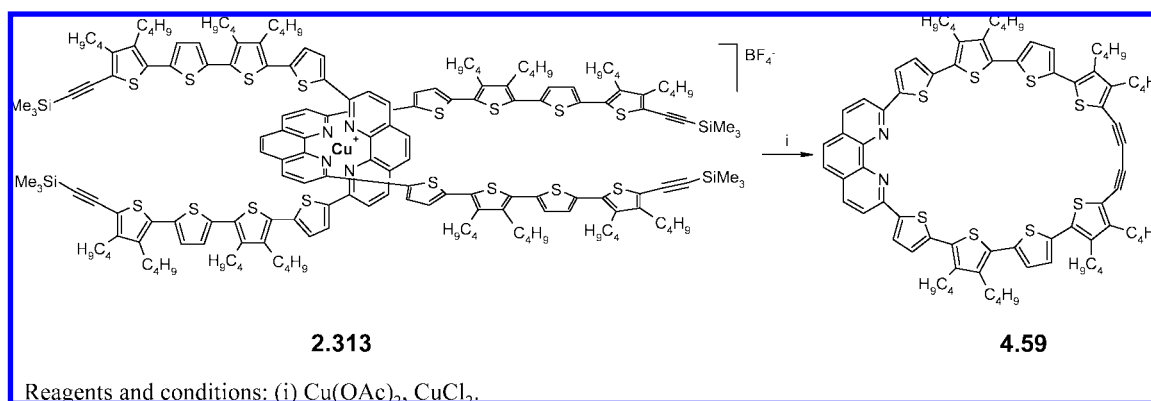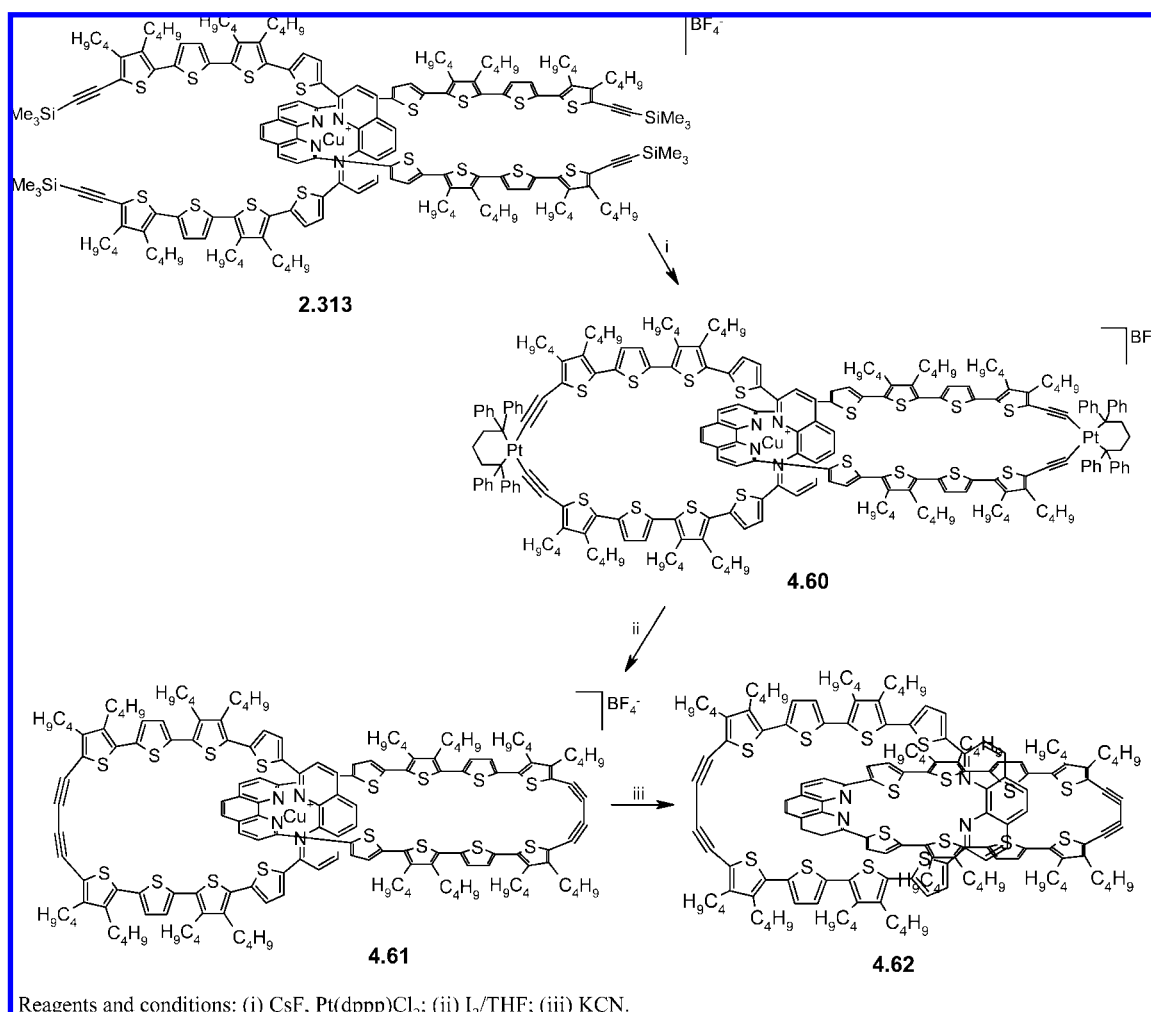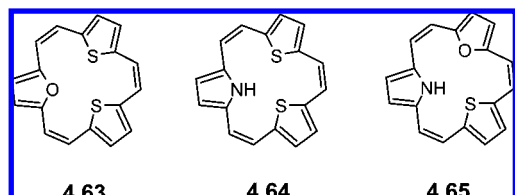
to an antiaromatic system in the Hückel sense and therefore is instable.

The first neutral porphyrinoid system containing only sulfur bridges, tetrathia[22]annulene[2,1,2,1] **4.75** was re-

ported by Cava et al.[685] The synthesis of this 22π system is depicted in Scheme 4.24. In contrast to the macrocyclic precursor, in the ¹H NMR spectrum of **4.75**, all protons were greatly deshielded (11.4−12.3 ppm), indicating an aromatic ring current. The strong absorption maximum at 417 nm and several absorptions at longer wavelengths (503−771 nm) correspond to the typical Soret- and Q-bands of porphyrins.

Interestingly, tetrathia[22]annulene[2,1,2,1] **4.75** was very recently taken up and investigated as a promising material for organic electronics. Zhu and Xu et al. showed that the molecule was almost coplanar and packed into sandwich−herringbone arrangements. The physical properties in thin films

Chart 4.9

4.66   **4.67**   **4.68**   **4.69**

Chart 4.10

4.70   **4.71**
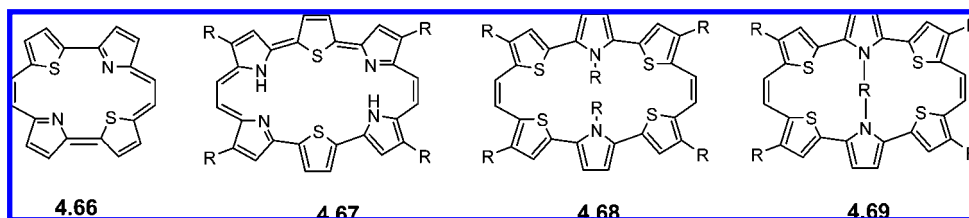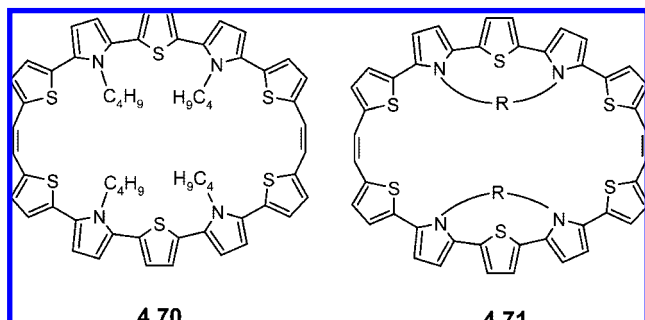
as well as the thermal stability were promising. As a very rare example of cyclic compounds, in OFETs, a quite high hole mobility of 0.05 cm^2 V^{-1} s^{-1} was found due to the favorable arrangement of the molecules in the solid state.[686]

Several mixed sytems containing thiophene and pyrrole rings were prepared in this line. Examples are presented in Chart 4.11 and range from thia-analogous porphyrins **4.76**−**4.78**[687,688] (18π) to modified expanded porphyrins which have more than 18π electrons in the conjugated pathway either due to an increased number of heterocyclic rings or due to multiple meso carbon bridges. Among them, thia-analogous pentaphyrin (sapphyrin) **4.79** (22π),[689] hexaphyrin (rubyrin) **4.80** (26π),[690] heptaphyrins **4.81** and **4.82** (30π),[691,692] and octaphyrins **4.83**−**4.85** (34−38π)[693,694] have been synthesized by efficient methods and were found to be mostly nonaromatic in nature. For octaphyrins, both planar and figure-eight conformations were found. Very recently, synthesis and structural characterization of the first example of planar [34]octaphyrin(1.1.0.1.1.0.0.0) **4.86** with three different heteroatoms (N, S, Se) and α-conjugated quaterthiophenes unit were disclosed. X-ray structure analysis showed a nearly coplanar structure and the quaterthiophene unit in an *all-syn* conformation, which in contrast to **4.83** is restricting the ring inversion.[695]

At this end, it should be noted that recently Sessler et al. synthesized cyclo[8]pyrroles **4.87** which respresent expanded porphyrins without meso-bridges and aromatic 30π octaphyrins through oxidative coupling of bipyrrole units (Chart 4.11). The resulting fully conjugated macrocycles exhibited interesting physical properties, such as intense Q-bands in the absorption spectra which are shifted to the NIR regime (1112 nm) and anion receptor properties.[696] As a macrocyclic α,α-connected oligopyrrole, it can be seen as a direct counterpart to the (antiaromatic) 32π cyclo[8]thiophene **4.31** (*vide supra*). However, it was never reported that it can be reduced to the corresponding 32π macrocycle.
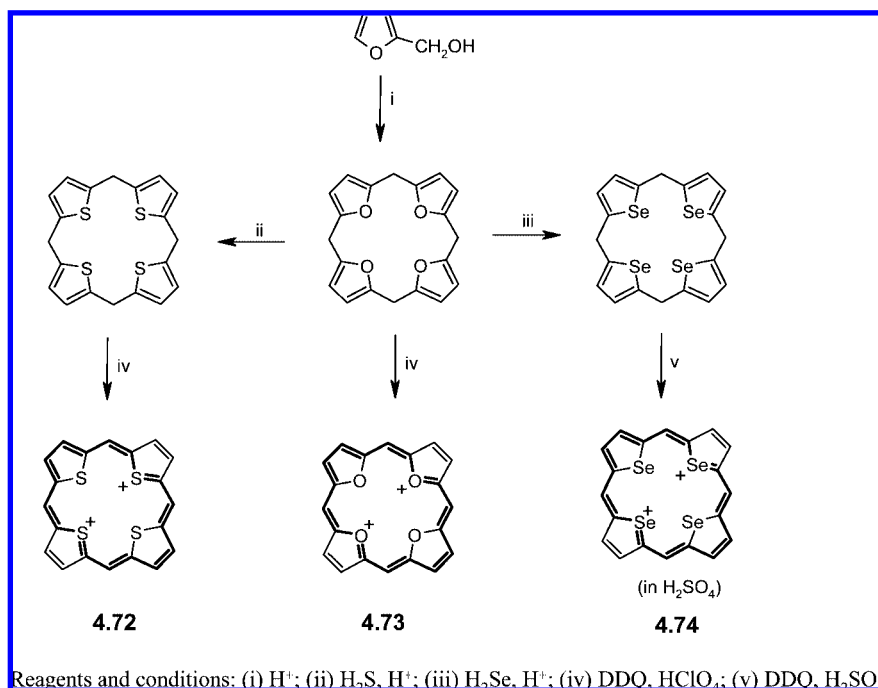
5. Dendritic Oligothiophenes

Three-dimensional branched architectures, generally termed as dendrimers, represent a class of synthetic macromolecules that have impacted dramatically the field of organic and polymer chemistry and created a new branch in synthetic and material chemistry. Since the last two decades, dendrimer research has been at the forefront of polymer research and was first postulated in the 1940s by Flory as a pioneer in polymer research and Nobel laureate in 1974 who proved the existence of branched chains and their potential role in "three-dimensional" (3D) macromolecular architectures.[697−699] Then it was in 1978 when Vögtle et al. developed an iterative cascade method for the synthesis of low molecular weight branched amines.[700] The real expansion of the field started after Tomalia[701] and Newkome[702] discovered the starburst effect, which shed light on a new chemical arena. Since then, dendrimer chemistry has been diversified worldwide in various fields, from biology to materials chemistry, and numerous attractive dendritic systems have been developed.[703,704] In general, dendrimers are globular, highly branched, fractal-like polymers of a precise molecular weight, 3D shape, and "well-defined" size that are constructed *via* iterative procedures. Synthesizing monodisperse dendrimers demands a high level of synthetic control, which is achieved through stepwise reactions *via* subsequent generations.[700] The high functional group density at the periphery of dendrimers, coupled with unique control over molecular structure, makes these synthetic materials exceptionally attractive candidates for a variety of surface applications. The basic importance of shape in defining the physical properties of macromolecules has been recognized in the past years, with diverse synthetic procedures and advanced architectural designs. A major effort has been directed toward achieving accurate control over the structure and composition as well as the overall macromolecular topology.

Synthetic methods used for the construction of these branched macromolecules generally rely on divergent or convergent approaches. The divergent method comprises sequential addition of building blocks or repeating units to the central multifunctional core. The build up of the dendrimers goes toward the periphery by protection and deprotection techniques. In contrast, in the convergent method, the building blocks are first constructed stepwise with different generations and then attached to a specific functional core unit.

A variety of dendrimers have been constructed to date with different core, periphery, and branching units, with flexible and rigid structures and also including the attachment of different functionalities. Recently, conjugated, rigid, and shape-persistent dendritic structures were constructed comprising phenylacetylene,[705,706] phenylenevinylene,[707] or exclusively phenylene units.[708] However, functionalization of dendrimers with oligothiophenes at the core or periphery as well as purely thiophene-based dendrimers was materialized just recently. Several star-shaped and tetrahedral structures were also developed which can be regarded as "small" dendrimers.

Scheme 4.23

4.72   **4.73**   **4.74**

(in H₂SO₄)

Reagents and conditions: (i) H⁺; (ii) H₂S, H⁺; (iii) H₂Se, H⁺; (iv) DDQ, HClO₄; (v) DDQ, H₂SO₄.

Scheme 4.24

4.75

Reagents and conditions: (i) TiCl₄/Zn, 75%; (ii) DDQ, hydrazine, 82%
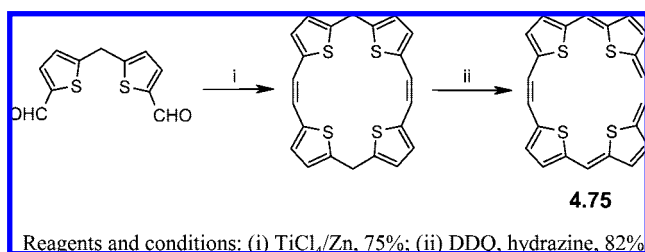
5.1. Star-Shaped Structures

Müllen et al. synthesized some hexasubstituted oligothienyl benzene derivatives **5.2** (*n* = 0−2) in yields of 32−61% by Co₂(CO)₈ catalyzed [2 + 2 + 2] cyclotrimerization of corresponding bis(oligothienyl)acetylenes **5.1** (Scheme 5.1).[709] All these compounds exhibited low transition temperatures and less ordered mesophases. Nevertheless, compounds **5.2** (*n* = 0, 1) formed discotic nematic mesophases at low temperature after annealing for a longer time.

Scherf et al. synthesized oligothiophene swivel-cruciforms **5.4−5.6** by using 4-fold Pd⁰-catalyzed coupling of tetrabromo-3,3′-bithiophene **5.3** and corresponding stannylated (oligo)thiophenes (Scheme 5.2).[710] In fact, in this type of compounds, two linear α-conjugated oligothiophenes were connected *via* a β−β linkage at the inner thiophene rings. Due to the branched structure, for **5.4−5.6**, an increased solubility in organic solvents was observed. The compounds were tested in OFET and gave relatively low field-effect mobilities of 3.7×10^{-5} cm² V⁻¹ s⁻¹ and moderate on/off ratios of 10^3. By attachment of hexyl side chains to the termini of the oligothiophene arms in **5.5**, a better soluble material **5.7** (Chart 5.1) for solution processing was obtained. An increased hole mobility of 1.2×10^{-2} cm² V⁻¹ s⁻¹ was measured in OFET devices.[711]

Zhu et al. very recently reported the synthesis of a series of smaller "X"-shaped oligothiophenes **5.8** and **5.9** (Chart 5.1). By utilizing Pd⁰-catalyzed Stille cross-coupling reactions, derivatives with 7 and 11 thiophene units were built

up.[712] Spectroscopic and electrochemical studies on these series showed broad absorption and emission bands. Application of the dendritic oligothiophenes in bulk-heterojunction OSCs with PCBM as acceptor gave increasing conversion efficiencies from 0.04% to 0.8% with increasing size of the molecules.[713] The same trend was seen for the photocurrents and internal photoconversion efficiencies, indicating improved charge separation and transport properties. A 3D-network formation has been proposed as a result of the electrochemical polymerizations of nonsubstituted derivatives **5.8** (*n* = 0, 1).

A series of star-shaped molecules **5.10−5.13** was prepared having a 3-, 4-, and 6-fold substituted phenylene or a tetrasubstituted thienylene as core and phenyl-capped terthienyl-ethynylenes arms (Chart 5.2).[714] The covalent attachment of the conjugated arms to the brominated core molecules was achieved by Sonogashira-type coupling reactions. By increasing the number of arms around the benzene core, bathochromic shifts of the absorption and emission maxima were observed. Thus, for the corresponding linear oligothiophene arm, the absorption and emission maxima were observed at 374 and 493 nm, respectively, while the corresponding star-shaped derivative, for example, **5.11**, showed red-shifted absorption and emission maxima at 417 and 576 nm, respectively. A smaller bathochromic shift was observed for analogue **5.13** due to the thienylene core (λ_{abs} = 402 nm, λ_{em} = 570 nm). This behavior suggested a delocalized π-conjugation though the core molecules. This finding was corroborated by a decrease of the oxidation potential measured in cyclic voltammograms. Casado et al.[715] have also studied the Raman spectroscopy and electrochemistry of multiarmed structures **5.10−5.13** and showed that the terthienyl-ethynylene units are only weakly coupled to the core unit due to cross-conjugation within the core, which prevents further π-electron delocalization.

Miller et al. prepared tris[4-(2-thienyl)phenyl]amine **5.14a** by Pd⁰-catalyzed coupling of 2-thienylmagnesium bromide with tris(4-bromophenyl)amine in 79% yield (Chart 5.3).[716] Yamamoto et al.[717] synthesized an analogous bithiophene

Chart 4.11

4.76 4.77 4.78 4.79 4.80

4.81 4.82: X = S/Se 4.83 4.86

4.84 4.85 4.87

Scheme 5.1

5.1: n = 0-2   **5.2**: n = 0-2

Reagents and conditions: (i) 0.15 eq. Co₂(CO)₈, dioxane, reflux
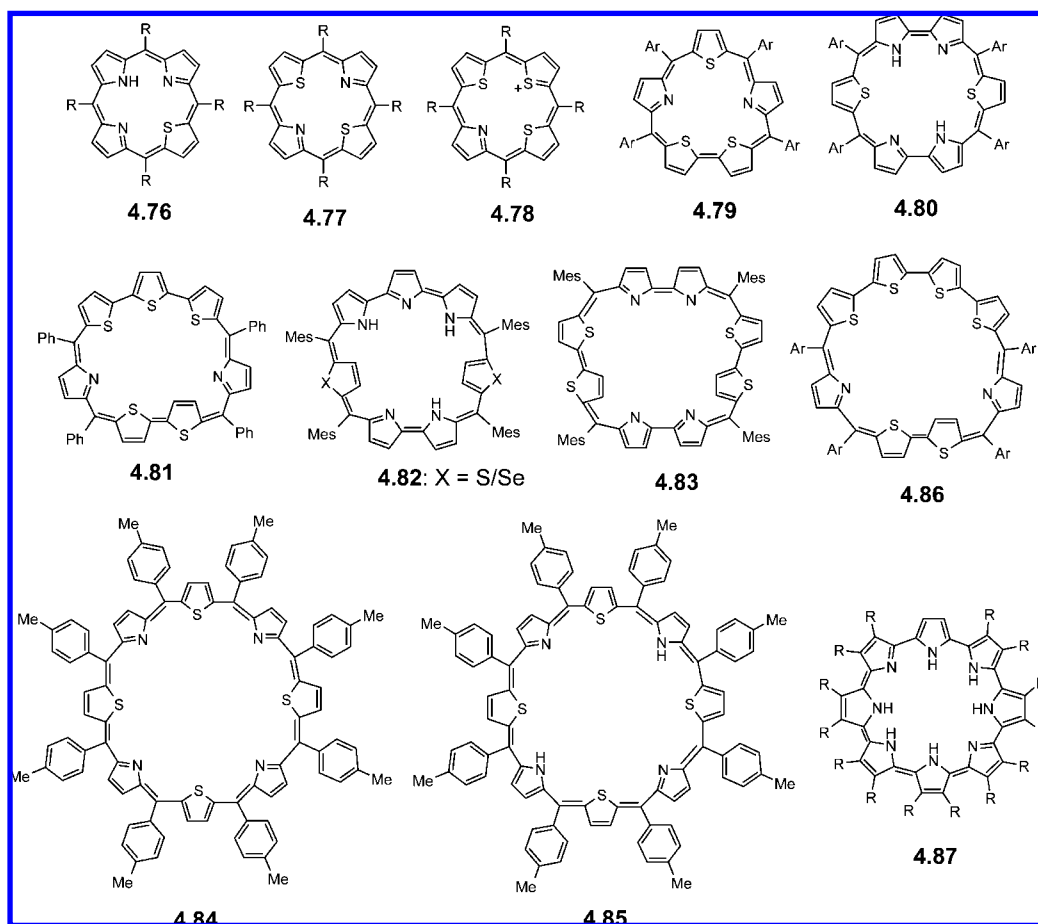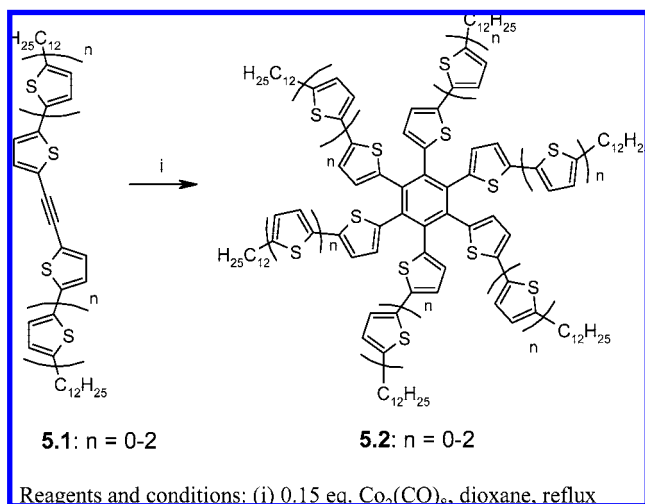
derivative **5.14b** by bromination of **5.14a** with NBS followed by coupling with 2-thienylmagnesium bromide in 76% yield. Coupling of terthiophene boronic acid with tris(bromophenyl)amine using Pd⁰-catalyzed coupling afforded terthiophene analogue **5.14c** in 32% yield. Phenyl-capped derivative **5.14d** was synthesized by coupling the Grignard reagent of 2-bromo-5-phenylthiophene and tris(4-iodophenyl)amine. The star-shaped oligothiophene **5.14a** as an amorphous glass showed a high hole drift mobility of 10^{-2} cm² V⁻¹ s⁻¹ at an electric field of 10^{-5} V cm⁻¹ in time-of-flight measurement.[718] A corresponding starburst polymer **P5.14a** was prepared on indium−tin oxide (ITO) electrodes by elec-

tropolymerization of **5.14a** and implemented in OLEDs.[719] A decrease in operating voltage and an increase in current density and luminance was reported for a bilayer ITO/**P5.14a**/Alq₃/Mg:Ag device, where p-doped polymer **P5.14a** acted as the hole-transporting layer and Alq₃ as the emissive layer.[720]

Electropolymerization of star-shaped oligomers **5.14a**−**c** resulted in the formation of highly redox active, cross-linked hyperbranched polymers, which led to systems with good conductivities, indicating the presence of multiple pathways for charge carriers provided by the branching units.[721]

Branched structure **5.15** (Chart 5.3) was synthesized by C−C coupling reactions of monostannylated tris(thienylphenyl)amine and the corresponding monobromo derivative in 88% yield. Compound **5.15** exhibited a high glass transition temperature (T_g = 135 °C) and acted in OLEDs as a good hole-transporting and emitting amorphous material. By using Alq₃ as electron transporting layer, a bilayer device showed high luminance.[722]

Recently, Roncali et al. synthesized similar star-shaped oligothiophenes **5.16** and **5.17** with triphenylamine as core (Chart 5.3).[723] The stannyl derivatives of the terthiophene arms were coupled to trisbromophenylamine by utilizing standard Pd⁰-catalyzed reactions. Compared to the case of derivative **5.16**, optical spectra of **5.17** showed a red shift of the absorption and emission maxima as well as a decrease in oxidation potential. These findings indicated a strong electron donating effect of the EDOT units along with a structural rigidification. OLEDs with the layer sequence ITO/PEDOT:PSS/**5.16** or **5.17**/Al showed very low turn-on voltages around 2 V due to efficient charge-injection and
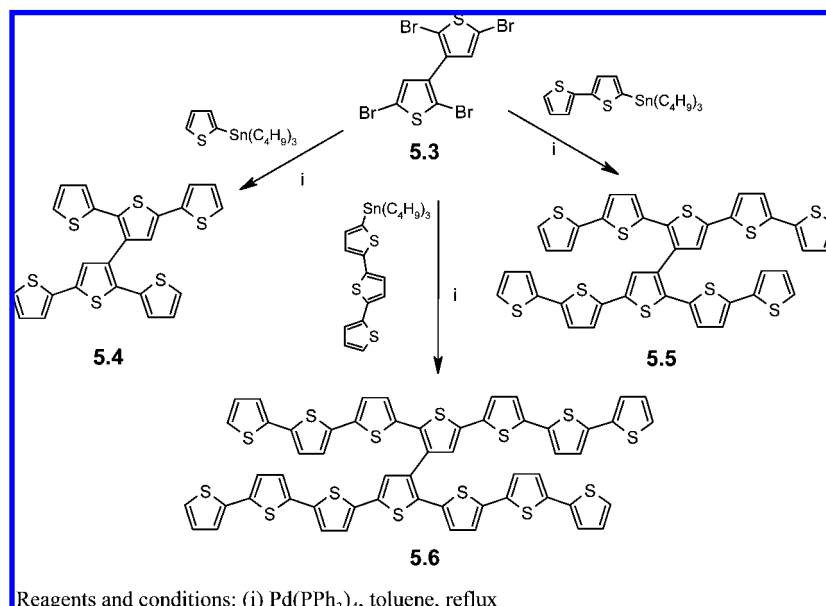
Scheme 5.2

Reagents and conditions: (i) Pd(PPh₃)₄, toluene, reflux

Chart 5.1

5.7   5.8: n = 0, 1   5.9
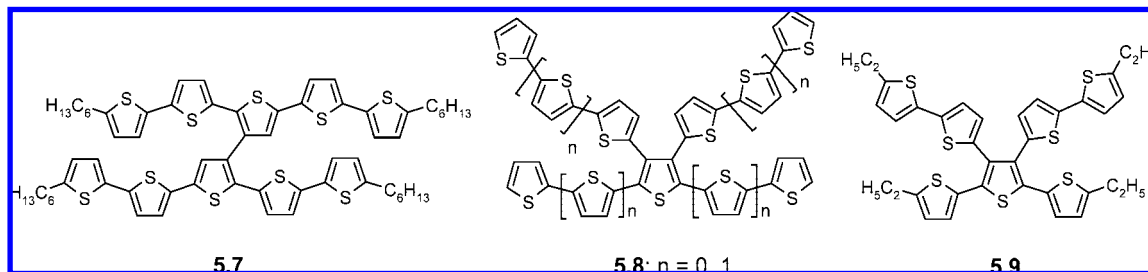
Chart 5.2

5.10   5.11   5.12   5.13

R =
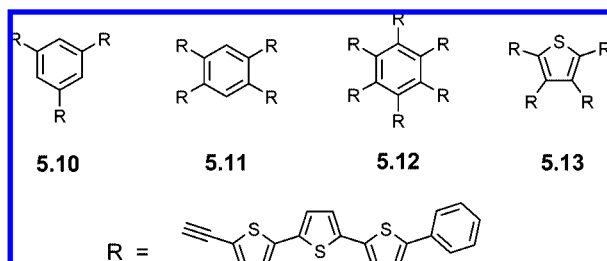
good transport properties in the oligothiophene layer. In OSCs, relatively low power conversion efficiencies (**5.16**, 0.32%; **5.17**, 0.14%) were reported, whereas a quite high hole mobility (1.1×10^{-2} cm^2 V^{-1} s^{-1}) was observed in OFET measurements.

Employing Stille-type reactions, Dunsch et al. prepared star-shaped thiophene-based compounds **5.18** and **5.19** ($n =$ 0, 1) (Chart 5.3) containing triphenylamine-, benzene, and 1,3,5-triphenylbenzene as core.[724] These compounds were characterized by cyclic voltammetry and UV−vis/NIR spectroelectrochemistry, and tuning of their electrochemical properties was investigated. Compounds **5.18** and **5.19** (n = 1) showed multistep reversible electron transfer processes. Increased stability of the charged states by the incorporation of a bithiophene moiety in **5.19** (n = 0) has been discussed.

Star-shaped D−A systems **5.20a−d** based on a triphenylamine core and thienylenevinylene arms as the donor part as well as terminal dicyanovinylene groups as acceptors were synthesized by the Roncali group (Chart 5.4).[725] Compound

5.20a was prepared in 70% yield from tris[4-(2-thienyl)phenyl]amine by Vilsmeier−Haack formylation followed by Wittig−Horner olefination with thienylmethylphosphonate. Compounds **5.20b−d** were obtained in 19%, 48%, and 70% yield by Knoevenagel condensation of the appropriate aldehyde precursor and malononitrile. **5.20a** showed a $\pi-\pi^*$ absorption band at 424 nm and an emission at 506 nm. The successive introduction of electron-withdrawing dicyanovinyl groups in **5.20b−d** further shifted the absorption (~510 nm) and emission (~630 nm) maxima toward lower energies. These compounds were used for the fabrication of bilayer heterojunction photovoltaic cells by successive thermal evaporation of the donor and the acceptor C₆₀. Power conversion efficiencies of ca. 1.2% were observed under white light illumination.[725] In a recent report, by using a LiF layer between the acceptor C₆₀ and the Al cathode for compound **5.20d**, the efficiency was increased to 1.85%.[726]

Cremer and Briehn reported oligothienyl-triphenylamines **5.21** (Chart 5.4), comprising head-to-tail coupled oligo(3-hexylthiophenes) as arms linked to a triphenylamine core.[727] The oligomers were built up *via* Pd⁰-catalyzed cross-coupling reaction of a triphenylamine boronic ester and bromooligothiophenes in 70−75% yields. These oligomers showed strong absorption and emission transitions in the visible region with high fluorescence quantum yields reaching 65% for **5.21** (n = 1).

Soluble star-shaped C_3-symmetric oligothiophene-functionalized truxenes were reported by Pei et al.[728] Suzuki-type coupling of 2,7,12-tribromo-5,5,10,10,15,15-hexahexyltruxene **5.22** with thienyl-2-boronic acid gave thiophene-

Chart 5.3

5.14a: n = 1, R = H
b: n = 2, R = H
c: n = 3, R = H
d: n = 1, R = Ph

5.15

5.16

5.17

5.18

5.19: n = 0, 1

Chart 5.4

5.20

5.21: n = 0, 1, 2, 3

a: R = R^1 = R^2 =

b: R = R^1 =   R^2 =

c: R =   R^1 = R^2 =

d: R = R^1 = R^2 =
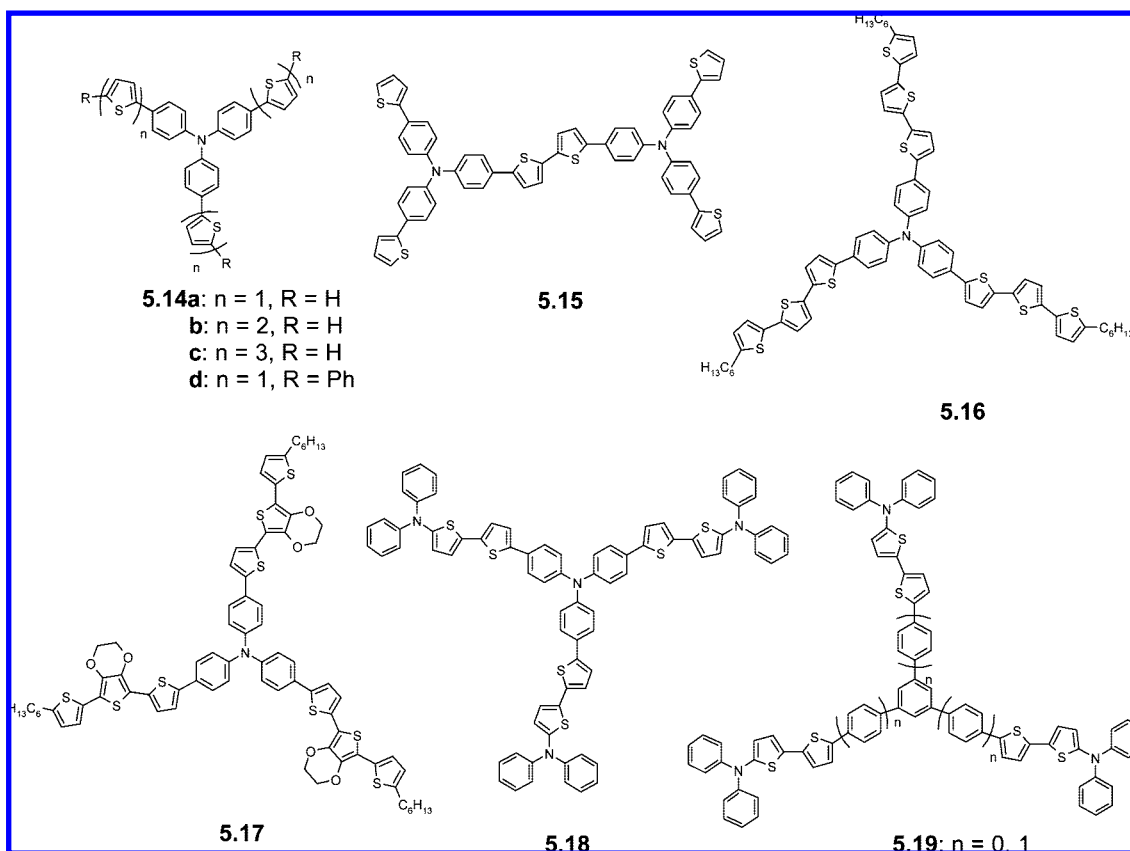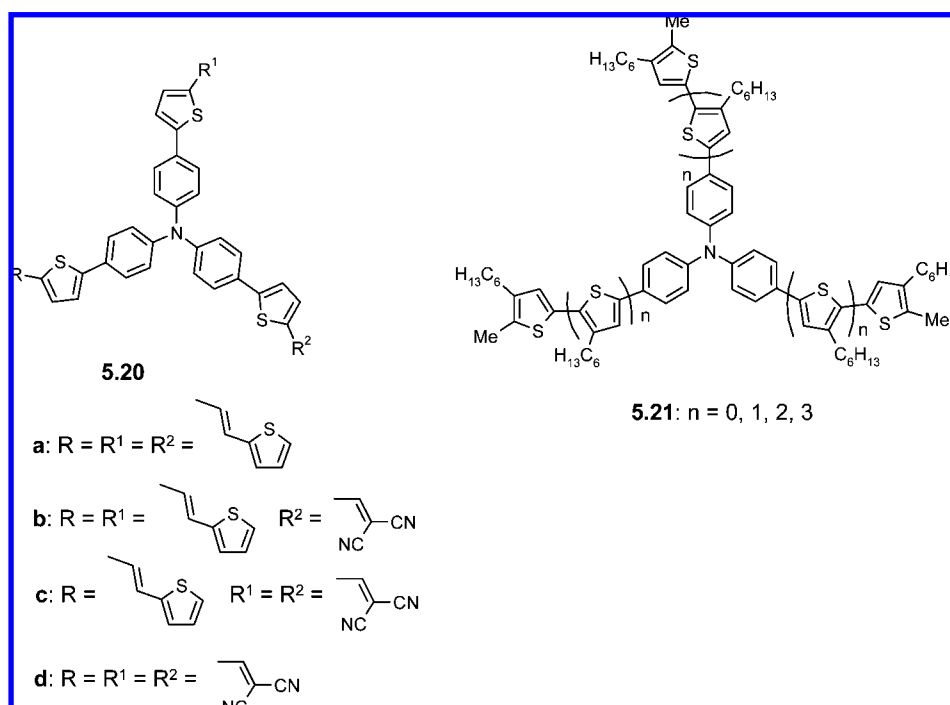
substituted truxene **5.23** (*n* = 1). The thiophene arms were elongated step-by-step *via* bromination with NBS followed by Pd^0-catalyzed coupling with thiophene-2-boronic acid to yield bithiophene **5.23** (*n* = 2), terthiophene **5.23** (*n* = 3), and quaterthiophene derivative **5.23** (*n* = 4) (Scheme 5.4). In comparison to the absorption of the corresponding arms, their UV−vis spectra showed successively red-shifted ab-

sorption maxima with increasing length of the oligothiophene arms, suggesting an extended π-conjugation through the truxene core. Due to the high solubility of **5.23** in organic solvents, solution-processed OFETs were fabricated.[729] Mobilities up to 1.03×10^{-3} cm^2 V^{-1} s^{-1} and on/off ratios of ∼10^3 were observed for **5.23** (*n* = 1), but the mobilities decreased with increasing length of the oligothiophene arms.

Scheme 5.4

5.22

5.23: n = 1-4

Reagent and condition: (i) Thiophene-2-boronic acid, Pd(PPh₃)₄, THF, NaHCO₃/H₂O. (ii) NBS, CHCl₃.
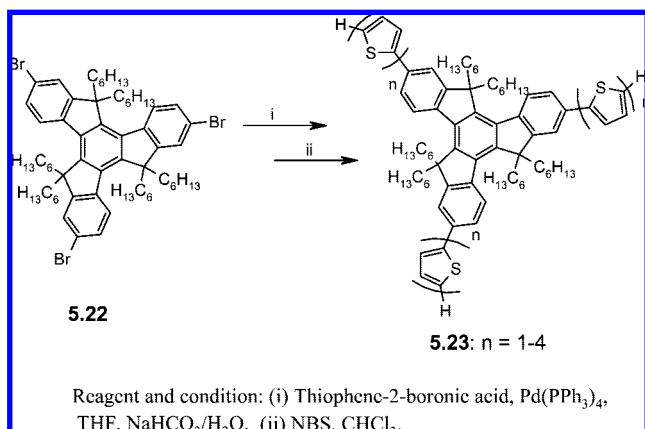
This rather unexpected result might be due to unfavorable film morphologies. Oxidative polymerization of **5.23** (*n* = 1) by FeCl₃ in chloroform afforded a hyperbranched polymer, which is highly soluble in organic solvents and showed bathochromically shifted absorption and emission compared to the monomer due to further extension of conjugation in the polymer.[728]

The same authors recently employed a divergent/convergent approach to prepare π-conjugated first and second generation dendrimers **5.24** and **5.25** bearing oligothienylene−ethynylene branches attached to the truxene core (Chart 5.5).[730] These dendrimers not only showed broad absorption bands and high absorptivities but also have an intrinsic energy gradient from the periphery toward the core through the branching units, resulting in efficient energy migration. The maximum emission wavelengths for **5.24** and **5.25** were at 444 and 468 nm in THF solution and at 508 and 521 nm in thin films, respectively, independent of the excitation wavelength. This finding suggested an efficient intermolecular and/or intramolecular energy transfer from the periphery to the longest conjugated segment.

Pei et al. developed an efficient approach toward the formation of star-shaped chiral amines through asymmetric allylation of optically active imines bearing chiral functionalities.[731] The (oligo)thiophene-substituted homoallylic amines **5.28** were prepared with high diastereoselectivity by Ce-catalyzed addition of allylic zinc to chiral imines **5.27** which were obtained from condensation of 2-thienyl- or 5-bithienylcarboxaldehyde **5.26** and the methylester of α-amino acid valine (Scheme 5.5). The application of such an addition reaction to aldehydes of truxene **5.23** (*n* = 1, 2) yielded chiral star-shaped, amino-functionalized (oligo)thiophene-truxenes **5.29** in excellent diastereoselectivity (Chart 5.6). The optical properties were not significantly different from

Chart 5.5

5.24: R = C₆H₁₃, n = 1, m = 0
5.25: R = C₆H₁₃, n = 3, m = 1

Scheme 5.5

5.26: n = 1, 2   **5.27**: n = 1, 2   **5.28**: n = 1, 2

Reagents and conditions: (i) Toluene, reflux; (ii) Zn/THF, 25 °C, CeCl₃.7H₂O

Chart 5.6

5.29 a: n = 1
b: n = 2

5.30: R₁ = H, n = 1-4, R = C₆H₁₃

5.31: R₁R₁ = ⟨O—O⟩, n = 1, 2, R = C₆H₁₃

R = C₆H₁₃

5.32: X = —; **5.33**: X = ⌒⌒; **5.34**: X = ═══

5.35
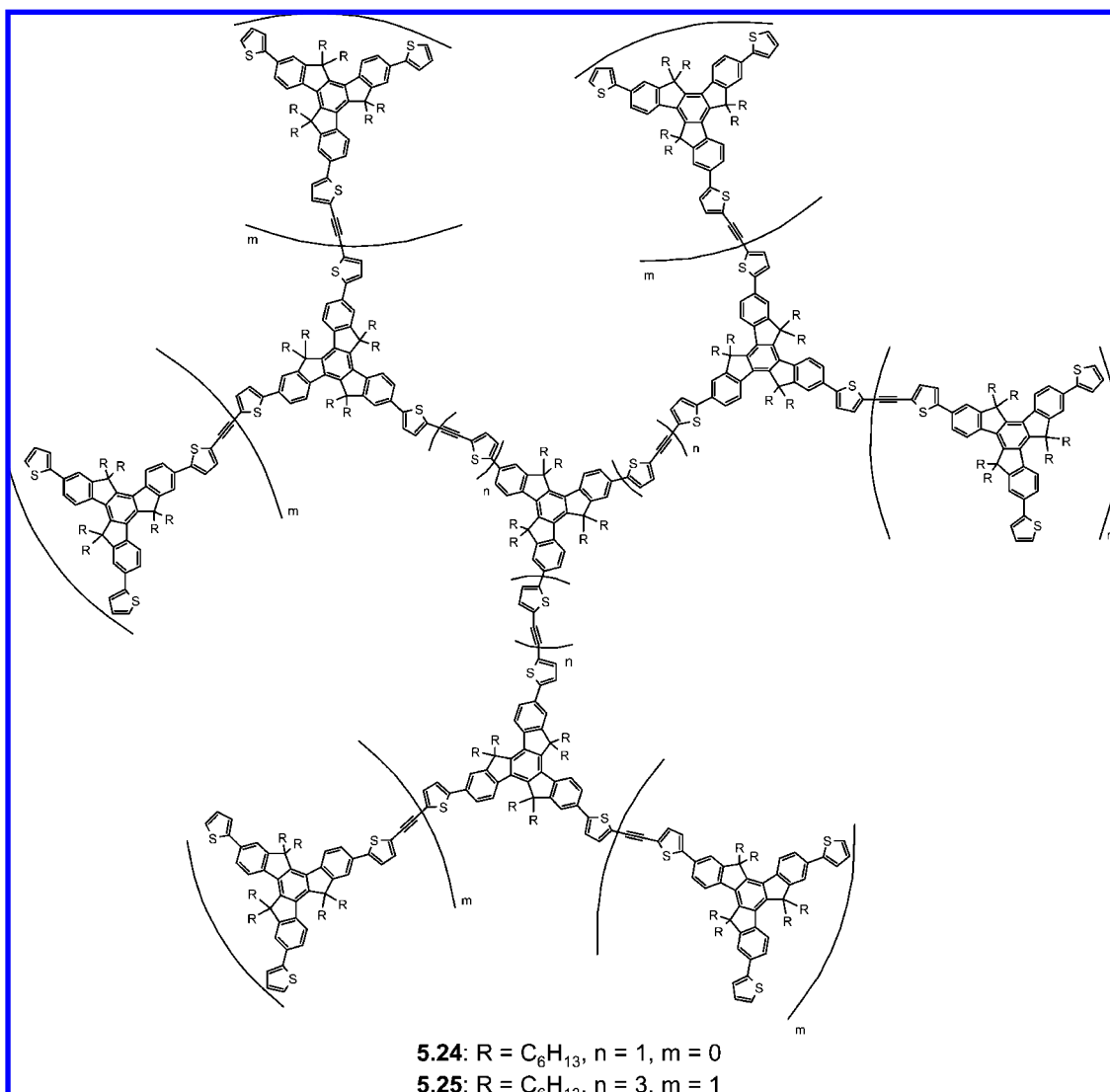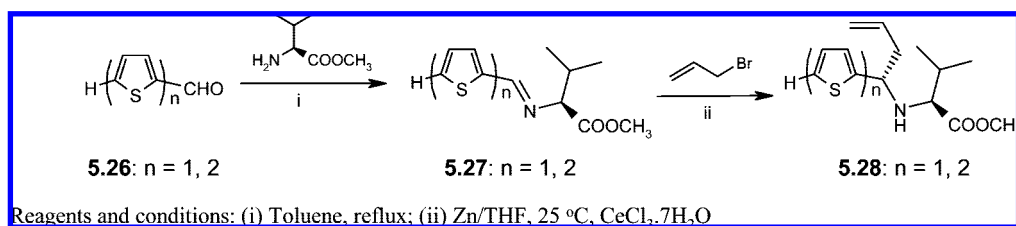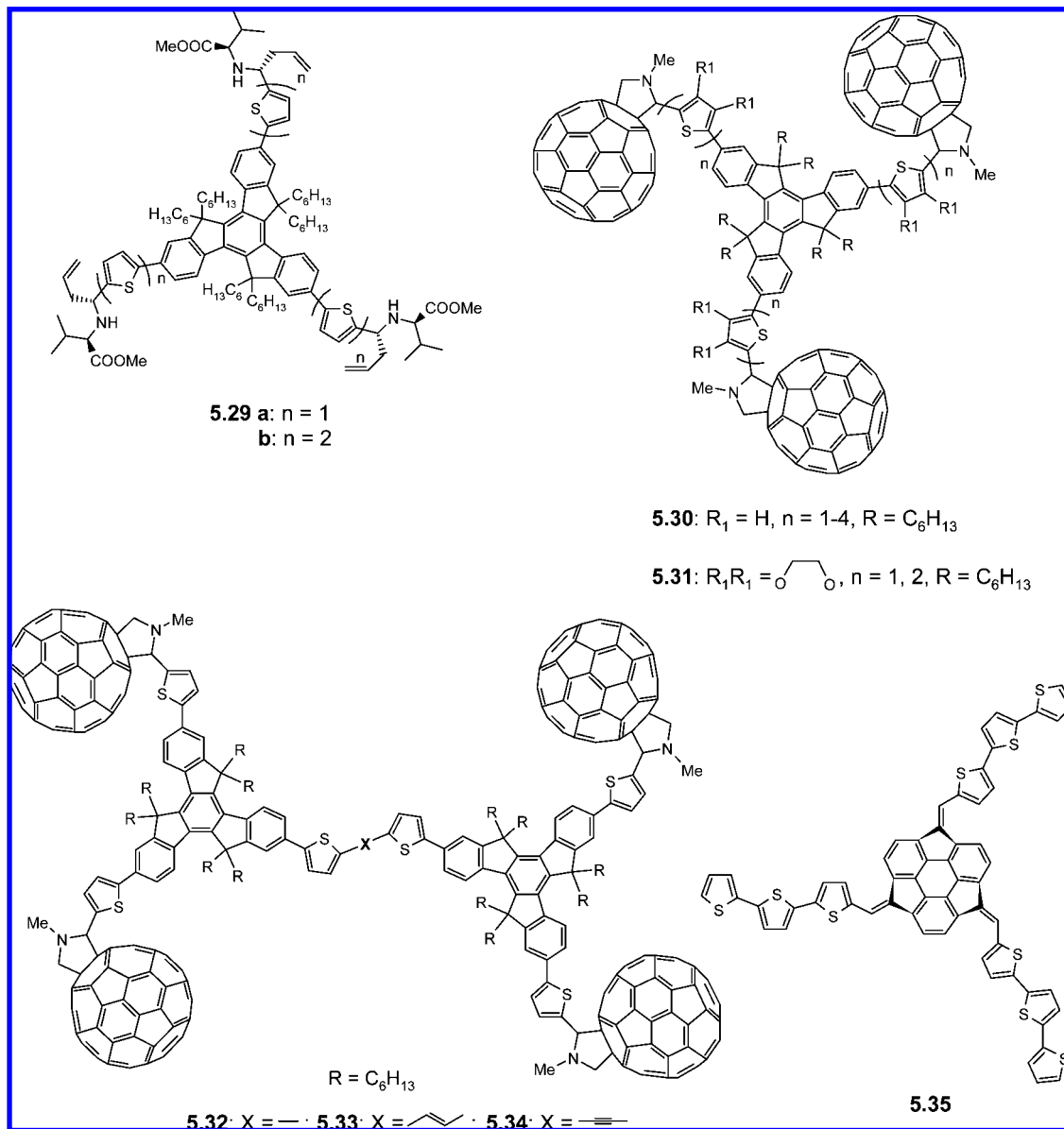
those of corresponding parent compounds **5.23** (n = 1, 2). In CD spectra, a negative Cotton effect was found for the star-shaped structures, whereas an inverse positive effect has been measured for the linear chiral (oligo)thiophene-amine arms.

The peripheral decoration of star-shaped oligothiophene-truxenes with fullerene units was also realized by Pei's group (Chart 5.6).[732] C₆₀-moieties were attached to the arms of the star-shaped molecules by the Prato-reaction to give D−A systems **5.30** and **5.31** in 25−35% yield. Thus, by dipolar cycloaddition C₆₀ was coupled to the aldehyde-terminated oligothiophene arms with the aid of N-methylglycine.[30]

Structures **5.32−5.34** were obtained by connecting two of the star-shaped systems with single, double, or triple bonds, respectively. Typical Pd⁰-catalyzed Suzuki-, Negishi-, and Sonogashira-type cross-couplings as well as McMurry reactions were used to bridge the two π-conjugated systems. Although there is no change in the absorption spectrum for **5.32−5.34**, the emission maxima shifted to longer wavelengths in the order **5.34** (446 nm) < **5.32** (460 nm) < **5.33** (483 nm). A strong quenching of the emission was observed due to an efficient photoinduced intramolecular charge transfer between the oligomers and the C₆₀ moieties.

Chart 5.7

5.36: n = 0, 1
R = H, CH₃

5.37
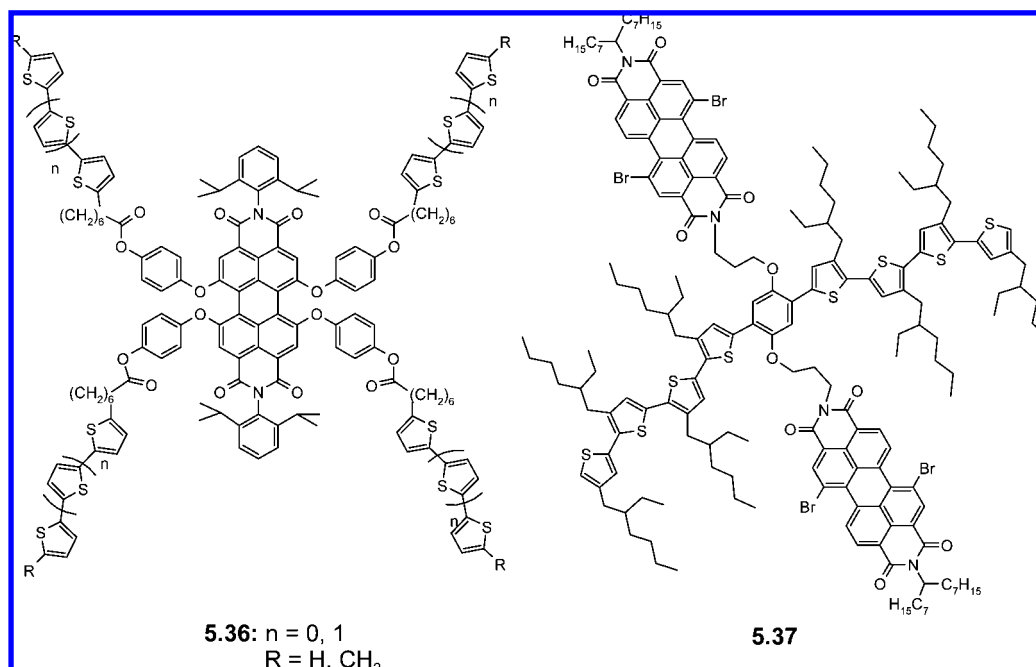
A terthiophene-substituted π-extended bowl-shaped conjugated material **5.35** (Chart 5.6) was synthesized by condensation of the benzylic anion of rigid sumanene and formylated terthiophene in the presence of NaOH as base and tetrabutylammonium bromide as phase-transfer reagent.[733] UV–vis spectra of **5.35** showed red-shifted absorptions at 434 and 545 nm and a band gap of 1.99 eV due to the rigid molecular structure and expanded π-conjugation.

The formation of a hyperbranched polymeric network by electropolymerization of oligothiophene-functionalized perylene bisimides was reported by Würthner et al. (Chart 5.7).[734,735] Monomers **5.36** were synthesized by esterification of hydroxyphenoxy-substituted perylene bisimide with heptanoic acid-substituted bi- and terthiophenes in the presence of dicyclohexylcarbodiimide and dimethylaminopyridine as coupling reagents. No ground-state electronic interaction between the various chromophores was observed in the absorption spectrum of **5.36** (n = 1, R = H), which showed peaks at 362 nm due to the oligothiophene and at 573 nm due to the perylene unit. The emission at 605 nm only came from the perylene core irrespective of the excitation wavelength, indicating an efficient energy transfer process from the oligothiophene arms to the perylene core. The polymer network formed by electropolymerization revealed remarkable p-type conductivity. Significantly, two separate regimes of electrical conductance have been observed for the films generated from **5.36** (n = 1, R = H).

Chen et al. prepared an oligothiophene–perylene-based D–A system **5.37**, where two perylenediimide and two quaterthiophene units are attached to a phenyl core (Chart 5.7).[736] Although there is weak electronic interaction in the ground state, absorption spectra of **5.37** in chloroform showed broad overlapping oligothiophene and perylene diimide absorptions. The emission at 535 nm came only from the perylene core irrespective of the excitation wavelength. This suggested an efficient energy transfer process from the oligothiophene arms to the perylene units with strong quenching of the oligothiophene emission. Cyclic voltammetry measurement of **5.37** showed three reversible oxidation

waves corresponding to the oligothiophene moieties and two reduction waves for the perylene diimide, further indicative of weak electronic interactions between the donor and acceptor moieties in the ground state. Transient absorption spectroscopy measurements showed two different dynamics of charge separation and charge recombination processes associated with two types of donor/acceptor conformation of **5.37** in solution.

Bäuerle et al. reported the synthesis of a series of star-shaped oligothiophene–perylene D–A systems **5.40** (Scheme 5.6).[737] The structures were built up in 62, 54, and 43% yield by 3-fold reaction of iodinated perylene-functionalized bi-, quater-, or sexithiophene **5.38** (n = 1–3) with triphenylamine boronic ester **5.39**. Here, head-to-tail coupled oligo(3-alkylthiophenes) mimicking the corresponding polymer were used as building blocks. The fabrication of OSCs based on a blend of **5.40** (n = 2) with PCBM revealed moderate power conversion efficiencies of 0.25% under a simulated terrestrial sun spectrum. The charge-transfer properties of two derivatives were studied by photoinduced absorption spectroscopy. Due to a fast photoinduced electron transfer (τ = 2 ps), a strong quenching of the emission was observed.[738] It turned out that the triphenylamine plus the oligothiophene arms acted as donor with enhanced conjugation and improved donor properties.

5.2. Tetrahedral Oligothiophenes

Tetrahedral oligothienyl silane derivatives **5.41** were recently prepared by modification of the tetravinylsilane core with oligothiophenes of different chain length using hydrosilylation and Stille coupling reactions (Chart 5.8).[739] Roncali et al. have prepared tetrahedral oligothienyl silane derivatives **5.42** and **5.43** by reaction of lithiated terthiophenes with SiCl₄ (Chart 5.8).[740] In comparison to the linear parent terthiophenes, the tetrahedral structures gave a red shift of 17–19 nm in the absorption spectra. These materials were implemented as donor component in bilayer heterojunction solar cells showing a significant increase in performance (η

Scheme 5.6

5.38: n = 1-3

+

5.39

5.40: n = 1-3

Reagent and condition: (i) Pd(PPh₃)₄, DME, NaOH, 80 °C

Chart 5.8

5.41: n = 0; R = H
n = 0; R = CHO
n = 1; R = H
n = 1; R = CHO
n = 2; R = H

5.42: R = n-C₆H₁₃
5.43: R = S-n-C₆H₁₃

5.44: n = 1, 2

5.45: n = 0, 1

5.46

Scheme 5.7

5.48: n = 1, 2   **5.47**: n = 1, 2

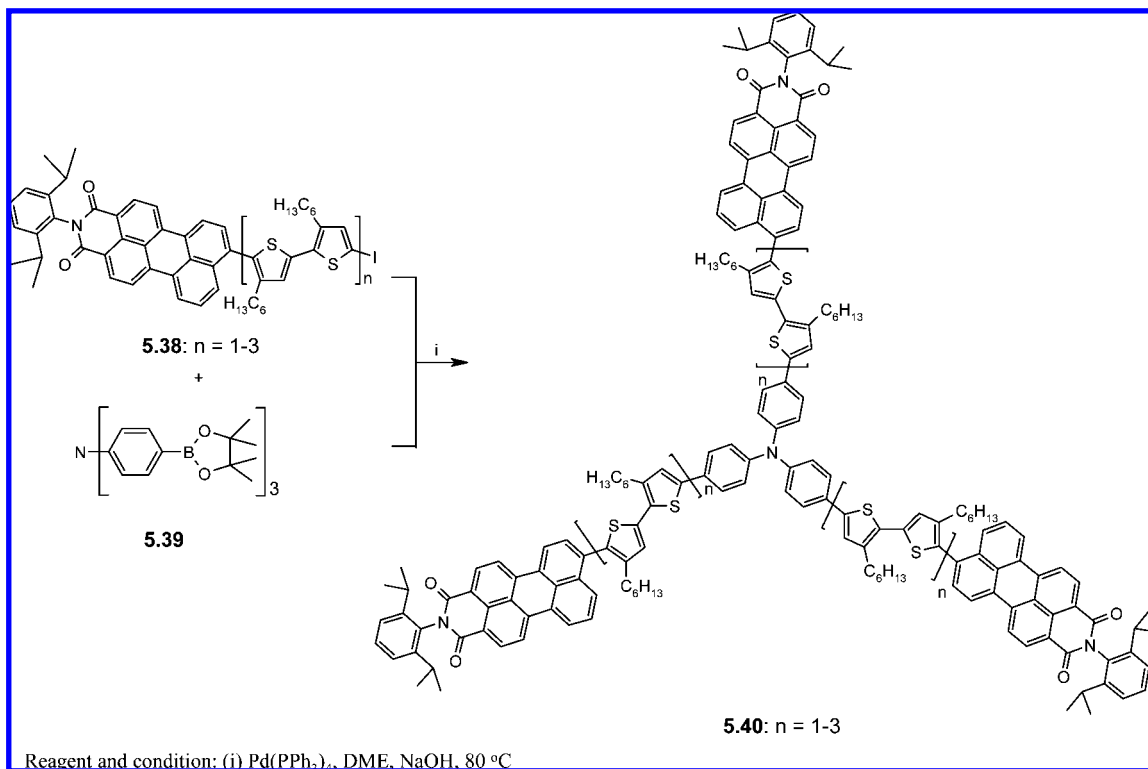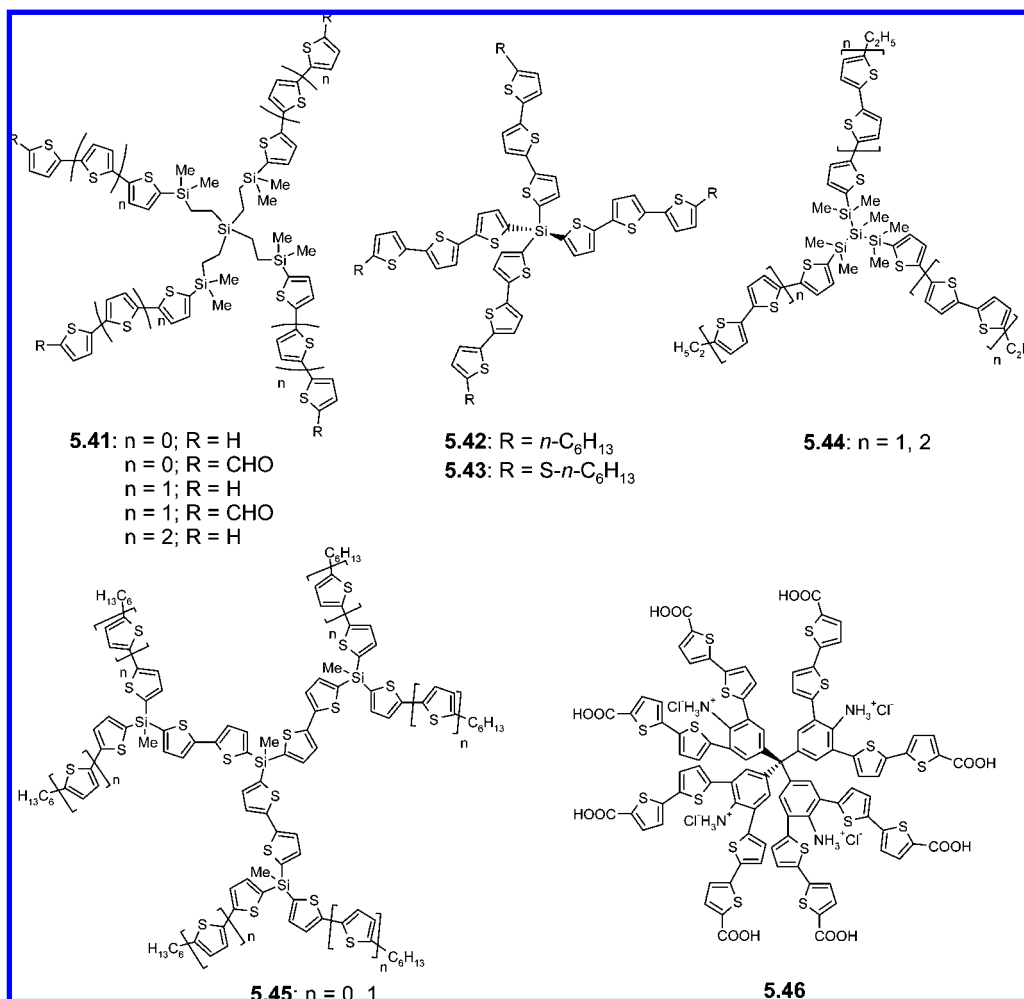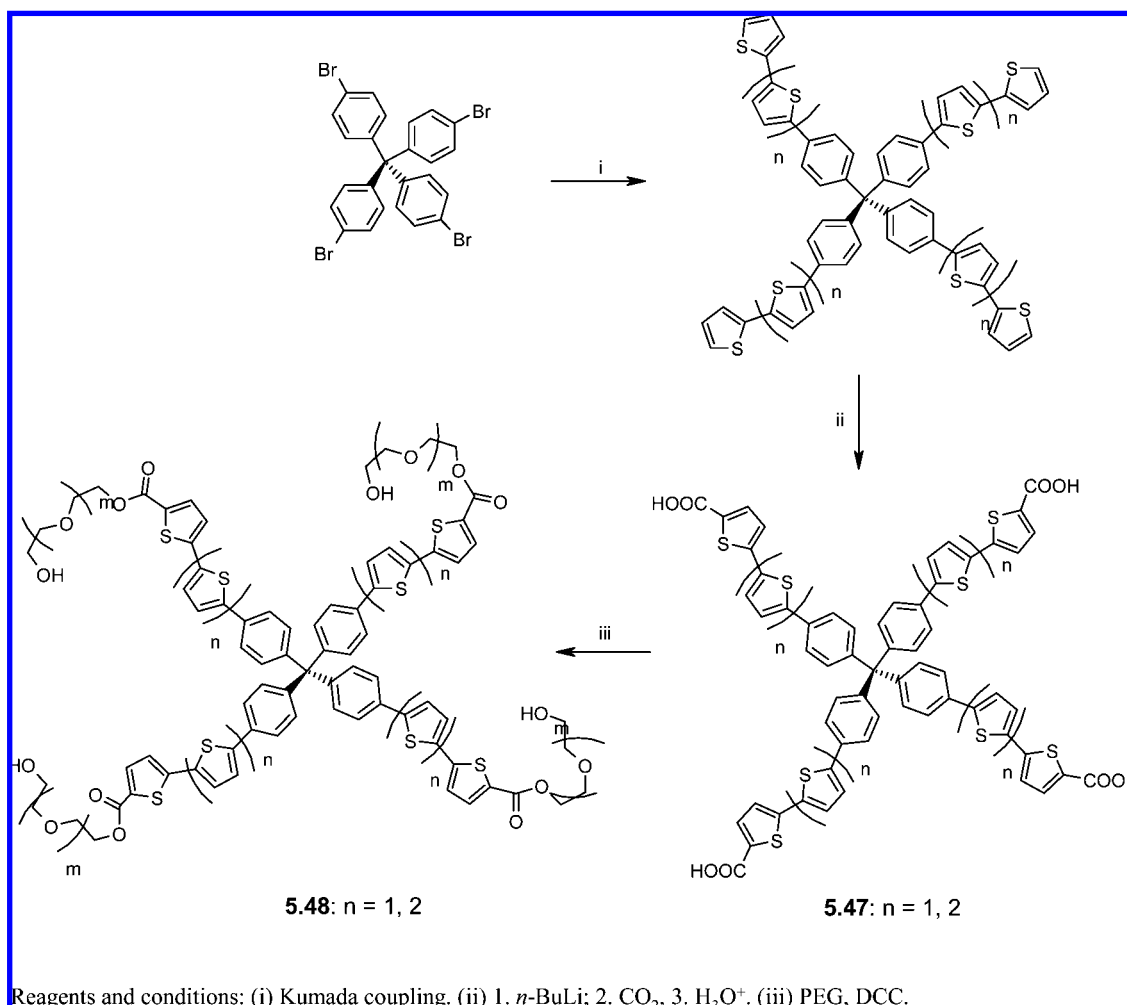Reagents and conditions: (i) Kumada coupling. (ii) 1. *n*-BuLi; 2. CO₂; 3. H₃O⁺. (iii) PEG, DCC.

≤ 0.20%) compared to cells including only the linear dihexylterthiophene ($\eta = 0.04\%$) as active material, which was attributed to the isotropic absorption and hole transport associated with the 3D geometry. In bulk-heterojunction solar cells with PCBM as acceptor, compound **5.43** showed an efficiency of 0.3%, which nevertheless is quite low compared to standard P3HT-PCBM solar cells.[272,273,741−744]

Small generation dendrimers based on oligothiophene-silanes have been reported including **5.44** ($n = 1, 2$)[745] and **5.45** ($n = 0, 1$)[746] (Chart 5.8). Terthienyl-silane **5.44** ($n = 1$) was synthesized by the reaction of lithiated alkylter-thiophene with tris(chlorodimethylsilyl)methylsilane in 56% yield. On the other hand, Stille-type reaction of stannylated alkylterthiophene and tris[5-(bromobithienyl)dimethylsilyl-]methylsilane afforded quinquethiophene-silane **5.44** ($n = 2$) in 60% yield. Bithiophene-silane dendrimers **5.45** ($n = 0, 1$) were prepared in low yields using Kumada coupling for the derivative with $n = 0$ and a Suzuki coupling reaction for the derivative with $n = 1$, in which tris(5-bromo-2-thienyl)methylsilane was used as core. Red-shifted absorp-tions due to $\sigma-\pi$ conjugation and strong fluorescence were reported when compared to corresponding oligothiophenes. These Si-linked oligomers showed high thermal stability.

A modification of a tetrahedral oligothiophene−tetraphenylmethane **5.46** consisting of eight fluorescent carboxyl-terminated bithiophene units as branching arms and four amino groups in the *p*-position of the phenyl groups was prepared (Chart 5.8).[747] The compound showed high pH

sensitivity with an emission at ∼430 nm in acidic solution and at ∼500 nm at pH 5−13, which represented a good example of pH-sensitive fluorescent probes for biological systems.

Using tetraphenylmethane as a core, Liu et al. have prepared tetrahedral branched bi- and terthiophenes **5.47** ($n = 1, 2$) and **5.48** ($n = 1, 2$) by Pd⁰-catalyzed aryl−aryl coupling methods (Scheme 5.7).[748] The linkage of polyeth-yleneglycol (PEG) units to the fluorescent oligothiophene arms in compound **5.48** increased the water solubility of the tetrahedral chromophores. At the same time, in comparison to their parent carboxylic acids **5.47**, the fluorescence quantum yields of **5.48** increased by a factor of 6−7 due to intermolecular interactions of the chromophores and reduced nonemissive energy loss.

The synthesis of oligothiophenes and oligothienylethy-nylenes attached to orthogonally arranged spiro-cores has been reported by Tour et al.[16,749,750] In this respect, Pei et al. developed a convenient synthesis of similar oligothiophene-spirobifluorenes (**5.49**, $n = 1−3$).[751] Mono-, bi-, and terthie-nylzinc chloride were prepared by lithiation of the corre-sponding (oligo)thiophenes, which were reacted by subsequent transmetalation with anhydrous zinc chloride. Then, Pd⁰-catalyzed Negishi-type coupling of the organozinc (oligo)th-ienyls with 2,2′,7,7′-tetrabromo-9,9′-spirobifluorene as a core afforded tetrahedron-shaped derivatives **5.49** (Scheme 5.8).

The same group synthesized an analogous spirobifluorene-based structure **5.50**, comprising regioregular oligo(3-hexy-

Scheme 5.8

Reagents and Conditions: (i) n-BuLi, TMEDA, ZnCl₂, THF; ii) Pd(PPh₃)₄, 2,2',7,7'-tetrabromo-9,9'-spirobifluorene

Chart 5.9

5.50: n = 0, 1, 2

5.51
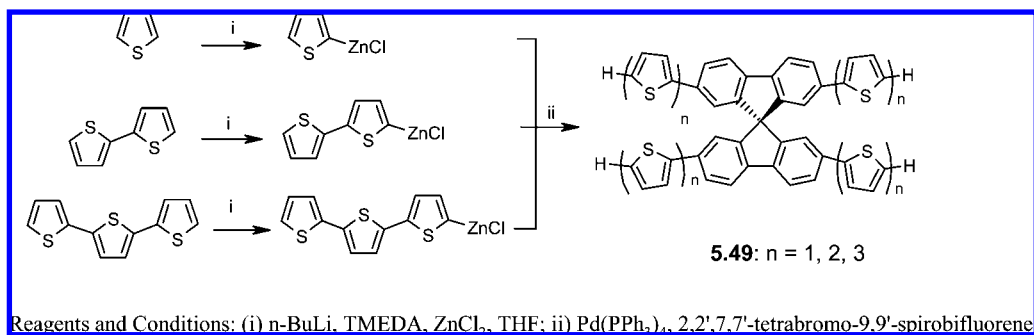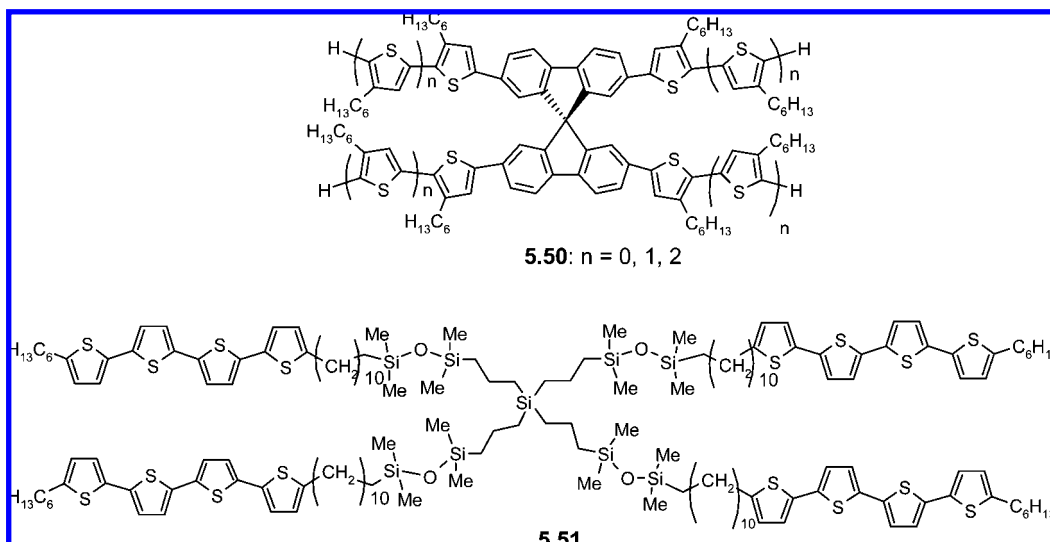
lthiophenes), by employing Suzuki-type cross-coupling reactions. Reaction of sodium 4-n-hexyl-2-thienylboronate with 2,2′,7,7′-tetrabromo-9,9′-spirobifluorene gave the 4-fold hexylthiophene-substituted derivatives **5.50** (n = 0) in 97% yield. Subsequent bromination with NBS and Pd⁰-catalyzed coupling with sodium 4-n-hexyl-2-thienylboronate afforded corresponding head-to-tail coupled oligothiophene **5.50** (n = 1, 2) in ∼98% yield (Chart 5.9).[751] Electrochemical measurement indicated that the radical cations of the oligothiophene-modified 9,9′-spirobifluorenes are more stable than those of the corresponding linear oligothiophenes. The band gaps (2.34−2.89 V) of **5.50** (n = 0−2) were estimated from the onset potentials of n-doping and p-doping.[752]

The attachment of hexyl-capped quaterthiophenes to a carbosilane core *via* longer alkyl side chains was achieved by hydrosilylation reactions. Kirchmeyer et al. obtained quaterthiophene-functionalized tetrahedral structure **5.51** (Chart 5.9), which was highly soluble in organic solvents. In OFETs, these solution-processable materials showed excellent charge carrier mobility values of 10^{-2} cm² V⁻¹ s⁻¹ and on/off ratios of 10^6. Because of the high portion of saturated parts in the core, this result is rather unexpected and was explained by an ordering of the molecules in a way that the peripheral conjugated π-systems can stack.[753]

5.3. Functionalization of Dendrimers with Oligothiophenes at the Periphery

The peripheral functionalization of conventional dendrimers containing flexible and saturated spacers with oligothiophenes was reported by Miller et al. Bi- and quater-

Chart 5.10

5.52: R =

5.53: R =
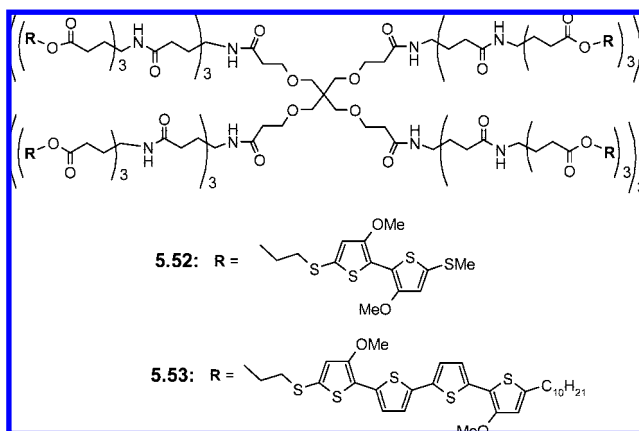
thiophenes were attached to the periphery of the acid-terminated *G2*-dendrimer through esterification with a (2-hydroxyethyl)thio linker (Chart 5.10).[754] The moderate conductivity of I₂-doped films of dendrimers **5.52** and **5.53** increased by 2 orders of magnitude when they were exposed to solvent vapors.

Advincula et al. decorated conventional dendrimers with conjugated dendrons at the periphery. Formylated terthiophene dendron **5.54**, which was prepared by Vilsmeyer−Haack formylation of dendron **5.73a** (*vide infra*), was linked to the periphery of a *G4*-polyamidoamine (PAMAM) dendrimer by reductive amination. The incorporation of Pd- or Au-nanoparticles into the dendrimer created new hybrid nanomaterials **5.55** (Scheme 5.9).[755] As a consequence of

Scheme 5.9. Representative Core-Shell Architecture of the PAMAM−Oligothiophene Conjugate

Reagents and conditions: (i) a. G4-PAMAM-(NH$_2$)$_{64}$, CH$_2$Cl$_2$/MeOH; b. NaBH$_3$CN; (ii) Pd(OAc)$_2$, NaBH$_4$ or HAuCl$_4$.3H$_2$O. NH$_2$NH$_2$. (N represents peripheral NH$_2$. NH. groups on the PAMAM surface)
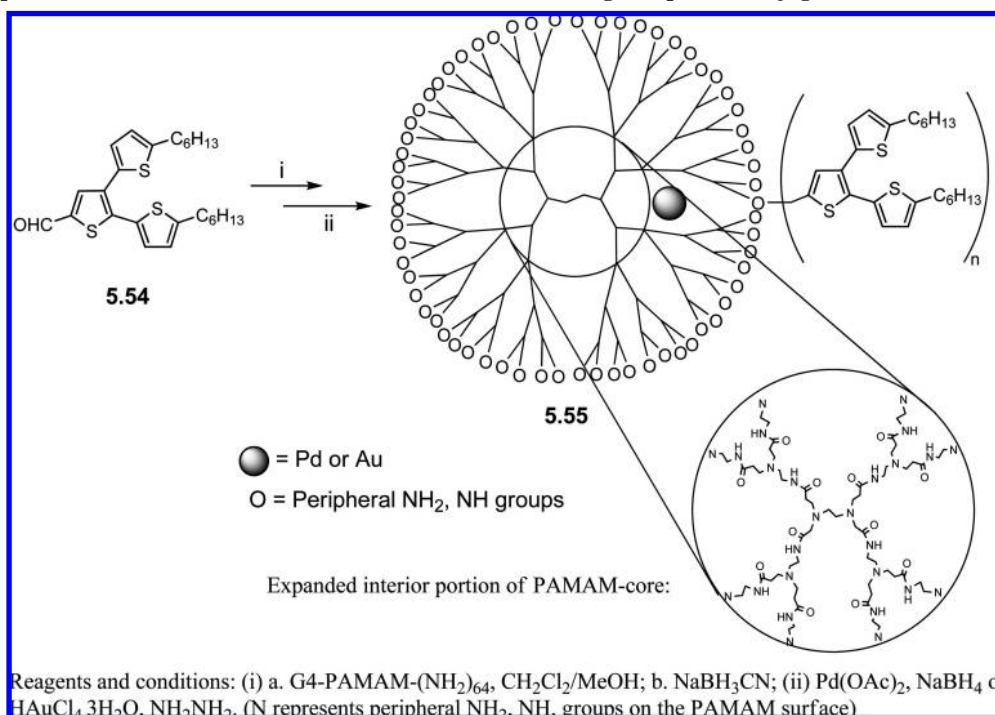
the dendritic architecture, the emission properties of the thiophene dendrons enhanced due to efficient energy transfer between the metal nanoparticle and the dendrons. Attachment of these terthiophene dendrons to gold nanoparticles *via* thiol/phosphonate functionalization has been reported recently. Photovoltaic devices fabricated with CdSe nanoparticles which were jacketed by phosponate-functionalized terthiophene dendrons showed a moderate power conversion efficiency of 0.29%.[756] As a comparison, OSCs having a blend of CdSe nanoparticles and regioregular poly(3-hexylthiophene) as active layer gave external power conversion efficiencies of 1.7%.[757]

Decoration of phenylene cores with oligothiophenes was realized in the star-shaped systems **5.56** and **5.57** and in dendritic **5.58** by Kirchmeyer et al. (Chart 5.11).[758] The bi- and terthiophene derivatives were synthesized by Kumada-type cross-coupling of 1,3,5-tribromobenzene or 1,3,5-(4-bromophenyl)benzene and the Grignard reagents of α-decyloligothiophenes by using Pd(dppf)Cl$_2$ as a catalyst. The absorption maxima were found at 365 nm for **5.56** ($n = 1$) and at 405 nm for **5.56** ($n = 2$), respectively, suggesting that the oligothiophene units were not fully conjugated with each other due to the *meta*-substitution in the core. Moderate field-effect mobilities of 2×10^{-4} cm^2 V^{-1} s^{-1} in OFET devices were found for **5.56**. In comparison to the terthienyl derivative **5.56** ($n = 2$), in compound **5.57** one thiophene unit is replaced by a phenyl unit. This structural variation resulted in a blue shift of the absorption maximum to 372 nm and a significant decrease in charge carrier mobility. The same trend can be observed for the extended phenylene−thienylene dendrimer **5.58**, which consisted of 10 phenylene units in the center and 12 alkylterthiophene branches and was also prepared by Kirchmeyer et al. In OFETs, a hole mobility of 10^{-4} cm^2 V^{-1} s^{-1} has been determined for dendrimer **5.58**.[759]

In a similar way, by using a convergent route, Mitchell et al. synthesized dendrimers **5.61** and **5.62**, consisting of a tri- or tetrasubstituted benzene core and oligothiophene dendrons

of the Advincula-type (Scheme 5.10).[760] The build up was achieved by Stille-type coupling of 2-(tributylstannyl)thiophene and 1,3,5-tribromo- or 1,2,4,5-tetrabromobenzene, respectively, to give thienyl−phenyl precursors **5.59** and **5.60**. Subsequent bromination with NBS and Stille-type coupling with stannylated terthiophene or septithiophene dendrons (**5.73** and **5.74**; see Scheme 5.13) gave dendrimers **5.61a,b** in 93 and 96% yield and derivatives **5.62a,b** in 85% and 11% yield, respectively. The absorption and emission spectra suggested that conjugation is involved between the dendrons through the benzene core.

The same group further prepared dendrimer **5.63** by inserting a bithiophene unit between the core of **5.60** and the periphery (Chart 5.11). Despite its relatively large optical band gap of 2.1 eV, fabrication of OSCs based on a blend of **5.63** and PCBM (1:4) revealed a power conversion efficiency of 1.3% under simulated AM1.5 illumination.[761]

Giant shape-persistent and globular polyphenylene dendrimers **5.64** (R = H, CH$_3$) which were decorated at the periphery with terthiophenes were reported by Müllen and Heinze et al. (Scheme 5.11).[762] A terthiophene-substituted tetraphenylcyclopentadione was prepared by Pd^0-catalyzed coupling of 5-bromoterthiophene and tetraphenylcyclopentadienone diboronic ester. Subsequent Diels−Alder cycloaddition of cyclopentadione and an ethynylated phenylene dendrimer gave large hybrid dendrimers **5.64** (R = H, CH$_3$) in 69 and 71% yield, respectively. By electropolymerization of **5.64** (R = H), 3D networks with good conductivities were formed. Depending on the charging level of the electroactive components used as building blocks for the dendrimer core and the perimeter, two regimes of electrical conductivity were observed.

5.4. Oligothiophenes used as Cores in Dendrimers

Oligothiophenes end-capped with polybenzylether dendrons were prepared by the Fréchet group (Scheme 5.12).[763] Benzyl ester-substituted quinquethiophene **5.65** was depro-

Chart 5.11

5.56 (n = 1, 2)

5.57

5.58

5.63
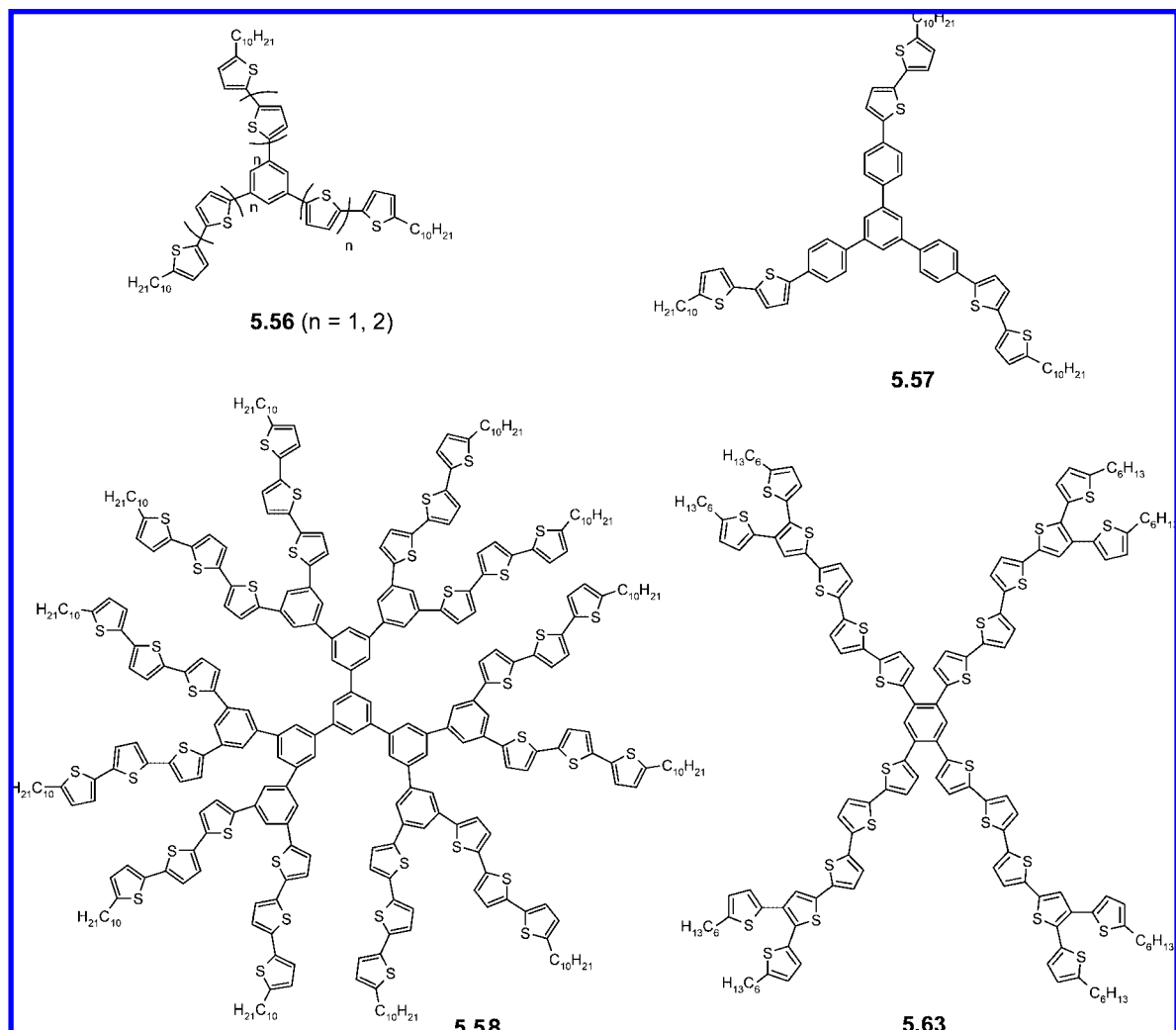
tected in basic medium to the carboxylic acid and converted to the corresponding acid chloride using oxalyl chloride. This was now connected to a *G3*-hydroxyl-terminated Fréchet dendron by ester linkages. Stille-type coupling of the terminally brominated quinquethiophene and 2,5-bis(trimethylstannyl)thiophene afforded the highly soluble dendron-capped undecithiophene **5.66** in 84% yield. A similar synthetic strategy has been employed to prepare homologous dumbbell-shaped dendron-capped heptadecathiophene **5.67** (Chart 5.12).[764] Electrochemical investigation showed that the oxidation of the oligothiophene core resulted in the removal of two electrons, thus leading to dicationic states consisting of two individual radical cations on the oligothiophene chain rather than of a dication. The finding also corroborates the view that, in the solid state, long doubly oxidized oligothiophenes accommodate two polarons rather than a bipolaron on a single chain.[765]

Fréchet et al. later on prepared dendronized oligothiophenes **5.68** and **5.69** up to a nonamer. The aliphatic ether dendrons were either attached to the α-position of a terminal or to the β-position of a central thiophene unit (Chart 5.12).[766] The syntheses were performed by iterative NBS brominations and Pd[0]-catalyzed Stille-type coupling reactions. These materials revealed that the attachment of dendrons to the rather stiff π-conjugated backbone enhanced solubility, reduced the melting point, and increased conjugation, as

indicated by the red-shifted absorptions relative to alkylated oligothiophenes.

Further peripheral decoration of the latter type of dendronized oligothiophenes with coumarin dyes gave compounds **5.70** and **5.71** as models to study energy transfer processes in light-harvesting systems (Chart 5.13).[767] The dye molecules in the periphery of the dendrons acted as an antenna system and by excitation at the coumarin absorption maximum ($\lambda = 343$ nm), the energy is efficiently transferred to the oligothiophene core, which emits at longer wavelengths ($\lambda = 500-650$ nm). The same concept has been pursued with dendronized quinquethiophene **5.72**, which bears hole transporting triarylamines at the periphery (Chart 5.13).[768] Excitation of the triarylamine groups at 310 nm led to green emission at 550 nm coming from the quinquethiophene unit. Fabrication of OLEDs using **5.72** as hole transporting and emitting layer and 2-(4-biphenyl)-5-(4-*tert*-butylphenyl)-1,3,4-oxadiazole as electron transport layer showed green luminescence at 560 nm with an external quantum efficiency of 0.12%.

5.5. Functionalized *all*-Thiophene Dendrimers

Although quite a number of conjugated dendrimers has been reported in the past few years along with a few small generational thiophene-based dendrimers with silane moieties (*vide supra*), the first examples of *all*-thiophene dendrimers

Scheme 5.10

Reagents and condition: (i) Tributyl(thiophene-2-yl)stannane, PdCl$_2$(PPh$_3$)$_2$, DMF, 90 °C; (ii) NBS, AcOH, CHCl$_3$, 0 °C then rt.; (iii) Stannylated dendron, Pd(PPh$_3$)$_4$, DMF, 90 °C.
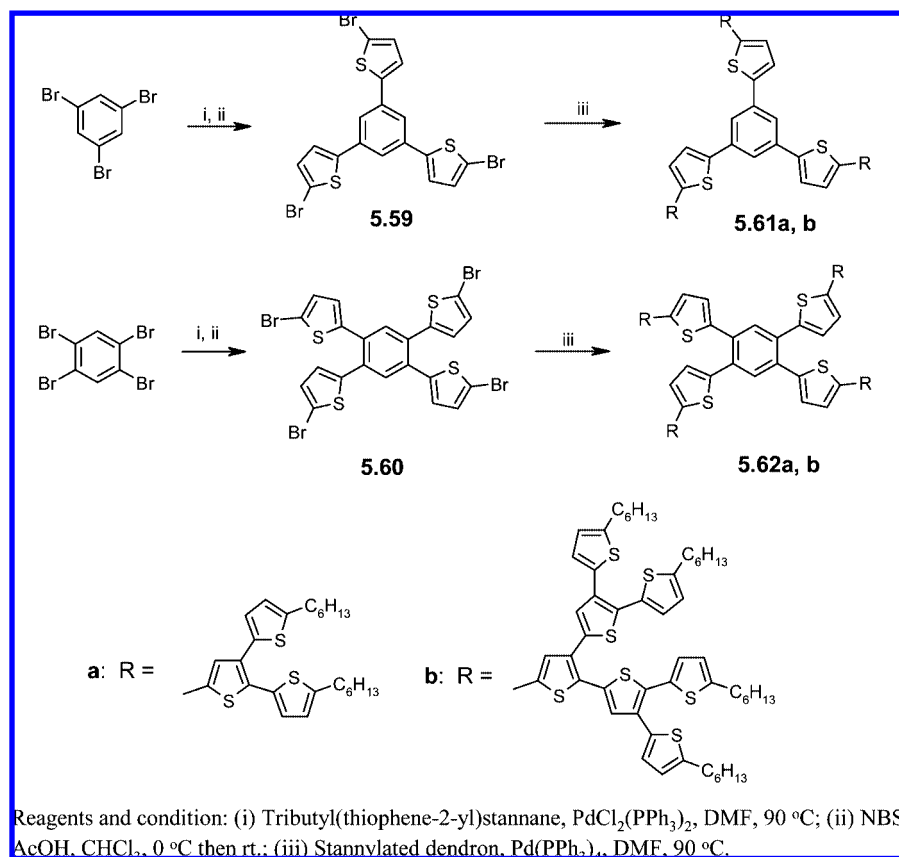
were reported by Advincula et al. (Scheme 5.13).[769] They synthesized dendritic oligothiophenes up to a third generation (*G3*) by a convergent approach using transition-metal-catalyzed Kumada- and Stille-type couplings. The central building block was α,β-branched terthiophene **5.73**, carrying hexyl side chains at the periphery, which made them highly soluble in common organic solvents. *G2*-dendron **5.74a** (7T) was obtained by coupling stannylated terthiophene **5.73b** and 2,3-dibromothiophene (Scheme 5.13). *G3*-dendron **5.75** (15T) was obtained by further coupling of stannylated *G2*-dendron **5.74b** and 2,3-dibromothiophene (Scheme 5.13).

G2-dendrimer **5.76**, consisting of 30 thiophene units, was then synthesized by C−C cross-coupling of tetrabromo-bithiophene and the stannyl derivative of G2-dendron **5.74b** (Scheme 5.14).[770] Investigations of the optical properties revealed broad absorption bands compared to the cases of linear oligothiophenes. AFM measurements of dendrimer **5.76** on a mica surface showed the formation of uniform globular aggregates. On the other hand, self-assembled monolayers on a graphite surface were observed by STM investigations of **5.76** (Figure 5.1).

Our group recently developed an effective approach to novel functionalized dendritic oligothiophenes (DOTs) with the aim to create 3D semiconducting nanoparticles which can be further functionalized at the periphery with, e.g., dyes or redox active, self-organizing, or biological groups and easily attached to core structures of interesting geometric and electronic properties. As a basic building block, trimethylsilyl (TMS)-protected branched terthiophene **5.77** was used to directly allow selective reactions at the free α-position to build up higher generational DOTs (Scheme 5.15).[771] In contrast to Advincula's systems, in this case, the TMS-protecting groups allowed further transformations at the other

α-positions and can either be cleaved off to give the "pure" oligothiophenes or be converted to other functional groups by electrophilic *ipso*-reactions. Thus, the first series of protected and nonsubstituted DOTs have been synthesized up to the fourth generation (*G4*), including a monodisperse and highly soluble 45T (**5.84**) dendron and 90T dendrimers (**5.85**, **5.86**).

Branched terthiophene **5.77** was synthesized by Kumada-type cross-coupling of the Grignard reagent of 2-bromo-5-trimethylsilyl (TMS)-thiophene and 2,3-dibromothiophene in 79% yield. Higher generational DOTs were built up from **5.77** *via* electrophilic *ipso*-reaction with iodine monochloride, which very effectively led to the exchange of TMS groups by iodine to give activated dendron **5.78** (98%). On the other hand, lithiation of **5.77** with *n*-BuLi and subsequent reaction with a dioxaborolane gave the other modular building block, TMS-protected boronic ester **5.79** (93%). Cross-coupling of the two components in a Pd⁰-catalyzed Suzuki-type reaction gave TMS-protected **5.80** as a *G2*-wedge (84%). Deprotected derivative **5.81** was quantitatively obtained by desilylation of **5.80** with tetrabutylammonium fluoride (Scheme 5.15).

Repetition of the sequential divergent−convergent protocol with TMS-protected nonithiophene **5.80** led to boronic ester **5.82** (82% yield) on one hand and the tetraiodinated derivative **5.83** (98%) on the other. Pd⁰-catalyzed cross-coupling of the latter molecule with 4 equiv of boronic ester **5.82** directly resulted in *G4*-dendron **5.84** in one step (yield 80%, Scheme 5.16).

Subsequently, the only free α-position of *G4*-dendron **5.84** was lithiated with *n*-BuLi and oxidatively homocoupled to *G4*-dendrimer **5.85** by CuCl$_2$ (54%). Desilylation of **5.85** by fluoride quantitatively gave *all*-thiophene dendrimer **5.86**, built up from 90 thiophene units, which is a monodisperse

Scheme 5.11

5.64 R = H
R = CH$_3$

Reagents and conditions: (i) o-xylene, Ph$_2$O, 190 °C
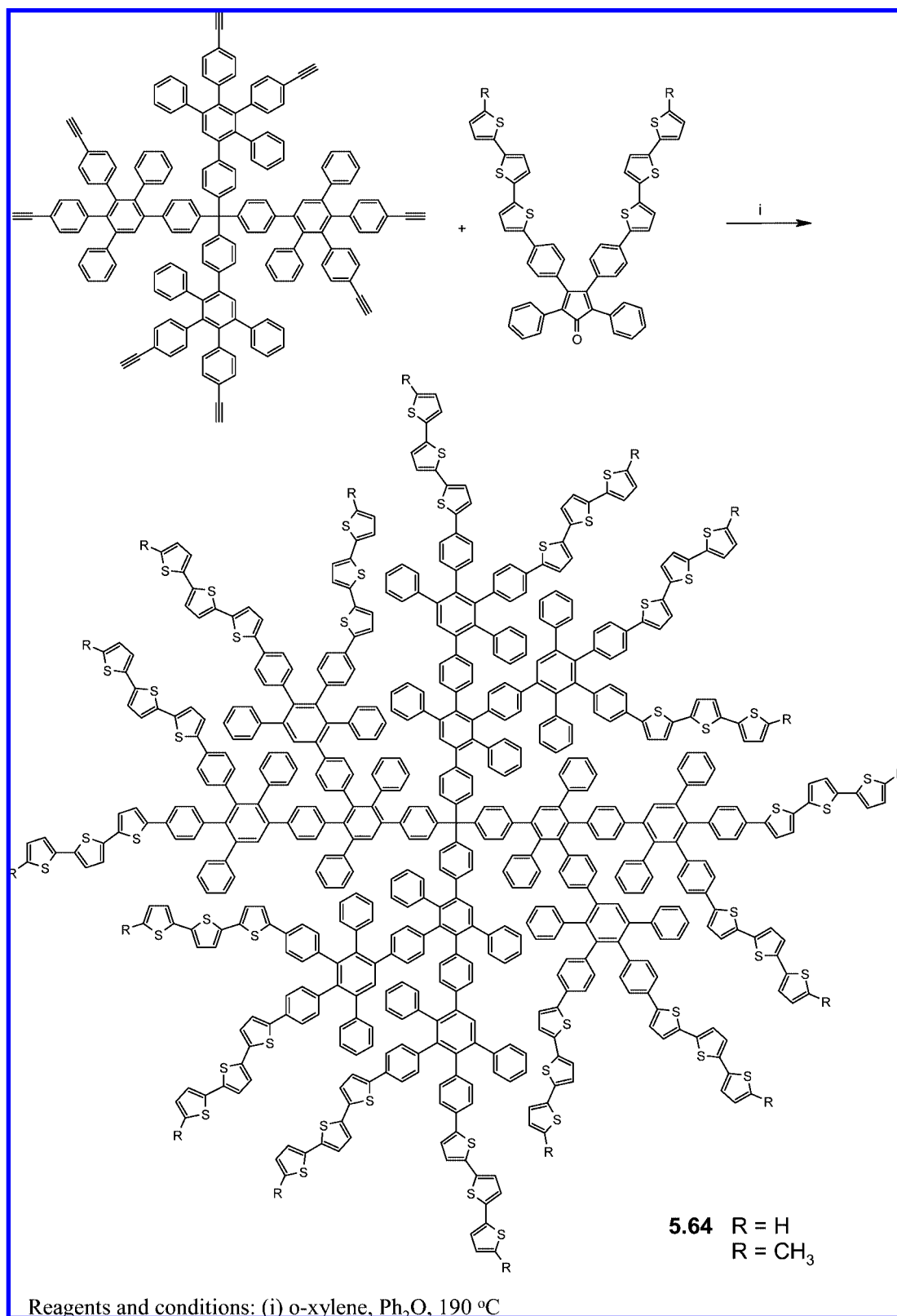
compound and well soluble in common organic solvents (Scheme 5.17).

Investigations of the optical properties resulted in absorption spectra exhibiting intensive and very broad bands which were red-shifted with increasing generational size. The optical band gap (≥ 2.24 eV) depended on the size of the nanostructure and was in the range of linear semiconducting oligo- and polythiophenes. The full spectra were a superimposition of multiple chromophores which correlate to α-conjugated subunits in the DOTs, whereby shorter chain lengths prevail. Deconvolution of the spectra and corroborative calculations clearly revealed that conjugation paths along the $\alpha-\beta$ connections exist as additional chromophoric subunits. Fluorescence typically was emitted from the longest

Scheme 5.12

Reagents and conditions: (i) KOH, THF/H$_2$O. (ii) Oxalyl chloride, THF. (iii) OH-polybenzyl ether dendron, K$_2$CO$_3$, 18-crown-6. (iv) 2,5-Bis(trimethylstannyl)thiophene, Pd(PPh$_3$)$_2$Cl$_2$, DMF.
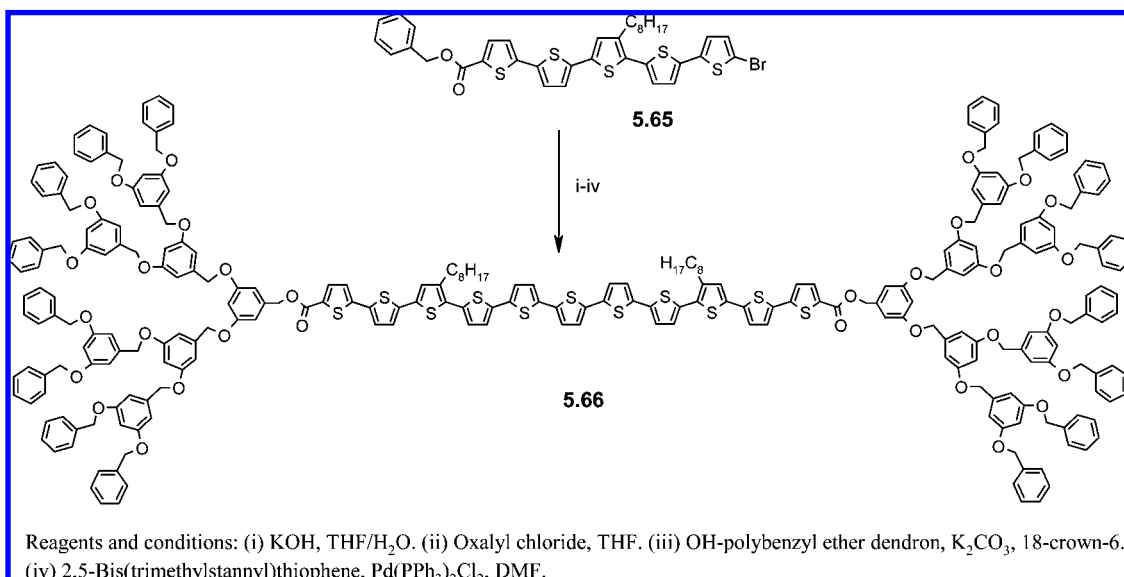
Chart 5.12
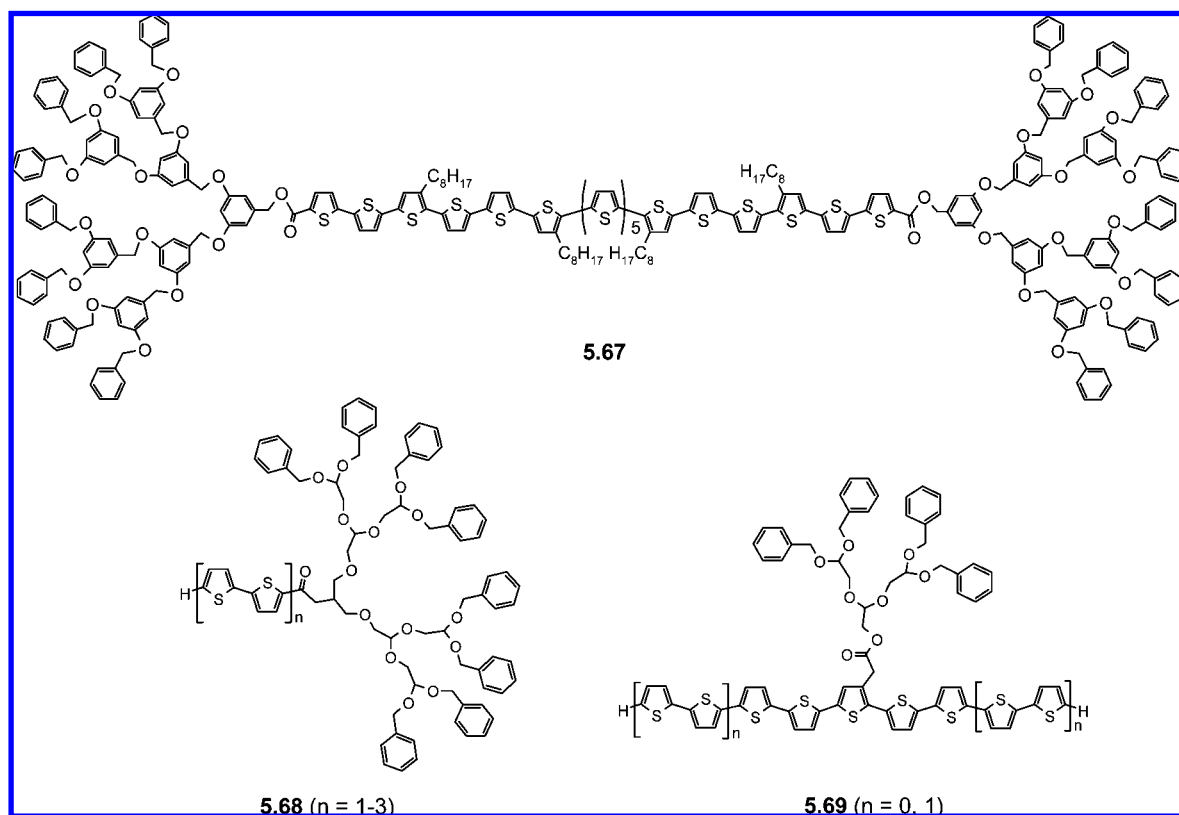
chromophoric α-conjugated pathway and was invariant to the excitation wavelength. This behavior, together with the very low fluorescence quantum yields, clearly indicated intramolecular energy transfer from shorter chromophores to the longest one, which then emits.

Lin et al. synthesized branched oligothiophenes **5.87** and **5.88** by Stille-type cross-coupling reactions where the periphery was functionalized with triarylamine groups (Chart 5.14).[772] These materials formed amorphous glasses due to the presence of asymmetric amine moieties together with β-branching in the oligothiophene units, which is responsible for the nonplanar molecular structures. High glass transition temperatures (T_g) and the presence of triarylamine groups

rendered them too good candidates for hole-transporting materials in electroluminescent devices. A bilayer device containing ITO/**5.87**/Alq$_3$/Mg:Ag showed good performance, including an external quantum efficiency of 1.36%.

Ng and co-workers recently prepared semiflexible dendrons **5.89** up to the third generation using ester-terminated quaterthiophene and 3,5-dibromophenol as precursor building blocks, where quaterthiophene moieties were used as branching and peripheral units (Chart 5.15).[773] Spectroscopic studies revealed that solvent polarity has a strong influence on the absorption and emission spectra of the dendrons. Thus, an increase in the solvent polarity produced a bathochromic shift

Chart 5.13

5.70

5.71

5.72
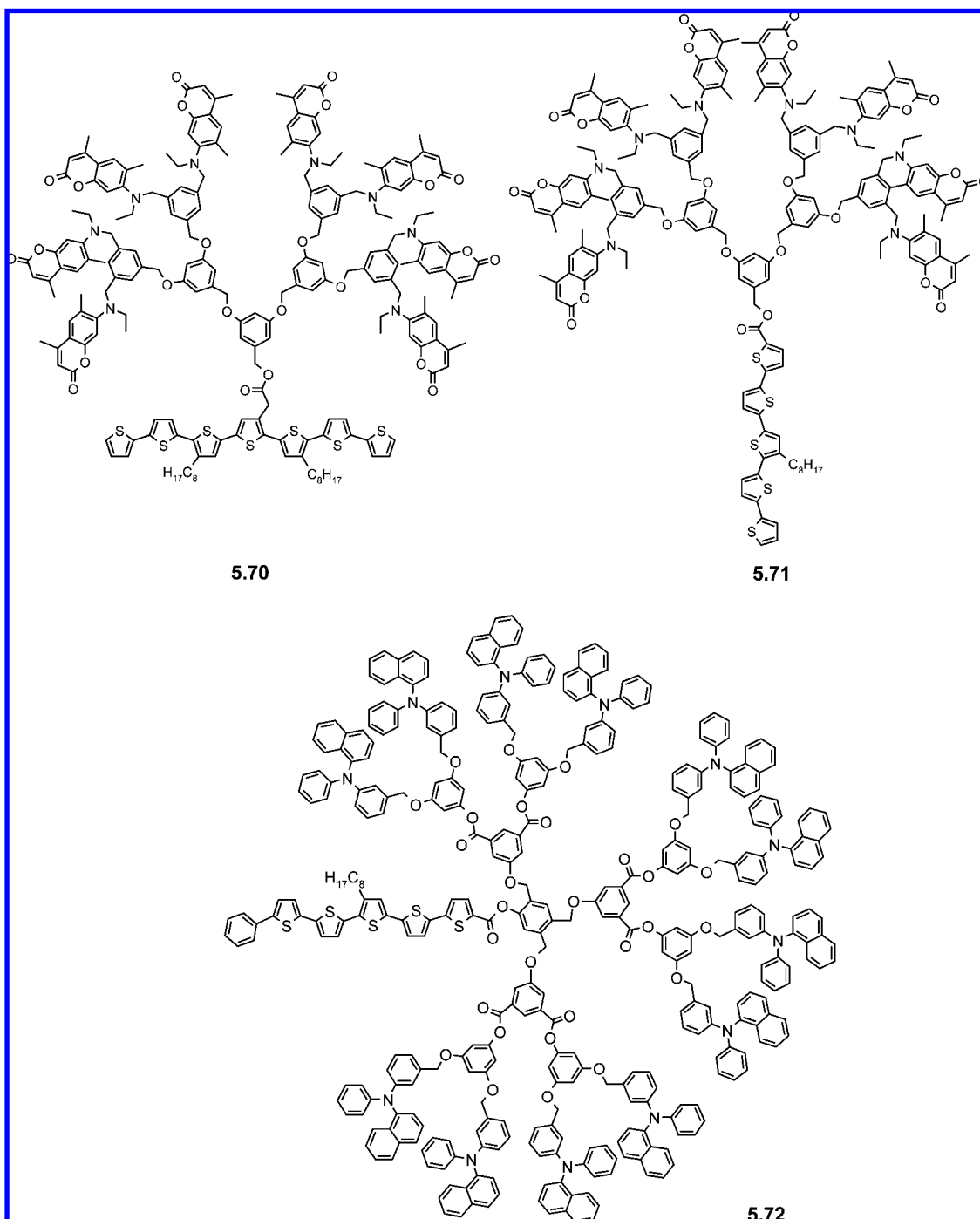
in absorption and emission spectra as well as a dramatic decrease of the fluorescence quantum yield.

Very recently, Aso et al. prepared another series of dendrimers containing quaterthiophene as repeating conjugated bridges and benzene rings as branching centers.[774] The dendron was synthesized by employing selective Stille-type coupling reactions of a stannylated quaterthiophene and 1,3,5-tribromobenzene. Deprotection of the TMS group using KOH followed by a Cu-catalyzed Eglinton homocoupling of the terminal ethynyl group gave dendrimer **5.90**, which on treatment with Na$_2$S afforded **5.91** in ~40% overall yield (Scheme 5.18). The dendrimers were characterized by NMR and MALDI-TOF mass spectroscopy. UV−vis spectroscopy showed absorption bands corresponding to the quaterthiophene-phenyl and nonithiophene-phenyl system because

of the interruption of conjugation through *meta*-substitution at the core benzene rings. OFET devices fabricated using **5.91** (R = Ph) as active material showed a moderate field-effect mobility of 2×10^{-4} cm^2 V^{-1} s^{-1}.[774]

6. Conclusions and Prospects

This review intended to describe and to highlight recent developments in the area of functional oligothiophenes, which can be considered as a third generation of advanced π-conjugated oligomers with defined structure and became enormously relevant as very promising materials in organic and molecular electronics. From the vast number of publications (around 770 cited here), it becomes clear that this field represents an exploding area. This steep development is

Scheme 5.13

Reagents and conditions: (i) BuLi, 1-bromohexane; (ii) NBS, DMF; (iii) 1. Mg, 2. 2,3-dibromothiophene NidpppCl$_2$; (iv) BuLi, Bu$_3$SnCl; (v) 2,3-dibromothiophene, Pd(PPh$_3$)$_4$, DMF

Scheme 5.14

Reagents and conditions: (i) Pd(PPh$_3$)$_4$, DMF
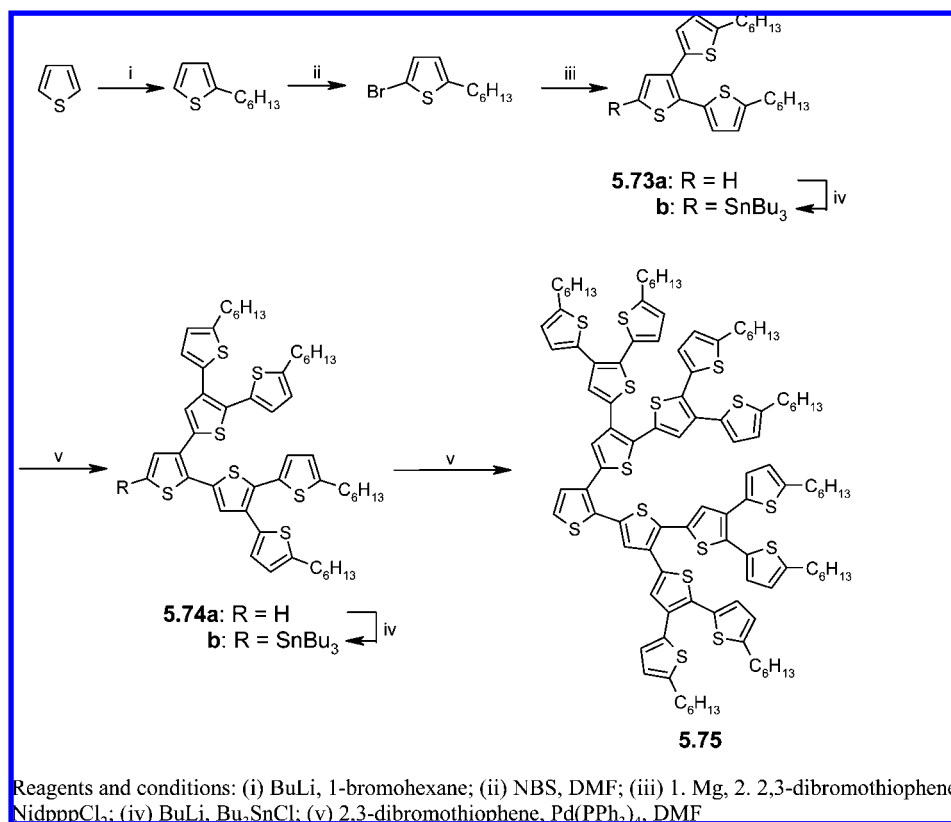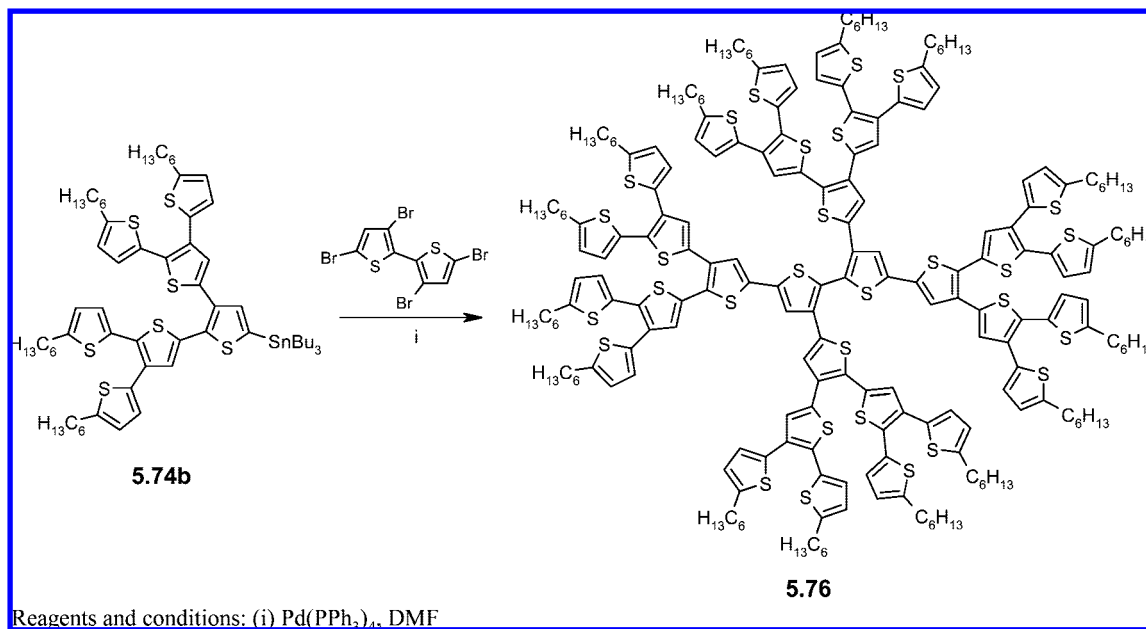
definitely due to the excellent control and understanding of a manifold of specific synthetic reactions to build up π-conjugated core molecules which either tolerate various functional groups already attached or bear reactive sites to subsequently connect the functional units. It was quickly recognized that, with functional groups, additional properties to the specific ones of the π-conjugated systems can be created.

In this respect, the aspect of ordering and self-assembly is very important for active materials in organic electronics, and thus, linear oligothiophenes functionalized with surface-

active groups, which serve for the formation of self-assembled monolayers and supramolecular organization as well as liquid crystalline oligothiophenes, represent a viable approach to this issue. Combinations with classical polymers give rise to ordering phenomena, e.g., from block copolymers, and to good processing by maintaining the particular electronic properties of the conjugated backbone.

A huge variety of functionalized oligothiophenes have been prepared under the aspect to widen or to tune the electronic properties by attaching donor and acceptor groups, dyes, or transition metal complexes. In particular, energy or
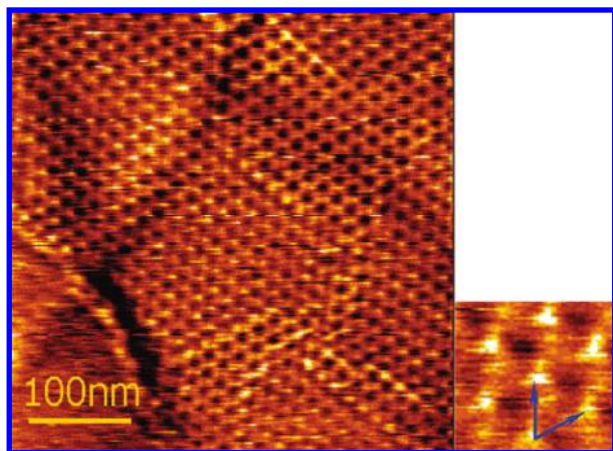
Figure 5.1. STM topographic image of the self-assembled hexagonal structure of **5.76** on HOPG. The unit cell dimensions are $a = b = 10 \pm 2$ nm and $\alpha = 62° \pm 2°$. (Reproduced with permission from ref 770. Copyright 2004 American Chemical Society.)

electron transfer processes were widely investigated in these systems as elementary processes in materials for energy conversion.

Oligothiophenes decorated with groups which specifically recognize guest molecules as well as derivatives which bear biologically active groups recently became very interesting in sensory materials. In particular, the combination of an oligothiophene with a "bio"-component is a newly emerging field and highly promising in order to create novel biological sensory materials as well as to investigate novel self-ordering processes due to the specific intermolecular interactions of the "bio"-moieties.

In the search for novel building blocks in π-conjugated oligomers and polymers for organic electronics, fused thiophenes were (re)discovered, because they provide flat π-systems with excellent charge transport properties and special electronic features, such as a quinoidal contribution in the ground-state which is used to design low band gap materials. By implementing fused thiophenes as building blocks into co-oligomers and polymers, the electronic properties of the resulting conjugated system can be widely tuned.

Very recently, another trend was recognizable in the field of oligothiophenes which also could be followed for other π-conjugated systems: This is the search for systems with increased dimensionality. In this respect, novel molecular architectures including more complicated conjugated structures and sophisticated topologies other than linear have emerged as a consequence of increased versatility of thiophene chemistry, and they currently represent a most interesting and quickly spreading field of research in academics and industry. On the basis of known basic structures, many intriguing molecules with increased dimensionalities, such as star-shaped and dendritic structures, were synthesized in the meanwhile and came recently into play in materials science. Linear oligothiophenes decorated with classical dendrons or dendrimers, which are substituted by smaller oligothiophenes, appeared on the scene. Then, in the past few years, *all*-thiophene dendritic structures came up as highly promising conjugated materials, because they represent rather stiff and shape-persistent organic functional nanoparticles, which can be applied in organic electronic devices.

Since our last review on oligothiophenes which appeared 10 years ago and mostly described synthetic methods and the properties of the basic (alkylated) linear oligomer series in light of structure–property relationships and the model character for corresponding polythiophenes,[37] a profound change in philosophy and a huge extension of possible structures has taken place and surely will continue. The integration of functionalized and specifically tuned (oligo)thiophenes into controlled nanoarchitectures and complicated conjugated structures will in the future provide more promising materials and possibilities for applications. It is evident that the basis for the future development of such sophisticated materials lies in the parallel occurring steep development of novel synthetic methods and novel catalyst systems for transition-metal-catalyzed coupling reactions. Both fields together provide a newly emerging playground for us: With many challenges remaining, one can be curious to see further development in the area of thiophene-based structures. Why should it not be possible in the near future to synthesize most sophisticated molecules with still unknown properties? For instance, defined linear or branched oligothiophenes having much more than the 96 thiophene units, which at the moment mark the "world record",[775] or a fully conjugated trefoil knot, as has been already presented and calculated by Fomine et al.,[676] or maybe a Möbius band with unique electronic properties consisting of only thiophenes could be worth being tackled and prepared.

7. Appendix

In this review article, we have comprehensively portrayed the results based on functional oligothiophenes published until the end of 2007. Rapid advances in this area have afforded numerous reports during manuscript production. In this section, we provide a brief account of some recent developments in the field as of January 2008.

Scherf et al. reviewed recent developments in oligothiophene-based organic semiconductors for solution-processable OFETs.[776] Meijer et al. demonstrated that trace amounts of impurities ($<0.4\%$) present in oligothiophenes **2.34** ($m = 4$, 5, β) can have a dramatic influence on the molecular packing and self-assembled structures.[777] The synthesis and spectroscopic properties of a series of cyclophanes consisting of oligothiophene units as π-dimeric model compounds were reported.[778]

A variety of new linear donor–acceptor-substituted oligothiophenes,[779–783] thieno[3,2-*b*]thiophene,[782] and dithieno[3,2-*b*:2′,3′-*d*]thiophene[783,784] was synthesized and tested as sensitizer in DSSCs. Electronegative oligothiophenes based on difluorodioxocyclopentene-annelated thiophenes[785] and hexafluorocyclopenta[*c*]thiophene homooligomers up to a hexamer[786,787] were synthesized. Organic field-effect transistors based on these oligomers showed n-type semiconducting behavior. Shinkai et al. studied an effective self-sorting supramolecular organogel formation using p-type oligothiophene **2.45** ($n = 2$) and n-type perylene derivatives bearing two cholesterol groups at each terminus.[788]

Leo and Bäuerle et al. demonstrated an approach toward tandem solar cells using **2.110** ($n = 1$) and C_{60} fullerene.[789] A novel oligothiophene-BODIPY-based donor–acceptor system for light harvesting was synthesized and characterized by absorption and emission spectroscopy, which indicated tunable and efficient resonance energy transfer from the quaterthiophene donor to the BODIPY acceptor.[790] Solvent-dependent ultrafast intramolecular photoinduced charge-

Scheme 5.15

Reagents and conditions: (i) 1. Mg/diethyl ether, 2. 2,3-dibromothiophene/Ni(dppp)Cl$_2$; (ii) ICl/THF; (iii) 1. n-BuLi/THF, 2. 2-isopropyloxy-4,4,5,5-tetramethyl-1,3,2-dioxaborolane; (iv) Pd$_2$dba$_3$·CHCl$_3$/HP(t-Bu)$_3$BF$_4$/K$_3$PO$_4$/THF; (v) Bu$_4$NF/THF

Scheme 5.16

Reagents and conditions: (i) 1. n-BuLi/THF, 2. 2-isopropyloxy-4,4,5,5-tetramethyl-1,3,2-dioxaborolane; (ii) ICl/THF; (iii) Pd$_2$dba$_3$· CHCl$_3$/HP(t-Bu)$_3$BF$_4$/K$_3$PO$_4$/THF.
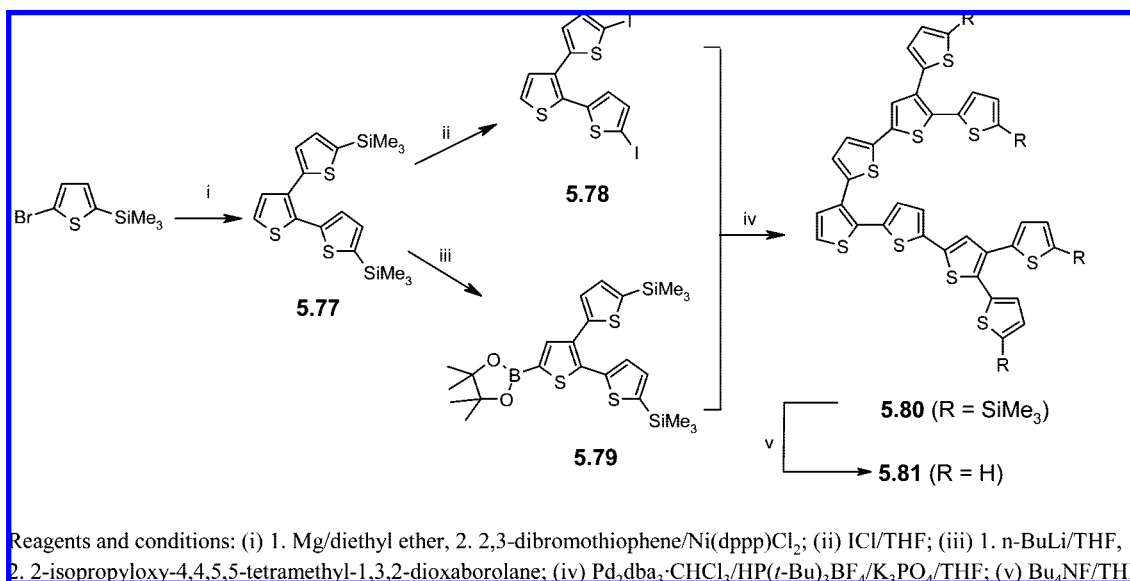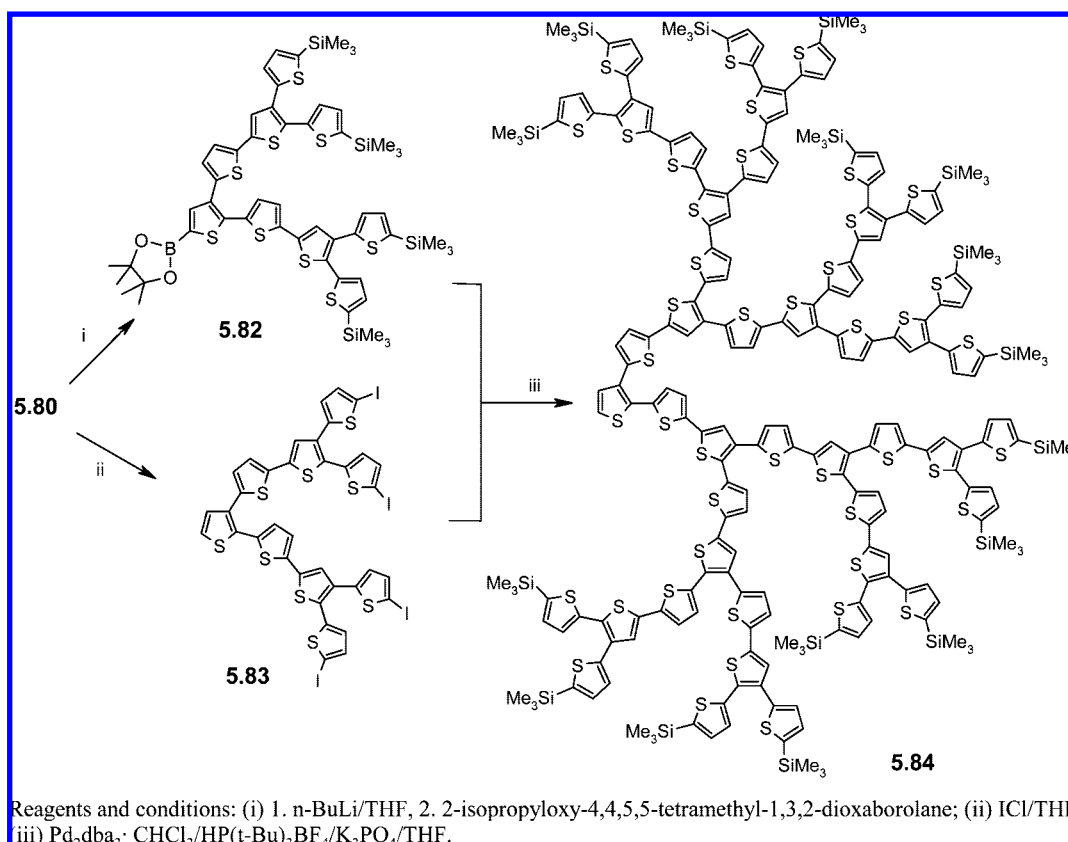
transfer properties of a quaterthiophene−anthraquinone dyad were reported.[791] A variety of donor−acceptor substituted oligothiophenes attached to chiral binaphthalene linkers was synthesized and studied by means of UV−vis and CD spectroscopy in order to obtained fundamental insight into the chiroptical properties of conjugated polymers with optically active side chains in both the neutral and oxidized state.[792] Low band gap solution-processable oligothiophenes functionalized with an electron-withdrawing diketopyrrolopyrrole core were synthesized and characterized by UV−vis and AFM techniques. These oligomers showed intense absorption that extended from the visible to the near-IR

region.[793,794] Bulk heterojunction solar cells using blend solutions of hexyl-terminated oligomer and PCBM exhibited power conversion efficiencies as high as 2.3% when the donor/acceptor ratio was 70:30 with external quantum efficiencies close to 30% between 550 and 750 nm.[793] Hole-transporting triphenylamine-oligothiophene hybrid materials were reported.[795]

Photoinduced electron transfer dynamics in π-conjugated oligothiophene-perylene bisimide dyads **2.166** was studied.[796] Pentathiophene−perylene bisimide dyads with a flexible alkyl linker were synthesized. The photoinduced processes such as charge separation, charge recombination, and energy
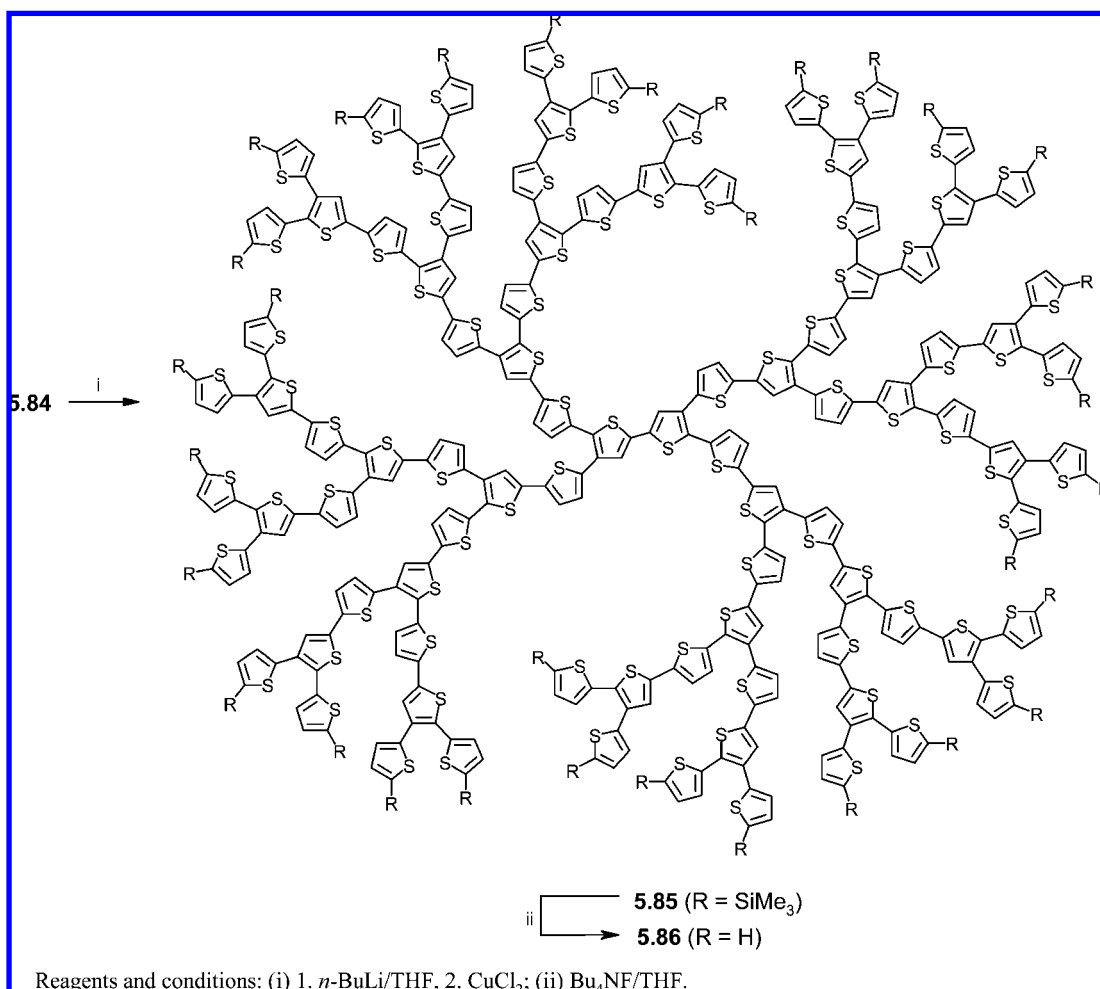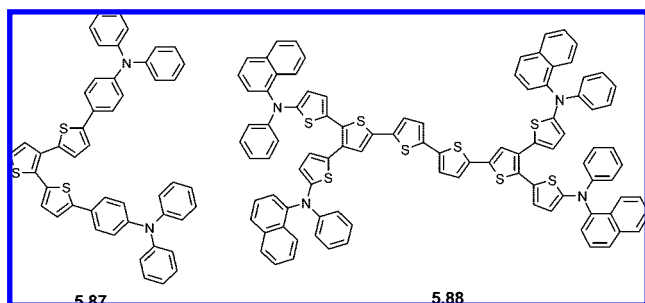
Scheme 5.17

5.85 (R = SiMe₃)
5.86 (R = H)

Reagents and conditions: (i) 1. *n*-BuLi/THF, 2. CuCl₂; (ii) Bu₄NF/THF.

Chart 5.14

transfer in the dyads were investigated by using femtosecond transient absorption spectroscopy.[797] Various alkylphenyl-terminated oligothiophenes were synthesized, and their thin-film transistor properties were reported.[798,799] Kato et al. synthesized a new electrochromic liquid crystalline material comprising of an imidazolium group as an ion-conductive part and a π-conjugated phenylterthiophene moiety associated as hole-transporter.[800] Aida et al. prepared a liquid crystalline oligothiophene−C₆₀ dyad with hydrophilic and hydrophobic wedges which not only prevented donor−acceptor interactions leading to the trapping of charge carrier but also confirmed a long-range conducting pathway.[801] Photoinduced excitation energy transfer dynamics in oligothiophene−fullerene dyads **2.180** (*n* = 1−3) were investigated by a femtosecond fluorescence up-conversion study.[802]

Oligothienyl-bridged dinuclear tris(2,2′-bipyridine)ruthenium(II) complexes have been prepared, and the isomeric effects on luminescence lifetimes and electrochemistry were discussed.[803] A Ru(II) complex based on dicarboxylated bipyridine and octylthienothiophene-substituted bipyridine was prepared and demonstrated as a highly efficient photo-sensitizer for DSSCs, yielding a power conversion efficiency of 10.53% under AM 1.5G illumination.[804] Binuclear ruthenocenes bridged by ethenes and thiophene derivatives, Rc−CH=CH−Z−CH=CH−Rc (Z = thiophene, thieno[3,2-*b*]thiophene, 2,2′-bithiophene; Rc = ruthenocene), were prepared which showed one-step two-electron redox waves in cyclic voltammograms.[805] A series of oligothienyl dicarboxylate bridged M−M (M = Mo or W) quadruply bonded complexes has been prepared and characterized by electrochemical, steady-state absorption as well as transient absorption and emission spectroscopy. These complexes showed intense absorption spanning the region of 300−800 nm and long-lived photoexcited states which could be useful for solar energy conversion.[806,807]

Among biologically active oligothiophenes, water-soluble, electroactive, and photoluminescent quaterthiophene-dinucleotide hybrids, which led to the formation of chiral supramolecular assemblies,[808] and oligothiophene-functionalized guanosine, which formed supramolecular arrays via H-bonding between guanosines,[809] have been published. Bäuerle et al. synthesized complementary thymidine- and adenosine-functionalized quaterthiophenes using a "click" reaction protocol.

Chart 5.15

5.89
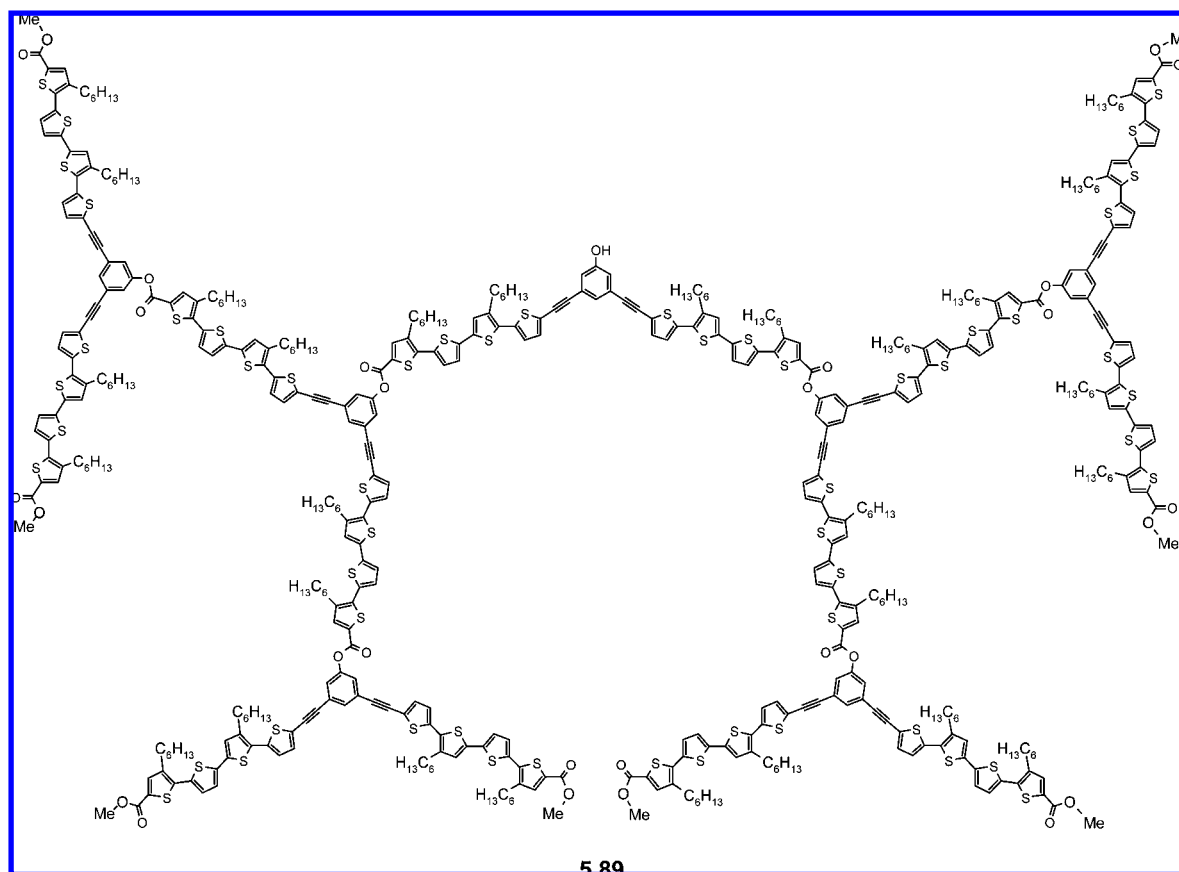
Recognition-driven self-assembled superstructures via hydrogen bonding and intermolecular interactions were studied in solution and in the solid state.[810] Stupp et al. synthesized a terthiophene-tripeptide amphiphile which was self-assembled to form one-dimentional helical nanofibers. In addition, hierarchical double- and triple-stranded helices were observed for this amphiphile, which could be related with terthiophene J-aggregate interactions among fibers.[811]

Oligothiophene-labeled deoxyuridines were synthesized for the detection of single nucleotide polymorphisms.[812] Bifunctional conjugates based on the linkage of inorganic magnetic nanoparticles to oligothiophene fluorophores mediated by polyethylene glycol bridging units were prepared. *In vitro* studies on human tumor cells showed that these conjugates emitting at different wavelengths can be used for multiplexing detection. It was also reported that, in the case of oligothiophene—Fe$_2$O$_3$ nanoparticle conjugates, the fluorescent and magnetic properties can be maintained after cellular uptake.[813] Push—pull-type fluorophores comprising MeO-, HO-, and Me$_2$N- groups as donor and dicyanovinylene as acceptor were synthesized as NIR contrast agents for biomedical applications.[814]

Hong et al. synthesized two air-stable p-type organic semiconductors, which have a symmetrically substituted 2,7-divinylbenzothieno[3,2-b]benzothiophene backbone. They showed good electrical performances on a SiO$_2$/Si substrate and high field-effect mobilities up to 0.4 cm^2 V^{-1} s^{-1}.[815] Polarized light emission studies from uniaxially aligned thin films of a biphenylthienothiophene co-oligomer were reported.[816] Various annulated and nonannulated functional thieno[2,3-b]thiophenes have been synthesized and characterized by NMR and X-ray structure analysis.[817−819] Face-to-face π-stacked structures in the crystal lattice were achieved

with bipolar molecules containing alternate electron-rich thieno[3,2-b]thiophene and electron-deficient pyrimidine or benzothiazole units.[820] Alkylenesulfanyl-bridged bithienyls were prepared by a highly effective ring-closing reaction via arylalkylsulfonium intermediates and used as inner cores in oligothiophenes. Their electronic, film-forming, and thermal properties were studied.[821] Rasmussen et al. reported that direct addition of tetracyanoethylene to *N*-(*p*-hexylphenyl)dithieno[3,2-b:2′,3′-d]pyrrole yielded not only aromatic mono- and bis-tricyanovinyl-substituted products but also a quinoidal product with dicyanomethylene groups.[822]

Perepichka et al. studied the thin-film transistor behavior of isomeric tetrathienoanthracenes, which were synthesized using Stille-type coupling of 2- and 3-(tributylstannyl)thiophene derivatives with tetrabromobenzene followed by oxidative cyclization. Structural studies using X-ray crystallography and scanning tunneling microscopy revealed a completely planar structure and strong intermolecular interaction for these isomers. Hole mobilities of up to 7.4 × 10^{-2} cm^2 V^{-1} s^{-1} were measured for vacuum-deposited films of these isomers.[823] Pei et al. prepared a highly substituted hole-transporting benzo[b]thiophene derivative which was used as dopant in polymer light emitting diodes (PLEDs). OFET measurements showed that the formation of nanowires of the dopant within the conjugated polymer matrix improved the hole mobility of the emissive layer. In PLEDs the luminous efficiency and external quantum efficiency were increased by a factor of 2 for the doped device in comparison to the one without dopant.[824]

A series of low band gap thiophene end-capped oligo(2,3-alkylthieno[3,4-b]pyrazine)s were synthesized by Karsten and Janssen. With increasing number of thienopyrazine units, the absorption wavelength of these oligomers rapidly shifted to

Scheme 5.18

5.90: R = H, Ph

5.91: R = H, Ph

Reagents and conditions: (i) Na₂S•9H₂O, THF, reflux
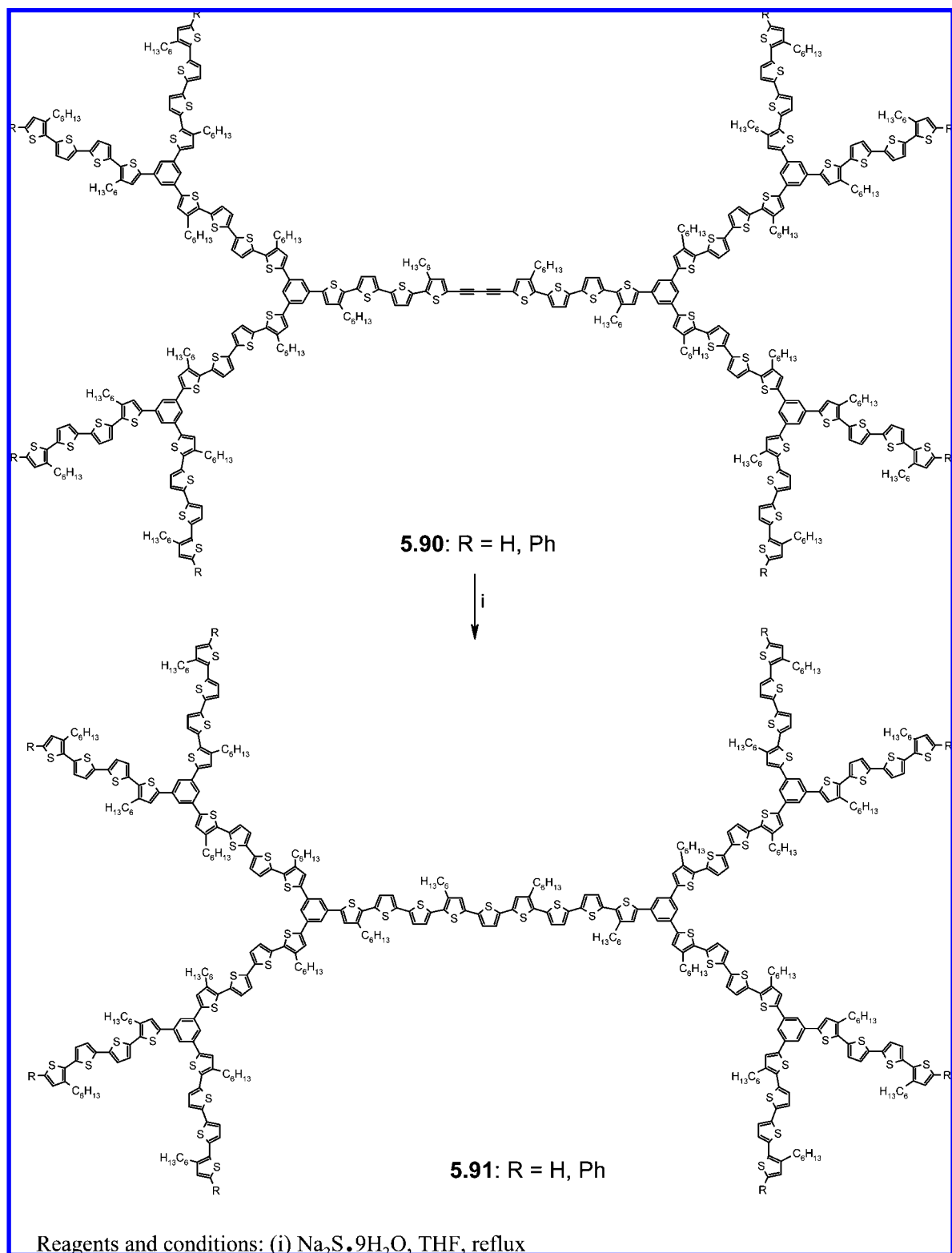
lower energies, having an absorption onset close to 900 nm for the system with three thieno[3,4-*b*]pyrazines.[825] Yamaguchi et al. reported that the incorporation of boryl and phosphanyl groups to the thienylethynylene skeleton resulted in a nucleophilic cascade cyclization, thus furnishing the zwitterionic structure.[826] Chemical oxidation of pentathienoacene **3.133** with *m*-chloroperbenzoic acid produced a series of oxidized derivatives containing one or two thiophene-*S*,*S*-dioxide units. The resulting *S*,*S*-dioxides have lower HOMO energy levels and smaller band gaps then the parent compound.[827] The effect of position and degree of sulfur oxidation on the electronic and solid-state properties of a series of fused thieno[3,2-*b*]thiophene *S*,*S*-dioxides was reported.[828] Agawa et al. recently confirmed the planar structure of **3.182** by X-ray single crystal analysis.[829]

Theoretical investigations on cyclo[8]thiophene **4.31** revealed that the interaction between π-orbitals of individual macrocycles favors tubular aggregates. It has been shown

that the binding of cations between macrocycles is higher compared to that of neutral aggregates, favoring self-assembling on oxidation. The oxidation of neutral aggregates led to polaron formation, which delocalized toward the tube axes, and most of it is located at the central macrocycles.[830] Haley et al. studied the structure property relationships of a series of electron-rich butyl end-capped annulated terthiophenes which were prepared from dehydrothieno[14]annulenes by reaction with sodium sulfide.[831,832] Recently, a large two-photon absorption cross section as high as 100 000 GM in the visible spectral region was reported for a series of similar π-conjugated thienylene−ethynylene−vinylene-based macrocycles **4.54**.[833] Functional macrocycles comprising thiophene and hexafluorocyclopentene building blocks with photochromic reactivity were prepared and investigated by Liu et al.[834]

Dendritic compounds involving a thiophene, a bithiophene, and a terthiophene unit fully substituted with 2,2′-bithiophen-5-yl pendants were reported.[835] The excited-state dynamics and nonlinear optical properties of a series of oligothiophene dendrons were investigated. It was observed that the excitation is delocalized over a large number of thiophene units in the dendron and there is an ultrafast energy transfer (200−300 fs) to the longest conjugated chain. A linear increase of the two-photon absorption cross section with increasing generation was also reported.[836] Swivel-cruciform type oligothiophene dimers **5.4**−**5.7** were used as semiconductor in OFETs. XRD and AFM analysis of the resulting thin films revealed the highly crystalline nature of these cruciforms.[837]

Bithiophenesilane dendrons and dendrimers consisting of 2,2′-bithiophen-5,5′-diyl units up to the third generation were prepared and characterized by absorption and photoluminescence spectroscopy.[838] A series of dendrimers comprising a truxene unit as node and oligo(thienylethynylene)s as branching units were synthesized and analyzed by spectroscopic, AFM, and dynamic light scattering techniques.[839] Synthesis of star-shaped oligothiophenes grafted on a phosphorus or on a phosphine oxide node was reported.[840]

8. Acknowledgments

9. References

(1) *Handbook of Oligo- and Polythiophenes*; Fichou, D., Ed.; Wiley-VCH: Weinheim, 1999.
(2) *Electronic Materials: The Oligomer Approach*; Müllen, K., Wegner, G., Eds.; Wiley-VCH: Weinheim, 1998.
(3) Gronowitz, S. Thiophene and Its Derivatives. In *The Chemistry of Heterocyclic Compounds*; Weissberger, A., Taylor, E. C., Eds.; John Wiley & Sons: New York, 1985−1992; Vol. 44, Parts 1−5.
(4) Gronowitz, S.; Hörnfeldt, A.-B. *Thiophenes*; Elsevier Academic Press: San Diego, CA, 2004.
(5) *Metal Catalyzed Cross-Coupling Reactions*; Diedrich, F., Stang, P. J., Eds.; Wiley-VCH: Weinheim, 1998 and 2006.
(6) Horowitz, G.; Fichou, D.; Peng, X.; Xu, Z.; Garnier, F. *Solid State Commun.* **1989**, *72*, 381–384.
(7) Garnier, F.; Horowitz, G.; Peng, X.; Fichou, D. *Adv. Mater.* **1990**, *2*, 592–594.
(8) Geiger, F.; Stoldt, M.; Schweizer, H.; Bäuerle, P.; Umbach, E. *Adv. Mater.* **1993**, *5*, 922–925.
(9) Noma, N.; Tsuzuki, T.; Shirota, Y. *Adv. Mater.* **1995**, *7*, 647–648.
(10) Garnier, F.; Horowitz, G.; Fichou, D. *Synth. Met.* **1989**, *28*, 705–714.
(11) Bäuerle, P. *Adv. Mater.* **1992**, *4*, 102–107.
(12) Hotta, S. Molecular conductive materials: Polythiophenes and oligothiophenes. In *Handbook of Organic Conductive Molecules and Polymers*; Nalwa, H. S., Ed.; Wiley: Chicheste, U.K., 1997; Vol. 2, Chapter 8; pp 309−387.
(13) Roncali, J. *Chem. Rev.* **1997**, *97*, 173–206.
(14) Spangler, C.; He, M. Charge-state incorporation in dithienylpolyenes and thienylene polyenylene oligomers and polymers. In *Handbook of Organic Conductive Molecules and Polymers*; Nalwa, H. S., Ed.; John Wiley & Sons: Weinheim, 1997; Vol. 2; pp 389−414.
(15) Roncali, J. *Acc. Chem. Res.* **2000**, *33*, 147–156.
(16) Tour, J. M. *Acc. Chem. Res.* **2000**, *33*, 791–804.
(17) Fichou, D. *J. Mater. Chem.* **2000**, *10*, 571–588.
(18) Shirota, Y. *J. Mater. Chem.* **2000**, *10*, 1–25.
(19) Mitschke, U.; Bäuerle, P. *J. Mater. Chem.* **2000**, *10*, 1471–1507.
(20) Katz, H. E.; Bao, Z.; Gilat, S. L. *Acc. Chem. Res.* **2001**, *34*, 359–369.
(21) Hassan, J.; Seívignon, M.; Gozzi, C.; Schulz, E.; Lemaire, M. *Chem. Rev.* **2002**, *102*, 1359–1470.
(22) Otsubo, T.; Aso, Y.; Takimiya, K. *J. Mater. Chem.* **2002**, *12*, 2565–2575.
(23) Roncali, J.; Blanchard, P.; Frère, P. *J. Mater. Chem.* **2005**, *15*, 1589–1610.
(24) Ozturk, T.; Ertas, E.; Mert, O. *Tetrahedron* **2005**, *61*, 11055–11077.
(25) Schwab, P. F. H.; Smith, J. R.; Michl, J. *Chem. Rev.* **2005**, *105*, 1197–1279.
(26) Hoeben, F. J. M.; Jonkheijm, P.; Meijer, E. W.; Schenning, A. P. H. J. *Chem. Rev.* **2005**, *105*, 1491–1546.
(27) Perepichka, I. F.; Perepichka, D. F.; Meng, H.; Wudl, F. *Adv. Mater.* **2005**, *17*, 2281–2305.
(28) Sun, Y.; Liu, Y.; Zhu, D. B. *J. Mater. Chem.* **2005**, *15*, 53–65.
(29) Roncali, J. *Chem. Soc. Rev.* **2005**, *34*, 483–495.
(30) Segura, J. L.; Martín, N.; Guldi, D. M. *Chem. Soc. Rev.* **2005**, *34*, 31–47.
(31) Barbarella, G.; Melucci, M.; Sotgiu, G. *Adv. Mater.* **2005**, *17*, 1581–1593.
(32) Collins, S. K.; Vachon, M. P. *Org. Biomol. Chem.* **2006**, *4*, 2518–2524.

(33) Torroba, T.; García-Valverde, M. *Angew. Chem., Int. Ed.* **2006**, *45*, 8092–8096.

(34) Blanchard, P.; Leriche, P.; Frère, P.; Roncali, J. Advanced Functional Polythiophenes Based on Tailored Precursors. In *Handbook of Conducting Polymers*; 3rd ed.; Skotheim, T. A., Reynolds, J. R., Eds.; CRC Press: New York, 2007; pp 1−77.

(35) Murphy, A. R.; Fréchet, J. M. J. *Chem. Rev.* **2007**, *107*, 1066–1096.

(36) Mallik, A. B.; Locklin, J.; Mannsfeld, S. C. B.; Reese, C.; Roberts, M. E.; Senatore, M. L.; Zi, H.; Bao, Z. Design, Synthesis, and Transistor Performance of Organic Semiconductors. In *Organic Field-Effect Transistors*; Bao, Z., Locklin, J., Eds.; CRC Press: 2007; pp 159−228.

(37) Bäuerle, P. Sulfur-Containing Oligomers. In *Electronic Materials: The Oligomer Approach*; Müllen, K., Wegner, G., Eds.; Wiley-VCH: Weinheim, 1998; pp 105−197.

(38) Otsubo, T.; Aso, Y.; Takimiya, K. *Bull. Chem. Soc. Jpn.* **2001**, *74*, 1789–1801.

(39) Garnier, F.; Hajlaoui, R.; Yassar, A.; Srivastava, P. *Science* **1994**, *265*, 1684–1686.

(40) Sirringhaus, H.; Kawase, T.; Friend, R.; Shimoda, T.; Inbasekaran, M.; Wu, W.; Woo, E. *Science* **2000**, *290*, 2123–2126.

(41) Ong, B. S.; Wu, Y.; Liu, P.; Gardner, S. *J. Am. Chem. Soc.* **2004**, *126*, 3378–3379.

(42) Waldauf, C.; Schilinsky, P.; Perisutti, M.; Hauch, J.; Brabec, C. J. *Adv. Mater.* **2003**, *15*, 2084–2088.

(43) Holliday, B. J.; Swager, T. M. *Chem. Commun.* **2005**, 23–36.

(44) Swager, T. M. *Acc. Chem. Res.* **1998**, *31*, 201–207.

(45) Rockel, H.; Huber, J.; Gleiter, R.; Schuhmann, W. *Adv. Mater.* **1994**, *6*, 568–571.

(46) Pande, R.; Kamtekar, S.; Ayyagari, M. S.; Kamath, M.; Marx, K. A.; Kumar, J.; Tripathy, S. K.; Kaplan, D. L. *Bioconjugate Chem.* **1996**, *7*, 159–164.

(47) Kumar, A.; Welsh, D. M.; Morvant, M. C.; Piroux, F.; Abboud, K. A.; Reynolds, J. R. *Chem. Mater.* **1998**, *10*, 896–902.

(48) Welsh, D. M.; Kumar, A.; Meijer, E. W.; Reynolds, J. R. *Adv. Mater.* **1999**, *11*, 1379–1382.

(49) Garnier, F. *Adv. Mater.* **1989**, *1*, 117–121.

(50) Tamao, K.; Sumitani, S.; Kiso, Y.; Zembayashi, M.; Fujioka, A.; Kodama, S.; Nakajima, I.; Minato, A.; Kumada, M. *Bull. Chem. Soc. Jpn.* **1976**, *49*, 1958–1969.

(51) Suzuki, A. *Pure Appl. Chem.* **1991**, *63*, 419–422.

(52) Kotha, S.; Lahiri, K.; Kashinath, D. *Tetrahedron* **2002**, *58*, 9633–9695.

(53) Sonogashira, K.; Tohda, Y.; Hagihara, N. *Tetrahedron Lett.* **1975**, *16*, 4467–4470.

(54) Stille, J. K. *Angew. Chem., Int. Ed.* **1986**, *25*, 508–524.

(55) Miyasaka, M.; Rajca, A. *Synlett* **2004**, 177–181.

(56) Chinchilla, R.; Nájera, C.; Yus, M. *Chem. Rev.* **2004**, *104*, 2667–2722.

(57) Jäckel, F.; Watson, M. D.; Müllen, K.; Rabe, J. P. *Phys. Rev. Lett.* **2004**, *92*, 188303.

(58) Mena-Osteritz, E.; Bäuerle, P. *Adv. Mater.* **2006**, *18*, 447–451.

(59) Purcell, S. T.; Garcia, N.; Binh, V. T.; Jones, L., II; Tour, J. M. *J. Am. Chem. Soc.* **1994**, *116*, 11985–11989.

(60) Tour, J. M.; Jones, L.; Pearson, D. L.; Lamba, J. J. S.; Burgin, T. P.; Whitesides, G. M.; Allara, D. L.; Parikh, A. N.; Atre, S. V. *J. Am. Chem. Soc.* **1995**, *117*, 9529–9534.

(61) Pearson, D. L.; Tour, J. M. *J. Org. Chem.* **1997**, *62*, 1376–1387.

(62) Tamura, M.; Fujihara, H. *J. Am. Chem. Soc.* **2003**, *125*, 15742–15743.

(63) Sih, B. C.; Teichert, A.; Wolf, M. O. *Chem. Mater.* **2004**, *16*, 2712–2718.

(64) Moorlag, C.; Sih, B. C.; Stott, T. L.; Wolf, M. O. *J. Mater. Chem.* **2005**, *15*, 2433–2436.

(65) Liedberg, B.; Yang, Z.; Engquist, I.; Wirde, M.; Gelius, U.; Götz, G.; Bäuerle, P.; Rummel, R. M.; Ziegler, C.; Gopel, W. *J. Phys. Chem. B* **1997**, *101*, 5951–5962.

(66) Michalitsch, R.; Lang, P.; Yassar, A.; Nauer, G.; Garnier, F. *Adv. Mater.* **1997**, *9*, 321–326.

(67) Michalitsch, R.; El Kassmi, A.; Yassar, A.; Lang, P.; Garnier, F. *J. Electroanal. Chem.* **1998**, *457*, 129–139.

(68) Michalitsch, R.; El Kassmi, A.; Yassar, A.; Garnier, F. *J. Heterocycl. Chem.* **2001**, *38*, 649–653.

(69) Michalitsch, R.; Nogues, C.; Najari, A.; El Kassmi, A.; Yassar, A.; Lang, P.; Garnier, F. *Synth. Met.* **1999**, *101*, 5–6.

(70) Zhu, L.; Tang, H.; Harima, Y.; Yamashita, K.; Hirayama, D.; Aso, Y.; Otsubo, T. *Chem. Commun.* **2001**, 1830–1831.

(71) Zhu, L.; Tang, H.; Harima, Y.; Yamashita, K.; Aso, Y.; Otsubo, T. *J. Mater. Chem.* **2002**, *12*, 2250–2254.

(72) Hirayama, D.; Yamashiro, T.; Takimiya, K.; Aso, Y.; Otsubo, T.; Norieda, H.; Imahori, H.; Sakata, Y. *Chem. Lett.* **2000**, *29*, 570–571.

(73) Hirayama, D.; Takimiya, K.; Aso, Y.; Otsubo, T.; Hasobe, T.; Yamada, H.; Imahori, H.; Fukuzumi, S.; Sakata, Y. *J. Am. Chem. Soc.* **2002**, *124*, 532–533.

(74) De Boer, B.; Meng, H.; Perepichka, D. F.; Zhang, J.; Frank, M. M.; Chabal, Y. J.; Bao, Z. *Langmuir* **2003**, *19*, 4272–4284.

(75) Taniguchi, S.; Minamoto, M.; Matsushita, M. M.; Sugawara, T.; Kawada, Y.; Bethell, D. *J. Mater. Chem.* **2006**, *16*, 3459–3465.

(76) Huang, W.; Masuda, G.; Maeda, S.; Tanaka, H.; Ogawa, T. *Chem.—Eur. J.* **2006**, *12*, 607–619.

(77) Vercelli, B.; Zotti, G.; Berlin, A. *Chem. Mater.* **2007**, *19*, 443–452.

(78) Endou, M.; Ie, Y.; Kaneda, T.; Aso, Y. *J. Org. Chem.* **2007**, *72*, 2659–2661.

(79) Bong, D.; Tam, I.; Breslow, R. *J. Am. Chem. Soc.* **2004**, *126*, 11796–11797.

(80) Tam, I. W.; Yan, J.; Breslow, R. *Org. Lett.* **2006**, *8*, 183–185.

(81) Guo, X.; Small, J. P.; Klare, J. E.; Wang, Y.; Purewal, M. S.; Tam, I. W.; Hong, B. H.; Caldwell, R.; Huang, L.; O'Brien, S.; Yan, J.; Breslow, R.; Wind, S. J.; Hone, J.; Kim, P.; Nuckolls, C. *Science* **2006**, *311*, 356–359.

(82) Lehn, J.-M. *Science* **2002**, *295*, 2400–2403.

(83) Hong, Y.; Miller, L. L. *Chem. Mater.* **1995**, *7*, 1999–2000.

(84) Kunugi, Y.; Miller, L. L.; Maki, T.; Canavesi, A. *Chem. Mater.* **1997**, *9*, 1061–1062.

(85) Kilbinger, A. F. M.; Feast, W. J. *J. Mater. Chem.* **2000**, *10*, 1777–1784.

(86) Henze, O.; Feast, W. J. *J. Mater. Chem.* **2003**, *13*, 1274–1278.

(87) Kilbinger, A. F. M.; Schenning, A. P. H. J.; Goldoni, F.; Feast, W. J.; Meijer, E. W. *J. Am. Chem. Soc.* **2000**, *122*, 1820–1821.

(88) Schenning, A. P. H. J.; Kilbinger, A. F. M.; Biscarini, F.; Cavallini, M.; Cooper, H. J.; Derrick, P. J.; Feast, W. J.; Lazzaroni, R.; Leclére, P.; McDonell, L. A.; Meijer, E. W.; Meskers, S. C. J. *J. Am. Chem. Soc.* **2002**, *124*, 1269–1275.

(89) Henze, O.; Feast, W. J.; Gardebien, F.; Jonkheijm, P.; Lazzaroni, R.; Leclere, P.; Meijer, E. W.; Schenning, A. P. *J. Am. Chem. Soc.* **2006**, *128*, 5923–5929.

(90) Leclére, P.; Surin, M.; Viville, P.; Lazzaroni, R.; Kilbinger, A. F. M.; Henze, O.; Feast, W. J.; Cavallini, M.; Biscarini, F.; Schenning, A. P. H. J.; Meijer, E. W. *Chem. Mater.* **2004**, *16*, 4452–4466.

(91) Leclére, P.; Surin, M.; Lazzaroni, R.; Kilbinger, A. F. M.; Henze, O.; Jonkheijm, P.; Biscarini, F.; Cavallini, M.; Feast, W. J.; Meijer, E. W.; Schenning, A. P. H. J. *J. Mater. Chem.* **2004**, *14*, 1959–1963.

(92) Shklyarevskiy, I. O.; Jonkheijm, P.; Christianen, P. C. M.; Schenning, A. P. H. J.; Meijer, E. W.; Henze, O.; Kilbinger, A. F. M.; Feast, W. J.; Del Guerzo, A.; Desvergne, J.-P.; Maan, J. C. *J. Am. Chem. Soc.* **2005**, *127*, 1112–1113.

(93) Westenhoff, S.; Abrusci, A.; Feast, W. J.; Henze, O.; Kilbinger, A. F. M.; Schenning, A. P. H. J.; Silva, C. *Adv. Mater.* **2006**, *18*, 1281–1285.

(94) Locklin, J.; Youk, J. H.; Xia, C.; Park, M. K.; Fan, X.; Advincula, R. C. *Langmuir* **2002**, *18*, 877–883.

(95) Xia, C.; Locklin, J.; Youk, J. H.; Fulghum, T.; Advincula, R. C. *Langmuir* **2002**, *18*, 955–957.

(96) Brustolin, F.; Surin, M.; Lemaur, V.; Romanazzi, G.; Sun, Q.; Cornil, J.; Lazzaroni, R.; Sommerdijk, N. A. J. M.; Leclère, P.; Meijer, E. W. *Bull. Chem. Soc. Jpn.* **2007**, *80*, 1703–1715.

(97) Hempenius, M. A.; Langeveld-Voss, B. M. W.; Haare, J. A. E. H. v.; Janssen, R. A. J.; Sheiko, S. S.; Spatz, J. P.; Möller, M.; Meijer, E. W. *J. Am. Chem. Soc.* **1998**, *120*, 2798–2804.

(98) Li, W.; Maddux, T.; Yu, L. *Macromolecules* **1996**, *29*, 7329–7334.

(99) Hayakawa, T.; Yokoyama, H. *Langmuir* **2005**, *21*, 10288–10291.

(100) Kawano, S.-i.; Fujita, N.; Shinkai, S. *Chem.—Eur. J.* **2005**, *11*, 4735–4742.

(101) Albano, V. G.; Bandini, M.; Melucci, M.; Monari, M.; Piccinelli, F.; Tommasi, S.; Umani-Ronchi, A. *Adv. Synth. Catal.* **2005**, *347*, 1507–1512.

(102) Melucci, M.; Barbarella, G.; Gazzano, M.; Cavallini, M.; Biscarini, F.; Bongini, A.; Piccinelli, F.; Monari, M.; Bandini, M.; Umani-Ronchi, A.; Biscarini, P. *Chem.—Eur. J.* **2006**, *12*, 7304–7312.

(103) Bandini, M.; Eichholzer, A.; Tommasi, S.; Umani-Ronchi, A. *Synthesis* **2007**, 1587–1588.

(104) Nawa, K.; Imae, I.; Noma, N.; Shirota, Y. *Macromolecules* **1995**, *28*, 723–729.

(105) Imae, I.; Nawa, K.; Ohsedo, Y.; Noma, N.; Shirota, Y. *Macromolecules* **1997**, *30*, 380–386.

(106) Ohsedo, Y.; Imae, I.; Shirota, Y. *J. Polym. Sci., B: Polym. Phys.* **2003**, *41*, 2471–2484.

(107) Melucci, M.; Barbarella, G.; Zambianchi, M.; Benzi, M.; Biscarini, F.; Cavallini, M.; Bongini, A.; Fabbroni, S.; Mazzeo, M.; Anni, M.; Gigli, G. *Macromolecules* **2004**, *37*, 5692–5702.

(108) Hayakawa, T.; Horiuchi, S. *Angew. Chem., Int. Ed.* **2003**, *42*, 2285–2289.

(109) Melucci, M.; Dionigi, C.; Lanzani, G.; Viola, I.; Gigli, G.; Barbarella, G. *Macromolecules* **2005**, *38*, 10050–10054.

(110) Zhao, C.; Zhang, Y.; Wang, C.; Rothberg, L.; Ng, M. K. *Org. Lett.* **2006**, *8*, 1585–1588.

(111) Hajlaoui, R.; Fichou, D.; Horowitz, G.; Nessakh, B.; Constant, M.; Garnier, F. *Adv. Mater.* **1997**, *9*, 557–561.

(112) Katz, H. E.; Lovinger, A. J.; Laquindanum, J. G. *Chem. Mater.* **1998**, *10*, 457–459.

(113) Katz, H. E.; Laquindanum, J. G.; Lovinger, A. J. *Chem. Mater.* **1998**, *10*, 633–638.

(114) Kwon, J.-H.; Seo, J.-H.; Kang, H.; Choi, D. H.; Ju, B.-K. *J. Appl. Phys.* **2007**, *101*, 064502.

(115) Byron, D.; Matharu, A.; Wilson, R.; Wright, G. *Mol. Cryst. Liq. Cryst.* **1995**, *265*, 61–76.

(116) Azumi, R.; Götz, G.; Bäuerle, P. *Synth. Met.* **1999**, *101*, 544–545.

(117) Ponomarenko, S.; Kirchmeyer, S. *J. Mater. Chem.* **2003**, *13*, 197–202.

(118) Leroy, J.; Levin, J.; Sergeyev, S.; Geerts, Y. *Chem. Lett.* **2006**, *35*, 166–167.

(119) Funahashi, M.; Hanna, J.-I. *Appl. Phys. Lett.* **2000**, *76*, 2574–2576.

(120) Yamada, T.; Azumi, R.; Tachibana, H.; Sakai, H.; Abe, M.; Bäuerle, P.; Matsumoto, M. *Chem. Lett.* **2001**, *30*, 1022–1023.

(121) Funahashi, M.; Zhang, F.; Tamaoki, N. *Adv. Mater.* **2007**, *19*, 353–358.

(122) Zhang, F.; Funahashi, M.; Tamaoki, N. *Appl. Phys. Lett.* **2007**, *91*, 063515(1)−063515(3)..

(123) Leroy, J.; Boucher, N.; Sergeyev, S.; Sferrazza, M.; Geerts, Y. H. *Eur. J. Org. Chem.* **2007**, 1256–1261.

(124) Sung, A.; Ling, M. M.; Tang, M. L.; Bao, Z.; Locklin, J. *Chem. Mater.* **2007**, *19*, 2342–2351.

(125) Vaidyanathan, S.; Dotz, F.; Katz, H. E.; Lawrentz, U.; Granstrom, J.; Reichmanis, E. *Chem. Mater.* **2007**, *19*, 4676–4681.

(126) Mohapatra, S.; Holmes, B. T.; Newman, C. R.; Prendergast, C. F.; Frisbie, C. D.; Ward, M. D. *Adv. Funct. Mater.* **2004**, *14*, 605–609.

(127) Fritz, S. E.; Mohapatra, S.; Holmes, B. T.; Anderson, A. M.; Prendergast, C. F.; Frisbie, C. D.; Ward, M. D.; Toney, M. F. *Chem. Mater.* **2007**, *19*, 1355–1361.

(128) Facchetti, A.; Letizia, J.; Yoon, M.-H.; Mushrush, M.; Katz, H. E.; Marks, T. J. *Chem. Mater.* **2004**, *16*, 4715–4727.

(129) Zhang, H.; Shiino, S.; Shishido, A.; Kanazawa, A.; Tsutsumi, O.; Shiono, T.; Ikeda, T. *Adv. Mater.* **2000**, *12*, 1336–1339.

(130) Yaegashi, M.; Shishido, A.; Shiono, T.; Ikeda, T. *Chem. Mater.* **2005**, *17*, 4304–4309.

(131) Van Breemen, A. J. J. M.; Herwig, P. T.; Chlon, C. H. T.; Sweelssen, J.; Schoo, H. F. M.; Setayesh, S.; Hardeman, W. M.; Martin, C. A.; de Leeuw, D. M.; Valeton, J. J. P.; Bastiaansen, C. W. M.; Broer, D. J.; Popa-Merticaru, A. R.; Meskers, S. C. J. *J. Am. Chem. Soc.* **2006**, *128*, 2336–2345.

(132) Huisman, B.-H.; Valeton, J. J. P.; Nijssen, W.; Lub, J.; Ten Hoeve, W. *Adv. Mater.* **2003**, *15*, 2002–2005.

(133) McCulloch, I.; Zhang, W.; Heeney, M.; Bailey, C.; Giles, M.; Graham, D.; Shkunov, M.; Sparrowe, D.; Tierney, S. *J. Mater. Chem.* **2003**, *13*, 2436–2444.

(134) Funahashi, M.; Hanna, J.-I. *Adv. Mater.* **2005**, *17*, 594–598.

(135) Funahashi, M.; Tamaoki, N. *ChemPhysChem* **2006**, *7*, 1193–1197.

(136) Funahashi, M.; Tamaoki, N. *Mol. Cryst. Liq. Cryst.* **2007**, *475*, 123–135.

(137) Funahashi, M.; Tamaoki, N. *Chem. Mater.* **2007**, *19*, 608–617.

(138) Lightowler, S.; Hird, M. *Chem. Mater.* **2005**, *17*, 5538–5549.

(139) Liu, P.; Zhang, Y.; Feng, G.; Hu, J.; Zhou, X.; Zhao, Q.; Xu, Y.; Tong, Z.; Deng, W. *Tetrahedron* **2004**, *60*, 5259–5264.

(140) Liu, P.; Liu, M.; Deng, W. *Synth. Commun.* **2006**, *36*, 685–692.

(141) Yasuda, T.; Kishimoto, K.; Kato, T. *Chem. Commun.* **2006**, 3399–3401.

(142) Kimura, M.; Yasuda, T.; Kishimoto, K.; Götz, G.; Bäuerle, P.; Kato, T. *Chem. Lett.* **2006**, *35*, 1150–1151.

(143) Didier, D.; Sergeyev, S.; Geerts, Y. H. *Tetrahedron* **2007**, *63*, 941–946.

(144) Prehm, M.; Götz, G.; Bäuerle, P.; Liu, F.; Zeng, X.; Ungar, G.; Tschierske, C. *Angew. Chem., Int. Ed.* **2007**, *46*, 7856–7859.

(145) Melucci, M.; Favaretto, L.; Bettini, C.; Gazzano, M.; Camaioni, N.; Maccagnani, P.; Ostoja, P.; Monari, M.; Barbarella, G. *Chem.−Eur. J.* **2007**, *13*, 10046–10054.

(146) Bäuerle, P.; Segelbacher, U.; Maier, A.; Mehring, M. *J. Am. Chem. Soc.* **1993**, *115*, 10217–10223.

(147) Bäuerle, P.; Segelbacher, U.; Gaudl, K. U.; Huttenlocher, D.; Mehring, M. *Angew. Chem., Int. Ed.* **1993**, *32*, 76–78.

(148) Miller, L. L.; Mann, K. R. *Acc. Chem. Res.* **1996**, *29*, 417–423.

(149) Graf, D. D.; Duan, R. G.; Campbell, J. P.; Miller, L. L.; Mann, K. R. *J. Am. Chem. Soc.* **1997**, *119*, 5888–5899.

(150) Kaikawa, T.; Takimiya, K.; Aso, Y.; Otsubo, T. *Org. Lett.* **2000**, *2*, 4197–4199.

(151) Satou, T.; Sakai, T.; Kaikawa, T.; Takimiya, K.; Otsubo, T.; Aso, Y. *Org. Lett.* **2004**, *6*, 997–1000.

(152) Sakai, T.; Satou, T.; Kaikawa, T.; Takimiya, K.; Otsubo, T.; Aso, Y. *J. Am. Chem. Soc.* **2005**, *127*, 8082–8089.

(153) Edder, C.; Fréchet, J. M. J. *Org. Lett.* **2003**, *5*, 1879–1882.

(154) Knoblock, K. M.; Silvestri, C. J.; Collard, D. M. *J. Am. Chem. Soc.* **2006**, *128*, 13680–13681.

(155) Steybe, F.; Effenberger, F.; Beckmann, S.; Kramer, P.; Glania, C.; Wortmann, R. *Chem. Phys.* **1997**, *219*, 317–331.

(156) Steybe, F.; Effenberger, F.; Gubler, U.; Bosshard, C.; Gunter, P. *Tetrahedron* **1998**, *54*, 8469–8480.

(157) Raimundo, J. M.; Blanchard, P.; Gallego-Planas, N.; Mercier, N.; Ledoux-Rak, I.; Hierle, R.; Roncali, J. *J. Org. Chem.* **2002**, *67*, 205–218.

(158) Casado, J.; Pappenfus, T. M.; Miller, L. L.; Mann, K. R.; Ortí, E.; Viruela, P. M.; Pou-Amérigo, R.; Hernández, V.; López Navarrete, J. T. *J. Am. Chem. Soc.* **2003**, *125*, 2524–2534.

(159) Ruiz Delgado, M. C.; Hern, V.; Casado, J.; López Navarrete, J. T.; Raimundo, J.-M.; Blanchard, P.; Roncali, J. *Chem.−Eur. J.* **2003**, *9*, 3670–3682.

(160) Raposo, M. M. M.; Fonseca, A. M. C.; Kirsch, G. *Tetrahedron* **2004**, *60*, 4071–4078.

(161) Effenberger, F.; Würthner, F.; Steybe, F. *J. Org. Chem.* **1995**, *60*, 2082–2091.

(162) Noda, T.; Shirota, Y. *J. Am. Chem. Soc.* **1998**, *120*, 9714–9715.

(163) Shirota, Y.; Noda, T.; Ogawa, H. *Proc. SPIE−Int. Soc. Opt. Eng.* **1999**, *3797*, 158–169.

(164) Doi, H.; Kinoshita, M.; Okumoto, K.; Shirota, Y. *Chem. Mater.* **2003**, *15*, 1080–1089.

(165) Noda, T.; Imae, I.; Noma, N.; Shirota, Y. *Adv. Mater.* **1997**, *9*, 239–241.

(166) Noda, T.; Ogawa, H.; Noma, N.; Shirota, Y. *J. Mater. Chem.* **1999**, *9*, 2177–2181.

(167) Castro, C. M.; Ruiz Delgado, M. C.; Hernández, V.; Shirota, Y.; Casado, J.; López Navarrete, J. T. *J. Phys. Chem. B* **2002**, *106*, 7163–7170.

(168) Clot, O.; Selmarten, D.; McNevin, M. J. *J. Mater. Chem.* **2005**, *15*, 4934–4942.

(169) Sundararaman, A.; Venkatasubbaiah, K.; Victor, M.; Zakharov, L. N.; Rheingold, A. L.; Jäkle, F. *J. Am. Chem. Soc.* **2006**, *128*, 16554–16565.

(170) Li, H.; Sundararaman, A.; Venkatasubbaiah, K.; Jäkle, F. *J. Am. Chem. Soc.* **2007**, *129*, 5792–5793.

(171) Wakamiya, A.; Mori, K.; Yamaguchi, S. *Angew. Chem., Int. Ed.* **2007**, *46*, 4273–4276.

(172) Götz, G.; Scheib, S.; Klose, R.; Heinze, J.; Bäuerle, P. *Adv. Funct. Mater.* **2002**, *12*, 723–728.

(173) Wong, K.-T.; Hung, T. H.; Chou, C. H.; Su, Y. O.; Kao, S. C. *Chem. Commun.* **2001**, 1628–1629.

(174) Gerstner, P.; Rohde, D.; Hartmann, H. *Synthesis* **2002**, 2487–2489.

(175) Tabet, A.; Schroder, A.; Hartmann, H.; Rohde, D.; Dunsch, L. *Org. Lett.* **2003**, *5*, 1817–1820.

(176) Tabet, A.; Hartmann, H. *Synthesis* **2005**, 610–616.

(177) Rohde, D.; Dunsch, L.; Tabet, A.; Hartmann, H.; Fabian, J. *J. Phys. Chem. B* **2006**, *110*, 8223–8231.

(178) Zrig, S.; Koeckelberghs, G.; Verbiest, T.; Andrioletti, B.; Rose, E.; Persoons, A.; Asselberghs, I.; Clays, K. *J. Org. Chem.* **2007**, *72*, 5855–5858.

(179) Chou, C.-F.; Huang, T.-H.; Lin, J. T.; Hsieh, C.-c.; Lai, C.-H.; Chou, P.-T.; Tsai, C. *Tetrahedron* **2006**, *62*, 8467–8473.

(180) Meng, H.; Bao, Z.; Lovinger, A. J.; Wang, B.; Mujsce, A. M. *J. Am. Chem. Soc.* **2001**, *123*, 9214–9215.

(181) Meng, H.; Zheng, J.; Lovinger, A. J.; Wang, B.-C.; Van Patten, P. G.; Bao, Z. *Chem. Mater.* **2003**, *15*, 1778–1787.

(182) Promarak, V.; Punkvuang, A.; Meunmat, D.; Sudyoadsuk, T.; Saengsuwan, S.; Keawin, T. *Tetrahedron Lett.* **2007**, *48*, 919–923.

(183) Promarak, V.; Punkvuang, A.; Jungsuttiwong, S.; Saengsuwan, S.; Sudyoadsuk, T.; Keawin, T. *Tetrahedron Lett.* **2007**, *48*, 3661–3665.

(184) Promarak, V.; Pankvuang, A.; Ruchirawat, S. *Tetrahedron Lett.* **2007**, *48*, 1151–1154.

(185) Promarak, V.; Ruchirawat, S. *Tetrahedron* **2007**, *63*, 1602–1609.

(186) Promarak, V.; Punkvuang, A.; Sudyoadsuk, T.; Jungsuttiwong, S.; Saengsuwan, S.; Keawin, T.; Sirithip, K. *Tetrahedron* **2007**, *63*, 8881–8890.

(187) Surin, M.; Sonar, P.; Grimsdale, A. C.; Müllen, K.; Feyter, S. D.; Habuchi, S.; Sarzi, S.; Braeken, E.; Heyen, A. V.; Auweraer, M. V. d.; Schryver, F. C. D.; Cavallini, M.; Moulin, J.-F.; Biscarini, F.; Femoni, C.; Lazzaroni, R.; Leclère, P. *J. Mater. Chem.* **2007**, *17*, 728–735.

(188) Li, Z. H.; Wong, M. S.; Fukutani, H.; Tao, Y. *Chem. Mater.* **2005**, *17*, 5032–5040.

(189) Li, Z. H.; Wong, M. S.; Tao, Y.; Fukutani, H. *Org. Lett.* **2007**, *9*, 3659–3662.

(190) Skabara, P. J.; Berridge, R.; Serebryakov, I. M.; Kanibolotsky, A. L.; Kanibolotskaya, L.; Gordeyev, S.; Perepichka, I. F.; Sariciftci, N. S.; Winder, C. *J. Mater. Chem.* **2007**, *17*, 1055–1062.

(191) Kanibolotsky, A. L.; Kanibolotskaya, L.; Gordeyev, S.; Skabara, P. J.; McCulloch, I.; Berridge, R.; Lohr, J. E.; Marchioni, F.; Wudl, F. *Org. Lett.* **2007**, *9*, 1601–1604.

(192) Barclay, T. M.; Cordes, A. W.; MacKinnon, C. D.; Oakley, R. T.; Reed, R. W. *Chem. Mater.* **1997**, *9*, 981–990.

(193) Melucci, M.; Barbarella, G.; Zambianchi, M.; Di Pietro, P.; Bongini, A. *J. Org. Chem.* **2004**, *69*, 4821–4828.

(194) Zotti, G.; Zecchin, S.; Vercelli, B.; Berlin, A.; Casado, J.; Hernández, V.; Ortiz, R. P.; López Navarrete, J. T.; Orti, E.; Viruela, P. M.; Milian, B. *Chem. Mater.* **2006**, *18*, 1539–1545.

(195) Joshi, M. V.; Cava, M. P.; Lakshmikantham, M. V.; Metzger, R. M.; Abdeldayem, H.; Henry, M.; Venkateswarlu, P. *Synth. Met.* **1993**, *57*, 3974–3979.

(196) Pappenfus, T. M.; Burand, M. W.; Janzen, D. E.; Mann, K. R. *Org. Lett.* **2003**, *5*, 1535–1538.

(197) Bader, M. M.; Custelcean, R.; Ward, M. D. *Chem. Mater.* **2003**, *15*, 616–618.

(198) Higuchi, H.; Nakayama, T.; Koyama, H.; Ojima, J.; Wada, T.; Sasabe, H. *Bull. Chem. Soc. Jpn.* **1995**, *68*, 2363–2377.

(199) Pappenfus, T. M.; Chesterfield, R. J.; Frisbie, C. D.; Mann, K. R.; Casado, J.; Raff, J. D.; Miller, L. L. *J. Am. Chem. Soc.* **2002**, *124*, 4184–4185.

(200) Janzen, D. E.; Burand, M. W.; Ewbank, P. C.; Pappenfus, T. M.; Higuchi, H.; da Silva Filho, D. A.; Young, V. G.; Brédas, J.-L.; Mann, K. R. *J. Am. Chem. Soc.* **2004**, *126*, 15295–15308.

(201) Takahashi, T.; Matsuoka, K.; Takimiya, K.; Otsubo, T.; Aso, Y. *J. Am. Chem. Soc.* **2005**, *127*, 8928–8929.

(202) Ortiz, R. P.; Casado, J.; Hernández, V.; López Navarrete, J. T.; Ortí, E.; Viruela, P. M.; Milián, B.; Hotta, S.; Zotti, G.; Zecchin, S.; Vercelli, B. *Adv. Funct. Mater.* **2006**, *16*, 531–536.

(203) Chesterfield, R. J.; Newman, C. R.; Pappenfus, T. M.; Ewbank, P. C.; Haukaas, M. H.; Mann, K. R.; Miller, L. L.; Frisbie, C. D. *Adv. Mater.* **2003**, *15*, 1278–1282.

(204) Ortiz, R. P.; Casado, J.; Hernández, V.; López Navarrete, J. T.; Viruela, P. M.; Ortí, E.; Takimiya, K.; Otsubo, T. *Angew. Chem., Int. Ed.* **2007**, *46*, 9057–9061.

(205) Handa, S.; Miyazaki, E.; Takimiya, K.; Kunugi, Y. *J. Am. Chem. Soc.* **2007**, *129*, 11684–11685.

(206) Casado, J.; Ortiz, R. P.; Ruiz Delgado, M. C.; Azumi, R.; Oakley, R. T.; Hernández, V.; López Navarrete, J. T. *J. Phys. Chem. B* **2005**, *109*, 10115–10125.

(207) Newman, C. R.; Frisbie, C. D.; da Silva Filho, D. A.; Bredas, J. L.; Ewbank, P. C.; Mann, K. R. *Chem. Mater.* **2004**, *16*, 4436–4451.

(208) Schulze, K.; Uhrich, C.; Schüppel, R.; Leo, K.; Pfeiffer, M.; Brier, E.; Reinold, E.; Bäuerle, P. *Adv. Mater.* **2006**, *18*, 2872–2875.

(209) Schulze, K.; Uhrich, C.; Schüppel, R.; Leo, K.; Pfeiffer, M.; Brier, E.; Reinold, E.; Bäuerle, P. *Proc. SPIE—Int. Soc. Opt. Eng.* **2006**, *6192*, 61920C(1−6)..

(210) Uhrich, C.; Schueppel, R.; Petrich, A.; Pfeiffer, M.; Leo, K.; Brier, E.; Kilickiran, P.; Bäuerle, P. *Adv. Funct. Mater.* **2007**, *17*, 2991–2999.

(211) Schueppel, R.; Uhrich, C.; Pfeiffer, M.; Leo, K.; Brier, E.; Reinold, E.; Bäuerle, P. *ChemPhysChem* **2007**, *8*, 1497–1503.

(212) Takahashi, T.; Takimiya, K.; Otsubo, T.; Aso, Y. *Org. Lett.* **2005**, *7*, 4313–4316.

(213) Uno, M.; Seto, K.; Masuda, M.; Ueda, W.; Takahashi, S. *Tetrahedron Lett.* **1985**, *26*, 1553–1556.

(214) Uno, M.; Seto, K.; Takahashi, S. *J. Chem. Soc., Chem. Commun.* **1984**, 932–933.

(215) O'Regan, B.; Grätzel, M. *Nature* **1991**, *353*, 737–740.

(216) Koumura, N.; Wang, Z. S.; Mori, S.; Miyashita, M.; Suzuki, E.; Hara, K. *J. Am. Chem. Soc.* **2006**, *128*, 14256–14257.

(217) Chen, R.; Yang, X.; Tian, H.; Wang, X.; Hagfeldt, A.; Sun, L. *Chem. Mater.* **2007**, *19*, 4007–4015.

(218) Kim, S.; Lee, J. K.; Kang, S. O.; Ko, J.; Yum, J. H.; Fantacci, S.; De Angelis, F.; Di Censo, D.; Nazeeruddin, M. K.; Grätzel, M. *J. Am. Chem. Soc.* **2006**, *128*, 16701–16707.

(219) Kim, S.; Choi, H.; Kim, D.; Song, K.; Kang, S. O.; Ko, J. *Tetrahedron* **2007**, *63*, 9206–9212.

(220) Choi, H.; Lee, J. K.; Song, K.; Kang, S. O.; Ko, J. *Tetrahedron* **2007**, *63*, 3115–3121.

(221) Kim, D.; Lee, J. K.; Kang, S. O.; Ko, J. *Tetrahedron* **2007**, *63*, 1913–1922.

(222) Choi, H.; Lee, J. K.; Song, K. H.; Song, K.; Kang, S. O.; Ko, J. *Tetrahedron* **2007**, *63*, 1553–1559.

(223) Li, S.-L.; Jiang, K.-J.; Shao, K.-F.; Yang, L.-M. *Chem. Commun.* **2006**, 2792–2794.

(224) Babudri, F.; Farinola, G. M.; Naso, F.; Ragni, R. *Chem. Commun.* **2007**, 1003–1022.

(225) Tian, H.; Yang, S. *Chem. Soc. Rev.* **2004**, *33*, 85–97.

(226) Facchetti, A.; Deng, Y.; Wang, A.; Koide, Y.; Sirringhaus, H.; Marks, T. J.; Friend, R. H. *Angew. Chem., Int. Ed.* **2000**, *39*, 4547–4551.

(227) Facchetti, A.; Mushrush, M.; Katz, H. E.; Marks, T. J. *Adv. Mater.* **2003**, *15*, 33–38.

(228) Yoon, M.-H.; DiBenedetto, S. A.; Facchetti, A.; Marks, T. J. *J. Am. Chem. Soc.* **2005**, *127*, 1348–1349.

(229) Yoon, M. H.; DiBenedetto, S. A.; Russell, M. T.; Facchetti, A.; Marks, T. J. *Chem. Mater.* **2007**, *19*, 4864–4881.

(230) Facchetti, A.; Mushrush, M.; Yoon, M. H.; Hutchison, G. R.; Ratner, M. A.; Marks, T. J. *J. Am. Chem. Soc.* **2004**, *126*, 13859–13874.

(231) Yoon, M.-H.; Kim, C.; Facchetti, A.; Marks, T. J. *J. Am. Chem. Soc.* **2006**, *128*, 12851–12869.

(232) Facchetti, A.; Yoon, M.-H.; Stern, C. L.; Katz, H. E.; Marks, T. J. *Angew. Chem., Int. Ed.* **2003**, *42*, 3900–3903.

(233) Yoon, M.-H.; Facchetti, A.; Stern, C. E.; Marks, T. J. *J. Am. Chem. Soc.* **2006**, *128*, 5792–5801.

(234) Letizia, J. A.; Facchetti, A.; Stern, C. L.; Ratner, M. A.; Marks, T. J. *J. Am. Chem. Soc.* **2005**, *127*, 13476–13477.

(235) Cai, X.; Gerlach, C. P.; Frisbie, C. D. *J. Phys. Chem. C* **2007**, *111*, 452–456.

(236) Ie, Y.; Umemoto, Y.; Kaneda, T.; Aso, Y. *Org. Lett.* **2006**, *8*, 5381–5384.

(237) Ie, Y.; Nitani, M.; Ishikawa, M.; Nakayama, K. i.; Tada, H.; Kaneda, T.; Aso, Y. *Org. Lett.* **2007**, *9*, 2115–2118.

(238) Tanaka, K.; Wang, S.; Yamabe, T. *Synth. Met.* **1989**, *30*, 57–65.

(239) Barbarella, G.; Pudova, O.; Arbizzani, C.; Mastragostino, M.; Bongini, A. *J. Org. Chem.* **1998**, *63*, 1742–1745.

(240) Barbarella, G.; Favaretto, L.; Sotgiu, G.; Zambianchi, M.; Antolini, L.; Pudova, O.; Bongini, A. *J. Org. Chem.* **1998**, *63*, 5497–5506.

(241) Miller, L. L.; Yu, Y. *J. Org. Chem.* **1995**, *60*, 6813–6819.

(242) Barbarella, G.; Favaretto, L.; Zambianchi, M.; Pudova, O.; Arbizzani, C.; Bongini, A.; Mastragostino, M. *Adv. Mater.* **1998**, *10*, 551–554.

(243) Jiang, B.; Tilley, T. D. *J. Am. Chem. Soc.* **1999**, *121*, 9744–9745.

(244) Barbarella, G.; Favaretto, L.; Sotgiu, G.; Zambianchi, M.; Bongini, A.; Arbizzani, C.; Mastragostino, M.; Anni, M.; Gigli, G.; Cingolani, R. *J. Am. Chem. Soc.* **2000**, *122*, 11971–11978.

(245) Bongini, A.; Barbarella, G.; Favaretto, L.; Sotgiu, G.; Zambianchi, M.; Casarini, D. *Tetrahedron* **2002**, *58*, 10151–10158.

(246) Barbarella, G.; Favaretto, L.; Sotgiu, G.; Zambianchi, M.; Fattori, V.; Cocchi, M.; Cacialli, F.; Gigli, G.; Cingolani, R. *Adv. Mater.* **1999**, *11*, 1375–1379.

(247) Gigli, G.; Barbarella, G.; Favaretto, L.; Cacialli, F.; Cingolani, R. *Appl. Phys. Lett.* **1999**, *75*, 439–441.

(248) Gigli, G.; Inganäs, O.; Anni, M.; De Vittorio, M.; Cingolani, R.; Barbarella, G.; Favaretto, L. *Appl. Phys. Lett.* **2001**, *78*, 1493–1495.

(249) Camaioni, N.; Ridolfi, G.; Fattori, V.; Favaretto, L.; Barbarella, G. *Appl. Phys. Lett.* **2004**, *84*, 1901–1903.

(250) Amir, E.; Rozen, S. *Angew. Chem., Int. Ed.* **2005**, *44*, 7374–7378.

(251) Casado, J.; Zgierski, M. Z.; Ewbank, P. C.; Burand, M. W.; Janzen, D. E.; Mann, K. R.; Pappenfus, T. M.; Berlin, A.; Perez-Inestrosa, E.; Ortiz, R. P.; López Navarrete, J. T. *J. Am. Chem. Soc.* **2006**, *128*, 10134–10144.

(252) Pappenfus, T. M.; Melby, J. H.; Hansen, B. B.; Sumption, D. M.; Hubers, S. A.; Janzen, D. E.; Ewbank, P. C.; McGee, K. A.; Burand, M. W.; Mann, K. R. *Org. Lett.* **2007**, *9*, 3721–3724.

(253) Jousselme, B.; Blanchard, P.; Gallego-Planas, N.; Delaunay, J.; Allain, M.; Richomme, P.; Levillain, E.; Roncali, J. *J. Am. Chem. Soc.* **2003**, *125*, 2888–2889.

(254) Jousselme, B.; Blanchard, P.; Allain, M.; Levillain, E.; Dias, M.; Roncali, J. *J. Phys. Chem. A* **2006**, *110*, 3488–3494.

(255) Hara, K.; Kurashige, M.; Dan-oh, Y.; Kasada, C.; Shinpo, A.; Suga, S.; Sayama, K.; Arakawa, H. *New J. Chem.* **2003**, *27*, 783–785.

(256) Hara, K.; Wang, Z. S.; Sato, T.; Furube, A.; Katoh, R.; Sugihara, H.; Dan-oh, Y.; Kasada, C.; Shinpo, A.; Suga, S. *J. Phys. Chem. B* **2005**, *109*, 15476–15482.

(257) Hara, K.; Miyamoto, K.; Abe, Y.; Yanagida, M. *J. Phys. Chem. B* **2005**, *109*, 23776–23778.

(258) Wang, Z.-S.; Cui, Y.; Hara, K.; Dan-oh, Y.; Kasada, C.; Shinpo, A. *Adv. Mater.* **2007**, *19*, 1138–1141.

(259) Cremer, J.; Mena-Osteritz, E.; Pschierer, N. G.; Müllen, K.; Bäuerle, P. *Org. Biomol. Chem.* **2005**, *3*, 985–995.

(260) Cremer, J.; Bäuerle, P. *Eur. J. Org. Chem.* **2005**, 3715–3723.

(261) Fron, E.; Lor, M.; Pilot, R.; Schweitzer, G.; Dincalp, H.; De Feyter, S.; Cremer, J.; Bäuerle, P.; Müllen, K.; Van der Auweraer, M.; De Schryver, F. C. *Photochem. Photobiol. Sci.* **2005**, *4*, 61–68.

(262) Chen, S.; Liu, Y.; Qiu, W.; Sun, X.; Ma, Y.; Zhu, D. *Chem. Mater.* **2005**, *17*, 2208–2215.

(263) Moustrou, C.; Rebière, N.; Samat, A.; Guglielmetti, R.; Yassar, A.; Dubest, R.; Aubard, J. *Helv. Chim. Acta* **1998**, *81*, 1293–1302.

(264) Yassar, A.; Galy, N. R.; Frigoli, M.; Moustrou, C.; Samat, A.; Guglielmetti, R.; Jaafari, A. *Synth. Met.* **2001**, *124*, 23–27.

(265) Frigoli, M.; Moustrou, C.; Samat, A.; Guglielmetti, R. *Eur. J. Org. Chem.* **2003**, 2799–2812.

(266) Ortica, F.; Smimmo, P.; Favaro, G.; Mazzucato, U.; Delbaere, S.; Venec, D.; Vermeersch, G.; Frigoli, M.; Moustrou, C.; Samat, A. *Photochem. Photobiol. Sci.* **2004**, *3*, 878–885.

(267) Coen, S.; Moustrou, C.; Frigoli, M.; Julliard, M.; Samat, A.; Guglielmetti, R. *J. Photochem. Photobiol. A* **2001**, *139*, 1–4.

(268) Yassar, A.; Garnier, F.; Jaafari, H.; Rebiere-Galy, N.; Frigoli, M.; Moustrou, C.; Samat, A.; Guglielmetti, R. *Appl. Phys. Lett.* **2002**, *80*, 4297–4299.

(269) Zhao, W.; Carreira, E. M. *Chem.—Eur. J.* **2007**, *13*, 2671–2685.

(270) Sariciftci, N. S.; Smilowitz, L.; Heeger, A. J.; Wudl, F. *Science* **1992**, *258*, 1474–1476.

(271) Padinger, F.; Rittberger, R. S.; Sariiftci, N. S. *Adv. Funct. Mater.* **2003**, *13*, 85–88.

(272) Li, G.; Shrotriya, V.; Huang, J.; Yao, Y.; Moriarty, T.; Emery, K.; Yang, Y. *Nat. Mater.* **2005**, *4*, 864–868.

(273) Ma, W.; Yang, C.; Gong, X.; Lee, K.; Heeger, A. J. *Adv. Funct. Mater.* **2005**, *15*, 1617–1622.

(274) Granström, M.; Petritsch, K.; Arias, A. C.; Lux, A.; Andersson, M. R.; Friend, R. H. *Nature* **1998**, *395*, 257–260.

(275) Pettersson, L. A. A.; Lucimara, S. R.; Inganäs, O. *J. Appl. Phys.* **1999**, *86*, 487–496.

(276) Gadisa, A.; Svensson, M.; Andersson, M. R.; Inganäs, O. *Appl. Phys. Lett.* **2004**, *84*, 1609–1611.

(277) Cravino, A.; Sariciftci, N. S. *J. Mater. Chem.* **2002**, *12*, 1931–1943.

(278) Otsubo, T.; Aso, Y.; Takimiya, K. *Pure Appl. Chem.* **2005**, *77*, 2003–2010.

(279) Benincori, T.; Brenna, E.; Sannicoló, F.; Trimarco, L.; Zotti, G.; Sozzani, P. *Angew. Chem., Int. Ed.* **1996**, *35*, 648–651.

(280) Yassar, A.; Hmyene, M.; Loveday, D. C.; Ferraris, J. P. *Synth. Met.* **1997**, *84*, 231–232.

(281) Cravino, A.; Zerza, G.; Maggini, M.; Bucella, S.; Svensson, M.; Andersson, M. R.; Neugebauer, H.; Sariciftci, N. S. *Chem. Commun.* **2000**, 2487–2488.

(282) Cravino, A.; Zerza, G.; Neugebauer, H.; Maggini, M.; Bucella, S.; Menna, E.; Svensson, M.; Andersson, M. R.; Brabec, C. J.; Sariciftci, N. S. *J. Phys. Chem. B* **2002**, *106*, 70–76.

(283) Murata, Y.; Suzuki, M.; Komatsu, K. *Org. Biomol. Chem.* **2003**, *1*, 2624–2625.

(284) Kim, D. H.; Kang, B. S.; Lim, S. M.; Bark, K.-M.; Kim, B. G.; Shiro, M.; Shim, Y.-B.; Shin, S. C. *J. Chem. Soc., Dalton Trans.* **1998**, 1893–1898.

(285) Yamazaki, T.; Murata, Y.; Komatsu, K.; Furukawa, K.; Morita, M.; Maruyama, N.; Yamao, T.; Fujita, S. *Org. Lett.* **2004**, *6*, 4865–4868.

(286) Wang, F.; Wilson, M. S.; Rauh, R. D.; Schottland, P.; Thompson, B. C.; Reynolds, J. R. *Macromolecules* **2000**, *33*, 2083–2091.

(287) Sonmez, G.; Shen, C. K. F.; Rubin, Y.; Wudl, F. *Adv. Mater.* **2005**, *17*, 897–900.

(288) Sivula, K.; Ball, Z. T.; Watanabe, N.; Fréchet, J. M. J. *Adv. Mater.* **2006**, *18*, 206–210.

(289) Effenberger, F.; Grube, G. *Synthesis* **1998**, 1372–1379.

(290) Knorr, S.; Grupp, A.; Mehring, M.; Grube, G.; Effenberger, F. *J. Chem. Phys.* **1999**, *110*, 3502–3508.

(291) Liu, S.-G.; Shu, L.; Rivera, J.; Liu, H.; Raimundo, J.-M.; Roncali, J.; Gorgues, J.; Echegoyen, L. *J. Org. Chem.* **1999**, *64*, 4884–4886.

(292) Yamashiro, T.; Aso, Y.; Otsubo, T.; Tang, H.; Harima, Y.; Yamashita, K. *Chem. Lett.* **1999**, *28*, 443–444.

(293) Maggini, M.; Scorrano, G.; Prato, M. *J. Am. Chem. Soc.* **1993**, *115*, 9798–9799.

(294) Fujitsuka, M.; Ito, O.; Yamashiro, T.; Aso, Y.; Otsubo, T. *J. Phys. Chem. A* **2000**, *104*, 4876–4881.

(295) Fujitsuka, M.; Masuhara, A.; Kasai, H.; Oikawa, H.; Nakanishi, H.; Ito, O.; Yamashiro, T.; Aso, Y.; Otsubo, T. *J. Phys. Chem. B* **2001**, *105*, 9930–9934.

(296) Negishi, N.; Yamada, K.; Takimiya, K.; Aso, Y.; Otsubo, T.; Harima, Y. *Chem. Lett.* **2003**, *32*, 404–405.

(297) van Hal, P. A.; Knol, J.; Langeveld-Voss, B. M. W.; Meskers, S. C. J.; Hummelen, J. C.; Janssen, R. A. J. *J. Phys. Chem. A* **2000**, *104*, 5974–5988.

(298) Negishi, N.; Takimiya, K.; Otsubo, T.; Harima, Y.; Aso, Y. *Chem. Lett.* **2004**, *33*, 654–655.

(299) Kunugi, Y.; Takimiya, K.; Negishi, N.; Otsubo, T.; Aso, Y. *J. Mater. Chem.* **2004**, *14*, 2840–2841.

(300) Negishi, N.; Takimiya, K.; Otsubo, T.; Harima, Y.; Aso, Y. *Synth. Met.* **2005**, *152*, 125–128.

(301) Kanato, H.; Takimiya, K.; Otsubo, T.; Aso, Y.; Nakamura, T.; Araki, Y.; Ito, O. *J. Org. Chem.* **2004**, *69*, 7183–7189.

(302) Nakamura, T.; Kanato, H.; Araki, Y.; Ito, O.; Takimiya, K.; Otsubo, T.; Aso, Y. *J. Phys. Chem. A* **2006**, *110*, 3471–3479.

(303) Oswald, F.; Islam, D. M. S.; Araki, Y.; Troiani, V.; De la Cruz, P.; Moreno, A.; Ito, O.; Langa, F. *Chem.—Eur. J.* **2007**, *13*, 3924–3933.

(304) Elandaloussi, E.; Frère, P.; Roncali, J. *Chem. Commun.* **1997**, 301–302.

(305) Martineau, C.; Blanchard, P.; Rondeau, D.; Delaunay, J.; Roncali, J. *Adv. Mater.* **2002**, *14*, 283–287.

(306) Apperloo, J. J.; Martineau, C.; van Hal, P. A.; Roncali, J.; Janssen, R. A. J. *J. Phys. Chem. A* **2002**, *106*, 21–31.

(307) Obara, Y.; Takimiya, K.; Aso, Y.; Otsubo, T. *Tetrahedron Lett.* **2001**, *42*, 6877–6881.

(308) Aso, Y.; Obara, Y.; Okai, T.; Nishiguchi, S.; Otsubo, T. *Mol. Cryst. Liq. Cryst.* **2002**, *376*, 153–158.

(309) van Hal, P. A.; Beckers, E. H. A.; Meskers, S. C. J.; Janssen, R. A. J.; Jousselme, B.; Blanchard, P.; Roncali, J. *Chem.—Eur. J.* **2002**, *8*, 5415–5429.

(310) Jousselme, B.; Blanchard, P.; Levillain, E.; De Bettignies, R.; Roncali, J. *Macromolecules* **2003**, *36*, 3020–3025.

(311) Narutaki, M.; Takimiya, K.; Otsubo, T.; Harima, Y.; Zhang, H.; Araki, Y.; Ito, O. *J. Org. Chem.* **2006**, *71*, 1761–1768.

(312) Kanato, H.; Narutaki, M.; Takimiya, K.; Otsubo, T.; Harima, Y. *Chem. Lett.* **2006**, *35*, 668–669.

(313) McClenaghan, N. D.; Grote, Z.; Darriet, K.; Zimine, M.; Williams, R. M.; De Cola, L.; Bassani, D. M. *Org. Lett.* **2005**, *7*, 807–810.

(314) Huang, C. H.; McClenaghan, N. D.; Kuhn, A.; Hofstraat, J. W.; Bassani, D. M. *Org. Lett.* **2005**, *7*, 3409–3412.

(315) Huang, C.-H.; McClenaghan, N. D.; Kuhn, A.; Bravic, G.; Bassani, D. M. *Tetrahedron* **2006**, *62*, 2050–2059.

(316) Nishizawa, T.; Tajima, K.; Hashimoto, K. *J. Mater. Chem.* **2007**, *17*, 2440–2445.

(317) Würthner, F.; Vollmer, M. S.; Effenberger, F.; Emele, P.; Meyer, D. U.; Port, H.; Wolf, H. C. *J. Am. Chem. Soc.* **1995**, *117*, 8090–8099.

(318) Vollmer, M. S.; Würthner, F.; Effenberger, F.; Emele, P.; Meyer, D. U.; Stümpfig, T.; Port, H.; Wolf, H. C. *Chem.—Eur. J.* **1998**, *4*, 260–269.

(319) Lindsey, J. S.; Schreiman, I. C.; Hsu, H. C.; Kearney, P. C.; Marguerettaz, A. M. *J. Org. Chem.* **1987**, *52*, 827–836.

(320) Krebs, F. C.; Spanggaard, H. *Sol. Energy Mater. Sol. Cells* **2005**, *88*, 363–375.

(321) Odobel, F.; Suresh, S.; Blart, E.; Nicolas, Y.; Quintard, J. P.; Janvier, P.; Le Questel, J. Y.; Illien, B.; Rondeau, D.; Richomme, P.; Haupl, T.; Wallin, S.; Hammarstrom, L. *Chem.—Eur. J.* **2002**, *8*, 3027–3046.

(322) Zhang, T. G.; Zhao, Y.; Asselberghs, I.; Persoons, A.; Clays, K.; Therien, M. J. *J. Am. Chem. Soc.* **2005**, *127*, 9710–9720.

(323) Schäferling, M.; Bäuerle, P. *Synth. Met.* **1999**, *101*, 38–39.

(324) Schäferling, M.; Bäuerle, P. *J. Mater. Chem.* **2004**, *14*, 1132–1141.

(325) Takeuchi, M.; Shioya, T.; Swager, T. M. *Angew. Chem., Int. Ed.* **2001**, *40*, 3372–3375.

(326) Collis, G. E.; Campbell, W. M.; Officer, D. L.; Burrell, A. K. *Org. Biomol. Chem.* **2005**, *3*, 2075–2084.

(327) Ikemoto, J.; Takimiya, K.; Aso, Y.; Otsubo, T.; Fujitsuka, M.; Ito, O. *Org. Lett.* **2002**, *4*, 309–311.

(328) Nakamura, T.; Ikemoto, J.; Fujitsuka, M.; Araki, Y.; Ito, O.; Takimiya, K.; Aso, Y.; Otsubo, T. *J. Phys. Chem. B* **2005**, *109*, 14365–14374.

(329) Oswald, F.; Islam, D. M. S.; Araki, Y.; Troiani, V.; Caballero, R.; Cruz, P. D. L.; Ito, O.; Langa, F. *Chem. Commun.* **2007**, 4498–4500.

(330) Oike, T.; Kurata, T.; Takimiya, K.; Otsubo, T.; Aso, Y.; Zhang, H.; Araki, Y.; Ito, O. *J. Am. Chem. Soc.* **2005**, *127*, 15372–15373.

(331) Higuchi, H.; Ishikura, T.; Miyabayashi, K.; Miyake, M.; Yamamoto, K. *Tetrahedron Lett.* **1999**, *40*, 9091–9095.

(332) Higuchi, H.; Ishikura, T.; Mori, K.; Takayama, Y.; Yamamoto, K.; Tani, K.; Miyabayashi, K.; Miyake, M. *Bull. Chem. Soc. Jpn.* **2001**, *74*, 889–906.

(333) Hayashi, N.; Matsuda, A.; Chikamatsu, E.; Mori, K.; Higuchi, H. *Tetrahedron Lett.* **2003**, *44*, 7155–7158.

(334) Hayashi, N.; Murayama, M.; Mori, K.; Matsuda, A.; Chikamatsu, E.; Tani, K.; Miyabayashi, K.; Miyake, M.; Higuchi, H. *Tetrahedron* **2004**, *60*, 6363–6383.

(335) Hayashi, N.; Naoe, A.; Miyabayashi, K.; Miyake, M.; Higuchi, H. *Tetrahedron Lett.* **2005**, *46*, 6961–6965.

(336) Justin Thomas, K. R.; Lin, J. T.; Wen, Y. S. *Organometallics* **2000**, *19*, 1008–1012.

(337) Wong, W.-Y.; Lu, G.-L.; Ng, K.-F.; Choi, K.-H.; Lin, Z. *J. Chem. Soc., Dalton Trans.* **2001**, 3250–3260.

(338) Zhu, Y.; Wolf, M. O. *J. Am. Chem. Soc.* **2000**, *122*, 10121–10125.

(339) Sato, M. A.; Sakamoto, M. A.; Kashiwagi, S. I.; Suzuki, T.; Hiroi, M. *Bull. Chem. Soc. Jpn.* **2001**, *74*, 1737–1742.

(340) Sato, M.; Fukui, K.; Sakamoto, M.; Kashiwagi, S.; Hiroi, M. *Thin Solid Films* **2001**, *393*, 210–216.

(341) Higgins, S. J.; Christopher, L. J.; Francis, S. M. *Synth. Met.* **1999**, *98*, 211–214.

(342) Zhu, Y.; Wolf, M. O. *Chem. Mater.* **1999**, *11*, 2995–3001.

(343) Wolf, M. O.; Zhu, Y. *Adv. Mater.* **2000**, *12*, 599–601.

(344) Chen, J.; Burrell, A. K.; Collis, G. E.; Officer, D. L.; Swiegers, G. F.; Too, C. O.; Wallace, G. G. *Electrochim. Acta* **2002**, *47*, 2715–2724.

(345) Collis, G. E.; Burrell, A. K.; Officer, D. L. *Tetrahedron Lett.* **2001**, *42*, 8733–8735.

(346) Justin Thomas, K. R.; Lin, J. T. *J. Organomet. Chem.* **2001**, *637–639*, 139–144.
(347) Schubert, U. S.; Eschbaumer, C. *Angew. Chem., Int. Ed.* **2002**, *41*, 2892–2926.
(348) Hofmeier, H.; Schubert, U. S. *Chem. Soc. Rev.* **2004**, *33*, 373–399.
(349) Pickup, P. G. *J. Mater. Chem.* **1999**, *9*, 1641–1653.
(350) McQuade, D. T.; Pullen, A. E.; Swager, T. M. *Chem. Rev.* **2000**, *100*, 2537–2574.
(351) Wolf, M. O. *Adv. Mater.* **2001**, *13*, 545–553.
(352) Constable, E. C.; Housecroft, C. E.; Schofield, E. R.; Encinas, S.; Armaroli, N.; Barigelletti, F.; Flamigni, L.; Figgemeier, E.; Vos, J. G. *Chem. Commun.* **1999**, 869–870.
(353) Encinas, S.; Flamigni, L.; Barigelletti, F.; Constable, E. C.; House-croft, C. E.; Schofield, E. R.; Figgemeier, E.; Fenske, D.; Neuburger, M.; Vos, J. G.; Zhehnder, M. *Chem.—Eur. J.* **2002**, *8*, 137–150.
(354) Constable, E. C.; Handel, R.; Housecroft, C. E.; Neuburger, M.; Schofield, E. R.; Zehnder, M. *Polyhedron* **2004**, *23*, 135–143.
(355) Hjelm, J.; Handel, R. W.; Hagfeldt, A.; Constable, E. C.; Housecroft, C. E.; Forster, R. J. *J. Phys. Chem. B* **2003**, *107*, 10431–10439.
(356) Hjelm, J.; Handel, R. W.; Hagfeldt, A.; Constable, E. C.; Housecroft, C. E.; Forster, R. J. *Inorg. Chem.* **2005**, *44*, 1073–1081.
(357) Hjelm, J.; Constable, E. C.; Figgemeier, E.; Hagfeldt, A.; Handel, R. W.; Housecroft, C. E.; Forster, R. J.; Mukhtar, E.; Schofield, E. *Chem. Commun.* **2002**, 284–285.
(358) De Nicola, A.; Ringenbach, C.; Ziessel, R. *Tetrahedron Lett.* **2003**, *44*, 183–187.
(359) Ringenbach, C.; De Nicola, A.; Ziessel, R. *J. Org. Chem.* **2003**, *68*, 4708–4719.
(360) Barbieri, A.; Ventura, B.; Barigelletti, F.; De Nicola, A.; Quesada, M.; Ziessel, R. *Inorg. Chem.* **2004**, *43*, 7359–7368.
(361) Balzani, V.; Juris, A.; Venturi, M.; Campagna, S.; Serroni, S. *Chem. Rev.* **1996**, *96*, 759–834.
(362) Houarner, C.; Blart, E.; Buvat, P.; Odobel, F. *Photochem. Photobiol. Sci.* **2005**, *4*, 200–204.
(363) Hagemann, O.; Jørgensen, M.; Krebs, F. C. *J. Org. Chem.* **2006**, *71*, 5546–5559.
(364) Bidan, G.; De Nicola, A.; Enee, V.; Guillerez, S. *Chem. Mater.* **1998**, *10*, 1052–1058.
(365) Trouillet, L.; De Nicola, A.; Guillerez, S. *Chem. Mater.* **2000**, *12*, 1611–1621.
(366) Walters, K. A.; Trouillet, L.; Guillerez, S.; Schanze, K. S. *Inorg. Chem.* **2000**, *39*, 5496–5509.
(367) Lafolet, F.; Genoud, F.; Divisia-Blohorn, B.; Aronica, C.; Guillerez, S. *J. Phys. Chem. B* **2005**, *109*, 12755–12761.
(368) Pappenfus, T. M.; Mann, K. R. *Inorg. Chem.* **2001**, *40*, 6301–6307.
(369) Barbieri, A.; Ventura, B.; Flamigni, L.; Barigelletti, F.; Fuhrmann, G.; Bäuerle, P.; Goeb, S.; Ziessel, R. *Inorg. Chem.* **2005**, *44*, 8033–8043.
(370) Liu, Y.; De Nicola, A.; Reiff, O.; Ziessel, R.; Schanze, K. S. *J. Phys. Chem. A* **2003**, *107*, 3476–3485.
(371) Bair, J. S.; Harrison, R. G. *J. Org. Chem.* **2007**, *72*, 6653–6661.
(372) Clot, O.; Wolf, M. O.; Yap, G. P. A.; Patrick, B. O. *Dalton Trans.* **2000**, 2729–2737.
(373) Moorlag, C.; Wolf, M. O.; Bohne, C.; Patrick, B. O. *J. Am. Chem. Soc.* **2005**, *127*, 6382–6393.
(374) Moorlag, C.; Clot, O.; Wolf, M. O.; Patrick, B. O. *Chem. Commun.* **2002**, 3028–3029.
(375) Moorlag, C.; Sarkar, B.; Sanrame, C. N.; Bäuerle, P.; Kaim, W.; Wolf, M. O. *Inorg. Chem.* **2006**, *45*, 7044–7046.
(376) Zhu, S. S.; Kingsborough, R. P.; Swager, T. M. *J. Mater. Chem.* **1999**, *9*, 2123–2131.
(377) Jousselme, B.; Blanchard, P.; Oçafrain, M.; Allain, M.; Levillain, E.; Roncali, J. *J. Mater. Chem.* **2004**, *14*, 421–427.
(378) Chen, C.-Y.; Wu, S.-J.; Wu, C.-G.; Chen, J.-G.; Ho, K.-C. *Angew. Chem., Int. Ed.* **2006**, *45*, 5822–5825.
(379) Chen, C.-Y.; Lu, H. C.; Wu, C. G.; Chen, J. G.; Ho, K. C. *Adv. Funct. Mater.* **2007**, *17*, 29–36.
(380) Araki, K.; Endo, H.; Masuda, G.; Ogawa, T. *Chem.—Eur. J.* **2004**, *10*, 3331–3340.
(381) Ziessel, R.; Bäuerle, P.; Ammann, M.; Barbieric, A.; Barigelletti, F. *Chem. Commun.* **2005**, 802–804.
(382) Lundin, N. J.; Blackman, A. G.; Gordon, K. C.; Officer, D. L. *Angew. Chem., Int. Ed.* **2006**, *45*, 2582–2584.
(383) Ammann, M.; Bäuerle, P. *Org. Biomol. Chem.* **2005**, *3*, 4143–4152.
(384) Bäuerle, P.; Ammann, M.; Wilde, M.; Götz, G.; Mena-Osteritz, E.; Rang, A.; Schalley, C. A. *Angew. Chem., Int. Ed.* **2007**, *46*, 363–368.
(385) Ammann, M.; Rang, A.; Schalley, C. A.; Bäuerle, P. *Eur. J. Org. Chem.* **2006**, 1940–1948.
(386) Reddinger, J. L.; Reynolds, J. R. *Macromolecules* **1997**, *30*, 673–675.
(387) Reddinger, J. L.; Reynolds, J. R. *Chem. Mater.* **1998**, *10*, 1236–1243.
(388) Reddinger, J. L.; Reynolds, J. R. *Chem. Mater.* **1998**, *10*, 3–5.
(389) Kang, B. S.; Kim, D. H.; Jung, T. S.; Jang, E. K.; Pak, Y.; Shin, S. C.; Park, D.-S.; Shim, Y.-B. *Synth. Met.* **1999**, *105*, 9–12.
(390) Higgins, T. B.; Mirkin, C. A. *Chem. Mater.* **1998**, *10*, 1589–1595.
(391) Lewis, J.; Long, N. C.; Raithby, P. R.; Shields, G. P.; Wong, W.-Y.; Younus, M. *J. Chem. Soc., Dalton Trans.* **1997**, 4283–4288.
(392) Weinberger, D. A.; Higgins, T. B.; Mirkin, C. A.; Liable-Sands, L. M.; Rheingold, A. L. *Angew. Chem., Int. Ed.* **1999**, *38*, 2565–2568.
(393) Graf, D. D.; Day, N. C.; Mann, K. R. *Inorg. Chem.* **1995**, *34*, 1562–1575.
(394) Graf, D. D.; Mann, K. R. *Inorg. Chem.* **1997**, *36*, 150–157.
(395) Clot, O.; Wolf, M. O.; Patrick, B. O. *J. Am. Chem. Soc.* **2000**, *122*, 10456–10457.
(396) Clot, O.; Wolf, M. O.; Patrick, B. O. *J. Am. Chem. Soc.* **2001**, *123*, 9963–9973.
(397) Zhu, Y.; Millet, D. B.; Wolf, M. O.; Rettig, S. J. *Organometallics* **1999**, *18*, 1930–1938.
(398) Stott, T. L.; Wolf, M. O.; Patrick, B. O. *Can. J. Chem.* **2007**, *85*, 383–391.
(399) Myrex, R. D.; Gray, G. M.; Spivey, A. G. V.; Lawson, C. M. *Organometallics* **2006**, *25*, 5045–5050.
(400) Kim, D. H.; Kim, J. H.; Kim, T. H.; Kang, D. M.; Kim, Y. H.; Shim, Y. B.; Shin, S. C. *Chem. Mater.* **2003**, *15*, 825–827.
(401) Clot, O.; Akahori, Y.; Moorlag, C.; Leznoff, D. B.; Wolf, M. O.; Batchelor, R. J.; Patrick, B. O.; Ishii, M. *Inorg. Chem.* **2003**, *42*, 2704–2713.
(402) Albano, V. G.; Bandini, M.; Barbarella, G.; Melucci, M.; Monari, M.; Piccinelli, F.; Tommasi, S.; Umani-Ronchi, A. *Chem.—Eur. J.* **2006**, *12*, 667–675.
(403) Bandini, M.; Melucci, M.; Piccinelli, F.; Sinisi, R.; Tommasi, S.; Umani-Ronchi, A. *Chem. Commun.* **2007**, 4519–4521.
(404) Bandini, M.; Piccinelli, F.; Tommasi, S.; Umani-Ronchi, A.; Ventrici, C. *Chem. Commun.* **2007**, 616–618.
(405) Albano, V. G.; Bandini, M.; Moorlag, C.; Piccinelli, F.; Pietrangelo, A.; Tommasi, S.; Umani-Ronchi, A.; Wolf, M. O. *Organometallics* **2007**, *26*, 4373–4375.
(406) Grüner, G.; Debaerdemaeker, T.; Bäuerle, P. *Chem. Commun.* **1999**, 1097–1098.
(407) Grüner, G. Ph.D. Thesis, University of Ulm, 2000.
(408) Gao, L. B.; Kan, J.; Fan, Y.; Zhang, L. Y.; Liu, S. H.; Chen, Z. N. *Inorg. Chem.* **2007**, *46*, 5651–5664.
(409) Marsella, M. J.; Newland, R. J.; Carroll, P. J.; Swager, T. M. *J. Am. Chem. Soc.* **1995**, *117*, 9842–9848.
(410) Yu, H.-H.; Xu, B.; Swager, T. M. *J. Am. Chem. Soc.* **2003**, *125*, 1142–1143.
(411) Yu, H.-H.; Pullen, A. E.; Büschel, M. G.; Swager, T. M. *Angew. Chem., Int. Ed.* **2004**, *43*, 3700–3703.
(412) Giannetto, M.; Mori, G.; Notti, A.; Pappalardo, S.; Parisi, M. F. *Chem.—Eur. J.* **2001**, *7*, 3354–3362.
(413) Rizzo, S.; Sannicolò, F.; Benincori, T.; Schiavon, G.; Zecchin, S.; Zotti, G. *J. Mater. Chem.* **2004**, *14*, 1804–1811.
(414) Vigalok, A.; Swager, T. M. *Adv. Mater.* **2002**, *14*, 368–371.
(415) Sun, X. H.; Chan, C. S.; Wong, M. S.; Wong, W. Y. *Tetrahedron* **2006**, *62*, 7846–7853.
(416) Sakamoto, K.; Takashima, Y.; Yamaguchi, H.; Harada, A. *J. Org. Chem.* **2007**, *72*, 459–465.
(417) Bäuerle, P.; Scheib, S. *Adv. Mater.* **1993**, *5*, 848–853.
(418) Scheib, S.; Bäuerle, P. *J. Mater. Chem.* **1999**, *9*, 2139–2150.
(419) Sannicolò, F.; Brenna, E.; Benincori, T.; Zotti, G.; Zecchin, S.; Schiavon, G.; Pilati, T. *Chem. Mater.* **1998**, *10*, 2167–2176.
(420) Bäuerle, P.; Scheib, S. *Acta Polym.* **1995**, *46*, 124–129.
(421) Rimmel, G.; Bäuerle, P. *Synth. Met.* **1999**, *102*, 1323–1324.
(422) Berlin, A.; Zotti, G.; Zecchin, S.; Schiavon, G. *Synth. Met.* **2002**, *131*, 149–160.
(423) Blanchard, P.; Huchet, L.; Levillain, E.; Roncali, J. *Electrochem. Commun.* **2000**, *2*, 1–5.
(424) Jousselme, B.; Blanchard, P.; Levillain, E.; Delaunay, J.; Allain, M.; Richomme, P.; Rondeau, D.; Gallego-Planas, N.; Roncali, J. *J. Am. Chem. Soc.* **2003**, *125*, 1363–1370.
(425) Demeter, D.; Blanchard, P.; Allain, M.; Grosu, I.; Roncali, J. *J. Org. Chem.* **2007**, *72*, 5285–5290.
(426) Hiller, M.; Kranz, C.; Huber, J.; Bäuerle, P.; Schuhmann, W. *Adv. Mater.* **1996**, *8*, 219–222.
(427) Faïd, K.; Leclerc, M. *J. Am. Chem. Soc.* **1998**, *120*, 5274–5278.
(428) Ho, H.-A.; Boissinot, M.; Bergeron, M. G.; Corbeil, G.; Doré, K.; Boudreau, D.; Leclerc, M. *Angew. Chem., Int. Ed.* **2002**, *41*, 1548–1551.
(429) Bäuerle, P.; Hiller, M.; Scheib, S.; Sokolowski, M.; Umbach, E. *Adv. Mater.* **1996**, *8*, 214–218.
(430) Meyer, A. Ph.D. Thesis, University of Ulm, 2000.
(431) Emge, A.; Bäuerle, P. *Synth. Met.* **1997**, *84*, 213–214.
(432) Bäuerle, P.; Emge, A. *Adv. Mater.* **1998**, *10*, 324–330.

(433) Emge, A.; Bäuerle, P. *Synth. Met.* **1999**, *102*, 1370–1373.

(434) Barbarella, G. *Chem.—Eur. J.* **2002**, *8*, 5072–5077.

(435) Barbarella, G.; Zambianchi, M.; Pudova, O.; Paladini, V.; Ventola, A.; Cipriani, F.; Gigli, G.; Cingolani, R.; Citro, G. *J. Am. Chem. Soc.* **2001**, *123*, 11600–11607.

(436) Sotgiu, G.; Zambianchi, M.; Barbarella, G.; Aruffo, F.; Cipriani, F.; Ventola, A. *J. Org. Chem.* **2003**, *68*, 1512–1520.

(437) Klok, H. A.; Rösler, A.; Götz, G.; Mena-Osteritz, E.; Bäuerle, P. *Org. Biomol. Chem.* **2004**, *2*, 3541–3544.

(438) Kirschbaum, T.; Briehn, C. A.; Bäuerle, P. *J. Chem. Soc., Perkin Trans. 1* **2000**, 1211–1216.

(439) Kirschbaum, T.; Bäuerle, P. *Synth. Met.* **2001**, *119*, 127–128.

(440) Strässler, C.; Davis, N. E.; Kool, E. T. *Helv. Chim. Acta* **1999**, *82*, 2160–2171.

(441) Kawai, K.; Sugimoto, A.; Yoshida, H.; Tojo, S.; Fujitsuka, M.; Majima, T. *Bioorg. Med. Chem. Lett.* **2005**, *15*, 4547–4549.

(442) Capobianco, M. L.; Naldi, M.; Zambianchi, M.; Barbarella, G. *Tetrahedron Lett.* **2005**, *46*, 8181–8184.

(443) Barbarella, G.; Zambianchi, M.; Sotgiu, G.; Ventola, A.; Galeotti, M.; Gigli, G.; Cazzato, A.; Capobianco, M. L. *J. Non-Cryst. Solids* **2006**, *352*, 2465–2467.

(444) Barbarella, G.; Zambianchi, M.; Ventola, A.; Fabiano, E.; DellaSala, F.; Gigli, G.; Anni, M.; Bolognesi, A.; Polito, L.; Naldi, M.; Capobianco, M. *Bioconjugate Chem.* **2006**, *17*, 58–67.

(445) Zambianchi, M.; Barbieri, A.; Ventola, A.; Favaretto, L.; Bettini, C.; Galeotti, M.; Barbarella, G. *Bioconjugate Chem.* **2007**, *18*, 1004–1009.

(446) Herland, A.; Nilsson, K. P. R.; Olsson, J. D. M.; Hammarström, P.; Konradsson, P.; Inganäs, O. *J. Am. Chem. Soc.* **2005**, *127*, 2317–2323.

(447) Herland, A.; Björk, P.; Nilsson, K. P. R.; Olsson, J. D. M.; Åsberg, P.; Konradsson, P.; Hammarström, P.; Inganäs, O. *Adv. Mater.* **2005**, *17*, 1466–1471.

(448) Mouffouk, F.; Brown, S. J.; Demetriou, A. M.; Higgins, S. J.; Nichols, R. J.; Rajapakse, R. M. G.; Reeman, S. *J. Mater. Chem.* **2005**, *15*, 1186–1196.

(449) Nakazumi, H.; Ohta, T.; Etoh, H.; Uno, T.; Colyer, C. L.; Hyodo, Y.; Yagi, S. *Synth. Met.* **2005**, *153*, 33–36.

(450) Xiang, Z.; Nesterov, E. E.; Skoch, J.; Lin, T.; Hyman, B. T.; Swager, T. M.; Bacskai, B. J.; Reeves, S. A. *J. Histochem. Cytochem.* **2005**, *53*, 1511–1516.

(451) Nesterov, E. E.; Skoch, J.; Hyman, B. T.; Klunk, W. E.; Bacskai, B. J.; Swager, T. M. *Angew. Chem., Int. Ed.* **2005**, *44*, 5452–5456.

(452) Kertesz, M.; Choi, C. H.; Yang, S. *Chem. Rev.* **2005**, *105*, 3448–3481.

(453) Wudl, F.; Kobayashi, M.; Heeger, A. J. *J. Org. Chem.* **1984**, *49*, 3382–3384.

(454) Neugebauer, H.; Kvarnstrom, C.; Brabec, C.; Sariciftci, N. S.; Kiebooms, R.; Wudl, F.; Luzzati, S. *J. Chem. Phys.* **1999**, *110*, 12108–12115.

(455) Lee, B. L.; Yamamoto, T. *Macromolecules* **1999**, *32*, 1375–1382.

(456) Kobayashi, M.; Chen, J.; Chung, T. C.; Moraes, F.; Heeger, A. J.; Wudl, F. *Synth. Met.* **1984**, *9*, 77–86.

(457) Kobayashi, M.; Colaneri, N.; Boysel, M.; Wudl, F.; Heeger, A. J. *J. Chem. Phys.* **1985**, *82*, 5717–5723.

(458) Pomerantz, M.; Chaloner-Gill, B.; Harding, L. O.; Tseng, J. J.; Pomerantz, W. J. *Synth. Met.* **1993**, *55*, 960–965.

(459) Vangeneugden, D. L.; Kiebooms, R. H. L.; Vanderzande, D. J. M.; Gelan, J. M. J. V. *Synth. Met.* **1999**, *101*, 120–121.

(460) Hung, T.-T.; Chen, S.-A. *Polymer* **1999**, *40*, 3881–3884.

(461) Lorcy, D.; Cava, M. P. *Adv. Mater.* **1992**, *4*, 562–564.

(462) Bäuerle, P.; Götz, G.; Emele, P.; Port, H. *Adv. Mater.* **1992**, *4*, 564–568.

(463) Musmanni, S.; Ferraris, J. P. *J. Chem. Soc., Chem. Commun.* **1993**, 172–174.

(464) Kiebooms, R. H. L.; Adriaensens, P. J. A.; Vanderzande, D. J. M.; Gelan, J. M. J. V. *J. Org. Chem.* **1997**, *62*, 1473–1480.

(465) Ikenoue, Y. *Synth. Met.* **1990**, *35*, 263–270.

(466) Lakshmikantham, M. V.; Lorcy, D.; Scordilis-Kelley, C.; Wu, X.-L.; Parakka, J. P.; Metzger, R. M.; Cava, M. P. *Adv. Mater.* **1993**, *5*, 723–726.

(467) Mitschke, U.; Bäuerle, P. *J. Chem. Soc., Perkin Trans. 1* **2001**, 740–753.

(468) Bäuerle, P. The Synthesis of Oligothiophenes. In *Handbook of Oligo and Polythiophenes*; Fichou, D., Ed.; Wiley-VCH: Weinheim, 1999; pp 89–181.

(469) Mohanakrishnan, A. K.; Amaladass, P.; Arul Clement, J. *Tetrahedron Lett.* **2007**, *48*, 779–784.

(470) Mohanakrishnan, A. K.; Lakshmikantham, M. V.; McDougal, C.; Cava, M. P.; Baldwin, J. W.; Metzger, R. M. *J. Org. Chem.* **1998**, *63*, 3105–3112.

(471) Kisselev, R.; Thelakkat, M. *Chem. Commun.* **2002**, 1530–1531.

(472) Vangeneugden, D. L.; Vanderzande, D. J. M.; Salbeck, J.; van Hal, P. A.; Janssen, R. A. J.; Hummelen, J. C.; Brabec, C. J.; Shaheen, S. E.; Sariciftci, N. S. *J. Phys. Chem. B* **2001**, *105*, 11106–11113.

(473) Meng, H.; Wudl, F. *Macromolecules* **2001**, *34*, 1810–1816.

(474) Meng, H.; Tucker, D.; Chaffins, S.; Chen, Y.; Helgeson, R.; Dunn, B.; Wudl, F. *Adv. Mater.* **2003**, *15*, 146–149.

(475) Sonmez, G.; Meng, H.; Wudl, F. *Chem. Mater.* **2003**, *15*, 4923–4929.

(476) Nicolas, Y.; Blanchard, P.; Roncali, J.; Allain, M.; Mercier, N.; Deman, A. L.; Tardy, J. *Org. Lett.* **2005**, *7*, 3513–3516.

(477) Deman, A. L.; Tardy, J.; Nicolas, Y.; Blanchard, P.; Roncali, J. *Synth. Met.* **2004**, *146*, 365–371.

(478) Laquindanum, J. G.; Katz, H. E.; Lovinger, A. J. *J. Am. Chem. Soc.* **1998**, *120*, 664–672.

(479) Payne, M. M.; Odom, S. A.; Parkin, S. R.; Anthony, J. E. *Org. Lett.* **2004**, *6*, 3325–3328.

(480) Payne, M. M.; Parkin, S. R.; Anthony, J. E.; Kuo, C. C.; Jackson, T. N. *J. Am. Chem. Soc.* **2005**, *127*, 4986–4987.

(481) Lloyd, M. T.; Mayer, A. C.; Subramanian, S.; Mourey, D. A.; Herman, D. J.; Bapat, A. V.; Anthony, J. E.; Malliaras, G. G. *J. Am. Chem. Soc.* **2007**, *129*, 9144–9149.

(482) Yamamoto, T.; Takimiya, K. *J. Am. Chem. Soc.* **2007**, *129*, 2224–2225.

(483) Takimiya, K.; Ebata, H.; Sakamoto, K.; Izawa, T.; Otsubo, T.; Kunugi, Y. *J. Am. Chem. Soc.* **2006**, *128*, 12604–12605.

(484) Laquindanum, J. G.; Katz, H. E.; Lovinger, A. J.; Dodabalapur, A. *Adv. Mater.* **1997**, *9*, 36–39.

(485) Pan, H.; Li, Y.; Wu, Y.; Liu, P.; Ong, B. S.; Zhu, S.; Xu, G. *J. Am. Chem. Soc.* **2007**, *129*, 4112–4113.

(486) Takimiya, K.; Kunugi, Y.; Ebata, H.; Otsubo, T. *Chem. Lett.* **2006**, *35*, 1200–1201.

(487) Liu, W. J.; Zhou, Y.; Ma, Y.; Cao, Y.; Wang, J.; Pei, J. *Org. Lett.* **2007**, *9*, 4187–4190.

(488) Zhou, Y.; Liu, W. J.; Ma, Y.; Wang, H.; Qi, L.; Cao, Y.; Wang, J.; Pei, J. *J. Am. Chem. Soc.* **2007**, *129*, 12386–12387.

(489) Nicolas, Y.; Blanchard, P.; Levillain, E.; Allain, M.; Mercier, N.; Roncali, J. *Org. Lett.* **2004**, *6*, 273–276.

(490) De Bettignies, R.; Nicolas, Y.; Blanchard, P.; Levillain, E.; Nunzi, J.-M.; Roncali, J. *Adv. Mater.* **2003**, *15*, 1939–1943.

(491) Ferraris, J. P.; Bravo, A.; Kim, W.; Hrncir, D. C. *J. Chem. Soc., Chem. Commun.* **1994**, 991–992.

(492) Pomerantz, M.; Chaloner-Gill, B.; Harding, L. O.; Tseng, J. J.; Pomerantz, W. J. *J. Chem. Soc., Chem. Commun.* **1992**, 1672–1673.

(493) Kastner, J.; Kuzmany, H.; Vegh, D.; Landl, M.; Cuff, L.; Kertesz, M. *Macromolecules* **1995**, *28*, 2922–2929.

(494) Armand, J.; Bellec, C.; Boulares, L.; Chaquin, P.; Masure, D.; Pinson, J. *J. Org. Chem.* **1991**, *56*, 4840–4845.

(495) Kenning, D. D.; Mitchell, K. A.; Calhoun, T. R.; Funfar, M. R.; Sattler, D. J.; Rasmussen, S. C. *J. Org. Chem.* **2002**, *67*, 9073–9076.

(496) Kenning, D. D.; Rasmussen, S. C. *Macromolecules* **2003**, *36*, 6298–6299.

(497) Kitamura, C.; Tanaka, S.; Yamashita, Y. *J. Chem. Soc., Chem. Commun.* **1994**, 1585–1586.

(498) Campos, L. M.; Tontcheva, A.; Günes, S.; Sonmez, G.; Neugebauer, H.; Sariciftci, N. S.; Wudl, F. *Chem. Mater.* **2005**, *17*, 4031–4033.

(499) Akoudad, S.; Roncali, J. *Chem. Commun.* **1998**, 2081–2082.

(500) Perepichka, I. F.; Levillain, E.; Roncali, J. *J. Mater. Chem.* **2004**, *14*, 1679–1681.

(501) Berlin, A.; Zotti, G.; Zecchin, S.; Schiavon, G.; Vercelli, B.; Zanelli, A. *Chem. Mater.* **2004**, *16*, 3667–3676.

(502) Casado, J.; Ortiz, R. P.; Ruiz Delgado, M. C.; Hern, V.; López Navarrete, J. T.; Raimundo, J. M.; Blanchard, P.; Allain, M.; Roncali, J. *J. Phys. Chem. B* **2005**, *109*, 16616–16627.

(503) Sonmez, G. *Chem. Commun.* **2005**, 5251–5259.

(504) Sonmez, G.; Wudl, F. *J. Mater. Chem.* **2005**, *15*, 20–22.

(505) Sonmez, G.; Sonmez, H. B.; Shen, C. K. F.; Jost, R. W.; Rubin, Y.; Wudl, F. *Macromolecules* **2005**, *38*, 669–675.

(506) Sonmez, G.; Sonmez, H. B.; Shen, C. K. F.; Wudl, F. *Adv. Mater.* **2004**, *16*, 1905–1908.

(507) Sonmez, G.; Shen, C. K. F.; Rubin, Y.; Wudl, F. *Angew. Chem., Int. Ed.* **2004**, *43*, 1498–1502.

(508) Wienk, M. M.; Turbiez, M. G. R.; Struijk, M. P.; Fonrodona, M.; Janssen, R. A. J. *Appl. Phys. Lett.* **2006**, *88*, 153511(1)153511(3)..

(509) Nishida, J. I.; Murakami, S.; Tada, H.; Yamashita, Y. *Chem. Lett.* **2006**, *35*, 1236–1237.

(510) Blanco, R.; Gomez, R.; Seoane, C.; Segura, J. L.; Mena-Osteritz, E.; Bäuerle, P. *Org. Lett.* **2007**, *9*, 2171–2174.

(511) Tanaka, S.; Yamashita, Y. *Synth. Met.* **1993**, *55*, 1251–1254.

(512) Tanaka, S.; Yamashita, Y. *Synth. Met.* **1995**, *69*, 599–600.

(513) Tanaka, S.; Yamashita, Y. *Synth. Met.* **1997**, *84*, 229–230.

(514) Ruiz Delgado, M. C.; Hernández, V.; López Navarrete, J. T.; Tanaka, S.; Yamashita, Y. *J. Phys. Chem. B* **2004**, *108*, 2516–2526.

(515) Kitamura, C.; Tanaka, S.; Yamashita, Y. *Chem. Mater*. **1996**, *8*, 570–578.
(516) Wienk, M. M.; Struijk, M. P.; Janssen, R. A. J. *Chem. Phys. Lett*. **2006**, *422*, 488–491.
(517) Bundgaard, E.; Krebs, F. C. *Macromolecules* **2006**, *39*, 2823–2831.
(518) Ishii, A.; Nakayama, J.; Kazami, J.; Ida, Y.; Nakamura, T.; Hoshino, M. *J. Org. Chem*. **1991**, *56*, 78–82.
(519) Wynberg, H.; Zwanenburg, D. J. *Tetrahedron Lett*. **1967**, *8*, 761–764.
(520) Pomerantz, M.; Gu, X. *Synth. Met*. **1997**, *84*, 243–244.
(521) Pomerantz, M.; Gu, X.; Zhang, S. X. *Macromolecules* **2001**, *34*, 1817–1822.
(522) Neef, C. J.; Brotherston, I. D.; Ferraris, J. P. *Chem. Mater*. **1999**, *11*, 1957–1958.
(523) Lee, K.; Sotzing, G. A. *Macromolecules* **2001**, *34*, 5746–5747.
(524) Sotzing, G. A.; Lee, K. *Macromolecules* **2002**, *35*, 7281–7286.
(525) Kumar, A.; Buyukmumcu, Z.; Sotzing, G. A. *Macromolecules* **2006**, *39*, 2723–2725.
(526) Lee, B.; Seshadri, V.; Palko, H.; Sotzing, G. A. *Adv. Mater*. **2005**, *17*, 1792–1795.
(527) Lee, B.; Seshadri, V.; Sotzing, G. A. *Langmuir* **2005**, *21*, 10797–10802.
(528) Lee, B.; Seshadri, V.; Sotzing, G. A. *Synth. Met*. **2005**, *152*, 177–180.
(529) Lee, B.; Yavuz, M. S.; Sotzing, G. A. *Macromolecules* **2006**, *39*, 3118–3124.
(530) Seshadri, V.; Wu, L.; Sotzing, G. A. *Langmuir* **2003**, *19*, 9479–9485.
(531) Danieli, R.; Taliani, C.; Zamboni, R.; Giro, G.; Biserni, M.; Mastragostino, M.; Testoni, A. *Synth. Met*. **1986**, *13*, 325–328.
(532) Rutherford, D. R.; Stille, J. K.; Elliott, C. M.; Reichert, V. R. *Macromolecules* **1992**, *25*, 2294–2306.
(533) Fuller, L. S.; Iddon, B.; Smith, K. A. *J. Chem. Soc., Perkin Trans. 1* **1997**, 3465–3470.
(534) Lim, E.; Jung, B.-J.; Shim, H.-K. *Macromolecules* **2003**, *36*, 4288–4293.
(535) Lim, E.; Jung, B.-J.; Lee, J.; Shim, H.-K.; Lee, J.-I.; Yang, Y. S.; Do, L.-M. *Macromolecules* **2005**, *38*, 4531–4535.
(536) Zotti, G.; Zecchin, S.; Vercelli, B.; Berlin, A.; Grimoldi, S.; Groenendaal, L.; Bertoncello, R.; Natali, M. *Chem. Mater*. **2005**, *17*, 3681–3694.
(537) Noh, Y.-Y.; Kim, D.-Y.; Yoshida, Y.; Yase, K.; Jung, B.-J.; Lim, E.; Shim, H.-K.; Azumi, R. *J. Appl. Phys*. **2005**, *97*, 104504–7.
(538) Noh, Y.-Y.; Kim, D.-Y.; Yoshida, Y.; Yase, K.; Jung, B.-J.; Lim, E.; Shim, H.-K.; Azumi, R. *Appl. Phys. Lett*. **2004**, *85*, 2953–2955.
(539) Noh, Y.-Y.; Kim, D.-Y.; Yoshida, Y.; Yase, K.; Jung, B.-J.; Lim, E.; Shim, H.-K. *Appl. Phys. Lett*. **2005**, *86*, 043501(1)043501(3)..
(540) Kim, H. S.; Kim, Y. H.; Kim, T. H.; Noh, Y. Y.; Pyo, S.; Yi, M. H.; Kim, D. Y.; Kwon, S. K. *Chem. Mater*. **2007**, *19*, 3561–3567.
(541) Kim, K. H.; Chi, Z.; Cho, M. J.; Jin, J.-I.; Cho, M. Y.; Kim, S. J.; Joo, J.-S.; Choi, D. H. *Chem. Mater*. **2007**, *19*, 4925–4932.
(542) San Miguel, L.; Matzger, A. J. *Macromolecules* **2007**, *40*, 9233–9237.
(543) Zhang, X.; Köhler, M.; Matzger, A. J. *Macromolecules* **2004**, *37*, 6306–6315.
(544) McCulloch, I.; Heeney, M.; Bailey, C.; Genevicius, K.; MacDonald, I.; Shkunov, M.; Sparrowe, D.; Tierney, S.; Wagner, R.; Zhang, W.; Chabinyc, M. L.; Kline, R. J.; McGehee, M. D.; Toney, M. F. *Nat. Mater*. **2006**, *5*, 328–333.
(545) Turbiez, M.; Frére, P.; Leriche, P.; Mercier, N.; Roncali, J. *Chem. Commun*. **2005**, 1161–1163.
(546) San Miguel, L.; Porter, W. W.; Matzger, A. J. *Org. Lett*. **2007**, *9*, 1005–1008.
(547) Zhang, X.; Johnson, J. P.; Kampf, J. W.; Matzger, A. J. *Chem. Mater*. **2006**, *18*, 3470–3476.
(548) Heeney, M.; Bailey, C.; Genevicius, K.; Shkunov, M.; Sparrowe, D.; Tierney, S.; McCulloch, I. *J. Am. Chem. Soc*. **2005**, *127*, 1078–1079.
(549) Shkunov, M.; Simms, R.; Heeney, M.; Tierney, S.; McCulloch, I. *Adv. Mater*. **2005**, *17*, 2608–2612.
(550) Heeney, M.; McCulloch, I.; Bailey, C. U.S. Patent 0,090,640, 2005.
(551) Hergué, N.; Frère, P. *Org. Biomol. Chem*. **2007**, *5*, 3442–3449.
(552) Li, X.-C.; Sirringhaus, H.; Garnier, F.; Holmes, A. B.; Moratti, S. C.; Feeder, N.; Clegg, W.; Teat, S. J.; Friend, R. H. *J. Am. Chem. Soc*. **1998**, *120*, 2206–2207.
(553) Gao, J.; Li, R.; Li, Q.; Meng, Q.; Jiang, H.; Li, H.; Hu, W. *Adv. Mater*. **2007**, *19*, 3008–3011.
(554) Sun, Y.; Ma, Y. Q.; Liu, Y. Q.; Lin, Y. Y.; Wang, Z.; Wang, Y.; Di, C. A.; Xiao, K.; Chen, X.; Qiu, W.; Zhang, B.; Yu, G.; Hu, W.; Zhu, D. *Adv. Funct. Mater*. **2006**, *16*, 426–432.
(555) Iosip, M. D.; Destri, S.; Pasini, M.; Porzio, W.; Pernstich, K. P.; Batlogg, B. *Synth. Met*. **2004**, *146*, 251–257.
(556) Takimiya, K.; Niihara, N.; Otsubo, T. *Synthesis* **2005**, 1589–1592.

(557) Cicoira, F.; Santato, C.; Melucci, M.; Favaretto, L.; Gazzano, M.; Muccini, M.; Barbarella, G. *Adv. Mater*. **2006**, *18*, 169–174.
(558) Mazzeo, M.; Vitale, V.; Sala, F. D.; Anni, M.; Barbarella, G.; Fabaretto, L.; Sotgiu, G.; Cingolani, R.; Gigli, G. *Adv. Mater*. **2005**, *17*, 34–39.
(559) Ortiz, R. P.; Ruiz Delgado, M. C.; Casado, J.; Hernández, V.; Kim, O.-K.; Woo, H. Y.; López Navarrete, J. T. *J. Am. Chem. Soc*. **2004**, *126*, 13363–13376.
(560) Kim, O. K.; Lee, K. S.; Woo, H. Y.; Kim, K. S.; He, G. S.; Swiatkiewicz, J.; Prasad, P. N. *Chem. Mater*. **2000**, *12*, 284–286.
(561) Lee, K.-S.; Yang, D.-Y.; Park, S. H.; Kim, R. H. *Polym. Adv. Technol*. **2006**, *17*, 72–82.
(562) Barbarella, G.; Favaretto, L.; Sotgiu, G.; Antolini, L.; Gigli, G.; Cingolani, R.; Bongini, A. *Chem. Mater*. **2001**, *13*, 4112–4122.
(563) Tedesco, E.; Sala, F. D.; Favaretto, L.; Barbarella, G.; Albesa-Jove, D.; Pisignano, D.; Gigli, G.; Cingolani, R.; Harris, K. D. M. *J. Am. Chem. Soc*. **2003**, *125*, 12277–12283.
(564) Sotgiu, G.; Barbarella, G. *J. Org. Chem*. **2007**, *72*, 4925–4931.
(565) Murata, H.; Kafafi, Z. H.; Uchida, M. *Appl. Phys. Lett*. **2002**, *80*, 189–191.
(566) Ohshita, J.; Kai, H.; Takata, A.; Iida, T.; Kunai, A.; Ohta, N.; Komaguchi, K.; Shiotani, M.; Adachi, A.; Sakamaki, K.; Okita, K. *Organometallics* **2001**, *20*, 4800–4805.
(567) Lee, T.; Jung, I.; Song, K. H.; Lee, H.; Choi, J.; Lee, K.; Lee, B. J.; Pak, J. Y.; Lee, C.; Kang, S. O.; Ko, J. *Organometallics* **2004**, *23*, 5280–5285.
(568) Ohshita, J.; Sumida, T.; Kunai, A.; Adachi, A.; Sakamaki, K.; Okita, K. *Macromolecules* **2000**, *33*, 8890–8893.
(569) Liu, M. S.; Luo, J.; Jen, A. K.-Y. *Chem. Mater*. **2003**, *15*, 3496–3500.
(570) Coppo, P.; Turner, M. L. *J. Mater. Chem*. **2005**, *15*, 1123–1133.
(571) Zotti, G.; Schiavon, G.; Berlin, A.; Fontana, G.; Pagani, G. *Macromolecules* **1994**, *27*, 1938–1942.
(572) Lambert, T. L.; Ferraris, J. P. *J. Chem. Soc., Chem. Commun*. **1991**, 752–754.
(573) Ferraris, J. P.; Lambert, T. L. *J. Chem. Soc., Chem. Commun*. **1991**, 1268–1270.
(574) Kozaki, M.; Tanaka, S.; Yamashita, Y. *J. Org. Chem*. **1994**, *59*, 442–450.
(575) Benincori, T.; Consonni, V.; Gramatica, P.; Pilati, T.; Rizzo, S.; Sannicolo, F.; Todeschini, R.; Zotti, G. *Chem. Mater*. **2001**, *13*, 1665–1673.
(576) Loganathan, K.; Cammisa, E. G.; Myron, B. D.; Pickup, P. G. *Chem. Mater*. **2003**, *15*, 1918–1923.
(577) Loganathan, K.; Pickup, P. G. *Electrochim. Acta* **2005**, *51*, 41–46.
(578) Ogawa, K.; Rasmussen, S. C. *J. Org. Chem*. **2003**, *68*, 2921–2928.
(579) Berlin, A.; Pagani, G.; Zotti, G.; Schiavon, G. *Makromol. Chem*. **1992**, *193*, 399–409.
(580) Radke, K. R.; Ogawa, K.; Rasmussen, S. C. *Org. Lett*. **2005**, *7*, 5253–5256.
(581) Koeckelberghs, G.; DeCremer, L.; Vanormelingen, W.; Verbiest, T.; Persoons, A.; Samyn, C. *Macromolecules* **2005**, *38*, 4545–4547.
(582) Baumgartner, T.; Wilk, W. *Org. Lett*. **2006**, *8*, 503–506.
(583) Neumann, T.; Dienes, Y.; Baumgartner, T. *Org. Lett*. **2006**, *8*, 495–497.
(584) Baumgartner, T.; Bergmans, W.; Kárpáti, T.; Neumann, T.; Nieger, M.; Nyulászi, L. *Chem.—Eur. J*. **2005**, *11*, 4687–4699.
(585) Zhang, X.; Côtè, A. P.; Matzger, A. J. *J. Am. Chem. Soc*. **2005**, *127*, 10502–10503.
(586) Sato, N.; Mazaki, Y.; Kobayashi, K.; Kobayashi, T. *J. Chem. Soc., Perkin Trans. 2* **1992**, 765–770.
(587) Mazaki, Y.; Kobayashi, K. *Tetrahedron Lett*. **1989**, *30*, 3315–3318.
(588) Xiao, K.; Liu, Y.; Qi, T.; Zhang, W.; Wang, F.; Gao, J.; Qiu, W.; Ma, Y.; Cui, G.; Chen, S.; Zhan, X.; Yu, G.; Qin, J.; Hu, W.; Zhu, D. *J. Am. Chem. Soc*. **2005**, *127*, 13281–13286.
(589) He, M.; Zhang, F. *J. Org. Chem*. **2007**, *72*, 442–451.
(590) Okamoto, T.; Kudoh, K.; Wakamiya, A.; Yamaguchi, S. *Chem.—Eur. J*. **2007**, *13*, 548–556.
(591) Okamoto, T.; Kudoh, K.; Wakamiya, A.; Yamaguchi, S. *Org. Lett*. **2005**, *7*, 5301–5304.
(592) Yamaguchi, S.; Xu, C.; Okamoto, T. *Pure Appl. Chem*. **2006**, *78*, 721–730.
(593) Yamada, K.; Okamoto, T.; Kudoh, K.; Wakamiya, A.; Yamaguchi, S.; Takeya, J. *Appl. Phys. Lett*. **2007**, *90*, 072102(1)072102(3)..
(594) Oyaizu, K.; Iwasaki, T.; Tsukahara, Y.; Tsuchida, E. *Macromolecules* **2004**, *37*, 1257–1270.
(595) Zhang, X.; Matzger, A. J. *J. Org. Chem*. **2003**, *68*, 9813–9815.
(596) Janssen, M. J.; Jong, F. D. *J. Org. Chem*. **1971**, *36*, 1645–1648.
(597) Miyasaka, M.; Rajca, A. *J. Org. Chem*. **2006**, *71*, 3264–3266.
(598) Nenajdenko, V. G.; Sumerin, V. V.; Chernichenko, K. Y.; Balenkova, E. S. *Org. Lett*. **2004**, *6*, 3437–3439.

(599) Chernichenko, K. Y.; Sumerin, V. V.; Shpanchenko, R. V.; Balenkova, E. S.; Nenajdenko, V. G. *Angew. Chem., Int. Ed.* **2006**, *45*, 7367–7370.

(600) Kabir, S. M. H.; Miura, M.; Sasaki, S.; Harada, G.; Kuwatani, Y.; Yoshida, M.; Iyoda, M. *Heterocycles* **2000**, *52*, 761–774.

(601) Rajca, A.; Miyasaka, M.; Pink, M.; Wang, H.; Rajca, S. *J. Am. Chem. Soc.* **2004**, *126*, 15211–15222.

(602) Rajca, A.; Wang, H.; Pink, M.; Rajca, S. *Angew. Chem., Int. Ed.* **2000**, *39*, 4481–4483.

(603) Miyasaka, M.; Rajca, A.; Pink, M.; Rajca, S. *J. Am. Chem. Soc.* **2005**, *127*, 13806–13807.

(604) Miyasaka, M.; Rajca, A.; Pink, M.; Rajca, S. *Chem.—Eur. J.* **2004**, *10*, 6531–6539.

(605) Shepherd, M. K. *J. Chem. Soc., Chem. Commun.* **1985**, 880–881.

(606) Hart, H.; Sasaoka, M. *J. Am. Chem. Soc.* **1978**, *100*, 4326–4327.

(607) Patra, A.; Wijsboom, Y. H.; Shimon, L. J. W.; Bendikov, M. *Angew. Chem., Int. Ed.* **2007**, *46*, 8814–8818.

(608) Jayasuriya, N.; Kagan, J.; Owens, J. E.; Kornak, E. P.; Perrine, D. M. *J. Org. Chem.* **1989**, *54*, 4203–4205.

(609) Proetzsch, R.; Bieniek, D.; Korte, F. *Tetrahedron Lett.* **1972**, *13*, 543–544.

(610) Imamura, K.; Takimiya, K.; Otsubo, T.; Aso, Y. *Chem. Commun.* **1999**, 1859–1860.

(611) Kauffmann, T.; Greving, B.; König, J.; Mitschker, A.; Woltermann, A. *Angew. Chem., Int. Ed.* **1975**, *14*, 713–714.

(612) Irngartinger, H.; Huber-Patz, U.; Rodewald, H. *Acta Crystallogr., Sect. C: Cryst. Struct. Commun.* **1985**, *C41*, 1088–1089.

(613) Zhou, Z.-H.; Yamamoto, T. *J. Organomet. Chem.* **1991**, *414*, 119–127.

(614) Kauffmann, T. *Angew. Chem., Int. Ed.* **1979**, *18*, 1–19.

(615) Marsella, M. J.; Reid, R. J. *Macromolecules* **1999**, *32*, 5982–5984.

(616) Marsella, M. J. *Acc. Chem. Res.* **2002**, *35*, 944–951.

(617) Marsella, M. J.; Kim, I. T.; Tham, F. *J. Am. Chem. Soc.* **2000**, *122*, 974–975.

(618) Marsella, M. J.; Yoon, K.; Tham, F. S. *Org. Lett.* **2001**, *3*, 2129–2131.

(619) Tol, A. J. W. *Synth. Met.* **1995**, *74*, 95–98.

(620) Zhao, D.; Moore, J. S. *Chem. Commun.* **2003**, 807–818.

(621) Grave, C.; Schlüter, A. D. *Eur. J. Org. Chem.* **2002**, 3075–3098.

(622) Höger, S. *J. Polym. Sci., A: Polym. Chem.* **1999**, *37*, 2685–2698.

(623) De Meijere, A.; Kozhushkov, S. I. *Top. Curr. Chem.* **1999**, *201*, 1–42.

(624) Haley, M. M.; Pak, J. J.; Brand, S. C. *Top. Curr. Chem.* **1999**, *201*, 81–130.

(625) Krömer, J.; Rios-Carreras, I.; Fuhrmann, G.; Musch, C.; Wunderlin, M.; Debaerdemacker, T.; Mena-Osteritz, E.; Bäuerle, P. *Angew. Chem., Int. Ed.* **2000**, *39*, 3481–3486.

(626) Fuhrmann, G.; Krömer, J.; Bäurele, P. *Synth. Met.* **2001**, *119*, 125–126.

(627) Fuhrmann, G. Ph.D. Thesis, University of Ulm, 2006.

(628) Perrine, D. M.; Kagan, J. *Heterocycles* **1986**, *24*, 365–368.

(629) Krömer, J.; Bäuerle, P. *Tetrahedron* **2001**, *57*, 3785–3794.

(630) Kauffmann, T.; Greving, B.; Kriegesmann, R.; Mitschker, A.; Woltermann, A. *Chem. Ber.* **1978**, *111*, 1330–1336.

(631) Kauffmann, T.; Mackowiak, H. P. *Chem. Ber.* **1985**, *118*, 2343–2352.

(632) Jung, S.-H.; Pisula, W.; Rouhanipour, A.; Räder, H. J.; Josemon, J.; Müllen, K. *Angew. Chem., Int. Ed.* **2006**, *45*, 4685–4690.

(633) Desiraju, G. R. *Nature* **2001**, *412*, 397–400.

(634) Schneider, H.-J.; Yatsimirsky, A. *Principles and Methods in Supramolecular Chemistry*; Wiley, Chicester, 1999.

(635) *Comprehensive Supramolecular Chemistry*; Atwood, J. L., Davies, J. E. D., MacNicol, D. D., Vögtle, F., Eds.; Pergamon: Oxford, 1996.

(636) Lehn, J.-M. *Supramolecular Chemistry*; VCH: Weinheim, 1995.

(637) Mascal, M. *Contemp. Org. Synth.* **1994**, *1*, 31–46.

(638) Lehn, J.-M. *Science* **1985**, *227*, 849–856.

(639) Fujita, M. *Chem. Soc. Rev.* **1998**, *27*, 417–425.

(640) Leininger, S.; Olenyuk, B.; Stang, P. J. *Chem. Rev.* **2000**, *100*, 853–908.

(641) Holliday, B. J.; Mirkin, C. A. *Angew. Chem., Int. Ed.* **2001**, *40*, 2022–2043.

(642) Rossi, R.; Carpita, A.; Bigelli, C. *Tetrahedron Lett.* **1985**, *26*, 523–526.

(643) Liu, Q.; Burton, D. J. *Tetrahedron Lett.* **1997**, *38*, 4371–4374.

(644) Fuhrmann, G.; Debaerdemaeker, T.; Bäuerle, P. *Chem. Commun.* **2003**, 948–949.

(645) Mena-Osteritz, E.; Bäuerle, P. *Adv. Mater.* **2001**, *13*, 243–246.

(646) Mena-Osteritz, E. *Adv. Mater.* **2002**, *14*, 609–616.

(647) Hoofman, R. J. O. M.; de Haas, M. P.; Siebbeles, L. D. A.; Warman, J. M. *Nature* **1998**, *392*, 54–56.

(648) Sirringhaus, H.; Brown, P. J.; Friend, R. H.; Nielsen, M. M.; Bechgaard, K.; Langeveld-Voss, B. M. W.; Spiering, A. J. H.;

(649) Janssen, R. A. J.; Meijer, E. W.; Herwig, P.; de Leeuw, D. M. *Nature* **1999**, *401*, 685–688.

(649) Engelkamp, H.; Middelbeek, S.; Nolte, R. J. M. *Science* **1999**, *284*, 785–788.

(650) Chi, L. F.; Jacobi, S.; Anczykowski, B.; Overs, M.; Schäfer, H. J.; Fuchs, H. *Adv. Mater.* **2000**, *12*, 25–30.

(651) Kolb, G.; Engelmann, G. E.; Ziegler, J. C. *Angew. Chem., Int. Ed.* **2000**, *39*, 1123–1125.

(652) Maruccio, G.; Cingolani, R.; Rinaldi, R. *J. Mater. Chem.* **2004**, *14*, 542–554.

(653) Bednarz, M.; Reineker, P.; Mena-Osteritz, E.; Bäuerle, P. *J. Lumin.* **2004**, *110*, 225–231.

(654) Bhaskar, A.; Ramakrishna, G.; Hagedorn, K.; Varnavski, O.; Mena-Osteritz, E.; Bäuerle, P.; Goodson, T., III *J. Phys. Chem. B* **2007**, *111*, 946–954.

(655) Zade, S. S.; Bendikov, M. *J. Org. Chem.* **2006**, *71*, 2972–2981.

(656) Fabian, J.; Hartmann, H. *J. Phys. Org. Chem.* **2007**, *20*, 554–567.

(657) Marsella, M. J.; Piao, G.; Tham, F. S. *Synthesis* **2002**, *9*, 1133–1135.

(658) Marsella, M. J.; Wang, Z. Q.; Reid, R. J.; Yoon, K. *Org. Lett.* **2001**, *3*, 885–887.

(659) Solooki, D.; Bradshaw, J. D.; Tessier, C. A.; Youngs, W. J. *Organometallics* **1994**, *13*, 451–455.

(660) Zhang, D.; Tessier, C. A.; Youngs, W. J. *Chem. Mater.* **1999**, *11*, 3050–3057.

(661) Youngs, W. J.; Tessier, C. A.; Bradshaw, J. D. *Chem. Rev.* **1999**, *99*, 3153–3180.

(662) Sarkar, A.; Haley, M. M. *Chem. Commun.* **2000**, 1733–1734.

(663) Nitschke, J. R.; Don Tilley, T. *J. Organomet. Chem.* **2003**, *666*, 15–22.

(664) Jung, I.; Choi, H.; Kim, E.; Lee, C.-H.; Kang, S. O.; Ko, J. *Tetrahedron* **2005**, *61*, 12256–12263.

(665) Badger, G. M.; Elix, J. A.; Lewis, G. E. *Aust. J. Chem.* **1965**, *18*, 70–89.

(666) Hu, Z.; Atwood, J. L.; Cava, M. P. *J. Org. Chem.* **1994**, *59*, 8071–8075.

(667) Ellinger, F.; Gieren, A.; Hübner, T.; Lex, J.; Lucchesini, F.; Merz, A.; Neidlein, R.; Salbeck, J. *Monatsh. Chem.* **1993**, *124*, 931–943.

(668) Hu, Z.; Scordilis-Kelley, C.; Cava, M. P. *Tetrahedron Lett.* **1993**, *34*, 1879–1882.

(669) Kawase, T.; Darabi, H. R.; Uchimiya, R.; Oda, M. *Chem. Lett.* **1995**, *24*, 499–500.

(670) Kurata, H.; Baba, H.; Oda, M. *Chem. Lett.* **1997**, *26*, 571–572.

(671) Nakao, K.; Nishimura, M.; Tamachi, T.; Kuwatani, Y.; Miyasaka, H.; Nishinaga, T.; Iyoda, M. *J. Am. Chem. Soc.* **2006**, *128*, 16740–16747.

(672) Iyoda, M. *Heteroat. Chem.* **2007**, *18*, 460–466.

(673) Tobe, Y.; Utsumi, N.; Nagano, A.; Sonoda, M.; Naemura, K. *Tetrahedron* **2001**, *57*, 8075–8083.

(674) Meth-Cohn, O.; Jiang, H. *J. Chem. Soc., Perkin Trans. 1* **1998**, 3737–3746.

(675) Mayor, M.; Didschies, C. *Angew. Chem., Int. Ed.* **2003**, *42*, 3176–3179.

(676) Fomine, S.; Guadarrama, P. *J. Phys. Chem. A* **2006**, *110*, 10098–10105.

(677) Fomine, S.; Guadarrama, P.; Flores, P. *J. Phys. Chem. A* **2007**, *111*, 3124–3131.

(678) Badger, G. M.; Lewis, G. E.; Singh, U. P. *Aust. J. Chem.* **1966**, *19*, 1461–1476.

(679) Badger, G. M.; Lewis, G. E.; Singh, U. P. *Aust. J. Chem.* **1967**, *20*, 1635–1642.

(680) Johnson, M. R.; Miller, D. C.; Bush, K.; Becker, J. J.; Ibers, J. A. *J. Org. Chem.* **1992**, *57*, 4414–4417.

(681) De Munno, G.; Lucchesini, F.; Neidlein, R. *Tetrahedron* **1993**, *49*, 6863–6872.

(682) Kozaki, M.; Parakka, J. P.; Cava, M. P. *J. Org. Chem.* **1996**, *61*, 3657–3661.

(683) Vogel, E.; Röhrig, P.; Sicken, M.; Knipp, B.; Herrmann, A.; Pohl, M.; Schmickler, H.; Lex, J. *Angew. Chem., Int. Ed.* **1989**, *28*, 1651–1655.

(684) Vogel, E.; Pohl, M.; Herrmann, A.; Wiss, T.; König, C.; Lex, J.; Gross, M.; Gisselbrecht, J. P. *Angew. Chem., Int. Ed.* **1996**, *35*, 1520–1524.

(685) Hu, Z.; Cava, M. P. *Tetrahedron Lett.* **1994**, *35*, 3493–3496.

(686) Zhao, T.; Wei, Z.; Song, Y.; Xu, W.; Hu, W.; Zhu, D. *J. Mater. Chem.* **2007**, *17*, 4377–4381.

(687) Latos-Grazyński, L.; Lisowski, J.; Szterenberg, L.; Olmstead, M. M.; Balch, A. L. *J. Org. Chem.* **1991**, *56*, 4043–4045.

(688) Rachlewicz, K.; Sprutta, N.; Chmielewski, P. J.; Latos-Grayński, L. *J. Chem. Soc., Perkin Trans. 2* **1998**, 969–976.

(689) Srinivasan, A.; Anand, V. G.; Narayanan, S. J.; Pushpan, S. K.; Kumar, M. R.; Chandrashekar, T. K.; Sugiura, K.-I.; Sakata, Y. *J. Org. Chem.* **1999**, *64*, 8693–8697.

(690) Narayanan, S. J.; Sridevi, B.; Chandrashekar, T. K.; Vij, A.; Roy, R. *J. Am. Chem. Soc.* **1999**, *121*, 9053–9068.

(691) Anand, V. G.; Pushpan, S. K.; Venkatraman, S.; Narayanan, S. J.; Dey, A.; Chandrashekar, T. K.; Roy, R.; Joshi, B. S.; Deepa, S.; Sastry, G. N. *J. Org. Chem.* **2002**, *67*, 6309–6319.

(692) Anand, V. R. G.; Pushpan, S. K.; Srinivasan, A.; Narayanan, S. J.; Sridevi, B.; Chandrashekar, T. K.; Roy, R.; Joshi, B. S. *Org. Lett.* **2000**, *2*, 3829–3832.

(693) Anand, V. G.; Pushpan, S. K.; Venkatraman, S.; Dey, A.; Chandrashekar, T. K.; Joshi, B. S.; Roy, R.; Teng, W.; Senge, K. R. *J. Am. Chem. Soc.* **2001**, *123*, 8620–8621.

(694) Sprutta, N.; Latos-Grazynski, L. *Chem.—Eur. J.* **2001**, *7*, 5099–5112.

(695) Kumar, R.; Misra, R.; Chandrashekar, T. K.; Suresh, E. *Chem. Commun.* **2007**, 43–45.

(696) Seidel, D.; Lynch, V.; Sessler, J. L. *Angew. Chem., Int. Ed.* **2002**, *41*, 1422–1425.

(697) Flory, P. J. *J. Am. Chem. Soc.* **1941**, *63*, 3091–3096.

(698) Flory, P. J. *J. Am. Chem. Soc.* **1941**, *63*, 3096–3100.

(699) Flory, P. J. *J. Am. Chem. Soc.* **1952**, *74*, 2718–2723.

(700) Buhleier, E.; Wehner, W.; Vögtle, F. *Synthesis* **1978**, 155–158.

(701) Tomalia, D. A.; Baker, H.; Dewald, J.; Hall, M.; Kallos, G.; Martin, S.; Roeck, J.; Ryder, J.; Smith, P. *Polym. J.* **1985**, *17*, 117–132.

(702) Newkome, G. R.; Yao, Z.; Baker, G. R.; Gupta, V. K. *J. Org. Chem.* **1985**, *50*, 2003–2004.

(703) Newkome, G. R.; Moorefield, C. N.; Vögtle, F. *Dendrimers and Dendrons: Concepts, Syntheses, Applications*; Wiley-VCH: Weinheim, Germany, 2001.

(704) Moorefield, C. N.; Newkome, G. R.; Mishra, A. In *Encyclopedia of Supramolecular Chemistry*; Atwood, J. L., Steed, J. W., Eds.; Marcel Dekker: New York, 2004.

(705) Moore, J. S. *Acc. Chem. Res.* **1997**, *30*, 402–413.

(706) Gong, L.; Hu, Q.; Pu, L. *J. Org. Chem.* **2001**, *66*, 2358–2367.

(707) Dev, S. K.; Maddux, T. M.; Yu, L. *J. Am. Chem. Soc.* **1997**, *119*, 9079–9080.

(708) Berresheim, A. J.; Müller, M.; Müllen, K. *Chem. Rev.* **1999**, *99*, 1747–1785.

(709) Geng, Y.; Fechtenkötter, A.; Müllen, K. *J. Mater. Chem.* **2001**, *11*, 1634–1641.

(710) Bilge, A.; Zen, A.; Forster, M.; Li, H.; Galbrecht, F.; Nehls, B. S.; Farrell, T.; Neher, D.; Scherf, U. *J. Mater. Chem.* **2006**, *16*, 3177–3182.

(711) Zen, A.; Bilge, A.; Galbrecht, F.; Alle, R.; Meerholz, K.; Grenzer, J.; Neher, D.; Scherf, U.; Farrell, T. *J. Am. Chem. Soc.* **2006**, *128*, 3914–3915.

(712) Sun, X.; Liu, Y.; Chen, S.; Qiu, W.; Yu, G.; Ma, Y.; Qi, T.; Zhang, H.; Xu, X.; Zhu, D. *Adv. Funct. Mater.* **2006**, *16*, 917–925.

(713) Sun, X.; Zhou, Y.; Wu, W.; Liu, Y.; Tian, W.; Yu, G.; Qiu, W.; Chen, S.; Zhu, D. *J. Phys. Chem. B* **2006**, *110*, 7702–7707.

(714) Pappenfus, T. M.; Mann, K. R. *Org. Lett.* **2002**, *4*, 3043–3046.

(715) Casado, J.; Pappenfus, T. M.; Mann, K. R.; Hern, V.; López Navarrete, J. T. *J. Chem. Phys.* **2004**, *120*, 11874–11881.

(716) Tabakovic, I.; Kunugi, Y.; Canavesi, A.; Miller, L. L. *Acta Chem. Scand.* **1998**, *52*, 131–136.

(717) Yamamoto, K.; Higuchi, M.; Uchida, K.; Kojima, Y. *Macromolecules* **2002**, *35*, 5782–5788.

(718) Ohishi, H.; Tanaka, M.; Kageyama, H.; Shirota, Y. *Chem. Lett.* **2004**, *33*, 1266–1267.

(719) Kunugi, Y.; Tabakovic, I.; Canavesi, A.; Miller, L. L. *Synth. Met.* **1997**, *89*, 227–229.

(720) Kunugi, Y.; Niwa, Y.; Zhu, L.; Harima, Y.; Yamashita, K. *Chem. Lett.* **2001**, *30*, 656–657.

(721) Yamamoto, K.; Higuchi, M.; Uchida, K.; Kojima, Y. *Macromol. Rapid Commun.* **2001**, *22*, 266–270.

(722) Cho, J.-S.; Kojima, Y.; Yamamoto, K. *Polym. Adv. Technol.* **2003**, *14*, 52–57.

(723) Cravino, A.; Roquet, S.; Aleveque, O.; Leriche, P.; Frere, P.; Roncali, J. *Chem. Mater.* **2006**, *18*, 2584–2590.

(724) Rapta, P.; Tabet, A.; Hartmann, H.; Dunsch, L. *J. Mater. Chem.* **2007**, *17*, 4998–5007.

(725) Roquet, S.; Cravino, A.; Leriche, P. O. A.; Frére, P.; Roncali, J. *J. Am. Chem. Soc.* **2006**, *128*, 3459–3466.

(726) Cravino, A.; Leriche, P.; Alévêque, O.; Roquet, S.; Roncali, J. *Adv. Mater.* **2006**, *18*, 3033–3037.

(727) Cremer, J.; Briehn, C. A. *Chem. Mater.* **2007**, *19*, 4155–4165.

(728) Pei, J.; Wang, J. L.; Cao, X. Y.; Zhou, X. H.; Zhang, W. B. *J. Am. Chem. Soc.* **2003**, *125*, 9944–9945.

(729) Sun, Y. M.; Xiao, K. Y.; Liu, Q.; Wang, J. L.; Pei, J.; Yu, G.; Zhu, D. B. *Adv. Funct. Mater.* **2005**, *15*, 818–822.

(730) Wang, J. L.; Luo, J.; Liu, L. H.; Zhou, Q. F.; Ma, Y.; Pei, J. *Org. Lett.* **2006**, *8*, 2281–2284.

(731) Wang, H.; Wang, J.-L.; Yuan, S.-C.; Jian, P.; Pei, W.-W. *Tetrahedron* **2005**, *61*, 8465–8474.

(732) Wang, J. L.; Duan, X. F.; Jiang, B.; Gan, L. B.; Pei, J.; He, C.; Li, Y. F. *J. Org. Chem.* **2006**, *71*, 4400–4410.

(733) Amaya, T.; Mori, K.; Wu, H.-L.; Ishida, S.; Nakamura, J.-I.; Murata, K.; Hirao, T. *Chem. Commun.* **2007**, 1902–1904.

(734) You, C. C.; Saha-Möller, C. R.; Würthner, F. *Chem. Commun.* **2004**, 2030–2031.

(735) You, C.-C.; Espindola, P.; Hippius, C.; Heinze, J.; Würthner, F. *Adv. Funct. Mater.* **2007**, *17*, 3764–3772.

(736) Chen, L. X.; Xiao, S.; Yu, L. *J. Phys. Chem. B* **2006**, *110*, 11730–11738.

(737) Cremer, J.; Bäuerle, P. *J. Mater. Chem.* **2006**, *16*, 874–884.

(738) Petrella, A.; Cremer, J.; De Cola, L.; Bäuerle, P.; Williams, R. M. *J. Phys. Chem. A* **2005**, *109*, 11687–11695.

(739) Arsenyan, P.; Pudova, O.; Popelis, J.; Lukevics, E. *Tetrahedron Lett.* **2004**, *45*, 3109–3111.

(740) Roquet, S.; de Bettignies, R.; Leriche, P.; Cravino, A.; Roncali, J. *J. Mater. Chem.* **2006**, *16*, 3040–3045.

(741) Reyes-Reyes, M.; Kim, K.; Carroll, D. L. *Appl. Phys. Lett.* **2005**, *87*, 083506(1)−083506(3)..

(742) Mihailetchi, V. D.; Xie, H. X.; de Boer, B.; Koster, L. J. A.; Blom, P. W. M. *Adv. Funct. Mater.* **2006**, *16*, 699–708.

(743) Kim, Y.; Cook, S.; Tuladhar, S. M.; Choulis, S. A.; Nelson, J.; Durrant, J. R.; Bradley, D. D. C.; Giles, M.; McCulloch, I.; Ha, C.-S.; Ree, M. *Nat. Mater.* **2006**, *5*, 197–203.

(744) Kim, J. Y.; Lee, K.; Coates, N. E.; Moses, D.; Nguyen, T.-Q.; Dante, M.; Heeger, A. J. *Science* **2007**, *317*, 222–225.

(745) Fujitsuka, M.; Cho, D. W.; Ohshita, J.; Kunai, A.; Majima, T. *J. Phys. Chem. C* **2007**, *111*, 1993–1998.

(746) Borshchev, O. V.; Ponomarenko, S. A.; Surin, N. M.; Kaptyug, M. M.; Buzin, M. I.; Pleshkova, A. P.; Demchenko, N. V.; Myakushev, V. D.; Muzafarov, A. M. *Organometallics* **2007**, *26*, 5165–5173.

(747) Liu, X.-M.; He, C.; Huang, J. *Tetrahedron Lett.* **2004**, *45*, 6173–6177.

(748) Liu, X.-M.; He, C.; Xu, J.-W. *Tetrahedron Lett.* **2004**, *45*, 1593–1597.

(749) Wu, R.; Schumm, J. S.; Pearson, D. L.; Tour, J. M. *J. Org. Chem.* **1996**, *61*, 6906–6921.

(750) Tour, J. M. *Chem. Rev.* **1996**, *96*, 537–553.

(751) Pei, J.; Ni, J.; Zhou, X. H.; Cao, X. Y.; Lai, Y. H. *J. Org. Chem.* **2002**, *67*, 4924–4936.

(752) Pei, J.; Ni, J.; Zhou, X. H.; Cao, X. Y.; Lai, Y. H. *J. Org. Chem.* **2002**, *67*, 8104–8113.

(753) Ponomarenko, S. A.; Tatarinova, E. A.; Muzafarov, A. M.; Kirchmeyer, S.; Brassat, L.; Mourran, A.; Moeller, M.; Setayesh, S.; de Leeuw, D. *Chem. Mater.* **2006**, *18*, 4101–4108.

(754) Miller, L. L.; Kunugi, Y.; Canavesi, A.; Rigaut, S.; Moorefield, C. N.; Newkome, G. R. *Chem. Mater.* **1998**, *10*, 1751–1754.

(755) Deng, S.; Locklin, J.; Patton, D.; Baba, A.; Advincula, R. C. *J. Am. Chem. Soc.* **2005**, *127*, 1744–1751.

(756) Advincula, R. C. *Dalton Trans.* **2006**, 2778–2784.

(757) Huynh, W. U.; Dittmer, J. J.; Alivisatos, A. P. *Science* **2002**, *295*, 2425–2427.

(758) Ponomarenko, S. A.; Kirchmeyer, S.; Elschner, A.; Huisman, B. H.; Karbach, A.; Drechsler, D. *Adv. Funct. Mater.* **2003**, *13*, 591–596.

(759) Kirchmeyer, S.; Ponomarenko, S. U.S. Patent, 0,132,959, 2004.

(760) Mitchell, W. J.; Kopidakis, N.; Rumbles, G.; Ginley, D. S.; Shaheen, S. E. *J. Mater. Chem.* **2005**, *15*, 4518–4528.

(761) Kopidakis, N.; Mitchell, W. J.; Van de Lagemaat, J.; Ginley, D. S.; Rumbles, G.; Shaheen, S. E.; Rance, W. L. *Appl. Phys. Lett.* **2006**, *89*, 103524(1)−103524(3)..

(762) John, H.; Bauer, R.; Espindola, P.; Sonar, P.; Heinze, J.; Müllen, K. *Angew. Chem., Int. Ed.* **2005**, *44*, 2447–2451.

(763) Malenfant, P. R. L.; Groenendaal, L.; Fréchet, J. M. J. *J. Am. Chem. Soc.* **1998**, *120*, 10990–10991.

(764) Apperloo, J. J.; Janssen, R. A. J.; Malenfant, P. R. L.; Groenendaal, L.; Fréchet, J. M. J. *J. Am. Chem. Soc.* **2000**, *122*, 7042–7051.

(765) Van Haare, J. A. E. H.; Havinga, E. E.; Van Dongen, J. L. J.; Janssen, R. A. J.; Cornil, J.; Brédas, J.-L. *Chem.—Eur. J.* **1998**, *4*, 1509–1522.

(766) Malenfant, P. R. L.; Jayaraman, M.; Fréchet, J. M. J. *Chem. Mater.* **1999**, *11*, 3420–3422.

(767) Adronov, A.; Malenfant, P. R. L.; Fréchet, J. M. J. *Chem. Mater.* **2000**, *12*, 1463–1472.

(768) Freeman, A. W.; Koene, S. C.; Malenfant, P. R. L.; Thompson, M. E.; Fréchet, J. M. J. *J. Am. Chem. Soc.* **2000**, *122*, 12385–12386.

(769) Xia, C.; Fan, X.; Locklin, J.; Advincula, R. C. *Org. Lett.* **2002**, *4*, 2067–2070.

(770) Xia, C.; Fan, X.; Locklin, J.; Advincula, R. C.; Gies, A.; Nonidez, W. *J. Am. Chem. Soc.* **2004**, *126*, 8735–8743.

(771) Ma, C. Q.; Mena-Osteritz, E.; Debaerdemaeker, T.; Wienk, M. M.; Janssen, R. A.; Bäuerle, P. *Angew. Chem., Int. Ed.* **2007**, *46*, 1679–1683.

(772) Su, Y. Z.; Lin, J. T.; Tao, Y.-T.; Ko, C.-W.; Lin, S.-C.; Sun, S.-S. *Chem. Mater.* **2002**, *14*, 1884–1890.

(773) Zhang, Y.; Zhao, C.; Yang, J.; Kapiamba, M.; Haze, O.; Rothberg, L. J.; Ng, M. K. *J. Org. Chem.* **2006**, *71*, 9475–9483.

(774) Negishi, N.; Ie, Y.; Taniguchi, M.; Kawai, T.; Tada, H.; Kaneda, T.; Aso, Y. *Org. Lett.* **2007**, *9*, 829–832.

(775) Izumi, T.; Kobashi, S.; Takimiya, K.; Aso, Y.; Otsubo, T. *J. Am. Chem. Soc.* **2003**, *125*, 5286–5287.

(776) Allard, S.; Forster, M.; Souharce, B.; Thiem, H.; Scherf, U. *Angew. Chem., Int. Ed.* **2008**, *47*, 4070–4098.

(777) Wolffs, M.; Korevaar, P. A.; Jonkheijm, P.; Henze, O.; Feast, W. J.; Schenning, A. P. H. J.; Meijer, E. W. *Chem. Commun.* **2008**, 4613–4615.

(778) Tsuge, A.; Hara, T.; Moriguchi, T.; Yamaji, M. *Chem. Lett.* **2008**, *37*, 870–871.

(779) Justin Thomas, K. R.; Hsu, Y.-C.; Lin, J. T.; Lee, K.-M.; Ho, K.-C.; Lai, C.-H.; Cheng, Y.-M.; Chou, P.-T. *Chem. Mater.* **2008**, *20*, 1830–1840.

(780) Wang, Z.-S.; Koumura, N.; Cui, Y.; Takahashi, M.; Sekiguchi, H.; Mori, A.; Kubo, T.; Furube, A.; Hara, K. *Chem. Mater.* **2008**, *20*, 3993–4003.

(781) Choi, H.; Baik, C.; Kang, S. O.; Ko, J.; Kang, M.-S.; Nazeeruddin, M. K.; Grätzel, M. *Angew. Chem., Int. Ed.* **2008**, *47*, 327–330.

(782) Li, G.; Jiang, K.-J.; Li, Y.-F.; Li, S.-L.; Yang, L.-M. *J. Phys. Chem. C* **2008**, *112*, 11591–11599.

(783) Tian, H.; Yang, X.; Chen, R.; Zhang, R.; Hagfeldt, A.; Sun, L. *J. Phys. Chem. C* **2008**, *112*, 11023–11033.

(784) Qin, H.; Wenger, S.; Xu, M.; Gao, F.; Jing, X.; Wang, P.; Zakeeruddin, S. M.; Grätzel, M. *J. Am. Chem. Soc.* **2008**, *130*, 9202–9203.

(785) Ie, Y.; Umemoto, Y.; Okabe, M.; Kusunoki, T.; Nakayama, K. i.; Pu, Y. J.; Kido, J.; Tada, H.; Aso, Y. *Org. Lett.* **2008**, *10*, 833–836.

(786) Umemoto, Y.; Ie, Y.; Saeki, A.; Seki, S.; Tagawa, S.; Aso, Y. *Org. Lett.* **2008**, *10*, 1095–1098.

(787) Ie, Y.; Umemoto, Y.; Nitani, M.; Aso, Y. *Pure Appl. Chem.* **2008**, *80*, 589–597.

(788) Sugiyasu, K.; Kawano, S.-i.; Fujita, N.; Shinkai, S. *Chem. Mater.* **2008**, *20*, 2863–2865.

(789) Riede, M. K.; Schueppel, R.; Schulze, K.; Wynands, D.; Timmreck, R.; Uhrich, C.; Petrich, A.; Pfeiffer, M.; Brier, E.; Reinold, E.; Bäuerle, P.; Leo, K. *Proc. SPIE—Int. Soc. Opt. Eng.* **2008**, *7002*, 70020G(1−8)..

(790) Zrig, S.; Rémy, P.; Andrioletti, B.; Rose, E.; Asselberghs, I.; Clays, K. *J. Org. Chem.* **2008**, *73*, 1563–1566.

(791) Wan, J.; Ferreira, A.; Xia, W.; Chow, C. H.; Takechi, K.; Kamat, P. V.; Jones Ii, G.; Vullev, V. I. *J. Photochem. Photobiol. A* **2008**, *197*, 364–374.

(792) Cornelis, D.; Peeters, H.; Zrig, S.; Andrioletti, B.; Rose, E.; Verbiest, T.; Koeckelberghs, G. *Chem. Mater.* **2008**, *20*, 2133–2143.

(793) Tamayo, A. B.; Walker, B.; Nguyen, T.-Q. *J. Phys. Chem. C* **2008**, *112*, 11545–11551.

(794) Tamayo, A. B.; Tantiwiwat, M.; Walker, B.; Nguyen, T.-Q. *J. Phys. Chem. C* **2008**, *112*, 15543–15552.

(795) Li, J.-C.; Lee, S.-H.; Hahn, Y.-B.; Kim, K.-J.; Zong, K.; Lee, Y.-S. *Synth. Met.* **2008**, *158*, 150–156.

(796) Huang, J.; Fu, H.; Wu, Y.; Chen, S.; Shen, F.; Zhao, X.; Liu, Y.; Yao, J. *J. Phys. Chem. C* **2008**, *112*, 2689–2696.

(797) Fujitsuka, M.; Harada, K.; Sugimoto, A.; Majima, T. *J. Phys. Chem. A* **2008**, *112*, 10193–10199.

(798) Huang, J.; Sun, J.; Katz, H. E. *Adv. Mater.* **2008**, *20*, 2567–2572.

(799) Becerril, H. A.; Roberts, M. E.; Liu, Z.; Locklin, J.; Bao, Z. *Adv. Mater.* **2008**, *20*, 2588–2594.

(800) Yazaki, S.; Funahashi, M.; Kato, T. *J. Am. Chem. Soc.* **2008**, *130*, 13206–13207.

(801) Li, W.-S.; Yamamoto, Y.; Fukushima, T.; Saeki, A.; Seki, S.; Tagawa, S.; Masunaga, H.; Sasaki, S.; Takata, M.; Aida, T. *J. Am. Chem. Soc.* **2008**, *130*, 8886–8887.

(802) Nakamura, Y.; Araki, Y.; Ito, O.; Takimiya, K.; Otsubo, T. *J. Phys. Chem. A* **2008**, *112*, 1125–1132.

(803) Steen, R. O.; Nurkkala, L. J.; Angus-Dunne, S. J.; Schmitt, C. X.; Constable, E. C.; Riley, M. J.; Bernhardt, P. V.; Dunne, S. J. *Eur. J. Inorg. Chem.* **2008**, 1784–1794.

(804) Gao, F.; Wang, Y.; Zhang, J.; Shi, D.; Wang, M.; Humphry-Baker, R.; Wang, P.; Zakeeruddin, S. M.; Gratzel, M. *Chem. Commun.* **2008**, 2635–2637.

(805) Sato, M.; Kitamura, T.; Masiko, T.; Unoura, K. *J. Organomet. Chem.* **2008**, *693*, 247–256.

(806) Chisholm, M. H.; Chou, P.-T.; Chou, Y.-H.; Ghosh, Y.; Gustafson, T. L.; Ho, M.-L. *Inorg. Chem.* **2008**, *47*, 3415–3425.

(807) Burdzinski, G. T.; Chisholm, M. H.; Chou, P. T.; Chou, Y. H.; Feil, F.; Gallucci, J. C.; Ghosh, Y.; Gustafson, T. L.; Ho, M. L.; Liu, Y.; Ramnauth, R.; Turro, C. *Proc. Natl. Acad. Sci. U.S.A.* **2008**, *105*, 15247–15252.

(808) Alesi, S.; Brancolini, G.; Melucci, M.; Massimo, L.; Alessandro, C.; Camaioni, V. N.; Barbarella, G. *Chem.—Eur. J.* **2008**, *14*, 513–521.

(809) Spada, G. P.; Lena, S.; Masiero, S.; Pieraccini, S.; Surin, M.; Samorì, P. *Adv. Mater.* **2008**, *20*, 2433–2438.

(810) Jatsch, A.; Kopyshev, A.; Mena-Osteritz, E.; Bäuerle, P. *Org. Lett.* **2008**, *10*, 961–964.

(811) Tsai, W.-W.; Li, L.-s.; Cui, H.; Jiang, H.; Stupp, S. I. *Tetrahedron* **2008**, *64*, 8504–8514.

(812) Capobianco, M. L.; Cazzato, A.; Alesi, S.; Barbarella, G. *Bioconjugate Chem.* **2008**, *19*, 171–177.

(813) Quarta, A.; Di Corato, R.; Manna, L.; Argentiere, S.; Cingolani, R.; Barbarella, G.; Pellegrino, T. *J. Am. Chem. Soc.* **2008**, *130*, 10545–10555.

(814) Meek, S. T.; Nesterov, E. E.; Swager, T. M. *Org. Lett.* **2008**, *10*, 2991–2993.

(815) Um, M.-C.; Kwak, J.; Hong, J.-P.; Kang, J.; Yoon, D. Y.; Lee, S. H.; Lee, C.; Hong, J.-I. *J. Mater. Chem.* **2008**, *18*, 4698–4703.

(816) Noh, Y.-Y.; Kim, D.-Y.; Misaki, M.; Yase, K. *Thin Solid Films* **2008**, *516*, 7505–7510.

(817) Kadzimirsz, D.; Kramer, D.; Sripanom, L.; Oppel, I. M.; Rodziewicz, P.; Doltsinis, N. L.; Dyker, G. *J. Org. Chem.* **2008**, *73*, 4644–4649.

(818) Liu, M.-G.; Hu, Y.-G.; Ding, M.-W. *Tetrahedron* **2008**, *64*, 9052–9059.

(819) Mashraqui, S. H.; Sangvikar, Y. S.; Ghadigaonkar, S. G.; Ashraf, M.; Meetsma, M. *Tetrahedron* **2008**, *64*, 8837–8842.

(820) Chang, Y.-C.; Chen, Y.-D.; Chen, C.-H.; Wen, Y.-S.; Lin, J. T.; Chen, H.-Y.; Kuo, M.-Y.; Chao, I. *J. Org. Chem.* **2008**, *73*, 4608–4614.

(821) Navacchia, M. L.; Melucci, M.; Favaretto, L.; Zanelli, A.; Gazzano, M.; Bongini, A.; Barbarella, G. *Org. Lett.* **2008**, *10*, 3665–3668.

(822) Pappenfus, T. M.; Hermanson, B. J.; Helland, T. J.; Lee, G. G. W.; Drew, S. M.; Mann, K. R.; McGee, K. A.; Rasmussen, S. C. *Org. Lett.* **2008**, *10*, 1553–1556.

(823) Brusso, J. L.; Hirst, O. D.; Dadvand, A.; Ganesan, S.; Cicoira, F.; Robertson, C. M.; Oakley, R. T.; Rosei, F.; Perepichka, D. F. *Chem. Mater.* **2008**, *20*, 2484–2494.

(824) Niu, Q.; Zhou, Y.; Wang, L.; Peng, J.; Wang, J.; Pei, J.; Cao, Y. *Adv. Mater.* **2008**, *20*, 964–969.

(825) Karsten, B. P.; Janssen, R. A. J. *Org. Lett.* **2008**, *10*, 3513–3516.

(826) Fukazawa, A.; Yamada, H.; Yamaguchi, S. *Angew. Chem., Int. Ed.* **2008**, *47*, 5582–5585.

(827) Suzuki, Y.; Okamoto, T.; Wakamiya, A.; Yamaguchi, S. *Org. Lett.* **2008**, *10*, 3393–3396.

(828) Miguel, L. S.; Matzger, A. J. *J. Org. Chem.* **2008**, *73*, 7882–7888.

(829) Fujimoto, T.; Suizu, R.; Yoshikawa, H.; Awaga, K. *Chem.—Eur. J.* **2008**, *14*, 6053–6056.

(830) Flores, P.; Guadarrama, P.; Ramos, E.; Fomine, S. *J. Phys. Chem. A* **2008**, *112*, 3996–4003.

(831) O'Connor, M. J.; Haley, M. M. *Org. Lett.* **2008**, *10*, 3973–3976.

(832) O'Connor, M. J.; Yelle, R. B.; Zakharov, L. N.; Haley, M. M. *J. Org. Chem.* **2008**, *73*, 4424–4432.

(833) Williams-Harry, M.; Bhaskar, A.; Ramakrishna, G.; Goodson, T.; Imamura, M.; Mawatari, A.; Nakao, K.; Enozawa, H.; Nishinaga, T.; Iyoda, M. *J. Am. Chem. Soc.* **2008**, *130*, 3252–3253.

(834) Yin, J.; Lin, Y.; Cao, X.; Yu, G.-A.; Liu, S. H. *Tetrahedron Lett.* **2008**, *49*, 1582–1585.

(835) Benincori, T.; Capaccio, M.; Angelis, F. D.; Falciola, L.; Muccini, M.; Mussini, P.; Ponti, A.; Toffanin, S.; Traldi, P.; Sannicolò, F. *Chem.—Eur. J.* **2008**, *14*, 459–471.

(836) Ramakrishna, G.; Bhaskar, A.; Bäuerle, P.; Ma, C. Q.; Goodson, T., III *J. Phys. Chem. A* **2008**, *112*, 2018–2026.

(837) Zen, A.; Pingel, P.; Neher, D.; Scherf, U. *Phys. Status Solidi A* **2008**, *205*, 440–448.

(838) Luponosov, Y. N.; Ponomarenko, S. A.; Surin, N. M.; Muzafarov, A. M. *Org. Lett.* **2008**, *10*, 2753–2756.

(839) Wang, J.-L.; Yan, J.; Tang, Z.-M.; Xiao, Q.; Ma, Y.; Pei, J. *J. Am. Chem. Soc.* **2008**, *130*, 9952–9962.

(840) Leriche, P.; Aillerie, D.; Roquet, S.; Allain, M.; Cravino, A.; Frere, P.; Roncali, J. *Org. Biomol. Chem.* **2008**, *6*, 3202–3207.